Neural Plasticity

Reestablishing Neural Plasticity in Regenerated Spiral Ganglion Neurons and Sensory Hair Cells for Hearing Loss 2021

Lead Guest Editor: Renjie Chai
Guest Editors: Geng-lin Li, Jian Wang, Jing Zou, and Hai Huang

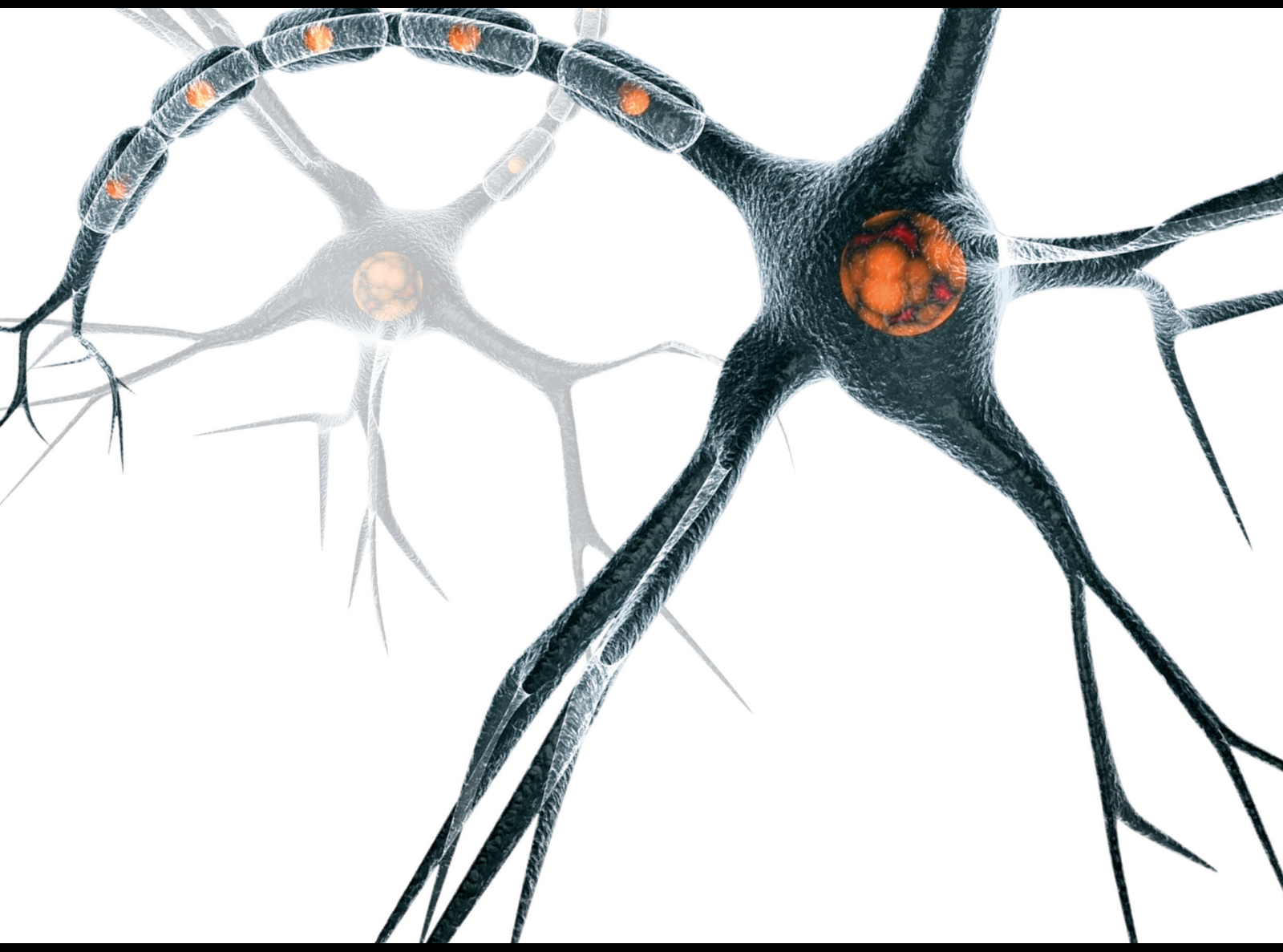

Reestablishing Neural Plasticity in Regenerated Spiral Ganglion Neurons and Sensory Hair Cells for Hearing Loss 2021

Neural Plasticity

Reestablishing Neural Plasticity in Regenerated Spiral Ganglion Neurons and Sensory Hair Cells for Hearing Loss 2021

Lead Guest Editor: Renjie Chai
Guest Editors: Geng-lin Li, Jian Wang, Jing Zou, and Hai Huang

Contents

Hindawi
Neural Plasticity
Volume 2022, Article ID 5567174, 12 pages
https://doi.org/10.1155/2022/5567174

Research Article

ROS-Induced Oxidative Damage and Mitochondrial Dysfunction Mediated by Inhibition of SIRT3 in Cultured Cochlear Cells

Lingjun Zhang, Zhengde Du, Lu He, Wenqi Liang, Ke Liu, and Shusheng Gong

Department of Otorhinolaryngology, Beijing Friendship Hospital, Capital Medical University, 95 Yongan Road, Xicheng District, Beijing 100050, China

Correspondence should be addressed to Ke Liu; liuke@ccmu.edu.cn and Shusheng Gong; gongss1962@163.com

Received 5 February 2021; Revised 23 April 2021; Accepted 28 December 2021; Published 19 January 2022

Academic Editor: Renjie Chai

Sensorineural hearing loss (SNHL) is one of the most common causes of disability worldwide. Previous evidence suggests that reactive oxygen species (ROS) may play an important role in the occurrence and development of SNHL, while its mechanism remains unclear. We cultured dissected organs of Corti in medium containing different concentrations (0, 0.25, 0.5, 0.75, 1, and 1.25 mM) of hydrogen peroxide (H_2O_2) and established a four-concentration model of 0, 0.5, 0.75, and 1 mM to study different degrees of damage. We examined ROS-induced mitochondrial damage and the role of sirtuin 3 (SIRT3). Our results revealed that the number of ribbon synapses and hair cells appeared significantly concentration-dependent decrease with exposure to H_2O_2. Outer hair cells (OHCs) and inner hair cells (IHCs) began to be lost, and activation of apoptosis of hair cells (HCs) was observed at 0.75 mM and 1 mM H_2O_2, respectively. In contrast with the control group, the accumulation of ROS was significantly higher, and the mitochondrial membrane potential (MMP) was lower in the H_2O_2-treated groups. Furthermore, the expression of SIRT3, FOXO3A, and SOD2 proteins declined, except for an initial elevation of SIRT3 between 0 and 0.75 mM H_2O_2. Administration of the selective SIRT3 inhibitor 3-(1H-1,2,3-triazol-4-yl) pyridine resulted in increased damage to the cochlea, including loss of ribbon synapses and hair cells, apoptosis of hair cells, more production of ROS, and reduced mitochondrial membrane potential. Thoroughly, our results highlight that ROS-induced mitochondrial oxidative damage drives hair cell degeneration and apoptosis. Furthermore, SIRT3 is crucial for preserving mitochondrial function and protecting the cochlea from oxidative damage and may represent a possible therapeutic target for SNHL.

1. Introduction

As life expectancy increases, sensorineural hearing loss has become more common, affecting people's living quality [1]. There are several types of sensorineural hearing loss (SNHL), such as noised-induced hearing loss (NIHL), age-related hearing loss (ARHL), ototoxic drug-induced hearing loss (ODIHL), and inherited hearing loss. ARHL or presbycusis is a progressive decline in hearing function that is the most prevalent type of SNHL in the elderly [2–5], which is characterized by higher hearing thresholds, beginning at high frequencies and spreading toward low frequencies, accompanied by the loss of HCs and spiral ganglion neurons (SGNs) from the basal to apical turn. Noise-induced hearing loss (NIHL) is the second most prevalent type of SNHL, behind presbycusis [3]. It is typically characterized by elevation in hearing thresholds and speech perception, tinnitus, and auditory processing disorders [6] due to damage to and/or death of cochlear hair cells, as well as primary auditory neurons after exposure to strong noise stimulation [7]. Platinum-based anticancer drugs and aminoglycoside antibiotics can lead to hearing loss at high frequencies and preferential damage to OHCs at the cochlea basal turn [8–10].

Reactive oxygen species (ROS) are mainly generated by the mitochondria in most mammalian cells [11, 12], including hydroxyl radicals and hydrogen peroxide (H_2O_2). Growing evidence has convincingly argued that ROS and oxidative stress are responsible for the pathogenesis of various cochlear disorders, especially SNHL, including noise exposure, senility, and ototoxicity [13, 14]. An immediate increase in ROS in the cochlea after noise exposure indicates

that ROS are associated with early damage to cochlear hair cells and persist for 7-10 days [15]. In a model of the senescence-accelerated mouse prone 8 (SAMP8), oxidative stress and impairment in activities of antioxidant enzyme were shown to be involved in premature ARHL [16]. Moreover, ototoxic drugs can induce generation of ROS [17, 18]. On the other hand, recent studies have suggested that before overt hearing loss happened, cochlear synaptopathy, which synapses between IHCs and cochlear afferent nerve fibers are disrupted, is more common taking place [19], although there is no direct evidence that ROS could cause loss of synapses. Rodent studies have indicated excessive release of glutamate from IHCs and insufficient energy supply can lead to cochlear synaptopathy [20, 21], while this all could be induced by ROS. In this study, we hoped to provide some direct evidence between ROS and cochlear synaptopathy. Much evidence implicates that mitochondrial dysfunction contributes to the occurrence and evolution of SNHL [22, 23]. As the major inducer of ROS, it is assumed that exposure to noise, aging, and ototoxic drugs causes mitochondrial damage and, in turn, increases ROS accumulation, which eventually results in apoptosis, necrosis, and tissue damage [6]. Mitochondrial damage, lipid peroxidation, and immune inflammatory reactions are strongly associated with ROS [24–26]. ROS can also lower mitochondrial membrane potential and induce calcium overload, further damaging the mitochondria and contributing to hair cell apoptosis or necrosis [25, 27].

Given the important role ROS play in SNHL, the development and application of antioxidant drugs are becoming increasingly common. Sirtuin proteins are histone deacetylases dependent on nicotinamide adenine dinucleotide (NAD^+); they have been shown to regulate the morphology and function of mitochondria and have become the focus of research in recent years. The NAD^+-dependent mitochondrial sirtuin, SIRT3, has been shown to be able to deacetylate mitochondrial respiratory chain complex subunit proteins and promote energy production [28]. SIRT3 not only increases the activity of intracellular antioxidant enzymes by activating FOXO3A but also directly deacetylates MnSOD to increase the antioxidant capacity of cells and reduce intracellular ROS levels [29, 30]. A recent study has suggested that administration of NAD^+ precursor, nicotinamide riboside, can prevent spiral ganglia neurite degeneration and NIHL, which is mediated by SIRT3 [31]. In vitro, overexpression of SIRT3 can ameliorate autophagic cell death, which is dependent on superoxide anions generated from mitochondria induced by cadmium [32]. However, the direct effect of SIRT3 in cochlear basilar membranes (CBMs) has not been documented yet.

Here, we explored the hypothesis that ROS induced by exposure to different concentrations of H_2O_2 may cause mitochondrial damage and loss of ribbon synapses in vitro, which may contribute to SNHL at the cellular level. In addition, we also explored the role of SIRT3 in cochlear oxidative damage in cultured organs of Corti in vitro, and possible protective mechanisms by SIRT3 involvement were investigated.

2. Materials and Methods

2.1. Animals. We purchased postnatal day 3 C57BL/6 mice from the Experimental Animal Department of the Capital Medical University. The experimental protocols conformed to the National Institutes of Health guidelines, which were revised in 1996 (NIH Publications). Our research had got permission from the Capital Medical University Animal Ethics Committee.

2.2. Cultures. After the skin was cleaned with 75% alcohol, the postnatal day 3 C57BL/6 mice were euthanized by cold CO_2 inhalation and decapitated painlessly. The skin was peeled off the scalp, and the skull was cut into two pieces posterior to the eye. The cochleae were removed and placed in Leibovitz's L-15 (Procell, PM151012, Wuhan, China). The organ of Corti was separated away from the stria vascularis and then adhered to separate culture plates. Each plate contained 1 ml/well of culture medium, which comprised Dulbecco's modified Eagle's medium/Ham's F-12 (DMEM/F-12; 1 : 1 Mix) (Sigma-Aldrich, D8437, St. Louis, MO, USA) with 10% bovine serum albumin (Sigma-Aldrich, A1595, St. Louis, MO, USA) and 30 U/mL penicillin G (Sigma-Aldrich, P3032, St. Louis, MO, USA). The organ of Corti explants was cultured in a humidified atmosphere with 5% CO_2 at 37°C.

2.3. H_2O_2-Induced Oxidative Stress. According to various studies, we chose to use H_2O_2 to induce oxidative stress in vitro. First, cochlear specimens were placed in a humidified incubator for 24 h. Then, the culture medium was discarded and substituted by fresh medium (DMEM/F-12) containing different concentrations of H_2O_2 (0, 0.25, 0.5, 0.75, 1, and 1.25 mM) for 24 h. Afterward, the medium was discarded, and the specimens were left and prepared according to subsequent studies' protocols.

Next, we evaluated the effect of SIRT3 on oxidative stress induced by H_2O_2 using 3-(1H-1,2,3-triazol-4-yl) pyridine (3-TYP) (MCE, HY-108331, Monmouth Junction, NJ, USA), an inhibitor of SIRT3. The organs of Corti were pretreated with 3-TYP (50 μM) for 2 h prior to H_2O_2 treatment. A 100 mM stock solution was prepared with 3-TYP dissolved in DMSO (Beyotime Biotechnology, ST038, Haimen, China) and was kept at -80°C until use. We further diluted the stock solution with culture medium to appropriate concentration for administration. The highest concentration of DMSO should be under 0.1%. Additionally, it has been previously shown that 50 μM 3-TYP does not significantly affect cell viability [32].

2.4. Immunofluorescence. The specimens were fixed with 4% paraformaldehyde for 2 min and then washed with PBS. Subsequently, they were incubated in 0.3% Triton X-100 containing 10% goat serum (ZSGB-BIO, ZLI-9021, Beijing, China) at room temperature for 15 min. Then, they were immunolabeled with monoclonal mouse anti-carboxyl-terminal binding protein 2 (CtBP2) (1 : 300, Abcam, ab204663, Cambridge, MA, USA) and rabbit anti-myosin VIIa antibody (1 : 300, Proteus Biosciences, 25-6790, Ramona, CA, USA) to label ribbon synapses and hair cells,

respectively, and incubated overnight at 4°C. The next day, the specimens were counterstained with secondary antibodies conjugated with Alexa FluorTM/® 568 and 647 (1 : 300, Invitrogen, A21124, A21245, Molecular Probes, Carlsbad, CA, USA) for 2 h. The specimens were washed in PBS for 10 min and mounted on glass slides with 4′,6-diamidino-2-phenylindole (DAPI) (ZSGB-BIO, ZLI-9557, Beijing, China). Finally, the specimens were observed under a laser confocal microscope (Leica Microsystems, Wetzlar, Germany).

2.5. Hair Cells and Ribbon Synapse Counting. We quantified the outer hair cells (OHCs), inner hair cells (IHCs), and ribbon synapses with a ×63 magnification oil-immersion objective mounted on a Leica TCS SP8 laser confocal microscope (Leica Microsystems, Wetzlar, Germany). Approximately 14–15 IHCs and 42–45 OHCs were included in each visual field. Five specimens were selected from each group to measure the average, and percentages were used to describe the survival of hair cells. We obtained the mean of ribbon synapses for each IHC using the sum of CtBP2-stained puncta divided by the sum of IHC nuclei.

2.6. Determination of Mitochondria-Derived ROS. To evaluate ROS, explants were cultured in a medium containing MitoSOX (1 : 1000, Invitrogen, M36008, Carlsbad, CA, USA) for 30 min at 37°C. Then, they were washed gently with PBS for 10 min and mounted on glass slides with DAPI. All steps of the procedure were protected from light. The fluorescence intensity was analyzed by laser confocal microscopy with an optimal excitation wavelength of 568 nm (red) and calculated by Image J (National Institutes of Health, Bethesda, Maryland, USA).

2.7. Laser Confocal Microscopy. The specimens were scanned hierarchically with an interval of 0.5 μm/layer by a ×63 magnification oil-immersion objective mounted on a Leica TCS SP8 laser confocal microscope (Leica Microsystems, Wetzlar, Germany). The final images were superimposed. The optimal excitation wavelengths of 568 nm (red), 647 nm (far-red), and 358 nm (blue) for DAPI were used.

2.8. Measurement of Mitochondrial Membrane Potential. Mitochondria extraction was performed with the Tissue Mitochondria Isolation Kit (Beyotime Biotechnology, C3606, Haimen, China) based on the manufacturer's instructions as preparation. Mitochondrial membrane potential was measured using the potential-sensitive fluorescent dye JC-1 (Beyotime Biotechnology, C2006, Haimen, China). The results were detected using a multimode plate reader (EnSpireTM, Perkin Elmer Singapore Pte. Ltd. Singapore) and expressed as the ratio of the readings.

2.9. Western Blot. To determine the levels of SIRT3 and the SIRT3-related proteins, FOXO3A and SOD2, western blot was adopted. We use radioimmunoprecipitation assay lysis buffer (Beyotime Biotechnology, P0013, Haimen, China) to extract total protein and an enhanced BCA Protein Assay Kit (Beyotime Biotechnology, P0010S, Haimen, China) to quantify protein concentration. Sodium dodecyl sulfate-polyacrylamide gel electrophoresis was used to isolated protein lysates. Then, we transferred protein lysates onto polyvinylidene difluoride membranes and incubated in a 5% fat-free milk blocking solution for 1 h. After washing in tris-buffered saline, the membranes were incubated with the primary antibodies anti-SIRT3 (1 : 1000 CST, D22A3, Shanghai, China), anti-FOXO3A (1 : 1000 CST, D19A7, Shanghai, China), and anti-SOD2 (1 : 1000 CST, D3X8F, Shanghai, China) at 4°C overnight. After washing for 7 min three times, the membranes were subsequently incubated with the appropriate horseradish peroxidase-conjugated secondary antibody (1 : 5000, Santa Cruz Biotechnology, SC-2357-CM, Santa Cruz, CA, USA) at room temperature for 1 h. Finally, the membranes were visualized using BeyoECL Plus (Beyotime Biotechnology, P0018S, Haimen, China). We used the Image-Pro Plus 6.0 software (Media Cybernetics, Rockville, MD, USA) to analyze quantification of these proteins.

2.10. Apoptosis Staining. We used a terminal deoxynucleotidyl transferase-mediated deoxy uridine triphosphate nick-end labeling staining kit TUNEL POD (Roche Molecular Biochemicals, 11772465001, Mannheim, Germany) to detect hair cell apoptosis. After being incubated in 0.3% Triton X-100 containing 10% goat serum (ZSGB-BIO, ZLI-9021, Beijing, China) at room temperature for 15 min, the specimens were immunolabeled with rabbit anti-myosin VIIa antibody (1 : 300, Proteus Biosciences, 25-6790, Ramona, CA, USA) and incubated overnight at 4°C. The next day, the specimens were first counterstained with secondary antibodies conjugated with Alexa FluorTM/® 647 (1 : 300, Invitrogen, A21124, A21245, Molecular Probes, Carlsbad, CA, USA) for 2 h. And then, the label reaction with TUNEL POD was carried out for 1 h at 37°C. Wash the specimens with PBS for 10 min and mount them on glass slides with DAPI (ZSGB-BIO, ZLI-9557, Beijing, China). Finally, the specimens were observed under a laser confocal microscope (Leica Microsystems, Wetzlar, Germany).

2.11. Statistical Analyses. We use GraphPad Prism 8 (GraphPad Software, Inc., La Jolla, CA, USA) to perform statistical cartography and illustrate our data with mean ± standard error. The paired-sample *t*-test was performed to evaluate differences between the different groups. Statistical significance was set at $P < 0.05$.

3. Results

3.1. H_2O_2 Induces Dose-Dependent Ribbon Synapse, and Hair Cells Decline: Model Building. First, we determined the changes in the number of ribbon synapses and the survival of hair cells under different H_2O_2 concentrations. Our findings showed that after a 24 h exposure to H_2O_2, the number of ribbon synapses and cochlear hair cells was significantly decreased in a concentration-dependent manner. We recorded the concentrations at which there was apparent loss of ribbon synapses with no loss of hair cells, apparent loss of ribbon synapses and OHCs, and apparent loss of IHCs (Figure 1(a)).

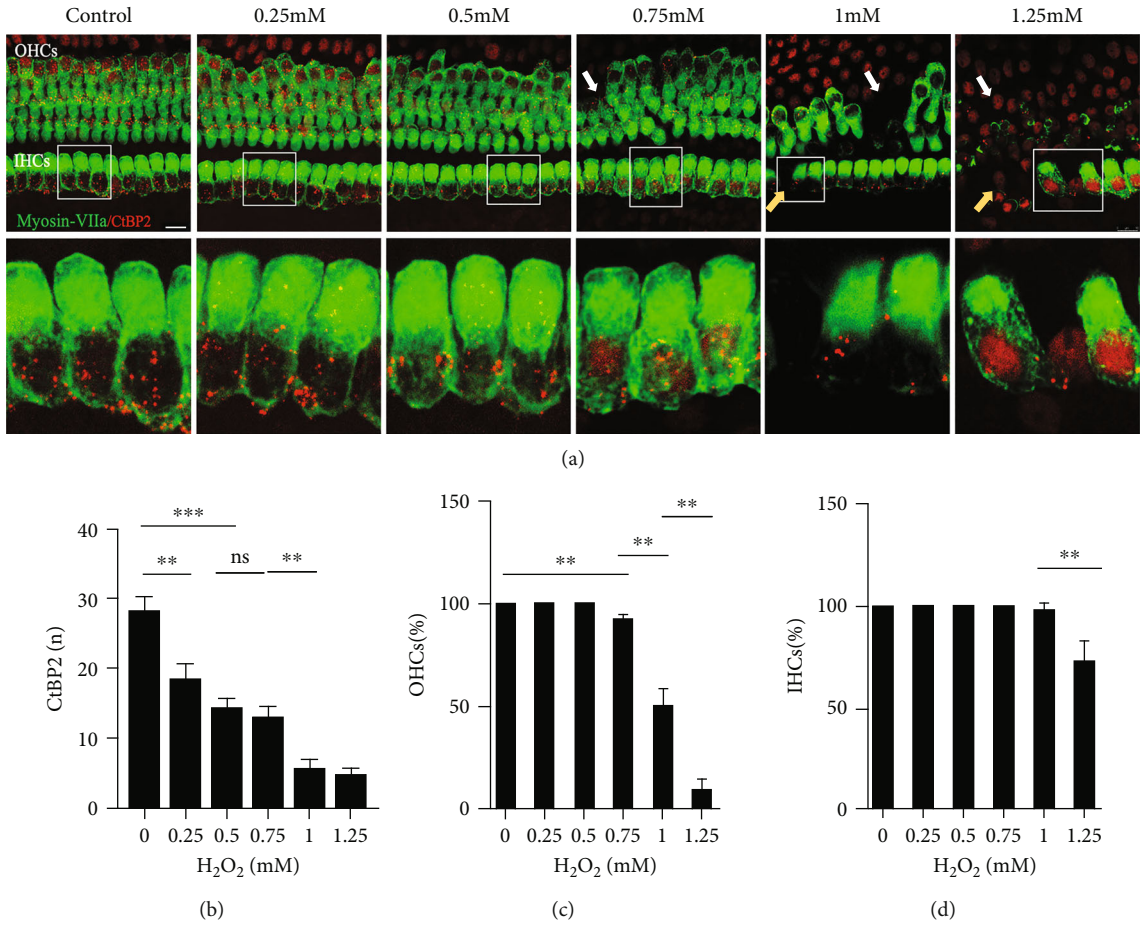

FIGURE 1: H_2O_2 induces dose-dependent loss of ribbon synapses and hair cells at the 0, 0.25, 0.5 0.75, 1, and 1.25 mM concentrations. (a) Confocal images showing ribbon synapses (red) and hair cells (green) in the middle region of cochlear explants at each concentration. The white arrows indicate OHC damaged areas. Yellow arrows indicate IHC damaged areas. (b) Quantification of ribbon synapses at each concentration. (c) Rate of OHC survival at each concentration. (d) Rate of IHC survival at each concentration. Data are expressed as means ± SD ($n = 5$ organ of Corti per concentration). $^*P < 0.05$, $^{**}P < 0.01$, and $^{***}P < 0.001$. Scale bar = 10 μm.

The number of ribbon synapses in the middle turn of the organ of Corti in the control, 0.25, 0.5, 0.75, 1, and 1.25 mM groups was 28.2 ± 81.99, 18.5 ± 2.11, 14.36 ± 1.37, 12.96 ± 1.63, 5.62 ± 1.36, and 4.75 ± 0.92, respectively (Figure 1(b)). In contrast with the 0.25 mM group, there were significantly fewer ribbon synapses in the 0.5 mM group in comparison with the control group ($P < 0.001$). There was no significant difference in the number of ribbon synapses in the 0.5 mM and 0.75 mM groups ($P > 0.05$), while the number of ribbon synapses in the 1 mM group was efficaciously lower than that in the 0.75 mM group ($P < 0.01$). And no significant difference was found in the number of ribbon synapses between the 1 mM and 1.25 mM groups.

Regarding the survival of hair cells, we investigated the whole cochlear basilar membranes (Figures 1(c) and 1(d)). In the 0.25 mM and 0.5 mM groups, hair cells remained intact, and there were no obvious alterations in their quantities, although the arrangement of hair cells in the apex of the cochlea was disordered in the 0.5 mM group. At a concentration of 0.75 mM H_2O_2, 92.75 ± 1.53% of OHCs ($P < 0.01$) and all IHCs remained. In the 1 mM group, approximately 50% of OHCs survived (50.10 ± 7.99%), which was significantly different compared with the 0.75 mM group ($P < 0.01$), and 97.92 ± 2.95% of IHC survived. There was extensive hair cell loss in the 1.25 mM group; only 9.13 ± 5.54% and 72.35 ± 9.79% of OHCs and IHCs survived, respectively, which was significantly different from the 1 mM group (both $P < 0.01$). According to the results above, we built a model of four concentrations: 0, 0.5, 0.75, and 1 mM for the following study.

3.2. Pharmacological Suppression of SIRT3 and Aggravated Oxidative Damage to the Cochlea. To investigate the impact of SIRT3 mitigation on H_2O_2-induced oxidative damage, we used a selective SIRT3 inhibitor, 3-TYP [33]. Previous research by Pi et al. revealed that 3-TYP can inhibit SIRT3 activity but does not downregulate protein expression [32].

We first quantified the number of ribbon synapses and analyzed the survival of hair cells in the groups established above. Our results revealed that the damage to ribbon synapses and hair cells was dependent on the concentration of

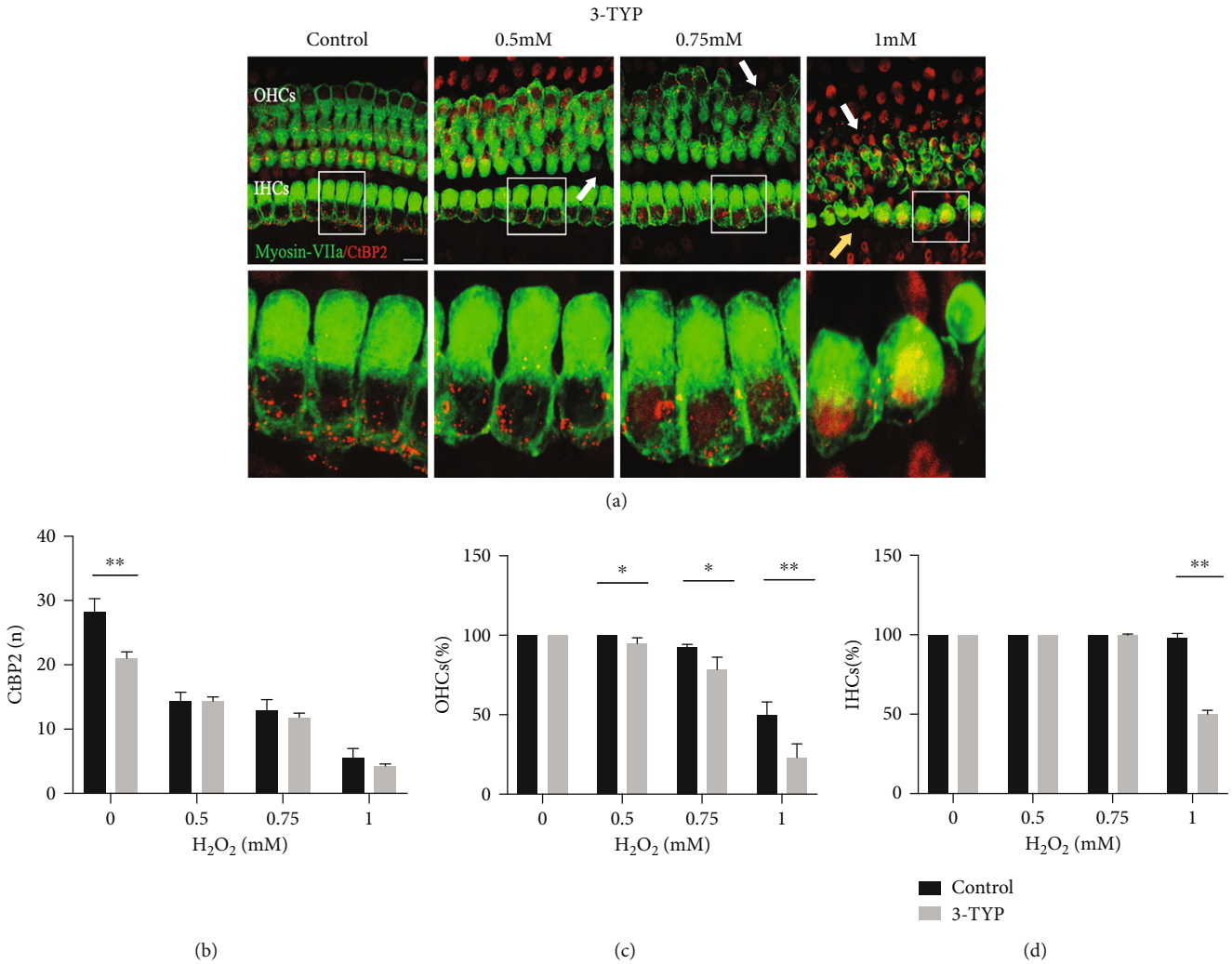

Figure 2: H_2O_2 induces aggravated oxidative damage to cochlear by suppression of SIRT3. (a) Representative images of ribbon synapses (red) and HCs (green) in the middle region of cochlear explants in 0, 0.5, 0.75, and 1 mM groups pretreated with 3-TYP. The white arrows indicate OHC damaged areas. Yellow arrows indicate IHC damaged areas. (b) Comparison of ribbon synapse at each concentration between matched and 3-TYP groups. (c) Comparison of OHC survival at each concentration between matched and 3-TYP groups. (d) Comparison of IHC survival at each concentration between matched and 3-TYP groups. Data are shown as means ± SD ($n = 5$ in each group). $^*P < 0.05$, $^{**}P < 0.01$, and $^{***}P < 0.001$. Scale bar = 10 μm.

H_2O_2 (Figure 2). In the presence of 3-TYP, the number of ribbon synapses in the middle turn of the organ of Corti in the control, 0.5, 0.75, and 1 mM groups declined with 21.03 ± 0.98, 14.31 ± 0.72, 11.85 ± 0.62, and 4.25 ± 0.33, respectively (Figure 2(b)). Interestingly, after pretreated with 3-TYP, no significant difference was discovered in the number of ribbon synapses between these H_2O_2 concentrations, except in the control group, in which the number was declined ($P < 0.01$) (Figure 2(b)).

However, after pretreated with 3-TYP, HCs in H_2O_2 groups appeared more disorganized and morphologically abnormal, as compared Figure 1(a) with Figure 2(a). Furthermore, as shown in Figure 2(c), there was a significantly lower rate of OHC survival in the 0.5 mM group compared with the group that was not treated with 3-TYP ($P < 0.05$). A similar tendency also appeared in the 0.75 mM and 1 mM groups ($P < 0.05$ and $P < 0.01$, respectively). Regarding the survival rate of IHCs (Figure 2(d)), in the 0.75 mM group, we observed that IHC loss began, and those that remained were chaotically arranged. In the 1 mM group treated with 3-TYP, only 49.91 ± 2.47% IHCs survived, compared with 97.92 ± 2.95% in the 1 mM group without 3-TYP ($P < 0.01$). However, there was no significant difference between the rate of IHC survival in both control and 0.5 mM groups. These results revealed that 3-TYP could inhibit intracellular antioxidant activity and aggravate oxidative stress, increasing the damage to the ribbon synapse and hair cells.

3.3. H_2O_2 Induces Increased Mitochondrial ROS in CBMs, and This Is Enhanced with 3-TYP Treatment. We measured the levels of mitochondrial ROS using MitoSOX staining. The red fluorescence intensity of MitoSOX staining in the groups treated with H_2O_2 was significantly more apparent than that in the control group, and the level was largely

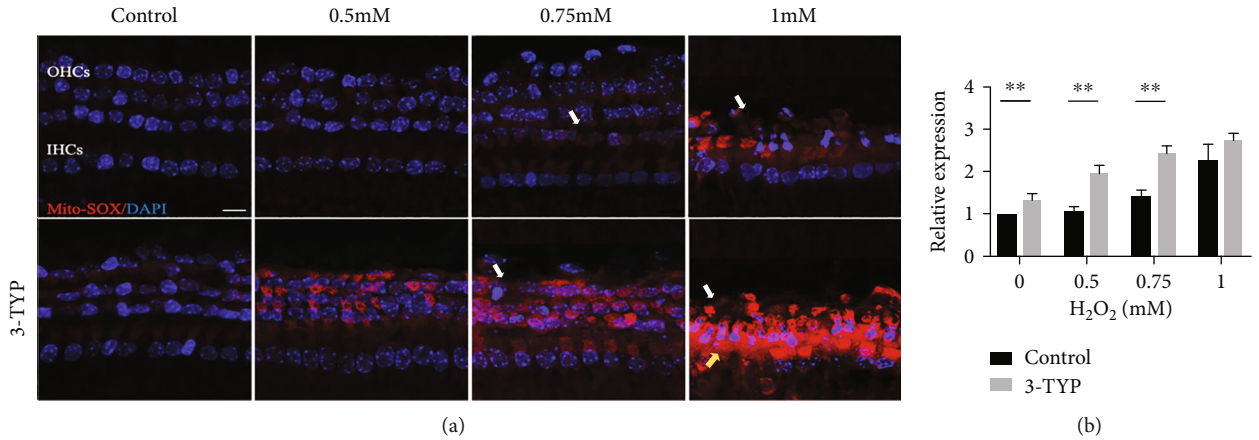

Figure 3: H_2O_2 induces ROS generation, which is enhanced by 3-TYP. (a) Confocal images of MitoSOX staining (red) in the 0, 0.5, 0.75, and 1 mM groups pretreated with or without 3-TYP. The white arrows indicate OHC damaged areas. Yellow arrows indicate IHC damaged areas. (b) Relative level of fluorescence intensity in each group. Data are expressed as means ± SD ($n = 5$ organ of Corti per concentration). $^{*}P < 0.05$, $^{**}P < 0.01$, and $^{***}P < 0.001$. Scale bar = 10 μm.

dependent on the concentrations of H_2O_2, with the highest in the 1 mM group, regardless of pretreatment with 3-TYP, as shown in Figure 3. The quantitative comparison was performed using red fluorescence intensity (Figure 3(b)). Relative staining in the 0.5, 0.75, and 1 mM groups rose by 1.07 ± 0.10 – fold, 1.42 ± 0.15 – fold, and 2.27 ± 0.37 – fold, respectively. No significant difference was shown in the relative ROS levels between the 0 and 0.5 mM groups. Relative fluorescence intensity in the 0.5 mM group was significantly lower than that in the 0.75 mM group ($P < 0.05$), and relative fluorescence intensity in the 0.75 mM group was significantly lower than that in the 1 mM group ($P < 0.05$).

After pre-treated with 3-TYP, the relative fluorescence intensity was increased in each concentration group (0, 0.5, 0.75, and 1 mM), by 1.33 ± 0.15 – fold, 1.96 ± 0.19 – fold, 2.43 ± 0.18 – fold, and 2.74 ± 0.16, respectively. Relative staining was significantly higher as H_2O_2 concentrations higher: control vs. 0.5 mM, $P < 0.01$, 0.5 vs. 0.75 mM, $P < 0.05$, and 0.75 vs. 1 mM, $P < 0.05$, respectively. Furthermore, the levels of relative fluorescence intensity in control, 0.5, and 0.75 mM 3-TYP pretreated groups were significantly higher than in the nontreated matched group with $P < 0.01$. Thus, it indicated that mitochondrial ROS levels increased in response to H_2O_2 treatment in vitro. Furthermore, this may be enhanced by inhibition of SIRT3.

3.4. H_2O_2 Induces Mitochondrial Dysfunction in CBMs, Which Is Intensified by 3-TYP Treatment. The MMP was used to evaluate mitochondrial function. As shown in Figure 4, MMP levels in the 0, 0.5, 0.75, and 1 mM groups were 2.23 ± 0.27, 1.76 ± 0.09, 1.67 ± 0.12, and 1.43 ± 0.10, respectively. Our results showed that mitochondrial function was inversely related to H_2O_2 concentration. The MMP level in the 0.5 mM and 0.75 mM groups was not significantly different. The MMP level in the 0.5 mM group was significantly lower than that in the control group ($P < 0.01$), as was the MMP level in the 1 mM group compared to that in the 0.75 mM group ($P < 0.01$). The result also illustrated the

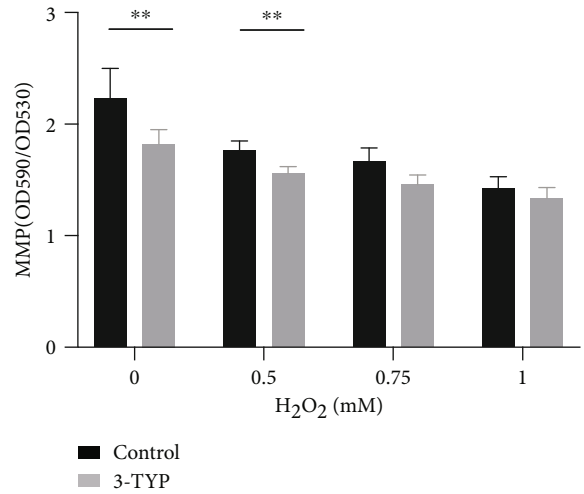

Figure 4: Comparison of MMP levels in the 0, 0.5, 0.75, and 1 mM groups between matched nontreated and 3-TYP-treated groups. Data are expressed as means ± SD ($n = 5$ organ of Corti per concentration). $^{*}P < 0.05$, $^{**}P < 0.01$, and $^{***}P < 0.001$.

MMP levels in the same concentration groups pretreated with 3-TYP; these were 1.82 ± 0.13, 1.56 ± 0.06, 1.46 ± 0.08, and 1.34 ± 0.10, respectively, which also demonstrated a concentration-dependent decline. There was a significant difference in MMP between the control and 0.5 mM groups ($P < 0.01$) and the 0.5 mM and 1 mM groups ($P < 0.05$). To investigate the effect of SIRT3 suppression, we compared the MMP level between the 3-TYP pretreated group and nontreated group. The MMP level in each 3-TYP pretreated group was lower than in the nontreated matched group, with a significant difference in the 0 and 0.5 mM groups ($P < 0.01$). Our findings indicated that H_2O_2 resulted in a concentration-dependent decrease in mitochondrial membrane potential, and SIRT3 played an important role in protecting mitochondrial function.

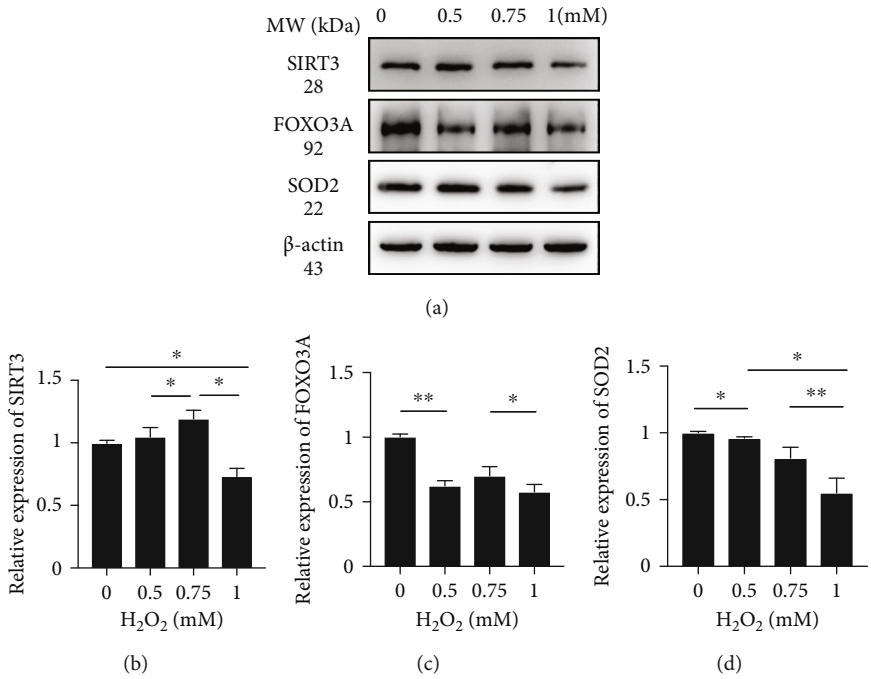

Figure 5: H_2O_2 induces downregulation of SIRT3, FOXO3A, and SOD2. (a) Representative western blot analysis using antibodies against SIRT3, FOXO3A, SOD2, and β-actin in CBMs. (b) Protein expression of SIRT3 in the 0, 0.5, 0.75, and 1 mM groups. (c) Protein expression of FOXO3A in the 0, 0.5, 0.75, and 1 mM groups. (d) Protein expression of SOD2 in the 0, 0.5, 0.75, and 1 mM groups. Data are expressed as means ± SD ($n = 5$ organ of Corti per concentration). $^{*}P < 0.05$, $^{**}P < 0.01$, and $^{***}P < 0.001$.

3.5. H_2O_2 Downregulates SIRT3 and SIRT3-Dependent Protein Expression. As previously mentioned, SIRT3 is crucial in oxidation resistance and protects cells from oxidative damage. We analyzed the expression of SIRT3 and the related proteins FOXO3A and SOD2 by western blotting to confirm this effect (Figure 5). As shown in Figure 5(b), the level of SIRT3 protein was significantly higher in the 0.75 mM group than in the 0.5 mM and control groups (1.19 ± 0.07 – fold vs. 1.05 ± 0.08 – fold, $P < 0.05$; 1.19 ± 0.07 – fold vs. 1.00 ± 0.02 – fold, $P < 0.05$, respectively). However, in the 1 mM group, the protein level was dramatically decreased to 0.73 ± 0.07 – fold, which was significantly lower than in any other group ($P < 0.05$). This suggested that stimulation by H_2O_2 initially elevated the level of SIRT3 protein, which could help cells to resist oxidative damage to a certain degree. However, this elevation was limited and finally declined. The level of FOXO3A protein, a downstream target of SIRT3, generally declined (Figure 5(c)). By contrast with the control group, the level of FOXO3A was decreased in the 0.5 mM, 0.75 mM, and 1 mM groups by 0.62 ± 0.04 – fold ($P < 0.01$), 0.70 ± 0.07 – fold ($P < 0.05$), and 0.58 ± 0.06 – fold ($P < 0.01$), respectively. Compared with the control group, the expression of SOD2 protein declined stably to 0.96 ± 0.01 – fold in the 0.5 mM group ($P < 0.05$), 0.81 ± 0.08 – fold in the 0.75 mM group ($P < 0.05$), and 0.55 ± 0.11 – fold in the 1 mM group ($P < 0.05$). Moreover, the levels were significantly different between the 0.5 mM and 1 mM groups and the 0.75 mM and 1 mM groups, although no difference was noticed in expression levels between the 0.5 mM and 0.75 mM groups, which may be related to statistical error. The decrease in the expression of these two downstream proteins indicates that despite elevated SIRT3 expression, H_2O_2 activated the oxidative reaction and degraded the expression of antioxidant proteins, causing damage to tissues. Together, these results provide evidence that H_2O_2 could induce the downregulation of SIRT3 and SIRT3-related proteins, thus inhibiting the antioxidant reaction and causing damage.

3.6. Hair Cell Apoptosis Induced by H_2O_2 and Intensified by 3-TYP Treatment. As mentioned above, the loss of hair cells appeared significantly H_2O_2 concentration-dependent, which may due to the activation of apoptosis induced by H_2O_2. To confirm the occurrence of apoptosis, we used TUNEL POD staining. As shown in Figure 6, the TUNEL-positive cells were first observed in the OHC area in the 0.75 mM group. In the 1 mM group, a large number of OHCs appeared apoptosis and a portion of IHCs lost directly. After treatment with 3-TYP, apoptosis of hair cells occurred earlier and severer, as the TUNEL-positive cells were first observed in the OHC area in the 0.5 mM group and more TUNEL-positive OHCs were in the 0.75 mM group. Furthermore, in the 1 mM group, none of OHCs survived and almost half of IHCs lost directly. However, we still could observe a TUNEL-positive cell in IHC area. This suggests that H_2O_2 induces apoptosis of hair cells in the CBMs, and administration of 3-TYP could exacerbate the occurrence of apoptosis.

4. Discussion

Hair cells mainly function in turning the sound wave energy into electric signals [34]. Although SNHL could be caused by

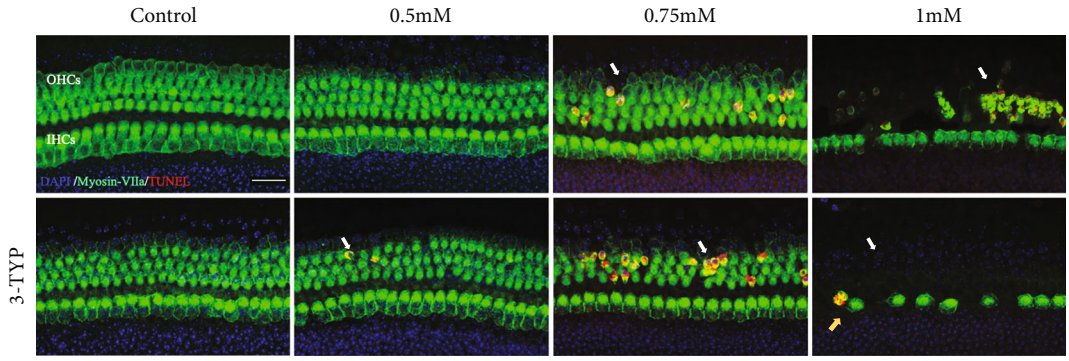

FIGURE 6: H_2O_2 induce occurrence of hair cell apoptosis, and this is intensified by 3-TYP. Representative images of TUNEL staining (red) and hair cells (green) in 0, 0.5, 0.75, and 1 mM groups pretreated with or without 3-TYP. The white arrows indicate TUNEL-positive cells in OHC areas. Yellow arrows indicate TUNEL-positive cells in IHC areas. Scale bar = 25 μm.

many factors, including genetic factors, aging, chronic cochlear infections, infectious diseases, ototoxic drugs, and noise exposure, most of the SNHL occurs due to the irreversible loss of HCs and spiral ganglion neurons (SGNs), both of which have limited regeneration ability in adult mammals [35]. Thus, how to protect the cochlear HC is a key scientific question in the hearing research field. As the human cochlear is inaccessible, in vitro animal models could be a crucial way to study SNHL. Here, we studied the oxidative damage to the organ of Corti caused by H_2O_2 and further investigated the changes of the oxidative damage after inhibition of SIRT3. Accumulation of ROS could result in various degrees of loss of hair cells and ribbon synapses, decrease of mitochondrial membrane potential, and decrease of SIRT3 and related protein expression. Furthermore, under the administration of 3-TYP, oxidative damage was aggravated.

4.1. Apoptosis May Contribute to Loss of HCs. It has been proven that hearing mostly depends on hair cells to convert mechanical stimulation to electrochemical activity and the IHC ribbon synapses to transmit electrochemical signals [36, 37]. OHCs are mainly responsible for the active mechanical amplification process, which facilitates high sensitivity and good frequency resolution. IHCs are responsible for sound detection and provide afferent auditory neurotransmission to the brain [11, 38, 39]. In this study, cochlear sensory hair cells and IHC ribbon synapses in cochlear explants exhibited dose-dependent cytotoxic effects when exposed to H_2O_2. At certain concentration group, we viewed an enormous loss of OHCs and a slight loss of IHCs. Previous research has shown that the degeneration and loss of hair cells are largely due to the activation of apoptosis [40, 41]. Apoptosis occurs in two ways: the extrinsic pathway, activated by death receptors, and the intrinsic pathway, initiated by a change in mitochondrial membrane permeability [42–44]. Mitochondrial dysfunction causes the permeability transition pore to open in an irreparable way, which subsequently leads to rise of the permeability of mitochondrial outer membrane [42, 45]. Moreover, the accumulation of ROS, decrease of the mitochondrial membrane potential, and release of apoptosis-related factors and cytochrome c were induced by mitochondrial dysfunction spark apoptotic and necrotic cell death pathways as well [44, 46].

4.2. Lack of Energy May Contribute to Synaptic Loss. Our results indicate that the intrinsic pathway of apoptosis due to mitochondrial dysfunction and overgeneration of ROS may contribute to the loss of hair cells in the cochlea. Our results also showed that exposure to H_2O_2 significantly decreased the number of ribbon synapses, even at low concentrations. The concomitant decline in the mitochondrial membrane potential decreases adenosine triphosphate (ATP) levels in the cochlea, which becomes insufficient for the transportation of ribbon synaptic vesicles and maintenance of ribbon synapses' function [41]. Considering oxidative stress, related studies have shown that inhibition of AMPK, a key cellular energy sensor related to ATP production, could attenuate the loss of outer hair cells and ribbon synapses and preserved auditory function after noise exposure [47]. Recent animal studies have shown that synaptic loss can occur without permanent hearing threshold shifts after noise exposure [48, 49], suggesting that synaptopathy is a significant marker of early noise-induced hearing loss.

4.3. Accumulation of ROS Reduces MMP and Triggers Oxidative Damage. To evaluate the level of ROS, we used MitoSOX staining, and our results demonstrated that the higher the concentration, the greater the accumulation of ROS and the more severe the damage to the cochlea. Most mammalian cells generate ROS, which are regarded as toxic products of cellular metabolism by the mitochondria, and can act as signalling molecules to regulate various physiological processes [50]. It is assumed that noise exposure induces mitochondrial damage and, in turn, increases ROS accumulation. A considerable amount of ROS can trigger progressive oxidative damage, promote oxidation of the mitochondrial DNA and proteins [51], and induce lipid peroxidation products, which can result in apoptosis and reduce cochlear blood flow [6]. Normal mitochondrial membrane potential is a prerequisite for maintaining oxidative phosphorylation of mitochondria and ATP production. The cumulative burden of ROS production can lead to MMP breakdown, which further results in energy deficiency and mitochondrial dysfunction [41, 52]. In this study, the

MMP levels in both groups (with and without 3-TYP) decreased as H_2O_2 concentration increased. In particular, the pharmacological inhibitor 3-TYP of SIRT3 intensified the decline of MMP.

4.4. Potential Role of SIRT3 in Hearing Protection and Mitohormesis. SIRT3 is the major mitochondrial deacetylase and is expressed in metabolically active tissues such as the liver, kidney, and heart [28]. It appears that it can resist various mitochondrial stresses, especially by utilizing cellular antioxidant systems to combat oxidative stress. FOXO3A is a forkhead transcription factor that is deacetylated by SIRT3 to increase the transcription of key antioxidant genes, including SOD2 and catalase, and protects mitochondria from further oxidative stress [53, 54]. SOD2 is responsible for reducing ROS and protecting against oxidative stress and is also activated by SIRT3-mediated deacetylation [30]. Additionally, SIRT3 directly deacetylates mitochondrial isocitrate dehydrogenase, IDH2, and stimulates its activity [55], which helps to maintain the mitochondrial pool of NADPH for conversion of reduced glutathione [56–58].

To detect the expression of SIRT3, FOXO3A, and SOD2 proteins, we performed western blot analysis. Our results revealed that under moderate amounts of ROS (i.e., the 0.5 mM and 0.75 mM H_2O_2 groups), the level of SIRT3 initially increased and subsequently decreased in the 1 mM group. We suggest that this may correspond with mitohormesis, which means that the effects caused by a stressor may be beneficial when its level is relatively low and deleterious when it is high [59]. It has been reported that the level of SIRT3 increases under calorie restriction (CR), fasting, and exercise training in different tissues [55, 60]. Under calorie restriction, a moderate increase in ROS can trigger oxidative stress resistance activities to attenuate oxidative cellular damage [59, 61]. However, large or chronic increases in ROS may result in damage or cell death, as they exceed the capacity to maintaining homeostasis; thus, the balance is broken. It is noteworthy that oxidative stress is commonly associated with mitochondrial hyperacetylation [60, 62]. We assume that the activities of antioxidants and related enzymes such as FOXO3A and SOD2 are dampened through direct acetylation [58, 63, 64]. In this study, we found that the levels of FOXO3A and SOD2 decreased as the H_2O_2 concentration increased. As mentioned above, a moderate ROS rise increases SIRT3 transcription, thus helping to achieve a new hormetic steady state. The increased levels of SIRT3 can then deacetylate FOXO3A and SOD2 to defend against oxidative stress, but this capacity is limited. Mitochondrial hyperacetylation fails in the function of antioxidant enzymes and excess neutralization with oxidation products and ultimately reduces the expression of SIRT3, FOXO3A, and SOD2 and worsens oxidative stress. Interestingly, the expression of FOXO3A protein rose slightly in the 0.75 mM H_2O_2 group, which may probably due to dramatical expression of its upstream protein SIRT3, as assumed. Also, statistical bias cannot be ruled out, either.

To provide direct evidence that SIRT3 is a key factor in the preservation of mitochondrial function and antioxidation, we performed biochemical experiments with the selective SIRT3 inhibitor, 3-TYP. 3-TYP inhibits SIRT3 activity but does not affect SIRT3 protein expression [32, 33]. Our findings illustrated that inhibition of SIRT3 exacerbated the level of ROS, loss of hair cells and ribbon synapses, and decreased MMP. A previous study in cultured HepG2 cells had suggested that activation of SIRT3 could suppress mitochondrial-derived ROS-stimulated autophagic cell death induced by cadmium through SIRT3/SOD2 pathway [32]. ROS is important for osteoclasts in differentiation and activation induced by receptor activator of NF-κB ligand (RANKL). Suppression of SOD2 activity by SIRT3-targeted siRNA could increase ROS levels and raise osteoclastogenesis [65]. High expression of xCT, which is the member 11 of solute carrier family 7 (SLC7A11), was commonly along with increased levels of ROS and sensitivity to glucose deprivation in breast cancer cells. Downregulation of SIRT3 further increased the levels of ROS and promoted xCT-related cell death [66]. Adjudin, a lonidamine analogue, could protect cochlear HCs from gentamicin-induced damage mediated by the SIRT3-ROS axis in vitro [67]. Furthermore, an in vivo study revealed that $SIRT3^{-/-}$ mice were more susceptible to NIHL, and $SIRT3^{-/-}$ mice treated with nicotinamide riboside exhibited less protection from both TTS and PTS after noise exposure [31]. On the other hand, it is interesting that significant reduction in the number of ribbon synapses was only discovered in the control group pretreated with 3-TYP. As mentioned above, great evidence shows that the level of SIRT3 increases under stress like CR. We have reason to believe that the protective effect for ribbon synapses of higher expression of SIRT3 induced by H_2O_2 is stronger than inhibition of activity, while in the control group, only the activity of SIRT3 was inhibited, and the loss of ribbon synapses became severer.

However, in vitro research provides the suggestion for studies in vivo but is different from in vivo research because of the complex internal environment and variable influencing factors. Next, we hope to further study the mitochondrial oxidative damage and deacetylation of SIRT3 in NIHL in vivo.

5. Conclusion

Overall, we propose that ROS and oxidative stress are major causes of SNHL. Furthermore, SIRT3 is crucial for preserving mitochondrial function and protecting the cochlea from oxidative damage. Additionally, we imitate different phases of SNHL in the organ of Corti in vitro and establish a novel in vitro model for investigation of the mechanisms of SNHL.

Data Availability

The data that support the findings of this study are openly available from the corresponding author upon reasonable request.

Conflicts of Interest

The authors declare that there is no conflict of interests regarding the publication of this paper.

Acknowledgments

This work was supported by grants from the National Natural Science Foundation of China (Grant Nos. 81830030, 81771016, and 81700917). We would like to thank all the authors who contributed to this special issue.

References

[1] D. M. P. Jayakody, P. L. Friedland, R. N. Martins, and H. R. Sohrabi, "Impact of aging on the auditory system and related cognitive functions: a narrative review," *Frontiers in Neuroscience*, vol. 12, p. 125, 2018.

[2] S. Someya, T. Yamasoba, R. Weindruch, T. A. Prolla, and M. Tanokura, "Caloric restriction suppresses apoptotic cell death in the mammalian cochlea and leads to prevention of presbycusis," *Neurobiology of Aging*, vol. 28, no. 10, pp. 1613–1622, 2007.

[3] M. Knipper, P. Van Dijk, I. Nunes, L. Ruttiger, and U. Zimmermann, "Advances in the neurobiology of hearing disorders: recent developments regarding the basis of tinnitus and hyperacusis," *Progress in Neurobiology*, vol. 111, pp. 17–33, 2013.

[4] X. Fu, X. Sun, L. Zhang et al., "Tuberous sclerosis complex-mediated mTORC1 overactivation promotes age-related hearing loss," *The Journal of Clinical Investigation*, vol. 128, no. 11, pp. 4938–4955, 2018.

[5] C. Cheng, Y. Wang, L. Guo et al., "Age-related transcriptome changes in Sox2+ supporting cells in the mouse cochlea," *Stem Cell Research & Therapy*, vol. 10, no. 1, p. 365, 2019.

[6] A. R. Fetoni, F. Paciello, R. Rolesi, G. Paludetti, and D. Troiani, "Targeting dysregulation of redox homeostasis in noise-induced hearing loss: oxidative stress and ROS signaling," *Free Radical Biology & Medicine*, vol. 135, pp. 46–59, 2019.

[7] S. G. Kujawa and M. C. Liberman, "Adding insult to injury: cochlear nerve degeneration after "temporary" noise-induced hearing loss," *The Journal of Neuroscience*, vol. 29, no. 45, pp. 14077–14085, 2009.

[8] C. Fujimoto and T. Yamasoba, "Mitochondria-targeted antioxidants for treatment of hearing loss: a systematic review," *Antioxidants*, vol. 8, no. 4, p. 109, 2019.

[9] M. Jiang, T. Karasawa, and P. S. Steyger, "Aminoglycoside-induced cochleotoxicity: a review," *Frontiers in Cellular Neuroscience*, vol. 11, p. 308, 2017.

[10] Z. Zhong, X. Fu, H. Li et al., "Citicoline protects auditory hair cells against neomycin-induced damage," *Frontiers in Cell and Development Biology*, vol. 8, p. 712, 2020.

[11] S. Morioka, H. Sakaguchi, T. Yamaguchi et al., "Hearing vulnerability after noise exposure in a mouse model of reactive oxygen species overproduction," *Journal of Neurochemistry*, vol. 146, no. 4, pp. 459–473, 2018.

[12] R. S. Balaban, S. Nemoto, and T. Finkel, "Mitochondria, oxidants, and aging," *Cell*, vol. 120, no. 4, pp. 483–495, 2005.

[13] Y. Ohinata, J. M. Miller, and J. Schacht, "Protection from noise-induced lipid peroxidation and hair cell loss in the cochlea," *Brain Research*, vol. 966, no. 2, pp. 265–273, 2003.

[14] N. Benkafadar, F. Francois, C. Affortit et al., "ROS-induced activation of DNA damage responses drives senescence-like state in postmitotic cochlear cells: implication for hearing preservation," *Molecular Neurobiology*, vol. 56, no. 8, pp. 5950–5969, 2019.

[15] H. Yamane, Y. Nakai, M. Takayama, H. Iguchi, T. Nakagawa, and A. Kojima, "Appearance of free radicals in the guinea pig inner ear after noise-induced acoustic trauma," *European Archives of Oto-Rhino-Laryngology*, vol. 252, no. 8, pp. 504–508, 1995.

[16] J. Menardo, Y. Tang, S. Ladrech et al., "Oxidative stress, inflammation, and autophagic stress as the key mechanisms of premature age-related hearing loss in SAMP8 mouse cochlea," *Antioxidants & Redox Signaling*, vol. 16, no. 3, pp. 263–274, 2012.

[17] D. Mukherjea, S. Jajoo, T. Kaur, K. E. Sheehan, V. Ramkumar, and L. P. Rybak, "Transtympanic administration of short interfering (si)RNA for the NOX3 isoform of NADPH oxidase protects against cisplatin-induced hearing loss in the rat," *Antioxidants & Redox Signaling*, vol. 13, no. 5, pp. 589–598, 2010.

[18] J. Guo, R. Chai, H. Li, and S. Sun, "Protection of hair cells from ototoxic drug-induced hearing loss," *Advances in Experimental Medicine and Biology*, vol. 1130, pp. 17–36, 2019.

[19] M. C. Liberman and S. G. Kujawa, "Cochlear synaptopathy in acquired sensorineural hearing loss: manifestations and mechanisms," *Hearing Research*, vol. 349, pp. 138–147, 2017.

[20] I. Varela-Nieto, S. Murillo-Cuesta, M. Calvino, R. Cediel, and L. Lassaletta, "Drug development for noise-induced hearing loss," *Expert Opinion on Drug Discovery*, vol. 15, no. 12, pp. 1457–1471, 2020.

[21] K. A. Fernandez, D. Guo, S. Micucci, V. De Gruttola, M. C. Liberman, and S. G. Kujawa, "Noise-induced cochlear synaptopathy with and without sensory cell loss," *Neuroscience*, vol. 427, pp. 43–57, 2020.

[22] H. Zhou, X. Qian, N. Xu et al., "Disruption of Atg7-dependent autophagy causes electromotility disturbances, outer hair cell loss, and deafness in mice," *Cell Death & Disease*, vol. 11, no. 10, p. 913, 2020.

[23] Q. Jieyu, Z. Liyan, T. Fangzhi et al., "Espin distribution as revealed by super-resolution microscopy of stereocilia," *American Journal of Translational Research*, vol. 12, no. 1, 2020.

[24] D. Yamashita, H. Y. Jiang, J. Schacht, and J. M. Miller, "Delayed production of free radicals following noise exposure," *Brain Research*, vol. 1019, no. 1-2, pp. 201–209, 2004.

[25] K. Baker and H. Staecker, "Low dose oxidative stress induces mitochondrial damage in hair cells," *The Anatomical Record*, vol. 295, no. 11, pp. 1868–1876, 2012.

[26] K. Wakabayashi, M. Fujioka, S. Kanzaki et al., "Blockade of interleukin-6 signaling suppressed cochlear inflammatory response and improved hearing impairment in noise-damaged mice cochlea," *Neuroscience Research*, vol. 66, no. 4, pp. 345–352, 2010.

[27] S. Orrenius, B. Zhivotovsky, and P. Nicotera, "Regulation of cell death: the calcium-apoptosis link," *Nature Reviews. Molecular Cell Biology*, vol. 4, no. 7, pp. 552–565, 2003.

[28] B. H. Ahn, H. S. Kim, S. Song et al., "A role for the mitochondrial deacetylase Sirt3 in regulating energy homeostasis," *Proceedings of the National Academy of Sciences of the United States of America*, vol. 105, no. 38, pp. 14447–14452, 2008.

[29] N. R. Sundaresan, M. Gupta, G. Kim, S. B. Rajamohan, A. Isbatan, and M. P. Gupta, "Sirt3 blocks the cardiac hypertrophic response by augmenting Foxo3a-dependent antioxidant defense mechanisms in mice," *The Journal of Clinical Investigation*, vol. 119, no. 9, pp. 2758–2771, 2009.

[30] R. Tao, M. C. Coleman, J. D. Pennington et al., "Sirt3-mediated deacetylation of evolutionarily conserved lysine 122 regulates MnSOD activity in response to stress," *Molecular Cell*, vol. 40, no. 6, pp. 893–904, 2010.

[31] K. D. Brown, S. Maqsood, J. Y. Huang et al., "Activation of SIRT3 by the NAD^+ Precursor Nicotinamide Riboside Protects from Noise-Induced Hearing Loss," *Cell Metabolism*, vol. 20, no. 6, pp. 1059–1068, 2014.

[32] H. Pi, S. Xu, R. J. Reiter et al., "SIRT3-SOD2-mROS-dependent autophagy in cadmium-induced hepatotoxicity and salvage by melatonin," *Autophagy*, vol. 11, no. 7, pp. 1037–1051, 2015.

[33] U. Galli, O. Mesenzani, C. Coppo et al., "Identification of a sirtuin 3 inhibitor that displays selectivity over sirtuin 1 and 2," *European Journal of Medicinal Chemistry*, vol. 55, pp. 58–66, 2012.

[34] Y. Wang, J. Li, X. Yao et al., "Loss of CIB2 causes profound hearing loss and abolishes mechanoelectrical transduction in mice," *Frontiers in Molecular Neuroscience*, vol. 10, p. 401, 2017.

[35] Z. Shasha, Q. Ruiying, D. Ying et al., "Hair cell regeneration from inner ear progenitors in the mammalian cochlea," *American Journal of Stem Cells*, vol. 9, no. 3, 2020.

[36] R. Taylor, A. Bullen, S. L. Johnson et al., "Absence of plastin 1 causes abnormal maintenance of hair cell stereocilia and a moderate form of hearing loss in mice," *Human Molecular Genetics*, vol. 24, no. 1, pp. 37–49, 2015.

[37] Y. Sergeyenko, K. Lall, M. C. Liberman, and S. G. Kujawa, "Age-related cochlear synaptopathy: an early-onset contributor to auditory functional decline," *The Journal of Neuroscience*, vol. 33, no. 34, pp. 13686–13694, 2013.

[38] J. D. Goutman, A. B. Elgoyhen, and M. E. Gomez-Casati, "Cochlear hair cells: the sound-sensing machines," *FEBS Letters*, vol. 589, no. 22, pp. 3354–3361, 2015.

[39] A. C. Wong and A. F. Ryan, "Mechanisms of sensorineural cell damage, death and survival in the cochlea," *Frontiers in Aging Neuroscience*, vol. 7, p. 58, 2015.

[40] G. C. Kujoth, A. Hiona, T. D. Pugh et al., "Mitochondrial DNA mutations, oxidative stress, and apoptosis in mammalian aging," *Science*, vol. 309, no. 5733, pp. 481–484, 2005.

[41] B. Guo, Q. Guo, Z. Wang et al., "D-Galactose-induced oxidative stress and mitochondrial dysfunction in the cochlear basilar membrane: an In Vitro aging model," *Biogerontology*, vol. 21, no. 3, pp. 311–323, 2020.

[42] T. Kamogashira, C. Fujimoto, and T. Yamasoba, "Reactive oxygen species, apoptosis, and mitochondrial dysfunction in hearing loss," *BioMed Research International*, vol. 2015, Article ID 617207, 7 pages, 2015.

[43] S. W. Tait and D. R. Green, "Caspase-independent cell death: leaving the set without the final cut," *Oncogene*, vol. 27, no. 50, pp. 6452–6461, 2008.

[44] A. Kurabi, E. M. Keithley, G. D. Housley, A. F. Ryan, and A. C. Wong, "Cellular mechanisms of noise-induced hearing loss," *Hearing Research*, vol. 349, pp. 129–137, 2017.

[45] V. Warnsmann, N. Meyer, A. Hamann, D. Kogel, and H. D. Osiewacz, "A novel role of the mitochondrial permeability transition pore in (−)-gossypol-induced mitochondrial dysfunction," *Mechanisms of Ageing and Development*, vol. 170, pp. 45–58, 2018.

[46] T. N. Le, L. V. Straatman, J. Lea, and B. Westerberg, "Current insights in noise-induced hearing loss: a literature review of the underlying mechanism, pathophysiology, asymmetry, and management options," *Journal of Otolaryngology - Head & Neck Surgery*, vol. 46, no. 1, p. 41, 2017.

[47] K. Hill, H. Yuan, X. Wang, and S. H. Sha, "Noise-induced loss of hair cells and cochlear synaptopathy are mediated by the activation of AMPK," *The Journal of Neuroscience*, vol. 36, no. 28, pp. 7497–7510, 2016.

[48] M. Kobel, C. G. Le Prell, J. Liu, J. W. Hawks, and J. Bao, "Noise-induced cochlear synaptopathy: past findings and future studies," *Hearing Research*, vol. 349, pp. 148–154, 2017.

[49] J. B. Jensen, A. C. Lysaght, M. C. Liberman, K. Qvortrup, and K. M. Stankovic, "Immediate and delayed cochlear neuropathy after noise exposure in pubescent mice," *PLoS One*, vol. 10, no. 5, article e0125160, 2015.

[50] L. A. Sena and N. S. Chandel, "Physiological roles of mitochondrial reactive oxygen species," *Molecular Cell*, vol. 48, no. 2, pp. 158–167, 2012.

[51] E. P. Yu and M. R. Bennett, "The role of mitochondrial DNA damage in the development of atherosclerosis," *Free Radical Biology & Medicine*, vol. 100, pp. 223–230, 2016.

[52] Z. D. Du, S. Yu, Y. Qi et al., "NADPH oxidase inhibitor apocynin decreases mitochondrial dysfunction and apoptosis in the ventral cochlear nucleus of D-galactose-induced aging model in rats," *Neurochemistry International*, vol. 124, pp. 31–40, 2019.

[53] A. H. Tseng, S. S. Shieh, and D. L. Wang, "SIRT3 deacetylates FOXO3 to protect mitochondria against oxidative damage," *Free Radical Biology & Medicine*, vol. 63, pp. 222–234, 2013.

[54] C. Han and S. Someya, "Maintaining good hearing: calorie restriction, Sirt3, and glutathione," *Experimental Gerontology*, vol. 48, no. 10, pp. 1091–1095, 2013.

[55] S. Someya, W. Yu, W. C. Hallows et al., "Sirt3 mediates reduction of oxidative damage and prevention of age-related hearing loss under caloric restriction," *Cell*, vol. 143, no. 5, pp. 802–812, 2010.

[56] B. Osborne, N. L. Bentley, M. K. Montgomery, and N. Turner, "The role of mitochondrial sirtuins in health and disease," *Free Radical Biology & Medicine*, vol. 100, pp. 164–174, 2016.

[57] W. He, J. C. Newman, M. Z. Wang, L. Ho, and E. Verdin, "Mitochondrial sirtuins: regulators of protein acylation and metabolism," *Trends in Endocrinology and Metabolism*, vol. 23, no. 9, pp. 467–476, 2012.

[58] W. Yu, K. E. Dittenhafer-Reed, and J. M. Denu, "SIRT3 Protein Deacetylates Isocitrate Dehydrogenase 2 (IDH2) and Regulates Mitochondrial Redox Status," *The Journal of Biological Chemistry*, vol. 287, no. 17, pp. 14078–14086, 2012.

[59] M. Ristow and K. Zarse, "How increased oxidative stress promotes longevity and metabolic health: the concept of mitochondrial hormesis (mitohormesis)," *Experimental Gerontology*, vol. 45, no. 6, pp. 410–418, 2010.

[60] M. D. Hirschey, T. Shimazu, E. Jing et al., "SIRT3 deficiency and mitochondrial protein hyperacetylation accelerate the development of the metabolic syndrome," *Molecular Cell*, vol. 44, no. 2, pp. 177–190, 2011.

[61] D. A. Sinclair, "Toward a unified theory of caloric restriction and longevity regulation," *Mechanisms of Ageing and Development*, vol. 126, no. 9, pp. 987–1002, 2005.

[62] M. D. Hirschey, T. Shimazu, E. Goetzman et al., "SIRT3 regulates mitochondrial fatty-acid oxidation by reversible enzyme deacetylation," *Nature*, vol. 464, no. 7285, pp. 121–125, 2010.

[63] P. I. Merksamer, Y. Liu, W. He, M. D. Hirschey, D. Chen, and E. Verdin, "The sirtuins, oxidative stress and aging: an emerging link," *Aging (Albany NY)*, vol. 5, no. 3, pp. 144–150, 2013.

[64] O. Ozden, S. H. Park, H. S. Kim et al., "Acetylation of MnSOD directs enzymatic activity responding to cellular nutrient status or oxidative stress," *Aging (Albany NY)*, vol. 3, no. 2, pp. 102–107, 2011.

[65] H. Kim, Y. D. Lee, H. J. Kim, Z. H. Lee, and H. H. Kim, "SOD2 and Sirt3 control osteoclastogenesis by regulating mitochondrial ROS," *Journal of Bone and Mineral Research*, vol. 32, no. 2, pp. 397–406, 2017.

[66] M. C. Chen, L. L. Hsu, S. F. Wang, C. Y. Hsu, H. C. Lee, and L. M. Tseng, "ROS mediate xCT-dependent cell death in human breast cancer cells under glucose deprivation," *Cell*, vol. 9, no. 7, p. 1598, 2020.

[67] Y. Quan, L. Xia, J. Shao et al., "Adjudin protects rodent cochlear hair cells against gentamicin ototoxicity via the SIRT3-ROS pathway," *Scientific Reports*, vol. 5, no. 1, p. 8181, 2015.

Hindawi
Neural Plasticity
Volume 2021, Article ID 6151973, 8 pages
https://doi.org/10.1155/2021/6151973

Research Article

Hearing Screening Combined with Target Gene Panel Testing Increased Etiological Diagnostic Yield in Deaf Children

Le Xie, Yue Qiu, Yuan Jin, Kai Xu, Xue Bai, Xiao-Zhou Liu, Xiao-Hui Wang, Sen Chen, and Yu Sun

Department of Otorhinolaryngology, Union Hospital, Tongji Medical College, Huazhong University of Science and Technology, Wuhan 430022, China

Correspondence should be addressed to Sen Chen; senchen@hust.edu.cn and Yu Sun; sunyu@hust.edu.cn

Received 21 April 2021; Revised 9 June 2021; Accepted 11 July 2021; Published 23 July 2021

Academic Editor: Geng lin Li

Genetic testing is the gold standard for exploring the etiology of congenital hearing loss. Here, we enrolled 137 Chinese patients with congenital hearing loss to describe the molecular epidemiology by using 127 gene panel testing or 159 variant testing. Sixty-three deaf children received 127 gene panel testing, while seventy-four patients received 159 variant testing. By use of 127 gene panel testing, more mutant genes and variants were identified. The most frequent mutant genes were *GJB2*, *SLC26A4*, *MYO15A*, *CDH23*, and *OTOF*. By analyzing the patients who received 127 gene panel testing, we found that 51 deaf children carried variants which were not included in 159 variant testing. Therefore, a large number of patients would be misdiagnosed if only 159 variant testing is used. This study highlights the advantage of 127 gene panel testing, and it suggests that broader genetic testing should be done to identify the genetic etiology of congenital hearing loss.

1. Introduction

Congenital hearing loss (HL) is a common disease, and about 1 to 2 per 1000 live births suffer from congenital hearing loss in the world. The prevalence of hearing loss increases with age. Among the kids in the primary school, the prevalence is 2.83/1000. Furthermore, in adolescents, it will rise to 3.5/1000 [1–3]. According to the latest date, approximately 50%-60% of congenital HL is caused by genetic factors [4, 5]. However, genetic disorder can also cause late-onset deafness in children and adolescents [2]. Both congenital or late-onset deafness caused by genetic disorder can be attributed to hereditary hearing loss. To date, more than 150 deafness-related genes and 6000 variants have been identified [6] (https://hereditaryhearingloss.org). The hearing loss genes and hot variants showed distinctly in different ethnic groups. Among these hearing loss genes, *GJB2* and *SLC26A4* gene variants were most common in Chinese deaf population [4]. For *GJB2* gene variants, the most frequent etiological factor of nonsyndromic hereditary hearing loss, the hotspots were described as c.235delC and c.109G>A, common in Asian, c.35delG, found in European, and c.71G > A, predominant in the Indian [7, 8]. Although *GJB2* and *SLC26A4* mutations account for a large part of causes of hereditary deafness, there are still a large number of known or unknown gene mutations that cause hearing loss. How to quickly and accurately detect causes of patients with suspected hereditary deafness is an important issue in the diagnosis and treatment of deafness.

Genetic testing is the gold standard for exploring the etiology of congenital and late-onset deafness. In addition, medical history and other auditory physiology tests are also very important. For hereditary deafness, genetic testing is a crucial step. Except for finding causes, it also could help diagnosis and intervention of syndromic hearing loss because some children only exhibited hearing loss without other symptoms at a young age. Besides, genetic testing was beneficial to protecting children with some variants such as m.1555A > G or variants in *KCNQ1* gene from avoidable risk factors [9–12]. DNA sequencing first

Table 1: The basic information of patients recruited in this research.

	127 gene panel	159 variants	Total
Male	35	39	74
Female	28	35	63
Total	63	74	137

Table 2: The genetic spectrum of hereditary hearing loss patients detected by 127 gene panel testing.

Gene	Patients carried variant	Pathogenic variant	Likely pathogenic variant	VUS variant
GJB2	33	32	0	1
SLC26A4	16	15	0	1
OTOF	5	1	3	1
MYO15A	5	1	1	3
CDH23	5	0	2	3
TECTA	4	0	1	3
MYO7A	4	0	0	4
WFS1	3	1	0	2
PTPRQ	2	1	0	1
COCH	2	0	2	0
GJB3	2	0	1	1
OTOA	2	0	1	1
USH2A	2	0	1	1
ESPN	2	0	0	2
TRIOBP	2	0	0	2
GRXCR1	1	1	0	0
ALMS1	1	1	0	0
COL4A3	1	0	1	0
ILDR1	1	0	1	0
ADGRV1	1	0	0	1
CLDN14	1	0	0	1
CRYM	1	0	0	1
DIAPH3	1	0	0	1
EDNRB	1	0	0	1
LOXHD1	1	0	0	1
MITF	1	0	0	1
MYH14	1	0	0	1
PCDH15	1	0	0	1
PDSS1	1	0	0	1
SLC17A8	1	0	0	1
TJP2	1	0	0	1
TMC1	1	0	0	1

described 44 years ago has evolved from single-mutation sequencing (Sanger sequencing) to high-throughput sequencing (Next generation sequencing, NGS) [5, 13]. Compared to Sanger sequencing, NGS was able to simultaneously sequence millions of small fragments at a reasonable cost and reduced runtime [13]. Targeted gene panel, a common NGS technique, has been widely applied in deaf population. It was targeted to the detection of variants in the massively known hearing loss genes. Considering the cost and time consuming, different panels were designed in clinical applications [1, 4, 12, 14, 15].

Table 3: The genetic spectrum of hereditary hearing loss patients detected by 159 variant testing.

Gene	Patients with mutant gene	Percentage
GJB2	45	0.608108
SLC26A4	27	0.364865
GJB3	2	0.027027
MT-RNR1	1	0.013514

As the spectrum of gene mutations is distinct in different ethnic group, studying mutated character of Chinese deaf children and choosing the appropriate gene panel are critical for clinical diagnosis and treatment. In this study, we enrolled 137 Chinese children with sensorineural hearing loss to describe the molecular epidemiology by using 127 gene panel testing and 159 variants in 22 gene testing.

2. Materials and Methods

2.1. Patients and Samples. A total of 137 patients under the age of twelve with sensorineural hearing loss were recruited from the Wuhan Union Hospital from 2018 to 2020. All patients failed pass the neonatal hearing screening and underwent 127 gene panel testing (targeting the exon regions and exon-intron boundaries of 127 known deafness-causing nuclear genes as well as deafness-causing mitochondrial regions) or 159 variants in 22 gene testing (detecting a total of 159 hotspot variants in 22 known deafness-causing genes). Informed consent was obtained from all patients or their legal guardians. This study was approved by the Institutional Review Board of the BGI in accordance with the Declaration of Helsinki (1964). Written informed consent, clinical evaluations, and blood samples were obtained from all the participants or their legal guardians. The study of the protocols was approved by the review boards of the ethics committees of the Tongji Medical College of Huazhong University of Science and Technology.

Peripheral venous blood samples were collected from all recruited patients. Genomic DNA was obtained and purified using a QIAamp DSP DNA Blood Mini Kit (61104, Qiagen Inc., Valencia, CA, USA).

2.2. Library Preparation, Sequencing, and Bioinformatics. Fragmented DNA (a size of 350–400 base pairs) were prepared using Covaris LE220 ultrasonicator (Covaris Inc., Woburn, Massachusetts, USA). Then end-repair and adaptor ligation were performed for library construction. After array hybridization, elution, and postcapture amplification, targeted DNA fragments were sequenced on the BGISEQ-500 platform. After sequencing and quality control, the clean reads derived from targeted high-throughput sequencing

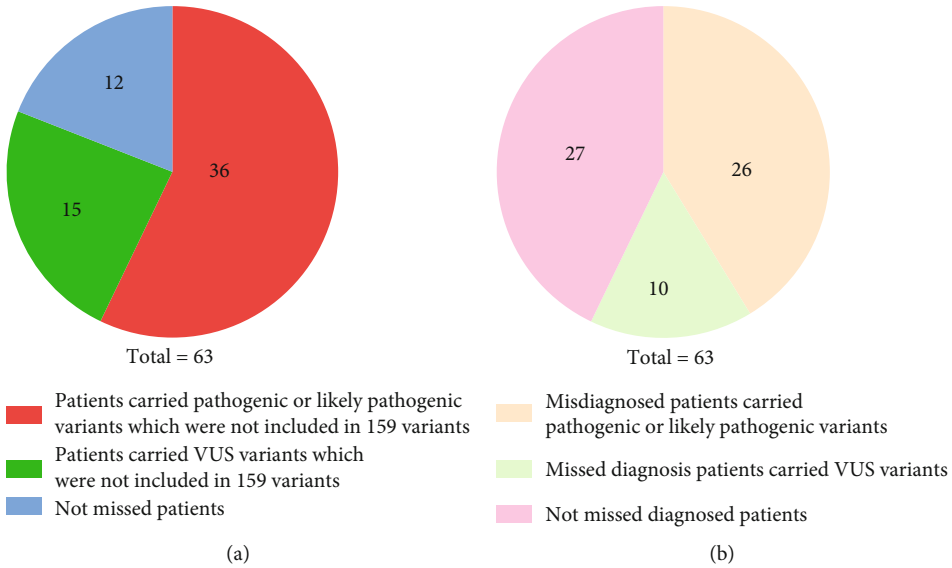

Figure 1: Analyze the genetic etiology of patients who received 127 gene panel testing compared with 159 variants. (a) 36 patients carried pathogenic or likely pathogenic variants which were not included in 159 variants, fifteen patients carried VUS variants which were not included in 159 variants, and 12 patients do not carry the variants which were not included in 159 variants. (b) 26 patients who carried pathogenic or likely pathogenic variants would misdiagnose if they were only detected by 159 variant testing, ten patients who carried VUS might miss diagnosis, and twenty-seven patients would not miss diagnosis.

were aligned to the GRCh37/hg19 using the BWA (Burrows Wheeler Aligner) Multi-Vision software package. After alignment, the variants of single-nucleotide variants (SNVs) and inserts and deletions (InDels) were detected by GATK software. Then, filtered SNVs and InDels were compared with NCBI GenBank database, 1000 Genomes, ESP6500, dbSNP, HGMD, and ExAC. Candidate variants were classified into pathogenic variants, likely pathogenic variants, variants of uncertain significance (VUS), likely benign variants, and benign variants according to the American College of Medical Genetics and Genomics–Association for Molecular Pathology (ACMG–AMP) guideline. The method described in this study partly reproduces the wording in our previous article [16–18].

3. Result

3.1. Study Samples. A total of 137 patients were included in this research, seventy-four patients were male and sixty-three were female. Sixty-three patients (46%) received genetic testing by 127 gene panel, while seventy-four patients (54%) received 159 variant testing (Table 1). Tested genes are provided in supplement (Table S1 and S2.)

3.2. Genetic Spectrum. Among the 63 received 127 gene panel test, ninety-two variants in 32 genes were detected, the top five genes were *GJB2* (33 patients), *SLC26A4* (16 patients), *MYO15A* (5 patients), *CDH23* (5 patients), and *OTOF* (5 patients) (Table 2).

Among the 74 who received 159 variant testing, twenty-one variants in 4 genes were detected; the patients with mutation of *GJB2*, *SLC26A4*, *GJB3*, and *MT-RNR1* were 45, 27, 2, and 1, respectively (Table 3).

3.3. Different Diagnosis between 127 Gene Panel Testing and 159 Variant Testing. Among the 63 patients who received 127 gene testing, fifty-one patients were found to carry variants which were not included in 159 variant testing, thirty-six of them had been found to carry pathogenic or likely pathogenic variants. If these patients received 159 variant testing only, in 36 of them, the genetic etiology of the hearing loss would be missed, and 26 of the patients were found to carry the pathogenic or likely pathogenic variants (Figure 1). Twenty-two deafness gene mutation which was not included in 159 variant testing was found in 25 patients; nine of them carried pathogenic or likely pathogenic variants of these 22 deafness genes. In these 22 deafness genes which were not included in 159 variant testing, eighty-four variants were found, ten of them were pathogenic or likely pathogenic (Table 4).

3.4. GJB2 Variants. In 127 gene panel testing, six variants of *GJB2* were identified; c.109G>A, c.235delC, c.299_300del AT, c.176_191del GCTGCAAGAACGTGTG, c.139G>T, and c.88A>G were detected 18, 15, 5, 2, 1, and 1 times, respectively (Table 5). The patients who carried heterozygous variant of c.109G>A were the most, and secondary was heterozygous c.235delC mutation in 11 patients, and then was the homozygous c.109G>A mutation in 5 patients and homozygous c.235delC mutation in 4 patients. In the 11 patients who carried heterozygous c.235delC variants, four of them carried c.299_300del AT, 2 carried c.109G>A, and 2 carried c.176_191del GCTGCAAG AACGTGTG compound heterozygotes variants, respectively. In our study, a patient who carried a novel heterozygous variant was identified, the nucleotide change is c.88A>G, the protein change is p.Ile30Val, and the characterization of variant

Table 4: The variants would be missed if tested by 159 variant testing.

Gene	Variant	Effect on protein	Characterization of variant
ADGR V1	c.11704A>G	p.Met3902Val	VUS
	c.2899-10T>A		VUS
ALMS1	c.2035C>T	p.Arg679Ter	Pathogenic
	c.5067+1G>A		Likely pathogenic
	c.6604G>A	p.Asp2202Asn	Likely pathogenic
CDH23	c.1765G>A	p.Asp589Asn	VUS
	c.2368A>G	p.Met790Val	VUS
	c.3262G>A	p.Val1088Met	VUS
	c.4859T>A	p.Val1620Glu	VUS
	c.5051G>A	p.Arg1684His	VUS
CLDN14	c.805C>T	p.Arg269Trp	VUS
	c.449C>T	p.Pro150Leu	VUS
	c.694G>A	p.Gly232Arg	VUS
COCH	c.812_813insG	p.Val271Valfs X5	Likely pathogenic
COL4A3	c.4755+1G>A		Likely pathogenic
CRYM	c.849C>T	p.His283His	VUS
DIAPH3	c.3543_3544i nsC	p.Pro1181 Profs∗4	VUS
EDNRB	c.758G>A	p.Arg253Gln	VUS
ESPN	c.1828G>C	p.Ala610Pro	VUS
	c.2069C>T	p.Ser690Leu	VUS
GJB2	c.109G>A	p.Val37Ile	Pathogenic
	c.139G>T	p.Glu47Ter	Pathogenic
	c.88A>G	p.Ile30Val	VUS
GJB3	c.580G>A	p.Ala194Thr	Likely pathogenic
	c.595A>G	p.Ile199Val	VUS
GRXCR1	c.784C>T	p.Arg262Ter	Pathogenic
ILDR1	c.206C>A	p.Pro69His	Likely pathogenic
LOXHD1	EX31 DUP		VUS
MITF	c.950G>C	p.Arg317Thr	VUS
MYH14	c.4641C>T	p.Asp1547Asp	VUS
	c.10251_10253 delCTT		Pathogenic
	c.4642G>A	p.Ala1548Thr	Pathogenic
	c.8702_8703i nsT	p.Pro2901Pro fsX25	Likely pathogenic
MYO15A	c.3239G>A	p.Arg1080His	VUS
	c.3743G>A	p.Arg1248Gln	VUS
	c.5681T>C	p.Leu1894Pro	VUS
	c.6340G>A	p.Val2114Met	VUS
MYO7A	c.1901G>A	p.Arg634Gln	VUS
	c.1945C>T	p.Arg649Trp	VUS
	c.6235C>T	p.Arg2079Trp	VUS
	c.6470T>C	p.Ile2157Thr	VUS
OTOA	c.943delT	p.Ser315Profs ∗5	Likely pathogenic
	c.1172C>T	p.Ser391Leu	VUS
	c.2359G>T	p.Glu787Ter	VUS
	c.5816G>A	p.Arg1939Gln	Pathogenic
OTOF	c.4023+1G>A		Likely pathogenic
	c.5098G>C	p.Glu1700Gln	Likely pathogenic
	c.1194T>A	p.Asp398Glu	VUS
	c.3429G>A	p.Arg1143Arg	VUS

Table 4: Continued.

Gene	Variant	Effect on protein	Characterization of variant
PCDH15	c.2563C>A	p.Arg855Arg	VUS
PDSS1	EX1 DUP		VUS
	c.6475C>T	p.Arg2159Ter	Pathogenic
PTPRQ	c.6025-4_6025-2delACA		VUS
SLC17A8	c.6293T>C	p.Leu2098Ser	VUS
	c.1117T>C	p.Leu373Leu	VUS
	c.243G>A	p.Met81Ile	VUS
SLC26A4	c.1079C>T	p.Ala360Val	Pathogenic
	c.1339delA	p.Lys447Serfs∗8	Pathogenic
	c.1519delT	p.Leu507∗	Pathogenic
	c.164+1G>C		Pathogenic
	c.2000T>C	p.Phe667Ser	Pathogenic
	c.1001+5G>T		VUS
	c.1087A>C	p.Ile363Leu	VUS
	c.1340A>T	p.Lys447Met	VUS
	c.208C>A	p.Pro70Thr	VUS
	c.678T>C	p.Ala226Ala	VUS
	c.718C>T	p.Leu240Phe	VUS
	c.765+5G>A		VUS
TECTA	c.640G>T	p.Gly214Ter	Likely pathogenic
	c.235G>C	p.Val79Leu	VUS
	c.2936T>C	p.Phe979Ser	VUS
TJP2	c.576G>A	p.Thr192Thr	VUS
TMC1	c.474G>T	p.Arg158Ser	VUS
	c.1810C>G	p.Arg604Gly	VUS
	c.589G>A	p.Gly197Arg	VUS
TRIOBP	c.2133T>C	p.Pro711Pro	VUS
	c.2314T>C	p.Cys772Arg	VUS
	c.-60-1G>C		VUS
USH2A	c.6937G>T	p.Gly2313Cys	Likely pathogenic
	c.10740+7G>A		VUS
	c.7230A>T	p.Val2410Val	VUS
	c.2051C>T	p.Ala684Val	Pathogenic
WFS1	c.125G>T	p.Arg42Leu	VUS
	c.2458G>A	p.Gly820Ser	VUS

is VUS; this patient carried c.919-2A>G and c.1229C>T compound heterozygotes variants of SLC26A4 gene as well.

In 159 variant testing, eight variants of *GJB2* were identified; the frequency of these variants from high to low were c.235delC, c.299_300delAT, c.176_191del GCTGCAAGA ACGTGTG, c.139G>T, c.187G>T, c.257C>G, c.427C>T, and c.428G>A; the check-out times of these variants were 36, 9, 5, 2, 1, 1, 1, and 1, respectively. Nineteen patients carried heterozygous c.235delC variants, five of them carried c.299_300delAT compound heterozygotes variants, three patients carried c.176_191del GCTGCAAGAACGTGTG compound heterozygotes variants, and one carried c.257C>G compound heterozygotes variants. The homozygous c.235delC patients were seventeen. c.299_300delAT heterozygous variant was identified in 9 patients, two of them carried c.176_191delGCTGCAAGAACGTGTG compound heterozygotes variants.

3.5. SLC26A4 Variants. In 127 gene panel testing, seventeen variants were identified in *SLC26A4* gene, the most frequent variant detected was c.919-2A>G, eleven patients carried heterozygous c.919-2A>G variant, nine of them were compound heterozygotes variants with other SLC26A4 variants, and one homozygous c.919-2A>G was identified. Eight novel variants were identified in our research; c.1339delA,

Table 5: Variants frequency in *GJB2* gene.

Variants	Homozygous	Heterozygous	Total
Testing by 127 gene panel			
c.109G>A	5	13	18
c.235delC	4	11	15
c.299_300del AT	1	4	5
c.176_191del GCTGCAAG AACGTGTG	0	2	2
c.139G>T	1	0	1
c.88A>G	0	1	1
Testing by 159 variant testing			
c.235delC	17	19	36
c.299_300delAT	0	9	9
c.176_191delGCTGCAAGA ACGTGTG	0	5	5
c.139G>T	2	0	2
c.187G>T	0	1	1
c.427C>T	1	0	1
c.428G>A	0	1	1
c.257C>G	0	1	1

Table 6: Variants frequency in *SLC26A4* gene.

Variants	Homozygous	Heterozygous	Total
Testing by 127 gene panel			
c.919-2A>G	1	11	12
c.2000T>C	0	2	2
c.1087A>C	0	1	1
c.1174A>T	0	1	1
c.1339delA	0	1	1
c.164+1G>C	0	1	1
c.718C>T	0	1	1
c.1226G>A	0	1	1
c.678T>C	0	1	1
c.1519delT	0	1	1
c.1229C>T	0	1	1
c.1340A>T	0	1	1
Testing by 159 variant testing			
c.919-2A>G	5	14	19
c.1229C>T	0	5	5
c.2168A>G	0	4	4
c.1174A>T	0	1	1
c.1226G>A	0	1	1
c.1336C>T	0	1	1
c.1343C>A	0	1	1
c.1343C>T	0	1	1
c.1594A>C	0	1	1
c.1692dupA	0	1	1
c.1707+5G >A	0	1	1
c.589G>A	0	1	1

c.1519delT, c.164+1G>C, and c.2000T>C were likely pathogenic variants, while c.1340A>T, c.718C>T, c.765+5G>A, and c.208C>A were VUS variants (Table 6).

Twelve variants of *SLC26A4* were identified in 159 variant testing; the most common variant was c.919-2A>G same as the 127 gene panel testing, then was c.1229C>T and c.2168A>G. Nineteen patients carried c.919-2A>G variant, fourteen of them were heterozygous while 5 were homozygous.

4. Discussion

Hearing scanning combined with molecular genetic testing is an effective approach to diagnose hereditary hearing loss, while because of the high cost of genetic testing, such limited the usage of more comprehensive genetic testing. Through 127 gene panel testing, more genetic etiology of deaf children was identified. In 127 gene panel testing, thirty-two deafness genes were identified in patients. The five most frequent genes were *GJB2* (33 patients), *SLC26A4* (16 patients), *MYO15A* (5 patients), *OTOF* (5 patients), and *CDH23* (5 patients), while only four deafness genes were identified by 159 variant testing, and the frequency of these four genes was 45 (*GJB2*), 27 (*SLC26A4*), 2 (*GJB3*), and 1 (*MT-RNR1*), respectively. The genetic spectrum of 127 gene testing is consistent with the previous research in China [19]. The diagnostic rate of *GJB2* and *SLC26A4* is higher in 159 variant testing which may cause more mutant genes identified in 127 gene panel testing. Furthermore, eighty-four variants in 32 genes which were not included in 159 variant testing were identified, and ten variants of these were pathogenic or likely pathogenic. This result demonstrates that even though 159 variant testing contain hotspot deafness variants, it would still misdetect abundant of gene mutations.

Broader genetic testing can improve the diagnostic sensitivity and accuracy. By analyzing the patients who received 127 gene panel testing, we found that 25 patients had mutant genes which were not included in 159 variant testing, and nine of them carried pathogenic or likely pathogenic variants. Fifty-one patients carried variants that were not included in 159 variant testing, and thirty-six of them carried pathogenic or likely pathogenic variants. If these patients only received 159 variant testing, the genetic etiology would not be identified. This result revealed that even if the patients pass the traditional gene testing, they still could have genetic causes. Therefore, expanded gene testing should be done to identify the genetic etiology.

Moreover, accurate genetic testing can benefit patients in several aspects. Identifying genetic etiology can guide clinicians to determine treatment strategies. In our research, we found several patients carried variants in *CDH23*, *WFS1*, and *PCDH15* by 127 gene panel testing. As reported in previous research, some patients with above gene mutation may have a poor prognosis of cochlear implantation (CI) [20]. Besides, early genetic diagnostic of hearing loss would provide more information on nature, mode of inheritance, and implications of genetic disorders, which would help individuals and families make informed medical and

personal decisions [14, 21]. Furthermore, the relationship between genotype and phenotype of hereditary hearing loss is complicated; finding novel variants would broaden the understanding of hereditary hearing loss.

Genetic testing should be optimized according to multiple dimensions. Firstly, the common detection of deafness genes and variants should vary by ethnicity and region. For example, in 127 gene panel testing, c.109G>A was the most frequent variant, then was the c.235delC. In our research, we did not select the ethnicity of the patients, which would influence the frequency of these variants. A previous research in Qinghai (China) has shown that c.109G>A was more common in minority patients, while c.235delC was more common in Han nationality [22]. Secondly, some gene mutation which might be associated with poor prognosis of CI such as *POU3F4*, *TMPRSS3*, *PJVK*, *CDH23*, and *PCDH15* should be added in genetic testing. The full sequence of these genes or at least the exon regions should be detected. If pathological mutations in these genes are missed, it may bring catastrophic consequences to patients and their families.

5. Conclusion

Congenital deafness is the number one congenital disease that endangers human health. The identification of the cause through hearing screening combined with genetic testing is an important basis for mechanism research, clinical intervention, and genetic counseling. With the development of sequencing technology, deeper and broader genetic testing by next-generation sequencing are efficient and affordable. More accurate and convenient genetic testing should be designed and recommended. It can increase the detection rate of patients with hereditary deafness, guide clinical treatment strategies, expand new deafness genes or variants, and provide help for future clinical work.

Data Availability

The data which support the conclusions of our study is upon the request.

Ethical Approval

The study of the protocols was approved by the review boards of the ethics committees of the Tongji Medical College of Huazhong University of Science and Technology.

Consent

Written informed consent, clinical evaluations, and blood samples were obtained from all the participants or their legal guardians.

Conflicts of Interest

The authors declare that they have no conflict of interest.

Authors' Contributions

Le Xie and Yue Qiu contributed equally to this work.

Acknowledgments

This work was supported by a grant from the National Nature Science Foundation of China (81771003 and 82071058).

Supplementary Materials

See Supplementary Tables S1 and S2 in the Supplementary Material. Tested genes among 127 gene panel testing are provided in Table S1, and tested variants in 159 variant testing are provided in Table S2. *(Supplementary Materials)*

References

[1] R. Cabanillas, M. Diñeiro, G. A. Cifuentes et al., "Comprehensive genomic diagnosis of non-syndromic and syndromic hereditary hearing loss in Spanish patients," *BMC Medical Genomics*, vol. 11, no. 1, p. 58, 2018.

[2] A. M. H. Korver, R. J. H. Smith, G. van Camp et al., "Congenital hearing loss," *Nature Reviews Disease Primers*, vol. 3, no. 1, 2017.

[3] A. van Wieringen, A. Boudewyns, A. Sangen, J. Wouters, and C. Desloovere, "Unilateral congenital hearing loss in children: challenges and potentials," *Hearing Research*, vol. 372, pp. 29–41, 2019.

[4] Y.-. B. Xiang, C.-. Y. Xu, Y.-. Z. Xu et al., "Next-generation sequencing identifies rare pathogenic and novel candidate variants in a cohort of Chinese patients with syndromic or nonsyndromic hearing loss," *Molecular Genetics & Genomic Medicine*, vol. 8, no. 12, 2020.

[5] K. D. Brodie, A. T. Moore, A. M. Slavotinek et al., "Genetic testing leading to early identification of childhood ocular manifestations of usher syndrome," *Laryngoscope*, vol. 131, no. 6, 2020.

[6] A. E. Shearer, M. S. Hildebrand, and R. J. H. Smith, "Hereditary hearing loss and deafness overview, in GeneReviews(®)," in *GeneReviews is a registered trademark of the University of Washington, Seattle*, M. P. Adam, Ed., University of Washington, Seattle Copyright © 1993-2021, University of Washington, Seattle, Seattle (WA), 1993.

[7] D. K. Chan and K. W. Chang, "GJB2-associated hearing loss: systematic review of worldwide prevalence, genotype, and auditory phenotype," *Laryngoscope*, vol. 124, no. 2, pp. E34–E53, 2014.

[8] F. F. Zhao, Y. B. Ji, D. Y. Wang et al., "Phenotype-genotype correlation in 295 Chinese deaf subjects with biallelic causative mutations in the GJB2 gene," *Genetic Testing and Molecular Biomarkers*, vol. 15, no. 9, pp. 619–625, 2011.

[9] G. Casazza and J. D. Meier, "Evaluation and management of syndromic congenital hearing loss," *Current Opinion in Otolaryngology & Head and Neck Surgery*, vol. 25, no. 5, pp. 378–384, 2017.

[10] A. Eftekharian and M. H. Mahani, "Jervell and Lange-Nielsen syndrome in cochlear implanted patients: our experience and a review of literature," *International Journal of Pediatric Otorhinolaryngology*, vol. 79, no. 9, pp. 1544–1547, 2015.

[11] T. Yang, L. Guo, L. Wang, and X. Yu, "Diagnosis, intervention, and prevention of genetic hearing loss," *Advances in Experimental Medicine and Biology*, vol. 1130, pp. 73–92, 2019.

[12] C. M. Sloan-Heggen, A. O. Bierer, A. E. Shearer et al., "Comprehensive genetic testing in the clinical evaluation of 1119 patients with hearing loss," *Human Genetics*, vol. 135, no. 4, pp. 441–450, 2016.

[13] T. Atik, G. Bademci, O. Diaz-Horta, S. H. Blanton, and M. Tekin, "Whole-exome sequencing and its impact in hereditary hearing loss," *Genetics Research*, vol. 97, 2015.

[14] G. García-García, A. Berzal-Serrano, P. García-Díaz et al., "Improving the management of patients with hearing loss by the implementation of an NGS panel in clinical practice," *Genes*, vol. 11, no. 12, 2020.

[15] Y. Sun, J. Xiang, Y. Liu et al., "Increased diagnostic yield by reanalysis of data from a hearing loss gene panel," *BMC Medical Genomics*, vol. 12, no. 1, p. 76, 2019.

[16] S. Chen, Y. Jin, L. Xie et al., "A novel spontaneous mutation of the SOX10 gene associated with Waardenburg Syndrome Type II," *Neural Plasticity*, vol. 2020, Article ID 9260807, 2020.

[17] Y. Qiu, S. Chen, K. X. Le Xie et al., "Auditory neuropathy spectrum disorder due to two novel compound heterozygous OTOF mutations in two Chinese families," *Neural Plasticity*, vol. 2019, Article ID 9765276, 2019.

[18] Y. Qiu, S. Chen, X. Wu et al., "Jervell and Lange-Nielsen syndrome due to a novel compound heterozygous KCNQ1 mutation in a Chinese family," *Neural Plasticity*, vol. 2020, Article ID 3569359, 2020.

[19] S. Chen, Z. Liang, B. Chen et al., "The prevalence of deafness-associated mutations in neonates: a meta-analysis of clinical trials," *International Journal of Pediatric Otorhinolaryngology*, vol. 121, pp. 99–108, 2019.

[20] H. Zhang, S. Chen, Y. Sun, and W. Kong, "The value of genetic diagnosis of deafness in evaluating the prognosis of cochlear implantation," *Lin Chung Er Bi Yan Hou Tou Jing Wai Ke Za Zhi*, vol. 35, no. 3, pp. 274–281, 2021.

[21] N. B. Urbančič, S. Battelino, T. Tesovnik, and K. T. Podkrajšek, "The importance of early genetic diagnostics of hearing loss in children," *Medicina*, vol. 56, no. 9, p. 471, 2020.

[22] S. Duan, Y. Guo, X. Chen, and Y. Li, "Genetic mutations in patients with nonsyndromic hearing impairment of minority and Han Chinese ethnicities in Qinghai, China," *Journal of International Medical Research*, vol. 49, no. 4, 2021.

Hindawi
Neural Plasticity
Volume 2021, Article ID 4784385, 16 pages
https://doi.org/10.1155/2021/4784385

Review Article

Noise-Induced Hearing Loss: Updates on Molecular Targets and Potential Interventions

Huanyu Mao[1,2] **and Yan Chen**[1,2]

[1]*ENT Institute and Department of Otorhinolaryngology, Eye & ENT Hospital, Fudan University, Shanghai 200031, China*
[2]*NHC Key Laboratory of Hearing Medicine (Fudan University), Shanghai 200031, China*

Correspondence should be addressed to Yan Chen; chenyan0528@fudan.edu.cn

Received 8 April 2021; Accepted 12 June 2021; Published 7 July 2021

Academic Editor: Hai Huang

Noise overexposure leads to hair cell loss, synaptic ribbon reduction, and auditory nerve deterioration, resulting in transient or permanent hearing loss depending on the exposure severity. Oxidative stress, inflammation, calcium overload, glutamate excitotoxicity, and energy metabolism disturbance are the main contributors to noise-induced hearing loss (NIHL) up to now. Gene variations are also identified as NIHL related. Glucocorticoid is the only approved medication for NIHL treatment. New pharmaceuticals targeting oxidative stress, inflammation, or noise-induced neuropathy are emerging, highlighted by the nanoparticle-based drug delivery system. Given the complexity of the pathogenesis behind NIHL, deeper and more comprehensive studies still need to be fulfilled.

1. Introduction

Hair cells (HCs) in the inner ear cochlea function in transducing sound waves into electric signals [1–4], while supporting cells function in supporting the HCs and providing the potential pool for HC regeneration [5–9]. Damages from a variety of sources can impair HC function, including mutations in deafness genes, aging, ototoxic drugs, chronic cochlear infections, and noise exposure [10–13]. Acoustic overexposure would result in sensorineural hearing loss characterized by high-frequency hearing threshold shift mainly, termed as noise-induced hearing loss (NIHL)[14], which is due to loss or damage of sensory HCs and degeneration of the spiral ganglion neurons (SGNs). Though noise susceptibility is quite individual, it is normally acknowledged that noise above 85 dB would be considered as hearing harmful [15, 16]. Studies [17–19] have shown that mild or moderate noise would only trigger temporary hearing threshold shift (TTS), because the noise-induced hair cell damage and auditory nerve fiber degeneration were still reversible. Hearing ability is commonly measured by auditory brainstem response (ABR) and distortion product otoacoustic emission (DPOAE) test [20]. The ABR threshold and DPOAE level would recover to prenoise level over time in TTS patients. However, severe noise exposure, referring as strong sound vibrations, or longtime exposure to harmful noise, or both, can lead to cochlear hair cell necrosis and apoptosis, causing permanent threshold shift (PTS)[16, 21]. Although the neonatal mammals still have very limited HC regeneration ability, the adults have lost this ability [22–26], leading to the irreversible loss of HCs after noise damage. Besides decrease of auditory sensitivity and language recognition ability, NIHL patients could suffer from headache, tinnitus, dizziness, hypertension, etc. [14, 17].

It is estimated that about 5% of the world's population suffer from disabling hearing loss [27]. Modern people are exposed to acoustic trauma with increasingly higher risk as the industrialization of society. Strikingly, evidence has shown that acoustic trauma-induced hearing impairment aggravates microglial deterioration around the hippocampus, indicating its potential causal role in the pathogenesis of dementia, which exacerbates the already overloading public health burden of NIHL [28]. Therefore, more and more attention has been focused on revealing the pathogenesis

mechanisms and effective therapeutics of NIHL. We review the updates on molecular targets about NIHL, summarize the approved and potential medications for NIHL treatment, and propose the controversies and foreseeing on NIHL.

2. Cellular Pathologies

Acoustic shock with strong sonic energy caused temporary or permanent cellular pathologies. Hair cells, especially outer hair cells (OHCs), are the main targets of noise trauma. Noise overexposure causes hair cells swelling and eventual irreversible death [29]. Noise-induced sensory hair cell impairment also accompanies by collapse and loss of stereocilia and destruction of their tip connection. Interestingly, the loss of tip links connecting adjacent stereocilia would increase noise susceptibility reversely [30–32]. Acoustic overstimulation can also cause the reduction of synaptic connections between hair cells and spiral ganglion cells, afferent fiber swelling, and auditory nerve deterioration [33–37].

It is widely recognized that noise with sound intensity > 85 dB is hearing harmful, while extremely high intensity noise like blast or gunshot could do much more harm to the hearing system within very short exposing time. The latter has been given a special name termed blast-induced hearing loss to highlight its difference from chronic NIHL [38]. Besides the damage of hair cells and spiral ganglion neurons, high intensity noise can result in middle ear damage like tympanic membrane perforation, ossicular chain dislocation, oval/round window rupture, and thus external lymph fistula [39]. The stria vascularis and spiral ligament are also attacked by intense noise, resulting in lower blood flow and lower vessel diameter in the stria vascularis [40]. Hearing impairment is the foremost clinical symptom of blast overexposure injury. Besides that, blast may also cause otitis media because of the rupture of tympanic membrane and secondary infection [41]. Vertigo and balance disorder occur in patients accompanied by labyrinthine damage and hemorrhage after blast exposure, which leaves headache and dizziness for a long time after the accident. Therefore, the treatment of blast-induced hearing loss often involves operations like tympanoplasty to repair tympanic membrane and rebuild ossicular chain [42].

3. Molecular Pathogenesis

Acoustic trauma features hair cell loss, synaptic ribbon deterioration, and acoustic nerve degeneration. Previous studies [43, 44] have proved that after noise exposure, both necrosis and apoptosis occurred in the sensory epithelium. However, the causative mechanisms inducing necrosis and apoptosis are much complex and intertwined (Figure 1).

3.1. Oxidative Stress. Though the exact mechanism behind NIHL is not fully explained yet, various studies [45–47] have suggested that oxidative stress in the cochlea contributes to the noise-induced hearing impairment. Ohlemiller et al. [45] have proved that the production of hydroxyl radical, a main kind of reactive oxygen species (ROS), increases over four times upon acoustic trauma in cochlear perilymph. ROS, mainly generated from the leaking electrons in the mitochondrial electron transport chain, is crucial for multiple physiological behaviors like cell proliferation and differentiation in relative low content [46, 48]. Under physiological circumstances, the production and scavenging of ROS are maintained at balance subtly and dynamically. Many stress stimulators like extensive sound exposure as well as ototoxic drugs like cisplatin [47] and aminoglycosides [49–56] can increase ROS production in hair cells, which is beyond the maximal cellular antioxidative ability, and threaten the integrity of DNA, protein, and other survival-crucial macromolecules [57]. Similar to ROS, reactive nitrogen species (RNS) also contribute to the noise-induced cochlear oxidative imbalance [58]. Overproduction of ROS/RNS in hair cells and spiral ganglion neurons is well studied [59, 60], whereas the role of oxidative stress in supporting cells still needs further explanation. Styrene was applied to induce specifically oxidative damage in cochlear supporting cells, and hearing ability was also apparently impaired [61]. However, how oxidative stress in supporting cells participates in NIHL progression requires deeper exploration.

The production and scavenging of ROS/RNS are mediated by various endogenous antioxidants and antioxidative enzymes [57]. The enzymes producing ROS/RNS are usually kept at low expressing level in hypermetabolic cells like acoustic hair cells, tumor cells, and cardiac myocytes, which are oxidative stress sensitive. The NADPH oxidase family (NOX) has been proved to catalyze the electron transport from NADPH to oxygen molecules to speed up ROS production [62]. The *NOX4* transgenic mice which constitutively expressed human *NOX4* were found to be noise susceptible while they had normal hearing threshold without acoustic stimulation, stressing the vital role of imbalance of redox homeostasis in NIHL [63].

Besides ROS/RNS overproduction, the inducible transient upregulation of antioxidative genes also features the pathogenesis of NIHL as a physical feedback mechanism. Nrf2, which is widely expressed in multiple tissues such as the heart, liver, and cochlea, can respond to oxidative stress and activate downstream antioxidative gene expression like glutathione peroxidase (GPx), NAD(P)H:quinone oxidoreductase 1 (NQO1), heme oxygenase-1 (HO-1), and catalase (CAT) [64–66]. Nrf2 signaling can also activate autophagy in hair cells via p62 protein for oxidative stress amelioration [67]. More and more researches [67, 68] have proved that targeting Nrf2 signaling is a promising therapeutic solution for NIHL.

Given the fact that oxidative stress is one of the key contributors to the pathogenesis of NIHL, it is reasonable to assume that genes involved in the redox homeostasis correlate to noise vulnerability of the cochlea [69]. Superoxide dismutase (SOD) and paraoxonases (PONs) are two antioxidative enzymes found in the cochlea; the former directly catalyzes superoxide radicals to less toxic hydrogen peroxide while the latter decreases lipid peroxidation activity [70]. It is reported that the polymorphisms of SOD2, PON1, and PON2 are related to susceptibility to NIHL in workers with high occupational noise trauma risk [69, 71]. Meanwhile, overexpression of SOD1 was found to provide a protective

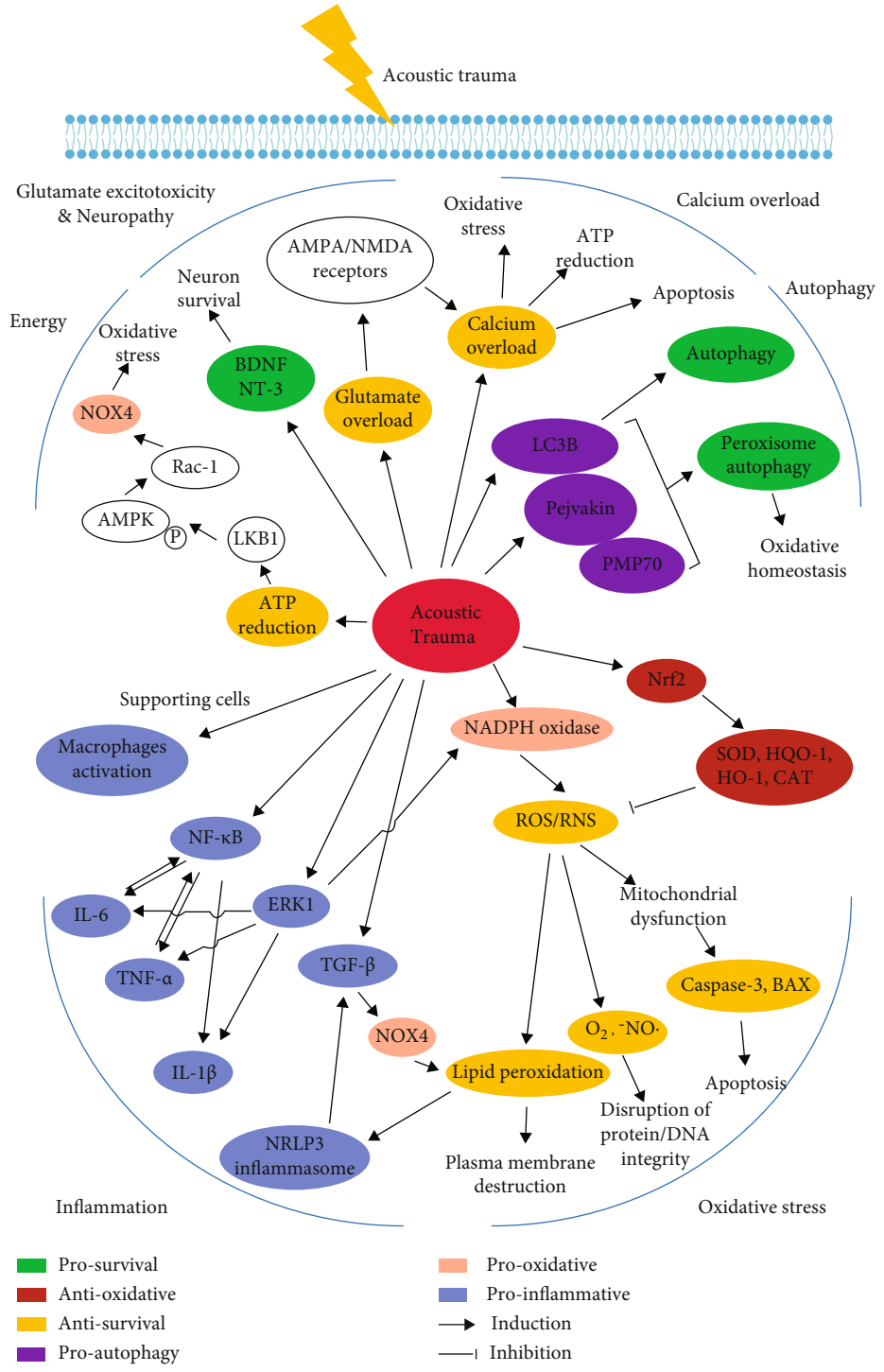

Figure 1: The molecular pathogenesis of NIHL.

effect on noise-related hearing loss [72]. Another newly emerging medication named nicotinamide, the NAD^+ precursor, can boost NAD^+ content and ameliorate NIHL in a SIRT3-dependent way [73]. SIRT3 plays an important role in maintaining the function of various antioxidative enzymes while impaired SIRT3 resulted in ROS overproduction and decreased levels of GSH [74, 75].

3.2. Autophagy. Autophagy, as a recently found endogenous self-defense mechanism, degrades damaged organelles by lysosome to maintain internal homeostasis and preserve energy providing for cell survival upon stress like nutrient deficiency, pathogen infection, protein misfolding, and oxidative stress [76–80]. Previous studies [81, 82] have shown that autophagy is upregulated in auditory hair cells after

intense noise exposure. The immunostaining results show the upregulation of LC3b, the indispensable component of autophagosome, and the colocalization of LC3b and Lamp1, indicating the enhanced fusion of autophagosome and lysosome. To test the hypothesis of autophagy as the cochlear endogenous defenses against NIHL, researchers analyzed whether the disruption of autophagy could exacerbate NIHL with autophagy direct inhibitor 3-MA and mTOR signaling agonist RAP. mTOR protein is one of the main negative regulators for autophagy induction because it can phosphorylate Atg13 to cut off the beginning phase of autophagosome formation [83]. Notably, the inhibition of autophagy worsened the noise-induced oxidative imbalance and the eventual hair cell loss and impaired hearing ability [81].

Pejvakin protein is recently identified as the oxidative sensor in auditory hair cells. Researchers applied immunostaining colocalization analysis and in situ PLA technology to testify the enhanced interactions between pejvakin and LC3B, as well as pejvakin and PMP70 (the marker of peroxisome) in hair cells after acoustic trauma or simply H_2O_2 treatment. Furthermore, pejvakin is found to mediate peroxisome autophagy after noise exposure, which is vital to secondary peroxisome proliferation and oxidative homeostasis maintenance afterwards. Pejvakin-mutated mice show impaired peroxisome proliferation and more severe oxidative stress in auditory hair cells after noise exposure [84].

3.3. Inflammation. The cochlea was used to be considered as immune exemption organ because of the blood-perilymph barrier [85]. However back in 2008, Okano et al. [86] transplanted the EGFP-positive hematopoietic stem cells (HSCs) into wide-type C57BL/6 mice to label the bone marrow-derived cells (BMDCs) with green fluorescence and found EGFP-positive cells in cochlear spiral ganglion and spiral ligament regions of the HSC transplanted mice. Interestingly, EGFP-positive cells were colocalized with F4/80, Iba1, and CD68 immunostaining marks, indicating the presence of bone marrow-derived cochlear resident macrophage-like cells. Like microglia in the nervous system, supporting cells can also be stained with various macrophage markers surprisingly. LPS treatment can induce phagocytosis of supporting cells, which is the direct functional evidence linking cochlear supporting cells with macrophages [87]. Recently, more and more researches suggest the key role of inflammation in aging, drug, and noise-induced ototoxicity [10]. It is notable to point out that inflammation is a dual sword that requires a very complicated and delicate regulatory network involving multiple genes and transcription factors. After acoustic trauma, inflammatory cells representing CD45, CD68, and Iba1 positive infiltrate and proliferate in the cochlea, especially in the stria vascularis, with high expression of CX3CR1, the receptor of a classic chemokine [88, 89]. These inflammatory cells can synthesize and release a variety of proinflammatory cytokines like interleukin-1β (IL-1β), interleukin-6 (IL-6), and tumor necrosis factor-α (TNF-α)[90]. IL-1β and IL-6, the markers of acute inflammation belonging to the interleukin superfamily, contribute to the mononuclear phagocyte infiltration and subsequent release of elastase and prostaglandin, bringing to excessive inflammation cascade activation resulting in microcirculation disturbance, tissue destruction, and eventual hearing impairment [88, 89, 91].

Targeting TNF-α inhibition by molecules or siRNA also attenuates the noise-induced cochlear inflammation and thus hearing threshold shift [92–94]. It is reported that noise-induced increase of TNF-α can be regulated by nuclear factor of activated T cells 4 (Nfatc4), a well-researched transcription factor served as proinflammatory cytokine inducer. Nfatc4 knockout mice show resistance to TNF-α-mediated hair cell apoptosis triggered by intense noise [95]. Notably, TNF-α is testified to be able to induce calcium influx through ERK-dependent activation of TRPV1. Desensitization of TRPV1 by capsaicin ameliorates TNF-α-induced calcium influx and hair cell apoptosis in NIHL modeling mice [96].

Tumor growth factor-β (TGF-β) has been proved to be pluri-regulatory in cochlear development and homeostasis maintenance such as otic capsule formation [97], spiral ganglion neuron survival [98, 99], and inflammation responses [100]. TGF-β initially serves as the inducer of adhesion and chemoattractive molecules for the chemotaxis and activation of leukocytes, and downregulates the interleukin production reversely as the inflammation progresses, indicating its double effects on inflammation regulation [101–103]. Reportedly, the mRNA expression level of TGF-β is upregulated in the cochleae upon noise trauma. Using P7 and P144, two peptides targeting TGF-β inhibition, significantly improves hearing compared to the control group in NIHL mouse model [104]. Further evidence indicates that TGF-β inhibitor decreased the NOX4 content, which is proved to promote NLRP3 inflammasome activation by oxidating fatty acids [105].

It is well testified that nuclear factor kappa B (NF-κB) and its target proinflammatory genes play the central roles in inflammation regulation. Previous researches [94, 106, 107] have found that NF-κB signaling cascade can be activated by noise trauma and inhibition of NF-κB can decrease the content of proinflammatory cytokines. Glucocorticoid is the most commonly used medication for the treatment of NIHL, and its pharmaceutical activity is reported to be partly mediated by NF-κB inhibition [108]. Another interesting discovery about NIHL is that mice show greater sensitivity to noise overexposure during the night [109]. The circadian sensitivity alteration of the cochlea is proved to be adrenal gland-derived endogenous glucocorticoid dependent for its key role on inflammation regulation [110]. Besides, proinflammatory meditators like cyclooxygenase-2 (COX2) and NADPH oxidase 3 (NOX3) are also found upregulated after noise exposure, verifying the indispensable role of inflammation in the pathogenesis of NIHL [94].

3.4. Glutamate Excitotoxicity and Neuropathy. The acute cochlear synaptic ribbon disruption and lasting acoustic neural degeneration also underlie the NIHL pathogenesis. Studies [111, 112] have proved that glutamate excessive accumulation serves as the contributor to acute and chronic deterioration of the auditory nervous system. Glutamate is subtly regulated and remains at a very low level in the synaptic cleft. The overloading of glutamate might dysregulate the cystine-

glutamate transporter and result in cystine and thus GSH deficiency, or constantly activate the glutamate receptor in the postsynaptic membrane and damage the afferent neural fibers [113, 114]. GLAST, one of the five classic glutamate transporters, is found to be expressed in supporting cells located around the inner hair cells. GLAST plays a crucial role in glutamate uptake for its rapid recirculation in the synaptic cleft between the inner hair cells and afferent auditory neural fibers, and depletion of GLAST leads to excessive accumulation of glutamate, which might trigger calcium overload in spiral ganglion neurons. The knockout of GLAST exacerbates the hearing loss in transgenic mice, indicating the potential role of glutamate excitotoxicity in NIHL [111]. The release of glutamate from inner hair cells is also vesicular glutamate transporter type-3 (vGlut3) dependent. Despite the fact that glutamate excitotoxicity relates to NIHL pathogenesis, glutamate also has its dual effects on the noise-induced synapses loss. vGlut3-KO mice show moderate to severe hearing loss due to the impaired synaptic connection development for IHCs and acoustic nerve fibers. And $Vglut3^{+/-}$ mice show disrupted synaptic ribbon recovery after acoustic trauma, indicating that glutamate also participates in the repair of ribbon synapses in TTS model of NIHL [112].

Previous studies [115, 116] have suggested that calcium overload as a vital contributor to glutamate excitotoxicity. There are two main kinds of glutamate receptors in the postsynaptic region, termed as N-methyl-d-aspartate (NMDA) receptor and α-amino-3-hydroxy-5-methyl-4-isoxazole-propionate (AMPA) receptor [117]. Though NMDA receptors play the key role in calcium influx and consequent excitotoxicity in the central nervous system, intratympanic injection of NMDA receptor antagonist AM-101 shows no obvious protective effect on the tone ABR threshold at any frequencies, indicating that calcium influx mediated by NMDA receptors is not the most important contributor of glutamate excitotoxicity in the cochlea [115].

As for AMPA receptor, it is an ionic channel type receptor of glutamate, containing four subunits, namely, GluA1, GluA2, GluA3, and GluA4. Once activated, AMPA receptors mediate fast moving of multiple ions crossing cellular membrane [117, 118]. GluA2 has been testified to decrease $Ca2^{+}$ permeability greatly [119–121]. Recent studies have revealed the existence of GluA2-lacking calcium-permeable AMPA receptors (CP-AMPARs) [116, 122]. Interestingly, IEM-1460, a CP-AMPAR inhibitor, significantly ameliorates the noise-induced decline of synapse integrity, as well as ABR threshold shift, shedding light on the therapeutic potential of NIHL by targeting CP-AMPARs [116].

The reduction of synaptic ribbons and acoustic neural degeneration is reversible in noise-induced transient hearing loss. It is reported that the recovery of cochlear synaptic ribbons after noise exposure is regulated by some endogenous neural factors named neurotrophins. Neurotrophins are endogenous molecules which are vital to the morphogenesis of nervous system development and neuron survival. Brain-derived neurotrophic factor (BDNF) and neurotrophin-3 (NT-3) are highly expressed in the inner hair cells and supporting cells to guide the auditory neural fibers to form precise synaptic connection in postnatal mice and stabilize the connection in adult mice [123]. Knockout of Ntf3 in supporting cells using Plp1-CreER mouse line impairs the high-frequency hearing while Bdnf depletion does not. Reversely, overexpression of Ntf3 or Bdnf in supporting cells and hair cells both attenuate the noise-induced synaptic ribbon reduction and eventual hearing loss [124]. Direct administration of NT-3 also attenuates NIHL progression [125]. Interestingly, as the detection technology develops into more microcosmic level, NT-3 is also found in the extracellular vesicles from human multipotent stromal cells (MSC-EVs). And administration of MSC-EVs not only raises the survival rate of spiral ganglion neurons cultured *in vitro* but also ameliorates the NIHL *in vivo* [126].

The effect of BDNF on NIHL is quite complicated and controversial. Many studies have reported that BDNF administration can enhance auditory neuron survival [127–129]. Meanwhile, tropomyosin-related kinase type B (TrkB, a selective BDNF receptor) agonist DHF [109], amitriptyline, and 7,8-dihydroxyflavone [130] increase resistance to acoustic trauma. However, genetically, depletion of Bdnf gene in adult mice shows protective effect against NIHL because of impaired glutamate release from IHCs, indicating the essential role of BDNF for maintenance of IHC function as well [131].

3.5. Calcium Overload. Calcium is one of the most important ions for the development and physiological function of the inner ear [132, 133]. Under physiological circumstances, calcium content in hair cells and spiral ganglion neurons is quite low [134, 135]. In response to the sound stimulation, calcium influx and calcium-induced calcium release (CICR) from the endoplasmic reticulum significantly increase intracellular calcium and trigger the release of neurotransmitter from the IHCs to transform mechanical signals to electrical signals [136, 137]. Moreover, the spontaneous calcium spike from the IHCs also participates in the formation and functional maturation of the afferent auditory nerve [138]. Calcium takes part in various physiological functions as one of the main second messenger molecules, while excessive accumulation of calcium under stress like ischemia-reperfusion injury [139] contributes to cell death in several pathways. Previous studies show that calcium is also involved in the acoustic ototoxicity [135, 140, 141]. Intracellular calcium concentration is significantly upregulated in auditory hair cells, especially outer hair cells shortly after acoustic overstimulation though returns to basal level within 30-45 minutes [135]. The calcium concentration is also found increased abruptly in endolymph of the cochlea after intense noise exposure [141]. Minami et al. have reported that the expression of calcineurin, a calcium/calmodulin-dependent phosphatase, is restrictedly increased in dying hair cells marked by propidium iodide after noise overstimulation [142]. Calcineurin can dephosphorylate and activate the classic proapoptotic protein BAD, and the systemic administration of calcineurin inhibitor FK506 reduced the apoptosis of hair cells evidently [142, 143].

Though strong evidence has proved that excessive calcium overload contributes to noise-induced hair cell death, the pharmacological drug development targeting calcium

overload is still contentious. Voltage-gated calcium channels (VGCCs) facilitating calcium influx are proved to be responsible for the noise-induced intracellular calcium overload. There are five different types of VGCCs, namely, L-, T-, N-, P/Q-, and R-type [144]. It is reported that administration of T-type calcium channel blockers like ethosuximide and trimethadione prior to noise exposure can effectively reduce the hearing threshold shift [145]. However, other researchers suggest that L-type calcium channel blockers [146] attenuate NIHL while T-type calcium channel blockers cannot.

3.6. Energy Metabolism. Transient ATP depletion in the cochlear perilymph following acoustic trauma has been proved by studies [147, 148]. Likewise, the extracellular ATP content in the inner ear also decreased upon ischemia stress [149]. Since either the production of endogenous antioxidants or the recovery of spiral ganglion cells upon noise exposure is energy consuming, researchers proposed the hypothesis that transient ATP depletion might weaken the defense ability of the cochlea against acoustic trauma. 5′-Adenosine monophosphate- (AMP-) activated protein kinase (AMPK), the energy sensor protein responding to fluctuation of intracellular AMP/ATP ration [150], has been reported to be activated by noise-induced ATP depletion and responsible for the pathogenesis of NIHL [44]. Parallel to transient energy exhaustion, AMPK activates Rac-1, belonging to GTPase family which can phosphate its downstream targets via hydrolyzing GTP and trigger p67 protein phosphorylation [151]. p67 is one of the functional subunits of NADPH oxidase 3 (NOX3), which contributes to noise overexposure-induced ROS overproduction in hair cells and eventual cell death [152]. Reversely, excessive ROS accumulation also activates the AMPKα signaling, marked by enhanced phosphorylated AMPKα, while systematical administration of antioxidant N-acetyl-L-cysteine (NAC) decreases both phosphorylated AMPKα and oxidative stress [153]. Noise-induced phosphorylation of AMPKα is also regulated by liver kinase B1 (LKB1), mediated by the transient intracellular ATP depletion. Indirect inhibition of AMPKα or its upstream regulatory gene LKB1 can ameliorate noise-induced necrosis of acoustic hair cells [147].

However, there is hardly any effective way to boost energy generation in hair cells after noise exposure. It is reported that transient increasing serum glucose level with administration of glucose can strengthen the cochlear defense system against NIHL by increasing ATP and NADPH content in hair cells [154]. Nevertheless, the diabetic mice with constant high blood glucose show much more severe noise-induced hair cell death and spiral ganglion neuron loss, which might be due to the blood flow ration reduction induced by chronic inflammation [155].

3.7. Others

3.7.1. Matrix Metalloproteinases. Matrix metalloproteinases (MMPs) play a key role in the extracellular matrix (ECM) homeostasis and remodeling. For example, MMP-2 is reported to be involved in synaptic remodeling after cochlear lesion [156]. Either overactivation or excessive inhibition of MMPs can lead to multiple disorders like carcinoma invasion and migration [157]. RNA sequencing data reveal that MMPs are upregulated in the acute phase after noise exposure and decreased gradually over time. A short-term administration of doxycycline, an inhibitor of MMPs, can attenuate noise-induced hearing loss while a seven-day application regimen exacerbates the hair cell death reversely [158]. MMPs are regulated by cysteinyl leukotriene and its type 1 receptor (CysLTR1), which is also increased in the cochlea after acoustic overstimulation. A four-day application of montelukast, a leukotriene receptor antagonist, can ameliorate NIHL damage [159].

3.7.2. Pannexins. Like the well-researched connexin channels, pannexin protein is also involved in the intracellular communication channel formation allowing the passage of the small molecules and ions. Panx3 is one of the main kinds of pannexin protein expressed in the cochlea [160]. A previous study [161] has proved that genetic depletion of paxn3 has no impact on the proper morphogenesis of the inner ear and hearing though the cochlear bone is slightly impaired. Strikingly, the panx3 knockout mice show decreased susceptibility to NIHL while the mechanism underlying its acoustic protective effect still requires further exploration.

4. Gene Variations Related to NIHL

Up to now, there are more than 30 gene variations reported to be relevant to NIHL in animal studies or human epidemiology investigations.

4.1. Oxidative Stress and DNA Repair-Related Gene Variations. Since oxidative stress contributes to the pathogenesis of NIHL, mutations of multiple genes involving in the antioxidative system have been proved to alter noise susceptibility. Catalase (CAT), superoxide dismutase (SOD2), and the antioxidant paraoxonase (PON) are three main proteins playing important roles in scavenging free radicals; mutation of which weakens the intracellular defensive ability against noise-induced oxidative damage [71, 162, 163]. NFL2E2 (also known as Nrf2) is a vital transcriptional factor regulating various antioxidative protein expressions such as HO-1, CAT, SOD, and GPx [65]. Polymorphisms of NFL2E2 (rs6726395 and rs77684420) have been confirmed as related to genetic vulnerability for NIHL in a Chinese population-based study [164]. Other genes, like NOX3 encoding NADPH oxidase-3 catalyzing the generation of superoxide [165], HSPA1L encoding chaperons assisting antioxidative proteins to fold correctly [166], and GST (glutathione S-transferase) family [167, 168] which participate in the metabolism of an intracellular antioxidant GSH, have been reported as NIHL-related genes.

Moreover, free radicals and lipid peroxide induced by acoustic trauma could do harm to DNA integrity and might cause mutations of certain sequences. APE1 [169] and OGG1 [170], encoding DNA repair enzymes to remove specific abnormal bases, are found to be associated with NIHL susceptibility as well.

4.2. Apoptosis-Related Gene Variations. Another case-control study [171] involving Chinese workers with or without noise exposure history identifies two SNPs of CASP3 (rs1049216 and rs6948) significantly correlated to decreased NIHL risk, due to impaired apoptosis of hair cells since caspase3 serves as the central role of apoptosis induction.

4.3. Gap Junction-Related Gene Variations. Connexin 26, which is encoded by GJB2, is involved in the gap junction establishment between hair cells, allowing intercellular communications of ions and other small molecules [172, 173]. GJB2 SNP (rs3751385) is identified as a NIHL susceptible genetic mutation in a study applied in Polish workers [174]. Meanwhile, another study including Chinese workers reports that GJB2 SNP (rs137852540) combined with SOD2 and CAT mutations increased the vulnerability to NIHL [162]. The correlation between GJB mutation and NIHL vulnerability is also confirmed in Cx26 knockdown mice [174].

4.4. Potassium Channel-Related Gene Variations. Gene polymorphisms associated with K ion circulation in the inner ear are also associated with resistance to noise-induced hearing loss. KCNQ1/KCNE1 variation affecting potassium recycling is identified related to NIHL [175, 176]. Mutations of other potassium channel-related genes like KCNQ4 [175], KCNJ10 [176], and KCNMA1 [177] are also related to NIHL vulnerability. Potassium channels located in the outer hair cells in the cochlea which are responsible for the K^+ influx regulate the excitability of OHCs. Reportedly, the potassium concentration in the cochlear endolymph of the guinea pig is upregulated shortly after acoustic injury [141, 178]. However, the exact mechanism behind potassium circulation disruption and NIHL is still lack of strong evidence.

4.5. Tip-Link-Related Gene Variations. The maturation of stereocilia in the hair cells is vital for hearing onset because it is where mechanical signals of sound waves are transformed into electrical signals that could be transported through hair cells and neurons. Tip-link, made of cadherins, plays an important part in the maintenance of ordered structure of stereocilia. A study revealed that mutations of PCDH15 and CDH23, two genes encoding cadherins for the integrity of stereocilia especially tip-link, are related to susceptibility to NIHL [179, 180].

4.6. Others. The purinergic receptor 2 (P2X2 receptor) is highly expressed in the cochlear sensory epithelium, especially in supporting cells of the greater epithelial ridge. P2X2 receptor can be activated by ATP [181] which is released from hair cells through connexins, and plays an important role in the development of the cochlea and hearing function [182]. A mutation of P2X2 gene (c.178G>T) is found responsible for progressive hearing loss and NIHL susceptibility in a Chinese family [183].

Another genome-wide association study suggested that AUTS2 SNP (rs35075890) and PTPRN2 SNP (rs10081191) are associated with NIHL vulnerability [184], which are commonly thought to be related to mental disorders and metabolic diseases according to previous studies [185].

There are quite more genes, with multiple physiological functions, reported to be NIHL-associated genetic factors, while the exact roles of which in the pathogenesis of NIHL still require deeper explorations (see more details in Table 1).

5. Therapeutics

It is widely acknowledged the lack of approved medications for NIHL treatment, and recent pharmaceutical explorations are heralding a new era in the field.

5.1. Approved Medications. Clinically, few medications have been identified as effective except glucocorticoid for NIHL. Glucocorticoid has been proved to exhibit various protective effects against NIHL, highlighted by its anti-inflammatory activity via inhibiting the synthesis and release of inflammatory molecules like prostaglandins and leukotrienes. Dexamethasone, as the most commonly used glucocorticoid in clinical practice, was administered postintense white noise with intratympanic or intraperitoneal injection. And two routines of administration show similar hearing recovery effects; both are significantly better than the saline group [194].

5.2. Drugs in Clinical Trials. The phase 2 trial report of ebselen has assessed its safety and efficacy on NIHL. Ebselen, the GPx1 mimic, aims at oxidative stress reduction. In this randomized, double-blind, placebo-controlled phase 2 trial, subjects receiving 400 mg ebselen show significantly protective effect on transient noise-induced hearing impairment with no side effects reported [195].

5.3. Potential Medications

5.3.1. Medications Targeting Oxidative Stress. Qter, the artificial analog of an endogenous antioxidant coenzyme Q10, was administered systematically to noise-exposed mice and significantly reduced the threshold shift after acoustic trauma and promoted outer hair cell survival [196]. Moreover, the dendrites of spiral ganglion cells and cortical neuronal morphology are significantly restored by Qter application for its role involved in free radicals scavenging and regeneration of antioxidants like reduced glutathione (GSH)[197]. And redox homeostasis is maintained by Qter treatment demonstrated by reduction of 4-HNE or DHE (the markers of lipid peroxidation) immunostaining-positive cells in the cochleae.

Parallel to Qter, a peptide derived from human telomerase called GV1001 attenuates sensory hair cell death targeting the noise-induced excessive ROS/RNS accumulation, as suggested by the byproducts of lipid peroxidation (4-HNE) and protein nitration (3-NT) [58]. Moreover, GV1001 can also ameliorate kanamycin-induced hearing loss in mice, indicating that excessive ROS/RNS and its downstream cascades like inflammation and apoptosis underlie the sharing pathological contributors for noise and aminoglycoside-induced ototoxicity. Taking into consideration previous studies regarding the therapeutic effects of GV1001, we hypothesize that GV1001 might also exert otoprotective effects against NIHL, because excessive ROS/RNS generation is thought to underlie the causative mechanisms of NIHL.

Table 1: NIHL-related gene variations.

Class		Gene name	Variations	Function
Oxidative stress	NOX3	NADPH oxidase-3	rs33652818 [165]	Generation of superoxide (O_2·-)
	CAT	Catalase	rs7943316 [162, 163]	Hydrogen peroxide decomposition
	GSTM1	Glutathione S-transferase mu 1	Null [167, 168]	GSH metabolism
	GSTP1	Glutathione S-transferase pi 1	Ile (105)/Ile (105) [167, 168]	GSH metabolism
	GSTT1	Glutathione S-transferase theta 1	Null [167, 168]	GSH metabolism
	NFL2E2	Nuclear factor erythroid-derived 2-like 2	rs6726395 rs77684420 [164]	Transcriptional factor regulating various antioxidative protein expression
	HSPA1L	Heat shock protein family A member 1 like	rs2227956 [166]	Antioxidative protein stabilizer
	PON2	Paraoxonase 2	S311C [71]	Antioxidative protein
	SOD2	Superoxide dismutase 2	IVS3-23T/G IVS3-60T/G [71]	Catalyzing the destruction of free radical
Apoptosis	CASP3	Caspase3	rs1049216 rs6948 [171]	Intracellular apoptosis promoter
DNA methylation	DNMT1	DNA methyltransferase 1	rs2228611 [186]	DNA methylation
	DNMT3A	DNA methyltransferase 3 alpha	rs749131 [186]	DNA methylation
Gap junction	GJB1	Gap junction protein beta1	rs1997625 [176]	Gap junction channels
	GJB2	Gap junction protein beta2	rs3751385 [162, 176]	Gap junction channels
	GJB4	Gap junction protein beta4	rs755931 [176]	Gap junction channels
DNA repair	APE1	Apurinic/apyrimidinic endodeoxy-ribonuclease 1	T1349G T656G [169]	Encoding the endonuclease, a DNA repair enzyme
	OGG1	8-Oxoguanine DNA glycosylase	Ser326Cys [170]	DNA repair enzyme
Ion channels	KCNMA1	Potassium calcium-activated channel subfamily M alpha1	rs696211 [177]	Ca^{2+}-activated K^+ channel
	KCNE1	Potassium voltage-gated channel subfamily E regulatory subunit 1	rs2070358 rs1805128 [175, 176]	K^+ channel
	KCNJ10	Potassium inwardly-rectifying channel subfamily J member 10	rs1130183 [176]	K^+ channel
	KCNQ1	Potassium voltage-gated channel subfamily Q member 1	rs7945327 rs11022922 rs718579 rs163171 rs2056892 [175, 176]	K^+ channel
	KCNQ4	Potassium voltage-gated channel subfamily Q member 4	rs4660468 [175]	K^+ channel
Stereocilia structure	PCDH15	Protocadherin related 15	rs11004085 rs7095441 [179]	Encoding cadherin for the integrity of stereocilia, especially tip-link
	CDH23	Cadherin 23	rs3752752 [180]	Encoding cadherin for the integrity of stereocilia, especially tip-link
	MYH14	Myosin heavy chain 14	rs667907 rs588035 [179]	Might contribute to tip-link integrity
Others	EYA4	EYA transcriptional coactivator and phosphatase 4	rs3813346 [187]	Multifunctional transcriptional factor
	FOXO3	Forkhead box O3	rs2802292 rs3777781 rs212769 [188]	Multifunctional transcriptional factor
	GRHL2	Grainyhead-like 2	rs611419 [189, 190]	Multifunctional transcriptional factor
	HOTAIR	HOX transcript antisense RNA	rs4759314 [191]	Regulatory lncRNA

Table 1: Continued.

Class	Gene name	Variations	Function
MYO1A	Myosin 1a	rs1552245 [177]	Actin-based molecular motors
NOTCH1	Notch receptor 1	rs3124594 rs3124603 [192]	Notch signaling transduction
NCL	Nucleolin	rs7598759 [193]	Ribosome biogenesis
P2RX2	Purinergic receptor P2X2	V60L [183]	Purinergic signaling transduction
AUTS2	Autism susceptibility candidate 2	rs35075890 [185]	Multifunctions
PTPRN2	Protein tyrosine phosphatase receptor type N2	rs10081191 [184]	Multifunctions

The systematical administration of methylene blue prior to noise trauma promotes the acoustic hair cell survival via ameliorating the oxidative stress-induced dysfunction of respiratory electron transport chain, featured by the reservation of complex IV activity and ATP production [198]. Moreover, methylene blue induces generation of neurotrophin-3 (NT-3) to preserve the synaptic ribbons around inner hair cells upon noise exposure [199].

5.3.2. Medications Targeting Inflammation. Avenanthramide-C (AVN-C), a natural flavonoid purified from oats, has shown anti-inflammatory and antioxidant activities in *in vitro* experiments. Notably, AVN-C has great water solubility and blood-labyrinth barrier permeability, suggesting pharmaceutical potential for NIHL treatment. Researchers have found that peritoneal injection of AVN-C protects hair cells from noise trauma by increasing antioxidant defense and decreasing proinflammatory cytokines like IL-1β and Tnf [200].

5.4. Medications Targeting Hearing Protective Genes. Isl1, which is highly expressed in prosensory region during otocyst development and no longer expressed in the postnatal cochlea, attenuates noise-triggered hair cell loss when artificially overexpressed specifically in postnatal hair cells. Though the exact mechanism behind the protective effect of Isl1 is not fully understood, it proposes a bold hypothesis that overexpression of acoustic progenitor developmental genes in the adult cochlea might increase the hair cell defense system against noise stress [201].

5.5. Emerging Nanoparticle Medications. Nanomedication, as a newly emerged therapy, was applied in the NIHL treatment. Nanosystems, including polyethylene glycol- (PEG-) coated poly lactic acid (PLA) nanoparticles and zeolitic imidazolate nanoparticles, were invented and applied to deliver steroid drugs to the inner ear. They show significant protective effect, even better than free steroid drugs, when administered systematically with better stability and biocompatibility [202, 203]. However, the efficacy and safety of nanoparticle-based medications still need further verification.

6. Conclusions

In this article, we systematically and comprehensively reviewed the epidemiology, mechanical and molecular pathogenesis, and therapeutic inventions about NIHL. Oxidative stress, inflammation, calcium overload, glutamate excitotoxicity, and energy metabolism are the main contributors to NIHL up to now. These pharmaceutical exploring studies not only shed light on the clinical treatment for NIHL but also make further steps on the systematical understanding of NIHL pathogenesis.

Controversies are engendered on certain disputations of NIHL: Firstly, the oxidative stress in supporting cells upon acoustic trauma has been verified, but how to promote hair cell survival through regulating supporting cells is still blank. Secondly, the excitotoxicity of excessive glutamate exacerbates the destruction of acoustic nerve while Vglut3 knockout mice show impaired neural fiber recovery. Similarly, administration of BDNF ameliorates NIHL, but depletion of Bdnf receptor gene also shows protective effect by inhibiting glutamate release. Therefore, given the complexity of glutamate and neurotrophins, what is the proper way of modulating glutamate and neurotrophins for the maximum protective effect? Thirdly, because of the blood-perilymph barrier, most medications administered systematically are hard to penetrate into the cochlea. The development of nanomedication would alter the stability and permeability of drugs, which might bring hope to the emergency of more efficacious and less toxic medication. Moreover, with the research progresses in the field of regeneration of cochlear hair cells and neural fibers [24, 204–208], NIHL might be curable one day in the future.

Conflicts of Interest

The authors claim that there are no conflicts of interest.

Acknowledgments

This work was supported by the National Natural Science Foundation of China (82071049, 81771010, and 81570911).

References

[1] Y. Liu, J. Qi, X. Chen et al., "Critical role of spectrin in hearing development and deafness," *Science Advances*, vol. 5, no. 4, 2019.

[2] Y. Wang, J. Li, X. Yao et al., "Loss of CIB2 causes profound hearing loss and abolishes mechanoelectrical transduction in mice," *Frontiers in Molecular Neuroscience*, vol. 10, p. 401, 2017.

[3] J. Qi, Y. Liu, C. Chu et al., "A cytoskeleton structure revealed by super-resolution fluorescence imaging in inner ear hair cells," *Cell Discovery*, vol. 5, no. 1, p. 12, 2019.

[4] Q. Fang, Y. Zhang, P. da et al., "Deletion of *Limk1* and *Limk2* in mice does not alter cochlear development or auditory function," *Scientific Reports*, vol. 9, no. 1, article 39769, p. 3357, 2019.

[5] S. Zhang, Y. Zhang, Y. Dong et al., "Knockdown of Foxg1 in supporting cells increases the trans-differentiation of supporting cells into hair cells in the neonatal mouse cochlea," *Cellular and Molecular Life Sciences : CMLS*, vol. 77, no. 7, article 3291, pp. 1401–1419, 2020.

[6] C. Cheng, Y. Wang, L. Guo et al., "Age-related transcriptome changes in Sox2+ supporting cells in the mouse cochlea," *Stem Cell Research & Therapy*, vol. 10, no. 1, article 1437, p. 365, 2019.

[7] X. Lu, S. Sun, J. Qi et al., "Bmi1 regulates the proliferation of cochlear supporting cells via the canonical Wnt signaling pathway," *Molecular Neurobiology*, vol. 54, no. 2, article 9686, pp. 1326–1339, 2017.

[8] S. Zhang, R. Qiang, Y. Dong et al., "Hair cell regeneration from inner ear progenitors in the mammalian cochlea," *American Journal of Stem Cells*, vol. 9, no. 3, pp. 25–35, 2020.

[9] B. Cox, R. Chai, A. Lenoir et al., "Spontaneous hair cell regeneration in the neonatal mouse cochlea in vivo," *Development (Cambridge, England)*, vol. 141, no. 4, pp. 816–829, 2014.

[10] Z. He, S. Y. Zou, M. Li et al., "The nuclear transcription factor FoxG1 affects the sensitivity of mimetic aging hair cells to inflammation by regulating autophagy pathways," *Redox Biology*, vol. 28, article 101364, 2020.

[11] P. Jiang, S. Zhang, C. Cheng et al., "The roles of exosomes in visual and auditory systems," *Frontiers in Bioengineering and Biotechnology*, vol. 8, p. 525, 2020.

[12] F. Qian, X. Wang, Z. Yin et al., "The *slc4a2b* gene is required for hair cell development in zebrafish," *Aging*, vol. 12, no. 19, article 103840, pp. 18804–18821, 2020.

[13] J. Lv, X. Fu, Y. Li et al., "Deletion of *Kcnj16* in mice does not alter auditory function," *Frontiers in Cell and Development Biology*, vol. 9, article 630361, 2021.

[14] W. Clark and B. Bohne, "Effects of noise on hearing," *JAMA*, vol. 281, no. 17, pp. 1658-1659, 1999.

[15] "Noise and hearing loss," *Lancet (London, England)*, vol. 338, no. 8758, pp. 21-22, 1991.

[16] The Cochrane Collaboration, E. Kateman, J. H. Verbeek et al., "Interventions to prevent occupational noise induced hearing loss," *The Cochrane Database of Systematic Reviews*, vol. 7, 2017.

[17] The Cochrane Collaboration, J. H. Verbeek, E. Kateman, T. C. Morata, W. Dreschler, and B. Sorgdrager, "Interventions to prevent occupational noise induced hearing loss," *The Cochrane Database of Systematic Reviews*, vol. 3, 2009.

[18] E. Lynch and J. Kil, "Compounds for the prevention and treatment of noise-induced hearing loss," *Drug Discovery Today*, vol. 10, no. 19, pp. 1291–1298, 2005.

[19] A. Fetoni, F. Paciello, R. Rolesi, G. Paludetti, and D. Troiani, "Targeting dysregulation of redox homeostasis in noise-induced hearing loss: oxidative stress and ROS signaling," *Free Radical Biology & Medicine*, vol. 135, pp. 46–59, 2019.

[20] G. Harding, B. Bohne, and M. Ahmad, "DPOAE level shifts and ABR threshold shifts compared to detailed analysis of histopathological damage from noise," *Hearing Research*, vol. 174, no. 1-2, pp. 158–171, 2002.

[21] M. Liberman, "Noise-induced hearing loss: permanent versus temporary threshold shifts and the effects of hair cell versus neuronal degeneration," *Advances in Experimental Medicine and Biology*, vol. 875, pp. 1–7, 2016.

[22] T. Wang, R. Chai, G. S. Kim et al., "Lgr5+ cells regenerate hair cells via proliferation and direct transdifferentiation in damaged neonatal mouse utricle," *Nature Communications*, vol. 6, no. 1, p. 6613, 2015.

[23] W. Li, D. You, Y. Chen, R. Chai, and H. Li, "Regeneration of hair cells in the mammalian vestibular system," *Frontiers in Medicine*, vol. 10, no. 2, pp. 143–151, 2016.

[24] S. Zhang, D. Liu, Y. Dong et al., "Frizzled-9+ supporting cells are progenitors for the generation of hair cells in the postnatal mouse cochlea," *Frontiers in Molecular Neuroscience*, vol. 12, p. 184, 2019.

[25] Y. Zhang, L. Guo, X. Lu et al., "Characterization of Lgr6+ cells as an enriched population of hair cell progenitors compared to Lgr5+ cells for hair cell generation in the neonatal mouse cochlea," *Frontiers in Molecular Neuroscience*, vol. 11, p. 147, 2018.

[26] Y. Chen, X. Lu, L. Guo et al., "Hedgehog signaling promotes the proliferation and subsequent hair cell formation of progenitor cells in the neonatal mouse cochlea," *Frontiers in Molecular Neuroscience*, vol. 10, p. 426, 2017.

[27] B. Wilson, D. L. Tucci, M. H. Merson, and G. M. O'Donoghue, "Global hearing health care: new findings and perspectives," *Lancet (London, England)*, vol. 390, no. 10111, pp. 2503–2515, 2017.

[28] H. Zhuang, J. Yang, Z. Huang et al., "Accelerated age-related decline in hippocampal neurogenesis in mice with noise-induced hearing loss is associated with hippocampal microglial degeneration," *Aging*, vol. 12, no. 19, article 103898, pp. 19493–19519, 2020.

[29] S. Park, S. A. Back, K. H. Park et al., "Comparison of functional and morphologic characteristics of mice models of noise-induced hearing loss," *Auris, Nasus, Larynx*, vol. 40, no. 1, pp. 11–17, 2013.

[30] W. Han, J. O. Shin, J. H. Ma et al., "Distinct roles of stereociliary links in the nonlinear sound processing and noise resistance of cochlear outer hair cells," *Proceedings of the National Academy of Sciences of the United States of America*, vol. 117, no. 20, pp. 11109–11117, 2020.

[31] C. Zhu, C. Cheng, Y. Wang et al., "Loss of ARHGEF6 causes hair cell stereocilia deficits and hearing loss in mice," *Frontiers in Molecular Neuroscience*, vol. 11, p. 362, 2018.

[32] J. Qi, L. Zhang, F. Tan et al., "Espin distribution as revealed by super-resolution microscopy of stereocilia," *American Journal of Translational Research*, vol. 12, no. 1, pp. 130–141, 2020.

[33] J. Jensen, A. C. Lysaght, M. C. Liberman, K. Qvortrup, and K. M. Stankovic, "Immediate and delayed cochlear neuropathy after noise exposure in pubescent mice," *PLoS One*, vol. 10, no. 5, article e0125160, 2015.

[34] L. Shi, K. Liu, H. Wang et al., "Noise induced reversible changes of cochlear ribbon synapses contribute to temporary hearing loss in mice," *Acta Oto-Laryngologica*, vol. 135, no. 11, pp. 1093–1102, 2015.

[35] W. Liu, X. Xu, Z. Fan et al., "Wnt signaling activates TP53-induced glycolysis and apoptosis regulator and protects against cisplatin-induced spiral ganglion neuron damage in the mouse cochlea," *Antioxidants & Redox Signaling*, vol. 30, no. 11, pp. 1389–1410, 2019.

[36] W. Yan, W. Liu, J. Qi et al., "A three-dimensional culture system with Matrigel promotes purified spiral ganglion neuron survival and function in vitro," *Molecular Neurobiology*, vol. 55, no. 3, pp. 2070–2084, 2018.

[37] R. Guo, X. Ma, M. Liao et al., "Development and application of cochlear implant-based electric-acoustic stimulation of spiral ganglion neurons," *ACS Biomaterials Science & Engineering*, vol. 5, no. 12, pp. 6735–6741, 2019.

[38] M. Mayorga, "The pathology of primary blast overpressure injury," *Toxicology*, vol. 121, no. 1, pp. 17–28, 1997.

[39] J. Patterson and R. Hamernik, "Blast overpressure induced structural and functional changes in the auditory system," *Toxicology*, vol. 121, no. 1, pp. 29–40, 1997.

[40] S. Shin, A. R. Lyu, S. H. Jeong, T. H. Kim, M. J. Park, and Y. H. Park, "Acoustic trauma modulates cochlear blood flow and vasoactive factors in a rodent model of noise-induced hearing loss," *International Journal of Molecular Sciences*, vol. 20, no. 21, p. 5316, 2019.

[41] P. Littlefield and D. Brungart, "Long-term sensorineural hearing loss in patients with blast-induced tympanic membrane perforations," *Ear and Hearing*, vol. 41, no. 1, pp. 165–172, 2020.

[42] K. Mizutari, "Update on treatment options for blast-induced hearing loss," *Current Opinion in Otolaryngology & Head and Neck Surgery*, vol. 27, no. 5, pp. 376–380, 2019.

[43] T. Nicotera, B. Hu, and D. Henderson, "The caspase pathway in noise-induced apoptosis of the chinchilla cochlea," *Journal of the Association for Research in Otolaryngology: JARO*, vol. 4, no. 4, pp. 466–477, 2003.

[44] H. Zheng, J. Chen, and S. Sha, "Receptor-interacting protein kinases modulate noise-induced sensory hair cell death," *Cell Death & Disease*, vol. 5, no. 5, article e1262, 2014.

[45] K. Ohlemiller, J. Wright, and L. Dugan, "Early elevation of cochlear reactive oxygen species following noise exposure," *Audiology & Neuro-Otology*, vol. 4, no. 5, pp. 229–236, 1999.

[46] J. Cobley, "Mechanisms of mitochondrial ROS production in assisted reproduction: the known, the unknown, and the intriguing," *Antioxidants (Basel, Switzerland)*, vol. 9, no. 10, p. 933, 2020.

[47] W. Zhang, H. Xiong, J. Pang et al., "Nrf2 activation protects auditory hair cells from cisplatin-induced ototoxicity independent on mitochondrial ROS production," *Toxicology Letters*, vol. 331, pp. 1–10, 2020.

[48] S. Chong, I. Low, and S. Pervaiz, "Mitochondrial ROS and involvement of Bcl-2 as a mitochondrial ROS regulator," *Mitochondrion*, vol. 19, pp. 39–48, 2014.

[49] C. Ojano-Dirain, P. Antonelli, and C. G. le Prell, "Mitochondria-targeted antioxidant MitoQ reduces gentamicin-induced ototoxicity," *American Neurotology Society [and] European Academy of Otology and Neurotology*, vol. 35, no. 3, pp. 533–539, 2014.

[50] Z. He, L. Guo, Y. Shu et al., "Autophagy protects auditory hair cells against neomycin-induced damage," *Autophagy*, vol. 13, no. 11, pp. 1884–1904, 2017.

[51] S. Gao, C. Cheng, M. Wang et al., "Blebbistatin inhibits neomycin-induced apoptosis in hair cell-like HEI-OC-1 cells and in cochlear hair cells," *Frontiers in Cellular Neuroscience*, vol. 13, p. 590, 2020.

[52] S. Sun, M. Sun, Y. Zhang et al., "In vivo overexpression of X-linked inhibitor of apoptosis protein protects against neomycin-induced hair cell loss in the apical turn of the cochlea during the ototoxic-sensitive period," *Frontiers in Cellular Neuroscience*, vol. 8, p. 248, 2014.

[53] Z. Zhong, X. Fu, H. Li et al., "Citicoline protects auditory hair cells against neomycin-induced damage," *Frontiers in Cell and Developmental Biology*, vol. 8, p. 712, 2020.

[54] Y. Zhang, W. Li, Z. He et al., "Pre-treatment with fasudil prevents neomycin-induced hair cell damage by reducing the accumulation of reactive oxygen species," *Frontiers in Molecular Neuroscience*, vol. 12, p. 264, 2019.

[55] X. Yu, W. Liu, Z. Fan et al., "c-Myb knockdown increases the neomycin-induced damage to hair-cell-like HEI- OC1 cells in vitro," *Scientific Reports*, vol. 7, no. 1, article 41094, 2017.

[56] M. Guan, Q. Fang, Z. He et al., "Inhibition of ARC decreases the survival of HEI-OC-1 cells after neomycin damage in vitro," *Oncotarget*, vol. 7, no. 41, article 11336, pp. 66647–66659, 2016.

[57] K. Prasad and S. Bondy, "Increased oxidative stress, inflammation, and glutamate: potential preventive and therapeutic targets for hearing disorders," *Mechanisms of Ageing and Development*, vol. 185, article 111191, 2020.

[58] S. Lee, J. J. Han, S. Y. Lee et al., "Outcomes of peptide vaccine GV1001 treatment in a murine model of acute noise-induced hearing loss," *Antioxidants (Basel, Switzerland)*, vol. 9, no. 2, p. 112, 2020.

[59] A. Li, D. You, W. Li et al., "Novel compounds protect auditory hair cells against gentamycin-induced apoptosis by maintaining the expression level of H3K4me2," *Drug Delivery*, vol. 25, no. 1, pp. 1033–1043, 2018.

[60] Z. He, S. Sun, M. Waqas et al., "Reduced TRMU expression increases the sensitivity of hair-cell-like HEI-OC-1 cells to neomycin damage in vitro," *Scientific Reports*, vol. 6, no. 1, article 29621, 2016.

[61] A. Fetoni, R. Rolesi, F. Paciello et al., "Styrene enhances the noise induced oxidative stress in the cochlea and affects differently mechanosensory and supporting cells," *Free Radical Biology & Medicine*, vol. 101, pp. 211–225, 2016.

[62] P. Wenzel, S. Kossmann, T. Münzel, and A. Daiber, "Redox regulation of cardiovascular inflammation - immunomodulatory function of mitochondrial and Nox-derived reactive oxygen and nitrogen species," *Free Radical Biology & Medicine*, vol. 109, pp. 48–60, 2017.

[63] S. Morioka, H. Sakaguchi, T. Yamaguchi et al., "Hearing vulnerability after noise exposure in a mouse model of reactive oxygen species overproduction," *Journal of Neurochemistry*, vol. 146, no. 4, pp. 459–473, 2018.

[64] M. Galicia-Moreno, S. Lucano-Landeros, H. C. Monroy-Ramirez et al., "Roles of Nrf2 in liver diseases: molecular, pharmacological, and epigenetic aspects," *Antioxidants (Basel, Switzerland)*, vol. 9, no. 10, p. 980, 2020.

[65] A. Cuadrado, A. I. Rojo, G. Wells et al., "Therapeutic targeting of the NRF2 and KEAP1 partnership in chronic diseases," *Drug Discovery*, vol. 18, no. 4, pp. 295–317, 2019.

[66] D. Moretti, S. Tambone, M. Cerretani et al., "NRF2 activation by reversible KEAP1 binding induces the antioxidant

response in primary neurons and astrocytes of a Huntington's disease mouse model," *Free Radical Biology & Medicine*, vol. 162, pp. 243–254, 2021.

[67] K. Hayashi, K. Dan, F. Goto et al., "The autophagy pathway maintained signaling crosstalk with the Keap1-Nrf2 system through p62 in auditory cells under oxidative stress," *Cellular Signalling*, vol. 27, no. 2, pp. 382–393, 2015.

[68] A. Fetoni, F. Paciello, R. Rolesi et al., "Rosmarinic acid up-regulates the noise-activated Nrf2/HO-1 pathway and protects against noise-induced injury in rat cochlea," *Free Radical Biology & Medicine*, vol. 85, pp. 269–281, 2015.

[69] L. Forsberg, U. de Faire, and R. Morgenstern, "Oxidative stress, human genetic variation, and disease," *Archives of Biochemistry and Biophysics*, vol. 389, no. 1, pp. 84–93, 2001.

[70] Q. Chen, S. E. Reis, C. M. Kammerer et al., "Association between the severity of angiographic coronary artery disease and paraoxonase gene polymorphisms in the National Heart, Lung, and Blood Institute-sponsored Women's Ischemia Syndrome Evaluation (WISE) study," *American Journal of Human Genetics*, vol. 72, no. 1, pp. 13–22, 2003.

[71] G. Fortunato, E. Marciano, F. Zarrilli et al., "Paraoxonase and superoxide dismutase gene polymorphisms and noise-induced hearing loss," *Clinical Chemistry*, vol. 50, no. 11, pp. 2012–2018, 2004.

[72] D. E. Coling, K. C. Y. Yu, D. Somand et al., "Effect of SOD1 overexpression on age- and noise-related hearing loss," *Free Radical Biology and Medicine*, vol. 34, no. 7, pp. 873–880, 2003.

[73] K. Brown, S. Maqsood, J. Y. Huang et al., "Activation of SIRT3 by the NAD^+ precursor nicotinamide riboside protects from noise-induced hearing loss," *Cell Metabolism*, vol. 20, no. 6, pp. 1059–1068, 2014.

[74] J. Wang, Y. Yang, and W. Li, "SIRT3 deficiency increases mitochondrial oxidative stress and promotes migration of retinal pigment epithelial cells," *Experimental Biology and Medicine (Maywood, N.J.)*, vol. 246, no. 8, pp. 877–887, 2021.

[75] S. Someya, W. Yu, W. C. Hallows et al., "Sirt3 mediates reduction of oxidative damage and prevention of age-related hearing loss under caloric restriction," *Cell*, vol. 143, no. 5, pp. 802–812, 2010.

[76] N. Mizushima and B. Levine, "Autophagy in human diseases," *The New England Journal of Medicine*, vol. 383, no. 16, pp. 1564–1576, 2020.

[77] H. Zhou, X. Qian, N. Xu et al., "Disruption of Atg7-dependent autophagy causes electromotility disturbances, outer hair cell loss, and deafness in mice," *Cell Death & Disease*, vol. 11, no. 10, p. 913, 2020.

[78] Y. Ding, W. Meng, W. Kong, Z. He, and R. Chai, "The role of FoxG1 in the inner ear," *Frontiers in Cell and Development Biology*, vol. 8, article 614954, 2020.

[79] Z. He, Q. Fang, H. Li et al., "The role of FOXG1 in the postnatal development and survival of mouse cochlear hair cells," *Neuropharmacology*, vol. 144, pp. 43–57, 2019.

[80] H. Li, Y. Song, Z. He et al., "Meclofenamic acid reduces reactive oxygen species accumulation and apoptosis, inhibits excessive autophagy, and protects hair cell-like HEI-OC1 cells from cisplatin-induced damage," *Frontiers in Cellular Neuroscience*, vol. 12, p. 139, 2018.

[81] H. Yuan, X. Wang, K. Hill et al., "Autophagy attenuates noise-induced hearing loss by reducing oxidative stress," *Antioxidants & Redox Signaling*, vol. 22, no. 15, pp. 1308–1324, 2015.

[82] P. Li, D. Bing, S. Wang et al., "Sleep deprivation modifies noise-induced cochlear injury related to the stress hormone and autophagy in female mice," *Frontiers in Neuroscience*, vol. 13, p. 1297, 2019.

[83] S. Pattingre, L. Espert, M. Biard-Piechaczyk, and P. Codogno, "Regulation of macroautophagy by mTOR and Beclin 1 complexes," *Biochimie*, vol. 90, no. 2, pp. 313–323, 2008.

[84] J. Defourny, A. Aghaie, I. Perfettini, P. Avan, S. Delmaghani, and C. Petit, "Pejvakin-mediated pexophagy protects auditory hair cells against noise-induced damage," *Proceedings of the National Academy of Sciences of the United States of America*, vol. 116, no. 16, pp. 8010–8017, 2019.

[85] M. Fujioka, H. Okano, and K. Ogawa, "Inflammatory and immune responses in the cochlea: potential therapeutic targets for sensorineural hearing loss," *Frontiers in Pharmacology*, vol. 5, p. 287, 2014.

[86] T. Okano, T. Nakagawa, T. Kita et al., "Bone marrow-derived cells expressing Iba1 are constitutively present as resident tissue macrophages in the mouse cochlea," *Journal of Neuroscience Research*, vol. 86, no. 8, pp. 1758–1767, 2008.

[87] Y. Hayashi, H. Suzuki, W. Nakajima et al., "Cochlear supporting cells function as macrophage-like cells and protect audiosensory receptor hair cells from pathogens," *Scientific Reports*, vol. 10, no. 1, article 63654, p. 6740, 2020.

[88] K. Hirose, C. M. Discolo, J. R. Keasler, and R. Ransohoff, "Mononuclear phagocytes migrate into the murine cochlea after acoustic trauma," *The Journal of Comparative Neurology*, vol. 489, no. 2, pp. 180–194, 2005.

[89] S. Tornabene, K. Sato, L. Pham, P. Billings, and E. M. Keithley, "Immune cell recruitment following acoustic trauma," *Hearing Research*, vol. 222, no. 1-2, pp. 115–124, 2006.

[90] M. Fujioka, S. Kanzaki, H. J. Okano, M. Masuda, K. Ogawa, and H. Okano, "Proinflammatory cytokines expression in noise-induced damaged cochlea," *Journal of Neuroscience Research*, vol. 83, no. 4, pp. 575–583, 2006.

[91] W. Wang, L. S. Zhang, A. K. Zinsmaier et al., "Neuroinflammation mediates noise-induced synaptic imbalance and tinnitus in rodent models," *PLoS Biology*, vol. 17, no. 6, article e3000307, 2019.

[92] H. Satoh, G. S. Firestein, P. B. Billings, J. P. Harris, and E. M. Keithley, "Tumor necrosis factor-alpha, an initiator, and etanercept, an inhibitor of cochlear inflammation," *The Laryngoscope*, vol. 112, no. 9, pp. 1627–1634, 2002.

[93] J. Rodrigues, A. L. L. Bachi, G. A. V. Silva et al., "New insights on the effect of TNF alpha blockade by gene silencing in noise-induced hearing loss," *International Journal of Molecular Sciences*, vol. 21, no. 8, p. 2692, 2020.

[94] F. Paciello, A. di Pino, R. Rolesi et al., "Anti-oxidant and anti-inflammatory effects of caffeic acid: *in vivo* evidences in a model of noise-induced hearing loss," *Food and Chemical Toxicology: An International Journal Published for the British Industrial Biological Research Association*, vol. 143, article 111555, 2020.

[95] Y. Zhang, D. Chen, L. Zhao et al., "Nfatc4 deficiency attenuates ototoxicity by suppressing Tnf-mediated hair cell apoptosis in the mouse cochlea," *Frontiers in Immunology*, vol. 10, p. 1660, 2019.

[96] A. Dhukhwa, P. Bhatta, S. Sheth et al., "Targeting inflammatory processes mediated by TRPVI and TNF-α for treating

noise-induced hearing loss," *Frontiers in Cellular Neuroscience*, vol. 13, p. 444, 2019.

[97] D. Frenz, V. Galinovic-Schwartz, W. Liu, K. C. Flanders, and T. R. van de Water, "Transforming growth factor β_1 is an epithelial-derived signal peptide that influences otic capsule formation," *Developmental Biology*, vol. 153, no. 2, pp. 324–336, 1992.

[98] H. Kim, K. Y. Kang, J. G. Baek, H. C. Jo, and H. Kim, "Expression of TGFbeta family in the developing internal ear of rat embryos," *Journal of Korean Medical Science*, vol. 21, no. 1, pp. 136–142, 2006.

[99] J. Okano, T. Takigawa, K. Seki, S. Suzuki, K. Shiota, and M. Ishibashi, "Transforming growth factor beta 2 promotes the formation of the mouse cochleovestibular ganglion in organ culture," *The International Journal of Developmental Biology*, vol. 49, no. 1, pp. 23–31, 2005.

[100] C. Stolfi, E. Troncone, I. Marafini, and G. Monteleone, "Role of TGF-beta and Smad7 in gut inflammation, fibrosis and cancer," *Biomolecules*, vol. 11, no. 1, p. 17, 2021.

[101] S. Wahl, "Transforming growth factor beta (TGF-beta) in inflammation: a cause and a cure," *Journal of Clinical Immunology*, vol. 12, no. 2, pp. 61–74, 1992.

[102] A. Yoshimura, Y. Wakabayashi, and T. Mori, "Cellular and molecular basis for the regulation of inflammation by TGF-beta," *Journal of Biochemistry*, vol. 147, no. 6, pp. 781–792, 2010.

[103] M. Nolte and C. Margadant, "Controlling immunity and inflammation through integrin-dependent regulation of TGF-β," *Trends in Cell Biology*, vol. 30, no. 1, pp. 49–59, 2020.

[104] S. Murillo-Cuesta, L. RodrÃ-guez-de la Rosa, J. Contreras et al., "Transforming growth factor Î²1 inhibition protects from noise-induced hearing loss," *Frontiers in Aging Neuroscience*, vol. 7, p. 32, 2015.

[105] J. Moon, K. Nakahira, K. P. Chung et al., "NOX4-dependent fatty acid oxidation promotes NLRP3 inflammasome activation in macrophages," *Nature Medicine*, vol. 22, no. 9, pp. 1002–1012, 2016.

[106] N. Sai, X. Shi, Y. Zhang et al., "Involvement of cholesterol metabolic pathways in recovery from noise-induced hearing loss," *Neural Plasticity*, vol. 2020, Article ID 6235948, 17 pages, 2020.

[107] G. Zhang, H. Zheng, I. Pyykko, and J. Zou, "The TLR-4/NF-κB signaling pathway activation in cochlear inflammation of rats with noise-induced hearing loss," *Hearing Research*, vol. 379, pp. 59–68, 2019.

[108] Y. Tahera, I. Meltser, P. Johansson et al., "NF-kappaB mediated glucocorticoid response in the inner ear after acoustic trauma," *Journal of Neuroscience Research*, vol. 83, no. 6, pp. 1066–1076, 2006.

[109] I. Meltser, C. R. Cederroth, V. Basinou, S. Savelyev, G. S. Lundkvist, and B. Canlon, "TrkB-mediated protection against circadian sensitivity to noise trauma in the murine cochlea," *Current Biology : CB*, vol. 24, no. 6, pp. 658–663, 2014.

[110] C. Cederroth, J. S. Park, V. Basinou et al., "Circadian regulation of cochlear sensitivity to noise by circulating glucocorticoids," *Current Biology: CB*, vol. 29, no. 15, pp. 2477–2487.e6, 2019.

[111] N. Hakuba, K. Koga, K. Gyo, S. I. Usami, and K. Tanaka, "Exacerbation of noise-induced hearing loss in mice lacking the glutamate transporter GLAST," *The Journal of Neuroscience: The Official Journal of the Society for Neuroscience*, vol. 20, no. 23, pp. 8750–8753, 2000.

[112] K. Kim, S. Payne, A. Yang-Hood et al., "Vesicular glutamatergic transmission in noise-induced loss and repair of cochlear ribbon synapses," *The Journal of Neuroscience: The Official Journal of the Society for Neuroscience*, vol. 39, no. 23, pp. 4434–4447, 2019.

[113] Á. Chamorro, U. Dirnagl, X. Urra, and A. M. Planas, "Neuroprotection in acute stroke: targeting excitotoxicity, oxidative and nitrosative stress, and inflammation," *The Lancet. Neurology*, vol. 15, no. 8, pp. 869–881, 2016.

[114] X. Dong, Y. Wang, and Z. Qin, "Molecular mechanisms of excitotoxicity and their relevance to pathogenesis of neurodegenerative diseases," *Acta Pharmacologica Sinica*, vol. 30, no. 4, pp. 379–387, 2009.

[115] D. Bing, S. C. Lee, D. Campanelli et al., "Cochlear NMDA receptors as a therapeutic target of noise-induced tinnitus," *Cellular Physiology and Biochemistry: International Journal of Experimental Cellular Physiology, Biochemistry, and Pharmacology*, vol. 35, no. 5, pp. 1905–1923, 2015.

[116] N. Hu, M. Rutherford, and S. Green, "Protection of cochlear synapses from noise-induced excitotoxic trauma by blockade of Ca2+-permeable AMPA receptors," *Proceedings of the National Academy of Sciences of the United States of America*, vol. 117, no. 7, pp. 3828–3838, 2020.

[117] T. Hanada, "Ionotropic glutamate receptors in epilepsy: a review focusing on AMPA and NMDA receptors," *Biomolecules*, vol. 10, no. 3, p. 464, 2020.

[118] A. Niedzielski and R. Wenthold, "Expression of AMPA, kainate, and NMDA receptor subunits in cochlear and vestibular ganglia," *The Journal of Neuroscience: The Official Journal of the Society for Neuroscience*, vol. 15, no. 3, pp. 2338–2353, 1995.

[119] H. Tanaka, S. Y. Grooms, M. V. L. Bennett, and R. S. Zukin, "The AMPAR subunit GluR2: still front and center-stage[1]," *Brain Research*, vol. 886, no. 1-2, pp. 190–207, 2000.

[120] M. Hollmann, M. Hartley, and S. Heinemann, "Ca2+ permeability of KA-AMPA–gated glutamate receptor channels depends on subunit composition," *Science (New York, N.Y.)*, vol. 252, no. 5007, pp. 851–853, 1991.

[121] T. Verdoorn, N. Burnashev, H. Monyer, P. Seeburg, and B. Sakmann, "Structural determinants of ion flow through recombinant glutamate receptor channels," *Science (New York, N.Y.)*, vol. 252, no. 5013, pp. 1715–1718, 1991.

[122] J. Sebe, S. Cho, L. Sheets, M. A. Rutherford, H. von Gersdorff, and D. W. Raible, "Ca2+-permeable AMPARs mediate glutamatergic transmission and excitotoxic damage at the hair cell ribbon synapse," *The Journal of Neuroscience: The Official Journal of the Society for Neuroscience*, vol. 37, no. 25, pp. 6162–6175, 2017.

[123] B. Fritzsch, L. Tessarollo, E. Coppola, and L. F. Reichardt, "Neurotrophins in the ear: their roles in sensory neuron survival and fiber guidance," *Progress in Brain Research*, vol. 146, pp. 265–278, 2004.

[124] G. Wan, M. E. Gómez-Casati, A. R. Gigliello, M. C. Liberman, and G. Corfas, "Neurotrophin-3 regulates ribbon synapse density in the cochlea and induces synapse regeneration after acoustic trauma," *eLife*, vol. 3, 2014.

[125] M. Duan, K. Agerman, P. Ernfors, and B. Canlon, "Complementary roles of neurotrophin 3 and a N-methyl-D-aspartate

antagonist in the protection of noise and aminoglycoside-induced ototoxicity," *Proceedings of the National Academy of Sciences of the United States of America*, vol. 97, no. 13, pp. 7597–7602, 2000.

[126] A. Warnecke, J. Harre, H. Staecker et al., "Extracellular vesicles from human multipotent stromal cells protect against hearing loss after noise trauma in vivo," *Clinical and Translational Medicine*, vol. 10, no. 8, article e262, 2020.

[127] A. Wise, R. Richardson, J. Hardman, G. Clark, and S. O'Leary, "Resprouting and survival of guinea pig cochlear neurons in response to the administration of the neurotrophins brain-derived neurotrophic factor and neurotrophin-3," *The Journal of Comparative Neurology*, vol. 487, no. 2, pp. 147–165, 2005.

[128] D. Rejali, V. A. Lee, K. A. Abrashkin, N. Humayun, D. L. Swiderski, and Y. Raphael, "Cochlear implants and ex vivo BDNF gene therapy protect spiral ganglion neurons," *Hearing Research*, vol. 228, no. 1-2, pp. 180–187, 2007.

[129] L. Pettingill, A. K. Wise, M. S. Geaney, and R. K. Shepherd, "Enhanced auditory neuron survival following cell-based BDNF treatment in the deaf guinea pig," *PLoS One*, vol. 6, no. 4, article e18733, 2011.

[130] K. Fernandez, T. Watabe, M. Tong et al., "Trk agonist drugs rescue noise-induced hidden hearing loss," *JCI Insight*, vol. 6, no. 3, 2021.

[131] A. Zuccotti, S. Kuhn, S. L. Johnson et al., "Lack of brain-derived neurotrophic factor hampers inner hair cell synapse physiology, but protects against noise-induced hearing loss," *The Journal of Neuroscience: The Official Journal of the Society for Neuroscience*, vol. 32, no. 25, pp. 8545–8553, 2012.

[132] R. Fettiplace and J. Nam, "Tonotopy in calcium homeostasis and vulnerability of cochlear hair cells," *Hearing Research*, vol. 376, pp. 11–21, 2019.

[133] I. Sziklai, "The significance of the calcium signal in the outer hair cells and its possible role in tinnitus of cochlear origin," *European Archives of Oto-Rhino-Laryngology*, vol. 261, no. 10, pp. 517–525, 2004.

[134] E. Ferrary, P. Tran Ba Huy, N. Roinel, C. Bernard, and C. Amiel, "Calcium and the inner ear fluids," *Acta Oto-Laryngologica. Supplementum*, vol. 460, pp. 13–17, 1988.

[135] H. Zuo, B. Cui, X. She, and M. Wu, "Changes in guinea pig cochlear hair cells after sound conditioning and noise exposure," *Journal of Occupational Health*, vol. 50, no. 5, pp. 373–379, 2008.

[136] M. Castellano-MuÃ±oz and A. Ricci, "Role of intracellular calcium stores in hair-cell ribbon synapse," *Frontiers in Cellular Neuroscience*, vol. 8, p. 162, 2014.

[137] R. Fettiplace, "The role of calcium in hair cell transduction," *Society of General Physiologists Series*, vol. 47, pp. 343–356, 1992.

[138] A. Brandt, J. Striessnig, and T. Moser, "CaV1.3 channels are essential for development and presynaptic activity of cochlear inner hair cells," *The Journal of Neuroscience: The Official Journal of the Society for Neuroscience*, vol. 23, no. 34, pp. 10832–10840, 2003.

[139] J. Fiolet and A. Baartscheer, "Cellular calcium homeostasis during ischemia; a thermodynamic approach," *Cardiovascular Research*, vol. 45, no. 1, pp. 100–106, 2000.

[140] A. Fridberger, A. Flock, M. Ulfendahl, and B. Flock, "Acoustic overstimulation increases outer hair cell Ca2+ concentrations and causes dynamic contractions of the hearing organ," *Proceedings of the National Academy of Sciences of the United States of America*, vol. 95, no. 12, pp. 7127–7132, 1998.

[141] K. Ikeda, J. Kusakari, and T. Takasaka, "Ionic changes in cochlear endolymph of the guinea pig induced by acoustic injury," *Hearing Research*, vol. 32, no. 2-3, pp. 103–110, 1988.

[142] S. Minami, D. Yamashita, J. Schacht, and J. M. Miller, "Calcineurin activation contributes to noise-induced hearing loss," *Journal of Neuroscience Research*, vol. 78, no. 3, pp. 383–392, 2004.

[143] M. Vicente-Torres and J. Schacht, "A BAD link to mitochondrial cell death in the cochlea of mice with noise-induced hearing loss," *Journal of Neuroscience Research*, vol. 83, no. 8, pp. 1564–1572, 2006.

[144] F. Neumaier, M. Dibué-Adjei, J. Hescheler, and T. Schneider, "Voltage-gated calcium channels: determinants of channel function and modulation by inorganic cations," *Progress in Neurobiology*, vol. 129, pp. 1–36, 2015.

[145] H. Shen, B. Zhang, J. H. Shin et al., "Prophylactic and therapeutic functions of T-type calcium blockers against noise-induced hearing loss," *Hearing Research*, vol. 226, no. 1-2, pp. 52–60, 2007.

[146] U. Heinrich, J. Maurer, and W. Mann, "Alteration of loosely bound calcium in the guinea pig organ of Corti after treatment with diltiazem as calcium channel blocker," *European Archives of Oto-Rhino-Laryngology: official journal of the European Federation of Oto-Rhino-Laryngological Societies (EUFOS) : affiliated with the German Society for Oto-Rhino-Laryngology-Head and Neck Surgery*, vol. 254, no. 5, pp. 223–229, 1997.

[147] K. Hill, H. Yuan, X. Wang, and S. H. Sha, "Noise-induced loss of hair cells and cochlear synaptopathy are mediated by the activation of AMPK," *The Journal of Neuroscience: The Official Journal of the Society for Neuroscience*, vol. 36, no. 28, pp. 7497–7510, 2016.

[148] S. Vlajkovic, G. D. Housley, D. J. B. Muñoz et al., "Noise exposure induces up-regulation of ecto-nucleoside triphosphate diphosphohydrolases 1 and 2 in rat cochlea," *Neuroscience*, vol. 126, no. 3, pp. 763–773, 2004.

[149] R. Thalmann, T. Miyoshi, and I. Thalmann, "The influence of ischemia upon the energy reserves of inner ear tissues," *The Laryngoscope*, vol. 82, no. 12, pp. 2249–2272, 1972.

[150] W. W. Winder and D. M. Thomson, "Cellular energy sensing and signaling by AMP-activated protein kinase," *Cell Biochemistry and Biophysics*, vol. 47, no. 3, pp. 332–347, 2007.

[151] F. Chen, H. W. Zheng, K. Hill, and S. H. Sha, "Traumatic noise activates Rho-family GTPases through transient cellular energy depletion," *The Journal of Neuroscience: The Official Journal of the Society for Neuroscience*, vol. 32, no. 36, pp. 12421–12430, 2012.

[152] H. Sumimoto, R. Minakami, and K. Miyano, "Soluble regulatory proteins for activation of NOX family NADPH oxidases," *Methods in Molecular Biology (Clifton, N.J.)*, vol. 1982, pp. 121–137, 2019.

[153] F. Wu, H. Xiong, and S. Sha, "Noise-induced loss of sensory hair cells is mediated by ROS/AMPKα pathway," *Redox Biology*, vol. 29, article 101406, 2020.

[154] H. Xiong, L. Lai, Y. Ye, and Y. Zheng, "Glucose protects cochlear hair cells against oxidative stress and attenuates noise-induced hearing loss in mice," *Neuroscience Bulletin*, vol. 37, no. 5, pp. 657–668, 2021.

[155] T. Fujita, D. Yamashita, S. Katsunuma, S. Hasegawa, H. Tanimoto, and K. I. Nibu, "Increased inner ear susceptibility to noise injury in mice with streptozotocin-induced diabetes," *Diabetes*, vol. 61, no. 11, pp. 2980–2986, 2012.

[156] M. Fredrich and R. Illing, "MMP-2 is involved in synaptic remodeling after cochlear lesion," *Neuroreport*, vol. 21, no. 5, pp. 324–327, 2010.

[157] C. Overall and C. López-Otín, "Strategies for MMP inhibition in cancer: innovations for the post-trial era," *Nature Reviews. Cancer*, vol. 2, no. 9, pp. 657–672, 2002.

[158] B. Hu, Q. Cai, Z. Hu et al., "Metalloproteinases and their associated genes contribute to the functional integrity and noise-induced damage in the cochlear sensory epithelium," *The Journal of Neuroscience: The Official Journal of the Society for Neuroscience*, vol. 32, no. 43, pp. 14927–14941, 2012.

[159] J. S. Park, S. J. Kang, M. K. Seo, I. Jou, H. G. Woo, and S. M. Park, "Role of cysteinyl leukotriene signaling in a mouse model of noise-induced cochlear injury," *Proceedings of the National Academy of Sciences*, vol. 111, no. 27, pp. 9911–9916, 2014.

[160] X. Wang, M. Streeter, Y. P. Liu, and H. B. Zhao, "Identification and characterization of pannexin expression in the mammalian cochlea," *The Journal of Comparative Neurology*, vol. 512, no. 3, pp. 336–346, 2009.

[161] J. Abitbol, J. J. Kelly, K. Barr, A. L. Schormans, D. W. Laird, and B. L. Allman, "Differential effects of pannexins on noise-induced hearing loss," *The Biochemical Journal*, vol. 473, no. 24, pp. 4665–4680, 2016.

[162] S. Wang, L. G. Yu, R. P. Liu et al., "Gene-gene interaction of GJB2, SOD2, and CAT on occupational noise-induced hearing loss in Chinese Han population," *Biomedical and Environmental Sciences: BES*, vol. 27, no. 12, pp. 965–968, 2014.

[163] A. Konings, L. van Laer, M. Pawelczyk et al., "Association between variations in CAT and noise-induced hearing loss in two independent noise-exposed populations," *Human Molecular Genetics*, vol. 16, no. 15, pp. 1872–1883, 2007.

[164] B. S. Wang, K. Xu, H. Zhang et al., "Association between NFE2L2 gene polymorphisms and noise-induced hearing loss in a Chinese population," *Biomedical and Environmental Sciences*, vol. 32, no. 6, pp. 465–470, 2019.

[165] J. Lavinsky, A. L. Crow, C. Pan et al., "Genome-wide association study identifies nox3 as a critical gene for susceptibility to noise-induced hearing loss," *PLoS Genetics*, vol. 11, no. 4, article e1005094, 2015.

[166] A. Konings, L. van Laer, S. Michel et al., "Variations in *HSP70* genes associated with noise-induced hearing loss in two independent populations," *European Journal of Human Genetics*, vol. 17, no. 3, pp. 329–335, 2009.

[167] C. Y. Lin, J. L. Wu, T. S. Shih, P. J. Tsai, Y. M. Sun, and Y. L. Guo, "Glutathione *S*-transferase M1, T1, and P1 polymorphisms as susceptibility factors for noise-induced temporary threshold shift," *Hearing Research*, vol. 257, no. 1-2, pp. 8–15, 2009.

[168] H. Shen, X. Huo, K. Liu et al., "Genetic variation in GSTM1 is associated with susceptibility to noise-induced hearing loss in a Chinese population," *Journal of Occupational and Environmental Medicine*, vol. 54, no. 9, pp. 1157–1162, 2012.

[169] H. Shen, J. Dou, L. Han et al., "Genetic variation in APE1 gene promoter is associated with noise-induced hearing loss in a Chinese population," *International Archives of Occupational and Environmental Health*, vol. 89, no. 4, article 1100, pp. 621–628, 2016.

[170] H. Shen, J. Cao, Z. Hong et al., "A functional Ser326Cys polymorphism in hOGG1 is associated with noise-induced hearing loss in a Chinese population," *PLoS One*, vol. 9, no. 3, article e89662, 2014.

[171] Y. Wu, J. Ni, M. Qi et al., "Associations of genetic variation in CASP3 gene with noise-induced hearing loss in a Chinese population: a case–control study," *Environmental Health*, vol. 16, no. 1, p. 78, 2017.

[172] C. Elfgang, R. Eckert, H. Lichtenberg-Fraté et al., "Specific permeability and selective formation of gap junction channels in connexin-transfected HeLa cells," *The Journal of Cell Biology*, vol. 129, no. 3, pp. 805–817, 1995.

[173] H. Zhao, N. Yu, and C. Fleming, "Gap junctional hemichannel-mediated ATP release and hearing controls in the inner ear," *Proceedings of the National Academy of Sciences of the United States of America*, vol. 102, no. 51, pp. 18724–18729, 2005.

[174] E. van Eyken, L. van Laer, E. Fransen et al., "The contribution of GJB2 (Connexin 26) 35delG to age-related hearing impairment and noise-induced hearing loss," *Otology & Neurotology*, vol. 28, no. 7, pp. 970–975, 2007.

[175] L. van Laer, P. I. Carlsson, N. Ottschytsch et al., "The contribution of genes involved in potassium-recycling in the inner ear to noise-induced hearing loss," *Human Mutation*, vol. 27, no. 8, pp. 786–795, 2006.

[176] M. Pawelczyk, L. van Laer, E. Fransen et al., "Analysis of gene polymorphisms associated with K ion circulation in the inner ear of patients susceptible and resistant to noise-induced hearing loss," *Annals of Human Genetics*, vol. 73, no. 4, pp. 411–421, 2009.

[177] X. Zhang, Y. Ni, Y. Liu et al., "Screening of noise-induced hearing loss (NIHL)-associated SNPs and the assessment of its genetic susceptibility," *Environmental Health*, vol. 18, no. 1, p. 30, 2019.

[178] B. M. Johnstone, R. Patuzzi, J. Syka, and E. Syková, "Stimulus-related potassium changes in the organ of Corti of guinea-pig," *The Journal of Physiology*, vol. 408, no. 1, pp. 77–92, 1989.

[179] A. Konings, L. van Laer, A. Wiktorek-Smagur et al., "Candidate gene association study for noise-induced hearing loss in two independent noise-exposed populations," *Annals of Human Genetics*, vol. 73, no. 2, pp. 215–224, 2009.

[180] T. J. Kowalski, M. Pawelczyk, E. Rajkowska, A. Dudarewicz, and M. Sliwinska-Kowalska, "Genetic variants of CDH23 associated with noise-induced hearing loss," *Otology & Neurotology*, vol. 35, no. 2, pp. 358–365, 2014.

[181] A. Brake, M. Wagenbach, and D. Julius, "New structural motif for ligand-gated ion channels defined by an ionotropic ATP receptor," *Nature*, vol. 371, no. 6497, pp. 519–523, 1994.

[182] F. Mazzarda, A. Delia, R. Massari et al., "Organ-on-chip model shows that ATP release through connexin hemichannels drives spontaneous Ca2+signaling in non-sensory cells of the greater epithelial ridge in the developing cochlea," *Lab on a Chip*, vol. 20, no. 16, pp. 3011–3023, 2020.

[183] D. Yan, Y. Zhu, T. Walsh et al., "Mutation of the ATP-gated P2X(2) receptor leads to progressive hearing loss and increased susceptibility to noise," *Proceedings of the National Academy of Sciences*, vol. 110, no. 6, pp. 2228–2233, 2013.

[184] Y. Niu, C. Xie, Z. Du et al., "Genome-wide association study identifies 7q11.22 and 7q36.3 associated with noise-induced hearing loss among Chinese population," *Journal of Cellular and Molecular Medicine*, vol. 25, no. 1, pp. 411–420, 2021.

[185] K. Hori, T. Nagai, W. Shan et al., "Cytoskeletal regulation by AUTS2 in neuronal migration and neuritogenesis," *Cell Reports*, vol. 9, no. 6, pp. 2166–2179, 2014.

[186] E. Ding, J. Liu, H. Guo et al., "*DNMT1* and *DNMT3A* haplotypes associated with noise-induced hearing loss in Chinese workers," *Scientific Reports*, vol. 8, no. 1, article 12193, 2018.

[187] X. Zhang, Y. Liu, L. Zhang et al., "Associations of genetic variations in *EYA4*, *GRHL2* and *DFNA5* with noise-induced hearing loss in Chinese population: a case-control study," *Environmental Health*, vol. 14, no. 1, p. 77, 2015.

[188] H. Guo, E. Ding, Y. Bai et al., "Association of genetic variations in FOXO3 gene with susceptibility to noise induced hearing loss in a Chinese population," *PLoS One*, vol. 12, no. 12, article e0189186, 2017.

[189] X. Li, X. Huo, K. Liu et al., "Association between genetic variations in GRHL2 and noise-induced hearing loss in Chinese high intensity noise exposed workers: a case-control analysis," *Industrial Health*, vol. 51, no. 6, pp. 612–621, 2013.

[190] X. Xu, Q. Yang, J. Jiao et al., "Genetic variation in *POU4F3* and *GRHL2* associated with noise-induced hearing loss in Chinese population: a case-control study," *International Journal of Environmental Research and Public Health*, vol. 13, no. 6, p. 561, 2016.

[191] B. Wang, E. Ding, H. Shen et al., "Association of TagSNP in lncRNA *HOTAIR* with susceptibility to noise-induced hearing loss in a Chinese population," *Hearing Research*, vol. 347, pp. 41–46, 2017.

[192] E. Ding, J. Liu, H. Shen et al., "Notch polymorphisms associated with sensitivity of noise induced hearing loss among Chinese textile factory workers," *BMC Medical Genetics*, vol. 19, no. 1, p. 168, 2018.

[193] Y. Grondin, M. E. Bortoni, R. Sepulveda et al., "Genetic polymorphisms associated with hearing threshold shift in subjects during first encounter with occupational impulse noise," *PLoS One*, vol. 10, no. 6, article e0130827, 2015.

[194] M. A. Han, "Therapeutic effect of dexamethasone for noise-induced hearing loss: systemic versus intratympanic injection in mice," *Otology & Neurotology*, vol. 36, no. 5, pp. 755–762, 2015.

[195] J. Kil, E. Lobarinas, C. Spankovich et al., "Safety and efficacy of ebselen for the prevention of noise-induced hearing loss: a randomised, double-blind, placebo-controlled, phase 2 trial," *Lancet (London, England)*, vol. 390, no. 10098, pp. 969–979, 2017.

[196] A. Fetoni, P. de Bartolo, S. L. M. Eramo et al., "Noise-induced hearing loss (NIHL) as a target of oxidative stress-mediated damage: cochlear and cortical responses after an increase in antioxidant defense," *The Journal of Neuroscience: The Official Journal of the Society for Neuroscience*, vol. 33, no. 9, pp. 4011–4023, 2013.

[197] G. Lenaz, R. Fato, G. Formiggini, and M. L. Genova, "The role of coenzyme Q in mitochondrial electron transport," *Mitochondrion*, vol. 7, pp. S8–S33, 2007.

[198] M. Oz, D. E. Lorke, M. Hasan, and G. A. Petroianu, "Cellular and molecular actions of methylene blue in the nervous system," *Medicinal Research Reviews*, vol. 31, no. 1, pp. 93–117, 2011.

[199] J. Park, I. Jou, and S. Park, "Attenuation of noise-induced hearing loss using methylene blue," *Cell Death & Disease*, vol. 5, no. 4, article e1200, 2014.

[200] A. Umugire, S. Lee, D. Kim, M. Choi, H. S. Kim, and H. H. Cho, "Avenanthramide-C prevents noise- and drug-induced hearing loss while protecting auditory hair cells from oxidative stress," *Cell Death Discovery*, vol. 5, no. 1, p. 115, 2019.

[201] M. Huang, A. Kantardzhieva, D. Scheffer, M. C. Liberman, and Z. Y. Chen, "Hair cell overexpression of Islet1 reduces age-related and noise-induced hearing loss," *The Journal of Neuroscience: The Official Journal of the Society for Neuroscience*, vol. 33, no. 38, pp. 15086–15094, 2013.

[202] R. Horie, T. Sakamoto, T. Nakagawa, T. Ishihara, M. Higaki, and J. Ito, "Stealth-nanoparticle strategy for enhancing the efficacy of steroids in mice with noise-induced hearing loss," *Nanomedicine (London, England)*, vol. 5, no. 9, pp. 1331–1340, 2010.

[203] X. Xu, K. Lin, Y. Wang et al., "A metal-organic framework based inner ear delivery system for the treatment of noise-induced hearing loss," *Nanoscale*, vol. 12, no. 30, pp. 16359–16365, 2020.

[204] L. Liu, Y. Chen, J. Qi et al., "Wnt activation protects against neomycin-induced hair cell damage in the mouse cochlea," *Cell Death & Disease*, vol. 7, no. 3, article e2136, 2016.

[205] Y. Zhang, S. Zhang, Z. Zhang et al., "Knockdown of *Foxg1* in Sox9+ supporting cells increases the trans-differentiation of supporting cells into hair cells in the neonatal mouse utricle," *Aging (Albany NY)*, vol. 12, no. 20, article 104009, pp. 19834–19851, 2020.

[206] R. Guo, S. Zhang, M. Xiao et al., "Accelerating bioelectric functional development of neural stem cells by graphene coupling: implications for neural interfacing with conductive materials," *Biomaterials*, vol. 106, pp. 193–204, 2016.

[207] R. Guo, M. Xiao, W. Zhao et al., "2D $Ti_3C_2T_x$MXene couples electrical stimulation to promote proliferation and neural differentiation of neural stem cells," *Acta Biomaterialia*, vol. -S1742-7061, no. 20, pp. 30749–30752, 2020.

[208] R. Guo, J. Li, C. Chen et al., "Biomimetic 3D bacterial cellulose-graphene foam hybrid scaffold regulates neural stem cell proliferation and differentiation," *Colloids and Surfaces. B, Biointerfaces*, vol. 200, article 111590, 2021.

Hindawi
Neural Plasticity
Volume 2021, Article ID 5511010, 11 pages
https://doi.org/10.1155/2021/5511010

Review Article

Autophagy: A Novel Horizon for Hair Cell Protection

Chang Liu,[1,2] Zhiwei Zheng,[1,2] Pengjun Wang,[3] Shuangba He,[4] and Yingzi He[1,2]

[1]*ENT Institute and Otorhinolaryngology Department, Eye and ENT Hospital, State Key Laboratory of Medical Neurobiology, Fudan University, Shanghai 200031, China*
[2]*NHC Key Laboratory of Hearing Medicine (Fudan University), Shanghai 200031, China*
[3]*Department of Otorhinolaryngology, Affiliated Sixth People's Hospital of Shanghai Jiaotong University, 600 Yishan Road, Shanghai 200233, China*
[4]*Department of Otolaryngology Head and Neck, Nanjing Tongren Hospital, School of Medicine, Southeast University, Nanjing, China China*

Correspondence should be addressed to Shuangba He; hesb@njtrh.org and Yingzi He; yingzihe09611@126.com

Received 10 February 2021; Accepted 21 June 2021; Published 30 June 2021

Academic Editor: Jian Wang

As a general sensory disorder, hearing loss was a major concern worldwide. Autophagy is a common cellular reaction to stress that degrades cytoplasmic waste through the lysosome pathway. Autophagy not only plays major roles in maintaining intracellular homeostasis but is also involved in the development and pathogenesis of many diseases. In the auditory system, several studies revealed the link between autophagy and hearing protection. In this review, we aimed to establish the correlation between autophagy and hair cells (HCs) from the aspects of ototoxic drugs, aging, and acoustic trauma and discussed whether autophagy could serve as a potential measure in the protection of HCs.

1. Introduction

As a general sensory disorder in human society, hearing loss was a major concern worldwide. The causes of hearing loss are infections, noise, aging, and ototoxic drugs. Autophagy is a common cellular reaction to stress that degrades cytoplasmic waste through the lysosome pathway. Autophagy not only plays major roles in maintaining intracellular homeostasis but is also involved in the development and pathogenesis of several diseases [1–6]. During a variety of pathological and physiological states, the activation of autophagy seems beneficial, as it removes damaged organelles or defends microbial infection and is important in various diseases related to metabolism or neurodegeneration [7].

Autophagy suppresses necroptosis and PARP-mediated cell death under cellular stress conditions. Early studies demonstrated that autophagy might be a prosurvival factor in many pathological processes [8]. In retinal ganglion cells, it was found that autophagy suppresses cell apoptosis and promotes cell survival, while the deletion of autophagy significantly decreases cell survival during the degeneration of the optic nerve [9]. In the auditory system, several studies revealed the link between autophagy and hearing protection and proved that the upregulation of autophagy might contribute to the alleviation of morphological damage in the inner ear [6, 10]. In this review, we aimed to establish the correlation between autophagy and hair cells (HCs), determined the effect of autophagy in hearing loss, and further discussed whether autophagy could serve as a potential measure in the protection of HCs.

2. Autophagy and Cochlear Development

Modulated by the growth factor signaling pathway, autophagy regulates cellular differentiation by providing energy and materials to the cells (such as immune cell [11]). Some studies proved the existence of autophagy in the inner ear of many species. For example, Atg4b$^{-/-}$ null mice showed a defect in vestibular otoconia development, which might lead to the aberration of equilibrium [12]. Autophagy is involved in the neurogenesis in chicken's auditory spiral ganglion [13]. Moreover, HCs might present autophagic morphological

features after ototoxic insults [14]. These data indicated that autophagy is crucial at the early stage of inner ear development. In the early postnatal stage of mice, auditory ribbon synapses are formed and matured with the development of cochlear HC stereocilia [15–18]. According to previous studies, although ATG5-deficient auditory HCs (including OHCs and IHCs) show well-functional morphology and mechanotransduction at P5, progressive accumulation of polyubiquitinated protein, as well as degeneration, is observed at P14 [19], which might eventually cause hearing loss. Furthermore, the treatment of postnatal mice with autophagy inhibitors before the onset stage of hearing induces long-term auditory disorders. The disruptions of autophagy have deleterious effects on the development of cochlear ribbon synapses in mice [20]. Together, these results strongly suggested that autophagy plays a critical role in the formation of HC morphology at the early postnatal stage.

3. Autophagy and Hearing Loss

Sensorineural hearing loss (SNHL) includes noise-induced hearing loss (NIHL), age-related hearing loss (ARHL), inherited hearing loss, and ototoxic drug-induced hearing loss (ODIHL). SNHL occurs because of the irreversible damage to hair cells (HCs) and spiral ganglion neurons (SGNs), both of which have very limited regeneration ability in adult mouse cochlea [21–26]. Thus, how to protect the cochlear HC is a key scientific question in the hearing research field.

3.1. Autophagy and Aminoglycoside-Induced Hearing Loss. As widely used clinical drugs, aminoglycosides (AGs) are famous for the broad antibacterial spectrum [27]. However, the application is limited because of the severe side-effects (including the ototoxicity), which might induce sensorineural hearing loss permanently and affect the life quality of patients significantly [28]. AGs cause damage to the outer hair cells (OHCs) of the basal turn, and with continuing drug exposure, damage spreads to the other turns as well as inner hair cells (IHCs) [29].

In the tissues with the need of high energy, such as HCs [30], phosphatase and tensin homolog- (PTEN-) induced putative kinase 1 (PINK1) is highly expressed [31]. According to a previous study, the suppression of PINK1 and the loss of HEI-OC1 cells were increased, with or without gentamicin (GM) exposure [32]. In addition, the PINK1 knockdown (KD) cells showed less expression of LC3B but a higher degree of p53 and activated caspase 3, indicating that PINK1 alleviates the GM-induced ototoxicity by inducing autophagy and resisting the level of p53 in HCs [32].

In the brain and neuroendocrine system, ubiquitin carboxyl-terminal hydrolase isozyme L1 (UCHL1) is highly expressed, which is important in maintaining synaptic structures, stabilizing ubiquitin, and regulating proteasomal or lysosomal degradation [33]. In the auditory system, UCHL1 was found to be downregulated in the cochlea by gentamicin (GM) in a time-dependent manner, and in damage or pathological condition, UCHL1 deficiency was found to be associated with the autophagy pathway [34, 35]. According to this study, UCHL1 was downregulated after GM treatment, and after GM exposure, siRNA or the pharmacological inhibitor (LDN-91946) treatment exacerbated the damage to the cochlear explants and HEI-OC1 cells [36]. The silencing of the UCHL1 protein blocked autophagic flux and the inhibition of LAMP1 and LC3 colocalization. These findings suggested that by downregulating UCHL1, GM might serve as a negative regulator to the autophagosome and lysosome fusion [36].

Fatty acids extracted from avocado oil have several functions, including promoting collagen synthesis, reducing inflammation, and wound healing [37]. In the brain tissue of diabetic rats, the seed oil attenuates oxidative stress and prevents mitochondrial dysfunction [38]. A recent study showed the protective effect of avocado oil on auditory HCs. Also, the avocado oil extract (DKB122) was shown to protect the HCs from neomycin-induced damage via upregulating antioxidant pathways, inhibiting inflammatory gene expression, and activating autophagy [39]. The level of p62 protein in HEI-OC1 cells is decreased in a dose-dependent manner after DKB122 treatment. Furthermore, p62 binds to LC3 and incorporates into the autophagosome; strikingly, the downregulation of intracellular p62 suggested that DKB122 upregulates the autophagy in HEI-OC1 cells.

3.2. Autophagy and Cisplatin-Induced Hearing Loss. Cisplatin is an anticancer drug used in clinical treatment. Based on the broad-spectrum chemotherapeutic effects, cisplatin is widely utilized in various cancers, such as testicular cancer, breast cancer, and head/neck cancer [40, 41]. However, progressive hearing loss could also be caused by high doses of cisplatin [6, 42–46]. Previous studies have shown that the accumulation of reactive oxygen species (ROS) after cisplatin treatment is a critical factor inducing HC damage [47–49].

m^6A is a fat mass and obesity-associated (FTO) demethylase that regulates mRNA metabolism by catalyzing demethylation of m^6A [50], while meclofenamic acid (MA), an anti-inflammatory drug, serves as a selective inhibitor [51]. A previous study reported that MA2 (a more active form of MA) treatment significantly reduces the apoptosis level of HEI-OC1 cells after cisplatin exposure. However, the effects of MA2 on cisplatin-induced HEI-OC1 death might not involve the participation of m^6A, because no significant increase of m^6A was observed after MA2 treatment [49]. The data showed that the level of autophagy was upregulated after cisplatin exposure, while after treatment of HEI-OC1 cells with MA2, the cisplatin-induced cell apoptosis and autophagy activation were significantly decreased [49]. These results suggested that the correlation between autophagy and cisplatin-induced apoptosis is complicated, and excessive autophagy might promote HC apoptosis.

As a Pou family transcription factor [52], Pou4f3 is necessary for HC differentiation, especially for the functional transduction and synaptic specialization [53, 54]. The mutation of Pou4f3 leads to the loss of HCs in the cochlea and subsequently results in severe hearing loss [55]. A recent study demonstrated that Pou4f3 participated in cisplatin-induced autophagy. After cisplatin treatment or AAV2-Pou4f3 shRNA transfection, Pou4f3 expression was decreased markedly. However, the levels of Beclin-1 and LC3-II were

upregulated, indicating that Pou4f3 mutation promotes cisplatin-induced autophagy [56]. In addition, as the autophagy activator, rapamycin promoted HC apoptosis, while 3-MA inhibited HC apoptosis. This Pou4f3 mutation promotes HC apoptosis in the cochlea via autophagy [56].

A regulator of cell death, STAT1, was also reported to be involved in cisplatin-induced HC death [57, 58]. A previous study used siRNA to knockdown *STAT1* gene expression; consequently, the reduction of cisplatin-induced HC death was observed in vivo and in vitro [57]. In order to reveal the potential correlation between STAT1 and autophagy, other studies investigated the effect of STAT1 ablation on HC damage induced by cisplatin or GM. As shown in the study, comparing to the WT mice, both LC3-II conversion and Beclin-1 expression were increased in the explants from $STAT1^{-/-}$ mice after cisplatin or GM treatment. However, 3-MA+cisplatin/GM treatment significantly reduced the level of surviving HCs in explants of $STAT1^{-/-}$ mice, suggesting that autophagy is a potential protector in preventing cisplatin- and GM-induced HC death [59].

As a regulatory protein, glycogen synthase kinase 3β (GSK-3β) participates in a variety of physiological processes and the occurrence of several diseases [60–65]. Some studies also showed that as a downstream factor of AKT, GSK-3β is involved in the regulation of autophagy, while in the normal state GSK-3β suppresses the activation of autophagy. However, when abnormal external stimuli occur, the upstream kinase in the cells promotes the phosphorylation and leads to the inactivation of GSK-3β and blocks the inhibition on autophagy [66, 67]. In auditory research, gene knockout restored the inhibitory effect of GSK-3β, and the autophagy and cytoprotective effects in HEI-OC1 cells were enhanced successfully [68]. Furthermore, the GSK-3β-KO HEI-OC1 cells showed higher viability and higher autophagy rate after cisplatin treatment as compared to that of GSK-3β-WT HEI-OC1 cells. Moreover, cotreatment with 3-MA results in the reduction of autophagy accompanied by an upregulation of cell apoptosis [68]. These findings suggested that autophagy could be activated by downregulating the expression of GSK-3β, and autophagy exerts a protective effect against ototoxicity drugs.

As a member of the nucleotide-binding and oligomerization domain- (NOD-) like receptor (NLR) family, NLRX1 is important in regulating autophagy, ROS generation, and cell death in various kinds of cell types, responding to different stimuli [69–73]. In auditory research, it was found that NLRX1 was localized in the mitochondria of HEI-OC1 cells, and by activating the ROS/JNK signaling pathway and autophagy, NLRX1 sensitized the HEI-OC1 cells to cisplatin ototoxicity [74, 75]. According to the study, after treating HEI-OC1 cells with cisplatin, the increased expression of NLRX1 was synchronized with the activation of autophagy. However, by silencing the expression of NLRX1, the level of autophagy activation was reduced, and cell viability was increased [75]. Mechanistic studies revealed that by inhibiting ROS generation, autophagy activation and cell apoptosis could be successfully prevented in both HEI-OC1 cells and cochlear explants, providing a novel strategy against cisplatin-induced ototoxicity [75–78].

3.3. Autophagy and Noise-Induced Hearing Loss. Increased ROS production or decreased antioxidant activity causes oxidative damage, which is a key element causing noise-induced hearing loss (NIHL). However, ROS was also able to induce cellular defense processes, such as autophagy [79]. A recent study found that the level of oxidative stress in OHCs is noise-dose dependent and that the activation of autophagy exerts a protective effect against NIHL by alleviating the oxidative stress. As described previously, oxidative stress induced by temporary threshold shift (TTS) noise increases the level of LC3B in OHCs, and rapamycin treatment diminishes 4-HNE and 3-NT levels and decreases noise-induced HC loss. On the other hand, the reduction in LC3B via 3-MA or LC3B-siRNA increases the level of 3-NT and noise-induced cell death in OHCs [80].

Pejvakin, a peroxisome-associated protein from the gasdermin family, plays a critical role in sound-induced peroxisome proliferation [81]. Moreover, pejvakin participates in an early autophagic degradation of peroxisomes (pexophagy) in HCs after noise exposure [82]. According to the studies, pejvakin-mediated pexophagy prior to peroxisome proliferation protects the HCs against oxidative damage [83, 84]. As the lipid peroxidation in HCs was investigated through the assessment of the immunoreactivity of 4-HNE, an inverse correlation was established between pexophagy and 4-HNE, which suggested that pejvakin-mediated pexophagy plays a critical role in redox homeostasis and HC protection against noise-induced damage [82]. These results were also confirmed by the rescue experiments in $Pjvk^{-/-}$ mice, as the viral transduction of Pjvk and LC3B cDNAs successfully restored the pexophagy and prevented the progress of oxidative stress [82]. Due to the similar clearance mechanisms owned by peroxisomes and mitochondria [85, 86], investigating whether mitochondrial autophagy has a protective effect against noise overexposure is essential.

Sleep deprivation (SD) also causes various inner ear diseases, such as hearing loss and tinnitus [87, 88]. The hypothalamic-pituitary-adrenal (HPA) axis is activated by successive SD, which subsequently leads to the upregulation of corticosterone [89], which in turn, activates the glucocorticoid receptors, resulting in the disruption of metabolic activity in the autophagy system [90]. The presence of corticosterone receptors in the auditory system has been demonstrated in many studies [91, 92], and it has been proved that high levels of corticosterone protect cochlear OHCs from various insults [93, 94]. Recently, the effects of SD on noise vulnerability were investigated with respect to the potential underlying mechanisms [95]. According to the study, the elevated expression of LC3B and autophagy activation is observed in the short-term SD+ acoustic trauma (AT) group, whereas repeated SD+AT group could not exert a similar effect. In addition, the SD+AT group exhibits high levels of corticosterone and severe OHC loss. This phenomenon could be attributed to the disruption of repeated SD to the homeostasis, resulting in the disorders of immunological malfunction [96, 97] and autophagy system disorder. However, the autophagy induced by short-term SD causes a protective effect on HCs in the apoptotic processes induced by oxidative stress. Thus, it is demonstrated that short-term

SD exerts protective effects on HCs by regulating corticosterone and activating autophagy after noise exposure [95].

3.4. Age-Related Hearing Loss and Autophagy. As a predominant neurodegenerative disease, age-related hearing loss (AHL) is a common form of hearing loss [5, 98–102]. It is prevalent in adults aged ≥70 years, which results in social isolation, communication disorders, and a decline in physical function [103]. The SAMP8 strain is a classic model in studying the influence of aging on biological processes [104]. A previous study has revealed the mechanisms of ARHL, using SAMP8 mice, involved in the participation of oxidative stress, inflammation, and autophagic stress [105].

MicroRNAs (miRNAs) are endogenous, small, noncoding RNAs that control the stability of messenger RNA (mRNA). Recently, the existence of miRNAs in the cochlea has been proved, which suggested that miRNAs are critical in cochlear pathology [106, 107]. As a regulator controlling autophagy and cell death, miR-34a restrains autophagic flux by inhibiting autophagy protein ATG9a in HEI-OC1 cells [10, 108, 109]. Notably, the inhibitory effect of miR-34a to autophagy is mediated through multiple targets, such as SIRT1 and Bcl-2 [110–112]. As an NAD^+-dependent histone deacetylase, SIRT1 is famous in the modulation of aging. The deacetylation of multiple autophagy-related proteins, including ATG7, ATG5, and ATG8 [113], or regulation of uncoupling protein 2 (UCP2) to stimulate mitophagy activates autophagy via SIRT1 [114]. According to a recent study, loss of HCs is observed in aged C57BL/6 mice, accompanied by the downregulation of autophagy and SIRT1 expression, and in HEI-OC1 cells, the decrease in SIRT1 leads to the reduction of LC3-II with an elevated level of p62. Moreover, silencing the expression of SIRT1 impaired the formation of the autophagosomes [115]. In addition, the long-term administration of resveratrol (SIRT1 activator) to the aging cochlea enhanced mitophagy, alleviated mitochondrial biogenesis, and improved the mitochondrial function [115]. Altogether, it suggested that the miR-34a/SIRT1 signaling pathway is a potential target for modulating autophagy, which is promising in delaying ARHL.

Inflammaging means a clinical condition in the elder with low-grade and chronic inflammation. Since it is related to several age-related diseases, it might increase the morbidity or mortality in the elderly. The long-term infection might alter the permeability and structure of the round window membrane [116], causing the permeation of lipopolysaccharide (LPS) into the inner ear [117]. When LPS enters the inner ear, it damages the HCs through multiple mechanisms, including inducing mitochondrial damage, accumulation of ROS, and activation of NF-κB, SAPK/JNK, caspases, or other apoptotic pathways [118–121]. FoxG1 is a critical transcription factor belonging to the forkhead family. It regulates the proliferation and differentiation of cells, and the mutations in the *Foxg1* gene affect the development of axon and neuron [122]. During the development of the inner ear, FoxG1 is critical in maintaining the formation of HCs and the morphology of the cochlea [46]. FoxG1 also regulates the metabolism and biosynthesis of mitochondria [123–125], and hence, the unusual expression of FoxG1 results in opposing consequences to the function of mitochondria. Moreover, another study showed that the susceptibility of aging OC-1 cells to LPS-induced inflammation is regulated by FoxG1 via activated autophagy [5], thereby providing a potential target in AHL treatment.

3.5. Inherited Hearing Loss and Autophagy. The defection of mitochondrial tRNA in posttranscriptional modification is thought to be related to a variety of human hereditary diseases, including inherited hearing loss [126]. Recently, the molecular mechanism of deafness-related tRNAIle4295A>G mutations was deeply studied. It was found that abnormal tRNA metabolism may lead to mitochondrial translation disorders, respiratory deficiency, increased level of reactive oxygen species, and autophagy promotion [127]. However, whether the upregulation of autophagy in HCs is protective or not was not demonstrated in this study.

4. Other Factors Related to Autophagy in the Inner Ear

IGF-1 is a trophic factor belonging to the insulin family. It is involved in the development of the nervous system in adults, and hence, the mutations cause human syndromic deafness [128]. The correlation between IGF-1 and autophagy has been demonstrated in many studies. For example, activation of mTOR and IGF-1 downregulates autophagy in mammary epithelial cells [129]. On the other hand, in cultures of Purkinje neurons, IGF-1 promotes autophagy through the induction of autophagosome fusion with lysosomes [130]. However, in the auditory system, the role of IGF-1 in regulating autophagy does not seem crucial, as no significant difference was detected in the autophagic flux between IGF-$1^{+/+}$ mice and IGF-$1^{-/-}$ mice [131]; however, the role of IGF-1 in regulating autophagy should not be excluded out. Hearing impairment is also caused by cochlear ischemia [132–134]. Reportedly, the patients with carotid arterial sclerosis might suffer severer NIHL [135].

Hearing impairment can also be induced by cochlear ischemia [132–134]. Reportedly, carotid arterial sclerosis exacerbates the effects of noise exposure. Arterial sclerosis might be a contributor to hearing loss in the elderly, especially in those exposed to noise [135, 136]. According to a recent study, autophagy exerts a protective effect in ischemia-induced hearing loss, as the activation of autophagy occurs simultaneously with the recovery of hearing after reperfusion [137]. However, additional studies are required to understand the underlying mechanism.

5. Future Aspect

5.1. Using Autophagy as an Antioxidative Therapy. The role of autophagy in the auditory system is that of an antioxidant to protect HCs and hearing [6, 80, 138]. The accumulation of intracellular free radicals and ROS is increased by oxidative stress after injuries, and once the protective ability of the antioxidant system is surpassed, HC death happens [139, 140]. Previously, antioxidative therapies mainly focused on decreasing the ROS release or enhancing the antioxidant

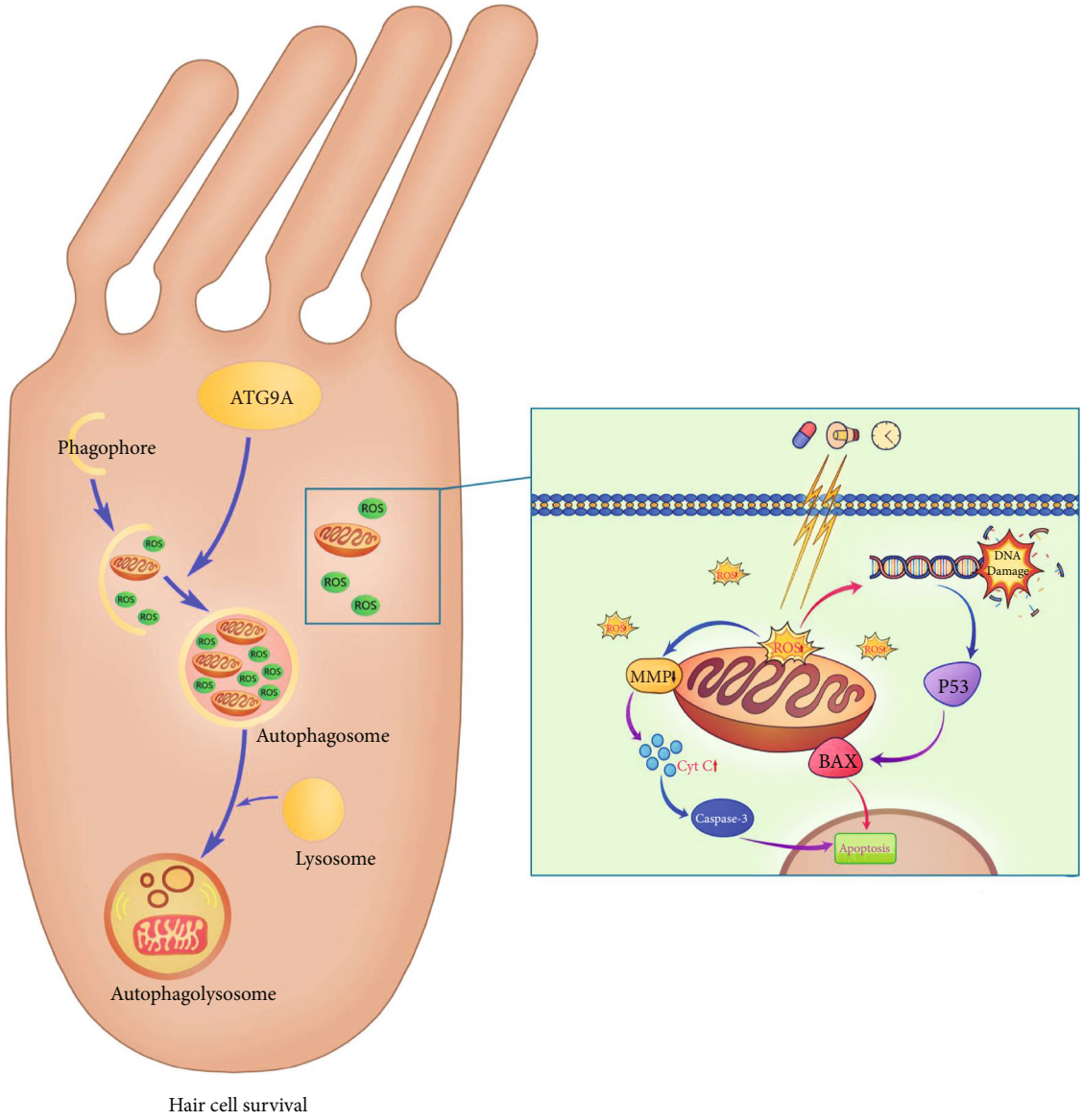

Figure 1: The correlation between autophagy and apoptosis in hair cell death.

capacity. However, the efficiency of the conventional antioxidants is obviously limited to the already damaged organelles [141]. As autophagy can remove both oxidized proteins and impaired mitochondria at the same time, it offers a novel measure for the protection of HCs by eliminating the already oxidized proteins and organelles. Thus, autophagy can not only remove ROS accumulation but also eliminate injured mitochondria, suggesting that autophagy is an ideal candidate for antioxidation therapy [142]. Several studies have confirmed that autophagy is a basic antioxidant measure. After exposure of HEI-OC-1 cells to neomycin, the activation of autophagy (by rapamycin) enhances the expression of antioxidant genes, while the inhibition of autophagy exerts an opposite effect [6]. The upregulation of autophagy level suppresses the oxidative stress, thus exerting a protective effect on the cells. Hence, the appropriate elevation of autophagy might prevent SNHL induced by multiple factors.

5.2. Epigenetic and Autophagy. As epigenetic modifications participate in various biological processes, including transcriptional regulation and cell differentiation [143, 144], the dysregulation of epigenetic modifications may lead to developmental disorders, as well as cancer [145]. Although epigenetic research was under intensive focus in other biological systems, the understanding of epigenetics in ototoxic drug/noise/aged-induced hearing loss is not yet clear. In addition to MIR-34 described above, MIR-96 is also a promising target involved in autophagy and hearing loss treatment. As the first miRNA mutation associated with human deafness, the mutation in MIR-96 results in nonsyndromic SNHL [146]. Although miRNA is an essential factor in mRNA regulation, the downstream genes of miR96 in the cochlea are yet to be identified. Recent studies on the tumor [147] and brain injury [148] suggested that ATG7 could be modulated by miR-96. ATG7 activates ATG12 and ATG8

that are the essential components in the formation of autophagosomes [149]. According to a previous study, the reduced expression of miR-96 may directly increase the level of ATG7, thereby elevating the autophagosome synthesis and autophagy hyperactivation and eventually resulting in neuronal degeneration and death [150]. However, the correlation between ATG7 and miR-96 in the auditory system remains to be elucidated.

6. Conclusion

Autophagy is involved in a variety of signaling pathways and plays a major role in the development and protection of HCs. Mitochondrion depolarization and ROS accumulation would happen when harmful stimulus exerted to HCs. If the damaged mitochondria cannot be cleared in time, the apoptosis pathway in HCs will be activated, leading to the death of HCs. However, with the activation of autophagy pathway, autophagosome could encapsulate the damaged mitochondria and fuse with lysosomes to form autophagosomes, thus degrading the damaged mitochondria and promoting the survival of HCs (Figure 1). However, autophagy seems to play a double-edged role in HC protection, some researchers believe that autophagy may aggravate HC damage, and others argue that autophagy can protect HCs from ototoxic factors, but the specific mechanism of autophagy is unclear. Along with the deepening of research, the mechanism of autophagy will be fully understood, and new treatments for hearing loss will be found in the future.

Conflicts of Interest

The authors declare no competing financial interests.

Authors' Contributions

Chang Liu, Zhiwei Zheng, and Pengjun Wang contributed equally to this work.

Acknowledgments

This work was supported by the National Natural Science Foundation of China (Nos. 82071045 and 81870728) and Shanghai Rising-Star Program (19QA1401800).

References

[1] N. Mizushima, B. Levine, A. M. Cuervo, and D. J. Klionsky, "Autophagy fights disease through cellular self-digestion," *Nature*, vol. 451, no. 7182, pp. 1069–1075, 2008.

[2] E. Janda, C. Isidoro, C. Carresi, and V. Mollace, "Defective autophagy in Parkinson's disease: role of oxidative stress," *Molecular Neurobiology*, vol. 46, no. 3, pp. 639–661, 2012.

[3] Y. Ohsumi, "Historical landmarks of autophagy research," *Cell Research*, vol. 24, no. 1, pp. 9–23, 2014.

[4] H. Zhou, X. Y. Qian, N. N. Xu et al., "Disruption of Atg7-dependent autophagy causes electromotility disturbances, outer hair cell loss, and deafness in mice," *Cell Death & Disease*, vol. 11, no. 10, p. 913, 2020.

[5] Z. H. He, S. Y. Zou, M. Li et al., "The nuclear transcription factor FoxG1 affects the sensitivity of mimetic aging hair cells to inflammation by regulating autophagy pathways," *Redox Biology*, vol. 28, 2020.

[6] Z. H. He, L. N. Guo, Y. L. Shu et al., "Autophagy protects auditory hair cells against neomycin-induced damage," *Autophagy*, vol. 13, no. 11, pp. 1884–1904, 2017.

[7] L. Yu, A. Alva, H. Su et al., "Regulation of an ATG7-beclin 1 program of autophagic cell death by caspase-8," *Science*, vol. 304, no. 5676, pp. 1500–1502, 2004.

[8] P. Boya, R. A. González-Polo, N. Casares et al., "Inhibition of macroautophagy triggers apoptosis," *Molecular and Cellular Biology*, vol. 25, no. 3, pp. 1025–1040, 2005.

[9] N. Rodriguez-Muela, F. Germain, G. Marino, P. S. Fitze, and P. Boya, "Autophagy promotes survival of retinal ganglion cells after optic nerve axotomy in mice," *Cell Death and Differentiation*, vol. 19, no. 1, pp. 162–169, 2012.

[10] J. Pang, H. Xiong, P. Lin et al., "Activation of miR-34a impairs autophagic flux and promotes cochlear cell death via repressing *ATG9A* : implications for age-related hearing loss," *Cell Death & Disease*, vol. 8, no. 10, article e3079, 2017.

[11] N. Germic, A. Hosseini, S. Yousefi, A. Karaulov, and H. U. Simon, "Regulation of eosinophil functions by autophagy," *Seminars in Immunopathology*, 2021.

[12] G. Mariño, A. F. Fernández, S. Cabrera et al., "Autophagy is essential for mouse sense of balance," *The Journal of Clinical Investigation*, vol. 120, no. 7, pp. 2331–2344, 2010.

[13] M. R. Aburto, J. M. Hurle, I. Varela-Nieto, and M. Magarinos, "Autophagy during vertebrate development," *Cell*, vol. 1, no. 3, pp. 428–448, 2012.

[14] M. P. Taylor and K. Kirkegaard, "Potential subversion of autophagosomal pathway by picornaviruses," *Autophagy*, vol. 4, no. 3, pp. 286–289, 2008.

[15] C. Jones and P. Chen, "Chapter Eight Primary cilia in planar cell polarity regulation of the inner ear," *Current Topics in Developmental Biology*, vol. 85, pp. 197–224, 2008.

[16] C. Petit and G. P. Richardson, "Linking genes underlying deafness to hair-bundle development and function," *Nature Neuroscience*, vol. 12, no. 6, pp. 703–710, 2009.

[17] S. F. Maison, J. C. Adams, and M. C. Liberman, "Olivocochlear innervation in the mouse: immunocytochemical maps, crossed versus uncrossed contributions, and transmitter colocalization," *The Journal of Comparative Neurology*, vol. 455, no. 3, pp. 406–416, 2003.

[18] H. M. Sobkowicz, J. E. Rose, G. E. Scott, and S. M. Slapnick, "Ribbon synapses in the developing intact and cultured organ of Corti in the mouse," *The Journal of Neuroscience*, vol. 2, no. 7, pp. 942–957, 1982.

[19] C. Fujimoto, S. Iwasaki, S. Urata et al., "Autophagy is essential for hearing in mice," *Cell Death & Disease*, vol. 8, no. 5, article e2780, 2017.

[20] W. Xiong, W. Wei, Y. Qi et al., "Autophagy is required for remodeling in postnatal developing ribbon synapses of cochlear inner hair cells," *Neuroscience*, vol. 431, pp. 1–16, 2020.

[21] S. Zhang, Y. Zhang, Y. Dong et al., "Knockdown of *Foxg1* in supporting cells increases the trans-differentiation of supporting cells into hair cells in the neonatal mouse cochlea," *Cellular and Molecular Life Sciences*, vol. 77, no. 7, pp. 1401–1419, 2020.

[22] Y. Zhang, S. Zhang, Z. Zhang et al., "Knockdown of *Foxg1* in Sox9+ supporting cells increases the trans-differentiation of supporting cells into hair cells in the neonatal mouse utricle," *Aging*, vol. 12, no. 20, pp. 19834–19851, 2020.

[23] S. S. Zhang, R. Y. Qiang, Y. Dong et al., "Hair cell regeneration from inner ear progenitors in the mammalian cochlea," *American Journal of Stem Cells*, vol. 9, no. 3, pp. 25–35, 2020.

[24] R. R. Guo, X. F. Ma, M. H. Liao et al., "Development and application of cochlear implant-based electric-acoustic stimulation of spiral ganglion neurons," *ACS Biomaterials Science & Engineering*, vol. 5, no. 12, pp. 6735–6741, 2019.

[25] S. S. Zhang, D. D. Liu, Y. Dong et al., "Frizzled-9+supporting cells are progenitors for the generation of hair cells in the postnatal mouse cochlea," *Frontiers in Molecular Neuroscience*, vol. 12, 2019.

[26] T. Wang, R. J. Chai, G. S. Kim et al., "Lgr5+ cells regenerate hair cells via proliferation and direct transdifferentiation in damaged neonatal mouse utricle," *Nature Communications*, vol. 6, no. 1, 2015.

[27] E. Durante-Mangoni, A. Grammatikos, R. Utili, and M. E. Falagas, "Do we still need the aminoglycosides?," *International Journal of Antimicrobial Agents*, vol. 33, no. 3, pp. 201–205, 2009.

[28] D. Baguley, D. McFerran, and D. Hall, "Tinnitus," *The Lancet*, vol. 382, no. 9904, pp. 1600–1607, 2013.

[29] J. Xie, A. E. Talaska, and J. Schacht, "New developments in aminoglycoside therapy and ototoxicity," *Hearing Research*, vol. 281, no. 1-2, pp. 28–37, 2011.

[30] Q. Yang, G. Sun, H. Yin et al., "PINK1 Protects Auditory Hair Cells and Spiral Ganglion Neurons from Cisplatin- induced Ototoxicity via Inducing Autophagy and Inhibiting JNK Signaling Pathway," *Free Radical Biology & Medicine*, vol. 120, pp. 342–355, 2018.

[31] A. M. Pickrell and R. J. Youle, "The Roles of PINK1, Parkin, and Mitochondrial Fidelity in Parkinson's Disease," *Neuron*, vol. 85, no. 2, pp. 257–273, 2015.

[32] Q. Yang, Y. Zhou, H. Yin et al., "PINK1 protects against gentamicin-induced sensory hair cell damage: possible relation to induction of autophagy and inhibition of p 53 signal pathway," *Frontiers in Molecular Neuroscience*, vol. 11, p. 403, 2018.

[33] G. Ristic, W. L. Tsou, and S. V. Todi, "An optimal ubiquitin-proteasome pathway in the nervous system: the role of deubiquitinating enzymes," *Frontiers in Molecular Neuroscience*, vol. 7, p. 72, 2014.

[34] F. E. Magraoui, C. Reidick, H. E. Meyer, and H. W. Platta, "Autophagy-related deubiquitinating enzymes involved in health and disease," *Cell*, vol. 4, no. 4, pp. 596–621, 2015.

[35] S. Costes, T. Gurlo, J. F. Rivera, and P. C. Butler, "UCHL1 deficiency exacerbates human islet amyloid polypeptide toxicity in β-cells," *Autophagy*, vol. 10, no. 6, pp. 1004–1014, 2014.

[36] Y. J. Kim, K. Kim, Y. Y. Lee, O. S. Choo, J. H. Jang, and Y. H. Choung, "Downregulated UCHL1 accelerates gentamicin-induced auditory cell death via autophagy," *Molecular Neurobiology*, vol. 56, no. 11, pp. 7433–7447, 2019.

[37] B. S. Nayak, S. S. Raju, and A. V. Chalapathi Rao, "Wound healing activity of Persea americana (avocado) fruit: a preclinical study on rats," *Journal of Wound Care*, vol. 17, no. 3, pp. 123–125, 2008.

[38] O. Ortiz-Avila, M. Esquivel-Martinez, B. E. Olmos-Orizaba, A. Saavedra-Molina, A. R. Rodriguez-Orozco, and C. Cortes-Rojo, "Avocado oil improves mitochondrial function and decreases oxidative stress in brain of diabetic rats," *Journal Diabetes Research*, vol. 2015, article 485759, 9 pages, 2015.

[39] T. N. M. Pham, S. Y. Jeong, D. H. Kim et al., "Protective mechanisms of avocado oil extract against ototoxicity," *Nutrients*, vol. 12, no. 4, p. 947, 2020.

[40] D. V. T. Catenacci, N. C. Tebbutt, I. Davidenko et al., "Rilotumumab plus epirubicin, cisplatin, and capecitabine as first-line therapy in advanced MET-positive gastric or gastro-oesophageal junction cancer (RILOMET-1): a randomised, double-blind, placebo-controlled, phase 3 trial," *The Lancet Oncology*, vol. 18, no. 11, pp. 1467–1482, 2017.

[41] M. L. Telli, K. M. Timms, J. Reid et al., "Homologous recombination deficiency (HRD) score predicts response to platinum-containing neoadjuvant chemotherapy in patients with triple-negative breast cancer," *Clinical Cancer Research*, vol. 22, no. 15, pp. 3764–3773, 2016.

[42] S. Gao, C. Cheng, M. H. Wang et al., "Blebbistatin inhibits neomycin-induced apoptosis in hair cell-like HEI-OC-1 cells and in cochlear hair cells," *Frontiers in Cellular Neuroscience*, vol. 13, 2020.

[43] Y. Q. Zhang, W. Li, Z. H. He et al., "Pre-treatment with fasudil prevents neomycin-induced hair cell damage by reducing the accumulation of reactive oxygen species," *Frontiers in Molecular Neuroscience*, vol. 12, 2019.

[44] L. Liu, Y. Chen, J. Qi et al., "Wnt activation protects against neomycin-induced hair cell damage in the mouse cochlea," *Cell Death & Disease*, vol. 7, no. 3, p. e2136, 2016.

[45] Z. H. Zhong, X. L. Fu, H. Li et al., "Citicoline protects auditory hair cells against neomycin-induced damage," *Frontiers in Cell and Development Biology*, vol. 8, 2020.

[46] Z. H. He, Q. J. Fang, H. Li et al., "The role of FOXG1 in the postnatal development and survival of mouse cochlear hair cells," *Neuropharmacology*, vol. 144, pp. 43–57, 2019.

[47] J. Choi, S. H. Kim, Y. C. Rah et al., "Effects of caffeic acid on cisplatin-induced hair cell damage in HEI-OC1 auditory cells," *International Journal of Pediatric Otorhinolaryngology*, vol. 78, no. 12, pp. 2198–2204, 2014.

[48] W. W. Liu, X. C. Xu, Z. M. Fan et al., "Wnt signaling activates TP53-induced glycolysis and apoptosis regulator and protects against cisplatin-induced spiral ganglion neuron damage in the mouse cochlea," *Antioxidants & Redox Signaling*, vol. 30, no. 11, pp. 1389–1410, 2019.

[49] H. Li, Y. D. Song, Z. H. He et al., "Meclofenamic acid reduces reactive oxygen species accumulation and apoptosis, inhibits excessive autophagy, and protects hair cell-like HEI-OC1 cells from cisplatin-induced damage," *Frontiers in Cellular Neuroscience*, vol. 12, 2018.

[50] X. Wang, Z. Lu, A. Gomez et al., "N^6-methyladenosine-dependent regulation of messenger RNA stability," *Nature*, vol. 505, no. 7481, pp. 117–120, 2014.

[51] Y. Huang, J. Yan, Q. Li et al., "Meclofenamic acid selectively inhibits FTO demethylation of m^6A over ALKBH5," *Nucleic Acids Research*, vol. 43, no. 1, pp. 373–384, 2015.

[52] B. Andersen and M. G. Rosenfeld, "POU domain factors in the neuroendocrine system: lessons from developmental biology provide insights into human disease," *Endocrine Reviews*, vol. 22, no. 1, pp. 2–35, 2001.

[53] H. J. Kim, H. H. Won, K. J. Park et al., "SNP linkage analysis and whole exome sequencing identify a novel *POU4F3* mutation in autosomal dominant late-onset nonsyndromic hearing loss (DFNA15)," *PLoS One*, vol. 8, no. 11, article e79063, 2013.

[54] M. Xiang, W. Q. Gao, T. Hasson, and J. J. Shin, "Requirement for Brn-3c in maturation and survival, but not in fate determination of inner ear hair cells," *Development*, vol. 125, no. 20, pp. 3935–3946, 1998.

[55] L. Erkman, R. J. McEvilly, L. Luo et al., "Role of transcription factors a Brn-3.1 and Brn-3.2 in auditory and visual system development," *Nature*, vol. 381, no. 6583, pp. 603–606, 1996.

[56] F. Xu, W. Yan, and Y. Cheng, "Pou4f3 gene mutation promotes autophagy and apoptosis of cochlear hair cells in cisplatin-induced deafness mice," *Archives of Biochemistry and Biophysics*, vol. 680, article 108224, 2020.

[57] T. Kaur, D. Mukherjea, K. Sheehan, S. Jajoo, L. P. Rybak, and V. Ramkumar, "Short interfering RNA against STAT1 attenuates cisplatin-induced ototoxicity in the rat by suppressing inflammation," *Cell Death & Disease*, vol. 2, no. 7, article e180, 2011.

[58] N. C. Schmitt, E. W. Rubel, and N. M. Nathanson, "Cisplatin-induced hair cell death requires STAT1 and is attenuated by epigallocatechin gallate," *The Journal of Neuroscience*, vol. 29, no. 12, pp. 3843–3851, 2009.

[59] S. Levano and D. Bodmer, "Loss of STAT1 protects hair cells from ototoxicity through modulation of STAT3, c-Jun, Akt, and autophagy factors," *Cell Death & Disease*, vol. 6, no. 12, article e2019, 2015.

[60] F. Takahashi-Yanaga, "Activator or inhibitor? GSK-3 as a new drug target," *Biochemical Pharmacology*, vol. 86, no. 2, pp. 191–199, 2013.

[61] D. Wu and W. Pan, "GSK3: a multifaceted kinase in Wnt signaling," *Trends in Biochemical Sciences*, vol. 35, no. 3, pp. 161–168, 2010.

[62] J. Y. Qi, L. Y. Zhang, F. Z. Tan et al., "Espin distribution as revealed by super-resolution microscopy of stereocilia," *American Journal of Translational Research*, vol. 12, no. 1, pp. 130–141, 2020.

[63] J. Y. Qi, Y. Liu, C. F. Chu et al., "A cytoskeleton structure revealed by super-resolution fluorescence imaging in inner ear hair cells," *Cell Discovery*, vol. 5, no. 1, 2019.

[64] A. Li, D. You, W. Y. Li et al., "Novel compounds protect auditory hair cells against gentamycin-induced apoptosis by maintaining the expression level of H3K4me2," *Drug Delivery*, vol. 25, no. 1, pp. 1033–1043, 2018.

[65] X. Y. Yu, W. W. Liu, Z. M. Fan et al., "c-Myb knockdown increases the neomycin-induced damage to hair-cell-like HEI- OC1 cells in vitro," *Scientific Reports*, vol. 7, no. 1, 2017.

[66] I. Azoulay-Alfaguter, R. Elya, L. Avrahami, A. Katz, and H. Eldar-Finkelman, "Combined regulation of mTORC1 and lysosomal acidification by GSK-3 suppresses autophagy and contributes to cancer cell growth," *Oncogene*, vol. 34, no. 35, pp. 4613–4623, 2015.

[67] J. Kubisch, D. Türei, L. Földvári-Nagy et al., "Complex regulation of autophagy in cancer - integrated approaches to discover the networks that hold a double-edged sword," *Seminars in Cancer Biology*, vol. 23, no. 4, pp. 252–261, 2013.

[68] T. Liu, S. Zong, P. Luo et al., "Enhancing autophagy by down-regulating GSK-3β alleviates cisplatin-induced ototoxicity in vivo and in vitro," *Toxicology Letters*, vol. 313, pp. 11–18, 2019.

[69] A. A. Abdul-Sater, N. Saïd-Sadier, V. M. Lam et al., "Enhancement of reactive oxygen species production and chlamydial infection by the mitochondrial Nod-like family member NLRX1," *The Journal of Biological Chemistry*, vol. 285, no. 53, pp. 41637–41645, 2010.

[70] Y. Lei, H. Wen, Y. Yu et al., "The mitochondrial proteins NLRX1 and TUFM form a complex that regulates type I interferon and autophagy," *Immunity*, vol. 36, no. 6, pp. 933–946, 2012.

[71] Y. Lei, H. Wen, and J. P. Ting, "The NLR protein, NLRX1, and its partner, TUFM, reduce type I interferon, and enhance autophagy," *Autophagy*, vol. 9, no. 3, pp. 432-433, 2013.

[72] E. Imbeault, T. M. Mahvelati, R. Braun, P. Gris, and D. Gris, "Nlrx1 regulates neuronal cell death," *Molecular Brain*, vol. 7, no. 1, 2014.

[73] S. Coutermarsh-Ott, A. Simmons, V. Capria et al., "NLRX1 suppresses tumorigenesis and attenuates histiocytic sarcoma through the negative regulation of NF-λB signaling," *Oncotarget*, vol. 7, no. 22, pp. 33096–33110, 2016.

[74] H. Yin, G. Sun, Q. Yang et al., "NLRX1 accelerates cisplatin-induced ototoxity in HEI-OC1 cells via promoting generation of ROS and activation of JNK signaling pathway," *Scientific Reports*, vol. 7, no. 1, article 44311, 2017.

[75] H. Yin, Q. Yang, Z. Cao et al., "Activation of NLRX1-mediated autophagy accelerates the ototoxic potential of cisplatin in auditory cells," *Toxicology and Applied Pharmacology*, vol. 343, pp. 16–28, 2018.

[76] Z. H. He, S. Sun, M. Waqas et al., "Reduced TRMU expression increases the sensitivity of hair-cell-like HEI-OC-1 cells to neomycin damage in vitro," *Scientific Reports*, vol. 6, no. 1, 2016.

[77] M. Guan, Q. J. Fang, Z. H. He et al., "Inhibition of ARC decreases the survival of HEI-OC-1 cells after neomycin damage in vitro," *Oncotarget*, vol. 7, no. 41, pp. 66647–66659, 2016.

[78] S. Sun, M. Z. Sun, Y. P. Zhang et al., "*In vivo* overexpression of X-linked inhibitor of apoptosis protein protects against neomycin-induced hair cell loss in the apical turn of the cochlea during the ototoxic-sensitive period," *Frontiers in Cellular Neuroscience*, vol. 8, 2014.

[79] P. J. Vernon and D. Tang, "Eat-me: autophagy, phagocytosis, and reactive oxygen species signaling," *Antioxidants & Redox Signaling*, vol. 18, no. 6, pp. 677–691, 2013.

[80] H. Yuan, X. Wang, K. Hill et al., "Autophagy attenuates noise-induced hearing loss by reducing oxidative stress," *Antioxidants & Redox Signaling*, vol. 22, no. 15, pp. 1308–1324, 2015.

[81] S. Delmaghani, J. Defourny, A. Aghaie et al., "Hypervulnerability to sound exposure through impaired adaptive proliferation of peroxisomes," *Cell*, vol. 163, no. 4, pp. 894–906, 2015.

[82] J. Defourny, A. Aghaie, I. Perfettini, P. Avan, S. Delmaghani, and C. Petit, "Pejvakin-mediated pexophagy protects auditory hair cells against noise-induced damage," *Proceedings of the National Academy of Sciences of the United States of America*, vol. 116, no. 16, pp. 8010–8017, 2019.

[83] J. J. Smith and J. D. Aitchison, "Peroxisomes take shape," *Nature Reviews. Molecular Cell Biology*, vol. 14, no. 12, pp. 803–817, 2013.

[84] M. Schrader, N. A. Bonekamp, and M. Islinger, "Fission and proliferation of peroxisomes," *Biochimica et Biophysica Acta*, vol. 1822, no. 9, pp. 1343–1357, 2012.

[85] A. L. Anding and E. H. Baehrecke, "Cleaning house: selective autophagy of organelles," *Developmental Cell*, vol. 41, no. 1, pp. 10–22, 2017.

[86] C. Lismont, M. Nordgren, P. P. Van Veldhoven, and M. Fransen, "Redox interplay between mitochondria and peroxisomes," *Frontiers in Cell and Development Biology*, vol. 3, 2015.

[87] J. M. Bhatt, N. Bhattacharyya, and H. W. Lin, "Relationships between tinnitus and the prevalence of anxiety and depression," *Laryngoscope*, vol. 127, no. 2, pp. 466–469, 2017.

[88] T. Pan, R. S. Tyler, H. Ji, C. Coelho, and S. A. Gogel, "Differences among patients that make their tinnitus worse or better," *American Journal of Audiology*, vol. 24, no. 4, pp. 469–476, 2015.

[89] R. E. Gonzalez-Castañeda, A. Y. Galvez-Contreras, C. J. Martínez-Quezada et al., "Sex-related effects of sleep deprivation on depressive- and anxiety-like behaviors in mice," *Experimental Animals*, vol. 65, no. 1, pp. 97–107, 2016.

[90] P. Bonaldo and M. Sandri, "Cellular and molecular mechanisms of muscle atrophy," *Disease Models & Mechanisms*, vol. 6, no. 1, pp. 25–39, 2013.

[91] K. E. Rarey, L. M. Curtis, and W. J. F. ten Cate, "Tissue specific levels of glucocorticoid receptor within the rat inner ear," *Hearing Research*, vol. 64, no. 2, pp. 205–210, 1993.

[92] Y. Tahera, I. Meltser, P. Johansson, A. C. Hansson, and B. Canlon, "Glucocorticoid receptor and nuclear factor-κB interactions in restraint stress-mediated protection against acoustic trauma," *Endocrinology*, vol. 147, no. 9, pp. 4430–4437, 2006.

[93] K. Takemura, M. Komeda, M. Yagi et al., "Direct inner ear infusion of dexamethasone attenuates noise-induced trauma in guinea pig," *Hearing Research*, vol. 196, no. 1-2, pp. 58–68, 2004.

[94] I. Meltser, Y. Tahera, and B. Canlon, "Glucocorticoid receptor and mitogen-activated protein kinase activity after restraint stress and acoustic trauma," *Journal of Neurotrauma*, vol. 26, no. 10, pp. 1835–1845, 2009.

[95] P. Li, D. Bing, S. Wang et al., "Sleep deprivation modifies noise-induced cochlear injury related to the stress hormone and autophagy in female mice," *Frontiers in Neuroscience*, vol. 13, p. 1297, 2019.

[96] C. Y. Chao, J. S. Wu, Y. C. Yang et al., "Sleep duration is a potential risk factor for newly diagnosed type 2 diabetes mellitus," *Metabolism*, vol. 60, no. 6, pp. 799–804, 2011.

[97] M. R. Irwin, "Why sleep is important for health: a psychoneuroimmunology perspective," *Annual Review of Psychology*, vol. 66, no. 1, pp. 143–172, 2015.

[98] M. Cheslock and O. De Jesus, *Presbycusis*, Stat Pearls, Treasure Island (FL), 2020.

[99] X. L. Fu, X. Y. Sun, L. Q. Zhang et al., "Tuberous sclerosis complex-mediated mTORC1 overactivation promotes age-related hearing loss," *The Journal of Clinical Investigation*, vol. 128, no. 11, pp. 4938–4955, 2018.

[100] Y. Y. Ding, W. Meng, W. J. Kong, Z. H. He, and R. J. Chai, "The role of FoxG1 in the inner ear," *Frontiers in Cell and Development Biology*, vol. 8, 2020.

[101] Y. Liu, J. Y. Qi, X. Chen et al., "Critical role of spectrin in hearing development and deafness," *Science Advances*, vol. 5, no. 4, p. eaav7803, 2019.

[102] C. Cheng, Y. F. Wang, L. Guo et al., "Age-related transcriptome changes in Sox2+supporting cells in the mouse cochlea," *Stem Cell Research & Therapy*, vol. 10, no. 1, 2019.

[103] N. C. Homans, R. M. Metselaar, J. G. Dingemanse et al., "Prevalence of age-related hearing loss, including sex differences, in older adults in a large cohort study," *The Laryngoscope*, vol. 127, no. 3, pp. 725–730, 2017.

[104] T. Takeda, M. Hosokawa, S. Takeshita et al., "A new murine model of accelerated senescence," *Mechanisms of Ageing and Development*, vol. 17, no. 2, pp. 183–194, 1981.

[105] J. Menardo, Y. Tang, S. Ladrech et al., "Oxidative stress, inflammation, and autophagic stress as the key mechanisms of premature age-related hearing loss in SAMP8 mouse cochlea," *Antioxidants & Redox Signaling*, vol. 16, no. 3, pp. 263–274, 2012.

[106] H. Xiong, J. Pang, H. Yang et al., "Activation of miR-34a/SIRT1/p53 signaling contributes to cochlear hair cell apoptosis: implications for age-related hearing loss," *Neurobiology of Aging*, vol. 36, no. 4, pp. 1692–1701, 2015.

[107] Q. Zhang, H. Liu, J. McGee, E. J. Walsh, G. A. Soukup, and D. Z. He, "Identifying MicroRNAs involved in degeneration of the organ of Corti during age-related hearing loss," *PLoS One*, vol. 8, no. 4, article e62786, 2013.

[108] J. Yang, D. Chen, Y. He et al., "MiR-34 modulates *Caenorhabditis elegans* lifespan via repressing the autophagy gene atg9," *Age*, vol. 35, no. 1, pp. 11–22, 2013.

[109] N. Liu, M. Landreh, K. Cao et al., "The microRNA miR-34 modulates ageing and neurodegeneration in *Drosophila*," *Nature*, vol. 482, no. 7386, pp. 519–523, 2012.

[110] Y. Yang, H. W. Cheng, Y. Qiu et al., "MicroRNA-34a plays a key role in cardiac repair and regeneration following myocardial infarction," *Circulation Research*, vol. 117, no. 5, pp. 450–459, 2015.

[111] R. Huang, Y. Xu, W. Wan et al., "Deacetylation of nuclear LC3 drives autophagy initiation under starvation," *Molecular Cell*, vol. 57, no. 3, pp. 456–466, 2015.

[112] R. Huang and W. Liu, "Identifying an essential role of nuclear LC3 for autophagy," *Autophagy*, vol. 11, no. 5, pp. 852-853, 2015.

[113] M. Morita, S. P. Gravel, V. Chénard et al., "mTORC1 controls mitochondrial activity and biogenesis through 4E-BP-dependent translational regulation," *Cell Metabolism*, vol. 18, no. 5, pp. 698–711, 2013.

[114] E. F. Fang, M. Scheibye-Knudsen, L. E. Brace et al., "Defective Mitophagy in XPA via PARP-1 Hyperactivation and NAD^+/-SIRT1 Reduction," *Cell*, vol. 157, no. 4, pp. 882–896, 2014.

[115] H. Xiong, S. Chen, L. Lai et al., "Modulation of miR-34a/SIRT1 signaling protects cochlear hair cells against oxidative stress and delays age-related hearing loss through coordinated regulation of mitophagy and mitochondrial biogenesis," *Neurobiology of Aging*, vol. 79, pp. 30–42, 2019.

[116] Y. J. Yoon and S. Hellstrom, "Ultrastructural characteristics of the round window membrane during pneumococcal otitis media in rat," *Journal of Korean Medical Science*, vol. 17, no. 2, pp. 230–235, 2002.

[117] H. Kawauchi, T. F. DeMaria, and D. J. Lim, "Endotoxin permeability through the round window," *Acta Oto-Laryngologica. Supplementum*, vol. 457, pp. 100–115, 1989.

[118] J. M. Platnich, H. Chung, A. Lau et al., "Shiga toxin/lipopolysaccharide activates caspase-4 and gasdermin D to trigger mitochondrial reactive oxygen species upstream of the NLRP3 inflammasome," *Cell Reports*, vol. 25, no. 6, pp. 1525–1536.e7, 2018.

[119] W. Abdulmahdi, D. Patel, M. M. Rabadi et al., "HMGB1 redox during sepsis," *Redox Biology*, vol. 13, pp. 600–607, 2017.

[120] S. da Silveira Cruz-Machado, C. E. Carvalho-Sousa, E. K. Tamura et al., "TLR4 and CD14 receptors expressed in rat pineal gland trigger NFKB pathway," *Journal of Pineal Research*, vol. 49, no. 2, pp. 183–192, 2010.

[121] M. A. Khan, A. Farahvash, D. N. Douda et al., "JNK activation turns on LPS- and gram-negative bacteria-induced NADPH oxidase-dependent suicidal NETosis," *Scientific Reports*, vol. 7, no. 1, p. 3409, 2017.

[122] C. H. Hwang, A. Simeone, E. Lai, and D. K. Wu, "*Foxg1* is required for proper separation and formation of sensory cristae during inner ear development," *Developmental Dynamics*, vol. 238, no. 11, pp. 2725–2734, 2009.

[123] M. Brancaccio, C. Pivetta, M. Granzotto, C. Filippis, and A. Mallamaci, "*Emx2* and *Foxg1* inhibit gliogenesis and promote neuronogenesis," *Stem Cells*, vol. 28, no. 7, pp. 1206–1218, 2010.

[124] S. G. Dastidar, P. M. Landrieu, and S. R. D'Mello, "FoxG1 promotes the survival of postmitotic neurons," *The Journal of Neuroscience*, vol. 31, no. 2, pp. 402–413, 2011.

[125] L. Pancrazi, G. di Benedetto, L. Colombaioni et al., "Foxg1 localizes to mitochondria and coordinates cell differentiation and bioenergetics," *Proceedings of the National Academy of Sciences of the United States of America*, vol. 112, no. 45, pp. 13910–13915, 2015.

[126] M. T. Bohnsack and K. E. Sloan, "The mitochondrial epitranscriptome: the roles of RNA modifications in mitochondrial translation and human disease," *Cellular and Molecular Life Sciences*, vol. 75, no. 2, pp. 241–260, 2018.

[127] F. Meng, M. Zhou, Y. Xiao et al., "A deafness-associated tRNA mutation caused pleiotropic effects on the m^1G37 modification, processing, stability and aminoacylation of $tRNA^{Ile}$ and mitochondrial translation," *Nucleic Acids Research*, vol. 49, no. 2, pp. 1075–1093, 2021.

[128] S. Murillo-Cuesta, L. Rodríguez-de la Rosa, R. Cediel, L. Lassaletta, and I. Varela-Nieto, "The role of insulin-like growth factor-I in the physiopathology of hearing," *Frontiers in Molecular Neuroscience*, vol. 4, p. 11, 2011.

[129] A. Sobolewska, M. Gajewska, J. Zarzynska, B. Gajkowska, and T. Motyl, "IGF-I, EGF, and sex steroids regulate autophagy in bovine mammary epithelial cells via the mTOR pathway," *European Journal of Cell Biology*, vol. 88, no. 2, pp. 117–130, 2009.

[130] M. Bains, M. L. Florez-McClure, and K. A. Heidenreich, "Insulin-like growth factor-I prevents the accumulation of autophagic vesicles and cell death in purkinje neurons by increasing the rate of autophagosome-to- lysosome fusion and degradation," *The Journal of Biological Chemistry*, vol. 284, no. 30, pp. 20398–20407, 2009.

[131] R. de Iriarte Rodríguez, S. Pulido, L. Rodríguez-de la Rosa, M. Magariños, and I. Varela-Nieto, "Age-regulated function of autophagy in the mouse inner ear," *Hearing Research*, vol. 330, no. Part A, pp. 39–50, 2015.

[132] C. Kim, J. H. Sohn, M. U. Jang et al., "Ischemia as a potential etiologic factor in idiopathic unilateral sudden sensorineural hearing loss: analysis of posterior circulation arteries," *Hearing Research*, vol. 331, pp. 144–151, 2016.

[133] C. D. Lin, I. H. Wei, M. H. Tsai et al., "Changes in guinea pig cochlea after transient cochlear ischemia," *Neuroreport*, vol. 21, no. 15, pp. 968–975, 2010.

[134] T. Yoshida, N. Hakuba, I. Morizane et al., "Hematopoietic stem cells prevent hair cell death after transient cochlear ischemia through paracrine effects," *Neuroscience*, vol. 145, no. 3, pp. 923–930, 2007.

[135] M. Yoshioka, Y. Uchida, S. Sugiura et al., "The impact of arterial sclerosis on hearing with and without occupational noise exposure: a population-based aging study in males," *Auris Nasus Larynx*, vol. 37, no. 5, pp. 558–564, 2010.

[136] B. Mazurek, H. Haupt, P. Georgiewa, B. F. Klapp, and A. Reisshauer, "A model of peripherally developing hearing loss and tinnitus based on the role of hypoxia and ischemia," *Medical Hypotheses*, vol. 67, no. 4, pp. 892–899, 2006.

[137] H. Yang, J. Pang, H. Xiong et al., "The protective effect of autophagy on ischemia/reperfusion-induced hearing loss: implications for sudden hearing loss," *Neuroreport*, vol. 28, no. 17, pp. 1157–1163, 2017.

[138] B. Fang and H. Xiao, "Rapamycin alleviates cisplatin-induced ototoxicity in vivo," *Biochemical and Biophysical Research Communications*, vol. 448, no. 4, pp. 443–447, 2014.

[139] T. Finkel and N. J. Holbrook, "Oxidants, oxidative stress and the biology of ageing," *Nature*, vol. 408, no. 6809, pp. 239–247, 2000.

[140] U. Lechowicz, A. Pollak, D. Raj-Koziak et al., "Tinnitus in patients with hearing loss due to mitochondrial DNA pathogenic variants," *European Archives of Oto-Rhino-Laryngology*, vol. 275, no. 8, pp. 1979–1985, 2018.

[141] H. Sies, "Oxidative stress: a concept in redox biology and medicine," *Redox Biology*, vol. 4, pp. 180–183, 2015.

[142] S. Giordano, V. Darley-Usmar, and J. Zhang, "Autophagy as an essential cellular antioxidant pathway in neurodegenerative disease," *Redox Biology*, vol. 2, pp. 82–90, 2014.

[143] M. J. Provenzano and F. E. Domann, "A role for epigenetics in hearing: establishment and maintenance of auditory specific gene expression patterns," *Hearing Research*, vol. 233, no. 1-2, pp. 1–13, 2007.

[144] W. Reik, "Stability and flexibility of epigenetic gene regulation in mammalian development," *Nature*, vol. 447, no. 7143, pp. 425–432, 2007.

[145] W. S. Layman and J. Zuo, "Epigenetic regulation in the inner ear and its potential roles in development, protection, and regeneration," *Frontiers in Cellular Neuroscience*, vol. 8, p. 446, 2015.

[146] Á. Mencía, S. Modamio-Høybjør, N. Redshaw et al., "Mutations in the seed region of human miR-96 are responsible for nonsyndromic progressive hearing loss," *Nature Genetics*, vol. 41, no. 5, pp. 609–613, 2009.

[147] Z. W. Zhang, Y. Wu, S. Yuan et al., "Glutathione peroxidase 4 participates in secondary brain injury through mediating ferroptosis in a rat model of intracerebral hemorrhage," *Brain Research*, vol. 1701, pp. 112–125, 2018.

[148] J. Gan, Q. Cai, Y. Qu et al., "miR-96 attenuates status epilepticus-induced brain injury by directly targeting Atg7

and Atg16L1," *Scientific Reports*, vol. 7, no. 1, article 10270, 2017.

[149] S. B. Hong, B. W. Kim, K. E. Lee et al., "Insights into noncanonical E1 enzyme activation from the structure of autophagic E1 Atg7 with Atg8," *Nature Structural & Molecular Biology*, vol. 18, no. 12, pp. 1323–1330, 2011.

[150] U. Bandyopadhyay, M. Nagy, W. A. Fenton, and A. L. Horwich, "Absence of lipofuscin in motor neurons of SOD1-linked ALS mice," *Proceedings of the National Academy of Sciences of the United States of America*, vol. 111, no. 30, pp. 11055–11060, 2014.

Hindawi
Neural Plasticity
Volume 2021, Article ID 8706400, 10 pages
https://doi.org/10.1155/2021/8706400

Research Article

Hyperoside Attenuate Inflammation in HT22 Cells via Upregulating SIRT1 to Activities Wnt/β-Catenin and Sonic Hedgehog Pathways

Jin Huang,[1] Liang Zhou,[2] Jilin Chen,[3] Tingbao Chen,[3] Bo Lei,[4,5] Niandong Zheng,[5] Xiaoqiang Wan,[5] Jianguo Xu,[4] and Tinghua Wang[1]

[1]*Institute of Neuroscience, Basic Medical College, Kunming Medical University, Kunming, Yunnan 650500, China*
[2]*Department of Neurology, Zhenxiong County People Hospital, Zhaotong, Yunnan Province, China*
[3]*Department of Animal Zoology, Kunming Medical University, Kunming, Yunnan Province, China*
[4]*Department of Neurosurgery, West-China Hospital, Sichuan University, Chengdu, Sichuan 610041, China*
[5]*Neurosurgery of the People's Hospital of Leshan, Leshan 614000, China*

Correspondence should be addressed to Tinghua Wang; wth20210506@163.com

Jin Huang and Liang Zhou contributed equally to this work.

Received 18 April 2021; Accepted 3 June 2021; Published 11 June 2021

Academic Editor: Renjie Chai

Neuroinflammation plays important roles in the pathogenesis and progression of altered neurodevelopment, sensorineural hearing loss, and certain neurodegenerative diseases. Hyperoside (quercetin-3-O-β-D-galactoside) is an active compound isolated from Hypericum plants. In this study, we investigate the protective effect of hyperoside on neuroinflammation and its possible molecular mechanism. Lipopolysaccharide (LPS) and hyperoside were used to treat HT22 cells. The cell viability was measured by MTT assay. The cell apoptosis rate was measured by flow cytometry assay. The mRNA expression levels of interleukin-1β (IL-1β), interleukin-6 (IL-6), interleukin-8 (IL-8), and tumor necrosis factor-α (TNF-α) were determined by quantitative reverse transcription polymerase chain reaction. The levels of oxidative stress indices superoxide dismutase (SOD), reactive oxygen species (ROS), catalase (CAT), glutathione (GSH), and malondialdehyde (MDA) were measured by the kits. The expression of neurotrophic factor and the relationship among hyperoside, silent mating type information regulation 2 homolog-1 (SIRT1) and Wnt/β-catenin, and sonic hedgehog was examined by western blotting. In the LPS-induced HT22 cells, hyperoside promotes cell survival; alleviates the level of IL-1β, IL-6, IL-8, TNF-α, ROS, MDA, Bax, and caspase-3; and increases the expression of CAT, SOD, GSH, Bcl-2, BDNF, TrkB, and NGF. In addition, hyperoside upregulated the expression of SIRT1. Further mechanistic investigation showed that hyperoside alleviated LPS-induced inflammation, oxidative stress, and apoptosis by upregulating SIRT1 to activate Wnt/β-catenin and sonic hedgehog pathways. Taken together, our data suggested that hyperoside acts as a protector in neuroinflammation.

1. Introduction

Neuroinflammation is a chronic inflammation of brain tissue, which plays an important role in the pathogenesis and progression of altered neurodevelopment, sensorineural hearing loss, and certain neurodegenerative diseases [1–5]. In the early stages of the central auditory pathway, noise-induced hearing loss and conductive hearing loss are related to neuroinflammation [6]. In addition, neuroinflammation contributes to neuronal death and neurological deterioration by increasing the production of proinflammatory factors and oxidative stress [7]. Numerous studies have shown that hippocampal neurons are susceptible to neuroinflammatory and cause neurological complications [8]. However, there are still no effective agents or methods to restore and prevent neuronal damage caused by neuroinflammation. Thus, the

identification of effective inflammatory protective candidate agents is crucial.

Hyperoside (quercetin3-O-β-D-galactoside) is an active compound isolated from Hypericum plants. It has antioxidant and anti-inflammatory activities, decreasing calcium overload and inhibiting apoptosis [9, 10]. Previous studies have confirmed that hyperoside effectively prevents neurological complications caused by neuroinflammation. In the hyperglycemia-induced oxidative stress and inflammation acute diabetes model, the administration of hyperoside prevented cognitive dysfunction, neuroinflammation, and oxidative stress caused by DM through the TNF-α/NF-κB/caspase-3 signaling pathway [11]. In diseases such as Parkinson's disease, hyperoside acts as a protective agent by attenuating LPS-induced activation of microglia [12]. So far, there are few studies on the protective effect of hyperoside on neuroinflammation, and the mechanism has not been fully elucidated.

Lipopolysaccharide (LPS) is widely used to activate the innate immune system. Previous studies have shown that LPS is usually used to prepare neuroinflammation models induced by inflammatory response [13, 14]. In this study, we exposed HT22 cells to LPS to mimic a cellular model of neuroinflammation. Simultaneously, the protective effect of hyperoside on neuroinflammation and its possible molecular mechanism were studied through this model. We found that hyperoside protects HT22 cells from LPS-induced inflammation; oxidative stress and apoptosis are closely related to SIRT1 levels. Further analysis showed that hyperoside alleviated LPS-induced inflammation, oxidative stress, and apoptosis by upregulating SIRT1 to activate Wnt/β-catenin and sonic hedgehog pathways.

2. Materials and Methods

2.1. Reagents and Drugs. LPS, hyperoside, and 3-(4,5-dimethyl-2-thiazolyl)-2,5-diphenyltetrazolium bromide (MTT) were purchased from Sigma-Aldrich (St. Louis, MO, USA). Dulbecco's modified Eagle medium containing 10% fetal bovine serum (FBS) was purchased from Gibco (Carlsbad, USA). 100 U/ml penicillin and 100 mg/ml streptomycin were purchased from Sigma-Aldrich (St. Louis, MO, USA). LiCl and sonic hedgehog agonist SAg were purchased from Merck (San Diego, CA, USA). Primary antibodies against Bcl-2, Bax, caspase-3, BDNF, NGF, SIRT1, Wnt1, β-catenin, Shh, Patch, and GAPDH and secondary antibodies were all purchased from Cell Signaling (Boston, MA, USA).

2.2. Cell Culture and Treatments. The HT22 murine neuronal cell line was purchased from Kunming Cell Bank of the Chinese Academy of Sciences (Kunming, China). HT22 cells were seeded at 2×10^4 cells/well in a 6-well plate and cultured in the DMEM with 10% fetal bovine serum, 100 U/ml penicillin, and 100 μg/ml streptomycin at 37°C in a 5% CO_2 humidified incubator. When HT22 reached 70% confluency after 24 h, cell transfection pretreated with different concentrations of hyperoside and LPS (1 μg/ml) was performed.

2.3. Cell Viability. Cell viability was determined by MTT assay. Briefly, the HT22 cells seeded into 24-well plates at a density of 2×10^4 cells/ml for 24 h. Cells were starved overnight and then pretreated with different concentrations of hyperoside for 24 h followed by incubation with LPS (1 μg/ml) for another 24 h. The medium was refreshed and incubated with 50 μl of MTT (5 mg/ml prepared in phosphate-buffered saline) for 4 h at 37°C. Next, the solution was removed and added DMSO to plates. The absorbance at 570 nm was measured using a plate reader.

2.4. Western Blotting. RIPA buffer added to HT22 cells (Invitrogen; USA) to collect the total protein; then the protein concentrations were determined assessed using the BCA method (Invitrogen, USA). The protein samples were mixed with a 5x loading buffer and denatured at the boil. The proteins were separated by 15% SDS-PAGE and transferred onto polyvinylidene fluoride membranes. Next, the membranes were incubated with primary antibodies (Bcl-2, Bax, caspase-3, BDNF, NGF, SIRT1, Wnt1, β-catenin, Shh, Patch, and GAPDH) at 4°C overnight. Then, the next day, the membranes were washed with PBS and incubated with secondary antibodies for 1 h. Finally, the protein bands were measured using the ImageJ software. The data were collected from at least three independent experiments.

2.5. qRT-PCR. Total RNA of HT22 cells was isolated using the TRIzol RNA Extraction Kit (Invitrogen, Grand Island, NY, USA), and the isolated total RNA was reverse-transcribed to cDNA using a reverse transcription kit (Takara, Kyoto, Japan). Next, SYBR Premix Ex Taq II (Takara, Kyoto, Japan) was used to perform qRT-PCR amplification. The IL-1β, IL-6, and TNF-α amplification primers were as follows: IL-1β, 5′-GATGGTCGCATTAGCTCC-3′ and 5′-GGCTGTAGCTGTAGCGTC-3′; IL-6, 5′-ATTG CGGCGGCTGACGCGTAG-3′ and 5′-GTCTGTTGCGC GAGCTGGTA-3′; IL-8, 5′-GTCGAGCTGCCGCGTAGCG T-3′ and 5′-CGCGATGCGTGCAGC-3′; and TNF-α, 5′ -CGTCAGCCGATTTGCTATCT-3′ and 5′-CGGACTCCG CAAAGTCTAAG-3′. The relative expression of mRNA was analyzed using the $2^{-\Delta\Delta Ct}$ method.

2.6. SOD, GSH, and MDA Assay. We measured oxygen species (ROS), catalase (CAT), superoxide dismutase (SOD), glutathione (GSH), and malondialdehyde (MDA) levels activity using the corresponding assay kits (Nanjing Jiancheng Bio Company, China).

2.7. Flow Cytometry. Flow cytometry assay was used to measure the cell apoptosis rate according to a previous report [15]. HT22 cells in each group were harvested and resuspended. The apoptotic cells were double-labeled with annexin V-FITC and PI using an annexin V-FITC/PI apoptosis detection kit (Beyotime Biotechnology, China) for 30 min at room temperature in the dark. Then, the fluorescence intensity of the cells was quantified by flow cytometry.

2.8. Statistical Analysis. In this study, the difference between two groups was compared by using a t-test, and that among groups was analyzed by one-way analysis of variance (ANOVA). All data were presented as the mean values ±

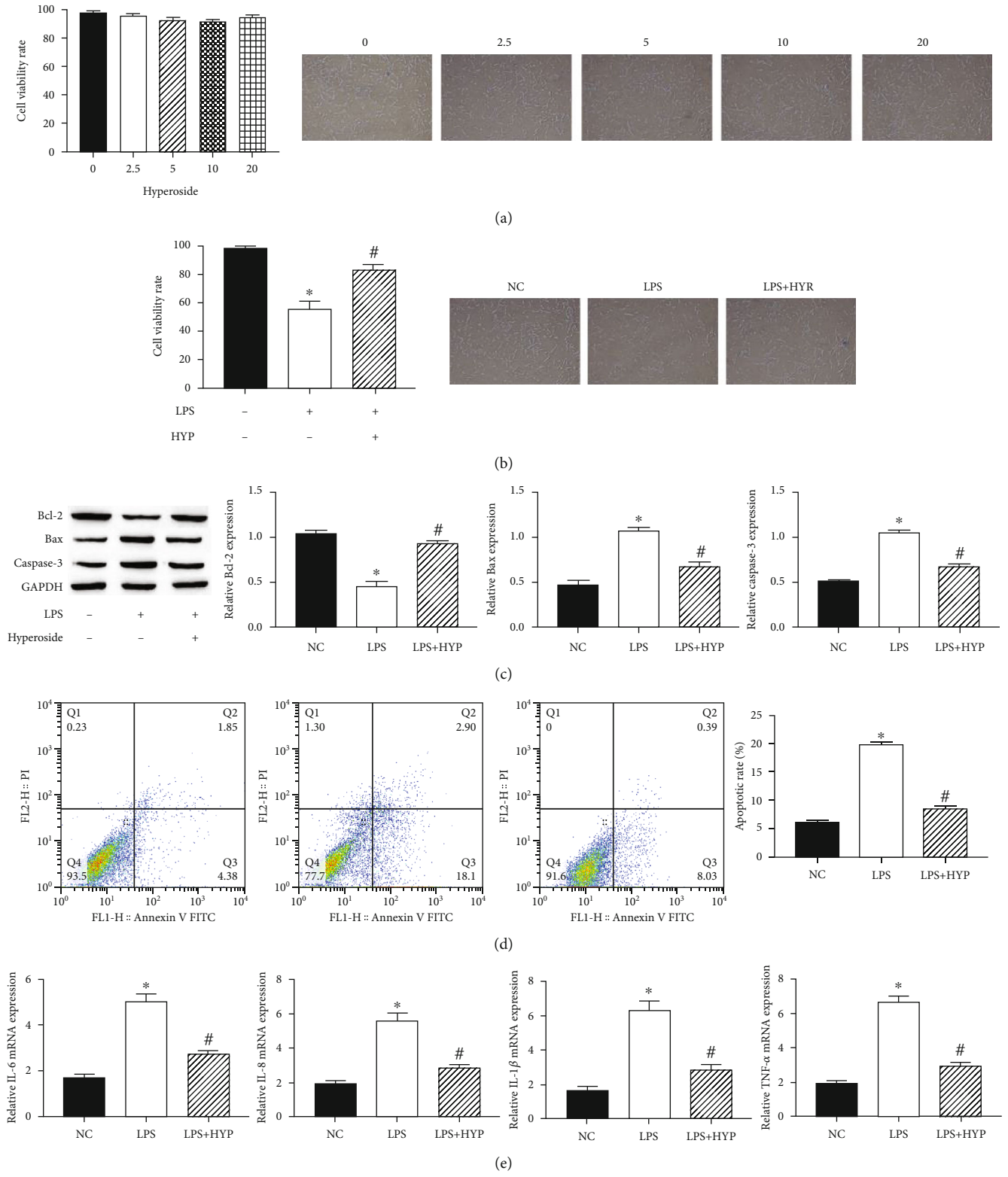

FIGURE 1: Hyperoside alleviated apoptosis and inflammation in the LPS-induced HT22 cells. HT22 cell viability was measured by the MTT assay. Cell viability was observed by a microscope (100x) (a, b). The expression of Bcl-2, Bax, and caspase-3 in HT22 cells was measured by western blotting (c). The HT22 cell apoptosis rate was measured by flow cytometry assay (d). The levels of IL-1β, IL-6, IL-8, and TNF-α mRNA in HT22 cells were measured by qRT-PCR (e); $*$ was considered significant compared to control ($^{*}P < 0.05$); # was considered significant compared to LPS ($^{\#}P < 0.05$).

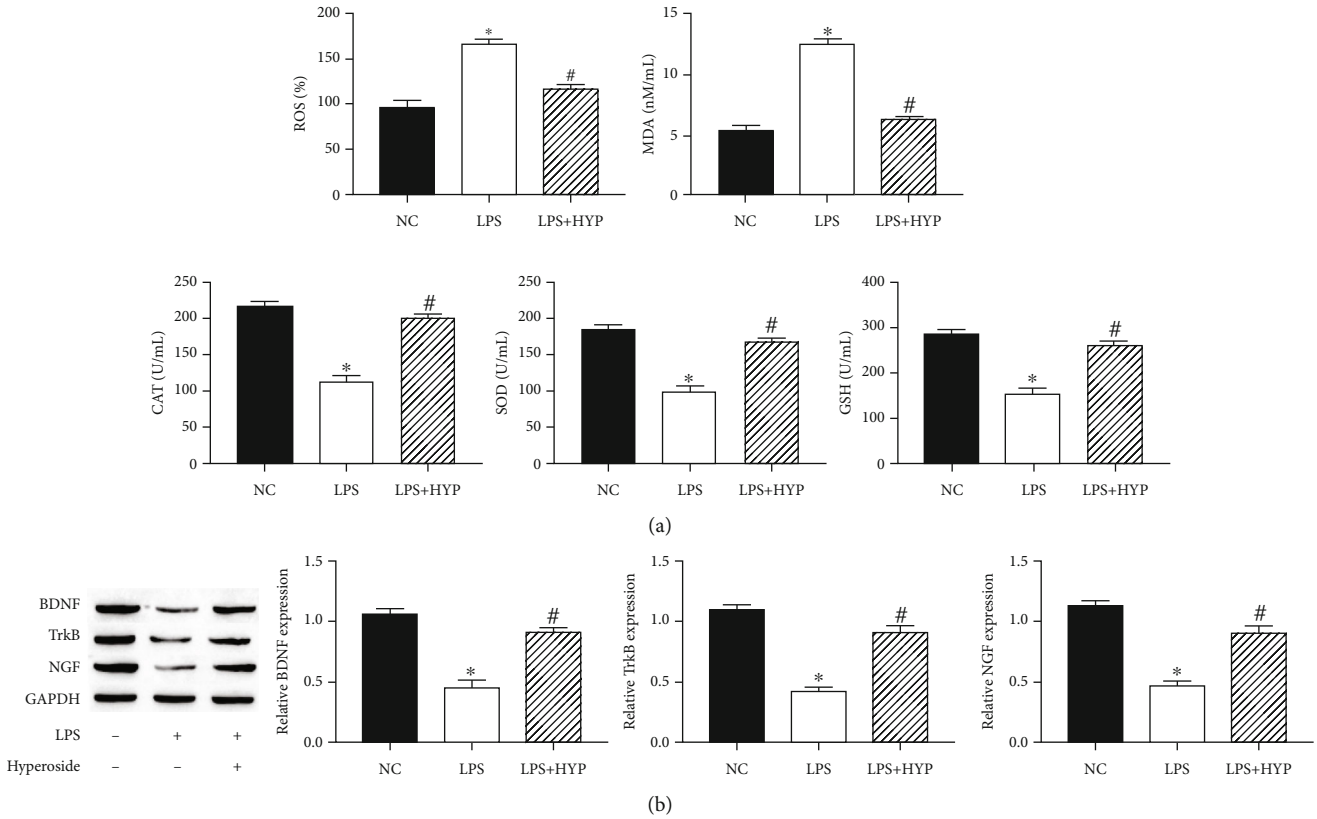

Figure 2: Hyperoside alleviated oxidative stress and reduction of neurotrophic factor in the LPS-induced HT22 cells. The levels of SOD, GSH, CAT, ROS, and MDA were measured by corresponding assay kits (a). The expression of BDNF, TrkB, and NGF in HT22 cells was measured by western blotting (b). $*$ was considered significant compared to control ($^{*}P < 0.05$); # was considered significant compared to LPS ($^{\#}P < 0.05$).

standard deviation (SD). Statistical analyses were performed by GraphPad Prism 7.0 software. $P < 0.05$ was considered to indicate a statistically significant difference.

3. Results

3.1. Hyperoside Alleviated Apoptosis and Inflammation in the LPS-Induced HT22 Cells. The viability of HT22 cells was detected using the MTT assay. The result showed that hyperoside had little effect on HT22 cell viability (Figure 1(a)). Compared with untreated cell, the treatment of LPS (1 μg/ml) significantly reduced HT22 cell viability (Figure 1(b)). Based on the MTT results, we choose 20 μM hyperoside to evaluate the protective effect on HT22 cells. The apoptotic protein expression of HT22 cells was detected using the western blotting; the results showed that treatment with 20 μM hyperoside significantly enhanced the antiapoptotic Bcl-2 expression and decreased the proapoptotic Bax and caspase-3 expression (Figure 1(c)). Simultaneously, 20 μM hyperoside treatment significantly inhibited LPS-induced apoptosis of HT22 cells (Figure 1(d)). Likewise, treatment with 20 μM hyperoside suppressed LPS-induced production of IL-1β, IL-6, IL-8, and TNF-α (Figure 1(e)). These results suggested that hyperoside alleviated apoptosis and inflammation in the LPS-induced HT22 cells.

3.2. Hyperoside Alleviated Oxidative Stress and Reduction of Neurotrophic Factor in the LPS-Induced HT22 Cells. The oxidative stress of HT22 cells increased, and the production of neurotrophic factors decreased after LPS treatment. Next, we studied the effect of hyperoside on oxidative stress and neurotrophic factors in LPS-induced HT22 cells. The results showed that treatment with 20 μM hyperoside significantly increased the levels of SOD, GSH, CAT, and neurotrophic factors BDNF, TrkB, NGF and decreased the levels of ROS and MDA (Figures 2(a) and 2(b)). These results suggested that hyperoside alleviated LPS-induced oxidative stress and reduction of neurotrophic factor in HT22 cells.

3.3. Hyperoside Inhibits LPS-Induced HT22 Cell Apoptosis and Inflammation through SIRT1. SIRT1 alleviated nerve damage; to find out whether hyperoside could ameliorate apoptosis and inflammation in the LPS-induced by acting on SIRT1, SITR1 inhibitors (nicotinamide (NAM)) were used to treat cells. Western blotting showed that SITR1 expression decreased in LPS-induced cells; simultaneously, compared with LPS induction, hyperoside treatment upregulated the expression level of SITR1. In addition, NAM treatment decreased the expression of SIRT1 in HT22 cells compared with the treatment of cells with LPS+hyperoside treatment (Figure 3(a)). Likewise, NAM treatment decreased the expression of Bcl-2 and enhanced the expression of Bax

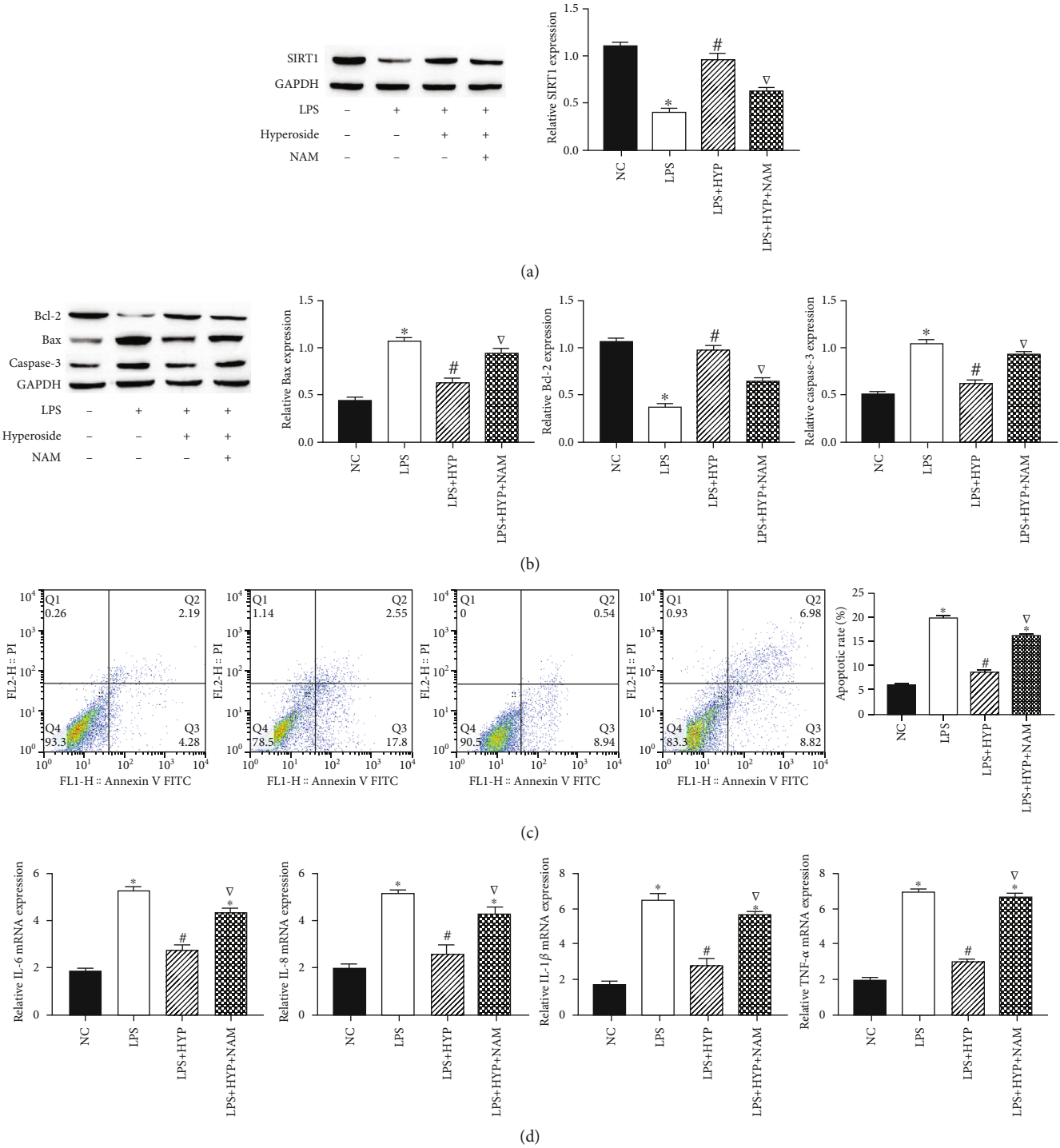

Figure 3: Hyperoside inhibits LPS-induced HT22 cell apoptosis and inflammation through SIRT1. The expression of SIRT cells was measured by western blotting (a). The expression of Bcl-2, Bax, and caspase-3 in HT22 cells was measured by western blotting (b). The HT22 cell apoptosis rate was measured by flow cytometry assay (c). The level of IL-1β, IL-6, IL-8, and TNF-α mRNA in HT22 cells was measured by qRT-PCR (d). $*$ was considered significant compared to control ($^{*}P < 0.05$); # was considered significant compared to LPS ($^{\#}P < 0.05$); ∇ was considered significant compared to LPS+HYP ($^{\nabla}P < 0.05$).

and caspase-3 in HT22 cells compared with the treatment of cells with LPS+hyperoside treatment (Figure 3(b)). Simultaneously, NAM treatment significantly increased apoptosis of HT22 cells (Figure 3(c)). In addition, NAM treatment increased the expression of IL-1β, IL-6, IL-8, and TNF-α, compared with the treatment of cells with LPS+hyperoside

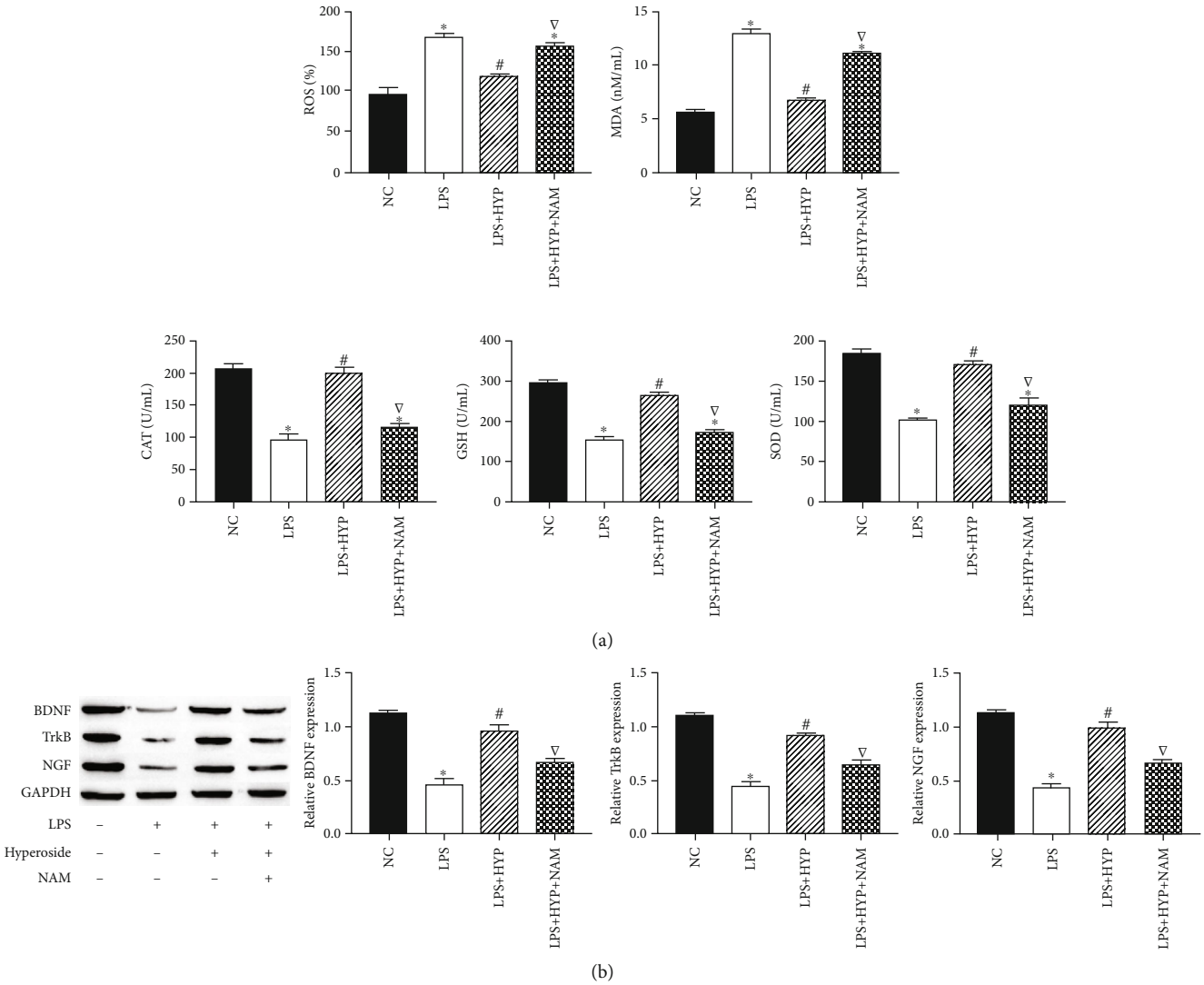

Figure 4: Hyperoside inhibits LPS-induced HT22 cell oxidative stress and reduction of neurotrophic factor through SIRT1. The level of SOD, GSH, CAT, ROS, and MDA were measured by corresponding assay kits (a). The expression of BDNF, TrkB, and NGF in HT22 cells was measured by western blotting (b). $*$ was considered significant compared to control ($^{*}P < 0.05$); # was considered significant compared to LPS ($^{\#}P < 0.05$); ∇ was considered significant compared to LPS + HYP ($^{\nabla}P < 0.05$).

treatment (Figure 3(d)). These results indicated that hyperoside inhibits LPS-induced HT22 cell apoptosis and inflammation by upregulating SIRT1.

3.4. Hyperoside Inhibits LPS-Induced HT22 Cell Oxidative Stress and Reduction of Neurotrophic Factor through SIRT1. We studied the effect of SIRT1 on oxidative stress and neurotrophic factors in LPS-induced HT22 cells. The results showed that NAM treatment decreased the levels of SOD, GSH, CAT, and neurotrophic factors BDNF and NGF and increased the levels of ROS and MDA in HT22 cells, compared with the treatment of cells with LPS+hyperoside treatment (Figures 4(a) and 4(b)). These results indicated that hyperoside inhibits oxidative stress and neurotrophic factor reduction in LPS-induced HT22 cells by upregulating SIRT.

3.5. Hyperoside Activates Wnt/β-Catenin and Sonic Hedgehog Pathways by Upregulating SIRT1. To clarify whether SIRT1 alleviates HT22 damage through the Wnt/β-catenin and sonic hedgehog pathways, we measured the expression levels of signaling molecules in the Wnt/β-catenin and sonic hedgehog pathways. The results showed that LPS significantly decreased the expression levels of Wnt1, β-catenin, Shh, and Patch; hyperoside treatment significantly increased the expression levels of Wnt1, β-catenin, Shh, and patch; in addition, NAM treatment decreased the expression levels of Wnt1, β-catenin, Shh, and patch. In addition, in HT22 cells, compared with NAM-treated cells, Wnt/β-catenin agonist (LiCl) and sonic hedgehog agonist (SAg) inhibited the inhibitory effect of NAM (Figures 5(a) and 5(b)). These results indicated that hyperoside activates Wnt/β-catenin and sonic hedgehog pathways by upregulating SIRT1.

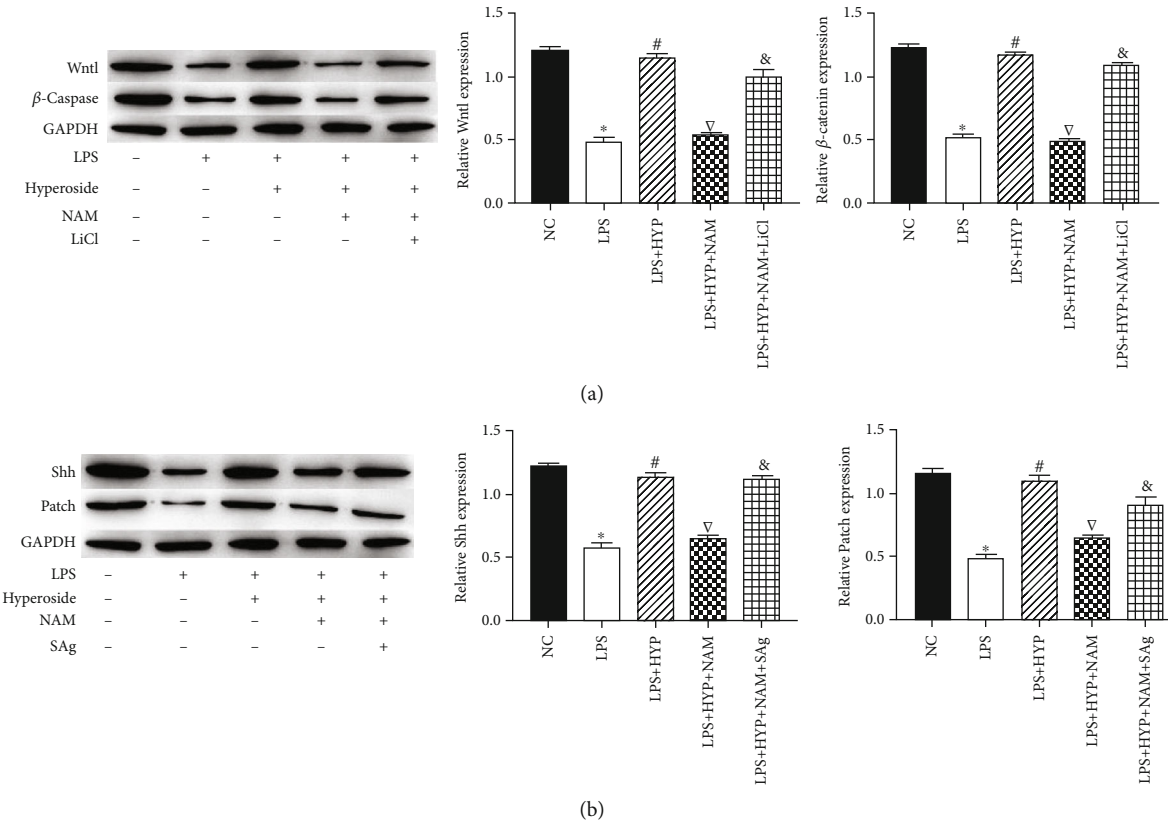

Figure 5: Hyperoside activates Wnt/β-catenin and sonic hedgehog pathways by upregulating SIRT1. The expression of Wnt1 and β-catenin in HT22 cells was measured by western blotting (a). The expression of Shh and patch in HT22 cells was measured by western blotting (b). $*$ was considered significant compared to control ($^{*}P < 0.05$); # was considered significant compared to LPS ($^{\#}P < 0.05$); ∇ was considered significant compared to LPS+HYP ($^{\nabla}P < 0.05$); & was considered significant compared to LPS+HYP+LiCl or LPS+HYP+SAg ($^{\&}P < 0.05$).

4. Discussion

Neuroinflammation is associated with the pathology of many neurological complications, including hearing loss, AD, PD, neuropathic pain, cognitive impairment, and cerebral ischemic injury [2, 16–24]. Identification of effective inflammatory protective candidate agents is one of the hot spots in the treatment of neurological complications [25]. Effective medical treatment reduces neuroinflammation or prevents neurodegeneration. Hyperoside has been reported to treat neuroinflammation in neurological complications [12], However, in recent years, there has been little research on the mechanism by which hyperoside alleviates neuroinflammation. In the present study, we explored the anti-inflammatory effects of hyperoside on LPS-induced HT22 neuroinflammation in mouse neuronal cells. We demonstrated that hyperoside attenuated apoptosis, inflammation, and oxidative stress and simultaneously restored the levels of neurotrophic factor proteins BDNF, TrkB, and NGF in HT22 cells induced by LPS. In addition, we provide evidence that STRI1 is highly expressed under the action of hyperoside and activates Wnt/β-catenin and sonic hedgehog pathways. In our study, hyperoside significantly inhibited the LPS-induced apoptosis, inflammation, and oxidative stress production by increased STRI and activating the Wnt/β-catenin and sonic hedgehog pathways.

Neurons are the basic structural and functional units of the nervous system [26]. Changes in the structure and function of neurons in the brain will cause nerve damage [27]. HT22 cells are a kind of mouse hippocampal neuronal cells, which are widely used as an in vitro neuronal model associated with neuroinflammation and nerve injury in studies to identify effective inflammatory protective candidate agents [28]. Previous studies have shown that systemic administration of LPS triggers nerve injury and neuroinflammation and in the brain, which induce neurodegeneration in mice [29, 30]. In the present study, we used HT22 cells as a neuronal cell model to examine the protective effect of hyperoside on LPS-activated neuroinflammation. We found that LPS inhibited HT22 activity, promoted the level of proinflammatory cytokines (TNF-α, IL-1β, IL-6, and IL-8) and apoptosis proteins Bax and xaspase-3, and activated oxidative stress. However, pretreatment with hyperoside significantly protected HT22 cells from LPS-induced cell growth inhibition by inhibiting apoptosis; down-regulating TNF-α, IL-1β, IL-6, IL-8, Bax, and caspase-3 levels; and inhibiting oxidative stress. These results are consistent with previous studies on hyperoside as antioxidants, anti-inflammatory agents, and antiapoptotic agents.

Regulation that protects neuronal survival is essential in the pathological process of alleviating neurological complications caused by neuroinflammation [2, 31]. In the development of neuronal, BDNF, as an important nerve growth factors, plays

an important role in the growth, survival, and differentiation of neurons [32]. BDNF enhances neuronal survival and protects synaptic function by binding to tropomyosin receptor kinase B (TrkB) [33, 34]. Simultaneously, BDNF promotes neuronal outward growth and recombination of dendritic spines, thereby improving neuronal connectivity [35]. NGF is a nerve cell growth regulator with dual biological functions of neuron nutrition and neurite outgrowth promotion. It has been proven to protect neurons by promoting nerve fiber regeneration [36, 37]. Previous studies have shown that LPS-induced inflammation is the main cause of neuronal death in the hippocampus. In this study, we found that the expression levels of BDNF, TrkB, and NGF in HT22 cells induced by LPS were significantly reduced and hyperoside treatment significantly restores the expression levels of BDNF, TrkB, and NGF.

SIRT1 is the main regulator of neurogenesis and plays a neuroprotective role in neurological diseases [38]. Previous studies showed that activation of SIRT1 reversed nerve damage in different neurological diseases by augmenting hippocampal neurogenesis [39]. Simultaneously, previous reports also demonstrated that activation of SIRT1 reduces the level of oxidative stress and the extent of inflammation [40]. In addition, crucially, Li et al. found that hyperoside enhances SIRT1 protein expression in a mechanism that protects ECV-304 cells from tert-butyl hydrogen peroxide-induced damage [41]. Thus, we speculate that hyperoside alleviating neuroinflammation may be related to the level of SIRT1. In this study, we found that hyperoside significantly increased the expression of SIRT1 in cells, while the SIRT1 inhibitor NAM effect attenuated the alleviating effect of hyperoside on neuroinflammation of induced by LPS. Wnt/β-catenin and sonic hedgehog pathways are confirmed to be regulated by SIRT1; SIRT1-mediated deacetylation in the process of c-myc degradation, which affected the stability of c-myc and increased the transcriptional activity of β-catenin, activates Wnt signaling through β-catenin [42]; simultaneously, SIRT1 agonist SRT1720 activated the sonic hedgehog signaling [43]. In addition, we have also observed that Wnt/β-catenin and sonic hedgehog signaling pathways are inhibited in neuroinflammation [44, 45]. Simultaneously, Wnt/β-catenin and sonic hedgehog signaling pathways are involved in the development of neuroinflammation-mediated hearing loss and other neurological diseases [46–55]. In this study, we found that hyperoside activates the expression of Wnt1, β-catenin, Shh, and patch by upregulating SIRT1.

In summary, the present study showed that hyperoside alleviated apoptosis, inflammation, oxidative stress, and reduction of neurotrophic factor in the LPS-induced HT22 cells. We further found that hyperoside alleviated nerve damage by upregulating SIRT1 to activate Wnt/β-catenin and sonic hedgehog signaling pathways. In conclusion, based on our findings, the therapeutic effect of hyperoside on neuroinflammation is further clarified, providing possible treatment basis for its clinical application for neuroinflammation.

Data Availability

The data used to support the findings of this study are available from the corresponding author upon reasonable request.

Conflicts of Interest

The authors declare no conflicts of interest.

Authors' Contributions

THW and JGX designed the experiments. JH and LZ wrote the article. JH, LZ, JC, TBC, BL, NDZ, and XQW performed experiments and analyzed data. All the authors read and approved the final manuscript. Jin Huang and Liang Zhou contributed equally to this work.

References

[1] S. Oka, J. Leon, K. Sakumi et al., "MTH1 and OGG1 maintain a low level of 8-oxoguanine in Alzheimer's brain, and prevent the progression of Alzheimer's pathogenesis," *Scientific Reports*, vol. 11, no. 1, p. 5819, 2021.

[2] M. A. Bonte, F. el Idrissi, B. Gressier, D. Devos, and K. Belarbi, "Protein network exploration prioritizes targets for modulating neuroinflammation in Parkinson's disease," *International Immunopharmacology*, vol. 95, article 107526, 2021.

[3] V. K. Arruri, C. Gundu, A. K. Kalvala, B. Sherkhane, D. K. Khatri, and S. B. Singh, "Carvacrol abates NLRP3 inflammasome activation by augmenting Keap1/Nrf-2/p62 directed autophagy and mitochondrial quality control in neuropathic pain," *Nutritional Neuroscience*, pp. 1–16, 2021.

[4] Z. H. He, S. Y. Zou, M. Li et al., "The nuclear transcription factor FoxG1 affects the sensitivity of mimetic aging hair cells to inflammation by regulating autophagy pathways," *Redox Biology*, vol. 28, article 101364, 2020.

[5] Y. Ding, W. Meng, W. Kong, Z. He, and R. Chai, "The role of FoxG1 in the inner ear," *Frontiers in Cell and Development Biology*, vol. 8, article 614954, 2020.

[6] W. Wang, L. S. Zhang, A. K. Zinsmaier et al., "Neuroinflammation mediates noise-induced synaptic imbalance and tinnitus in rodent models," *PLoS Biology*, vol. 17, no. 6, article e3000307, 2019.

[7] S. Ahmad, A. Khan, W. Ali et al., "Fisetin rescues the mice brains against D-galactose-induced oxidative stress, neuroinflammation and memory impairment," *Frontiers in Pharmacology*, vol. 12, article 612078, 2021.

[8] J. M. Li, R. Yu, L. P. Zhang et al., "Dietary fructose-induced gut dysbiosis promotes mouse hippocampal neuroinflammation: a benefit of short-chain fatty acids," *Microbiome.*, vol. 7, no. 1, p. 98, 2019.

[9] K. Sun, J. Luo, X. Jing et al., "Hyperoside ameliorates the progression of osteoarthritis: An _*in vitro*_ and _*in vivo*_ study," *Phytomedicine*, vol. 80, article 153387, 2021.

[10] J. Cao, C. Tang, M. Gao et al., "Hyperoside alleviates epilepsy-induced neuronal damage by enhancing antioxidant levels and reducing autophagy," *Journal of Ethnopharmacology*, vol. 257, article 112884, 2020.

[11] X. Chen, A. C. Famurewa, J. Tang, O. O. Olatunde, and O. J. Olatunji, "Hyperoside attenuates neuroinflammation, cognitive impairment and oxidative stress via suppressing TNF-α/NF-κB/caspase-3 signaling in type 2 diabetes rats," *Nutritional Neuroscience*, pp. 1–11, 2021.

[12] H. H. Fan, L. B. Zhu, T. Li et al., "Hyperoside inhibits lipopolysaccharide-induced inflammatory responses in

microglial cells via p38 and NFκB pathways," *International Immunopharmacology*, vol. 50, pp. 14–21, 2017.

[13] D. Zhao, L. J. Zhang, T. Q. Huang, J. Kim, M. Y. Gu, and H. O. Yang, "Narciclasine inhibits LPS-induced neuroinflammation by modulating the Akt/IKK/NF-κB and JNK signaling pathways," *Phytomedicine*, vol. 85, article 153540, 2021.

[14] Y. Xu, L. Yu, Y. Liu, X. Tang, and X. Wang, "Lipopolysaccharide-induced microglial neuroinflammation: attenuation by FK866," *Neurochemical Research*, vol. 46, no. 5, pp. 1291–1304, 2021.

[15] T. Shen, Y. Shang, Q. Wu, and H. Ren, "The protective effect of trilobatin against isoflurane-induced neurotoxicity in mouse hippocampal neuronal HT22 cells involves the Nrf2/ARE pathway," *Toxicology*, vol. 442, article 152537, 2020.

[16] H. J. Lee, S. G. Jeon, J. Kim et al., "Ibrutinib modulates Aβ/tau pathology, neuroinflammation, and cognitive function in mouse models of Alzheimer's disease," *Aging Cell*, vol. 20, no. 3, p. e13332, 2021.

[17] R. S. Toledo, D. J. Stein, P. R. S. Sanches et al., "rTMS induces analgesia and modulates neuroinflammation and neuroplasticity in neuropathic pain model rats," *Brain Research*, vol. 1762, article 147427, 2021.

[18] Y. Hu, X. Zhang, J. Zhang et al., "Activated STAT3 signaling pathway by ligature-induced periodontitis could contribute to neuroinflammation and cognitive impairment in rats," *Journal of Neuroinflammation*, vol. 18, no. 1, p. 80, 2021.

[19] X. Liu, M. Zhang, H. Liu et al., "Bone marrow mesenchymal stem cell-derived exosomes attenuate cerebral ischemia-reperfusion injury-induced neuroinflammation and pyroptosis by modulating microglia M1/M2 phenotypes," *Experimental Neurology*, vol. 341, article 113700, 2021.

[20] H. Zhou, X. Qian, N. Xu et al., "Disruption of Atg7-dependent autophagy causes electromotility disturbances, outer hair cell loss, and deafness in mice," *Cell Death & Disease*, vol. 11, no. 10, p. 913, 2020.

[21] Y. Zhang, S. Zhang, Z. Zhang et al., "Knockdown of Foxg1 in Sox9+ supporting cells increases the trans-differentiation of supporting cells into hair cells in the neonatal mouse utricle," *Aging*, vol. 12, no. 20, pp. 19834–19851, 2020.

[22] S. Zhang, Y. Zhang, P. Yu et al., "Characterization of Lgr5+ progenitor cell transcriptomes after neomycin injury in the neonatal mouse cochlea," *Frontiers in Molecular Neuroscience*, vol. 10, p. 213, 2017.

[23] C. Cheng, L. Guo, L. Lu et al., "Characterization of the transcriptomes of Lgr5+ hair cell progenitors and Lgr5- supporting cells in the mouse cochlea," *Frontiers in Molecular Neuroscience*, vol. 10, p. 122, 2017.

[24] Z. H. He, M. Li, Q. J. Fang et al., "FOXG1 promotes aging inner ear hair cell survival through activation of the autophagy pathway," *Autophagy*, pp. 1–22, 2021.

[25] W. Liu, L. Xu, X. Wang et al., "PRDX1 activates autophagy via the PTEN-AKT signaling pathway to protect against cisplatin-induced spiral ganglion neuron damage," *Autophagy*, pp. 1–23, 2021.

[26] Y. Fang, B. Shi, X. Liu et al., "Xiaoyao Pills Attenuate Inflammation and Nerve injury induced by lipopolysaccharide in hippocampal neurons in vitro," *Neural Plasticity*, vol. 2020, Article ID 8841332, 12 pages, 2020.

[27] K. Makowska and S. Gonkowski, "The influence of inflammation and nerve damage on the neurochemical characterization of calcitonin gene-related peptide-like immunoreactive (CGRP-LI) neurons in the enteric nervous system of the porcine descending colon," *International Journal of Molecular Sciences*, vol. 19, no. 2, p. 548, 2018.

[28] F. Guan, X. Zhou, P. Li et al., "MG53 attenuates lipopolysaccharide-induced neurotoxicity and neuroinflammation _via_ inhibiting TLR4/NF- κB pathway _in vitro_ and _in vivo_," *Progress in Neuro-Psychopharmacology and Biological Psychiatry*, vol. 95, article 109684, 2019.

[29] M. L. Aranda, D. Guerrieri, G. Piñero et al., "Critical role of monocyte recruitment in optic nerve damage induced by experimental optic neuritis," *Molecular Neurobiology*, vol. 56, no. 11, pp. 7458–7472, 2019.

[30] G. Fodelianaki, F. Lansing, P. Bhattarai et al., "Nerve growth factor modulates LPS - induced microglial glycolysis and inflammatory responses," *Experimental Cell Research*, vol. 377, no. 1-2, pp. 10–16, 2019.

[31] H. Liu, J. Zhang, X. Xu et al., "SARM1 promotes neuroinflammation and inhibits neural regeneration after spinal cord injury through NF-κB signaling," *Theranostics*, vol. 11, no. 9, pp. 4187–4206, 2021.

[32] F. Wang, X. X. Wei, L. S. Chang, L. Dong, Y. L. Wang, and N. N. Li, "Ultrasound combined with microbubbles loading BDNF retrovirus to open blood brain barrier for treatment of Alzheimer's disease," *Frontiers in Pharmacology*, vol. 12, article 615104, 2021.

[33] H. I. Kim, S. Lee, J. Lim et al., "ERRγ ligand HPB2 upregulates BDNF-TrkB and enhances dopaminergic neuronal phenotype," *Pharmacological Research*, vol. 165, article 105423, 2021.

[34] B. Yang, G. Luo, C. Zhang, L. Feng, X. Luo, and L. Gan, "Curcumin protects rat hippocampal neurons against pseudorabies virus by regulating the BDNF/TrkB pathway," *Scientific Reports*, vol. 10, no. 1, article 22204, 2020.

[35] I. Morella, H. Hallum, and R. Brambilla, "Dopamine D1 and glutamate receptors co-operate with brain-derived neurotrophic factor (BDNF) and TrkB to modulate ERK signaling in adult striatal slices," *Frontiers in Cellular Neuroscience*, vol. 14, article 564106, 2020.

[36] Y. Wang, X. Lai, D. Wu, B. Liu, N. Wang, and L. Rong, "Umbilical mesenchymal stem cell-derived exosomes facilitate spinal cord functional recovery through the miR-199a-3p/145-5p-mediated NGF/TrkA signaling pathway in rats," *Stem Cell Research & Therapy*, vol. 12, no. 1, p. 117, 2021.

[37] A. de León, J. Gibon, and P. A. Barker, "NGF-dependent and BDNF-dependent DRG sensory neurons deploy distinct degenerative signaling mechanisms," *eneuro*, vol. 8, no. 1, pp. - ENEURO.0277–ENEU20.2020, 2021.

[38] S. Kang, J. Li, Z. Yao, and J. Liu, "Cannabidiol induces autophagy to protects neural cells from mitochondrial dysfunction by upregulating SIRT1 to inhibits NF-κB and NOTCH pathways," *Frontiers in Cellular Neuroscience*, vol. 15, article 654340, 2021.

[39] C. Qu, C. Qu, L. Xu et al., "Nuclear receptor TLX may be through regulating the SIRT1/NF-κB pathway to ameliorate cognitive impairment in chronic cerebral hypoperfusion," *Brain Research Bulletin*, vol. 166, pp. 142–149, 2021.

[40] N. Mokarizadeh, P. Karimi, M. Erfani, S. Sadigh-Eteghad, N. Fathi Maroufi, and N. Rashtchizadeh, "β-Lapachone attenuates cognitive impairment and neuroinflammation in beta-amyloid induced mouse model of Alzheimer's disease," *International Immunopharmacology*, vol. 81, article 106300, 2020.

[41] H. B. Li, X. Yi, J. M. Gao, X. X. Ying, H. Q. Guan, and J. C. Li, "The mechanism of hyperoside protection of ECV-304 cells against tert-butyl hydroperoxide-induced injury," *Pharmacology*, vol. 82, no. 2, pp. 105–113, 2008.

[42] Y. Yao, Q. Hua, Y. Zhou, and H. Shen, "CircRNA has_*circ*_0001946 promotes cell growth in lung adenocarcinoma by regulating miR-135a-5p/SIRT1 axis and activating Wnt/β-catenin signaling pathway," *Biomedicine & Pharmacotherapy*, vol. 111, pp. 1367–1375, 2019.

[43] S. Guo, H. Liao, J. Liu et al., "Resveratrol activated sonic hedgehog signaling to enhance viability of NIH3T3 cells in vitro via regulation of Sirt1," *Cellular Physiology and Biochemistry*, vol. 50, no. 4, pp. 1346–1360, 2018.

[44] P. Jiang, Q. Jiang, Y. Yan, Z. Hou, and D. Luo, "Propofol ameliorates neuropathic pain and neuroinflammation through PPAR γ up-regulation to block Wnt/β-catenin pathway," *Neurological Research*, vol. 43, no. 1, pp. 71–77, 2021.

[45] G. M. Sullivan and R. C. Armstrong, "Transplanted adult neural stem cells express sonic hedgehog in vivo and suppress white matter neuroinflammation after experimental traumatic brain injury," *Stem Cells International*, vol. 2017, Article ID 9342534, 16 pages, 2017.

[46] D. You, L. Guo, W. Li et al., "Characterization of Wnt and Notch-responsive Lgr5+ hair cell progenitors in the striolar region of the neonatal mouse utricle," *Frontiers in Molecular Neuroscience*, vol. 11, p. 137, 2018.

[47] Y. Chen, X. Lu, L. Guo et al., "Hedgehog signaling promotes the proliferation and subsequent hair cell formation of progenitor cells in the neonatal mouse cochlea," *Frontiers in Molecular Neuroscience*, vol. 10, p. 426, 2017.

[48] X. Lu, S. Sun, J. Qi et al., "Bmi1 regulates the proliferation of cochlear supporting cells via the canonical Wnt signaling pathway," *Molecular Neurobiology*, vol. 54, no. 2, pp. 1326–1339, 2017.

[49] M. Waqas, S. Zhang, Z. He, M. Tang, and R. Chai, "Role of Wnt and Notch signaling in regulating hair cell regeneration in the cochlea," *Frontiers of Medicine*, vol. 10, no. 3, pp. 237–249, 2016.

[50] J. Wu, W. Li, C. Lin et al., "Co-regulation of the Notch and Wnt signaling pathways promotes supporting cell proliferation and hair cell regeneration in mouse utricles," *Scientific Reports*, vol. 6, no. 1, article 29418, 2016.

[51] L. Liu, Y. Chen, J. Qi et al., "Wnt activation protects against neomycin-induced hair cell damage in the mouse cochlea," *Cell Death & Disease*, vol. 7, no. 3, article e2136, 2016.

[52] S. Zhang, Y. Zhang, Y. Dong et al., "Knockdown of Foxg1 in supporting cells increases the trans-differentiation of supporting cells into hair cells in the neonatal mouse cochlea," *Cellular and Molecular Life Sciences*, vol. 77, no. 7, pp. 1401–1419, 2020.

[53] S. Zhang, D. Liu, Y. Dong et al., "Frizzled-9+ supporting cells are progenitors for the generation of hair cells in the postnatal mouse cochlea," *Frontiers in Molecular Neuroscience*, vol. 12, p. 184, 2019.

[54] Y. Zhang, L. Guo, X. Lu et al., "Characterization of Lgr6+ cells as an enriched population of hair cell progenitors compared to Lgr5 + cells for hair cell generation in the neonatal mouse cochlea," *Frontiers in Molecular Neuroscience*, vol. 11, p. 147, 2018.

[55] T. Wang, R. Chai, G. S. Kim et al., "Lgr5+ cells regenerate hair cells via proliferation and direct transdifferentiation in damaged neonatal mouse utricle," *Nature Communications*, vol. 6, no. 1, p. 6613, 2015.

Hindawi
Neural Plasticity
Volume 2021, Article ID 9919977, 12 pages
https://doi.org/10.1155/2021/9919977

Research Article

Dose-Dependent Pattern of Cochlear Synaptic Degeneration in C57BL/6J Mice Induced by Repeated Noise Exposure

Minfei Qian,[1,2,3,4] **Qixuan Wang**,[1,2,3] **Zhongying Wang**,[1,2,3] **Qingping Ma**,[1,2,3] **Xueling Wang**,[1,2,3] **Kun Han**,[1,2,3] **Hao Wu**,[1,2,3] **and Zhiwu Huang**[1,2,3]

[1]*Department of Otolaryngology-Head and Neck Surgery, Ninth People's Hospital, Shanghai Jiao Tong University School of Medicine, Shanghai 200011, China*
[2]*Ear Institute, Shanghai Jiao Tong University School of Medicine, Shanghai 200011, China*
[3]*Shanghai Key Laboratory of Translational Medicine on Ear and Nose Diseases, Shanghai 200011, China*
[4]*Department of Otolaryngology, Ren-Ji Hospital, Shanghai Jiao Tong University School of Medicine, Shanghai 200127, China*

Correspondence should be addressed to Hao Wu; wuhao@shsmu.edu.cn and Zhiwu Huang; huangzw86@126.com

Received 16 March 2021; Revised 1 April 2021; Accepted 25 May 2021; Published 10 June 2021

Academic Editor: Preston E. Garraghty

It is widely accepted that even a single acute noise exposure at moderate intensity that induces temporary threshold shift (TTS) can result in permanent loss of ribbon synapses between inner hair cells and afferents. However, effects of repeated or chronic noise exposures on the cochlear synapses especially medial olivocochlear (MOC) efferent synapses remain elusive. Based on a weeklong repeated exposure model of bandwidth noise over 2-20 kHz for 2 hours at seven intensities (88 to 106 dB SPL with 3 dB increment per gradient) on C57BL/6J mice, we attempted to explore the dose-response mechanism of prolonged noise-induced audiological dysfunction and cochlear synaptic degeneration. In our results, mice repeatedly exposed to relatively low-intensity noise (88, 91, and 94 dB SPL) showed few changes on auditory brainstem response (ABR), ribbon synapses, or MOC efferent synapses. Notably, repeated moderate-intensity noise exposures (97 and 100 dB SPL) not only caused hearing threshold shifts and the inner hair cell ribbon synaptopathy but also impaired MOC efferent synapses, which might contribute to complex patterns of damages on cochlear function and morphology. However, repeated high-intensity (103 and 106 dB SPL) noise exposures induced PTSs mainly accompanied by damages on cochlear amplifier function of outer hair cells and the inner hair cell ribbon synaptopathy, rather than the MOC efferent synaptic degeneration. Moreover, we observed a frequency-dependent vulnerability of the repeated acoustic trauma-induced cochlear synaptic degeneration. This study provides a sight into the hypothesis that noise-induced cochlear synaptic degeneration involves both afferent (ribbon synapses) and efferent (MOC terminals) pathology. The pattern of dose-dependent pathological changes induced by repeated noise exposure at various intensities provides a possible explanation for the complicated cochlear synaptic degeneration in humans. The underlying mechanisms remain to be studied in the future.

1. Introduction

Noise-induced hearing loss (NIHL) is a global public health issue. Hearing loss could be caused by genetic factors, aging, infectious diseases, ototoxic drugs, and noise exposure [1–6]. The reported mechanisms of noise-induced hair cells (HCs) and spiral ganglion neuron damage mainly include mechanical shearing forces and oxidative damage to HCs [7] and glutamate excitotoxicity to neurons [8–11]. In the past, noise exposure was considered harmful only when it causes a permanent threshold shift (PTS) [3, 12–16]. However, Kujawa and Liberman recently demonstrated that even a single acute noise exposure at moderate intensity that induces temporary threshold shift (TTS) could result in permanent loss of ribbon synapses, which was then known as synaptopathy [17]. Noise-induced cochlear synaptopathy has been the focus of attention in hearing research in these years. A number of studies further found that the loss of ribbon synapse between cochlear inner hair cells and type I afferent nerve (AN) fibers usually accompanies the abnormal suprathreshold auditory

brainstem response (ABR) [17–19]. More and more evidences indicate that cochlear synaptopathy might not only be the primary mechanism of hidden hearing loss (HHL) but also contribute to tinnitus and age-related hearing loss (ARHL) [20–23].

Despite the large number of pathological studies involving the effects of noise on the cochlear synaptopathy, most of the previous studies paid attention to the single or acute noise exposure that induced TTS with the loss of ribbon synapses [17, 19, 24, 25]. Although repeated noise exposure is more common in human daily life (such as noise at bars, cinemas, concerts, and traffics), relatively few studies focused on the effects of repeated or chronic noise exposures on the cochlear synaptopathy [26–28]. It remains inconsistent whether repeated noise exposure would cause more damage on cochlear synapses, since the noise exposure procedure and experimental animals in previous studies were quite various. For instance, 16-week-old Sprague-Dawley rats exposed to 8-16 kHz octave-band noise at 97 dB SPL for 2 hours in 4 repeated days did not produce similar ABR wave I amplitude decrement as acute noise exposure [27], while repeated white noise at 100 dB SPL for 2 hours even cause additional cochlear damages in C57BL/6J mice [26]. Moreover, a recent study suggested that the medial olivocochlear (MOC) efferent feedback protects the cochlea from loss of ribbon synapses under the weeklong exposure to moderate-intensity noise (84 dB SPL) in mice [29], while few studies reported chronic noise exposure-induced MOC efferent synaptic degeneration.

In this study, to explore the pattern of cochlear afferent and efferent synaptic degeneration induced by repeated noise exposure, we used seven gradient levels of noise exposure at low, moderate, and high intensity. Auditory function and cochlear immunofluorescence were measured at baseline and 1 day and 14 days post noise exposure to assess the pathological changes of ribbon and MOC efferent synapses in C57BL/6J mice. We proposed a hypothesis that dose-dependent cochlear synaptic degeneration in C57BL/6J mice was induced by repeated noise exposure.

2. Materials and Methods

2.1. Animals. C57BL/6J mice aged four weeks were obtained from the SIPPR-BK Laboratory Animal, Ltd. (Shanghai, China), which were derived from breeders originally purchased from The Jackson Laboratory. A total of about 82 male mice were used in this study to exclude potential sex differences in susceptibility to NIHL [30]. Animals were divided into one control group and seven experimental groups. Mice were housed under quiet laboratory conditions, which showed normal baseline ABR, and distortion product otoacoustic emission (DPOAE) thresholds were included in subsequent noise exposure experiments. Each group included 8-12 mice in the analyses. All experimental procedures followed the *Guide for the Care and Use of Laboratory Animals* and were approved by the University Ethics Committee for Laboratory Animals of Shanghai Jiao Tong University.

2.2. Repeated Noise Exposure Procedure. Noise exposure was performed by exposing conscious mice in a pie-shaped wire cage separated by eight compartments, in a calibrated reverberating chamber as described previously [31]. Bandpass-filtered noise of 2-20 kHz generated by MATLAB software (version 2007b) was delivered for 2 hours by an amplifier and loudspeaker (Yamaha) at seven gradients of intensity from 88 to 106 dB SPL. We defined the groups of relatively low intensity (88, 91, and 94 dB SPL), moderate intensity (97 and 100 dB SPL), and high intensity (103 and 106 dB SPL) in this study. An acoustimeter (type AWA6228+, Hangzhou Aihua) was used to calibrate noise exposure to the target sound pressure level. The exposure procedure was performed on seven exposed groups and their corresponding control groups of mice for continuous seven days repeatedly. The baseline was set at the day before the first day of noise exposure, ABRs were performed at baseline and 1 day and 14 days after NE, and DPOAEs were performed at baseline and 14 days after NE. Animals were sacrificed 14 days after NE (aged seven weeks) for observation of cochlear morphology using immunofluorescence (IF). Figure 1 shows the flowchart of the repeated noise exposure procedure.

2.3. ABR Tests. ABRs were performed at baseline and 1 day and 14 days after the repeated noise exposure procedure. Mice were anesthetized with xylazine (20 mg/kg) and ketamine (100 mg/kg) through intraperitoneal injection, and the body temperature was maintained near 37°C using a heating blanket (Harvard Apparatus, USA, 55-7020). Recordings were performed using three subcutaneous needle electrodes at the vertex (active), left mastoid area (reference), and right shoulder (ground), respectively. Short tone burst stimuli of 3 ms duration with 1 ms rise/fall times were generated by the RZ6 workstation (Tucker-Davis Technologies, USA). Stimulus sounds were delivered free-field via an MF-1 speaker placed 10 cm away from the vertex, in front of the mouse. Stimulus roved over frequencies of 32, 22.6, 16, 11.3, 8, and 4 kHz, and the sound level started from 90 to 0 dB sound pressure level (SPL) in 5 dB steps. For each ABR waveform, 400 responses were collected and averaged. ABR thresholds were identified as the minimal stimulus level that evoked any noticeable recording of waveforms at each frequency. Wave I amplitudes (μV) were measured by averaging the ΔV of both sides of the peak using the BioSigRZ software (Tucker-Davis Technologies, USA). Thresholds and amplitudes were measured by a researcher who was blind to the information of mice in groups.

2.4. DPOAE Tests. DPOAEs were performed at baseline and 14 days after repeated noise exposure of groups 88 dB SPL (representative low intensity) and moderate and high intensities, by the DPOAE workstation with BioSigRZ software (Tucker-Davis Technologies). For recordings, the left external auditory meatus of mice was coupled to a ER10B+ microphone (Etymotic Research). Two MF-1 speakers were used to deliver equal intensity primary tones, and the frequency ratio (f_2/f_1) was 1.2 of which [32]. The amplitude of distortion product (DP) at the frequency $2f_1$-f_2 was collected and averaged 512 times, in response to centre frequencies at 8, 16, and

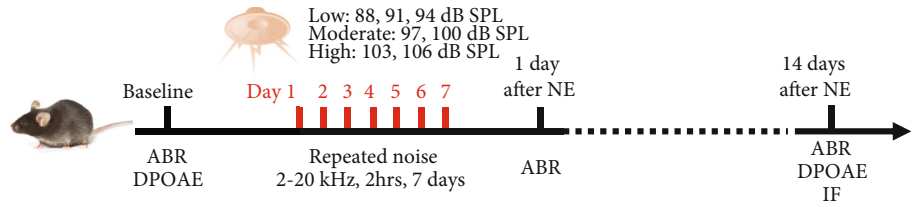

Figure 1: Flowchart of the repeated noise exposure procedure. NE: noise exposure; ABR: auditory brainstem response; DPOAE: distortion product otoacoustic emission; IF: immunofluorescence.

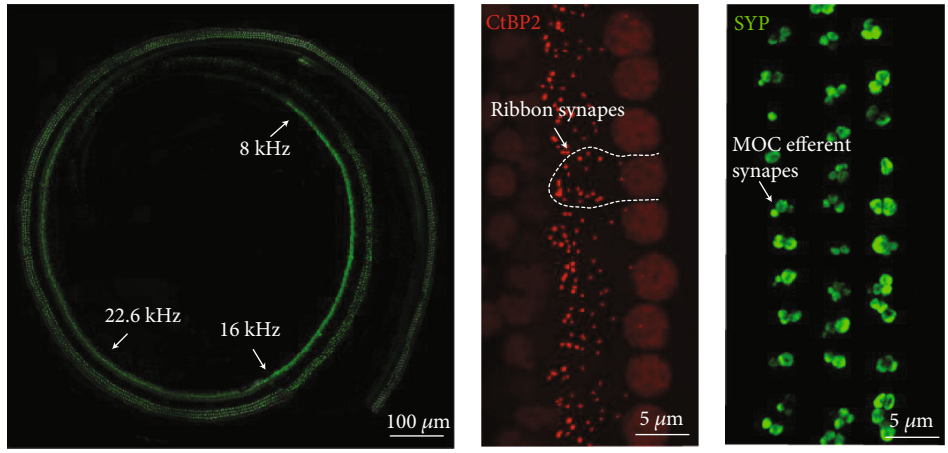

Figure 2: Morphometric analysis of frequency located ribbon and MOC efferent synapses: (a) frequency mapping on the organ of Corti; (b) ribbon synaptic counting; (c) MOC efferent synaptic measurement.

22.6 kHz presented from 80 to 20 dB SPL (in 5 dB increments). The DPOAE threshold was defined as the point where the DP can no longer be detected from noise [33]. Thresholds were measured by a researcher who was blind to the information of mice in groups.

2.5. Whole-Mount Cochlear Immunofluorescence. At 14 days after the noise exposure procedure, mice in different noise-exposed groups and nonexposed control groups were deeply anesthetized and sacrificed. Cochleae were immediately dissected from temporal bones in 10 mM phosphate buffer saline (PBS) solution (Sigma, USA) and then perfused with 4% paraformaldehyde (Sigma, USA) at 4°C overnight. The fixed cochlea was decalcified in 10% ethylene diamine tetraacetic acid (Sigma, USA) solution until it became boneless. The organ of Corti was dissected from the decalcified cochlea and then separated into three parts (the apical, middle, and basal turn) in the PBS solution. For immunofluorescence (IF), the tissue was blocked in 10% bovine serum albumin solution with 0.3% Triton X-100 (Sigma, USA) for one hour at room temperature. Primary antibodies mainly included rabbit anti-myosin VIIa (Abcam, UK, 1 : 500), mouse anti-CtBP2 immunoglobulin (Ig) G1 (BD Biosciences, USA, 1 : 200), and rabbit anti-synaptophysin (SYP) (Abcam, UK, 1 : 500). Secondary antibodies used were Alexa Fluor 633-conjugated goat anti-mouse IgG1 and Alexa Fluor 488-conjugated goat anti-rabbit IgG (Invitrogen, USA, 1 : 200). Images were acquired using a 40x water or 63x oil objective lens on a LSM880 confocal microscope (Carl Zeiss, Germany) with Z-stack scanning for 10 μm. The maximum intensity projection analysis was performed by using Zen software (Carl Zeiss, Germany, version 3.0).

2.6. Morphometric Analysis. In order to map the location of specific frequency on the organ of Corti in mice, we used a location-to-frequency relationship formula as previous studies described [34, 35]: $d\,(\%) = 156.5\text{-}82.5 \times \log\,(f)$, where d is the percentage of the distance from the base and f is the frequency in kHz. For morphometric analysis, confocal images at frequencies of 8, 16, and 22.6 kHz were mapped (Figure 2(a)). For ribbon synapses, spots of CtBP2 staining under each IHC were counted, and the counts of 10 to 12 continuous IHCs at a frequency were averaged for each sample (Figure 2(b)). For MOC efferent synapses [36, 37], the area of SYP staining of each Z-stack maximum intensity projection image was measured and calculated by using ImageJ software (National Institutes of Health, USA, version 1.8.0), which was expressed as the density of MOC efferent synapses of 5 to 6 continuous columns of three rows of outer hair cells (OHCs) for each sample (Figure 2(c)).

2.7. Data Processing and Statistical Analysis. Data processing and statistical analyses were performed using GraphPad Prism (GraphPad Software Inc., USA, version 8.0). Continuous variables are presented as the mean (standard

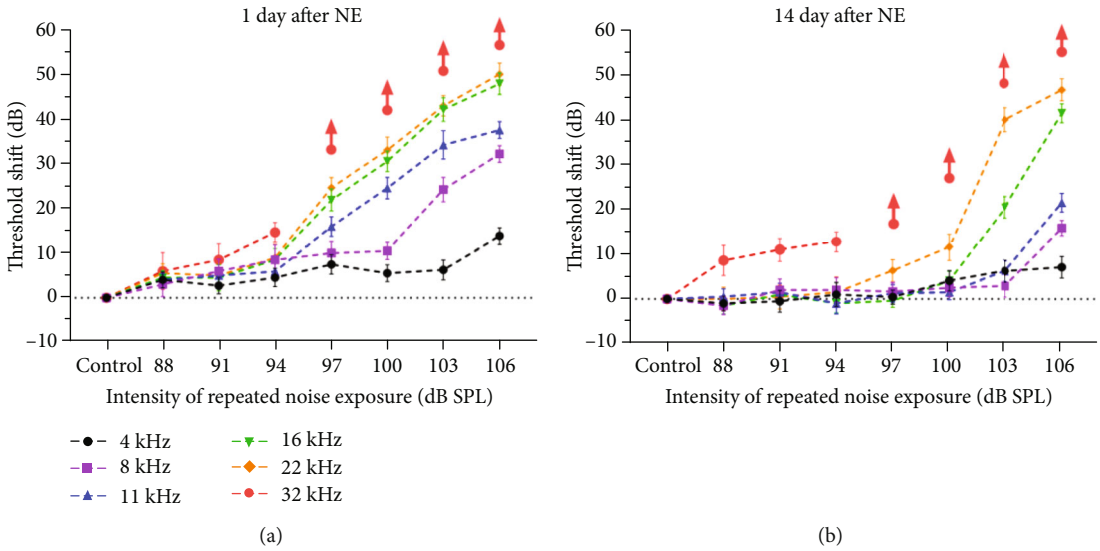

Figure 3: Dose-response relations between repeated noise exposure intensities with ABR threshold shifts at 1 day (a) and 14 days (b) after NE. The error bar represents the SEM for 8-12 mice in each group. Red arrows represent thresholds at 32 kHz frequency greater than 90 dB after the noise exposure.

deviation, SD) in tables. Cumulative distributions were tested by using the Kolmogorov-Smirnov test. Two-way ANOVA with Bonferroni post hoc tests was used to compare the difference between multiple groups. P value < 0.05 was considered statistically significant. In the figures, the error bar represents standard error of the mean (SEM), NS represents $P > 0.05$, $*$ represents $P < 0.05$, and $**$ represents $P < 0.01$.

3. Results

3.1. Dose-Response Relations for Repeated Noise-Induced ABR Threshold Shifts. ABR threshold shifts at 1 day after NE (Figure 3(a)) and 14 days after NE (Figure 3(b)) for groups of repeated noise exposure at various intensities were measured over frequencies from 4 kHz to 32 kHz. No significant threshold shifts were observed in groups of low-intensity noise exposures at 88, 91, and 94 dB SPL at any frequency except for 32 kHz (Table 1). Because the frequency of 32 kHz in C57 mice was extremely vulnerable to hearing loss related to a genetic defect of cadherin in the stereocilia [38, 39], this frequency was excluded from the following analyses in this study. For moderate- to high-intensity repeated noise exposures, threshold shifts at 1 day and 14 days after NE both showed a more striking increase at higher frequencies with intensity, while no significant PTSs showed at the frequency of 4 kHz even under the strongest noise exposure (106 dB SPL) at 14 days after NE. Moderate-intensity noise exposures (97 and 100 dB SPL) induced significant threshold shifts over frequencies from 8 kHz to 22 kHz at 1 day after NE, but no significant PTSs of which except for the 22 kHz in the group of intensity at 100 dB SPL (Table 1).

3.2. Not Significant Auditory Effects Induced by Low-Intensity Repeated Noise Exposure. For groups of low-intensity noise exposures at 88, 91, and 94 dB SPL without significant threshold shifts of ABR, we further analysed DPOAE threshold shifts (representative group of 88 dB SPL, Supplementary Figure 1), ABR wave I amplitudes (Figures 4(a)–4(c)), ribbon synaptic counts (Figures 4(d) and 4(f)), and the density of MOC efferent synapses (Figures 4(e) and 4(f)) at 14 days after repeated noise exposures, and no significant changes of which were observed at neither 8 kHz, 16 kHz, nor 22.6 kHz frequencies.

3.3. Moderate-Intensity Repeated Noise Exposure Impaired Cochlear Synaptic Morphology ahead of Function. For moderate-intensity noise exposures, the group of 97 dB SPL showed only TTSs at frequencies of 8, 16, and 22.6 kHz, while the group of 100 dB SPL showed more serious threshold shifts than that in the 97 dB SPL group and even a PTS (ABR and DPOAE threshold shifts) at the frequency of 22.6 kHz (Supplementary Figure 1). The frequency of 22.6 kHz was most vulnerable to repeated acoustic trauma on ABR wave I amplitudes, ribbon synapses, and MOC efferent synapses in groups of moderate-intensity noise exposures (Figures 5(c)–5(f)). Despite the considerable degree of threshold shifts at 1 day after NE (averaged 21.82 dB for group 97 dB SPL and 30.5 dB for group 100 dB SPL), 16 kHz was the most robust frequency against the synaptic degeneration from repeated noise exposures at 97 dB SPL; however, it showed a mild but significant decrease of wave I amplitudes and ribbon synaptic counts in the 100 dB SPL group (Figures 5(b) and 5(d)). Notably, changes at a frequency of 8 kHz indicated that the lower moderate-intensity (97 dB SPL) repeated noise exposures induced the cochlear ribbon and MOC efferent synaptic degeneration (Figures 5(d) and 5(e)) before ABR wave I amplitudes decreased (Figure 5(a)).

3.4. High-Intensity Repeated Noise Exposure Impaired Outer Hair Cells despite Cochlear Synaptic Degeneration. In

Table 1: ABR threshold shifts at 1 day and 14 days after repeated noise exposure at various intensities.

Intensity (dB SPL)	ABR threshold shifts (dB HL)											
	4 kHz		8 kHz		11.3 kHz		16 kHz		22.6 kHz		32 kHz	
	Mean (SD)	*P* value	Mean (SD)	*P* value	Mean (SD)	*P* value	Mean (SD)	*P* value	Mean (SD)	*P* value	Mean (SD)	*P* value
At 1 day after NE												
88 ($n = 10$)	4.00 (5.68)	0.3699	3.00 (8.56)	>0.9999	4.00 (4.59)	0.7544	4.50 (4.97)	0.131	5.50 (6.85)	0.2018	6.00 (13.08)	—
91 ($n = 11$)	2.73 (6.07)	>0.9999	6.00 (8.43)	0.357	5.00 (5.00)	0.5525	4.50 (9.26)	>0.9999	5.00 (8.50)	0.6249	8.50 (11.32)	—
94 ($n = 11$)	4.55 (6.88)	0.474	8.50 (10.55)	0.2195	5.91 (6.25)	0.0883	8.50 (7.84)	0.0525	9.00 (9.37)	0.0877	14.55 (7.23)	—
97 ($n = 12$)	7.50 (7.54)	0.0664	**10.00 (8.79)**	**0.0468**	**15.83 (7.64)**	**0.0381**	**21.82 (8.15)**	**<0.0001**	**24.58 (7.82)**	**<0.0001**	—	—
100 ($n = 10$)	5.50 (5.99)	0.1221	**10.50 (5.99)**	**0.0025**	**24.50 (7.62)**	**0.0006**	**30.50 (7.25)**	**<0.0001**	**33.00 (9.19)**	**<0.0001**	—	—
103 ($n = 12$)	6.25 (7.72)	0.1999	**24.17 (9.49)**	**0.0002**	**34.17 (11.04)**	**0.0013**	**42.08 (9.16)**	**<0.0001**	**42.92 (7.82)**	**<0.0001**	—	—
106 ($n = 8$)	**13.75 (5.18)**	**0.0007**	**32.14 (4.88)**	**<0.0001**	**37.50 (5.35)**	**0.0006**	**47.86 (6.36)**	**<0.0001**	**50.00 (7.50)**	**<0.0001**	—	—
At 14 days after NE												
88 ($n = 10$)	-1.00 (5.16)	>0.9999	-1.50 (6.26)	>0.9999	0.50 (5.50)	>0.9999	-1.50 (5.80)	>0.9999	0.00 (8.16)	>0.9999	8.50 (10.55)	—
91 ($n = 11$)	-0.50 (7.62)	>0.9999	2.00 (7.53)	>0.9999	1.50 (6.26)	>0.9999	1.00 (3.94)	>0.9999	0.45 (8.79)	>0.9999	10.91 (8.61)	—
94 ($n = 11$)	1.00 (8.43)	>0.9999	2.00 (8.56)	>0.9999	-1.00 (7.38)	>0.9999	-1.00 (6.58)	>0.9999	1.50 (10.55)	>0.9999	12.73 (7.54)	—
97 ($n = 12$)	0.42 (5.42)	>0.9999	1.67 (6.85)	>0.9999	1.25 (6.78)	>0.9999	-0.42 (4.98)	>0.9999	6.25 (8.56)	0.321	—	—
100 ($n = 10$)	4.00 (6.99)	0.7272	2.50 (6.35)	>0.9999	1.50 (5.30)	>0.9999	4.00 (6.58)	0.6079	**11.5 (9.44)**	**0.0273**	—	—
103 ($n = 12$)	6.25 (8.56)	0.3317	2.92 (8.65)	>0.9999	6.25 (8.01)	0.2999	**20.42 (8.38)**	**0.0003**	**40.00 (9.29)**	**<0.0001**	—	—
106 ($n = 8$)	7.14 (6.36)	0.1267	**15.71 (4.50)**	**0.0004**	**21.43 (5.56)**	**0.0002**	**41.43 (5.56)**	**<0.0001**	**46.67 (6.06)**	**<0.0001**	—	—

Two-way ANOVA with Bonferroni post hoc tests were used to compare the difference between ABR thresholds at 1 day or 14 days after NE with the baseline in each group of intensity. Bold type: $P < 0.05$.

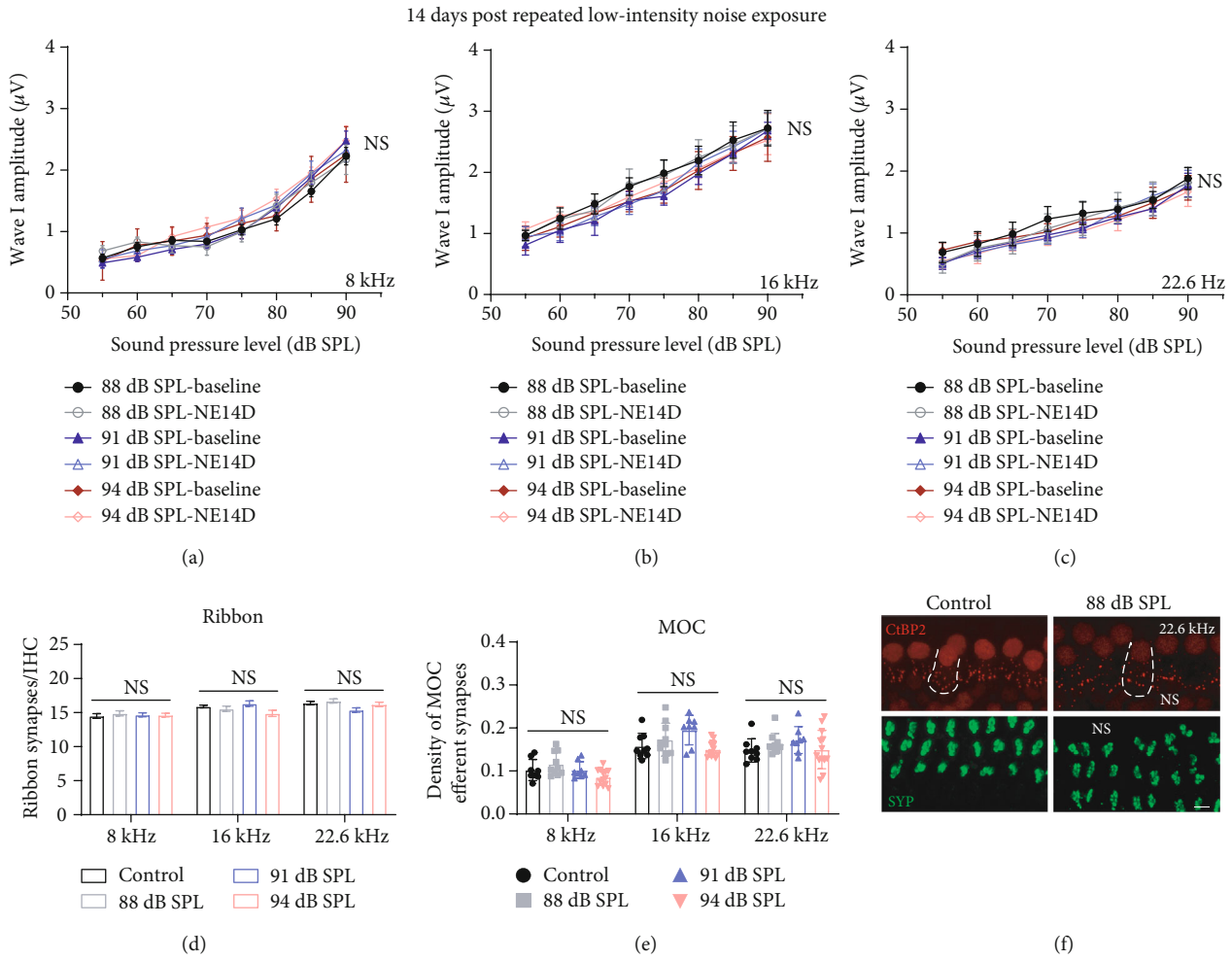

FIGURE 4: No significant permanent effects on (a–c) ABR wave I amplitudes, (d) ribbon synapse counts, and (e) MOC efferent synaptic measurement post low-intensity (88, 91, and 94 dB SPL) repeated noise exposure. (f) Representative IF images of morphometric analysis at frequency of 22.6 kHz (the scale bar indicates 10 μm). Two-way ANOVA with Bonferroni post hoc tests were used to compare the difference between groups. The error bar represents the SEM for 8-12 mice in each group. NE14D: 14 days after NE; NS: no significance. $^{*}P < 0.05$; $^{**}P < 0.01$.

consideration of PTSs induced by repeated high-intensity noise exposures, we performed DPOAE tests and HC counting at 14 days post exposures. No significant loss of HCs was found, even for the group of highest intensity (Supplementary Figure 2), while significant DPOAE threshold shifts were essentially consistent with PTSs at frequencies of 8, 16, and 22.6 kHz for each group (Table 1 and Figure 6(a)). In accordance with expectations, ABR wave I amplitudes and ribbon synaptic counts permanently reduced in high-intensity noise-exposed groups (Figures 6(b)–6(e)). However, to our surprise, the decrement of MOC efferent synapses was not significant after repeated noise exposures at high intensities except for that at the frequency of 22.6 kHz in the 106 dB SPL group (Figures 6(f)–6(h)).

4. Discussion

In this study, we explored and summarized the dose-dependent pattern of cochlear functional and morphological degeneration induced by repeated noise exposure at various intensities from 88 to 106 dB SPL in a 3 dB step increment.

Despite numerous studies that have demonstrated noise-induced cochlear synaptic degeneration in various animal models [18, 19, 25, 39–42], most of them used a single, short-duration noise exposure procedure extensively used in CBA/CaJ mice, Sprague-Dawley rats, guinea pigs, etc. The C57BL/6 strain mouse was not commonly used in previous NIHL studies, because it showed more severe ABR and DPOAE threshold shifts at high frequencies compared with CBA mice [39, 43], which was attributed to the genetic defect in the stereocilia of carrying $Cdh23^{ahl}$ alleles [38]. However, in recent years, since many laboratories have moved their mutant genes of interest to the C57BL/6 background [44], this strain was widely used for genetic studies, including many NIHL studies [45–47]. Moreover, previous strain comparisons revealed that C57 mice were more susceptible than CBAs in the older age group only [43], while a recent study indicated that the susceptibility of noise-induced cochlear ribbon synaptopathy in CBA mice was different from C57

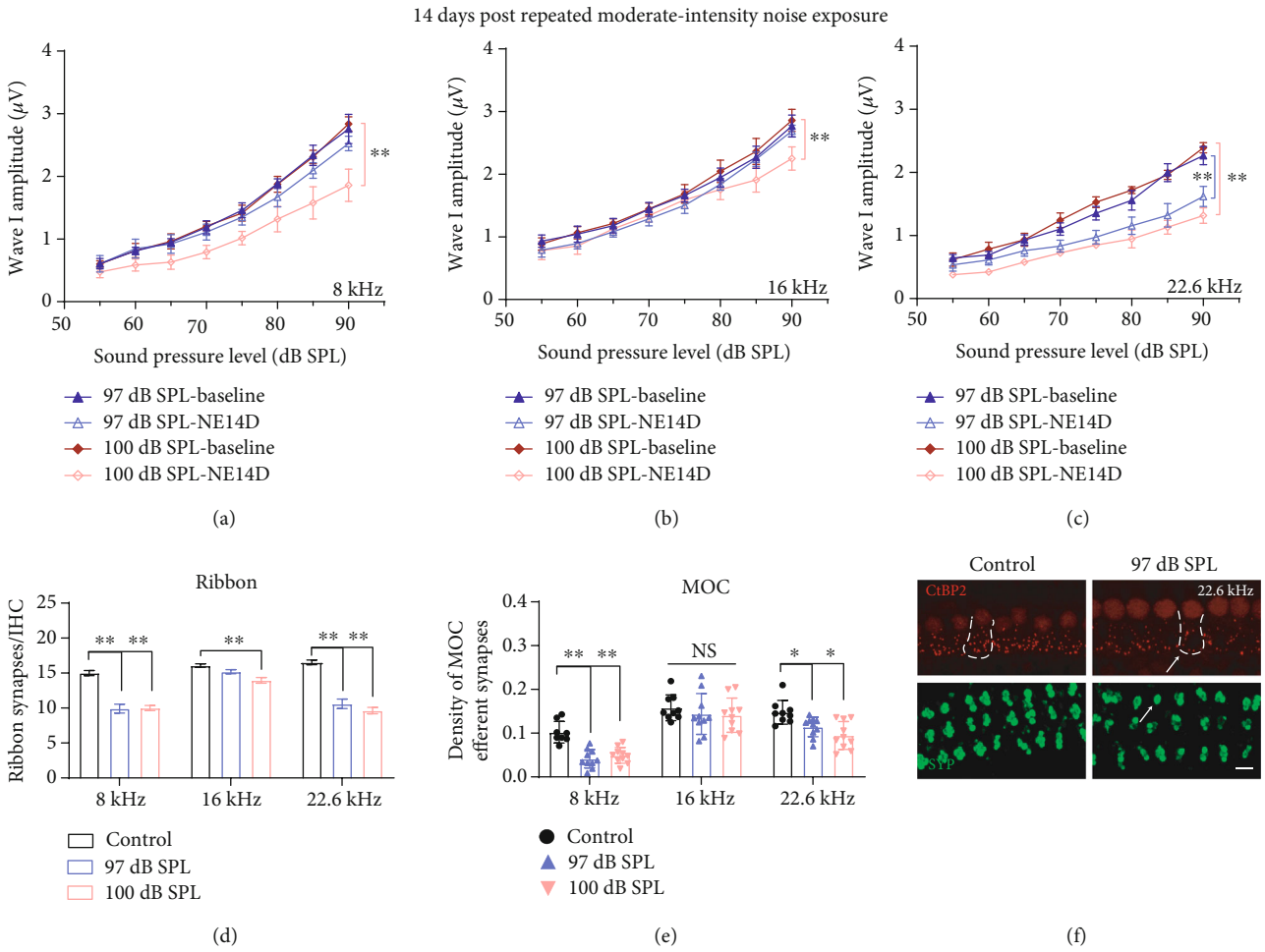

Figure 5: Moderate-intensity (97 and 100 dB SPL) repeated noise-induced permanent effects on (a–c) ABR wave I amplitudes, (d) ribbon synapse counts, and (e) MOC efferent synaptic quantification. (f) Representative IF images of morphometric analysis for group 97 dB SPL at a frequency of 22.6 kHz; white arrows indicate significant morphometric changes (the scale bar indicates 10 μm). Two-way ANOVA with Bonferroni post hoc tests were used to compare the difference between groups. The error bar represents the SEM for 8-12 mice in each group. NE14D: 14 days after NE; NS: no significance. $^{*}P < 0.05$; $^{**}P < 0.01$.

mice [31]. Thus, we chose to use young C57 mice aged four weeks and followed up to the age of 7 weeks. In this study, we provided the characterization of repeated noise-induced injury to cochlear function, synaptic morphology, and their dose-response relationships in C57BL/6J mice.

4.1. Smaller TTS Did Not Show Evidence of Cochlear or Synapse Pathology with Repeated Exposure. Given the compelling evidence that even moderate noise exposure can result in cochlear synaptic degeneration, numerous studies asked whether prolonged overexposure to various noise levels that had been considered "harmless" would add significant risk to NIHL [48, 49]. One challenge in understanding the cochlear consequence of noise is to overview damage patterns of the wide range of possible stimulus parameters. Referring to human daily exposures, we wondered if cochlear synaptic degeneration results from repeated exposures at lower SPLs.

Overall, in this study, one-week long repeated noise exposure at relatively low intensities seemed to be benign for young C57BL/6J mice during a moderate period (two weeks in our results). The "low" intensities (up to 94 dB SPL) of broadband noise used in this study are remarkably higher than that of environmental sounds, which did not induce even temporary impairments on cochlear function and synaptic morphology. These results could be supported by some previous studies. Morgan et al. [27] exposed Sprague-Dawley rats to 8-16 kHz octave-band noise at 97 dB SPL for 2 hours, which repeated for 4 consecutive days. They demonstrated that daily repeated exposures result in diminished TTS and recovered thresholds; moreover, no permanent reduction in suprathreshold ABR responses was observed. Mannström et al. exposed female Sprague-Dawley rats to 2-20 kHz broadband noise for 1.5 hours at various intensities, which was repeated every six weeks. They found that rats exposed to the repeated noise exposure at 101 and 104 dB SPL did not have any permanent impairment in thresholds or ABR wave I amplitudes in comparison with unexposed control rats [50]. Despite the species differences in the noise dose required to generate cochlear injuries [51, 52], our results suggested that in C57 mice [27], there is also a permissible dose of noise exposure that does not directly

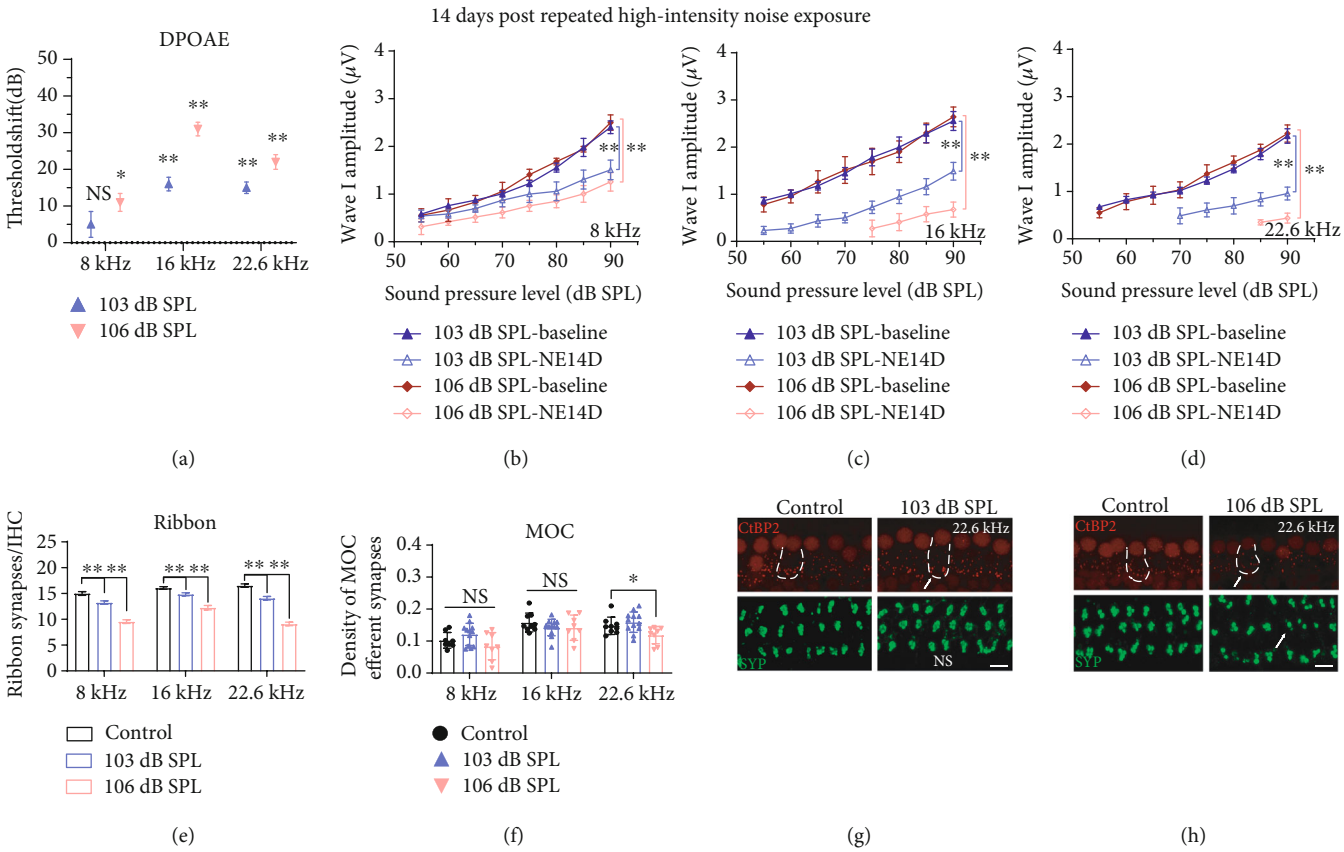

FIGURE 6: High-intensity (103 and 106 dB SPL) repeated noise-induced permanent effects on (a) DPOAE, (b–d) ABR wave I amplitudes, (e) ribbon synapse counts, and (f) MOC efferent synaptic quantification. Representative IF images of morphometric analysis for groups (g) 103 dB SPL and (h) 106 dB SPL at the frequency of 22.6 kHz; white arrows indicate significant morphometric changes (the scale bar indicates 10 μm). Two-way ANOVA with Bonferroni post hoc tests were used to compare the difference between groups. The error bar represents the SEM for 8-12 mice in each group. NE14D: 14 days after NE; NS: no significance. $^{*}P < 0.05$; $^{**}P < 0.01$.

cause the significant TTS as well as the cochlear synaptic degeneration. However, the long-term effects of accumulated noise-induced trauma in cochlea synapses should be further considered in future studies.

4.2. Damage Pattern of Repeated Noise Exposures. Noise-induced cochlear damage may take various patterns underlying different degrees and mechanisms for reversible or permanent impairments. To date, the sustained cochlear damage across all mammalian species studies seems to progress similarly with the noise dose increase, which first occurs in IHC ribbon synapses, then the stereocilia, later the loss of HCs and ANs [52, 53]. Different from the single octave band of noise extensively used in many previous studies [17, 18, 22], we used the repeated broadband noise at intensities from 97 to 106 dB SPL without producing significant loss of HCs, in order to focus on the cochlear synaptic degeneration and dysfunction of OHC stereocilia (reflected on DPOAE) and their vulnerability at various frequencies. Notably, we took not only ribbon synapses but also MOC efferent synapses into consideration of the cochlear synaptic degeneration.

As expected, repeated noise-induced hearing threshold shifts in C57 mice were more severe at higher frequencies, which should be attributed to the dysfunction or damage of OHC stereocilia. In this study, we further found that the vulnerability to repeated noise-induced cochlear synaptic degeneration was more remarkable at the higher frequency of 22.6 kHz and the lower frequency of 8 kHz, while the middle frequency of 16 kHz was most robust against synaptic degeneration. For all frequencies, TTSs first occurred with the increased doses of repeated noise exposure, which were not always accompanied by synaptic degeneration. Moreover, the change of ribbon synaptic counts appeared to be consistent with MOC efferent synapses under low- and moderate-intensity noise exposure. However, PTSs accompanied by damage on DPOAEs were more likely to result in loss of ribbon synapses rather than MOC efferent synapses (Table 2). To our knowledge, this present study showed for the first time that repeated noise exposure leading to cochlear synaptic degeneration could also cause reduction of MOC efferent synapses, which depended on the vulnerability of frequency and function of OHCs.

As previous studies indicated, the relationship between threshold shifts at 1 day after NE criterion change and ABR amplitudes or synaptic counts at each frequency was quite complicated [22, 51, 54, 55]. Among Sprague-Dawley rats, only the 8-16 kHz bandpass noise exposures producing TTSs at 1 day after NE greater than 30 dB could reduce ABR wave I amplitudes, while the degree of ABR wave I reduction was not related to the degree of threshold shifts [19]. However,

Table 2: Cochlear function and synaptic morphology changes related to repeated noise exposure at various intensities.

Frequency	Intensity (dB SPL)		Function			Synaptic morphology	
			Threshold shifts at 1 day after NE	Threshold shifts at 14 days after NE	Decreased ABR wave I amplitude	Ribbon synaptopathy	MOC efferent synaptic degeneration
8 kHz	Low	88, 91, 94	(-)	(-)	(-)	(-)	(-)
	Moderate	97	(+)	(-)	(-)	(+)	(+)
		100	(+)	(-)	(+)	(+)	(+)
	High	103	(+)	(-)	(+)	(+)	(-)
		106	(+)	(+)	(+)	(+)	(-)
16 kHz	Low	88, 91, 94	(-)	(-)	(-)	(-)	(-)
	Moderate	97	(+)	(-)	(-)	(-)	(-)
		100	(+)	(-)	(+)	(+)	(-)
	High	103	(+)	(+)	(+)	(+)	(-)
		106	(+)	(+)	(+)	(+)	(-)
22 kHz	Low	88, 91, 94	(-)	(-)	(-)	(-)	(-)
	Moderate	97	(+)	(-)	(+)	(+)	(+)
		100	(+)	(+)	(+)	(+)	(+)
	High	103	(+)	(+)	(+)	(+)	(-)
		106	(+)	(+)	(+)	(+)	(+)

(+) indicates significant change; (-) indicates nonsignificant change.

Maison et al. reported significant cochlear ribbon synaptopathy in CBA mice exposed to lower intensity but more prolonged octave noise that only produced a 15 dB TTS [29]. Here, we found that the degree of threshold shifts at 1 day after NE producing cochlear synaptic degeneration was particularly related to the frequency. Our results suggested that approximately 10 dB at 8 kHz, 30 dB at 16 kHz, and 20 dB at 22.6 kHz of threshold shifts at 1 day post exposure are able to result in permanent loss of ribbon synapses. Moreover, the degree of threshold shifts at 1 day after NE progress following PTSs was about 30 dB at 8 kHz and 22.6 kHz, which was higher than 40 dB at a frequency of 16 kHz (Table 1). The findings suggested that repeated or prolonged noise exposure might cause greater cochlear synaptic degeneration at lower and higher frequencies, in the order of ARHL patterns of IHC synapse loss observed in human temporal bones [56, 57]. Fernandez et al. previously demonstrated that CBA/CaJ mice exposed to 8-16 kHz noise at 91 dB SPL for 2 hours or 8 hours produced no loss of synapses at 16 kHz and below, while the synaptic loss increased with frequency for 8-hour exposure compared with the 2-hour exposure [22]. Repeated exposures to the single noise that induced only TTSs resulted in cumulative cochlear ribbon synaptopathy at frequencies of 16 kHz and above as well [58]. These results suggested that repeated noise overstimulation probably accelerates the cochlear synaptic degeneration in the animal model of ARHL [59].

4.3. Potential Effects on MOC Efferent Synapses of Repeated Noise Exposure. It is widely accepted that the feedback from the MOC efferent system can protect cochlear ribbon synaptopathy from both acute and chronic noise exposures [29, 60, 61]. Maison et al. removed all efferent feedback to the inner ear by cutting the efferent bundles, whereas the sectioning of the efferent fibers greatly exacerbated the ribbon synaptopathy in both basal and apical regions of the cochlea in CBA/CaJ mice under one-week exposure at 84 dB SPL [29]. A recent study used mice with a gain-of-function point mutation in the $\alpha 9$ subunit of the nicotinic acetylcholine receptor, which strengthened cochlear suppression of the MOC efferent system protecting the loss of ribbon synapses from acoustic injury [62]. The aging-induced MOC system decline has been demonstrated in numerous previous studies. The density of MOC efferent terminals decreased with age prior to OHC degeneration, as measured by contralateral suppression (CS) of DPOAEs in humans and CBA mice [63, 64].

However, it remains unclear whether noise exposure results in damage to MOC efferent nerves. Only a few studies have focused on damage to efferent nerve endings following noise exposure. Although the previous work failed to observe any effects on CS of acute recreational noise exposure in normal hearing threshold adults [65], Boero et al. first demonstrated that acute 1-16 kHz noise exposure at 100 dB SPL for 1 hour can produce degeneration of MOC terminals contacting the OHCs [60]. Consistently in this study, we first demonstrated that repeated noise exposure in C57 mice also results in MOC efferent synaptic degeneration. Our results indicated that the MOC efferent synapses showed strong resistance to noise damage, as well as partial protection from ribbon synaptopathy at middle frequencies of 16 kHz (Table 2), in accordance with the distribution of MOC terminals as previous observations [63, 66]. Further studies to reveal repeated noise-induced functional changes of MOC efferent nerves need to be performed in the future.

Notably, we found that various repeated noise-induced effects on patterns of TTSs, PTSs, ABR wave I amplitudes, ribbon, and MOC efferent synaptic degeneration were quite

complex. For instance, although both ribbon and MOC efferent synapses decreased at frequency of 8 kHz, ABR wave I amplitudes reduced in group 100 dB SPL rather than 97 dB SPL (Figure 4). We proposed that the different damage patterns may depend on balance of the degree of injury of various inner ear elements, especially the MOC efferent feedback. Besides, repeated high-intensity noise exposures enabled production of PTSs unexpectedly resulting in slighter MOC efferent synaptic degeneration than that under moderate-intensity noise. These results suggested that noise-induced PTS may alter synaptopathic outcomes. Fernandez et al. recently assessed the dose-response effects on ribbon synaptopathy and HC damage of acute 8-16 kHz octave-band noise exposure in CBA/CaJ mice. They also observed that higher-level noise exposure producing mixed sensory and neural loss resulted in smaller synapse losses, despite greater declines in suprathreshold ABR amplitudes [53]. Underlying mechanisms might involve HC injury attenuating the direct stimulus on synapses, which protected them from synaptic excitotoxicity [17].

5. Conclusions

In summary, we demonstrated the dose-dependent characterization of the repeated noise-induced injury to cochlear function, synaptic morphology, and their complex dose-response relationships in C57BL/6J mice. We proposed that the noise-induced various cochlear damage patterns attribute to the balance of degrees of injury on HCs, ribbon and MOC efferent synapses, etc. Notably, this study provided a sight into the hypothesis that the interruption in synaptic communication between MOC efferent terminals and OHCs, together with loss of ribbon synapses, contributes to prolonged noise-induced cochlear synaptic degeneration.

Data Availability

The analysed data used to support the findings of this study are included within the article; further inquiries are available from the corresponding authors upon request.

Conflicts of Interest

The authors declare that there is no conflict of interest regarding the publication of this paper.

Authors' Contributions

Minfei Qian and Qixuan Wang contributed equally to this work.

Acknowledgments

This study was supported by the Natural Science Foundation of Shanghai Science and Technology Committee (20ZR1431200), the Elite Program of Shanghai Ninth People's Hospital (JY201802), and the Shanghai Key Laboratory of Translational Medicine on Ear and Nose Diseases (14DZ2260300).

Supplementary Materials

Supplementary Figure 1: representative low-intensity (88 dB SPL) and moderate-intensity (97 and 100 dB SPL) repeated noise-induced DPOAE threshold shifts at 14 days after NE. Two-way ANOVA with Bonferroni post hoc tests were used to compare the difference compared with baseline. The error bar represents the SEM for 8-12 mice in each group. NS: no significance; $^*P < 0.05$. Supplementary Figure 2: whole-mount cochlear immunofluorescence at 14 days after 106 dB SPL repeated noise exposure. No significant HC loss was observed at frequencies of 8, 16, or 22.6 kHz. The scale bar indicates 20 μm. *(Supplementary Materials)*

References

[1] C. Zhu, C. Cheng, Y. Wang et al., "Loss of ARHGEF6 causes hair cell stereocilia deficits and hearing loss in mice," *Frontiers in Molecular Neuroscience*, vol. 11, p. 362, 2018.

[2] S. Gao, C. Cheng, M. Wang et al., "Blebbistatin inhibits neomycin-induced apoptosis in hair cell-like HEI-OC-1 cells and in cochlear hair cells," *Frontiers in Cellular Neuroscience*, vol. 13, p. 590, 2019.

[3] Y. Zhang, W. Li, Z. He et al., "Pre-treatment with fasudil prevents neomycin-induced hair cell damage by reducing the accumulation of reactive oxygen species," *Frontiers in Molecular Neuroscience*, vol. 12, p. 264, 2019.

[4] S. Zhang, Y. Zhang, Y. Dong et al., "Knockdown of Foxg1 in supporting cells increases the trans-differentiation of supporting cells into hair cells in the neonatal mouse cochlea," *Cellular and Molecular Life Sciences*, vol. 77, no. 7, pp. 1401–1419, 2020.

[5] F. Qian, X. Wang, Z. Yin et al., "The slc4a2b gene is required for hair cell development in zebrafish," *Aging*, vol. 12, no. 19, pp. 18804–18821, 2020.

[6] H. Zhou, X. Qian, N. Xu et al., "Disruption of Atg7-dependent autophagy causes electromotility disturbances, outer hair cell loss, and deafness in mice," *Cell Death & Disease*, vol. 11, no. 10, p. 913, 2020.

[7] A. Dhukhwa, P. Bhatta, S. Sheth et al., "Targeting inflammatory processes mediated by TRPVI and TNF-α for treating noise-induced hearing loss," *Frontiers in Cellular Neuroscience*, vol. 13, p. 444, 2019.

[8] R. Guo, M. Xiao, W. Zhao et al., "2D Ti3C2TxMXene couples electrical stimulation to promote proliferation and neural differentiation of neural stem cells," *Acta Biomaterialia*, 2020.

[9] L. Xia, Y. Shang, X. Chen et al., "Oriented neural spheroid formation and differentiation of neural stem cells guided by anisotropic inverse opals," *Frontiers in Bioengineering and Biotechnology*, vol. 8, p. 848, 2020.

[10] Y. Yang, Y. Zhang, R. Chai, and Z. Gu, "A polydopamine-functionalized carbon microfibrous scaffold accelerates the development of neural stem cells," *Frontiers in Bioengineering and Biotechnology*, vol. 8, p. 616, 2020.

[11] R. Guo, X. Ma, M. Liao et al., "Development and application of cochlear implant-based electric-acoustic stimulation of spiral ganglion neurons," *ACS Biomaterials Science & Engineering*, vol. 5, no. 12, pp. 6735–6741, 2019.

[12] A. Li, D. You, W. Li et al., "Novel compounds protect auditory hair cells against gentamycin-induced apoptosis by

maintaining the expression level of H3K4me2," *Drug Delivery*, vol. 25, no. 1, pp. 1033–1043, 2018.

[13] S. Sun, M. Sun, Y. Zhang et al., "In vivo overexpression of X-linked inhibitor of apoptosis protein protects against neomycin-induced hair cell loss in the apical turn of the cochlea during the ototoxic-sensitive period," *Frontiers in Cellular Neuroscience*, vol. 8, p. 248, 2014.

[14] Z. He, S. Sun, M. Waqas et al., "Reduced TRMU expression increases the sensitivity of hair-cell-like HEI-OC-1 cells to neomycin damage in vitro," *Scientific Reports*, vol. 6, p. 29621, 2016.

[15] X. Yu, W. Liu, Z. Fan et al., "c-Myb knockdown increases the neomycin-induced damage to hair-cell-like HEI-OC1 cells in vitro," *Scientific Reports*, vol. 7, p. 41094, 2017.

[16] Q. Wang, M. Qian, L. Yang et al., "Audiometric phenotypes of noise-induced hearing loss by data-driven cluster analysis and their relevant characteristics," *Frontiers in Medicine*, vol. 8, p. 331, 2021.

[17] S. G. Kujawa and M. C. Liberman, "Adding insult to injury: cochlear nerve degeneration after "temporary" noise-induced hearing loss," *The Journal of Neuroscience*, vol. 29, no. 45, pp. 14077–14085, 2009.

[18] G. Mehraei, A. E. Hickox, H. M. Bharadwaj et al., "Auditory brainstem response latency in noise as a marker of cochlear synaptopathy," *The Journal of Neuroscience*, vol. 36, no. 13, pp. 3755–3764, 2016.

[19] E. LOBARINAS, C. SPANKOVICH, and C. G. LE PRELL, "Evidence of "hidden hearing loss" following noise exposures that produce robust TTS and ABR wave-I amplitude reductions," *Hearing Research*, vol. 349, pp. 155–163, 2017.

[20] L. D. Liberman and M. C. Liberman, "Dynamics of cochlear synaptopathy after acoustic overexposure," *Journal of the Association for Research in Otolaryngology*, vol. 16, no. 2, pp. 205–219, 2015.

[21] Y. Sergeyenko, K. Lall, M. C. Liberman, and S. G. Kujawa, "Age-related cochlear synaptopathy: an early-onset contributor to auditory functional decline," *The Journal of Neuroscience*, vol. 33, no. 34, pp. 13686–13694, 2013.

[22] K. A. Fernandez, P. W. C. Jeffers, K. Lall, M. C. Liberman, and S. G. Kujawa, "Aging after noise exposure: acceleration of cochlear synaptopathy in "recovered" ears," *The Journal of Neuroscience*, vol. 35, no. 19, pp. 7509–7520, 2015.

[23] M. Qian, Q. Wang, L. Yang et al., "The effects of aging on peripheral and central auditory function in adults with normal hearing," *American Journal of Translational Research*, vol. 13, no. 2, pp. 549–564, 2021.

[24] K. Hill, H. Yuan, X. Wang, and S. H. Sha, "Noise-induced loss of hair cells and cochlear synaptopathy are mediated by the activation of AMPK," *The Journal of Neuroscience*, vol. 36, no. 28, pp. 7497–7510, 2016.

[25] A. C. Furman, S. G. Kujawa, and M. C. Liberman, "Noise-induced cochlear neuropathy is selective for fibers with low spontaneous rates," *Journal of Neurophysiology*, vol. 110, no. 3, pp. 577–586, 2013.

[26] Y. Luo, T. Qu, Q. Song et al., "Repeated moderate sound exposure causes accumulated trauma to cochlear ribbon synapses in mice," *Neuroscience*, vol. 429, pp. 173–184, 2020.

[27] D. S. Morgan, A. A. Arteaga, N. A. Bosworth et al., "Repeated temporary threshold shift and changes in cochlear and neural function," *Hearing Research*, vol. 381, p. 107780, 2019,.

[28] Z. Zhang, L. Fan, Y. Xing et al., "Temporary versus permanent synaptic loss from repeated noise exposure in guinea pigs and C57 mice," *Neuroscience*, vol. 432, pp. 94–103, 2020.

[29] S. F. Maison, H. Usubuchi, and M. C. Liberman, "Efferent feedback minimizes cochlear neuropathy from moderate noise exposure," *The Journal of Neuroscience*, vol. 33, no. 13, pp. 5542–5552, 2013.

[30] Q. Wang, X. Wang, L. Yang, K. Han, Z. Huang, and H. Wu, "Sex differences in noise-induced hearing loss: a cross-sectional study in China," *Biology of Sex Differences*, vol. 12, no. 1, p. 24, 2021.

[31] H. Liu, H. Peng, L. Wang et al., "Differences in calcium clearance at inner hair cell active zones may underlie the difference in susceptibility to noise-induced cochlea synaptopathy of C57BL/6J and CBA/CaJ mice," *Frontiers in Cell and Developmental Biology*, vol. 8, p. 635201, 2020.

[32] X.-Y. Zheng, D. Henderson, B.-H. Hu, D.-L. Ding, and S. L. McFadden, "The influence of the cochlear efferent system on chronic acoustic trauma," *Hearing Research*, vol. 107, no. 1-2, pp. 147–159, 1997.

[33] K. E. Froud, A. C. Y. Wong, J. M. E. Cederholm et al., "Type II spiral ganglion afferent neurons drive medial olivocochlear reflex suppression of the cochlear amplifier," *Nature Communications*, vol. 6, no. 1, 2015.

[34] M. Müller, K. . Hünerbein, S. Hoidis, and J. W. T. Smolders, "A physiological place-frequency map of the cochlea in the CBA/J mouse," *Hearing Research*, vol. 202, no. 1-2, pp. 63–73, 2005.

[35] L. Yang, D. S. Chen, T. F. Qu et al., "Maximal number of presynaptic ribbons are formed in cochlear region corresponding to middle frequency in mice," *Acta Oto-Laryngologica*, vol. 138, no. 1, pp. 25–30, 2018.

[36] B. CANLON, A. FRANSSON, and A. VIBERG, "Medial olivocochlear efferent terminals are protected by sound conditioning," *Brain Research*, vol. 850, no. 1-2, pp. 253–260, 1999.

[37] D. E. Vetter, M. C. Liberman, J. Mann et al., "Role of α9 nicotinic ACh receptor subunits in the development and function of cochlear efferent innervation," *Neuron*, vol. 23, no. 1, pp. 93–103, 1999.

[38] R. R. Davis, J. K. Newlander, X.-B. Ling, G. A. Cortopassi, E. F. Krieg, and L. C. Erway, "Genetic basis for susceptibility to noise-induced hearing loss in mice," *Hearing Research*, vol. 155, no. 1-2, pp. 82–90, 2001.

[39] S.-N. Park, S.-A. Back, K.-H. Park et al., "Comparison of functional and morphologic characteristics of mice models of noise-induced hearing loss," *Auris Nasus Larynx*, vol. 40, no. 1, pp. 11–17, 2013.

[40] M. D. Valero, J. A. Burton, S. N. Hauser, T. A. Hackett, R. Ramachandran, and M. C. Liberman, "Noise-induced cochlear synaptopathy in rhesus monkeys (Macaca mulatta)," *Hearing Research*, vol. 353, pp. 213–223, 2017.

[41] M. Kobel, C. G. Le Prell, J. Liu, J. W. Hawks, and J. Bao, "Noise-induced cochlear synaptopathy: past findings and future studies," *Hearing Research*, vol. 349, pp. 148–154, 2017.

[42] C. D. Escabi, M. D. Frye, M. Trevino, and E. Lobarinas, "The rat animal model for noise-induced hearing loss," *Journal of the Acoustical Society of America*, vol. 146, no. 5, p. 3692, 2019.

[43] K. K. Ohlemiller, J. S. Wright, and A. F. Heidbreder, "Vulnerability to noise-induced hearing loss in 'middle-aged' and young adult mice: a dose-response approach in CBA, C57BL, and BALB inbred strains," *Hearing Research*, vol. 149, no. 1-2, pp. 239–247, 2000.

[44] A. Kraev, "Parallel universes of Black Six biology," *Biology direct*, vol. 9, p. 18, 2014.

[45] N. J. Ingham, S. A. Pearson, V. E. Vancollie et al., "Mouse screen reveals multiple new genes underlying mouse and human hearing loss," *PLoS biology*, vol. 17, no. 4, p. e3000194, 2019.

[46] M. R. Bowl, M. M. Simon, N. J. Ingham et al., "A large scale hearing loss screen reveals an extensive unexplored genetic landscape for auditory dysfunction," *Nature communications*, vol. 8, no. 1, p. 886, 2017.

[47] K. K. Ohlemiller, S. M. Jones, and K. R. Johnson, "Application of mouse models to research in hearing and balance," *JARO: Journal of the Association for Research in Otolaryngology*, vol. 17, no. 6, pp. 493–523, 2016.

[48] S. G. Kujawa and M. C. Liberman, "Synaptopathy in the noise-exposed and aging cochlea: primary neural degeneration in acquired sensorineural hearing loss," *Hearing research*, vol. 330, pp. 191–199, 2015.

[49] P. M. Rabinowitz, D. Galusha, C. Dixon-Ernst, J. E. Clougherty, and R. L. Neitzel, "The dose-response relationship between in-ear occupational noise exposure and hearing loss," *Occupational and Environmental Medicine*, vol. 70, no. 10, pp. 716–721, 2013.

[50] P. M. Rabinowitz, D. Galusha, C. Dixon-Ernst, J. E. Clougherty, and R. L. Neitzel, "Repeated moderate noise exposure in the rat—an early adulthood noise exposure model," *Journal of the Association for Research in Otolaryngology*, vol. 16, no. 6, pp. 763–772, 2015.

[51] R. A. Dobie and L. E. Humes, "Commentary on the regulatory implications of noise-induced cochlear neuropathy," *International journal of audiology*, vol. 56, no. sup1, pp. 74–78, 2017.

[52] S. G. Kujawa and M. C. Liberman, "Translating animal models to human therapeutics in noise-induced and age-related hearing loss377," *Hearing research*, pp. 44–52, 2019.

[53] K. A. Fernandez, D. Guo, S. Micucci, V. De Gruttola, M. C. Liberman, and S. G. Kujawa, "Noise-induced cochlear synaptopathy with and without sensory cell loss," *Neuroscience*, vol. 427, pp. 43–57, 2020.

[54] A. E. Hickox and M. C. Liberman, "Is noise-induced cochlear neuropathy key to the generation of hyperacusis or tinnitus?," *Journal of Neurophysiology*, vol. 111, no. 3, pp. 552–564, 2014.

[55] J. B. Jensen, A. C. Lysaght, M. C. Liberman, K. Qvortrup, and K. M. Stankovic, "Immediate and delayed cochlear neuropathy after noise exposure in pubescent mice," *PLoS One*, vol. 10, no. 5, p. e0125160, 2015.

[56] P. Z. Wu, L. D. Liberman, K. Bennett, V. De Gruttola, J. T. O'Malley, and M. C. Liberman, "Primary neural degeneration in the human cochlea: evidence for hidden hearing loss in the aging ear," *Neuroscience*, vol. 407, pp. 8–20, 2019.

[57] L. M. Viana, J. T. O'Malley, B. J. Burgess et al., "Cochlear neuropathy in human presbycusis: confocal analysis of hidden hearing loss in post-mortem tissue," *Hearing research*, vol. 327, pp. 78–88, 2015.

[58] Y. WANG and C. REN, "Effects of repeated "benign" noise exposures in young CBA mice: shedding light on age-related hearing loss," *Journal of the Association for Research in Otolaryngology*, vol. 13, no. 4, pp. 505–515, 2012.

[59] J. C. Alvarado, V. Fuentes-Santamaría, M. C. Gabaldón-Ull, and J. M. Juiz, "Age-related hearing loss is accelerated by repeated short-duration loud sound stimulation," *Frontiers in neuroscience*, vol. 13, p. 77, 2019.

[60] L. E. Boero, V. C. Castagna, M. N. Di Guilmi, J. D. Goutman, A. B. Elgoyhen, and M. E. Gómez-Casati, "Enhancement of the medial olivocochlear system prevents hidden hearing loss," *The Journal of Neuroscience*, vol. 38, no. 34, pp. 7440–7451, 2018.

[61] G. Attanasio, M. Barbara, G. Buongiorno et al., "Protective effect of the cochlear efferent system during noise exposure," *Annals of the New York Academy of Sciences*, vol. 884, pp. 361–367, 1999.

[62] J. Taranda, S. F. Maison, J. A. Ballestero et al., "A point mutation in the hair cell nicotinic cholinergic receptor prolongs cochlear inhibition and enhances noise protection," *PLoS Biology*, vol. 7, no. 1, article e18, 2009.

[63] L. D. Liberman and M. C. Liberman, "Cochlear efferent innervation is sparse in humans and decreases with age," *The Journal of Neuroscience*, vol. 39, no. 48, pp. 9560–9569, 2019.

[64] X. Zhu, O. N. Vasilyeva, S. Kim et al., "Auditory efferent feedback system deficits precede age-related hearing loss: contralateral suppression of otoacoustic emissions in mice," *Journal of Comparative Neurology*, vol. 503, no. 5, pp. 593–604, 2007.

[65] Q. Wang, L. Yang, M. Qian et al., "Acute recreational noise-induced cochlear synaptic dysfunction in humans with normal hearing: a prospective cohort study," vol. 15, p. 659011, 2021.

[66] S. F. Maison and M. C. Liberman, "Predicting vulnerability to acoustic injury with a noninvasive assay of olivocochlear reflex strength," *The Journal of Neuroscience*, vol. 20, no. 12, pp. 4701–4707, 2000.

Hindawi
Neural Plasticity
Volume 2021, Article ID 9979157, 14 pages
https://doi.org/10.1155/2021/9979157

Research Article

Deletion of Clusterin Protects Cochlear Hair Cells against Hair Cell Aging and Ototoxicity

Xiaochang Zhao,[1] Heidi J. Henderson,[2] Tianying Wang,[1] Bo Liu,[1,3] and Yi Li[1]

[1]*Department of Otorhinolaryngology Head and Neck Surgery, Beijing Tongren Hospital, Capital Medical University, Beijing, China*
[2]*Department of Biomedical Sciences, Creighton University School of Medicine, Omaha, Nebraska 68178, USA*
[3]*Beijing Institute of Otolaryngology, Key Laboratory of Otolaryngology Head and Neck Surgery (Capital Medical University), Ministry of Education, Beijing, China*

Correspondence should be addressed to Bo Liu; trliubo@139.com and Yi Li; alinaliyi@163.com

Received 14 March 2021; Revised 15 April 2021; Accepted 28 April 2021; Published 30 May 2021

Academic Editor: Renjie Chai

Hearing loss is a debilitating disease that affects 10% of adults worldwide. Most sensorineural hearing loss is caused by the loss of mechanosensitive hair cells in the cochlea, often due to aging, noise, and ototoxic drugs. The identification of genes that can be targeted to slow aging and reduce the vulnerability of hair cells to insults is critical for the prevention of sensorineural hearing loss. Our previous cell-specific transcriptome analysis of adult cochlear hair cells and supporting cells showed that *Clu*, encoding a secreted chaperone that is involved in several basic biological events, such as cell death, tumor progression, and neurodegenerative disorders, is expressed in hair cells and supporting cells. We generated *Clu*-null mice (C57BL/6) to investigate its role in the organ of Corti, the sensory epithelium responsible for hearing in the mammalian cochlea. We showed that the deletion of *Clu* did not affect the development of hair cells and supporting cells; hair cells and supporting cells appeared normal at 1 month of age. Auditory function tests showed that *Clu*-null mice had hearing thresholds comparable to those of wild-type littermates before 3 months of age. Interestingly, *Clu*-null mice displayed less hair cell and hearing loss compared to their wildtype littermates after 3 months. Furthermore, the deletion of *Clu* is protected against aminoglycoside-induced hair cell loss in both *in vivo* and *in vitro* models. Our findings suggested that the inhibition of *Clu* expression could represent a potential therapeutic strategy for the alleviation of age-related and ototoxic drug-induced hearing loss.

1. Introduction

Hearing loss is one of the most common sensory impairments in humans, affecting approximately 1.3 billion people worldwide [1]. Sensorineural hearing loss, which accounts for a large proportion of hearing loss, is permanent and often caused by acoustic trauma, ototoxic drugs, aging, environmental factors, and genetic defects. Hearing loss affects speech understanding [2], which can lead to isolation, depression, and dementia [3]. However, to our knowledge, no drugs have been identified that can treat or prevent sensorineural hearing loss. The hair cells in the cochlea of the mammalian inner ear are mechanosensitive receptor cells that transduce mechanical stimuli into electrical signals. Two types of hair cells exist in the cochlea. The inner hair cells (IHCs) are the actual sensory receptors that relay electrical signals to the central auditory system through the spiral ganglion neurons, whereas outer hair cells (OHCs) amplify the mechanical signals in the cochlea [4]. Cochlear supporting cells maintain homeostasis of the ionic and chemical environment of the cochlea as well as contribute to the stiffness of the cochlear partition. Supporting cell defects can also lead to hair cell degeneration and hearing loss [5]. All hair cells, including those in the inner ear of nonmammals, are vulnerable to aging, noise, and ototoxicity drugs. The molecular mechanisms that underlie hair cell aging and vulnerability to mechanical and chemical insults remain unclear [6].

Clusterin (CLU) is a secreted chaperone protein involved in several basic biological events, such as cell death, tumor progression, and neurodegenerative disorders. CLU is expressed in many tissues in humans and animals, such as

the testis, epididymis, kidneys, heart, lungs, uterus, ovary, breast, and prostate [7]. Moreover, CLU has been found in the bodily fluids of almost all vertebrates, from zebrafish to humans [8, 9]. CLU plays important roles in protein homeostasis/proteostasis, the inhibition of cell death pathways, and the modulation of prosurvival signaling and transcriptional networks [10]. Previous studies have shown that CLU is associated with neurodegenerative diseases, immune diseases, aging, and cancer [10].

Our previous study used cell type-specific RNA sequencing (RNA-seq) analyses which show that *Clu* is expressed in hair cells and supporting cells [11, 12]. In the present study, we generated a *Clu*-null mouse model to examine the role of CLU in the inner ear. We compared changes in inner ear morphology and function between *Clu*-null and wild-type (WT) mice. We showed that deletion of *Clu* did not affect the development of cochlear hair cells and supporting cells; however, *Clu* deficiency delayed the onset and progression of age-related hearing loss (ARHL) and reduced aminoglycoside-induced hair cell and hearing loss.

2. Materials and Methods

2.1. Ethics Statement. All experimental procedures were approved by the Animal Ethics Review Committee of Capital Medical University. The usage of animals followed the Guide for Use of Laboratory Animals of the Capital Medical University in Beijing, China. *Clusterin* Knockout Mice and Genotyping *Clusterin* knockout mice were generated on C57BL/6 background by CRISPR/Cas9 technology. The *Clu* was deleted by replacing exon 3 of the *Clu* gene, which results in a 583 bp deletion. Genomic DNA was extracted from the tails of the newborn pups ($N = 4$ each group). The genomic DNA fragment around the guide RNA target site was amplified by *Clu*-KO-specific PCR primers as the following primer sets: forward:5′-CAACCGCATCAGGTAGA-3′; reverse:5′-ACCCAC AGCAAGGGTTAG-3′. F0 mice were bred to generate F1 mice. The PCR cycling parameters were as follows: 94°C for 3 min; 35 cycles of 94°C for 30 s, 56°C for 60 s, 72°C for 60 s; 72°Cfor 10 min. PCR products were separated on 1.5% agarose gel, and the expected band sizes for WT (wild-type) and knockout alleles were 1063 and 480 bps, respectively (Figure 1(b)). The DNA from the F1 offspring generation was sequenced to verify the mutation (Figure 1(c)). F2 generation was obtained by intercrossing heterozygous F1 offspring.

2.2. Auditory Brainstem Response (ABR) Measurements. ABR thresholds were measured with tone burst stimuli at frequencies of 8, 16, and 32 kHz in a sound-isolated chamber using a Tucker-Davis Technologies System workstation (RZ6) with SigGen32 software (Tucker-Davis Technologies Inc., Alachua, FL, USA). Mice were anesthetized with a ketamine/xylazine (18 : 2 mg/ml) solution (100/10 mg/kg body weight) and then placed on a soft pad. Subcutaneous electrodes were placed between the ears at the forehead for noninverting, underneath the left external ear for inverting, and back near the tail for ground lead. Auditory brainstem response (ABR) intensity series were collected with a descending series of stimulus levels in 5 dB steps beginning at 90 dB SPL. At least 6 mice per group/age were used for ABR hearing assessment. Following the ABR hearing measurements, tissues from the same mice were used to conduct histopathological and biochemical analyses.

2.3. Distortion Product Otoacoustic Emission (DPOAE) Measurements. DPOAE responses were recorded from anesthetized mice using TDT RZ6. The cubic (2f1-f2) DPOAE thresholds were obtained at a range of frequencies (4-32 kHz), evoked using two equal intensity primary stimuli about the test frequency, and applied to the ear canal using two speakers coupled via a microphone probe. Stimuli were decreased in intensity from 80 to 20 dB in 5 dB increments to establish thresholds. The threshold of DPOAE was defined as 6 dB above the noise floor. We used at least 6 mice per group for DPOAE assessment.

2.4. Cochlear Tissue Processing. After ABR testing, the mice were sacrificed by cervical dislocation and decapitation, and the cochleae were quickly separated from the temporal bone on the culture dish with 4% paraformaldehyde solution. Under a dissecting microscope, a hole was poked at the apex of the cochlea, and the round and oval windows were opened with a needle. The cochlea was perfused with 4% paraformaldehyde solution instead of lymph fluid via the apex and preserved with 4% paraformaldehyde solution at 4°C overnight. Then, the specimen was decalcified in 10% ethylenediaminetetraacetic acid (EDTA) solution for 1.5 hours. The cochlea shell was removed from the apex to base in PBS solution. The basilar membrane was harvested without the vestibular membrane and tectorial membrane. Six cochleae from 6 mice were used for histopathological assessment for each group/age.

2.5. Immunostaining and Laser Confocal Microscopy. The samples were washed three times in PBS and preincubated for 1 hour at room temperature in a blocking solution of 10% normal goat serum in 0.01 M PBS with 0.25% Triton X-100. Next, the samples were incubated with a combination of antibodies about rabbit antimyosin VIIa (1 : 300, Proteus Biosciences, 25-6790), left at 4°C overnight. After incubation, the samples were washed in PBS three times and incubated with the appropriate secondary antibodies coupled to Alexa Fluor in green, red channels at room temperature for 1 hour. After incubation, the samples were washed in PBS three times, and approximately 40 μL of DAPI (4, 6-diamidino-2-phenylindole; Santa Cruz) was applied for the nucleus staining.

Cochlear tissues were fixed with 4% paraformaldehyde in PBS overnight at 4°C. The specimens were decalcified over 12 h in 10% EDTA. The preparations then were dehydrated with graded alcohol series, cleared with xylene, and then embedded in paraffin. Paraffin-embedded specimens were cut into 10-μm-thick sections and then stained with H&E. Confocal images were acquired using Leica confocal microscope (TCS SP8 II; Leica Microsystems, Wetzlar, Germany). 20x magnification was used for imaging and cell counting.

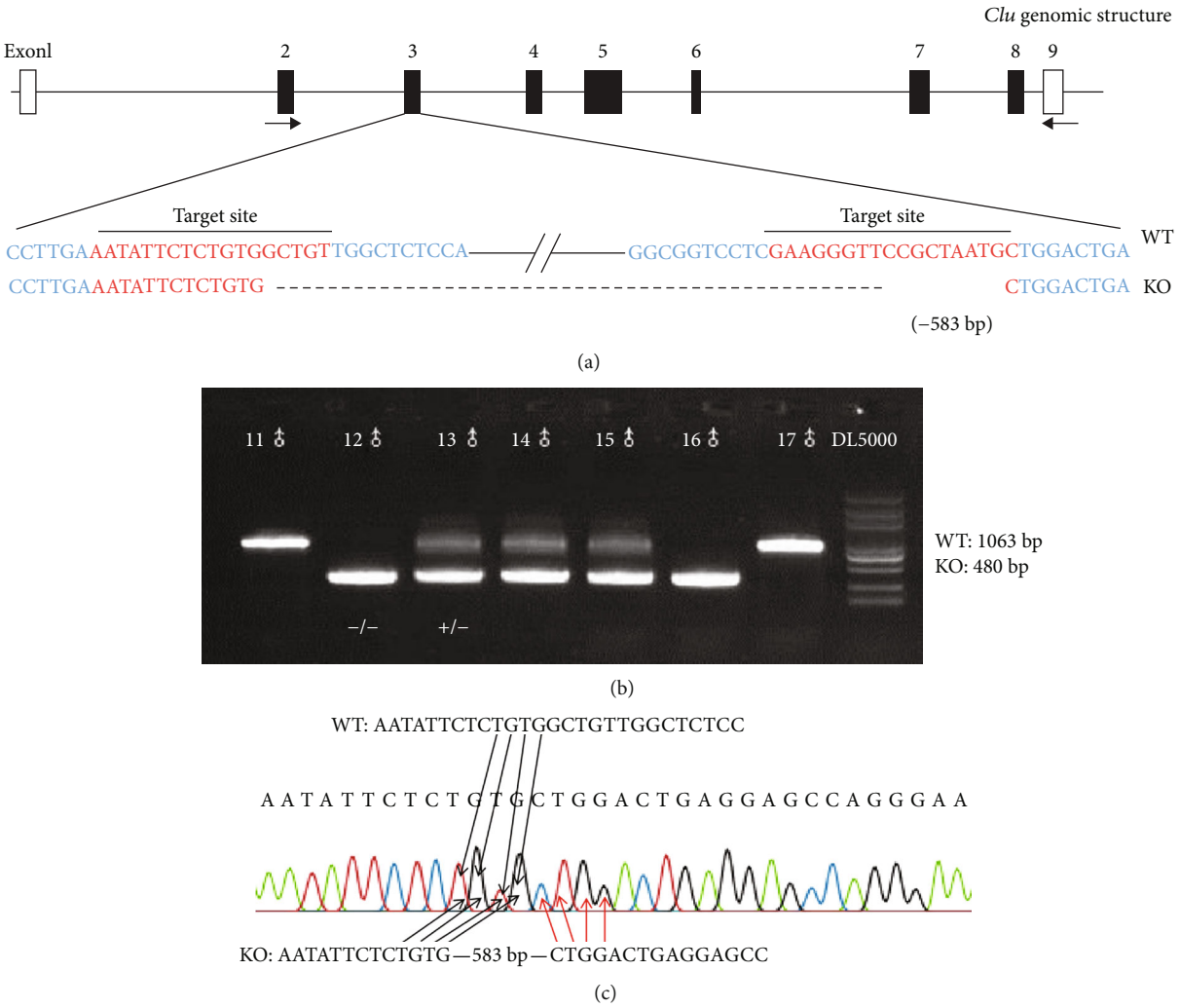

Figure 1: Construction of *Clu* knockout mice. (a) Schematic drawing showing the strategy used for *Clu* gene disruption. The target sites of clustered regularly interspaced short palindromic repeat (CRISPR)-Cas9 small guide RNAs (sgRNAs) in the *Clu* gene are indicated in red, and the deleted region of the *Clu* gene in knockout mice is indicated by dashes. The positions of RT-PCR primers are indicated by arrows. (b) PCR products were separated on a 1.5% agarose gel, and the expected band sizes for WT and knockout (KO) alleles were 1,063 and 480 bps, respectively. (c) Sequencing results for homozygotes. The black arrows represent wild-type sequences, and the red arrows represent sequences following the deleted fragment.

We used Myosin VIIa to label hair cells and DAPI to mark the nucleus of supporting cells underneath the hair cells for supporting cell count. To make cell count results comparable between mice of different ages and genotypes, we compared the actual number of supporting cells to the number of hair cells in the same cochlear location to obtain their relative percentages.

2.6. Drug Administration In Vivo. 6-week-old mice were divided into three groups: control group, WT group, and $Clu^{-/-}$ group ($N = 6$ for each group). In the control group, mice were given a subcutaneous injection of saline followed by an intraperitoneal injection of saline 30 minutes later. In the other two groups, mice were injected subcutaneously with kanamycin (0.1 mg/g of body weight; Sigma-Aldrich, St Louis, Missouri), dissolved in phosphate-buffered saline (PBS), followed by an intraperitoneal injection of furosemide (0.3 mg/g of body weight) 30 minutes later. For each group, ABR threshold was measured before injection and 10 days after coadministration of kanamycin and furosemide injection.

2.7. Organotypic Culture of the Organ of Corti and Drug Administration. Three-day-old mice were divided into three groups (control group, WT group, and $Clu^{-/-}$ group ($N = 6$ each group) for culture. The basilar membrane together with the organ of Corti were dissected out and place on the bottom of culture dish as previously described [12] in a humidified CO_2 incubator at 37°C. After 24 hours, the culture medium in the WT group and $Clu^{-/-}$ group was replace with fresh DMEM/F12 mediums containing 150 μM gentamicin, while the control group was replaced with DMEM/F12 medium. The culture continued for another 36 hours.

2.8. Small Molecule Fluorescent In Situ Hybridization. Cochleae from 21-day-old (C57BL/6) mice were dissected

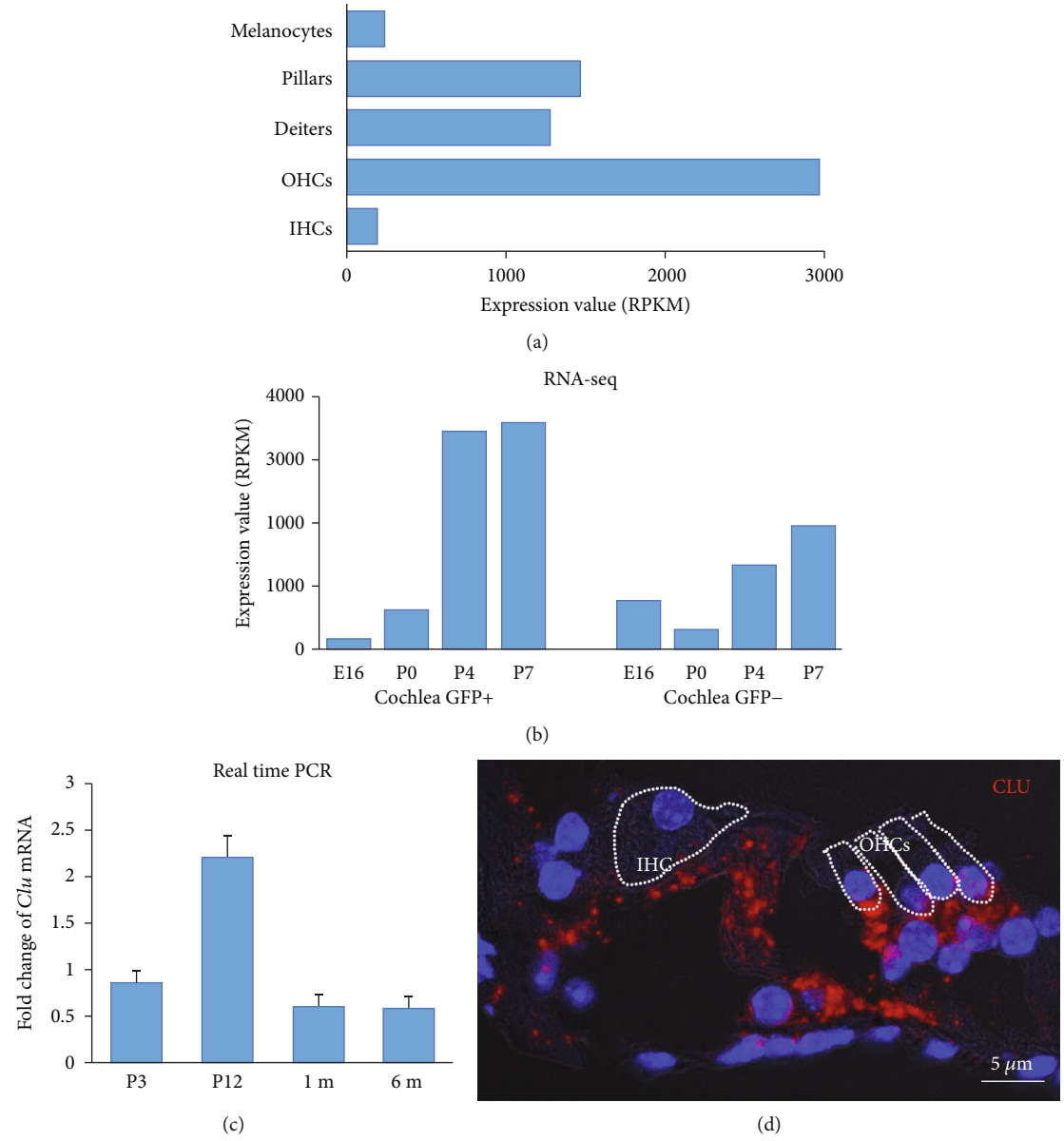

Figure 2: *Clu* expression in the organ of Corti of the cochlea. (a) RNA-seq in the adult CBA/J mouse cochlea showed *Clu* expression in OHCs, IHCs, pillar cells, Deiters' cells, and melanocytes, with strong expression in OHCs. (b) RNA-Seq examining gene expression during mouse inner ear development showed *Clu* expression in hair cells (GFP^+) and supporting cells (GFP^-) in the mouse cochlea, from E16 to P7. (c) Temporal expression patterns of *Clu* mRNA in the mouse inner ear. *Clu* mRNA transcripts were strongly expressed at P12, with slight but significantly decreased expression with aging. $N = 4$. (d) *In situ* hybridization performed in the WT cochlea at P21 showed *Clu* expression in OHCs and stronger expression in the pillar and Deiters' cells.

out and placed in 4% PFA in PBS at room temperature for 24 hours, followed by decalcified in 120 mM EDTA in 4%PFA at 4°Cfor 3 days until the bony tissue was soft and flexible. The tissues were washed in PBS, dehydrated using a standard ethanol series, followed by xylene. After the cochlear wall was removed, the tissues were embedded in paraffin. After paraffin embedding, the blocks were allowed to harden overnight before the tissues were sectioned along the perpendicular plane on a Leica microtome into 5-10 μm sections and mounted on Superfrost plus slides.

To examine the mRNA level expression of *Clu*, the RNAscope-based small molecule fluorescent *in situ* hybridization (smFISH) assay from Advanced Cell Diagnostics (ACD) was used. The paraffin-embedded sections mounted on the slides were baked for one hour at 60°C followed by deparaffinization step (xylene 5 min. 2x, 100% ethanol for 1 min. 2x, and dried at room temperature for 5 min.). A minimum of two sections from different cochlear regions were selected for smFISH. The tissue sections were covered with 5 to 8 drops of RNAscope hydrogen peroxide and incubated at room temperature for 10 min, followed by two washes in fresh distilled water. Slides were dried at room temperature, and a barrier was drawn around each tissue sample using an Immedge hydrophobic barrier pen. The protocol was

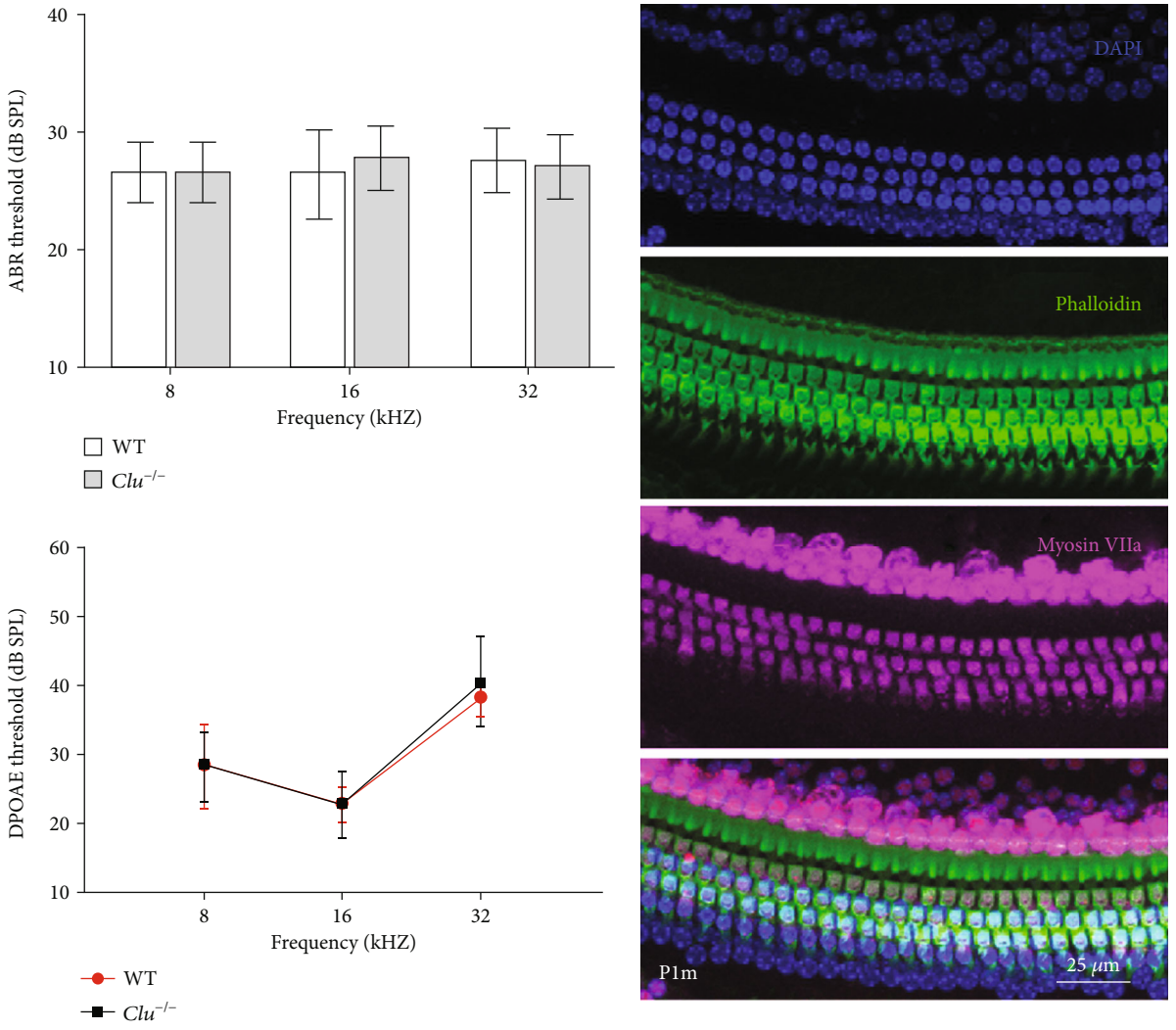

Figure 3: Continued.

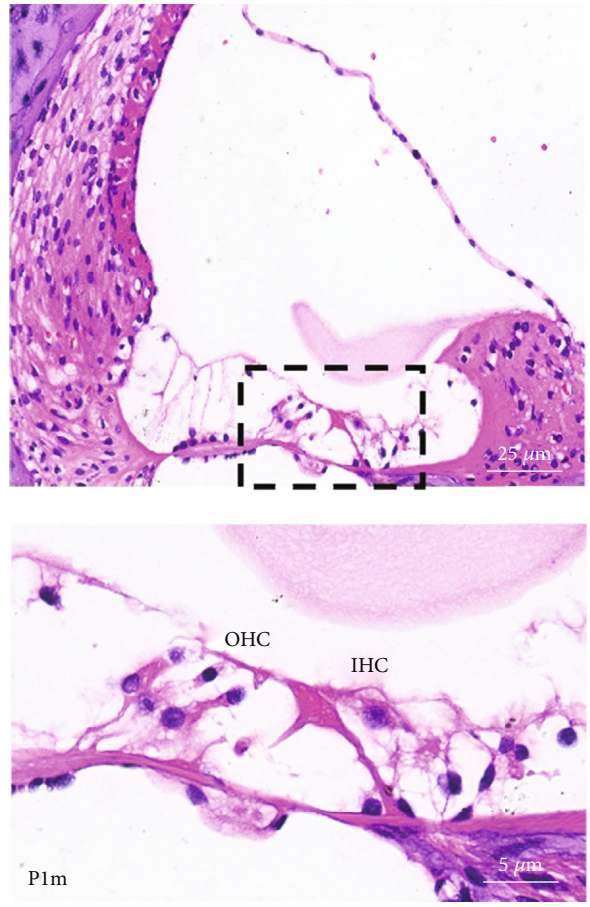

(c)

Figure 3: Hearing and basilar membrane morphology of *Clu*$^{-/-}$ mice in one month. (a) ABR hearing thresholds and DPOAE hearing threshold were measured at 32, 16, and 8 kHz in *Clu*$^{-/-}$ and WT mice at P1m. $N = 6$. (b) Cochlear basilar membrane morphology of *Clu*$^{-/-}$ mice at P1m. (c) Organ of Corti in the basal cochlear regions of P1m *Clu*$^{-/-}$ mice. No hair cells or supporting cell defects were observed.

conducted following the RNAscope 2.5 HD Detection Reagent, RED user manual, and published protocols. The proprietary gene-specific probe for *Clu* targets region n. 436 to 1335 (20 probe pairs). After completing the hybridization, amplification, and color detection steps, the slides were incubated with DAPI for 10 minutes. Finally, the slides were washed in 1X PBS and allowed to dry at room temperature. A drop of SlowFade (Invitrogen) was placed over the tissue and a coverslip was added to preserve the sample. Slides were imaged on a Zeiss LSM 710 confocal microscope. Images were analyzed using ImageJ.

2.9. RNA Extraction and Quantitative Real-Time Polymerase Chain Reaction (qRT-PCR). Total RNA was extracted from the inner ear of C57BL/6 wild-type mice using the RNeasy Mini kit (Tiangen, China). The RNase-free DNase set (Tiangen) was used to remove contaminated DNA. RNA concentration and purity were estimated via spectrophotometry by measuring the absorbance at 260 nm and 260/280 nm ratio, respectively. cDNA was synthesized from RNA using the High Capacity cDNA Reverse Transcription Kit (KAPA BIOSYSTEMS, USA) and oligo-dT primers. Subsequently, qRT-PCR was performed to analyze *Clu* expression at postnatal days 3 (P3), 12 (P12), 30 (1 m), and 180 (6 m). Four mice per group/age were used. qRT-PCR primers were designed based on published reference sequences in the National Center for Biotechnology Information database (NM_013492.3). qRT-PCR was performed using the KAPA SYBR®FAST qPCR Kit Master Mix (2X) Universal (KAPA BIOSYSTEMS) on a StepOnePlus Real-Time PCR System. Each sample was run in triplicate along with the housekeeping gene, GAPDH. Relative quantities of the transcripts were determined using $2^{-\Delta\Delta CT}$ method using GAPDH as a reference.

2.10. Statistical Analyses. Data have been expressed as means ± standard deviation. Statistical analyses were performed with SPSS 13.0 software (IBM, Chicago, IL, USA). A one-way analysis of variance was performed to compare groups. Differences between groups with $p < 0.05$ were considered statistically significant.

3. Results

3.1. Clu Expression in the Organ of Corti. We first examined the expression of *Clu* in the organ of Corti based on published transcriptomes from OHCs, IHCs, pillar cells, Deiters'

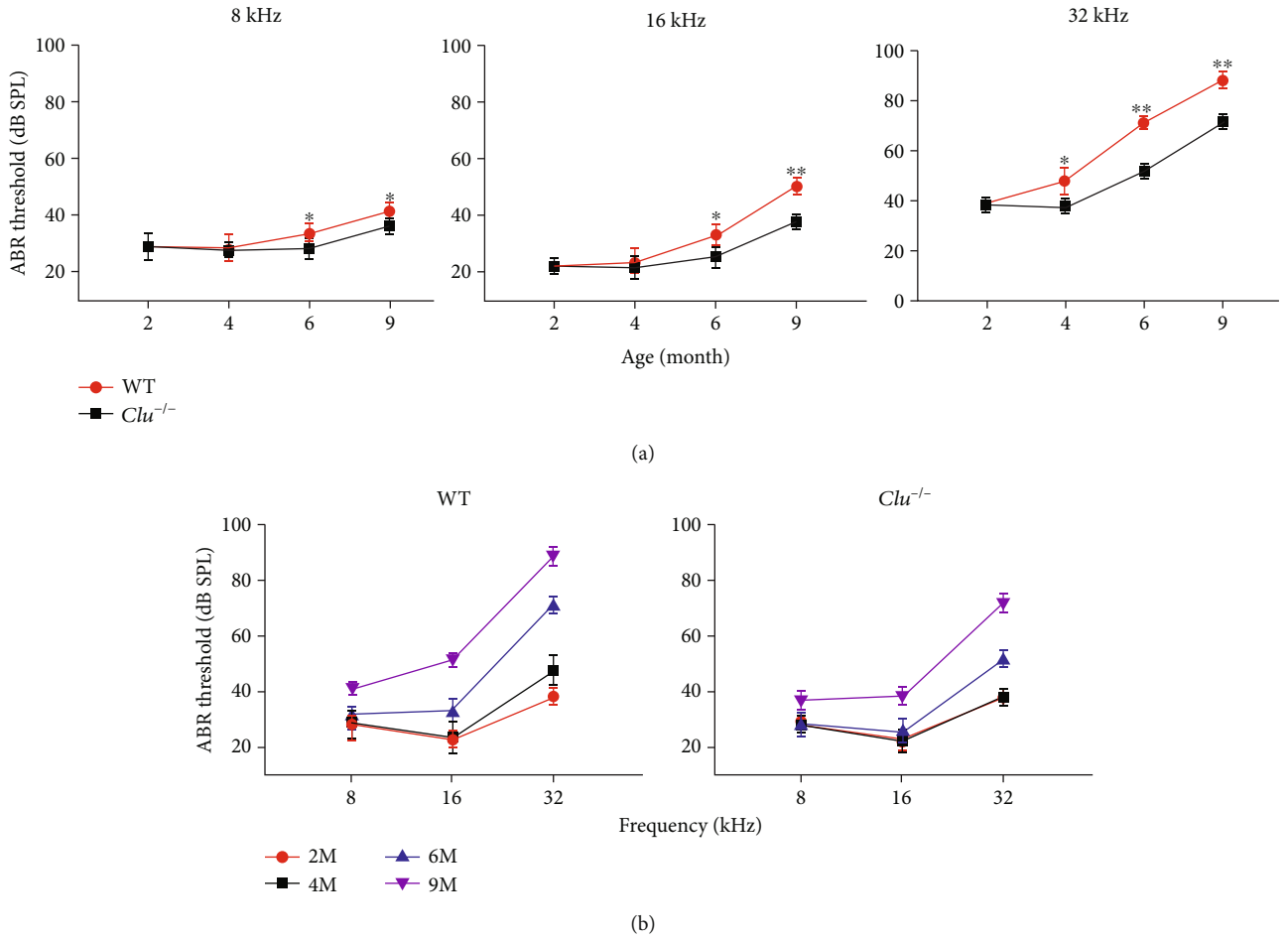

Figure 4: Assessment of age-related auditory dysfunction. (a) ABR hearing thresholds were measured at 32, 16, and 8 kHz in WT and $Clu^{-/-}$ mice at P2m, P4m, P6m, and P9m. *Clu* deficiency delayed ARHL in C57BL/6 mice. Data are presented as the mean ± SD. $^{*}p < 0.05$, $^{**}p < 0.01$. $N = 6$. (b) ABR thresholds of WT and $Clu^{-/-}$ mice at P2m, P4m, P6m, and P9m. $N = 6$.

cells, and stria melanocytes [11, 12]. As shown in Figure 2(a), *Clu* is expressed in hair cells and supporting cells. Figure 2(b) presents the expression of *Clu* in developing hair cells and supporting cells based on the dataset published by Scheffer et al. [13]. *Clu* was expressed in developing hair cells and supporting cells. To confirm the temporal patterns of *Clu* expression in the mouse inner ear, we performed quantitative real-time polymerase chain reaction (qRT-PCR) at P3, P12, P1m, and P6m. *Clu* mRNA transcripts were strongly expressed at P12, which slightly decreased with aging (i.e., at 1 m and 6 m) (Figure 2(c)). We also used smFISH to examine the spatial expression of *Clu* in the cochlea at P21. As shown in Figure 2(d), *Clu* was expressed in OHCs, but stronger expression was observed in the pillar and Deiters' cells.

3.2. Auditory Function of $Clu^{-/-}$ Mice. We measured ABR from $Clu^{-/-}$ and their WT littermates at P15 and P30. Figure 3(a) shows the mean ABR thresholds at 8, 16, and 32 kHz. We also measured DPOAE thresholds from these animals. It is clear from Figure 3(a) that the ABR and DPOAE thresholds of the $Clu^{-/-}$ mice are not statistically different from those of the WT mice. This indicated that deletion of *Clu* did not affect the development of hair cells and auditory function at 1 month of age.

3.3. Hair Cells and Supporting Cell Morphology in $Clu^{-/-}$ Mice. To investigate the morphology of the organ of Corti of $Clu^{-/-}$ mice, we performed histological analyses on cochlear sections from WT and $Clu^{-/-}$ mice at P3, P15, and P1m. Some examples are presented in Figure 3. We counted the total number of hair cells and found the numbers of hair cells and supporting cells in $Clu^{-/-}$ mice were not significantly different from the WT mice. Furthermore, we examined morphology of the organ of Corti in the basal turn in P15 and 1 m-old $Clu^{-/-}$ mice using HE staining. No defects were observed in either the hair cells or supporting cells in the $Clu^{-/-}$ cochleae. Thus, deletion of *Clu* did not affect the development of hair cells and supporting cells.

3.4. Clu Deficiency Delays Onset and Progression of Age-Related Hearing Loss. To investigate whether *Clu* plays a role in the maintenance of auditory function or ARHL, we conducted ABR tests in WT and $Clu^{-/-}$ mice at 2, 4, 6, and 9 months of age. The ABR thresholds at 8, 16, and 32 kHz are presented in Figure 4. It is apparent that the ABR thresholds

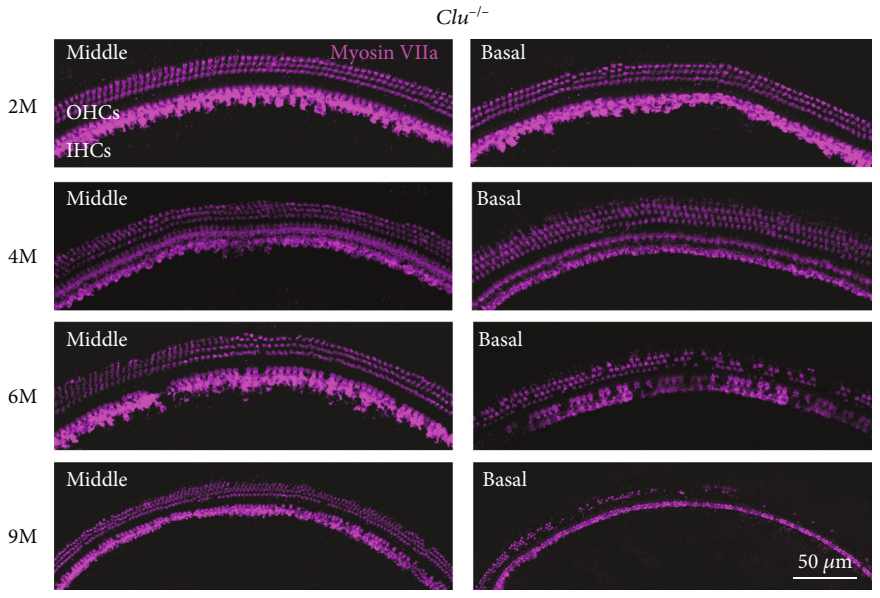

(a)

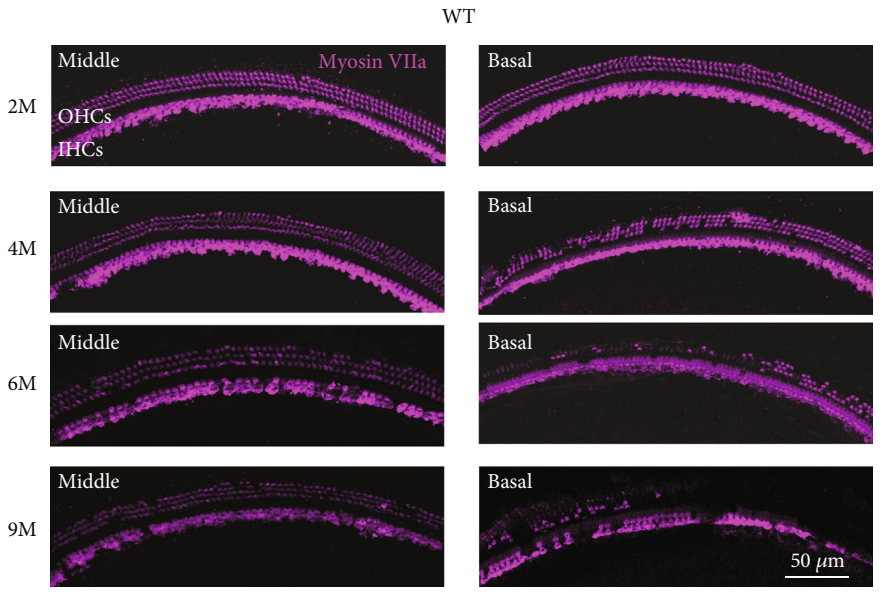

(b)

Figure 5: Continued.

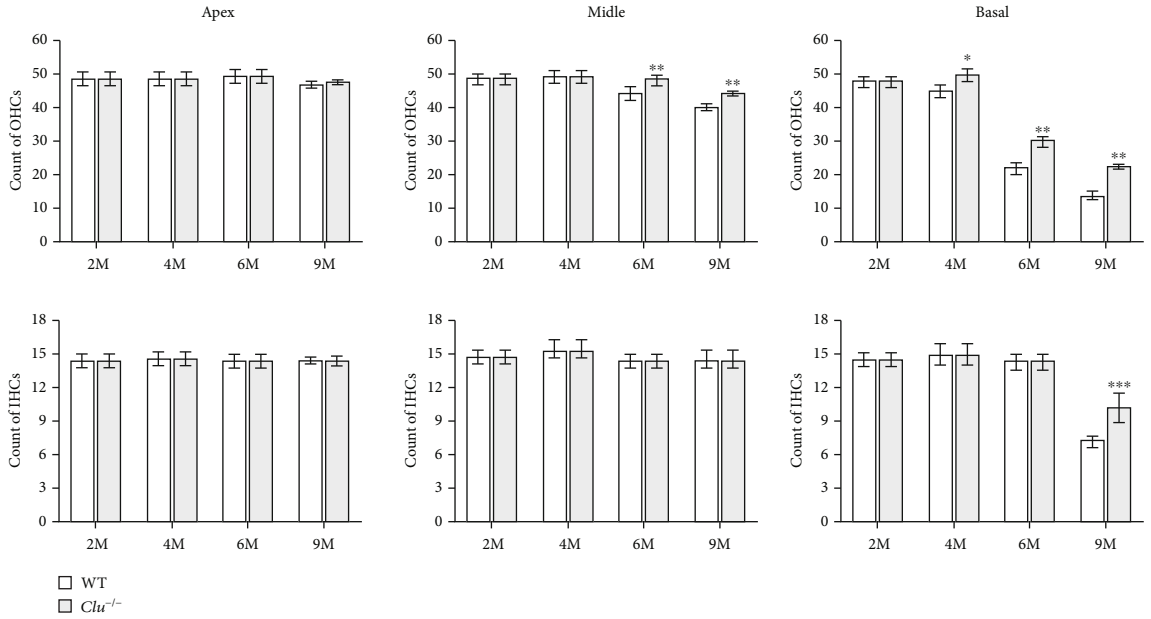

(c)

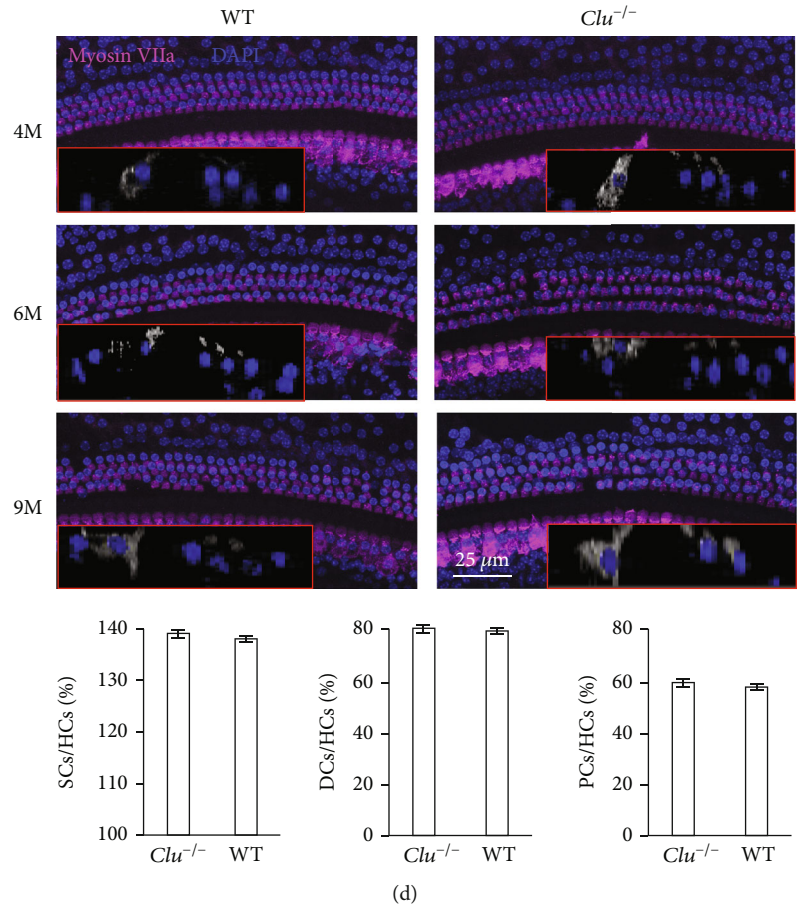

(d)

Figure 5: Assessment of age-related morphology of hair cells and supporting cells. (a) Cochlear basilar membrane immunostaining in P2m, P4m, P6m, and P9m $Clu^{-/-}$ mice. (b) Cochlear basilar membrane immunostaining in P2m, P4m, P6m, and P9m WT mice. The number of remaining hair cells in $Clu^{-/-}$ mice was significantly higher than that in WT mice at the same age. (c) Quantification of OHCs and IHCs in mice at P2m, P4m, P6m, and P9m across all tested frequencies in WT and $Clu^{-/-}$ mice. Data are presented as the mean ± SD. $^{*}p < 0.05$, $^{**}p < 0.01$. $N = 6$. (d) Quantification of supporting cells at P4m, P6m, and P9m in WT and $Clu^{-/-}$ mice. The red box shows a typical section after three-dimensional reconstruction. The percentages of supporting cells and hair cells showed no significant differences between WT and $Clu^{-/-}$ mice. $N = 6$.

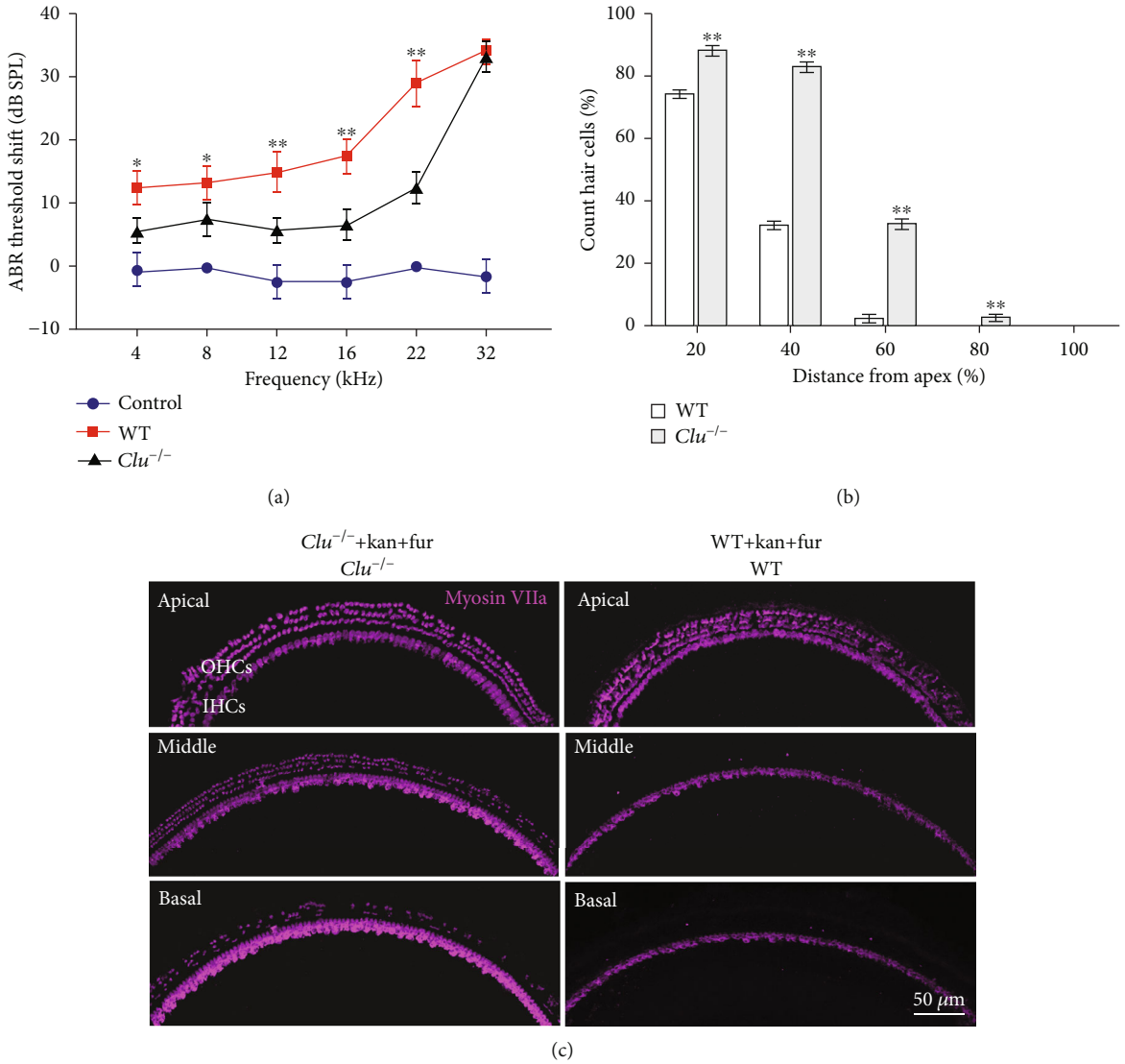

Figure 6: *Clu* deficiency protects hearing ability and inhibits sensory cell death induced by the coadministration of kanamycin and furosemide. (a) Assessment of auditory dysfunction in WT and $Clu^{-/-}$ mice treated with furosemide plus kanamycin. $N = 6$. (b) Quantification of OHCs and IHCs in WT and $Clu^{-/-}$ mice after treatment with furosemide plus kanamycin. Data are presented as the mean ± SD. $^{*}p < 0.05$, $^{**}p < 0.01$. $N = 6$. (c) Representative confocal microscopy images from WT and $Clu^{-/-}$ mice after treatment with furosemide plus kanamycin.

of WT at 16 and 32 kHz were elevated with age. Interestingly, the threshold elevation of $Clu^{-/-}$ mice at 16 and 32 kHz was significantly less comparing to that of the WT mice. This suggests that deletion of *Clu* has altered the onset and progression of ARHL.

ARHL in C57BL/6 mice develops as a result of the degeneration of sensory hair cells [2, 14–16]. We performed histological analyses on cochlear sections from WT and $Clu^{-/-}$ mice at 2, 4, 6, and 9 months. The cochleae from WT and $Clu^{-/-}$ mice at 2 m displayed no evidence of IHC or OHC loss. At 4 m, the basal region of the cochleae from WT mice displayed severe loss of OHCs, whereas the basal region of the cochlea from $Clu^{-/-}$ mice displayed no loss of hair cells. At 6 and 9 months, both WT and $Clu^{-/-}$ mice showed hair cell loss. However, the number of remaining OHCs in $Clu^{-/-}$ mice was significantly higher than that of the WT mice, in both the middle ($p < 0.05$) and basal turn ($p < 0.05$) of the cochleae. We also counted the number of Deiters' cells from WT and $Clu^{-/-}$ mice at these ages. The number of Deiters' cells was comparable that of OHCs (Figure 5(d)).

3.5. Clu Deficiency Protects Hair Cell Loss against Ototoxicity Induced by Coadministration of Kanamycin and Furosemide. Both WT and $Clu^{-/-}$ mice were treated with the combination of kanamycin and furosemide at 7–8 weeks to examine drug-induced hearing loss. Before drug treatment, the ABR threshold was measured to ensure that all mice used had normal auditory function. Figure 6 shows the ABR threshold shifts of WT and $Clu^{-/-}$ mice treated with furosemide and kanamycin. The threshold shifts were calculated by subtracting the ABR thresholds of the untreated control WT mice from the ABR thresholds of the treated WT and $Clu^{-/-}$ mice. The

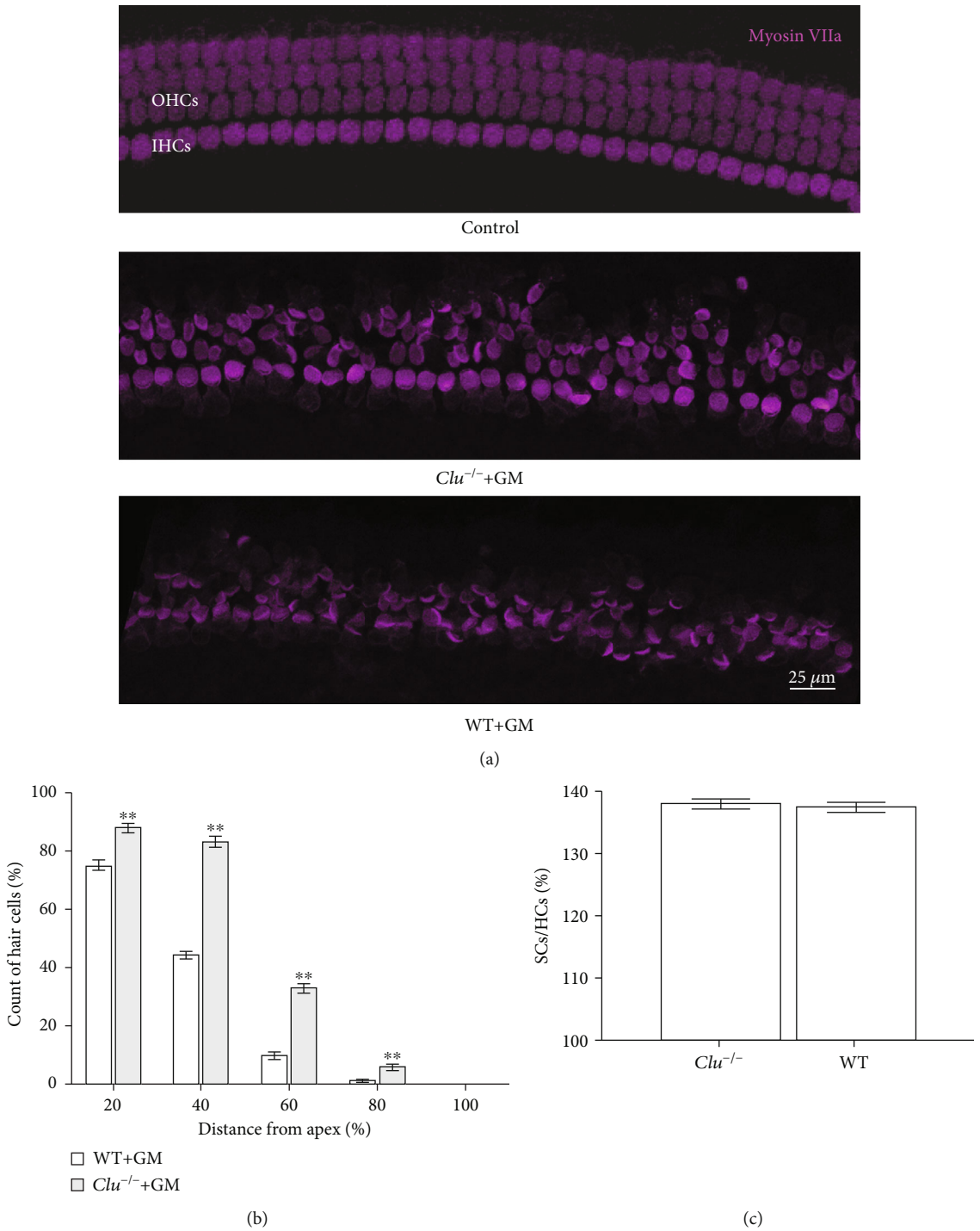

Figure 7: *Clu* deficiency attenuates gentamycin-induced cochlear hair cell death *in vitro*. (a) Representative images of myosin-stained hair cells in the CBM after exposure to the gentamycin (GM). $n = 6$ CBMS per condition. (b) Quantification of myosin staining in IHCs and OHCs. Data are presented as the mean ± SD. $^{*}p < 0.05$, $^{**}p < 0.01$. $N = 6$. (c) The percentages of supporting cells and hair cells showed no significant differences between WT and $Clu^{-/-}$ mice. $N = 6$.

results showed that 10 days after drug treatment, the ABR threshold shifts of WT mice were significantly greater than the $Clu^{-/-}$ mice, suggesting that *Clu* deficiency protected hearing loss against furosemide and kanamycin ototoxicity.

After the hearing test, we used immunohistochemistry to assess hair cell damage. The observed hair cell damage was consistent with the functional deficits indicated by the ABR measurements. The area of the basal turn showed more hair cell loss than the areas of the middle and apical turns, and OHC loss was much greater than IHC loss. In WT and $Clu^{-/-}$ mice, OHCs completely disappeared from the basal regions of the cochlea; however, the numbers of remaining

OHCs in the middle and basal turns were significantly higher in $Clu^{-/-}$ mice than in WT mice (Figure 6, $^{*}p < 0.05$), suggesting that *Clu* deficiency protested hair cell death. To confirm protection, we performed experiments in organotypic culture of the organ of Corti in which concentration of gentamicine can be controlled. As shown in Figure 7, treatment with 150 μM gentamicin after 36 hours significantly reduced the number of hair cells in cultured cochlear explants in culture from the WT mouse. The number of remaining hair cells in the cochlea derived from $Clu^{-/-}$ mice was significantly higher than that in cochlea derived from WT mice. This result was consistent with our in vivo findings, further validating the protective role played by *Clu* deficiency (Figure 7).

4. Discussion

HCs in the inner ear cochlea function in transducing sound waves into electric signals [17–21], while supporting cells function in supporting the HCs and providing the potential pool for HC regeneration [22–26]. Damages from a variety of sources can impair HC function, including genetic factors, aging, ototoxic drugs, chronic cochlear infections, and noise exposure [19, 27–31]. In this study, we reported the protective effect of *Clusterin* deficiency against age-related hearing loss and drug-induced ototoxicity, which are both due to irreversible loss of sensory HCs [32–36] and degeneration of the spiral ganglion neurons (SGNs) [37–42]. CLU is an extracellular chaperone protein that has been implicated in diverse physiological and pathophysiological cellular processes. *Clu* expression has been shown to be upregulated in response to cellular stress and under certain environmental conditions, such as during neurodegenerative diseases and cancer. In the current study, we investigated the role of CLU in the inner ear. We found that *Clu* deletion protected cochlear hair cells against aging and ototoxicity, which is the evidence that gene deletion can promote hair cell survival against aging and ototoxicity.

The RNA-seq data showed that *Clu* was expressed in both hair cells and supporting cells [13, 43]. Our RNAscope results showed that stronger expression was observed in the pillar and Deiters' cells, which is consistent with the results reported by Lee et al. [44]. These differences between the RNA-seq and *in situ* hybridization may be due to difference of sensitivity between RNA-seq and *in situ* hybridization.

We examined hearing thresholds and hair and supporting cell morphology in $Clu^{-/-}$ mice after birth. Compared with WT mice, the ABR and DPOAE thresholds of the $Clu^{-/-}$ mice were not significantly different from those of the WT mice within the first month after birth, which indicated that the deletion of *Clu* did not affect the development of hair cells and supporting cells. This also suggests that the biological processes involved with *Clu* are not related to differentiation and development of hair cells and supporting cells.

ARHL, or presbycusis, is a progressive decline in hearing function and is the most prevalent type of SNHL in the elderly. ARHL is characterized by higher hearing thresholds, beginning at high frequencies and spreading toward low frequencies, accompanied by the loss of HCs and SGNs from the basal to apical turn [45–48]. Surprisingly, we found that deletion of *Clu* slows onset and progression of age-related hair cell and hearing loss.

Clusterin is a glycoprotein that acts as a molecular chaperone to help cells cope with the presence of denatured, misfolded, or aggregated proteins. It often plays a protective role in the pathological processes of various diseases [10, 49]. Our results appeared to be contradictory to the traditional view of CLU function. However, studies of *Clu* mutations in Alzheimer's disease have suggested that CLU is associated with a high risk of late-onset Alzheimer's disease [50, 51]. No studies have been done to examine the relationship between CLU and hearing.

Many stress stimulators like ototoxic drugs had been testified to vast ROS production in HCs [52–58]. After observing the protective effects of *Clu* deficiency against ARHL and considering the importance of hair cells in drug-induced deafness, we evaluated whether *Clu* deficiency could confer protection against aminoglycoside ototoxicity by performing both *in vivo* and *in vitro* experiments. Our results showed that *Clu* deficiency protected hair cell death. The sensory hair cells of the inner ear are the primary target of aminoglycoside ototoxicity, and no therapies are currently available that can prevent ototoxicity. The mechanism through which *Clu* deficiency protects hair cells from ototoxic drugs remains unclear.

We speculate that the protective effects of *Clu* deficiency in hair cells may be the result of direct effects on hair cells, indirect effects mediated by supporting cells, or a combination of effects associated with both hair cells and supporting cells. Supporting cells may exert various effects on hair cells by providing an environment where hair cells can live [59, 60]. Some recent studies have shown that supporting cells may promote hair cell repair when *Atoh1* is overexpressed in Deiters' cells [61, 62]. Deiters' cells may also release organelles to promote survival of hair cells in response to stress [63].

In summary, our results revealed the protective effects of *Clu* deficiency in cochlear hair cells. Thus, *Clu* may be a good target gene for therapeutic interventions to slow ARHL and prevent ototoxic drug-induced hearing loss. Future work is necessary to determine the molecular mechanism through which *Clu* deletion protects against age-related hair cell apoptosis and aminoglycoside-induced hair cell loss.

Data Availability

The data used to support the findings of this study are included within the article, and the data are available.

Conflicts of Interest

The authors declare that the research was conducted in the absence of any commercial or financial relationships that could be construed as a potential conflict of interest.

Authors' Contributions

YL and BL designed the experiments. YL, BL, XCZ, HJH, and TYW performed the experiments. XCZ and YL wrote the manuscript.

Acknowledgments

The research is supported by the National Natural Science Foundation of China # 81600798.

References

[1] T. Vos, A. D. Flaxman, M. Naghavi et al., "Years lived with disability (YLDs) for 1160 sequelae of 289 diseases and injuries 1990-2010: a systematic analysis for the Global Burden of Disease Study 2010," *Lancet (London, England)*, vol. 380, no. 9859, pp. 2163–2196, 2012.

[2] G. Gates and J. Mills, "Presbycusis," *Lancet*, vol. 366, no. 9491, pp. 1111–1120, 2005.

[3] Y. Uchida, S. Sugiura, Y. Nishita, N. Saji, M. Sone, and H. Ueda, "Age-related hearing loss and cognitive decline – the potential mechanisms linking the two," *Auris Nasus Larynx*, vol. 46, no. 1, pp. 1–9, 2019.

[4] R. Fettiplace, "Hair cell transduction, tuning, and synaptic transmission in the mammalian cochlea," *Comprehensive Physiology*, vol. 7, no. 4, pp. 1197–1227, 2017.

[5] M. M. Mellado Lagarde, B. C. Cox, J. Fang, R. Taylor, A. Forge, and J. Zuo, "Selective ablation of pillar and Deiters' cells severely affects cochlear postnatal development and hearing in mice," *The Journal of Neuroscience*, vol. 33, no. 4, pp. 1564–1576, 2013.

[6] D. N. Furness, "Molecular basis of hair cell loss," *Cell and Tissue Research*, vol. 361, no. 1, pp. 387–399, 2015.

[7] M. R. Wilson and A. Zoubeidi, "Clusterin as a therapeutic target," *Expert Opinion on Therapeutic Targets*, vol. 21, no. 2, pp. 201–213, 2017.

[8] Y.-M. Jeong, T.-E. Jin, J.-H. Choi et al., "Induction of _clusterin_ expression by neuronal cell death in Zebrafish," *Yi Chuan Xue Bao*, vol. 41, no. 11, pp. 583–589, 2014.

[9] A. Londou, A. Mikrou, and I. K. Zarkadis, "Cloning and characterization of two clusterin isoforms in rainbow trout," *Molecular Immunology*, vol. 45, no. 2, pp. 470–478, 2008.

[10] P. Rohne, H. Prochnow, and C. Koch-Brandt, "The CLU-files: disentanglement of a mystery," *Biomolecular Concepts*, vol. 7, no. 1, pp. 1–15, 2016.

[11] H. Liu, L. Chen, K. P. Giffen et al., "Cell-specific transcriptome analysis shows that adult pillar and Deiters' cells express genes encoding machinery for specializations of cochlear hair cells," *Frontiers in Molecular Neuroscience*, vol. 11, p. 356, 2018.

[12] Y. Li, H. Liu, K. P. Giffen, L. Chen, K. W. Beisel, and D. Z. Z. He, "Transcriptomes of cochlear inner and outer hair cells from adult mice," *Sci Data*, vol. 5, no. 1, article 180199, 2018.

[13] D. I. Scheffer, J. Shen, D. P. Corey, and Z. Y. Chen, "Gene expression by mouse inner ear hair cells during development," *The Journal of Neuroscience*, vol. 35, no. 16, pp. 6366–6380, 2015.

[14] V. P. Spongr, D. G. Flood, R. D. Frisina, and R. J. Salvi, "Quantitative measures of hair cell loss in CBA and C57BL/6 mice throughout their life spans," *The Journal of the Acoustical Society of America*, vol. 101, no. 6, pp. 3546–3553, 1997.

[15] T. Yamasoba, F. R. Lin, S. Someya, A. Kashio, T. Sakamoto, and K. Kondo, "Current concepts in age-related hearing loss: epidemiology and mechanistic pathways," *Hearing Research*, vol. 303, pp. 30–38, 2013.

[16] Q. Zhang, H. Liu, G. A. Soukup, and D. Z. Z. He, "Identifying microRNAs involved in aging of the lateral wall of the cochlear duct," *PLoS One*, vol. 9, no. 11, article e112857, 2014.

[17] Y. Liu, J. Qi, X. Chen et al., "Critical role of spectrin in hearing development and deafness," *Science Advances*, vol. 5, no. 4, article eaav7803, 2019.

[18] Y. Wang, J. Li, X. Yao et al., "Loss of CIB2 causes profound hearing loss and abolishes mechanoelectrical transduction in mice," *Frontiers in Molecular Neuroscience*, vol. 10, p. 401, 2017.

[19] C. Zhu, C. Cheng, Y. Wang et al., "Loss of ARHGEF6 causes hair cell stereocilia deficits and hearing loss in mice," *Frontiers in Molecular Neuroscience*, vol. 11, p. 362, 2018.

[20] J. Qi, Y. Liu, C. Chu et al., "A cytoskeleton structure revealed by super-resolution fluorescence imaging in inner ear hair cells," *Cell Discovery*, vol. 5, no. 1, p. 12, 2019.

[21] J. Qi, L. Zhang, F. Tan et al., "Espin distribution as revealed by super-resolution microscopy of stereocilia," *American Journal of Translational Research*, vol. 12, no. 1, pp. 130–141, 2020.

[22] S. Zhang, Y. Zhang, Y. Dong et al., "Knockdown of Foxg1 in supporting cells increases the trans-differentiation of supporting cells into hair cells in the neonatal mouse cochlea," *Cellular and Molecular Life Sciences*, vol. 77, no. 7, pp. 1401–1419, 2020.

[23] C. Cheng, Y. Wang, L. Guo et al., "Age-related transcriptome changes in Sox2+ supporting cells in the mouse cochlea," *Stem Cell Research & Therapy*, vol. 10, no. 1, p. 365, 2019.

[24] X. Lu, S. Sun, J. Qi et al., "Bmi1 regulates the proliferation of cochlear supporting cells via the canonical Wnt signaling pathway," *Molecular Neurobiology*, vol. 54, no. 2, pp. 1326–1339, 2017.

[25] S. Zhang, R. Qiang, Y. Dong et al., "Hair cell regeneration from inner ear progenitors in the mammalian cochlea," *Am J Stem Cells*, vol. 9, no. 3, pp. 25–35, 2020.

[26] B. C. Cox, R. Chai, A. Lenoir et al., "Spontaneous hair cell regeneration in the neonatal mouse cochlea in vivo," *Development*, vol. 141, no. 4, pp. 816–829, 2014.

[27] Z. He, L. Guo, Y. Shu et al., "Autophagy protects auditory hair cells against neomycin-induced damage," *Autophagy*, vol. 13, no. 11, pp. 1884–1904, 2017.

[28] P. Jiang, S. Zhang, C. Cheng et al., "The roles of exosomes in visual and auditory systems," *Frontiers in Bioengineering and Biotechnology*, vol. 8, p. 525, 2020.

[29] Q. Fang, Y. Zhang, P. da et al., "Deletion of _Limk1_ and _Limk2_ in mice does not alter cochlear development or auditory function," *Scientific Reports*, vol. 9, no. 1, p. 3357, 2019.

[30] F. Qian, X. Wang, Z. Yin et al., "The slc4a2b gene is required for hair cell development in zebrafish," *Aging (Albany NY)*, vol. 12, no. 19, pp. 18804–18821, 2020.

[31] J. Lv, X. Fu, Y. Li et al., "Deletion of Kcnj16 in mice does not alter auditory function," *Frontiers in Cell and Development Biology*, vol. 9, p. 630361, 2021.

[32] L. Liu, Y. Chen, J. Qi et al., "Wnt activation protects against neomycin-induced hair cell damage in the mouse cochlea," *Cell Death & Disease*, vol. 7, no. 3, article e2136, 2016.

[33] Y. Zhang, S. Zhang, Z. Zhang et al., "Knockdown of Foxg1 in Sox9+ supporting cells increases the trans-differentiation of

supporting cells into hair cells in the neonatal mouse utricle," *Aging (Albany NY)*, vol. 12, no. 20, pp. 19834–19851, 2020.

[34] S. Zhang, D. Liu, Y. Dong et al., "Frizzled-9+ supporting cells are progenitors for the generation of hair cells in the postnatal mouse cochlea," *Frontiers in Molecular Neuroscience*, vol. 12, p. 184, 2019.

[35] A. Li, D. You, W. Li et al., "Novel compounds protect auditory hair cells against gentamycin-induced apoptosis by maintaining the expression level of H3K4me2," *Drug Delivery*, vol. 25, no. 1, pp. 1033–1043, 2018.

[36] Z. He, S. Sun, M. Waqas et al., "Reduced TRMU expression increases the sensitivity of hair-cell-like HEI-OC-1 cells to neomycin damage in vitro," *Scientific Reports*, vol. 6, no. 1, article 29621, 2016.

[37] R. Guo, S. Zhang, M. Xiao et al., "Accelerating bioelectric functional development of neural stem cells by graphene coupling: implications for neural interfacing with conductive materials," *Biomaterials*, vol. 106, pp. 193–204, 2016.

[38] R. Guo, M. Xiao, W. Zhao et al., "2D $Ti_3C_2T_x$MXene couples electrical stimulation to promote proliferation and neural differentiation of neural stem cells," *Acta Biomaterialia*, 2020.

[39] R. Guo, J. Li, C. Chen et al., "Biomimetic 3D bacterial cellulose-graphene foam hybrid scaffold regulates neural stem cell proliferation and differentiation," *Colloids and Surfaces. B, Biointerfaces*, vol. 200, p. 111590, 2021.

[40] W. Liu, X. Xu, Z. Fan et al., "Wnt signaling activates TP53-induced glycolysis and apoptosis regulator and protects against cisplatin-induced spiral ganglion neuron damage in the mouse cochlea," *Antioxidants & Redox Signaling*, vol. 30, no. 11, pp. 1389–1410, 2019.

[41] W. Yan, W. Liu, J. Qi et al., "A three-dimensional culture system with Matrigel promotes purified spiral ganglion neuron survival and function in vitro," *Molecular Neurobiology*, vol. 55, no. 3, pp. 2070–2084, 2018.

[42] R. Guo, X. Ma, M. Liao et al., "Development and application of cochlear implant-based electric-acoustic stimulation of spiral ganglion neurons," *ACS Biomaterials Science & Engineering*, vol. 5, no. 12, pp. 6735–6741, 2019.

[43] Y. Li, H. Liu, C. L. Barta et al., "Transcription factors expressed in mouse cochlear inner and outer hair cells," *PLoS One*, vol. 11, no. 3, article e0151291, 2016.

[44] S. Lee, J.-O. Shin, B. Sagong, U. K. Kim, and J. Bok, "Spatiotemporal expression patterns of clusterin in the mouse inner ear," *Cell and Tissue Research*, vol. 370, no. 1, pp. 89–97, 2017.

[45] Z. H. He, S. Y. Zou, M. Li et al., "The nuclear transcription factor FoxG1 affects the sensitivity of mimetic aging hair cells to inflammation by regulating autophagy pathways," *Redox Biology*, vol. 28, p. 101364, 2020.

[46] H. Zhou, X. Qian, N. Xu et al., "Disruption of Atg7-dependent autophagy causes electromotility disturbances, outer hair cell loss, and deafness in mice," *Cell Death & Disease*, vol. 11, no. 10, p. 913, 2020.

[47] Y. Ding, W. Meng, W. Kong, Z. He, and R. Chai, "The role of FoxG1 in the inner ear," *Frontiers in Cell and Development Biology*, vol. 8, p. 614954, 2020.

[48] Z. He, Q. Fang, H. Li et al., "The role of FOXG1 in the postnatal development and survival of mouse cochlear hair cells," *Neuropharmacology*, vol. 144, pp. 43–57, 2019.

[49] I. P. Trougakos, "The molecular chaperone apolipoprotein J/clusterin as a sensor of oxidative stress: implications in therapeutic approaches - a mini-review," *Gerontology*, vol. 59, no. 6, pp. 514–523, 2013.

[50] X. Yang, J. Li, B. Liu, Y. Li, and T. Jiang, "Impact of PICALM and CLU on hippocampal degeneration," *Human Brain Mapping*, vol. 37, no. 7, pp. 2419–2430, 2016.

[51] C. M. Karch and A. M. Goate, "Alzheimer's disease risk genes and mechanisms of disease pathogenesis," *Biological Psychiatry*, vol. 77, no. 1, pp. 43–51, 2015.

[52] H. Li, Y. Song, Z. He et al., "Meclofenamic acid reduces reactive oxygen species accumulation and apoptosis, inhibits excessive autophagy, and protects hair cell-like HEI-OC1 cells from cisplatin-induced damage," *Frontiers in Cellular Neuroscience*, vol. 12, p. 139, 2018.

[53] S. Gao, C. Cheng, M. Wang et al., "Blebbistatin inhibits neomycin-induced apoptosis in hair cell-like HEI-OC-1 cells and in cochlear hair cells," *Frontiers in Cellular Neuroscience*, vol. 13, p. 590, 2019.

[54] S. Sun, M. Sun, Y. Zhang et al., "In vivo overexpression of X-linked inhibitor of apoptosis protein protects against neomycin-induced hair cell loss in the apical turn of the cochlea during the ototoxic-sensitive period," *Frontiers in Cellular Neuroscience*, vol. 8, p. 248, 2014.

[55] Z. Zhong, X. Fu, H. Li et al., "Citicoline protects auditory hair cells against neomycin-induced damage," *Frontiers in Cell and Development Biology*, vol. 8, p. 712, 2020.

[56] Y. Zhang, W. Li, Z. He et al., "Pre-treatment with fasudil prevents neomycin-induced hair cell damage by reducing the accumulation of reactive oxygen species," *Frontiers in Molecular Neuroscience*, vol. 12, p. 264, 2019.

[57] X. Yu, W. Liu, Z. Fan et al., "c-Myb knockdown increases the neomycin-induced damage to hair-cell-like HEI- OC1 cells in vitro," *Scientific Reports*, vol. 7, no. 1, article 41094, 2017.

[58] M. Guan, Q. Fang, Z. He et al., "Inhibition of ARC decreases the survival of HEI-OC-1 cells after neomycin damage in vitro," *Oncotarget*, vol. 7, no. 41, pp. 66647–66659, 2016.

[59] S. Safieddine, A. El-Amraoui, and C. Petit, "The auditory hair cell ribbon synapse: from assembly to function," *Annual Review of Neuroscience*, vol. 35, no. 1, pp. 509–528, 2012.

[60] S. Riazuddin, Z. M. Ahmed, A. S. Fanning et al., "Tricellulin is a tight-junction protein necessary for hearing," *American Journal of Human Genetics*, vol. 79, no. 6, pp. 1040–1051, 2006.

[61] S. M. Yang, W. Chen, W. W. Guo et al., "Regeneration of stereocilia of hair cells by forced Atoh1 expression in the adult mammalian cochlea," *PLoS One*, vol. 7, no. 9, article e46355, 2012.

[62] M. Izumikawa, R. Minoda, K. Kawamoto et al., "Auditory hair cell replacement and hearing improvement by _Atoh1_ gene therapy in deaf mammals," *Nature Medicine*, vol. 11, no. 3, pp. 271–276, 2005.

[63] J. Defourny, S. Mateo Sánchez, L. Schoonaert et al., "Cochlear supporting cell transdifferentiation and integration into hair cell layers by inhibition of ephrin-B2 signalling," *Nature Communications*, vol. 6, no. 1, p. 7017, 2015.

Hindawi
Neural Plasticity
Volume 2021, Article ID 9950533, 11 pages
https://doi.org/10.1155/2021/9950533

Research Article

Canonical Wnt Signaling Pathway on Polarity Formation of Utricle Hair Cells

Di Deng,[1,2] **Xiaoqing Qian**,[2,3] **Binjun Chen**,[2,3] **Xiaoyu Yang**,[2,3] **Yanmei Wang**,[2,3] **Fanglu Chi**,[2,3] **Yibo Huang**,[2,3] **Yu Zhao**,[1] **and Dongdong Ren**[2,3]

[1]*Department of Otolaryngology, Head and Neck Surgery, West China Hospital, Sichuan University, Chengdu 610041, China*
[2]*NHC Key Laboratory of Hearing Medicine (Fudan University), Shanghai 200031, China*
[3]*ENT Institute and Department of Otorhinolaryngology, Eye & ENT Hospital, Fudan University, Shanghai 200031, China*

Correspondence should be addressed to Yibo Huang; adabobohuang@126.com, Yu Zhao; yutzhao@163.com, and Dongdong Ren; dongdongren@fudan.edu.cn

Received 31 March 2021; Revised 26 April 2021; Accepted 11 May 2021; Published 24 May 2021

Academic Editor: Renjie Chai

As part of the inner ear, the vestibular system is responsible for sense of balance, which consists of three semicircular canals, the utricle, and the saccule. Increasing evidence has indicated that the noncanonical Wnt/PCP signaling pathway plays a significant role in the development of the polarity of the inner ear. However, the role of canonical Wnt signaling in the polarity of the vestibule is still not completely clear. In this study, we found that canonical Wnt pathway-related genes are expressed in the early stage of development of the utricle and change dynamically. We conditionally knocked out β-catenin, a canonical Wnt signaling core protein, and found that the cilia orientation of hair cells was disordered with reduced number of hair cells in the utricle. Moreover, regulating the canonical Wnt pathway (Licl and IWP2) in vitro also affected hair cell polarity and indicated that Axin2 may be important in this process. In conclusion, our results not only confirm that the regulation of canonical Wnt signaling affects the number of hair cells in the utricle but also provide evidence for its role in polarity development.

1. Introduction

The cochlea and vestibule are important for hearing and balance, respectively. They detect sound and position signals through stereociliary bundle on the surface of hair cells (HCs) [1–4]. The vestibular system contains utricular maculae, saccular maculae, and three semicircular canal cristae. Planar polarity of the stereociliary bundle guarantees that the range of motion is detected properly by vestibular HCs [5]. In the inner ear, the stereocilia are arranged in an ascending cluster, with the highest being located adjacent to the kinocilium [6, 7]. The direction of stereociliary bundle between adjacent HCs are highly similar. Compared to the cochlea, an artificial line (line of polarity reversal, LPR) passes through the maculae. The maculae are divided into two regions: the kinocilium of the utricular maculae faces the LPR, while the kinocilium of the saccular maculae points away from the LPR [8].

In the canonical Wnt pathway, Wnt protein binds to Frizzled on the cell surface to inhibit the activity of the β-catenin-degrading complex composed of GSK-3, APC, and Axin. β-Catenin accumulates in the cytoplasm and is then transferred to the nucleus, where it controls embryogenesis and cell fate through T-cell factor/lymphoid enhancer-binding factor (TCF/LEF). The canonical Wnt signaling pathway and its downstream target genes play an important regulatory role in cell proliferation [9–13] and differentiation [14–18] during inner ear development [19], as well as in the survival of HCs [20–24] and spiral ganglion neurons [25]. During development, the expression of Wnt signaling significantly decreased with age in the inner ear [26]. The canonical Wnt pathway is essential to induce Pax2-positive otic placode cells to form an auditory sac [27]. In our previous studies, we found that polarity of striola in the medial region occurred earlier than in the lateral region, consistent with proliferation and differentiation in utricle HCs [28]. This

led us to hypothesize that the canonical Wnt signaling pathway is involved in polarity development in the utricle. Here, we found differences in the expression of Wnt pathway-related genes among different stages of polar formation in the utricle. We conditionally knocked out β-catenin, a core protein in the canonical Wnt signaling pathway, in Sox2-positive cells in mice. The number and polarity of HCs were also affected. Moreover, the polarity of the utricle was affected by treatment with an activator or inhibitor of the canonical Wnt pathway *in vitro*, and we found that Axin2 may be a key role in this process (Figure 1).

2. Materials and Methods

2.1. Animal Protocols. All protocols were approved by the Animal Care and Use Committee of the EENT Hospital of Fudan University. Healthy wild-type C57BL/6 mice were purchased from Shanghai SLAC Laboratory Animal Co., Ltd. (Shanghai, China). Female and male mice were mated in the same nest at 10 AM and recorded as E0. They were separated at 10 AM the next day and recorded as E0.5. In turn, E11.5 were recorded on day 12, E12.5 on day 13, and E13.5 on day 14. We also performed tap detection at E0.5.

$Sox2^{CreER}$ and $Ctnnb1^{flox(exon2-6)}$ mice were provided by Huawei Li at Fudan University and maintained in a mixed background of C57BL/6J and BALB/C. Standard PCR was performed to genotype transgenic mouse offspring. DNA was isolated by incubating the tail tip in a 100 μL mixture of Direct PCR and Protein K (100 : 2) at 55°C overnight and then at 95°C for 1 h. The primers used were as follows: GA486 (TGCCACGACCAAGTGACAGCAATG) and GA487 (ACCAGAGACGGAAATCCATCGCTC) for the Cre allele, with an expected fragment size of 300–400 bp; R15 (AAGGTAGAGTGATGAAAGTTGTT); and R16 (CAC CAT GTC CTC TGT CTA TTC) for the β-catenin knockout allele, with expected fragment sizes of ~300 and 223 bp for the mutant and wildtype, respectively. To activate Cre and avoid premature abortion due to tamoxifen, a tamoxifen/progesterone mixture dissolved in corn oil (Sigma Aldrich, St. Louis, MO, USA; 1 mL corn oil : 10 mg tamoxifen : 20 mg progesterone) was injected intraperitoneally once a day for 2 consecutive days. The dose on the first day (E11.5) was 0.1 μg/g tamoxifen, and the dose was halved on the following day (E12.5).

2.2. Utricle Harvest. The pregnant mice were anesthetized and killed. The embryo were removed from the uterus and quickly placed into a cold solution of 1× phosphate-buffered saline (PBS; pH = 7.4). The utricle was dissected with the microscope. P1 mice were anesthetized and killed; then, the utricle was harvested, and the otolith was removed with the microscope and harvest the utricle.

2.3. Tissue Culture In Vitro. The freshly dissected utricle was placed in Dulbecco's modified Eagle's medium (DMEM)/F12 medium (20% foetal bovine serum [FBS], B27 (1 : 100), streptomycin [100 U/mL]). The Petri dishes were incubated at 37°C, with a concentration of 5% CO_2 and humidity of 95%. Dimethyl sulfoxide (DMSO), lithium chloride (LiCl), or IWP2 was added 24 hours later. We treated cultures in the activator group with the canonical Wnt pathway activator LiCl (2.5 μM/mL). The canonical Wnt inhibitor IWP2 (1.0 μM/mL) was added to the inhibitor group. DMSO (1.0 μM/mL) was added to the control group. The final culture concentration depended on the growth of the utricle. The culture medium was replaced in full every 24 hours, and the tissue was removed and fixed on the day 5 after treatment. For all experiments, three biological replicates were used.

2.4. PCR and RT-qPCR. The reaction protocol for PCR was as follows: predenaturation at 94°C for 5 min, 32 cycles of denaturation at 94°C for 1 min, annealing at 55°C for 1 min, elongation at 72°C for 1.5 min, and a final elongation at 72°C for 10 min.

RNA was extracted from the utricle using the RNeasy Micro Kit (Qiagen, Hilden, Germany), and cDNA was synthesized using the GeneAmp® PCR System 9700 (Applied Biosystems, Foster City, CA, USA) by reverse transcription: 42°C for 15 min and 85°C for 5 s. The qPCR reaction protocol was as follows: 94°C for 30 s, followed by 45 cycles at 94°C for 5 s and 60°C for 30 s. Each sample was run in triplicate for analysis purposes. At the end of the PCR cycles, melting curve analysis was performed to validate the generation of the expected PCR product. The primer sequences were designed in the laboratory and synthesized by TsingKe Biotech (Beijing, China) based on the mRNA sequences obtained from the NCBI database, as follows:

GADPH (F: GCAAGGACACTGAGCAAGA; R:GGAT GGAAATTGTGAGGGAG), Apc (F: GCCTGGATGAG CCATTTATAC; R: AGTTTCATTCCCATTGTCGT), Wif1 (F: TTGTACCTGTGGATCGACG; R:GGCTTTCCTGAAA TCATGTGT), Camk2d (F: AGATCAAGGCCGGAGCTTA; R:CAGAGGCTGTGATACGTT), Fzd6 (F: CTTCAGTGG CCTGTATCTT; R:CCATGTCATCTCCCAGGT), Axin2 (F:AGAAGAGGAGTGGACGTGTG; R:AGCTGTTTCCG TGGATCTCA), Vangl2 (F:TCTCTGGCCCTGACACATTT; R:ACTGAGGAAGAGGGGAGACT), Prickle2 (F:ATGCCA CCTTCTTCCTCCTC; R:AGTAGGTGACAAATGGCCGA).

2.5. RNA-Sequencing (RNA-Seq) and Protein-Protein Interaction (PPI) Network. Total RNA was extracted from the utricle (E13.5 and P1,wild-type C57BL/6 mice) and then submitted to Otogenetics Corporation (Atlanta, GA, USA) for RNA-Seq assays. We assessed RNA integrity and purity using an Agilent Bioanalyzer (Agilent Technologies, Santa Clara, CA, USA). cDNA was generated from total RNA using the Clontech SMARTer PCR cDNA Synthesis Kit (Clontech Laboratories, Inc., Mountain View, CA USA, catalogue #634891). Bioruptor (Diagenode, Inc., Denville, NJ, USA) was used to fragment cDNA, an Agilent Bioanalyzer was used for profiling, and SPRIworks HT (catalogue #B06938; Beckman Coulter, Pasadena, CA, USA) was used to prepare the Illumina library. The quality, quantity, and size distribution of the Illumina library were determined using TapeStation (Agilent Technologies).

The DAVID database (https://david.ncifcrf.gov/) is a commonly used database for gene analyses. KEGG pathway

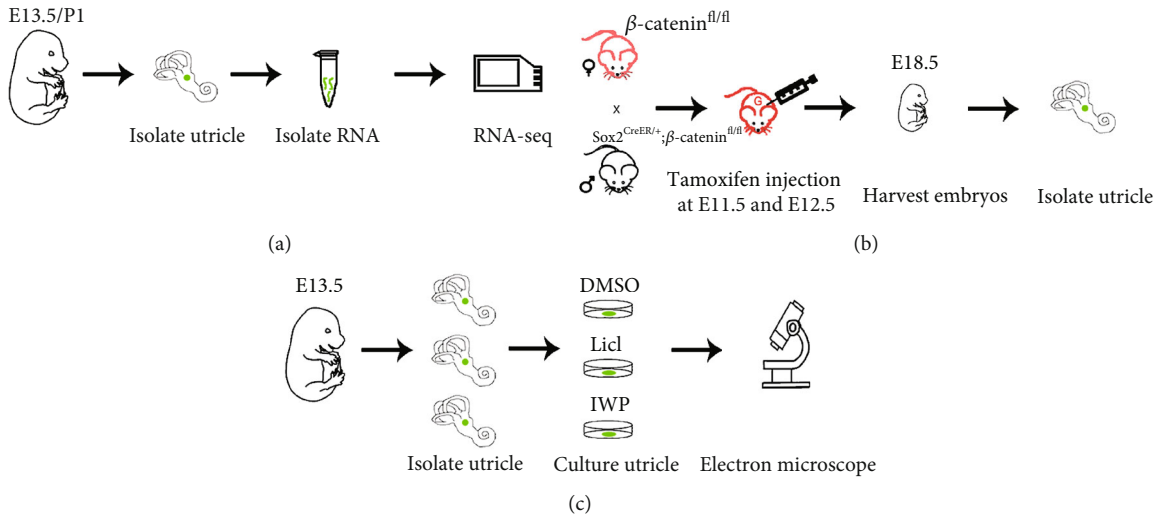

Figure 1: The experimental procedure. (a) RNA-sequencing of the utricle of E13.5 and P1 mice. (b) To conditionally knockout β-catenin, the β-catenin$^{f/f}$ female mice were mated with β-catenin$^{f/f}$ male mice with Sox2^{CreER+}; the pregnant mice were treated with tamoxifen injection at E11.5 and E12.5, and the utricle of the embryonic mice was harvested at E18.5. (c) Utricles of E13.5 mice were cultured *in vitro* with DMSO (control), LiCl (activator), and IWP2 (inhibitor).

enrichment analyses were performed using DAVID, and the TXT files of the results were downloaded for subsequent analysis. For the Bonferroni test, P values < 0.05 were set considered significant, and Log2 (fold_change) values between -1 and 1 were excluded from the analysis. STRING (https://string-db.org/) was used to analyse the interactions between proteins. Many signaling pathways play important roles in the development of the utricle. To better understand the role of the Wnt signaling pathway, we only included the Wnt pathway-related genes in this analysis.

2.6. Electron Microscope. Utricles were fixed with 2.5% glutaraldehyde at 4°C overnight and then processed using 2% tannin and 1% osmium acid. Graded ethanol series were used to dehydrate the samples, and liquid CO_2 (EM CPD300; Leica, Wetzlar, Germany) was used to dry them. An E-1045 sputter coater (Hitachi, Tokyo, Japan) was used to coat specimens with 100 Å Au. A NOV A NanoSEM 230 scanning electron microscope (FEI, Hillsboro, OR, USA) was used to scan the samples.

2.7. Whole-Mount Immunostaining. Mouse embryos were harvested at E18.5. Otocysts were dissected in cold PBS and fixed with 4% paraformaldehyde (Electron Microscopy Services, Hatfield, PA, USA) for 1 h at 4°C. After washing with PBS, utricles were dissected and blocked with 10% donkey serum, and 0.1% Triton-X in PBS for 30 min at room temperature, followed by incubating with primary antibodies diluted in PBS containing 5% donkey serum and 0.1% Triton-X overnight at 4°C. The next day, after washing extensively with PBS, tissues were incubated with secondary antibodies at 1 : 1,000 dilution in 0.1% Triton-X100 (in PBS) for 2 h at room temperature. After extensive PBS washing, samples were mounted in antifade Fluorescence Mounting Medium (Agilent Technologies) on coverslips. We used mouse anti-β-spectrin (1 : 500; catalogue #612562; BD Biosciences) primary antibody and Alexa Fluor 568 Donkey Anti-Mouse IgG (1 : 1,000; Invitrogen, Carlsbad, CA, USA) secondary antibody. FITC-conjugated phalloidin (1 : 1,000; Invitrogen) was used to visualize actin in the stereocilia of sensory HCs.

2.8. Quantification and Statistical Analyses. Whole-mount immunostaining images were acquired using a Zeiss LSM800 confocal microscope (Zeiss, Oberkochen, Germany) at 40× magnification, and the whole utricle image was obtained by flattening the overlapping parts of original images using Photoshop CS4 (Adobe Systems). The overall outline of a utricle was drawn on the stitched confocal image, and the area of the sensory epithelia was measured using the Zen image processing system (Zeiss). The number of HCs on the composite image was counted manually using Photoshop CS4 (Adobe Systems). Cell number was scored in two regions divided by LPR, defined as lateral and medial region. Hair bundle orientation was scored in three $40 \times 80\,\mu m^2$ regions in the middle of the utricle, defined as field 1, field 2, and field 3 (Figure 2(a)). The hair bundle angle was measured based on the position of kinocilium (spectrin-negative on the apical surface), by defining 0° as the anterior apex and 90° as the lateral side, and quantified using ImageJ64 (National Institutes of Health, Bethesda, MD, USA). A single kinocilium could be found directly in the electron microscope specimens. Matlab and Screen protractor were used to draw the angle distribution diagram. Statistical analyses were conducted using Prism 8 (GraphPad Software Inc., San Diego, CA, USA). A two-tailed, unpaired Student's t-test was used to determine statistical significance. $P < 0.05$ was considered significant. Data are shown as mean ± SD.

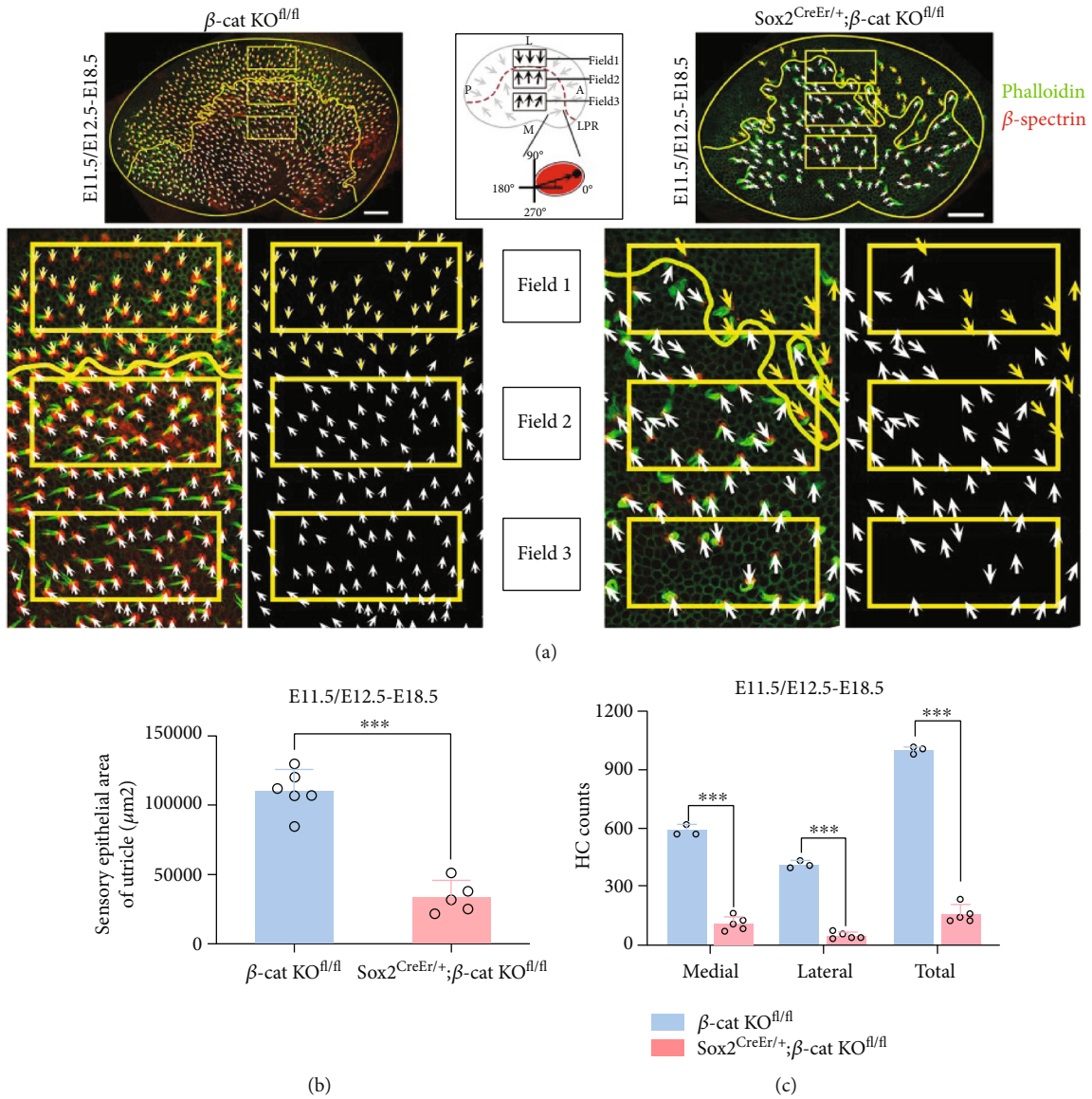

Figure 2: Continued.

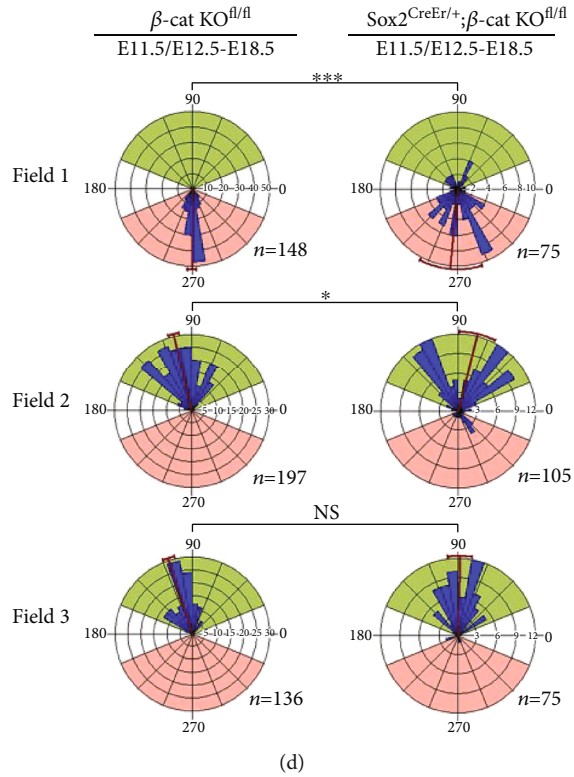

(d)

Figure 2: Knockout (KO) β-catenin in Sox2 positive cells influenced the orientation and number of vestibular hair cells. (a) Compared to the controls (left), $Sox2^{CreER/+}$ and β-$catenin^{fl/fl}$ (tamoxifen given at E11.5 and E12.5) utricles (right) showed a significant decrease in sensory epithelium area and HC number and a different extent of hair bundle orientation irregularity in fields 1–3. The schematic diagram in the middle black box defining regions of the utricle and illustrating the hair bundle polarity pattern. (b) Quantification of the sensory epithelium area of control and β-catenin KO utricles (controls, $n = 6$; mutants, $n = 5$). (c) Quantification of HC density on the lateral and medial sides of the LPR and the whole sensory epithelium, from control and β-catenin KO utricles (controls, $n = 3$; mutants, $n = 5$). (d) Circular histograms of the hair bundle orientation in field 1, field 2, and field 3 for control and β-catenin KO utricles (controls, $n = 3$; mutants, $n = 5$). LPR: line of polarity reversal; L: lateral; M: medial; A: anterior; P: posterior. $^{*}P < 0.05$, $^{***}P < 0.001$.

3. Result

3.1. Wnt Signaling Is Active in the E13.5 Utricle. Our previous studies showed that E13.5 is a critical period for the formation of polarity in the utricle [28]. Two clusters of HCs with opposite cilia began to appear in the utricle, gradually forming LPR. The Wnt signaling pathway is important for embryonic development and plays a variety of roles at different time points during development. Therefore, the primary purpose of our study is to understand the expression of Wnt pathway-related genes in the early utricle.

Wnt5a, Wnt7a, Wnt11, β-catenin, and Frizzled are important genes in the canonical/noncanonical Wnt signaling pathway. We detected these genes in the utricle by RT-PCR. Our research shows that these genes were expressed in the utricle of E13.5 mice (Figure 3(a)).

3.2. Changes of Wnt Signaling in the Early Development of the Utricle. To explore changes in Wnt signaling pathway activity during early development of the utricle, RNA from the utricle of P1 and E13.5 was extracted for RNA-Seq analysis.

Our results showed that Wnt pathway-related genes were differentially expressed. Compared to E13.5,the upregulated genes in P1 were Apc, Axin1, Axin2, Camk2d, Rac1, Fzd1, Fzd6, Dvl1, Wif1, Smad4, Wnt7a, Nkd1, Sfrp2, Ryk, Siah1a, Camk2g, Ctnnd2, Rspo3, Ppp3cb, Map3k7, Tcf7l1, Prkacb, Porcn, Cxxc4, Prkaca, Vangl1, Ppp3ca, Senp2, Prickle2, Nfatc1, Nfatc3, Nlk, Fzd4, Rock2, Prkcd, Prkce, Prkcz, Ctbp2, Prkci, Bambi, Mapk8, Csnk2a2, Frat1, Prickle1, Ppard, Gsk3a, Tle1, Tle4, Gpc1, Pygo2, Sdc3, and Sdc4. The downregulated genes included Camk2b, Psen1, Ruvbl1, Trp53, Ccnd1, Cacybp, Rhoa, Sfrp5, Csnk1g1, Csnk2b, Sdc1, Bcl9, Gpc2, Gpc3, Lgr5, Ccnd2, Cby1, Dkk2, Rbx1, Myc, Wnt7b, Ppp3r1, Frat2, Serpinf1, and Rhoc (Figure 3(b)). There were some representative genes of canonical Wnt signaling, such as Apc, Axin2, and Wif1. The protein interaction network of Wnt pathway-related genes showed their ranking (Figure 3(c)). Finally, we used RT-qPCR for verification and found that some canonical Wnt pathway-related genes differed in the expression levels of E13.5 and P1 (Figure 3(d)).

3.3. Conditional Knock-out β-Catenin Affects the Number and Polarity of Vestibular HCs. The areas of utricle maculae in the control and experimental groups were $96{,}326.63 \pm 36{,}029.13\ \mu m^2$ ($n = 7$) and $33{,}824.00 \pm 10{,}515.93\ \mu m^2$ ($n = 5$), respectively, $P < 0.05$ (Figure 2(b)). In the control group ($n = 3$), the total number of HCs was 995.67 ± 14.61, with 585.33 ± 33.40 and 410.33 ± 15.41 in the

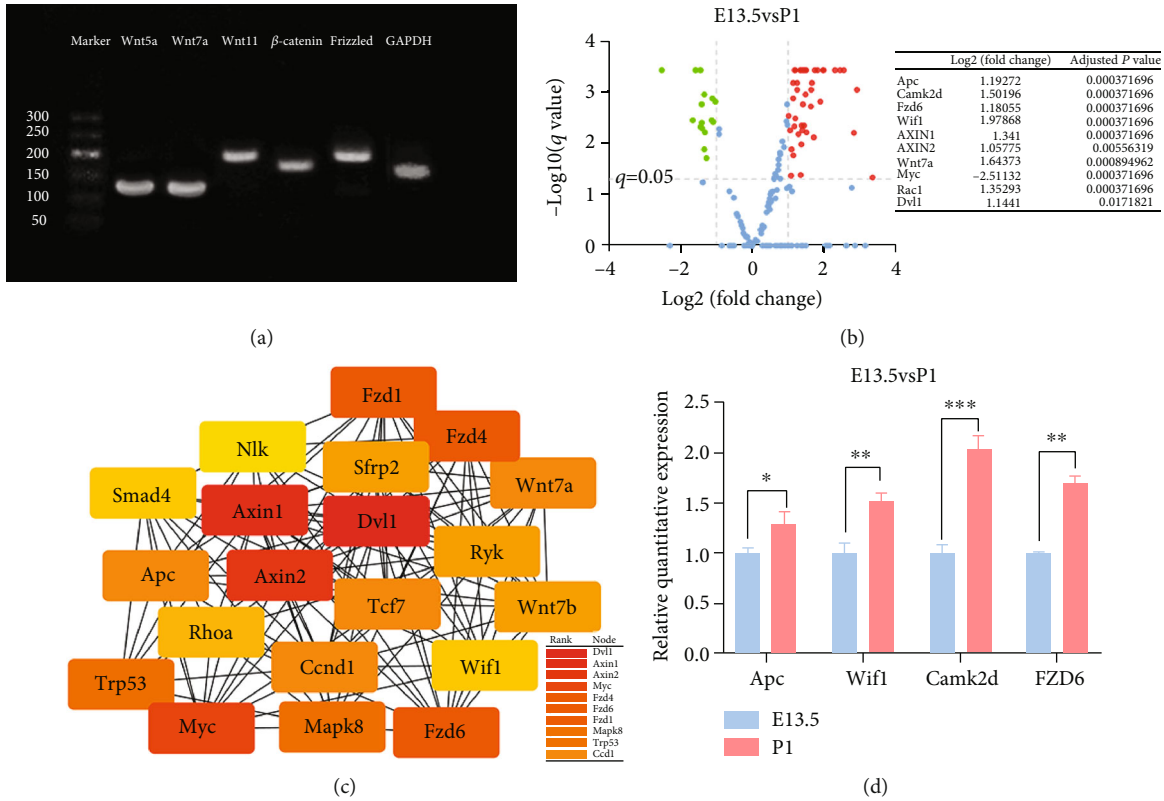

	Log2 (fold change)	Adjusted P value
Apc	1.19272	0.000371696
Camk2d	1.50196	0.000371696
Fzd6	1.18055	0.000371696
Wif1	1.97868	0.000371696
AXIN1	1.341	0.000371696
AXIN2	1.05775	0.00556319
Wnt7a	1.64373	0.000894962
Myc	−2.51132	0.000371696
Rac1	1.35293	0.000371696
Dvl1	1.1441	0.0171821

FIGURE 3: Wnt signaling pathway is active in the E13.5 utricle and changes during utricle development. (a) RT-PCR shows that Wnt5a, Wnt7a, Wnt11, β-catenin, and Frizzled were expressed in the utricle of E13.5 mice. (b) Differentially expressed Wnt pathway-related genes between the E13.5 and P1 utricle. The red dots represent the upregulated genes based on an adjusted P value < 0.05 and |log2 (fold change) | >1; the green dots represent the downregulated genes based on an adjusted P value < 0.05 and |log2 (fold change) | >1; the blue spots represent genes with no significant difference in expression. (c) PPI network of E13.5 and P1 utricle. Circles represent genes. Lines represent interactions between gene-encoded proteins, and the top 10 rankings are listed. (d) The relative levels of APC, Wif1, Camk2d, and Fzd6 were analysed by RT-qPCR. The data presented are based on at least three independent experiments. The data are presented as the mean ± SEM. $^{*}P < 0.05$, $^{**}P < 0.01$, $^{***}P < 0.001$.

medial and lateral regions, respectively, whereas in the experimental group ($n = 5$), the total number of HCs was 156.80 ± 40.09 with 109.00 ± 30.25 and 47.80 ± 15.46 in the medial and lateral regions, respectively, $P < 0.05$ (Figure 2(c)). As in the control group, β-catenin knockout mice still showed relatively clear LPRs, with the HCs on both sides having roughly normal directions (Figure 2(a)). However, it is worth noting that the direction of some HCs near LPR, in filed 1 and filed 2 regions, was disordered (Figure 2(d)).

3.4. Regulation of Wnt Signaling In Vitro Leads to Polarity Changes in the Utricle. To determine the role of the Wnt signaling pathway in the polarity of HCs in the utricle, we regulated Wnt signaling pathway activity *in vitro* using a Wnt/β-catenin inhibitor (IWP2) and a Wnt/β-catenin activator (LiCl) [29]. According to daily observations of the growth of the utricle, the final culture concentrations were 2.5 and 1.0 μM/mL for LiCl and IWP2, respectively.

Using a scanning electron microscope, we found that the polarity of the utricle was affected by treatment with the inhibitor or activator. Compared to the control group (Figures 4(a)and 4(b)), the position of the LPR in the activation group was changed (Figure 4, A' and B'), and the polarity of HCs on the lateral and medial side of the LPR was disturbed after adding the activator. In the inhibition group, the polarity of HCs on the lateral and medial sides of the LPR was disturbed (Figure 4, A" and B"). Circular histograms of the hair bundle orientation also showed the difference (Figure 4(c)).

3.5. Axin2 Is Decreased in Both the Activation and Inhibition Groups in mRNA. According to RNA-seq results and common Wnt pathway genes, RT-qPCR was performed to detect canonical Wnt signaling pathway-related genes (Apc, Wif1, and Axin2) and PCP core genes (Prickle2 and Vangl2) in cultured utricle in vitro to explore the possible mechanism of polarity change (Figure 5). We found that the expression of Wif1 decreased in the inhibitor group and increased in the activator group, while the expression of APC decreased in the activator group. PCP core genes (Prickle2 and Vangl2) did not change significantly in both groups. Interestingly, the expression of Axin2 was decreased in both groups, indicating that Axin2 may be an important role affecting the polarity of the utricle.

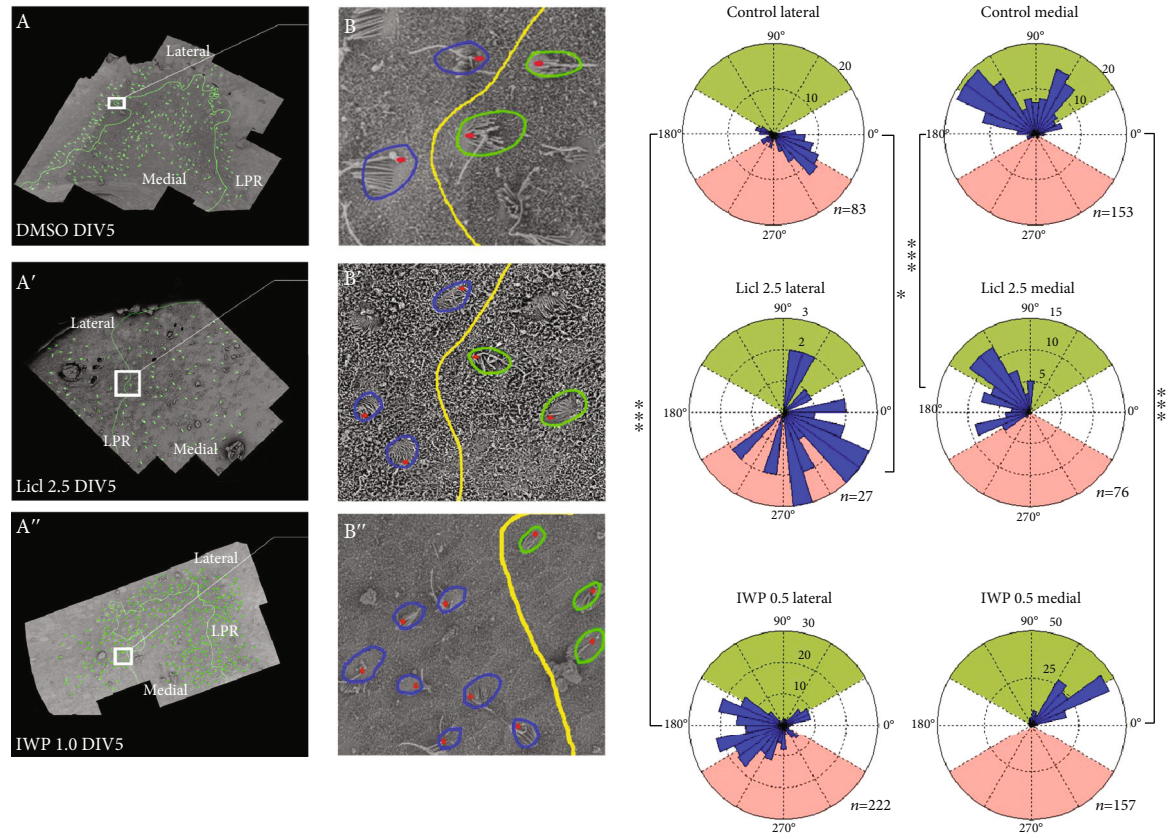

Figure 4: Regulation of Wnt signaling *in vitro*. (a) A' and A" correspond to the control, activation, and inhibition groups, respectively. DMSO, LiCl, and IWP2 were added into Petri dishes with E13.5 utricles and cultured for 5 days. Scanning electron microscopy showed the polarity and line of polarity reversal (LPR) of the hair cells (HCs) in the control group. The green line represents the LPR, and the green arrow represents the direction of the HC polarity. (b) B' and B" are the white boxes in (a) A' and A," respectively; the green circles represent the HCs on the medial side of the LPR, and the blue circles represent the HCs on the lateral side of the LPR; the red dots represent the position of the kinocilium. Circular histograms of the hair bundle orientation in lateral and medial regions for the control, activator, and inhibitor utricles. $^{*}P < 0.05$, $^{***}P < 0.001$.

4. Discussion

The utricle is the organ that senses balance. Proper utricle function depends on the polarization of hair bundles located on the HC surface. This cellular polarization has also been found in many epithelial cell types, including in the respiratory airway and lateral ventricles of the brain. The planar polarity of the utricle was described at three levels: subcellular, cellular, and tissue-wide [8]. In the inner ear, tissue polarity exists only in the vestibular organ. HCs are oriented such that their stereociliary bundles point toward the LPR in the mammalian utricle. LPR was intact in mouse embryos at E15 [30]. Our previous studies found that the HCs in the lateral extrastriolar region (E13.5) appear later than in the medial extrastriolar regions (E11.5). Thus, E13.5 is a critical period for the formation of polarity [28]. In this study, we treated utricles at or before E13.5, either by adding inhibitor or activator *in vitro* or by knocking out β-catenin *in vivo*. The results showed that the canonical Wnt signaling pathway played a role in polarity development of the utricle.

Wnt signaling is a marker of embryonic development and has multiple functions at a number of developmental time points. The Wnt signaling pathway includes both canonical and noncanonical forms. The Wnt signaling pathway has been studied in the early development of the cochlea. The Wnt signaling receptors (Fzd 1, 2, 3, 4, 6, Ryk, Ror2, and Lgr5) can be detected in the cochlea of mice at E14.5 [31–36]. The expression of Wnt7a, Wnt5a, Wnt2, Wnt10b, Wnt4, Wnt7b, Wnt8, and Wnt11 could be detected in the cochlea at E15 and E17 [37], and studies suggested a potential alternation between canonical and noncanonical signaling pathways [38, 39]. Our study also revealed both canonical and noncanonical Wnt pathway-related genes in the utricle during early development, and most Wnt pathway genes were also different between the two time periods of E13.5 and P1. These greatly altered genes may contribute to valid proliferation, differentiation, or innervation. When LiCl was added to activate the Wnt pathway *in vitro*, the proliferation domain of Sox2-positive cells in the cochlea (E12.5) was significantly expanded, indicating that the canonical Wnt pathway regulates the proliferation and differentiation of HCs during early development of the cochlea [14]. Furthermore, overexpression of β-catenin initiated proliferation of sensory precursors cells within the cochlear sensory

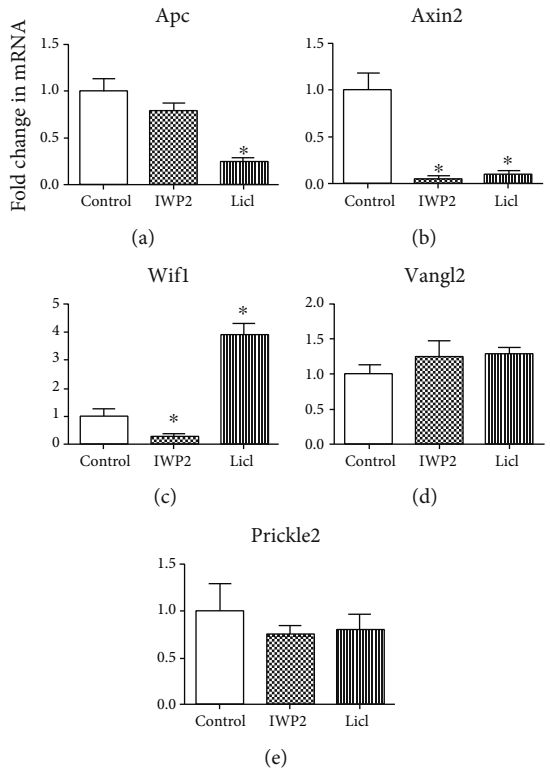

Figure 5: Analysis of Wnt pathway-related genes in vitro treatment at RNA level. (a) Compared with the control group, the expression of Apc was decreased with Licl treatment, and there was no statistical difference with IWP2 treatment. (b) The expression of Axin2 was decreased with IWP2 treatment or Licl treatment. (c) The expression of Wif1 was decreased with IWP2 treatment and was increased with Licl treatment. (d, e) Vangl2 and Prickle2 were no statistical difference with IWP2 treatment or Licl treatment, compared with the control group. $^*P < 0.05$.

epithelium [40]. Therefore, we hypothesized that the Wnt pathway might play the same role in the early development of the utricle. This was confirmed *in vivo* when we conditionally knocked out β-catenin that the number of utricle HCs was affected in the mic. In addition, we found changes in the polarity of hair cells.

Indeed, the Wnt pathway also plays an important role in inner ear polarity regulation. The polarity of HCs in the cochlea is mainly reflected in their convergence and extension, an identical ciliary direction among all HCs, and a V-shaped stereociliary bundle with a uniform direction [41]. In vestibular organs, the stereocilia arrangement and kinocilium displacement are in accordance with a subcellular polarity. HCs are surrounded by supporting cells, and all HCs showed directional coordination in this study. Regarding tissue polarity, cilia bundles of HCs are present on both sides of the LPR face, or move away from the LPR. The role of the Wnt/PCP pathway, a noncanonical Wnt pathway, in inner ear polarity has been studied extensively [34, 42–44]. The noncanonical Wnt/PCP signaling pathway mainly involves Wnt proteins, such as Wnt4, Wnt5A, and Wnt11 [45]. These proteins activate the DEP domain of the Dsh protein, to in turn activate downstream homologous paleogenesis by PCP core proteins, independent of the accumulation of β-catenin. Dislocation of the hair bundle is a common phenotype of Wnt/PCP pathway mutants in the inner ear. The cochlea of the Wnt5a mutant is wider and shorter, with stereociliary bundle misorientation in accordance with a subcellular polarity [35]. After knocking out Vangl or Frizzled, which are the core PCP genes, we observed a disturbance in the polarity of neighbouring cells that appeared relatively consistent, while its subcellular polarity remained intact [34, 46]. In addition, Testin, Celsr1, and Pk2 affect the PCP protein distribution in the vestibule according to the cellular polarity [44, 47, 48]. It is generally believed that the PCP axis is established by noncanonical Wnt signals for tissue polarity. Therefore, it is worth investigating whether canonical Wnt signals play a role in the polarity of the utricle.

Our results showed that the Wnt genes expressed on different days in the utricle were closely related to canonical Wnt/β-catenin pathway, such as Axin2. Thus, we suspect that the canonical Wnt pathway also plays an important role in regulating polarity. The canonical Wnt pathway has been implicated in the regulation of polarity in other organs and animals. Local activation of the canonical Wnt pathway regulates neuronal polarity and axonal outgrowth [49]. In addition, our previous study found that Rack1 is involved in cell membrane localization of the polarity core protein Vangl2, which is associated with zebrafish planar cell polarity formation, primarily by antagonizing the Wnt/β-catenin signaling pathway [50]. β-catenin is the core protein in the canonical Wnt pathway that controls the expression of downstream target genes. A mouse with conditional knockout of β-catenin in the dorsal neural folds will exhibit spina bifida

aperta, caudal axis bending, and tail truncation [51]. Similar polarity changes occurred in mouse kidneys with conditional knockout of β-catenin [52]. However, there are few studies on the canonical Wnt pathway in the context of polarity development in the inner ear, especially in the vestibule. Ankrd6 is asymmetrically distributed in the utricle and regulates polarity by inhibiting the canonical Wnt/β-catenin signaling pathway [53]. Some researchers suggested that the Wnt/β-catenin pathway is important in the ground hypothesis, which was suggested to explain the formation of LPR in the vestibule [54]; however, this has not been verified in mammals. Sox2 is expressed throughout the developing nervous system and plays a role in hair cell type formation [55]. We knocked out β-catenin in Sox2-positive cells and found that the utricle polarity was subsequently affected: the directions of some HCs were disordered near the LPR in the lateral and striolar regions. The changed polarity was also found after activating and inhibiting canonical Wnt pathways in vitro. The changed polarity was also found after activating and inhibiting canonical Wnt pathways in vitro, and PCP core genes (Vangl2 and Prickle2) were no statistical difference with IWP2 treatment or Licl treatment at the RNA level, compared with the control group. However, Axin2 unexpectedly decreased in the two treatment groups. Axin2, a scaffolding protein of glycogen synthase kinase 3, is a negative regulator of Wnt signaling. In addition, Axin2 feedback loop is important with many studies in Wnt pathway, which could help to limit Wnt-initiated signal [56]. Axin2 is involved in the development of the permanent teeth, hair, and eye brows and regulates calvarial suture closure in skull development [57, 58]. In the study of hair cells, a subset of hair cells is derived from Axin2-expressing tympanic border cells, and Axin2 cells were able to differentiate into hair cell-like cells [59]. These findings may suggest that Axin2 has the value in the polarity of utricle, which needs further study to elucidate.

5. Conclusion

In this study, we investigated expression changes of Wnt pathway-related genes during early development of the mouse utricle. In conditional knockout of β-catenin *in vivo*, our data showed the main effect is on hair cell number and may reveal an impact on stereociliary bundle orientation. Combined with the *in vitro* results, we believe that the canonical Wnt pathway is important for controlling HC polarity during mammalian utricle development. Our findings may stimulate future studies on vestibule polarity development.

Data Availability

All data used to support the findings of this study are available from the corresponding author upon request.

Conflicts of Interest

The authors have declared no conflict of interest.

Authors' Contributions

Di Deng, Xiaoqing Qian, and Binjun Chen have contributed equally to this work and share first authorship.

Acknowledgments

This study was supported by the National Natural Science Foundation of China (NSFC) (Grant nos. 81771017, 81970880, and 81970889).

References

[1] Y. Liu, J. Qi, X. Chen et al., "Critical role of spectrin in hearing development and deafness," *Science Advances*, vol. 5, no. 4, p. -eaav7803, 2019.

[2] Y. Wang, J. Li, X. Yao et al., "Loss of CIB2 causes profound hearing loss and abolishes mechanoelectrical transduction in mice," *Frontiers in Molecular Neuroscience*, vol. 10, p. 401, 2017.

[3] C. Zhu, C. Cheng, Y. Wang et al., "Loss of ARHGEF6 causes hair cell stereocilia deficits and hearing loss in mice," *Frontiers in Molecular Neuroscience*, vol. 11, p. 362, 2018.

[4] H. Zhou, X. Qian, N. Xu et al., "Disruption of Atg7-dependent autophagy causes electromotility disturbances, outer hair cell loss, and deafness in mice," *Cell Death & Disease*, vol. 11, no. 10, p. 913, 2020.

[5] P. G. Gillespie and U. Müller, "Mechanotransduction by hair cells: models, molecules, and mechanisms," *Cell*, vol. 139, no. 1, pp. 33–44, 2009.

[6] J. Qi, Y. Liu, C. Chu et al., "A cytoskeleton structure revealed by super-resolution fluorescence imaging in inner ear hair cells," *Cell Discovery*, vol. 5, no. 1, p. 12, 2019.

[7] J. Qi, L. Zhang, F. Tan et al., "Espin distribution as revealed by super-resolution microscopy of stereocilia," *American Journal of Translational Research*, vol. 12, no. 1, pp. 130–141, 2020.

[8] M. R. Deans, "A balance of form and function: planar polarity and development of the vestibular maculae," *Seminars in Cell & Developmental Biology*, vol. 24, no. 5, pp. 490–498, 2013.

[9] S. Zhang, D. Liu, Y. Dong et al., "Frizzled-9+ supporting cells are progenitors for the generation of hair cells in the postnatal mouse cochlea," *Frontiers in Molecular Neuroscience*, vol. 12, p. 184, 2019.

[10] Y. Chen, X. Lu, L. Guo et al., "Hedgehog signaling promotes the proliferation and subsequent hair cell formation of progenitor cells in the neonatal mouse cochlea," *Frontiers in Molecular Neuroscience*, vol. 10, p. 426, 2017.

[11] X. Lu, S. Sun, J. Qi et al., "Bmi1 regulates the proliferation of cochlear supporting cells via the canonical Wnt signaling pathway," *Molecular Neurobiology*, vol. 54, no. 2, pp. 1326–1339, 2017.

[12] J. Wu, W. Li, C. Lin et al., "Co-regulation of the Notch and Wnt signaling pathways promotes supporting cell proliferation and hair cell regeneration in mouse utricles," *Scientific Reports*, vol. 6, no. 1, p. 29418, 2016.

[13] T. Wang, R. Chai, G. S. Kim et al., "Lgr5+ cells regenerate hair cells via proliferation and direct transdifferentiation in damaged neonatal mouse utricle," *Nature Communications*, vol. 6, no. 1, p. 6613, 2015.

[14] S. Zhang, Y. Zhang, Y. Dong et al., "Knockdown of Foxg1 in supporting cells increases the trans-differentiation of

supporting cells into hair cells in the neonatal mouse cochlea," *Cellular and Molecular Life Sciences*, vol. 77, no. 7, pp. 1401–1419, 2020.

[15] S. Zhang, R. Qiang, Y. Dong et al., "Hair cell regeneration from inner ear progenitors in the mammalian cochlea," *American Journal of Stem Cells*, vol. 9, no. 3, pp. 25–35, 2020.

[16] B. C. Cox, R. Chai, A. Lenoir et al., "Spontaneous hair cell regeneration in the neonatal mouse cochlea in vivo," *Development*, vol. 141, no. 4, pp. 816–829, 2014.

[17] Y. Zhang, S. Zhang, Z. Zhang et al., "Knockdown of Foxg1 in Sox9+ supporting cells increases the trans-differentiation of supporting cells into hair cells in the neonatal mouse utricle," *Aging (Albany NY)*, vol. 12, no. 20, pp. 19834–19851, 2020.

[18] W. Li, D. You, Y. Chen, R. Chai, and H. Li, "Regeneration of hair cells in the mammalian vestibular system," *Frontiers in Medicine*, vol. 10, no. 2, pp. 143–151, 2016.

[19] R. van Amerongen and R. Nusse, "Towards an integrated view of Wnt signaling in development," *Development*, vol. 136, no. 19, pp. 3205–3214, 2009.

[20] L. Liu, Y. Chen, J. Qi et al., "Wnt activation protects against neomycin-induced hair cell damage in the mouse cochlea," *Cell Death & Disease*, vol. 7, no. 3, pp. e2136–e2136, 2016.

[21] Z. H. He, S. Y. Zou, M. Li et al., "The nuclear transcription factor FoxG1 affects the sensitivity of mimetic aging hair cells to inflammation by regulating autophagy pathways," *Redox Biology*, vol. 28, p. 101364, 2020.

[22] Y. Ding, W. Meng, W. Kong, Z. He, and R. Chai, "The role of FoxG1 in the inner ear," *Frontiers in Cell and Development Biology*, vol. 8, p. 614954, 2020.

[23] Z. He, Q. Fang, H. Li et al., "The role of FOXG1 in the postnatal development and survival of mouse cochlear hair cells," *Neuropharmacology*, vol. 144, pp. 43–57, 2019.

[24] S. Gao, C. Cheng, M. Wang et al., "Blebbistatin Inhibits Neomycin-Induced Apoptosis in Hair Cell-Like HEI-OC-1 Cells and in Cochlear Hair Cells," *Frontiers in Cellular Neuroscience*, vol. 13, p. 590, 2019.

[25] W. Liu, X. Xu, Z. Fan et al., "Wnt signaling activates TP53-induced glycolysis and apoptosis regulator and protects against cisplatin-induced spiral ganglion neuron damage in the mouse cochlea," *Antioxidants & Redox Signaling*, vol. 30, no. 11, pp. 1389–1410, 2019.

[26] C. Cheng, Y. Wang, L. Guo et al., "Age-related transcriptome changes in Sox2+ supporting cells in the mouse cochlea," *Stem Cell Research & Therapy*, vol. 10, no. 1, p. 365, 2019.

[27] T. Ohyama, O. A. Mohamed, M. M. Taketo, D. Dufort, and A. K. Groves, "Wnt signals mediate a fate decision between otic placode and epidermis," *Development*, vol. 133, no. 5, pp. 865–875, 2006.

[28] X. Yang, X. Qian, R. Ma et al., "Establishment of planar cell polarity is coupled to regional cell cycle exit and cell differentiation in the mouse utricle," *Scientific Reports*, vol. 7, no. 1, p. 43021, 2017.

[29] Z. Li, S. Chen, S. Chen, D. Huang, K. Ma, and Z. Shao, "Moderate activation of Wnt/β-catenin signaling promotes the survival of rat nucleus pulposus cells via regulating apoptosis, autophagy, and senescence," *Journal of Cellular Biochemistry*, vol. 120, no. 8, pp. 12519–12533, 2019.

[30] K. Denman-Johnson and A. Forge, "Establishment of hair bundle polarity and orientation in the developing vestibular system of the mouse," *Journal of Neurocytology*, vol. 28, no. 10/11, pp. 821–835, 1999.

[31] R. Chai, A. Xia, T. Wang et al., "Dynamic expression of Lgr5, a Wnt target gene, in the developing and mature mouse cochlea," *Journal of the Association for Research in Otolaryngology*, vol. 12, no. 4, pp. 455–469, 2011.

[32] M. L. Macheda, W. W. Sun, K. Kugathasan et al., "The Wnt receptor Ryk plays a role in mammalian planar cell polarity signaling," *The Journal of Biological Chemistry*, vol. 287, no. 35, pp. 29312–29323, 2012.

[33] H. Yu, P. M. Smallwood, Y. Wang, R. Vidaltamayo, R. Reed, and J. Nathans, "Frizzled 1 and frizzled 2 genes function in palate, ventricular septum and neural tube closure: general implications for tissue fusion processes," *Development*, vol. 137, no. 21, pp. 3707–3717, 2010.

[34] Y. Wang, N. Guo, and J. Nathans, "The role of Frizzled3 and Frizzled6 in neural tube closure and in the planar polarity of inner-ear sensory hair cells," *The Journal of Neuroscience*, vol. 26, no. 8, pp. 2147–2156, 2006.

[35] D. Qian, C. Jones, A. Rzadzinska et al., "Wnt5a functions in planar cell polarity regulation in mice," *Developmental Biology*, vol. 306, no. 1, pp. 121–133, 2007.

[36] Y. Wang, D. Huso, H. Cahill, D. Ryugo, and J. Nathans, "Progressive cerebellar, auditory, and esophageal dysfunction caused by targeted disruption of the frizzled-4 gene," *The Journal of Neuroscience*, vol. 21, no. 13, pp. 4761–4771, 2001.

[37] A. Dabdoub, M. J. Donohue, A. Brennan et al., "Wnt signaling mediates reorientation of outer hair cell stereociliary bundles in the mammalian cochlea," *Development*, vol. 130, no. 11, pp. 2375–2384, 2003.

[38] A. J. Mikels and R. Nusse, "Purified Wnt5a protein activates or inhibits beta-catenin-TCF signaling depending on receptor context," *PLoS Biology*, vol. 4, no. 4, article e115, 2006.

[39] J. D. Berndt, A. Aoyagi, P. Yang, J. N. Anastas, L. Tang, and R. T. Moon, "Mindbomb 1, an E3 ubiquitin ligase, forms a complex with RYK to activate Wnt/β-catenin signaling," *The Journal of Cell Biology*, vol. 194, no. 5, pp. 737–750, 2011.

[40] R. Chai, B. Kuo, T. Wang et al., "Wnt signaling induces proliferation of sensory precursors in the postnatal mouse cochlea," *Proceedings of the National Academy of Sciences of the United States of America*, vol. 109, no. 21, pp. 8167–8172, 2012.

[41] A. Li, J. Xue, and E. H. Peterson, "Architecture of the mouse utricle: macular organization and hair bundle heights," *Journal of Neurophysiology*, vol. 99, no. 2, pp. 718–733, 2008.

[42] X. Lu, A. G. Borchers, C. Jolicoeur, H. Rayburn, J. C. Baker, and M. Tessier-Lavigne, "PTK7/CCK-4 is a novel regulator of planar cell polarity in vertebrates," *Nature*, vol. 430, no. 6995, pp. 93–98, 2004.

[43] H. Yin, C. O. Copley, L. V. Goodrich, and M. R. Deans, "Comparison of phenotypes between different vangl2 mutants demonstrates dominant effects of the Looptail mutation during hair cell development," *PLoS One*, vol. 7, no. 2, article e31988, 2012.

[44] J. S. Duncan, M. L. Stoller, A. F. Francl, F. Tissir, D. Devenport, and M. R. Deans, "Celsr1 coordinates the planar polarity of vestibular hair cells during inner ear development," *Developmental Biology*, vol. 423, no. 2, pp. 126–137, 2017.

[45] H. Peradziryi, N. S. Tolwinski, and A. Borchers, "The many roles of PTK7: a versatile regulator of cell-cell communication," *Archives of Biochemistry and Biophysics*, vol. 524, no. 1, pp. 71–76, 2012.

[46] M. L. Stoller, O. Roman Jr., and M. R. Deans, "Domineering non-autonomy in Vangl1;Vangl2 double mutants

demonstrates intercellular PCP signaling in the vertebrate inner ear," *Developmental Biology*, vol. 437, no. 1, pp. 17–26, 2018.

[47] D. D. Ren, M. Kelly, S. M. Kim, C. M. Grimsley-Myers, F. L. Chi, and P. Chen, "Testin interacts with vangl2 genetically to regulate inner ear sensory cell orientation and the normal development of the female reproductive tract in mice," *Developmental Dynamics*, vol. 242, no. 12, pp. 1454–1465, 2013.

[48] M. R. Deans, D. Antic, K. Suyama, M. P. Scott, J. D. Axelrod, and L. V. Goodrich, "Asymmetric distribution of prickle-like 2 reveals an early underlying polarization of vestibular sensory epithelia in the inner ear," *The Journal of Neuroscience*, vol. 27, no. 12, pp. 3139–3147, 2007.

[49] E. Stanganello, E. E. Zahavi, M. Burute et al., "Wnt Signaling Directs Neuronal Polarity and Axonal Growth," *iScience*, vol. 13, pp. 318–327, 2019.

[50] S. Li, R. Esterberg, V. Lachance et al., "Rack1 is required for Vangl2 membrane localization and planar cell polarity signaling while attenuating canonical Wnt activity," *Proceedings of the National Academy of Sciences of the United States of America*, vol. 108, no. 6, pp. 2264–2269, 2011.

[51] T. Zhao, Q. Gan, A. Stokes et al., "β-catenin regulates Pax3 and Cdx2 for caudal neural tube closure and elongation," *Development*, vol. 141, no. 1, pp. 148–157, 2014.

[52] T. D. Marose, C. E. Merkel, A. P. McMahon, and T. J. Carroll, "β-Catenin is necessary to keep cells of ureteric bud/Wolffian duct epithelium in a precursor state," *Developmental Biology*, vol. 314, no. 1, pp. 112–126, 2008.

[53] C. Jones, D. Qian, S. M. Kim et al., "_Ankrd6_ is a mammalian functional homolog of _Drosophila_ planar cell polarity gene _diego_ and regulates coordinated cellular orientation in the mouse inner ear," *Developmental Biology*, vol. 395, no. 1, pp. 62–72, 2014.

[54] J. L. Green, T. Inoue, and P. W. Sternberg, "Opposing Wnt pathways orient cell polarity during organogenesis," *Cell*, vol. 134, no. 4, pp. 646–656, 2008.

[55] J. Lu, L. Hu, B. Ye et al., "Increased type I and decreased type II hair cells after deletion of _Sox2_ in the developing mouse utricle," *Neuroscience*, vol. 422, pp. 146–160, 2019.

[56] E. H. Jho, T. Zhang, C. Domon, C. K. Joo, J. N. Freund, and F. Costantini, "Wnt/beta-catenin/Tcf signaling induces the transcription of Axin2, a negative regulator of the signaling pathway," *Molecular and Cellular Biology*, vol. 22, no. 4, pp. 1172–1183, 2002.

[57] H.-M. I. Yu, B. Jerchow, T.-J. Sheu et al., "The role of Axin2 in calvarial morphogenesis and craniosynostosis," *Development*, vol. 132, no. 8, pp. 1995–2005, 2005.

[58] S. K. Macklin Mantia, S. L. Hines, K. L. Chaichana et al., "Case report expanding the germline AXIN2- related phenotype to include olfactory neuroblastoma and gastric adenoma," *BMC Medical Genetics*, vol. 21, no. 1, p. 161, 2020.

[59] T. A. Jan, R. Chai, Z. N. Sayyid et al., "Tympanic border cells are Wnt-responsive and can act as progenitors for postnatal mouse cochlear cells," *Development*, vol. 140, no. 6, pp. 1196–1206, 2013.

Hindawi
Neural Plasticity
Volume 2021, Article ID 9957712, 9 pages
https://doi.org/10.1155/2021/9957712

Research Article

Identification of Novel Compound Heterozygous *MYO15A* Mutations in Two Chinese Families with Autosomal Recessive Nonsyndromic Hearing Loss

Xiao-Hui Wang,[1] Le Xie,[1] Sen Chen,[1] Kai Xu,[1] Xue Bai,[1] Yuan Jin,[1] Yue Qiu,[1] Xiao-Zhou Liu,[1] Yu Sun,[1] and Wei-Jia Kong[1,2]

[1]*Department of Otorhinolaryngology, Union Hospital, Tongji Medical College, Huazhong University of Science and Technology, Wuhan 430022, China*
[2]*Institute of Otorhinolaryngology, Tongji Medical College, Huazhong University of Science and Technology, 430022 Wuhan, China*

Correspondence should be addressed to Yu Sun; sunyu@hust.edu.cn and Wei-Jia Kong; entwjkong@hust.edu.cn

Received 30 March 2021; Revised 14 April 2021; Accepted 4 May 2021; Published 15 May 2021

Academic Editor: Geng lin Li

Congenital deafness is one of the most common causes of disability in humans, and more than half of cases are caused by genetic factors. Mutations of the *MYO15A* gene are the third most common cause of hereditary hearing loss. Using next-generation sequencing combined with auditory tests, two novel compound heterozygous variants c.2802_2812del/c.5681T>C and c.5681T>C/c.6340G>A in the *MYO15A* gene were identified in probands from two irrelevant Chinese families. Auditory phenotypes of the probands are consistent with the previously reported for recessive variants in the *MYO15A* gene. The two novel variants, c.2802_2812del and c.5681T>C, were identified as deleterious mutations by bioinformatics analysis. Our findings extend the *MYO15A* gene mutation spectrum and provide more information for rapid and precise molecular diagnosis of congenital deafness.

1. Introduction

Congenital deafness is one of the most common birth defects, with an incidence of approximately 1.4 per 1000 newborns screened. More than 60% of neonates with congenital deafness can be attributable to genetic factors [1]. Most of these cases are nonsyndromic hearing loss (NSHL), and autosomal recessive inheritance accounts for up to 80% of NSHL [2]. *GJB2*, *SLC26A4*, and *MYO15A* are the top three common genes responsible for hereditary hearing loss [3, 4]. Mutations in the *MYO15A* gene have been found to lead to autosomal recessive nonsyndromic hearing loss 3 (DFNB3) [5], and new mutations of this gene are constantly being detected.

The *MYO15A* gene spans 71 kb of genomic DNA on chromosome 17p11.2. It contains 66 exons and encodes unconventional myosin-XV protein which is composed of 3530 amino acids [6]. The protein it encodes mainly localizes in the tips of mammalian hair cell stereocilia, which plays a crucial role in the development of stereocilia and the formation of normal auditory function [7, 8]. It shares a structural organization consisting of a N-terminal domain, an ATPase motor domain, a neck region with myosin light chain binding, and a globular tail domain [6, 9]. The integrity of a protein plays a crucial role for its function. Therefore, the truncating mutation which is interrupted by a stop codon may lead to a pathogenic protein. Besides, more than 40 missense mutations have been identified in the moto domain of the *MYO15A* gene associated with autosomal recessive nonsyndromic hearing loss (ARNSHL), where the most mutations occur. In the mouse model, the mutation in the motor domain results shorter stereocilia with an abnormal staircase structure which leads to deafness [4].

Hearing screening combined with genetic diagnosis can help us recognize more pathogenic gene mutations. The

mutation spectrum of the *MYO15A* gene is highly heterogeneous which refers to two heterozygous variants present in trans configuration within the same genomic region of interest. Through the study of two independent *MYO15A* gene mutant families, we identified two novel compound heterozygous mutations: c.2802_2812del/c.5681T>C and c.5681T>C/c.6340G>A. Besides, the known pathogenic variant of c.6340G>A provides more evidence to deduce the pathogenicity of the first two novel mutations by the verification between pedigrees.

2. Materials and Methods

2.1. Family Description. In this study, two Chinese families affected by congenital NSHL were recruited. These two Chinese families contain three family members (daughter/-son, mother, and father), respectively. The affected member II-1 of Family 1 (Figure 1(a)): a 2-year-old girl, failed to pass hearing screening and diagnosed with congenital NSHL. The proband II-1 of Family 2 (Figure 1(d)): a 1-year and 5-month-old boy, diagnosed with congenital NSHL as well. Other individuals had no history of hearing impairment.

2.2. Clinical Examination. All affected family members underwent clinical evaluation in the Department of Otorhinolaryngology, Union Hospital, Tongji Medical College, Huazhong University of Science and Technology, Wuhan, China. A series of audiological examinations were performed on probands, which included otoscopic examination, behavioral observation audiometry (BOA), auditory immittance, auditory brainstem response (ABR), auditory steady-state evoked response (ASSR), and distortion product otoacoustic emission (DPOAE). The DPOAE were detected in 750, 1000, 1500, 2000, 3000, 4000, 6000, and 8000 Hz frequencies. The degree of hearing loss was defined as mild (26–40 dB HL), moderate (41–55 dB HL), moderately severe (56–70 dB HL), severe (71–90 dB HL), and profound (>90 dB HL). The computed tomography (CT) scan and MRI (Magnetic Resonance Imaging) were also performed on probands. In addition, physical examinations were also performed to rule out other systemic diseases. The probands' parents provided family history and clinical questionnaires, and informed consent was obtained from the whole family for inclusion in the study.

2.3. Mutation Detection and Analysis. HDNPL_9957712After obtaining informed consent, 3-5 mL peripheral venous blood samples were obtained from all the family members for NGS+Sanger sequencing. Genomic DNA was extracted from the blood samples according to the manufacturer's standard procedure using the QIAamp DNA Blood Midi Kit (Qiagen Inc., Hilden, Germany). Agarose gel electrophoresis was performed for evaluating the quality and quantity of DNA samples according to the routine protocol. DNA from the proband were performed whole-exome sequencing. Whole-exome capture was performed using the BGI-Exome kit V4 and sequenced by BGI-seq500 with 100 bp paired-end sequencing. Sequenced reads were collected and aligned to the human genome reference (UCSCGRCh37/hg19) by the Burrows-Wheeler Aligner (BWA-MEM, version 0.7.10) [10]. In order to validate the mutations identified in the proband and confirm their cosegregation in the pedigree, DNA from all members of the family was performed Sanger sequenced. After polymerase chain reaction (PCR) amplification and purified the amplified fragments, Sanger sequencing was performed with an ABI3730xl DNA Sequence and the results were analyzed using the Sequencing Analysis 5.2 software (Thermo Fisher Scientific, USA) [11]. The names of variants were referred to the HGVS nomenclature guidelines (http://www.hgvs.org/mutnomen). The methods have been published in our previous studies [12, 13].

2.4. Predictions of the Pathogenic Variations. Several different computer algorithms were used to predict the pathogenic features of missense variants: MutationTaster (http://www.mutationtaster.org/), PROVEAN (http://provean.jcvi.org/), and PolyPhen-2 (http://genetics.bwh.harvard.edu/pph2/). The PROVEAN scores indicated deleterious and neutral function, with a cut-off score set at -2.5. The PolyPhen-2 score ranges from 0.0 to 1.0. Variants with scores of 0.0 are predicted to be benign. Values closer to 1.0 are more confidently predicted to be deleterious. Phylogenetic analysis of different sequence alignments was performed by Clustal Omega (https://www.ebi.ac.uk/Tools/msa/clustalo/). The orthologous *MYO15A* protein sequences include mouse, chimpanzee, rat, and macaque. The mutations were detected in the 1000 Genomes database, the dbSNP database, and the Exome Aggregation Consortium database (ExAC). Pathogenicity of the variants was classified based on the guidelines of ACMG 2015 [14].

3. Results

3.1. Clinical Data

3.1.1. Family 1. The proband II-1 of Family 1 test results were as follows. BOA showed poor hearing, and acoustic immittance test results show that the tympanograms were type As (left ear) and type A (right ear). The thresholds of ASSR were 80 dB nHL at 500 Hz, 90 dB nHL at 1 kHz, 100 dB nHL at 2 kHz, and 100 dB nHL at 4 kHz (right ear) and 90 dB nHL at 500 Hz, 60 dB nHL at 1 kHz, 110 dB nHL at 2 kHz, and 110 dB nHL at 4 kHz (left ear) (Figure 1(b)). The wave V thresholds of ABR of both ears were 90 dB, and DPOAE were absent bilaterally (Figure 1(c)). Tympanogram indicated almost normal function of the middle ear. The temporal bone CT scan suggested the proband without any malformation of middle or inner ear.

3.1.2. Family 2. The proband II-1 of Family 2 suffered from profound hearing loss, which was shown by the auditory examination. The wave V thresholds of ABR of both ears were not extracted in 105 dB. The thresholds of ASSR were all 100 dB nHL at every frequency (Figure 1(e)) of each ear, and bilateral DPOAE were absent (Figure 1(f)). Tympanogram revealed a type A curve indicating a normal function

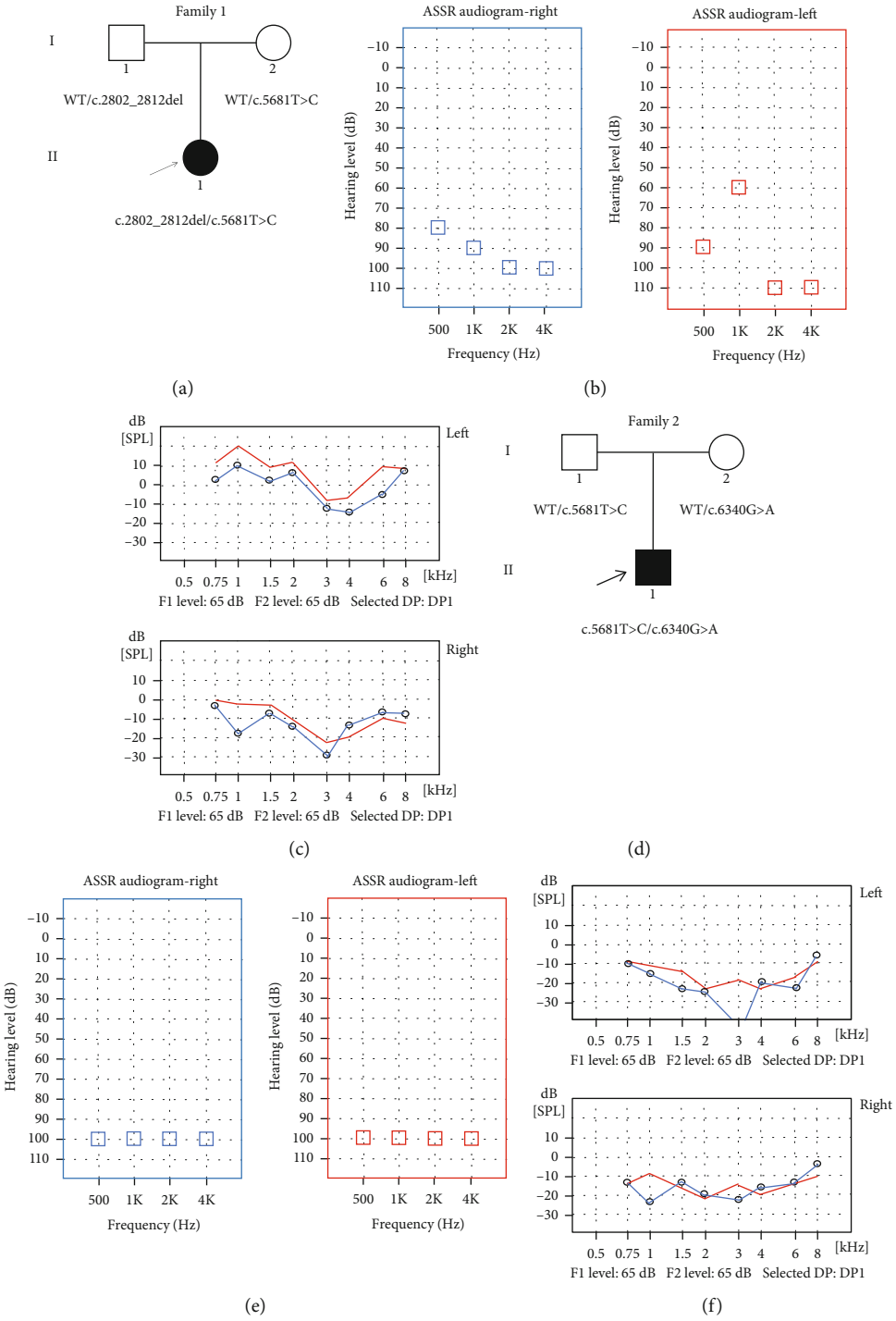

Figure 1: Pedigrees of the affected Family 1 (a) and Family 2 (d) associated with NSHL. The novel compound heterozygous mutations were found in family members. The probands are shown in black. WT: wild type. (b) Auditory steady-state response (ASSR) audiogram of the proband II-1 of Family 1. (c) Distortion product otoacoustic emission (DPOAE) audiogram of both ears of the proband II-1 of Family 1. (e) ASSR audiogram of the proband II-1 of Family 2. (f) DPOAE audiogram of both ears of the proband II-1 of Family 2.

of the middle ear. Temporal bone CT scans and MRI showed no obvious abnormalities. There was no family history of congenital deafness and no underlying environmental causes of hearing loss. The detailed clinical information is summarized in Table 1.

3.2. Mutation Identification and Analysis. Using deafness panel sequencing, 159 loci of 22 genes that cause congenital deafness were excluded. Whole-exome sequencing results were compared with the human reference genome (GRCh37/hg19). We found novel compound heterozygous mutation c.2802_2812del/c.5681T>C in Family 1 and c.5681T>C/c.6340G>A in Family 2. In Family 1, the c.2802_

Table 1: The clinical information of the patients.

Proband number	Age	Gender	Age onset	Hearing impairment	ABR	DPOAE	Tympanogram	MRI/CT
1	2 yr	F	0	Profound	85 dB	Absent	As(L)/A(R)	Normal
2	1 yr	M	0	Profound	105 dB	Absent	A(L)/A(R)	Normal

ABR: auditory brainstem response; DPOAE: distortion product otoacoustic emissions; A: A type; As: As type.

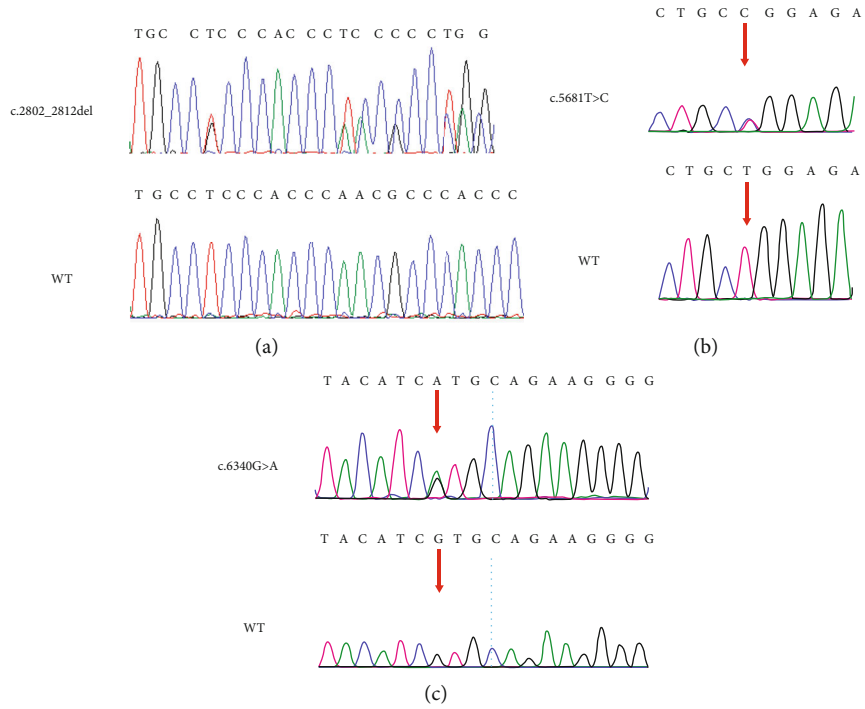

Figure 2: Sanger sequencing results of the c.2802_2812del (a), c.5681T>C (b), and c.6340G>A (c) mutations in the family members. Red arrows: sites of nucleotide changes.

2812del mutation, which was located in exon 2 and passed on from her clinically normal father (Figure 2(a)), led to a frame-shifting change in the N-terminal domain (p.Gln937Leufs∗39) and truncate mRNA translation resulting in lack of complete amino acid sequence. Occurring in exon 24, the c.5681T>C mutation, which was inherited from the unaffected mother (Figure 2(b)), led to a single substitution from leucine to proline at amino acid position 1894 in the ATPase motor domain (p.Leu1894Pro). Both of them were predicted to be deleterious variants based on the result of computer algorithms PolyPhen-2 and PROVEAN (Table 2), and these two variants were not seen in public databases dbSNP, 1000 Genomes Project, and ExAC. According to the American College of Medical Genetics and Genomics–Association for Molecular Pathology (ACMG–AMP) guidelines, the variant c.2802_2812del and c.5681T>C were classified pathogenic (PSV1+PM2+PM3+PM4+PP3) and likely pathogenic (PM2+PM3+PP3), respectively.

Interestingly, the variant c.5681T>C (p.Leu1894Pro) was also found in Family 2 and his unaffected father, and another variant was a reported variant c.6340G>A (p.Val2114Met) in exon 30, which was also detected in his mother (Figure 2(c)). The mutation c.6340G>A of the *MYO15A* gene, a known pathogenic missense mutation, leads to an alternation of a Valine with a Methionine at amino acid position 2114 in the MyTH4 domain. The c.6340G>A mutation was previously reported in another Chinese family and in two Egyptian families which is predicted to weaken the function of MyTH4 [15, 16]. It was predicted as deleterious by computational tools. Following the ACMG guidelines, the c.6340G>A variant was classified as pathogenic (PVS1+PM2+PM3+PP1+PP3). Detailed information of variants is shown in Table 2.

3.3. Functional Analysis of the Mutant Protein. Myosin-XV differs from other myosin proteins in that it has a long N-terminal extending in front of the conserved motor region. It includes a N-terminal domain encoded by giant exon 2 (Figure 3(a)), the ATPase motor domain, a lever arm that consists of three IQ motifs, and a globular tail domain that contains MyTH4, FERM, SH3, and PDZ ligand (Figure 3(b)). The locations of the mutations in this study have been shown in Figure 4. The mutation c.2802_2812del identified in the proband II-1 of Family 1 results in a frameshift, and no. 975 amino acid was converted into a termination codon, which generated a truncated protein (Figure 4(a)). The evolutionary conservation result

Table 2: Identified pathogenic variants in the MYO15A gene in this study and their prediction results by computer algorithms.

Nucleotide change	Type of variation	Gene subregion	Amino acid change	MutationTaster[a]	PROVEAN[b]	PolyPhen-2[c]	Novelty
c.2802_2812del	Truncation	Exon 2	p.Gln937Leufs∗39	DC	Deleterious (score -65.157)	—	Novel
c.5681T>C	Missense	Exon 24	p.Leu1894Pro	DC	Deleterious (score -6.817)	Probably damaging (score 0.988)	Novel
c.6340G>A	Missense	Exon 30	p.Val2114Met	DC	Deleterious (score -2.696)	Probably damaging (score 0.982)	[15, 16]

[a]DC: disease causing; PO: polymorphism. [b]The PROVEAN scores indicated deleterious and neutral function, respectively, with a cut-off score set at -2.5. Variants with a score equal to or below -2.5 are considered "deleterious"; variants with a score above -2.5 are considered "neutral." [c]The PolyPhen-2 score ranges from 0.0 to 1.0. Variants with scores of 0.0 are predicted to be benign. Values closer to 1.0 are more confidently predicted to be deleterious. The score can be interpreted as follows: 0.0 to 0.15: benign; 0.15 to 1.0: possibly damaging; 0.85 to 1.0: probably damaging.

proved that the amino acid residues at the mutation sites were highly conserved among multiple species (Figure 4(b)). This strongly demonstrates the importance of these residues for the normal function of the protein.

4. Discussion

Hair cells (HCs) in the inner ear contribute to transducing sound waves into electric signals [17–21]. Hearing loss is one of the major disabilities worldwide, which is often induced by irreversible loss of sensory HCs and degeneration of the spiral ganglion neurons. Congenital hearing loss could be caused by genetic factors, cochlear infections, ototoxic drugs, and noise exposure, and genetic factors account for more than 60% of congenital hearing loss [22]. Each cochlear hair cell has a bundle of actin-based stereocilia that detect sound. The *MYO*15A gene encodes an unconventional myosin that is expressed in the cochlea, which traffics and delivers critical molecules required for stereocilia development and thus is essential for building the mechanosensory hair bundle [7, 23, 24]. Mouse models' studies show that *MYO15A* mutations can lead to abnormal hearing function caused by short stereocilia and by loss of the normal staircase structure of stereocilia in hair cells [25, 26].

The mutation c.2802_2812del results in a truncated protein caused by the frameshift. Like many previously reported pathogenic truncating mutations in the *MYO15A* gene, the c.2802_2812del variant is predicted to result in a truncated protein product without motor, IQ, MyTH4, FERM, SH3, and PDZ domains. Since DFNB3 is an autosomal recessive disorder and the proband's father is a heterozygous carrier, we strongly speculate that the variant c.2802_2812del might cause hearing loss related to the incomplete protein structure. A previous study indicated that pathogenic mutations that reside in the N-terminal domain are associated with a variety of mild hearing loss phenotypes [27–29]. In combination with other studies [30], our study suggests that a truncated mutation c.2802_2812del in the N-terminal domain of the *MYO15A* gene may contribute to a severe phenotype. These evidences indicate the diversity of auditory phenotypes due to *MYO15A* variation [31].

The c.5681T>C mutation leads to a single substitution from leucine to proline at amino acid position 1894. This variant is located in the motor domain of the *MYO15A* gene. Our literature review illustrated that the motion domain is a hot region affected by *MYO15A* variation and more and more variants were detected in this domain [32, 33]. This region contains actin and ATP binding sites that generate the force to transport actin filaments in vitro [34]. It is reasonable that motor domain dysfunction will lead to abnormal stereocilia associated with a severe deafness phenotype. A recent mechanism study revealed that the myosin-XV motor domain may exhibit strain sensitivity, suggesting that it could also act as a force-sensitive element bridging the membrane and actin cytoskeleton at the stereocilia tip which, in turn, makes a significant influence on human deafness of *MYO15A* mutation [24]. Profound hearing loss and null DPAOE response may be caused by this novel compound heterozygous mutations of the *MYO15A* gene. The c.6340G>A mutation is a known disease mutation (https://www.ncbi.nlm.nih.gov/snp/rs377385081) which was first reported by Yang et al. in 2013 [15]. In Yang's study, the biallelic mutations c.6340G>A/c.6956+9C>G were also found in the proband's deaf relatives for which they were identified as disease mutations. The c.6340G>A mutation is a missense mutation resulting in an alternation of a Valine with a Methionine at amino acid position 2114 in the first MyTH4 domain in myosin-XV. The MyTH4 domain of myosin has some roles in microtubule as well as actin binding at the plasma membrane. Mutations in this domain can disrupt the protein-protein interaction which is important for the normal function of hearing [35, 36].

Here, we found c.5681T>C was compound heterozygous with c.2802_2812del and c.6340G>A in these two irrelevant pedigrees. We concluded the c.5681T>C variant to be pathogenic for several reasons: (a) the amino acid residues at the mutation sites were highly conserved; (b) several pathogenic mutations have been found near this location; (c) detected in 2 sporadic pedigrees with similar DFNB3 phenotype; (d) the *MYO15A* gene is highly heterogeneous, and c.6340G>A mutation is a known disease mutation, which combined with c.5681T>C causing deafness. Moreover, both the 2 novel mutations were cosegregated with the profound deafness and were predicted to be pathogenic mutations by computer algorithms. These all

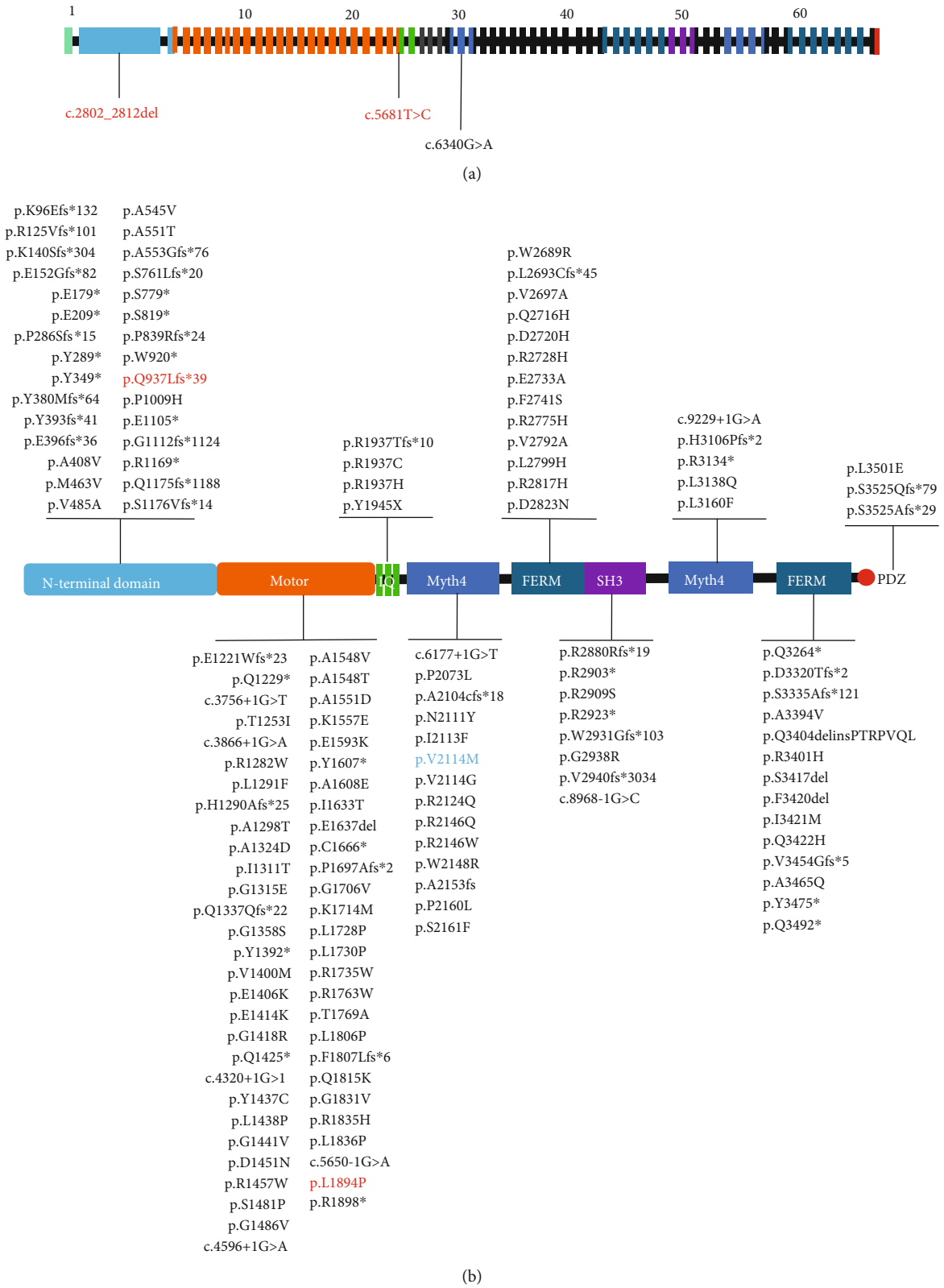

Figure 3: (a) Schematic diagram of 66 exons of the *MYO15A* gene is shown with all pathogenic mutations (arrows) of two families. Novel compound heterozygous *MYO15A* mutations are indicated in red. Previously reported mutation is indicated in black. (b) Overview of the reported *MYO15A* variants and their locations in the protein structure. The red words indicate the novel mutations, and the blue one refers to the reported variant that was detected in the proband in this study.

(a)

	p.Leu1894Pro *		p.Val2114Met *	
Mutation	KLFLKEHLYQ P LESMREHVLNL	1904	GHLEVPAELAGLLQA M AGLGLA	2020
Homo sapiens	KLFLKEHLYQ L LESMREHVLNL	1904	GHLEVPAELAGLLQA V AGLGLA	2020
Mus musculus	KLFLKEHLHQ L LESMRERVQNR	1888	RHLEVPAEVAGLLQA A AGLKLS	2004
Pan troglodytes	KLFLKEHLYQ L LESMREHVLNL	1896	GHLEVPAELAGLLQA V AGLGLA	2012
Rattus norvegious	KLFLKEHLHQ L LESMRERVLNR	1889	RHLEVPAEVAGLLQA A AGLKPS	2005
Maoaoa mulatta	KLFLKEHLYQ L LESMREHVLNL	1903	GHLEVPAELAGLLQA V AGLRLA	2019

(b)

Figure 4: (a) Codon and amino acid coding diagram of the variant c.2802_2812del (p.Gln937Leufs∗39) of the proband II-1 of Family 1. The red letters indicate the changed amino acids and the site of the stop codon. In the mutant, no. 975 amino acid was converted into a termination codon. (b) Evolutionary conservation of no. 1894 and no. 2114 amino acid (red). Mutated site is indicated by an asterisk.

suggested that c.5681T>C is a relevant and pathogenic mutation in the *MYO15A* gene responsible for the profound hearing loss of the probands.

In conclusion, our study demonstrated that two compound heterozygous mutations in the *MYO15A* gene (c.2802_2812del/c.5681T>C and c.5681T>C/c.6340G>A) were the pathogenic variants in two ARNSHL families. The c.2802_2812del and c.5681T>C mutations are reported for the first time, and both were strongly speculated as pathogenic mutations in the *MYO15A* gene. Our finding further extends the *MYO15A* gene mutation spectrum and enriches our knowledge of genotype-phenotype correlation in *MYO15A*-related deafness.

Data Availability

The data which supports the conclusions of our study is available upon request.

Consent

Written informed consent to participate in this study was provided by the participants' legal guardians.

Conflicts of Interest

The authors declare that they have no conflict of interest.

Authors' Contributions

Xiao-Hui Wang, Le Xie, and Sen Chen contributed equally to this work.

Acknowledgments

The authors thank the family for their participation in this study. This work was supported by grants from the National Nature Science Foundation of China (81771003 and 82071058).

References

[1] R. J. Smith, J. F. Bale Jr., and K. R. White, "Sensorineural hearing loss in children," *The Lancet*, vol. 365, no. 9462, pp. 879–890, 2005.

[2] C. C. Morton and W. E. Nance, "Newborn hearing screening–a silent revolution," *The New England Journal of Medicine*, vol. 354, no. 20, pp. 2151–2164, 2006.

[3] D. Duman and M. Tekin, "Autosomal recessive nonsyndromic deafness genes: a review," *Frontiers in Bioscience*, vol. 17, no. 7, pp. 2213–2236, 2012.

[4] N. Hilgert, R. J. H. Smith, and G. Van Camp, "Forty-six genes causing nonsyndromic hearing impairment: which ones should be analyzed in DNA diagnostics?," *Mutation Research*, vol. 681, no. 2-3, pp. 189–196, 2009.

[5] A. Wang, Y. Liang, R. A. Fridell et al., "Association of unconventional myosin MYO15 mutations with human nonsyndromic deafness DFNB3," *Science*, vol. 280, no. 5368, pp. 1447–1451, 1998.

[6] Y. Liang, A. Wang, I. A. Belyantseva et al., "Characterization of the human and mouse unconventional myosin XV genes responsible for hereditary deafness DFNB3 and shaker 2," *Genomics*, vol. 61, no. 3, pp. 243–258, 1999.

[7] I. A. Belyantseva, E. T. Boger, and T. B. Friedman, "Myosin XVa localizes to the tips of inner ear sensory cell stereocilia and is essential for staircase formation of the hair bundle," *Proceedings of the National Academy of Sciences of the United States of America*, vol. 100, no. 24, pp. 13958–13963, 2003.

[8] I. A. Belyantseva, E. T. Boger, S. Naz et al., "Myosin-XVa is required for tip localization of whirlin and differential elongation of hair-cell stereocilia," *Nature Cell Biology*, vol. 7, no. 2, pp. 148–156, 2005.

[9] V. Mermall, P. L. Post, and M. S. Mooseker, "Unconventional myosins in cell movement, membrane traffic, and signal transduction," *Science*, vol. 279, no. 5350, pp. 527–533, 1998.

[10] Y. Zhou, M. Tariq, S. He, U. Abdullah, J. Zhang, and S. M. Baig, "Whole exome sequencing identified mutations causing hearing loss in five consanguineous Pakistani families," *BMC Medical Genetics*, vol. 21, no. 1, p. 151, 2020.

[11] X. Fan, Y. Wang, Y. Fan et al., "TCOF1 pathogenic variants identified by whole-exome sequencing in Chinese Treacher Collins syndrome families and hearing rehabilitation effect," *Orphanet Journal of Rare Diseases*, vol. 14, no. 1, p. 178, 2019.

[12] Y. Qiu, S. Chen, L. Xie et al., "Auditory neuropathy spectrum disorder due to two novel compound heterozygous OTOF mutations in two Chinese families," *Neural Plasticity*, vol. 2019, Article ID 9765276, 7 pages, 2019.

[13] Y. Qiu, S. Chen, X. Wu et al., "Jervell and Lange-Nielsen syndrome due to a novel compound heterozygous KCNQ1 mutation in a Chinese family," *Neural Plasticity*, vol. 2020, Article ID 3569359, 8 pages, 2020.

[14] R. L. Alford, K. S. Arnos, M. Fox et al., "American College of Medical Genetics and Genomics guideline for the clinical evaluation and etiologic diagnosis of hearing loss," *Genetics in Medicine*, vol. 16, no. 4, pp. 347–355, 2014.

[15] T. Yang, X. Wei, Y. Chai, L. Li, and H. Wu, "Genetic etiology study of the non-syndromic deafness in Chinese Hans by targeted next-generation sequencing," *Orphanet Journal of Rare Diseases*, vol. 8, no. 1, p. 85, 2013.

[16] B. S. Budde, M. A. Aly, M. R. Mohamed et al., "Comprehensive molecular analysis of 61 Egyptian families with hereditary nonsyndromic hearing loss," *Clinical Genetics*, vol. 98, no. 1, pp. 32–42, 2020.

[17] Y. Liu, J. Qi, X. Chen et al., "Critical role of spectrin in hearing development and deafness," *Science Advances*, vol. 5, no. 4, article eaav7803, 2019.

[18] Y. Wang, J. Li, X. Yao et al., "Loss of CIB2 causes profound hearing loss and abolishes mechanoelectrical transduction in mice," *Frontiers in Molecular Neuroscience*, vol. 10, p. 401, 2017.

[19] Y. Zhang, S. Zhang, Z. Zhang et al., "Knockdown of Foxg 1 in Sox 9+ supporting cells increases the trans-differentiation of supporting cells into hair cells in the neonatal mouse utricle," *Aging*, vol. 12, no. 20, pp. 19834–19851, 2020.

[20] X. Lu, S. Sun, J. Qi et al., "Bmi 1 regulates the proliferation of cochlear supporting cells via the canonical Wnt signaling pathway," *Molecular Neurobiology*, vol. 54, no. 2, pp. 1326–1339, 2017.

[21] S. Zhang, D. Liu, Y. Dong et al., "Frizzled-9+ supporting cells are progenitors for the generation of hair cells in the postnatal mouse cochlea," *Frontiers in Molecular Neuroscience*, vol. 12, p. 184, 2019.

[22] R. Belcher, F. Virgin, J. Duis, and C. Wootten, "Genetic and non-genetic workup for pediatric congenital hearing loss," *Frontiers in Pediatrics*, vol. 9, p. 536730, 2021.

[23] P. G. Barr-Gillespie, "Assembly of hair bundles, an amazing problem for cell biology," *Molecular Biology of the Cell*, vol. 26, no. 15, pp. 2727–2732, 2015.

[24] F. Jiang, Y. Takagi, A. Shams et al., "The ATPase mechanism of myosin 15, the molecular motor mutated in DFNB3 human deafness," *The Journal of Biological Chemistry*, vol. 296, p. 100243, 2021.

[25] F. J. Probst, R. A. Fridell, Y. Raphael et al., "Correction of deafness in shaker-2 mice by an unconventional myosin in a BAC transgene," *Science*, vol. 280, no. 5368, pp. 1444–1447, 1998.

[26] R. H. Holme, B. W. Kiernan, S. D. M. Brown, and K. P. Steel, "Elongation of hair cell stereocilia is defective in the mouse mutant whirler," *The Journal of Comparative Neurology*, vol. 450, no. 1, pp. 94–102, 2002.

[27] W. Li, L. Guo, Y. Li et al., "A novel recessive truncating mutation in MYO15A causing prelingual sensorineural hearing loss," *International Journal of Pediatric Otorhinolaryngology*, vol. 81, pp. 92–95, 2016.

[28] F. B. Cengiz, D. Duman, A. Sırmacı et al., "Recurrent and private MYO15A mutations are associated with deafness in the Turkish population," *Genetic Testing and Molecular Biomarkers*, vol. 14, no. 4, pp. 543–550, 2010.

[29] R. Bashir, A. Fatima, and S. Naz, "Prioritized sequencing of the second exon of MYO15A reveals a new mutation segregating in a Pakistani family with moderate to severe hearing loss," *European Journal of Medical Genetics*, vol. 55, no. 2, pp. 99–102, 2012.

[30] N. Nal, Z. M. Ahmed, E. Erkal et al., "Mutational spectrum of MYO15A: the large N-terminal extension of myosin XVA is required for hearing," *Human Mutation*, vol. 28, no. 10, pp. 1014–1019, 2007.

[31] J. Zhang, J. Guan, H. Wang et al., "Genotype-phenotype correlation analysis of MYO15A variants in autosomal recessive non-syndromic hearing loss," *BMC Medical Genetics*, vol. 20, no. 1, p. 60, 2019.

[32] P. Xu, J. Xu, H. Peng, and T. Yang, "Compound heterozygous mutations in TMC1 and MYO15A are associated with autosomal recessive nonsyndromic hearing loss in two Chinese Han families," *Neural Plasticity*, vol. 2020, Article ID 8872185, 7 pages, 2020.

[33] L. Wang, L. Zhao, H. Peng et al., "Targeted next-generation sequencing identified compound heterozygous mutations in MYO15A as the probable cause of nonsyndromic deafness in a Chinese Han family," *Neural Plasticity*, vol. 2020, Article ID 6350479, 6 pages, 2020.

[34] M. J. Redowicz, "Myosins and deafness," *Journal of Muscle Research and Cell Motility*, vol. 20, no. 3, pp. 241–248, 1999.

[35] K. L. Weber, A. M. Sokac, J. S. Berg, R. E. Cheney, and W. M. Bement, "A microtubule-binding myosin required for nuclear anchoring and spindle assembly," *Nature*, vol. 431, no. 7006, pp. 325–329, 2004.

[36] H. M. Woo, J. I. Baek, M. H. Park et al., "Whole-exome sequencing identifies MYO15A mutations as a cause of autosomal recessive nonsyndromic hearing loss in Korean families," *BMC Medical Genetics*, vol. 14, no. 1, p. 72, 2013.

Hindawi
Neural Plasticity
Volume 2021, Article ID 5528434, 12 pages
https://doi.org/10.1155/2021/5528434

Research Article

Next-Generation Sequencing Identifies Pathogenic Variants in *HGF*, *POU3F4*, *TECTA*, and *MYO7A* in Consanguineous Pakistani Deaf Families

Xueshuang Mei,[1] **Yaqi Zhou**,[2] **Muhammad Amjad**,[3] **Weiqiang Yang**,[1] **Rufei Zhu**,[1] **Muhammad Asif**,[3] **Hafiz Muhammad Jafar Hussain**,[4] **Tao Yang**,[5,6,7] **Furhan Iqbal**,[3] **and Hongyi Hu**[1]

[1]*Department of Otorhinolaryngology, Peking University Shenzhen Hospital, Shenzhen, China*
[2]*Department of Otorhinolaryngology, Peking University Shenzhen Hospital, Shenzhen Peking University-The Hong Kong University of Science and Technology Medical Center, Shenzhen, China*
[3]*Institute of Pure and Applied Biology, Bahauddin Zakariya University, Multan, Pakistan*
[4]*Department of Nephrology, Institute of Nephrology, Ruijin Hospital, Shanghai Jiao Tong University School of Medicine, Shanghai, China*
[5]*Department of Otorhinolaryngology-Head and Neck Surgery, Ninth People's Hospital, Shanghai Jiao Tong University School of Medicine, Shanghai, China*
[6]*Ear Institute, Shanghai Jiao Tong University School of Medicine, Shanghai, China*
[7]*Shanghai Key Laboratory of Translational Medicine on Ear and Nose Diseases, Shanghai, China*

Correspondence should be addressed to Tao Yang; yangtfxl@sina.com, Furhan Iqbal; furhan.iqbal@bzu.edu.pk, and Hongyi Hu; hyihu@pkuszh.com

Received 2 March 2021; Revised 1 April 2021; Accepted 11 April 2021; Published 22 April 2021

Academic Editor: Renjie Chai

Background. Approximately 70% of congenital deafness is attributable to genetic causes. Incidence of congenital deafness is known to be higher in families with consanguineous marriage. In this study, we investigated the genetic causes in three consanguineous Pakistani families segregating with prelingual, severe-to-profound deafness. *Results*. Through targeted next-generation sequencing of 414 genes known to be associated with deafness, homozygous variants c.536del (p. Leu180Serfs∗20) in *TECTA*, c.3719 G>A (p. Arg1240Gln) in *MYO7A*, and c.482+1986_1988del in *HGF* were identified as the pathogenic causes of enrolled families. Interestingly, in one large consanguineous family, an additional c.706G>A (p. Glu236Lys) variant in the X-linked *POU3F4* gene was also identified in multiple affected family members causing deafness. Genotype-phenotype cosegregation was confirmed in all participating family members by Sanger sequencing. *Conclusions*. Our results showed that the genetic causes of deafness are highly heterogeneous. Even within a single family, the affected members with apparently indistinguishable clinical phenotypes may have different pathogenic variants.

1. Background

Congenital hearing loss affects 1‰-2‰ of newborns worldwide. Among them, approximately 70% of deafness is attributable to genetic causes [1]. The genetics of hearing loss is extremely heterogeneous as, to date, more than 120 genes are reported to cause nonsyndromic hearing loss (Hereditary Hearing Loss Homepage; https://hereditaryhearingloss.org). Similarly, numerous genes are known to cause syndromic hearing loss [2–10]. In recent years, next-generation sequencing (NGS) has been increasingly implemented in the genetic diagnosis of heterogeneous diseases including hearing loss, providing a high-throughput, efficient approach to target hundreds of causative genes or even the whole exome for the identification of pathogenic variants [11, 12]. Due to the extremely high heterogeneity of genetic hearing

loss, however, determining the pathogenicity of the candidate variants can be challenging in many cases. For example, rare, benign variants are not always distinguishable from the true pathogenic variants following general guidelines for sequencing data interpretation [13, 14]. Reporting of rare variants with phenotypic cosegregation in large families, therefore, will provide valuable references for genetic diagnosis of deafness in isolated cases [14].

The deafness-associated genes play diverse roles in the development, function, and maintenance of the inner ear. Variants in these genes correspondently lead to variable auditory phenotypes in regard to onset, severity, progression, audiogram profile, and accompanying syndromic features [1]. In some cases, different variants in the same gene, such as *MYO7A*, may result in distinct phenotypes in nonsyndromic deafness *DFNA11* and *DFNB2* [15, 16] or syndromic deafness *USH1B* [17]. Documentation and analysis of the genotype-phenotype correlation covering a broad range of novel or previously less characterized variants are therefore necessary to facilitate genetic diagnosis of hearing loss.

Approximately 80% of genetic deafness are inherited in an autosomal recessive manner [18]. In many cases, they are closely related to consanguineous marriage, which is common in regions of the Middle East, South Asia, South America, and Africa [19, 20]. Studies in Iranian and Palestinian populations, for example, showed that, respectively, 65% and 58% of deaf children were born to parents having consanguineous marriage [21, 22]. A number of deafness-associated genes are discovered by linkage analyses based on homozygosity mapping of large consanguineous deaf families [23, 24].

In this study, we performed targeted NGS in three Pakistani consanguineous families and identified novel variants in *TECTA* and *POU3F4* and previously reported variants in *MYO7A* and *HGF* as the pathogenic causes for prelingual, severe-to-profound deafness. Interestingly, in a large, multigenerational consanguineous family, we identified two separated variants in *HGF* and *POU3F4*, illustrating the complex genetic heterogeneity of deafness.

2. Materials and Methods

2.1. Subjects and Clinical Evaluations. Three consanguineously married families (PK-DD-KA-01 (Figure 1), PK-DD-RP-01 (Figure 2), and PK-DB-OKA-01 (Figure 3)) were enrolled from three districts (Muzafargarh, Rajanpur, and Okara, respectively) in Punjab (Pakistan) with multiple individuals suffering from deafness. Written informed consents were obtained from all participants and/or their parents before their enrollment in this study. Family members affected with deafness were examined in the ear, nose, and throat (ENT) wards of their respective District Head Quarter Hospital by medical specialists. Clinical evaluations included complete medical history interview, comprehensive physical examination, and pure tone audiometry (PTA). Otoscopic examination was performed to exclude hearing loss due to infections, trauma, or other environmental factors. The vestibular function was evaluated by medical history inquiry and behavioral testing. This study was approved by the Research Ethics Committee of the Peking University Shenzhen Hospital.

2.2. Genetic Analysis. Genomic DNA was extracted from peripheral blood samples of the enrolled subjects by using the QIAamp DNA Blood Mini Kit (QIAGEN, Shanghai). Targeted NGS was performed in the proband from each family (arrows in Figures 1(a), 2(a), and 3(a)) plus individual IV-5 from Family PK-DB-OKA-01. The customized capture panel (MyGenostics, Beijing) targeted the exonic region of 414 known deafness-associated genes; in addition to the exonic region, the panel also included all intronic, intergenic, and noncoding regions containing variants that reported in HGMD (147 genes, 751 variants) (Supplementary Table S1). Candidate pathogenic variants were defined as nonsynonymous (including nonsense, missense, splice-site, and indels) variants with minor allele frequencies (MAFs) less than 0.005 in public databases including 1000 Genomes, dbSNP, and GnomAD. Potential pathogenic effect of the candidate variants was evaluated by *in silico* tools MutationTaster, PROVEAN, SIFT, and PolyPhen-2. Cosegregation of the deafness phenotype and the pathogenic variants was confirmed in participating family members by PCR amplification and Sanger sequencing; the results were shown in each pedigree map. Pathogenicity of the variants was classified following the guidelines of ACMG 2015 [13].

3. Results

3.1. Clinical Characterization. There are at least seven subjects in family PK-DD-KA-01 (Figure 1(a)), 2 in PK-DD-RP-01 (Figure 2(a)), and 22 in PK-DB-OKA-01 (Figure 3(a)) that were suffering from bilateral, prelingual, severe-to-profound sensorineural hearing loss (Figures 1(c), 2(c), and 3(c)). All affected subjects in Families PK-DD-KA-01 and PK-DD-RP-01 and half (11/22) of the affected subjects in Family PK-DB-OKA-01 were born to parents with consanguineous marriage. No ear malformation, vestibular dysfunction, developmental abnormality, or syndromic symptom were identified in enrolled subjects.

3.2. Identification of the Pathogenic Variants in Probands. Targeted NGS of 414 known deafness genes was performed on probands of the three families. Homozygous variants c.536del (p. Leu180Serfs∗20) in *TECTA* (NM_005422.4), c.3719 G>A (p. Arg1240Gln) in *MYO7A* (NM_001127180.2), and c.482+1986_1988del in *HGF* (NM_000601.6) were identified as the candidate pathogenic variants in probands IV-4 of Family PK-DD-KA-01 (Figure 1(a)), IV-4 of Family PK-DD-RP-01 (Figure 2(a)), and IV-24 of Family PK-DB-OKA-01 (Figure 3(a)), respectively. All candidate variants have minor allele frequencies lower than 0.0001 in the public database gnomAD and are categorized as likely pathogenic based on ACMG guidelines (Table 1).

3.3. Identification of a Second Pathogenic Variant in Family PK-DB-OKA-01. Sanger sequencing confirmed that homozygous variants c.536del (p. Leu180Serfs∗20) in *TECTA* and c.3719 G>A (p. Arg1240Gln) in *MYO7A* segregated with the deafness in all participating members in Families PK-

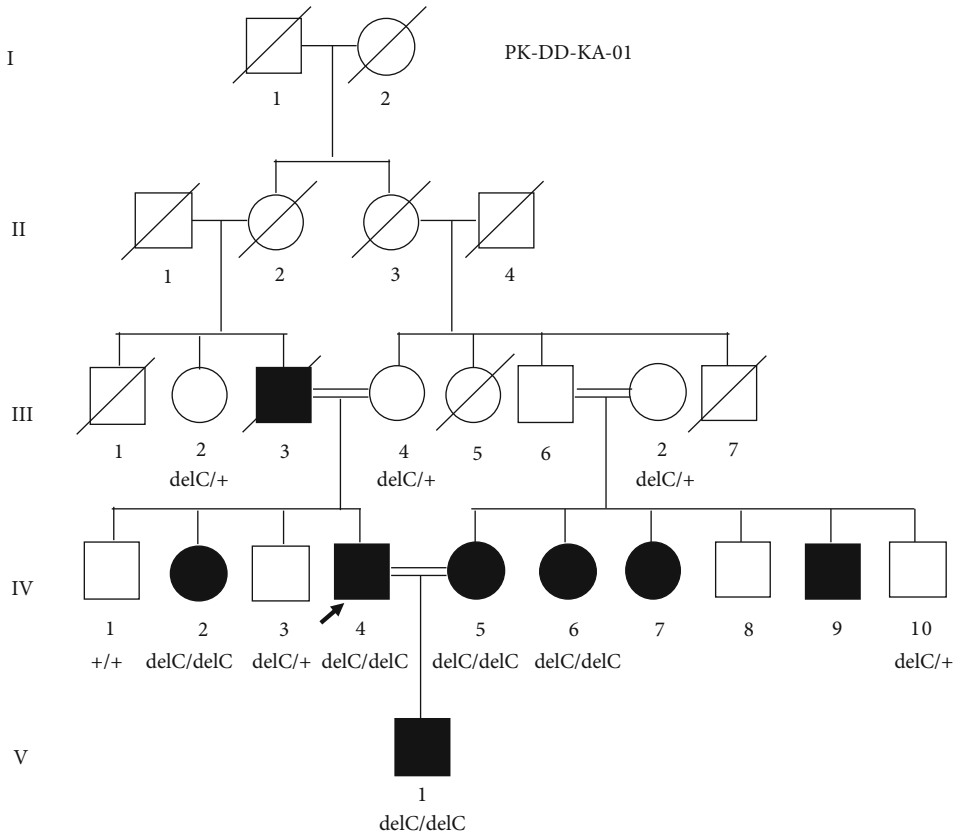

(a)

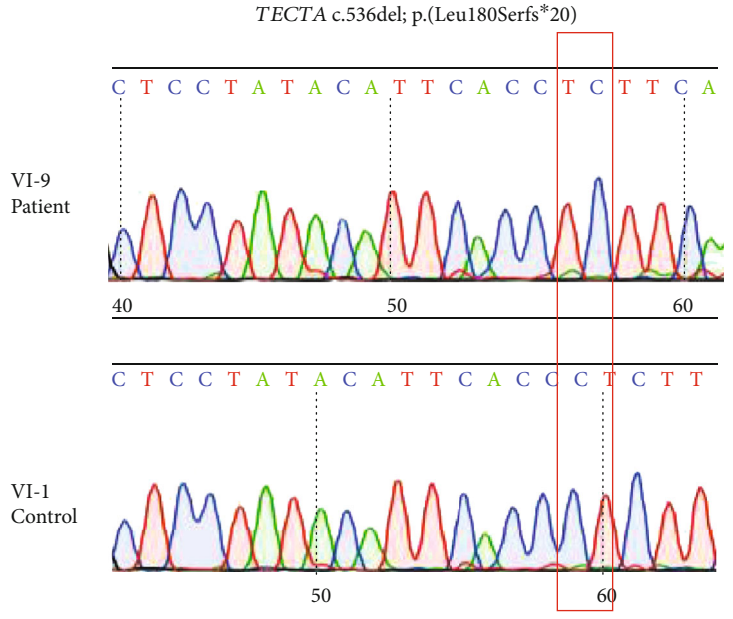

(b)

Figure 1: Continued.

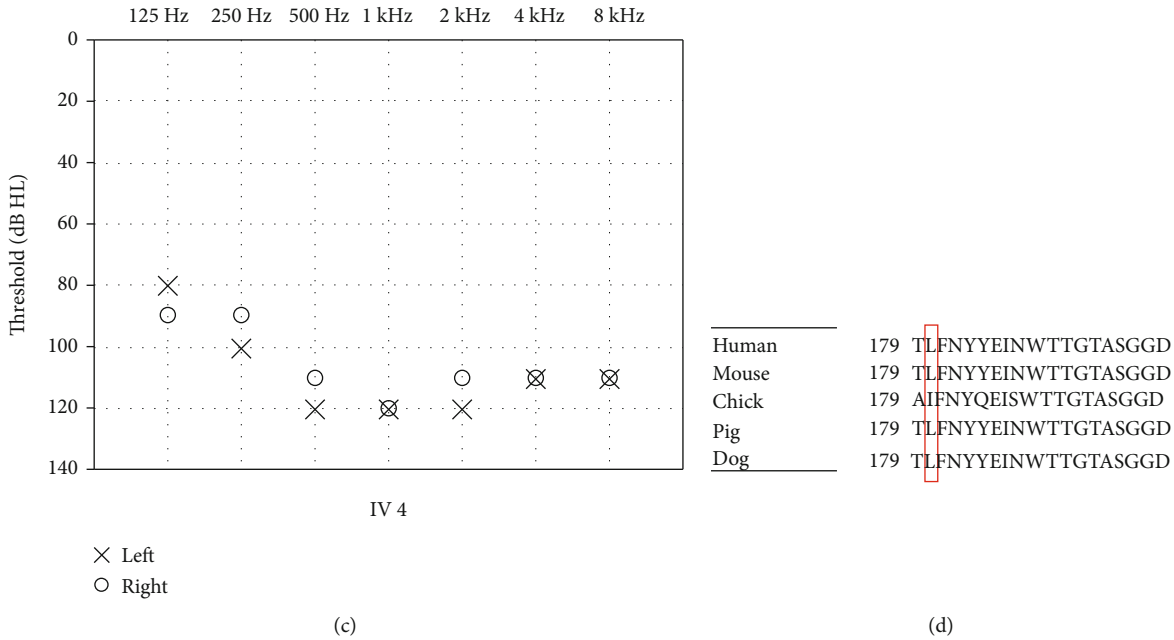

Figure 1: Genetic and phenotypic characterization of Family PK-DD-KA-01. (a) Pedigree and genotype showing the c.536del (p. Leu180Serfs∗20) variant in *TECTA*. (b) Sanger sequencing of the c.536del (p. Leu180Serfs∗20) variant in affected and unaffected family members. (c) Pure tone audiometry showing the bilateral profound hearing loss in affected family member IV-4. (d) Multiple sequence alignment showing the conservation of the L180 residue in different species.

DD-KA-01 (Figure 1(b)) and PK-DD-RP-01 (Figure 2(b)), respectively. In Family PK-DB-OKA-01, however, five deaf members (IV-4, IV-5, IV-6, III-10, and III-17, marked blue in (Figure 3(a))) were either heterozygous or wild type for variant c.482+1986_1988del in *HGF* (Figure 3(b)). A second round of targeted NGS on subject IV-5 in this family identified a hemizygous c.706G>A (p. Glu236Lys) variant in the X-chromosome gene *POU3F4* (NM_000307.5), a causative gene for X-linked nonsyndromic deafness *DFNX2*. The c.706G>A (p. Glu236Lys) variant segregated with the deafness in the five aforementioned male family members, but it was not detected in any other family members (Figures 3(a) and 3(b)). This novel variant is not seen in the gnomAD databases and has not been previously reported in association with hearing loss. It substitutes an evolutionarily conserved, acidic residue glutamic acid to an alkaline residue lysine at position 236 (Figure 3(e)) and is predicted to be deleterious or probably damaging by *in silico* tools MutationTaster, PROVEAN, SIFT, and PolyPhen-2 (Table 1).

4. Discussion

Hearing loss is one of the major disabilities worldwide, which is often induced by loss of sensory hair cells [25–29] and spiral ganglion neurons [30–34] in the inner ear cochlea. Hearing loss could be caused by genetic factors, aging, chronic cochlear infections, infectious diseases, ototoxic drugs, and noise exposure [35–42], and genetic factors account for around 70% of the hearing loss. In the present study, we are reporting the genetic causes of the prelingual, severe-to-profound deafness in three consanguineous Pakistani families through targeted NGS approach. Variants c.536del (p. Leu180Serfs∗20) in *TECTA* and c.706G>A (p. Glu236Lys) in *POU3F4* are novel, while c.3719 G>A (p. Arg1240Gln) in *MYO7A* and c.482 +1986_1988del in *HGF* were previously reported in only very limited cases associated with deafness [43, 44]. In support of their pathogenicity, all four variants segregated with multiple affected and unaffected family members consistent with the autosomal recessive or X-linked inheritance modes. Considering that homozygosity of rare variants is quite rare in the general population, the data generated during the present study will provide valuable genetic evidence regarding the genetic basis of deafness.

The phenotypes of the three families in this study are all characterized as prelingual, severe-to-profound sensorineural hearing loss. Consistently, a similar type of hearing loss has also been associated with many variants in *TECTA*, *MYO7A*, *HGF*, and *POU3F4* in previous reports. *TECTA* encodes *α*-tectorin, which is one of the main components to comprise the tectorial membrane in the cochlea [45]. Unlike dominant *TECTA* variants, which are associated with milder hearing loss DFNA8/12 (MIM 601543), the recessive *TECTA* variants often result in prelingual, severe-to-profound hearing loss (DFNB21, MIM 603629) [46–50]. Like several other recessive, truncating variants in *TECTA*, the c.536del (p. Leu180Serfs∗20) variant identified in this study causes a frameshift; this will result either in an abortive protein truncated in exon 4 or in no protein at all due to nonsense-mediated mRNA decay [51] and likely results in loss of function (Figure 4(a)). *MYO7A* is extensively expressed in the hair cells and plays an important role in maintaining stereocilia differentiation and morphology [52, 53]. The c.3719 G>A (p. Arg1240Gln) variant in *MYO7A* locates in the highly conserved first MyTH4 domain

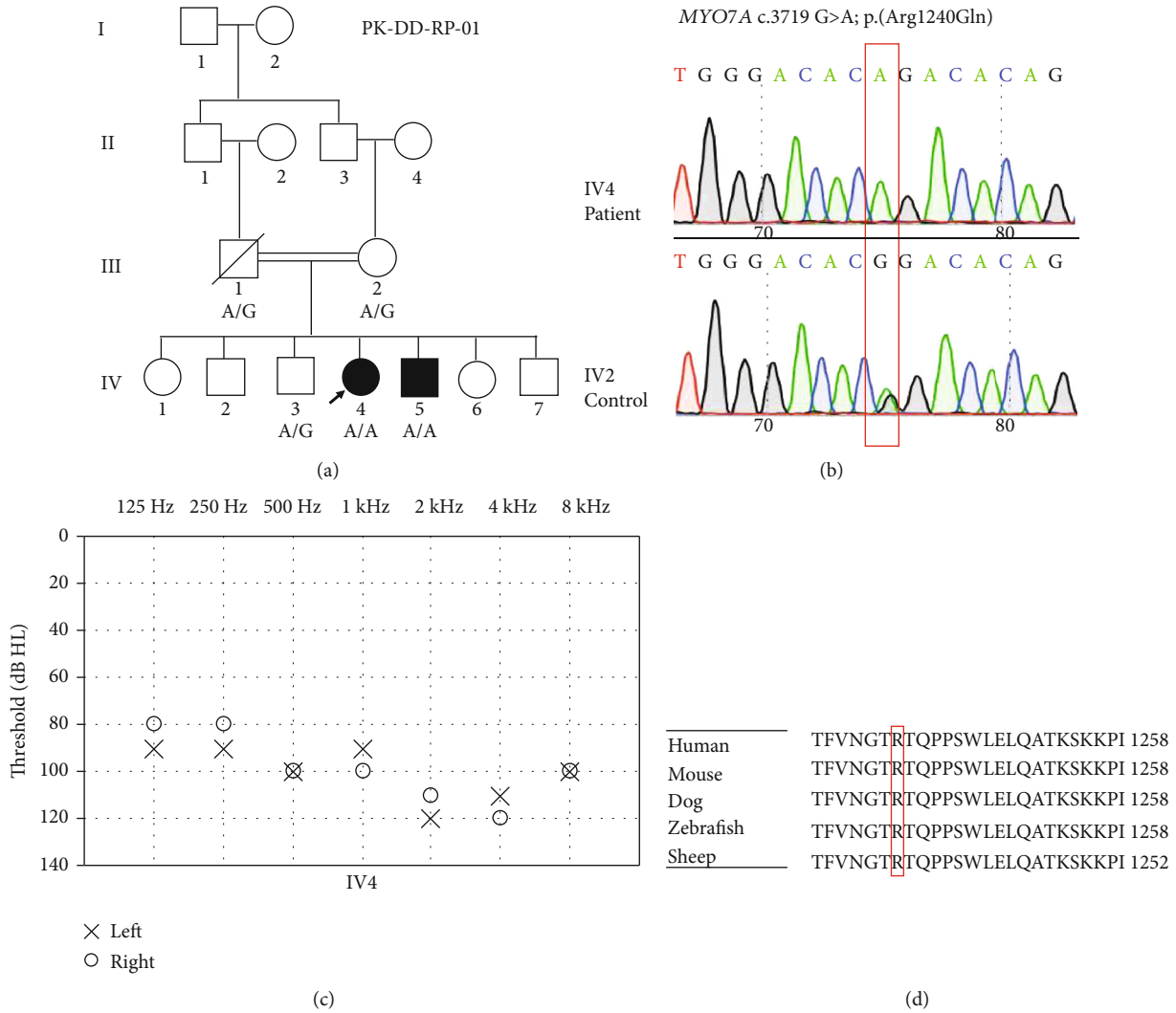

Figure 2: Genetic and phenotypic characterization of Family PK-DD-RP-01. (a) Pedigree and genotype showing the c.3719 G>A (p. Arg1240Gln) variant in *MYO7A*. (b) Sanger sequencing of the c.3719 G>A (p. Arg1240Gln) variant in affected and unaffected family members. (c) Pure tone audiometry showing the bilateral profound hearing loss in affected family member IV-4. (d) Multiple sequence alignment showing the conservation of the R1240 residue in different species.

(Figure 4(b)). It has been previously reported to be associated with Usher syndrome 1B (MIM 276900), characterized by congenital, severe-to-profound hearing loss, and late-onset retinitis pigmentosa before or after puberty [44, 54]. Since the two affected children with the c.3719 G>A (p. Arg1240Gln) homozygous variant in our study were 7 and 9 years old without apparent visual abnormality, the potential visual dysfunction remains to be determined at older age. *HGF* encodes a hepatocyte growth factor and is expressed in the stria vascularis of the mouse inner ear. The c.482+1986_1988del variant identified in this study has been previously reported to cause prelingual, profound deafness (DFNB39, MIM 608265) [43]. A *Hgf* 10 bp deletion in homozygous mutant mice, which fully encompasses the 3 bp deletion in humans, also displayed profound hearing loss at 4 weeks age (Figure 3(d)) [55]; *Hgf* 10 bp deletion in homozygous mice causes low expression of *Hgf* in the cochlea, which leads to developmental defect of the stria vascularis and reduced endocochlear potential in the cochlea [55]. The 3 bp deletion in the intronic region possibly has a similar mechanism to cause hearing loss. *POU3F4* encodes a POU domain transcription factor expressed in a spiral ligament and spiral limbus [56]. Most DFNX2 (MIM 304400) patients with *POU3F4* variants have profound hearing loss with or without developmental abnormality of the conductive components [57, 58]. Although the temporal bone abnormities could not be confirmed in this family, the PTA results of affected males in the family only presented sensorineural hearing loss, which is less common than mixed hearing loss in patients with POU3F4 variants. The novel c.706G>A (p. Glu236Lys) variant identified in this study is located in the highly conserved POU-specific domain (Figure 4(c)), which is similar to a previously reported c.707A>C; p. (Glu236Ala) variant in a Turkey family [59]. Overall, our results are consistent with known genotype-phenotype correlation of the corresponding genes.

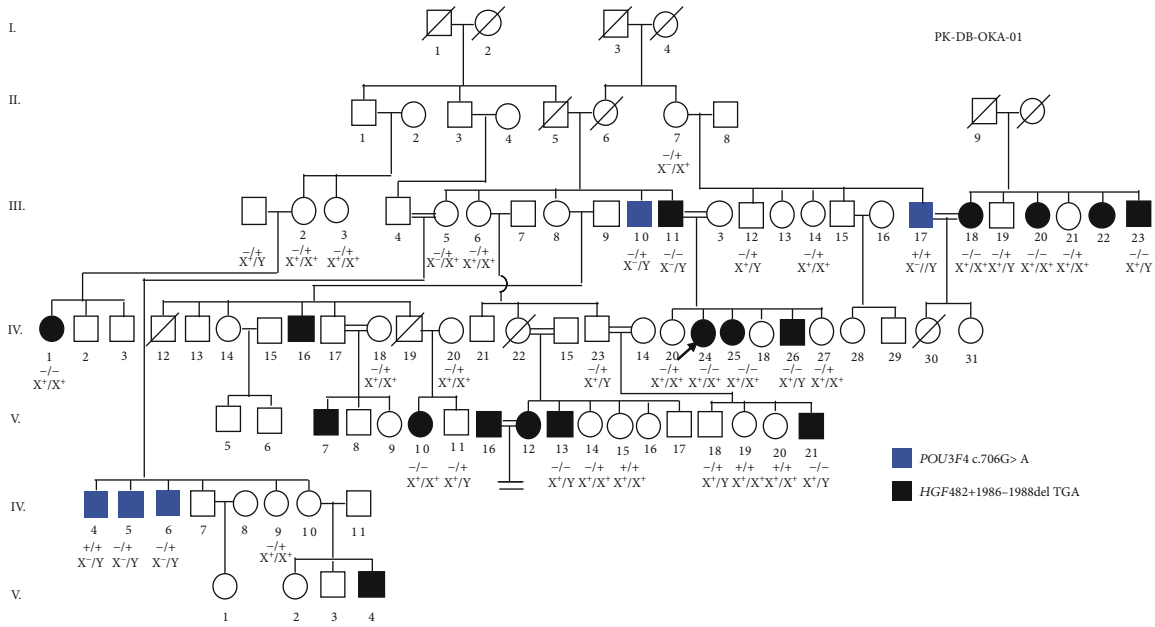

(a)

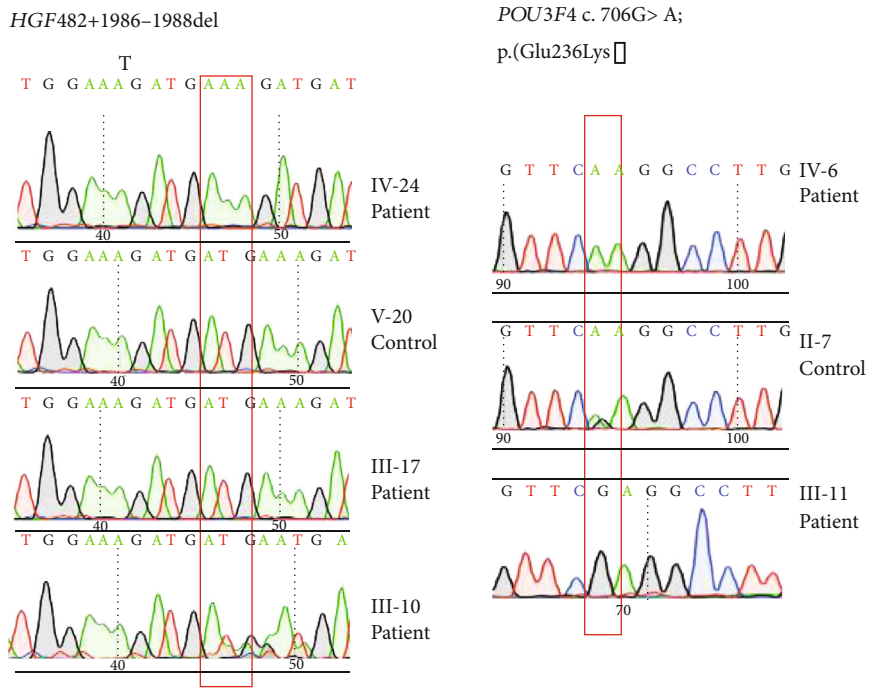

(b)

Figure 3: Continued.

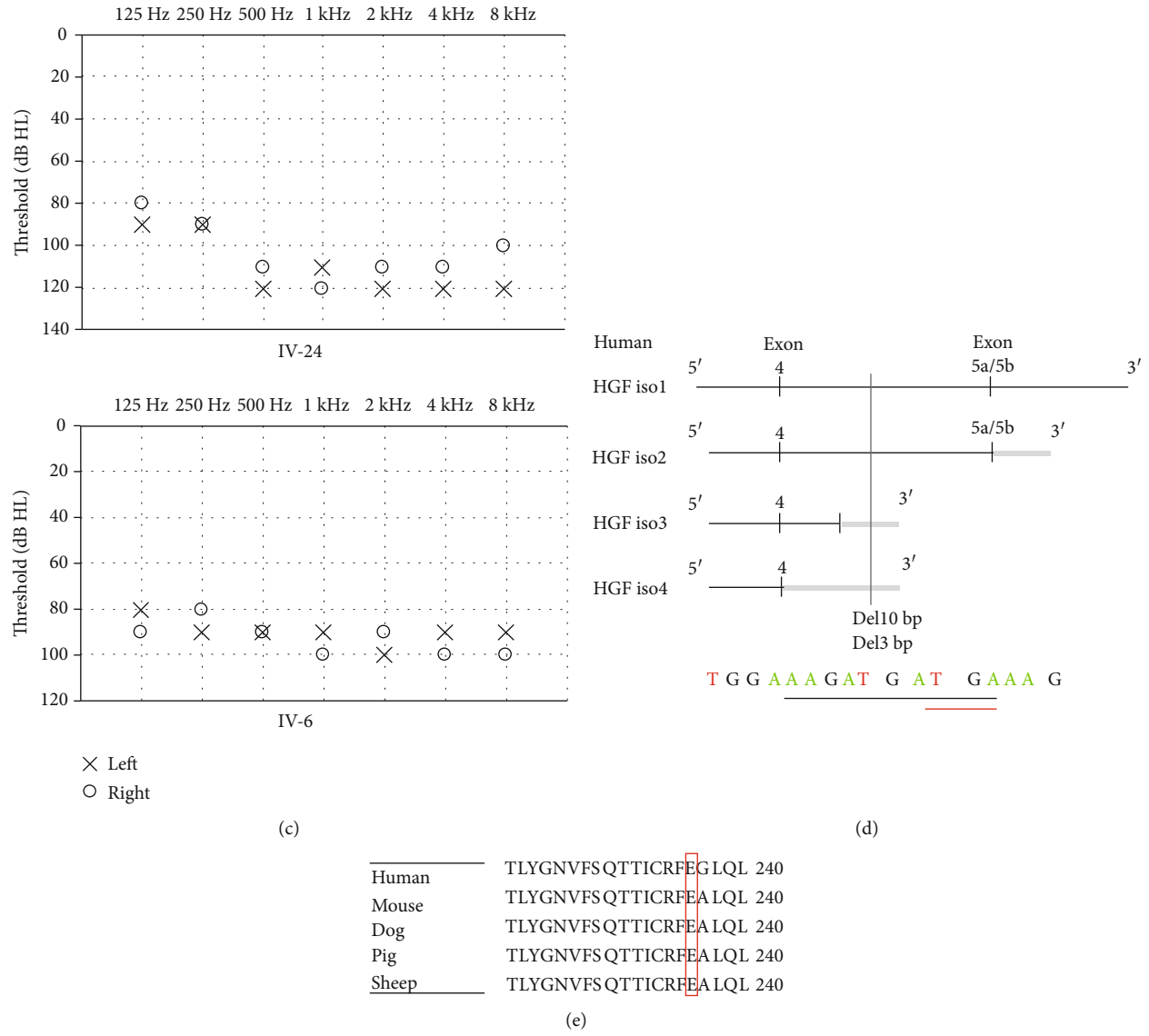

Figure 3: Genetic and phenotypic characterization of Family PK-DB-OKA-01. (a) Pedigree and genotypes showing the 482+1986-1988del variant in *HGF* (marked as -) and the c.706G>A (p. Glu236Lys) variant in *POU3F4* (marked as X¯). (b) Sanger sequencing of the 482 +1986-1988del and c.706G>A (p. Glu236Lys) variants. (c). Pure tone audiometry showing the bilateral profound hearing loss in affected family members IV-24 and IV-6. (d) Position of the 3 bp deletion in human *HGF* and the 10 bp deletion in mouse *Hgf* that both lead to profound hearing loss. (e) Multiple sequence alignment showing the conservation of the E236 residue in different species.

As summarized above, in this study, rare pathogenic variants were identified in four separate deafness-associated genes, *TECTA*, *MYO7A*, *HGF*, and *POU3F4*, which have distinct expression profiles and functions in the inner ear. Nevertheless, all four variants resulted in an almost uniformed type of prelingual, severe-to-profound deafness, representing yet another example of extremely high genetic heterozygosity for hearing loss. Interestingly, within the large pedigree of Family PK-DB-OKA-01 with multiple consanguineous marriages, five of the fifteen affected individuals actually have a hemizygous, X-linked variant as a separate cause of hearing loss irrelevant to the consanguineous marriage pattern (Figure 3(a)). Since most novel deafness-causative genes were originally identified through genetic analysis of such large pedigrees based on assumptions that all affected family members share a single pathogenic variant, our results suggested that caution should remain against such complexed inheritance patterns involving two or multiple genetic causes.

5. Conclusions

In summary, our study of three consanguineous families with prelingual, severe-to-profound deafness revealed a rather heterogeneous variant spectrum in the corresponding Pakistani deaf communities. Next-generation sequencing illustrates its advantages in resolving such complexed cases.

Table 1: Characterization and classification of the pathogenic variants.

Gene	Variants	MutationTaster	PROVEAN[a]	SIFT[b]	PolyPhen-2	ClinVar	MAF[c]	ACMG classification[d]
TECTA (NM_005422.4)	c.536del (p. Leu180Serfs∗20)[e]	Disease causing	—	—	—	—	0	Likely pathogenic
MYO7A (NM_001127180.2)	c.3719 G>A (p. Arg1240Gln)	Disease causing	Deleterious (-3.72)	Damaging (0.000)	Probably damaging	Pathogenic	0.0000745	Likely pathogenic
HGF (NM_000601.6)	482+1986-1988del	—	—	—	—	Pathogenic	0	Likely pathogenic
POU3F4 (NM_000307.5)	c.706G>A (p. Glu236Lys)[e]	Disease causing	Deleterious (-4.0)	Damaging (0.000)	Probably damaging	—	0	Likely pathogenic

[a]PROVEAN: negative score indicates deleterious, with the cut-off score set as −2.5. [b]SIFT: deleterious to neutral from scores 0 to 1, with the cut-off score set as 0.05. [c]The MAF was shown from gnomAD database. [d]The classification followed the ACMG guidelines for interpretation of sequence variants. [e]Novel variants identified in this study.

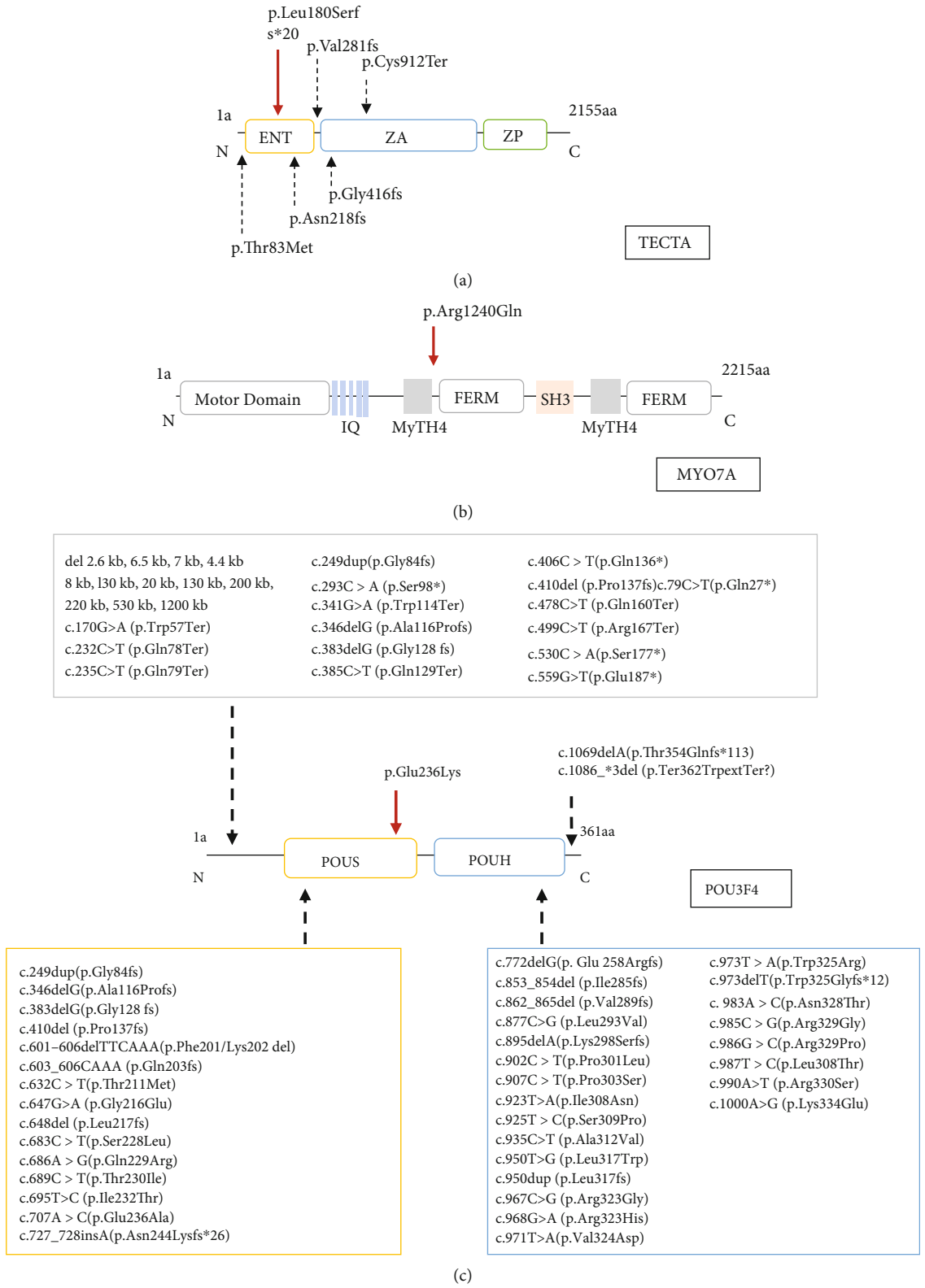

Figure 4: Domain structure and variant position of TECTA, MYO7A, and POU3F4 proteins. (a) α-Tectorin consists of entactin domain (ENT), zonadhesin (ZA) domain, and C-terminal zona pellucida (ZP) domain. Previously reported autosomal recessive variants in *TECTA* are presented, with the c.536del (p. Leu180Serfs∗20) variant highlighted by the red arrow. (b) Myosin VIIA consists of a motor domain, five IQ motif repeats, two large repeats of MyTH4 and FERM domains, and an SH3 domain. The c.3719 G>A (p. Arg1240Gln) variant is highlighted by the red arrow. (c) POU3F4 consists of a POU-specific domain (POUS) and a POU homeodomain (POUH). Previously reported *POU3F4* variants are presented, with the c.706G>A (p. Glu236Lys) variant highlighted by the red arrow.

Data Availability

The original data is available upon request by contacting the corresponding author.

Conflicts of Interest

The authors declare no conflict of interest.

Authors' Contributions

XM, YZ, Muhammad Amjad, TY, FI, and HH contributed to the conceptualization. XM, YZ, WY, RZ, Muhammad Asif, and HMJH contributed to the methodology. HH, YZ, and TY contributed to the funding acquisition. XM and YZ wrote the original draft. HH, TY, and FI contributed to the review and editing. All authors read and approved the final manuscript. Xueshuang Mei, Yaqi Zhou, and Muhammad Amjad contributed equally to this work.

Acknowledgments

This research was supported by the Shenzhen Sanming Project (SZSM201612076 to HH), the China Postdoctoral Science Foundation (2020M672757 to YZ), and the Shanghai Municipal Education Commission—Gaofeng Clinical Medicine Grant (20152519 to TY).

Supplementary Materials

Table S1: 414 genes associated with deafness that were sequenced by targeted NGS. *(Supplementary Materials)*

References

[1] C. C. Morton and W. E. Nance, "Newborn hearing screening–a silent revolution," *The New England Journal of Medicine*, vol. 354, no. 20, pp. 2151–2164, 2006.

[2] A. A. Dror and K. B. Avraham, "Hearing impairment: a panoply of genes and functions," *Neuron*, vol. 68, no. 2, pp. 293–308, 2010.

[3] I. Schrijver, "Hereditary non-syndromic sensorineural hearing loss: transforming silence to sound," *The Journal of Molecular Diagnostics: JMD*, vol. 6, no. 4, pp. 275–284, 2004.

[4] Y. He, X. Lu, F. Qian, D. Liu, R. Chai, and H. Li, "Insm1a is required for zebrafish posterior lateral line development," *Frontiers in Molecular Neuroscience*, vol. 10, no. 241, 2017.

[5] Y. Wang, J. Li, X. Yao et al., "Loss of CIB2 causes profound hearing loss and abolishes mechanoelectrical transduction in mice," *Frontiers in Molecular Neuroscience*, vol. 10, no. 401, 2017.

[6] C. Zhu, C. Cheng, Y. Wang et al., "Loss of ARHGEF6 causes hair cell stereocilia deficits and hearing loss in mice," *Frontiers in Molecular Neuroscience*, vol. 11, p. 362, 2018.

[7] Q. Fang, Y. Zhang, P. da et al., "Deletion of *Limk1* and *Limk2* in mice does not alter cochlear development or auditory function," *Scientific Reports*, vol. 9, no. 1, p. 3357, 2019.

[8] Z. He, Q. Fang, H. Li et al., "The role of FOXG1 in the postnatal development and survival of mouse cochlear hair cells," *Neuropharmacology*, vol. 144, pp. 43–57, 2019.

[9] F. Qian, X. Wang, Z. Yin et al., "The slc4a2b gene is required for hair cell development in zebrafish," *Aging*, vol. 12, no. 19, pp. 18804–18821, 2020.

[10] J. Lv, X. Fu, Y. Li et al., "Deletion of Kcnj16 in mice does not alter auditory function," *Frontiers in Cell and Developmental Biology*, vol. 9, no. 250, 2021.

[11] T. Yang, X. Wei, Y. Chai, L. Li, and H. Wu, "Genetic etiology study of the non-syndromic deafness in Chinese Hans by targeted next-generation sequencing," *Orphanet Journal of Rare Diseases*, vol. 8, no. 1, p. 85, 2013.

[12] S. Zou, X. Mei, W. Yang, R. Zhu, T. Yang, and H. Hu, "Whole-exome sequencing identifies rare pathogenic and candidate variants in sporadic Chinese Han deaf patients," *Clinical Genetics*, vol. 97, no. 2, pp. 352–356, 2020.

[13] on behalf of the ACMG Laboratory Quality Assurance Committee, S. Richards, N. Aziz et al., "Standards and guidelines for the interpretation of sequence variants: a joint consensus recommendation of the American College of Medical Genetics and Genomics and the Association for Molecular Pathology," *Genetics in Medicine: official journal of the American College of Medical Genetics.*, vol. 17, no. 5, pp. 405–423, 2015.

[14] L. He, X. Pang, H. Liu, Y. Chai, H. Wu, and T. Yang, "Targeted next-generation sequencing and parental genotyping in sporadic Chinese Han deaf patients," *Clinical Genetics*, vol. 93, no. 4, pp. 899–904, 2018.

[15] S. Riazuddin, S. Nazli, Z. M. Ahmed et al., "Mutation spectrum of MYO7A and evaluation of a novel nonsyndromic deafness DFNB2 allele with residual function," *Human Mutation*, vol. 29, no. 4, pp. 502–511, 2008.

[16] Y. Kaneko, A. Nakano, Y. Arimoto, K. Nara, H. Mutai, and T. Matsunaga, "The first sporadic case of DFNA11 identified by next-generation sequencing," *International Journal of Pediatric Otorhinolaryngology*, vol. 100, pp. 183–186, 2017.

[17] G. Lévy, F. Levi-Acobas, S. Blanchard et al., "Myosin VIIA gene: heterogeneity of the mutations responsible for Usher syndrome type IB," *Human Molecular Genetics*, vol. 6, no. 1, pp. 111–116, 1997.

[18] N. E. Morton, "Genetic epidemiology of hearing impairment," *Annals of the New York Academy of Sciences*, vol. 630, no. 1 Genetics of H, pp. 16–31, 1991.

[19] M. Fathzadeh, M. A. Babaie Bigi, M. Bazrgar, M. Yavarian, H. R. Tabatabaee, and S. M. Akrami, "Genetic counseling in southern Iran: consanguinity and reason for referral," *Journal of Genetic Counseling*, vol. 17, no. 5, pp. 472–479, 2008.

[20] D. Alnaqeb, H. Hamamy, A. M. Youssef, and K. Al-Rubeaan, "Assessment of knowledge, attitude and practice towards consanguineous marriages among a cohort of multiethnic health care providers in Saudi Arabia," *Journal of Biosocial Science*, vol. 50, no. 1, pp. 1–18, 2018.

[21] M. Ajallouyan, S. Radfar, S. Nouhi et al., "Consanguinity among parents of Iranian deaf children," *Iranian Red Crescent Medical Journal*, vol. 18, no. 11, p. e22038, 2016.

[22] A. Abu Rayyan, L. Kamal, S. Casadei et al., "Genomic analysis of inherited hearing loss in the Palestinian population," *Proceedings of the National Academy of Sciences of the United States of America*, vol. 117, no. 33, pp. 20070–20076, 2020.

[23] R. W. Collin, E. Kalay, J. Oostrik et al., "Involvement of DFNB59 mutations in autosomal recessive nonsyndromic hearing impairment," *Human Mutation*, vol. 28, no. 7, pp. 718–723, 2007.

[24] S. Y. Khan, S. Riazuddin, M. Tariq et al., "Autosomal recessive nonsyndromic deafness locus DFNB63 at chromosome 11q13.2-q13.3," *Human Genetics*, vol. 120, no. 6, pp. 789–793, 2007.

[25] J. Qi, L. Zhang, F. Tan et al., "Espin distribution as revealed by super-resolution microscopy of stereocilia," *American Journal of Translational Research*, vol. 12, no. 1, pp. 130–141, 2020.

[26] H. Zhou, X. Qian, N. Xu et al., "Disruption of Atg7-dependent autophagy causes electromotility disturbances, outer hair cell loss, and deafness in mice," *Cell Death & Disease*, vol. 11, no. 10, p. 913, 2020.

[27] Y. Liu, J. Qi, X. Chen et al., "Critical role of spectrin in hearing development and deafness," *Science Advances*, vol. 5, no. 4, article eaav7803, 2019.

[28] J. Qi, Y. Liu, C. Chu et al., "A cytoskeleton structure revealed by super-resolution fluorescence imaging in inner ear hair cells," *Cell Discovery*, vol. 5, no. 1, p. 12, 2019.

[29] Z. H. He, S. Y. Zou, M. Li et al., "The nuclear transcription factor FoxG1 affects the sensitivity of mimetic aging hair cells to inflammation by regulating autophagy pathways," *Redox Biology*, vol. 28, p. 101364, 2020.

[30] R. Guo, M. Xiao, W. Zhao et al., "2D Ti3C2TxMXene couples electrical stimulation to promote proliferation and neural differentiation of neural stem cells," *Acta Biomaterialia*, 2020.

[31] R. Guo, S. Zhang, M. Xiao et al., "Accelerating bioelectric functional development of neural stem cells by graphene coupling: implications for neural interfacing with conductive materials," *Biomaterials*, vol. 106, pp. 193–204, 2016.

[32] R. Guo, J. Li, C. Chen et al., "Biomimetic 3D bacterial cellulose-graphene foam hybrid scaffold regulates neural stem cell proliferation and differentiation," *Colloids and surfaces B, Biointerfaces*, vol. 200, article 111590, 2021.

[33] R. Guo, X. Ma, M. Liao et al., "Development and application of cochlear implant-based electric-acoustic stimulation of spiral ganglion neurons," *ACS Biomaterials Science & Engineering*, vol. 5, no. 12, pp. 6735–6741, 2019.

[34] W. Liu, X. Xu, Z. Fan et al., "Wnt signaling activates TP53-induced glycolysis and apoptosis regulator and protects against cisplatin-induced spiral ganglion neuron damage in the mouse cochlea," *Antioxidants & Redox Signaling*, vol. 30, no. 11, pp. 1389–1410, 2019.

[35] Z. He, L. Guo, Y. Shu et al., "Autophagy protects auditory hair cells against neomycin-induced damage," *Autophagy*, vol. 13, no. 11, pp. 1884–1904, 2017.

[36] C. Cheng, Y. Wang, L. Guo et al., "Age-related transcriptome changes in Sox2+ supporting cells in the mouse cochlea," *Stem Cell Research & Therapy*, vol. 10, no. 1, p. 365, 2019.

[37] F. Tan, C. Chu, J. Qi et al., "AAV-ie enables safe and efficient gene transfer to inner ear cells," *Nature Communications*, vol. 10, no. 1, p. 3733, 2019.

[38] Y. Zhang, W. Li, Z. He et al., "Pre-treatment with fasudil prevents neomycin-induced hair cell damage by reducing the accumulation of reactive oxygen species," *Frontiers in Molecular Neuroscience*, vol. 12, p. 264, 2019.

[39] S. Gao, C. Cheng, M. Wang et al., "Blebbistatin inhibits neomycin-induced apoptosis in hair cell-like HEI-OC-1 cells and in cochlear hair cells," *Frontiers in Cellular Neuroscience*, vol. 13, no. 590, 2020.

[40] S. Han, Y. Xu, J. Sun et al., "Isolation and analysis of extracellular vesicles in a Morpho butterfly wing- integrated microvortex biochip," *Biosensors & Bioelectronics*, vol. 154, p. 112073, 2020.

[41] S. Zhang, Y. Zhang, Y. Dong et al., "Knockdown of Foxg1 in supporting cells increases the trans-differentiation of supporting cells into hair cells in the neonatal mouse cochlea," *Cellular and Molecular Life Sciences: CMLS*, vol. 77, no. 7, pp. 1401–1419, 2020.

[42] Z. Zhong, X. Fu, H. Li et al., "Citicoline protects auditory hair cells against neomycin-induced damage," *Frontiers in Cell and Developmental Biology*, vol. 8, p. 712, 2020.

[43] J. M. Schultz, S. N. Khan, Z. M. Ahmed et al., "Noncoding mutations of HGF are associated with nonsyndromic hearing loss, DFNB39," *American Journal of Human Genetics*, vol. 85, no. 1, pp. 25–39, 2009.

[44] T. Jaijo, E. Aller, M. Beneyto et al., "MYO7A mutation screening in Usher syndrome type I patients from diverse origins," *Journal of Medical Genetics*, vol. 44, no. 3, article e71, 2007.

[45] D. K. Kim, J. A. Kim, J. Park, A. Niazi, A. Almishaal, and S. Park, "The release of surface-anchored α-tectorin, an apical extracellular matrix protein, mediates tectorial membrane organization," *Science Advances*, vol. 5, no. 11, article eaay6300, 2019.

[46] S. Asgharzade, M. A. Tabatabaiefar, M. H. Modarressi et al., "A novel TECTA mutation causes ARNSHL," *International Journal of Pediatric Otorhinolaryngology*, vol. 92, pp. 88–93, 2017.

[47] O. Diaz-Horta, D. Duman, J. Foster 2nd et al., "Whole-exome sequencing efficiently detects rare mutations in autosomal recessive nonsyndromic hearing loss," *PLoS One*, vol. 7, no. 11, article e50628, 2012.

[48] S. Naz, F. Alasti, A. Mowjoodi et al., "Distinctive audiometric profile associated with DFNB21 alleles of TECTA," *Journal of Medical Genetics*, vol. 40, no. 5, pp. 360–363, 2003.

[49] F. Alasti, M. H. Sanati, A. H. Behrouzifard et al., "A novel *TECTA* mutation confirms the recognizable phenotype among autosomal recessive hearing impairment families," *International Journal of Pediatric Otorhinolaryngology*, vol. 72, no. 2, pp. 249–255, 2008.

[50] A. Behlouli, C. Bonnet, S. Abdi et al., "A novel biallelic splice site mutation of TECTA causes moderate to severe hearing impairment in an Algerian family," *International Journal of Pediatric Otorhinolaryngology*, vol. 87, pp. 28–33, 2016.

[51] K. E. Baker and R. Parker, "Nonsense-mediated mRNA decay: terminating erroneous gene expression," *Current Opinion in Cell Biology*, vol. 16, no. 3, pp. 293–299, 2004.

[52] T. Self, T. Sobe, N. G. Copeland, N. A. Jenkins, K. B. Avraham, and K. P. Steel, "Role of myosin VI in the differentiation of cochlear hair cells," *Developmental Biology*, vol. 214, no. 2, pp. 331–341, 1999.

[53] S. Li, A. Mecca, J. Kim et al., "Myosin-VIIa is expressed in multiple isoforms and essential for tensioning the hair cell mechanotransduction complex," *Nature Communications*, vol. 11, no. 1, p. 2066, 2020.

[54] S. G. Jacobson, A. V. Cideciyan, T. S. Aleman et al., "Usher syndromes due to MYO7A, PCDH15, USH2A or GPR98 mutations share retinal disease mechanism," *Human Molecular Genetics*, vol. 17, no. 15, pp. 2405–2415, 2008.

[55] R. J. Morell, R. Olszewski, R. Tona et al., "Noncoding microdeletion in mouse Hgf disrupts neural crest migration into the stria vascularis, reduces the endocochlear potential, and suggests the neuropathology for human nonsyndromic deafness DFNB39," *The Journal of Neuroscience: the official journal of*

the Society for Neuroscience, vol. 40, no. 15, pp. 2976–2992, 2020.

[56] T. Parzefall, S. Shivatzki, D. R. Lenz et al., "Cytoplasmic mislocalization of POU3F4 due to novel mutations leads to deafness in humans and mice," *Human Mutation*, vol. 34, no. 8, pp. 1102–1110, 2013.

[57] Y. Su, X. Gao, S. S. Huang et al., "Clinical and molecular characterization of POU3F4 mutations in multiple DFNX2 Chinese families," *BMC Medical Genetics*, vol. 19, no. 1, p. 157, 2018.

[58] M. Bitner-Glindzicz, P. Turnpenny, P. Höglund et al., "Further mutations in brain 4 (POU3F4) clarify the phenotype in the X-linked deafness, DFN3," *Human Molecular Genetics*, vol. 4, no. 8, pp. 1467–1469, 1995.

[59] G. Bademci, A. Lasisi, K. O. Yariz et al., "Novel domain-specific POU3F4 mutations are associated with X-linked deafness: examples from different populations," *BMC Medical Genetics*, vol. 16, no. 1, p. 9, 2015.

Hindawi
Neural Plasticity
Volume 2021, Article ID 5585394, 14 pages
https://doi.org/10.1155/2021/5585394

Research Article

Transcriptomic Analysis Reveals an Altered Hcy Metabolism in the Stria Vascularis of the Pendred Syndrome Mouse Model

Wenyue Xue,[1,2,3] Yuxin Tian,[1,2,3] Yuanping Xiong,[4] Feng Liu,[1,2,3] Yanmei Feng,[1,2,3] Zhengnong Chen,[1,2,3] Dongzhen Yu,[1,2,3] and Shankai Yin[1,2,3]

[1]*Department of Otolaryngology-Head and Neck Surgery, Shanghai Jiao Tong University Affiliated Sixth People's Hospital, Shanghai, China*
[2]*Otolaryngology Institute of Shanghai Jiao Tong University, Shanghai, China*
[3]*Shanghai Key Laboratory of Sleep Disordered Breathing, Shanghai, China*
[4]*Department of Otolaryngology-Head and Neck Surgery, First Affiliated Hospital of Nanchang University, Nanchang, Jiangxi, China*

Correspondence should be addressed to Yanmei Feng; feng.yanmei@126.com and Dongzhen Yu; drdzyu@126.com

Received 1 February 2021; Revised 19 February 2021; Accepted 1 April 2021; Published 19 April 2021

Academic Editor: Laura Baroncelli

Purpose. *Slc26a4*$^{-/-}$ mice exhibit severer defects in the development of the cochlea and develop deafness, while the underlying mechanisms responsible for these effects remain unclear. Our study was to investigate the potential mechanism linking *SLC26A4* deficiency to hearing loss. *Materials and Methods*. RNA sequencing was applied to analyze the differential gene expression of the stria vascularis (SV) from wildtype and *Slc26a4*$^{-/-}$ mice. GO and KEGG pathway analysis were performed. Quantitative RT-PCR was applied to validate the expression of candidate genes affected by *Slc26a4*. ELISA and immunofluorescence technique were used to detect the homocysteine (Hcy) level in serum, brain, and SV, respectively. *Results*. 183 upregulated genes and 63 downregulated genes were identified in the SV associated with *Slc26a4* depletion. Transcriptomic profiling revealed that *Slc26a4* deficiency significantly affected the expression of genes associated with cell adhesion, transmembrane transport, and the biogenesis of multicellular organisms. The SV from *Slc26a4*$^{-/-}$ mice exhibited a higher expression of *Bhmt* mRNAs, as well as altered homocysteine (Hcy) metabolism. *Conclusions*. The altered expression of *Bhmt* results in a dramatic change in multiple biochemical reactions and a disruption of nutrient homeostasis in the endolymph which may contribute to hearing loss of *Slc26a4* knockout mouse.

1. Introduction

Pendred syndrome, characterized by deafness with enlargement of aqueduct and goiter, is caused by mutations of *SLC26A4*, one of the most prevalent causes of hereditary hearing loss globally [1]. A large-scale study showed mutations of *SLC26A4* that occur in approximately 5-10% sensorineural hearing loss children among a variety of different ethnic populations [2]. The onset of hearing loss in patients with Pendred syndrome is variable. Some patients may have hearing loss at birth, while others suffer fluctuating, or progressive hearing loss during their childhood, which may provide a window of opportunity for treatment [3].

To investigate the underlying mechanism of the Pendred syndrome, researchers have created a mouse model for study. The *Slc26a4* knockout mice suffer severe hearing loss and malformation of cochlea at birth. Previous studies looking at the *Slc26a4* knockout mice have found that pendrin, encoded by the *Slc26a4* gene, locates in root cells of the outer sulcus, cells overlying the spiral prominence, and spindle-shaped cells of the stria vascularis in cochlea. Meanwhile, three main changes occur in the inner ears of *Slc26a4* mutant mouse. (1) A lack of pendrin causes the acidification of the endolymph [4]. Pendrin is an anion exchange protein, similar to Cl^- and HCO_{3-} exchangers that participate in fluid regulation of the endolymph [5]. In the absence of pendrin, HCO_{3-} secretion into the endolymph is affected, which causes the endolymph to become acidic and leads to inhibition of Ca^{2+} reabsorption [4, 6]. (2) The scala media is enlarged due to the dysfunction of the endolymphatic sac.

Table 1: Primer used in this study.

Target	Forward (5'to3')	Reversed (5'to 3')
Slc26a7	GCATGATGAAACCTCGCAACA	TTCATTGCAGTTGCCGTTGG
Ace2	CACTCCTGCCACACCACGTT	TGGTCTTTAGGTCAAGTTTACAGCC
Gpr176	GGTGTTATGGTCAACTTGCCG	AGAGCATCGTATAGATCCACCAG
Lrrc8d	ATGTTTACCCTTGCGGAAGTTG	CATCAGCATAACGACTGCCAG
Padi1	TGTGTGCGTGGTAGGTGTG	TCGAGGGATCGTAGACCATGT
Arrb1	AAGGGACACGAGTGTTCAAGA	CCCGCTTTCCCAGGTAGAC
Alox15	CAGGGATCGGAGTACACGTT	GATTGTGCCATCCTTCCAGT
Bmht	CTGGGGAAGTGGTTTGGACA	GCCGGAAGCTATTCGCAGAT
Bhmt2	CTCCAGAAGCAGTGGTAGAACATC	CATCAGCTCCCGCTCTCAAG
Ahcy	TCGAAGTGTCCAATGTTACAGAC	CTTGGCCGGCACTTTGAG
Cbs	GCAGCGCTGTGTGGTCATC	GTCACTCAGGAACTTGGACATGTAGT

The cochlear lumen is formed by the balance of the fluid secretion in the vestibular labyrinth and fluid absorption in the endolymphatic sac, from embryonic day (E) 13.5 and 14.5 [7]. Thus, dysfunction of fluid absorption in the endolymphatic sac, due to *Slc26a4* mutation, results in an enlarged volume of the scala media [8, 9]. (3) The expression of Kcnj10 is reduced, and this inwardly rectifying K^+ channel subunit, located in the intermediate cells of the stria vascularis (SV), is responsible for the establishment of the endolymphatic potential (EP) [10, 11]. Wangemann et al. have reported an absence of Kcnj10 in the intermediate cells of *Slc26a4* mutant mice at 1-4 months of age, and this lack of channel protein causes a decrease in the EP, which may directly lead to deafness [12]. Among these three changes, the pathology in the SV is the initial and predominant cause of the hearing loss associated with *Slc26a4*$^{-/-}$ mice. However, how *Slc26a4* deficiency affects morphology and function of SV remains unknown.

In this study, we used RNA sequencing methodology to compare differences in the transcriptomes in the SV from wildtype and *Slc26a4* mutant mice. We found that *Slc26a4* deficiency significantly affected SV genes required for multicellular organism biogenesis. Furthermore, the SV from *Slc26a4*$^{-/-}$ mice exhibited higher expression of *Bhmt* mRNAs, as well as a dramatic reduction of Hcy, suggesting abnormality of Hcy metabolism as a novel mechanism by which *SLC26A4* affects hearing.

2. Materials and Methods

2.1. Animals. *Slc26a4* knockout mice were obtained from the Jackson Laboratory, and *Calca* knockout mice were from Cyagen Co. LTD. All animals were maintained in heterozygotes in SPF circumstances and adapted to the experimental circumstances for a week before the experiments. All experimental procedures were carried out in accordance with the Guide for the Care and Use of Laboratory Animals and were approved by the Animal Care and Use Committee of the Shanghai Jiao Tong University Affiliated Sixth People's Hospital [Permit number: SYXK 2016-0020].

2.2. RNA-seq. Wildtype and *Slc26a4*$^{-/-}$ mice were sacrificed at P14. The stria vascularis were isolated from inner ear and then lysed in Trizol (Invitrogen). Total RNA was isolated according to the manufacturer's instructions. All samples were sequenced on an Illumina HiSeq2500 platform at 15 million 100-bp single reads per sample. After quality control of the sequencing libraries, reads were trimmed and mapped against the Ensembl genome annotation and the human genome assembly (hg19/GRCh38) using Tophat2. Reads mapping to ribosomal RNAs or the mitochondrial genome were removed.

2.3. Quantitative Real-Time RT-PCR. Total RNA from wildtype and *Slc26a4*$^{-/-}$ stria vascularis was extracted with TRIzol reagent according to the manufacturer's instructions (Invitrogen). One microgram of total RNA was reverse transcribed using the ReverTra Ace® qPCR RT Kit (Toyobo, FSQ-101) according to the manufacturer's instructions. A SYBR RT-PCR kit (Toyobo, QPK-212) was used for quantitative real-time PCR analysis. The relative mRNA expression of different genes was calculated by comparison with the control gene *Gapdh* (encoding GAPDH) using the $2^{-\triangle\triangle Ct}$ method (Table 1).

2.4. Immunostaining. Wildtype and *Slc26a4*$^{-/-}$ mice were sacrificed at P14. The cochleae were isolated from temporal bone, fixed by 4% PFA, dehydrated by 30% sucrose, and cut into frozen sections. The section was then permeabilized with 0.1% Triton X-100 in PBS and blocked with 1% BSA in PBS. The samples were incubated with anti-Hcy (PAD984Ge01, Clonecloud) at 4°C overnight and then secondary antibody or DAPI at room temperature for 30 min. The stria vascularis were dissected from lateral wall and its actin structure were shown by phalloidin staining. Samples were examined and the figures were acquired with an LSM 710 confocal laser-scanning microscope (Carl Zeiss, Oberkochen, Germany) at 20x or 63x magnification.

2.5. Enzyme-Linked Immunosorbent Assay. The blood plasma and brain homogenate from wildtype and *Slc26a4*$^{-/-}$ mice were prepared and persevered at -20°C until analysis.

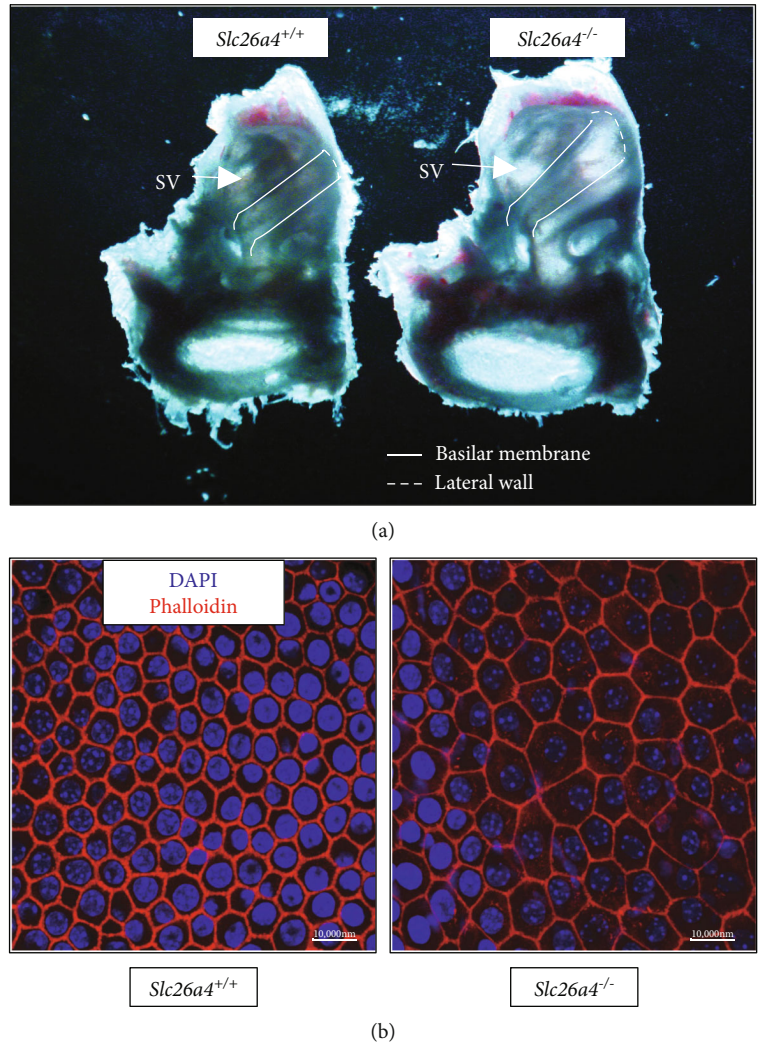

Figure 1: The dramatic morphological changes occurred in stria vascularis from *Slc26a4*$^{-/-}$ mice. (a) The scala media, formed by basilar membrane, lateral wall, and vestibular membrane, is significantly enlarged in *Slc26a4*$^{-/-}$ mice. SV: stria vascularis. The outline of stria vascularis, which is visualized through pigmentation in intermediate cells, is clearer in *Slc26a4*$^{+/+}$ mice. (b) Marginal cells in stria vascularis from wildtype or *Slc26a4*$^{-/-}$ mice were coated on coverlips and sent for phalloidin staining.

Hcy level was measured using ELISA Kit for Homocysteine (CED984Ge, Clone-Cloud) according to the manufacture's instruction. Absorbance was assessed by an ELISA microplate reader at 450 nm and the results were expressed in pg/ml.

2.6. ABR Threshold Testing. The hearing condition of mice was detected by auditory brain stem response (ABR) thresholds. The mice used for ABR testing were fully anesthetized by a mixture of ketamine and xylazine. The initial dose of ketamine and xylazine was 85 and 15 mg/kg, respectively. The stimulus generation and biosignal acquisition parameters were similar to those used in a previous study [13]. Auditory stimuli were presented from a speaker 10 cm ahead of the mouse's head, needle electrodes were positioned in the vertex of the head and the reference, and grounding electrodes were positioned posterior to the external auditory canals. The tone bursts were generated by TDT RP2.1 Real-time signal processor, (10-ms duration with 0.5-ms rise/fall time presented at 21.1/s intervals) at 4, 8, 16, 24, and 32 kHz with SigGen software. The biological signals picked up by the electrodes were led to a RA4PA preamplifier from Tucker-Davis Technologies (TDT System III; Alachua, FL, USA). The evoked ABR responses were amplified 20x by a PA4 preamplifier (TDT) and averaged 1000 times. The intensity of tone bursts started at 90 dB SPL and declined by a step of 10 dB, except around threshold where it was 5 dB. The threshold was determined based on visibility and reproducibility of negative–positive waves. Threshold was defined as the lowest sound level that produces a reproducible response.

2.7. Statistical Analysis. The results are represented as the mean ± s.e.m., and statistical significance between groups was determined using an unpaired t-test or the Mann–Whitney U test. The GraphPad Prism software 8.0 was used for all analyses, and a $^{*}p < 0.05$ was considered statistically significant.

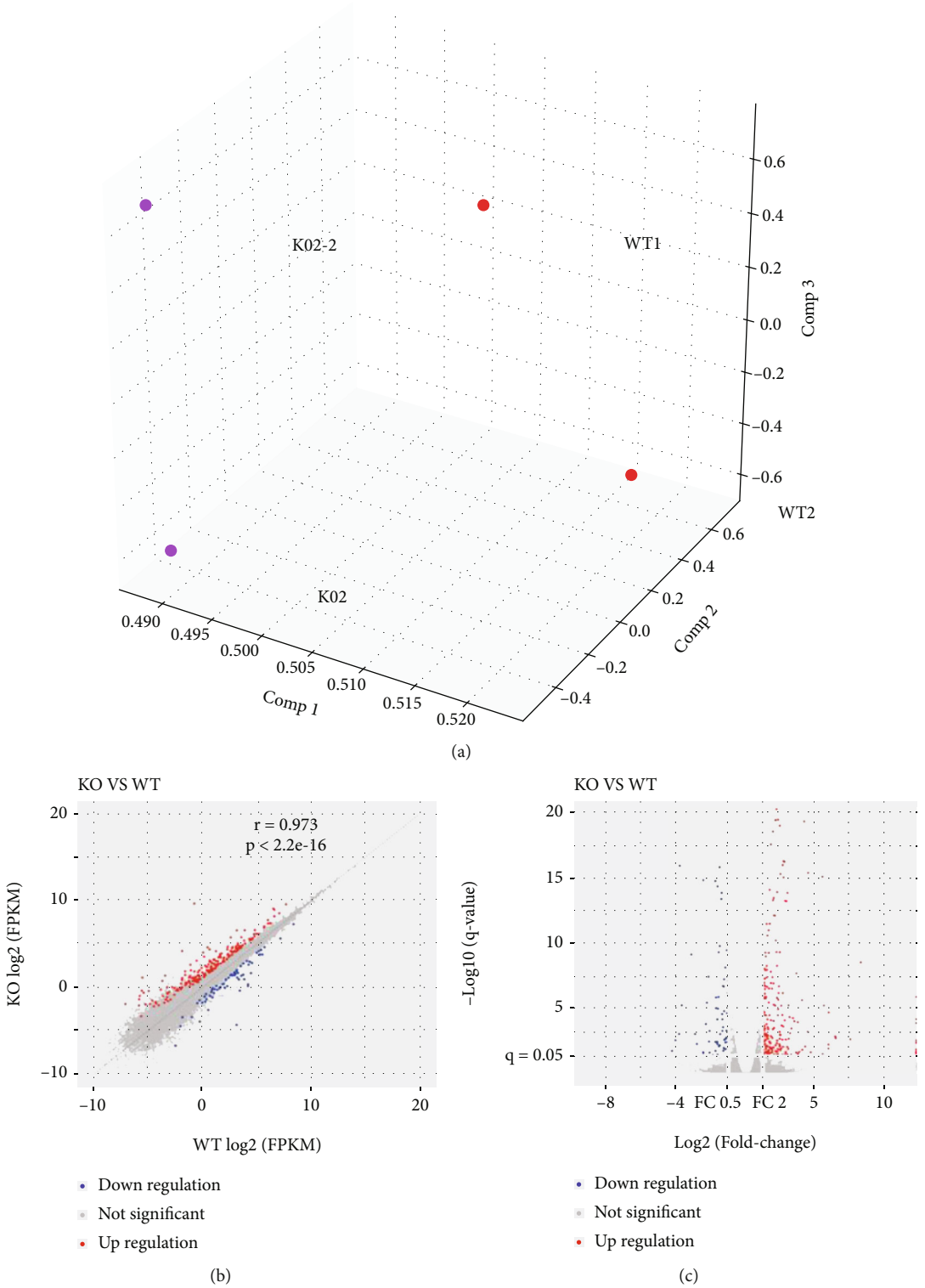

Figure 2: Transcripts regulated in stria vascularis of *Slc26a4* deletion. (a) Principal component analysis of RNAs from stria vascularis of wildtype (WT) and *Slc26a4*$^{-/-}$ (KO) mice. (b, c) Scatter plot (b) and Volcano plot (c) indicate individual RNAs sequenced.

3. Results

3.1. Dramatic Morphological Changes in the Stria Vascularis from Slc26a4$^{-/-}$ *Mice.* *Slc26a4*$^{-/-}$ mice typically have larger inner ears due to the dysfunction of the endolymphatic sac. Compared to those from *Slc26a4*$^{+/+}$ mice, the cochlear lumen of the inner ears, isolated from 6-week-old *Slc26a4*$^{-/-}$ mice, is significantly enlarged. Furthermore, the SV can be visualized

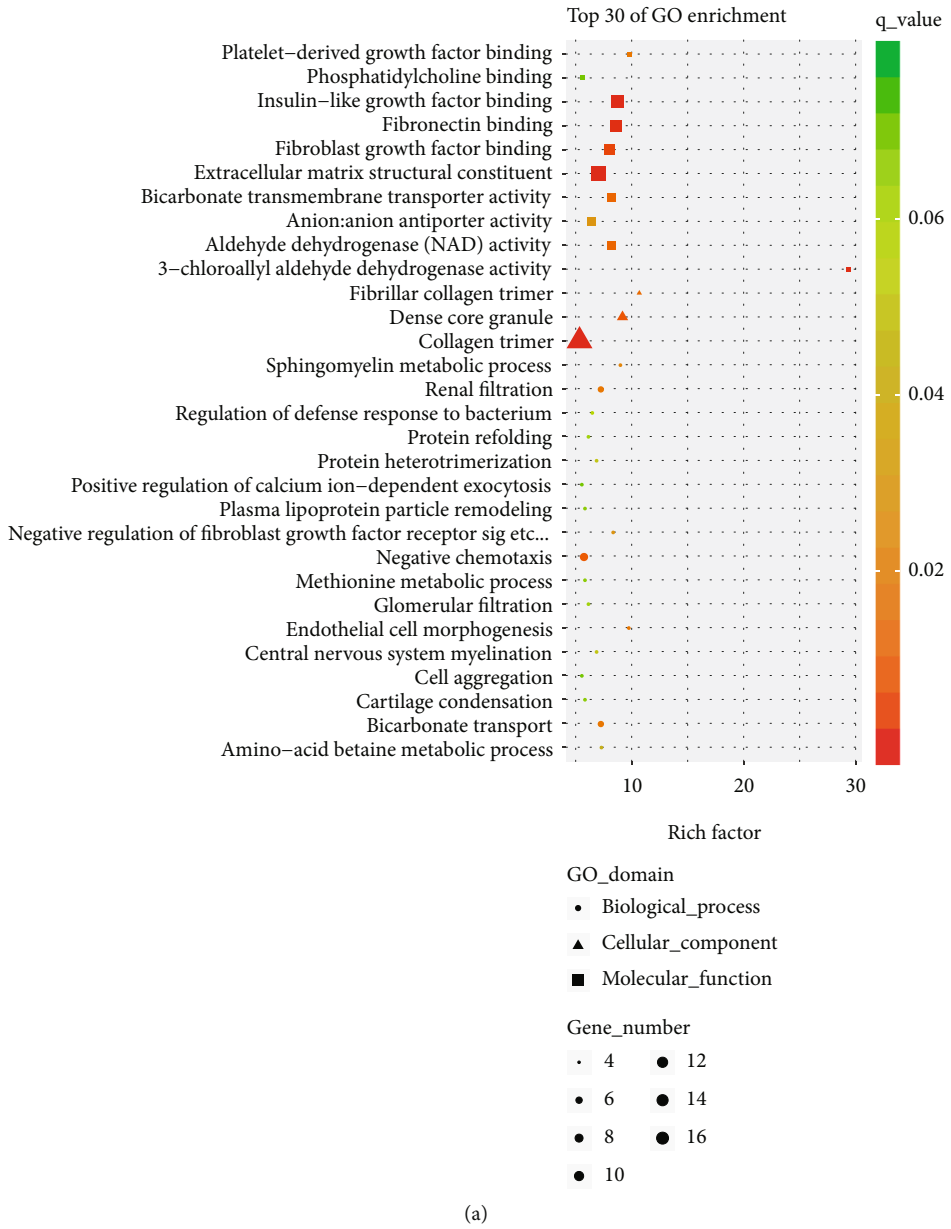

(a)

Figure 3: Continued.

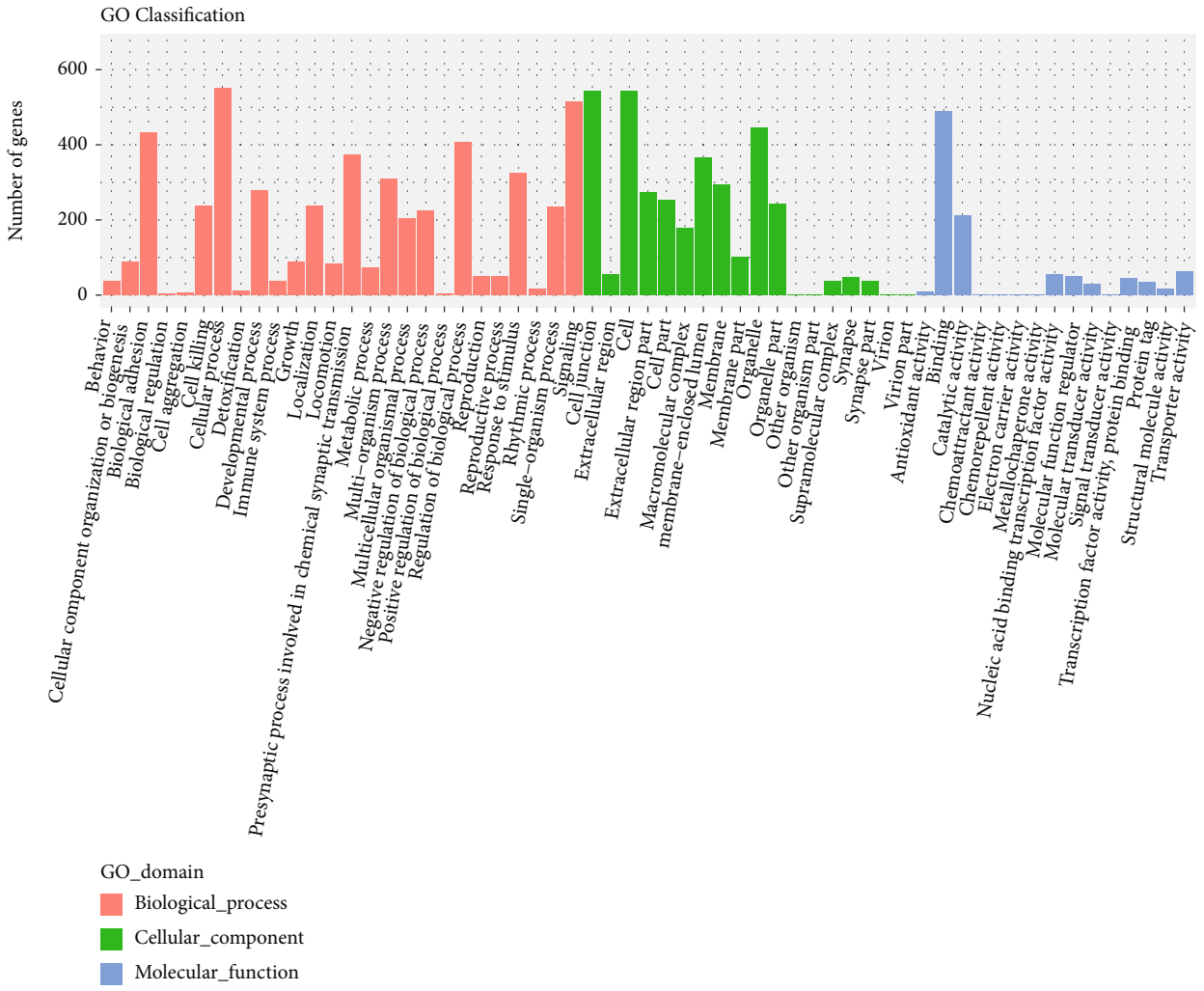

(b)

Figure 3: Continued.

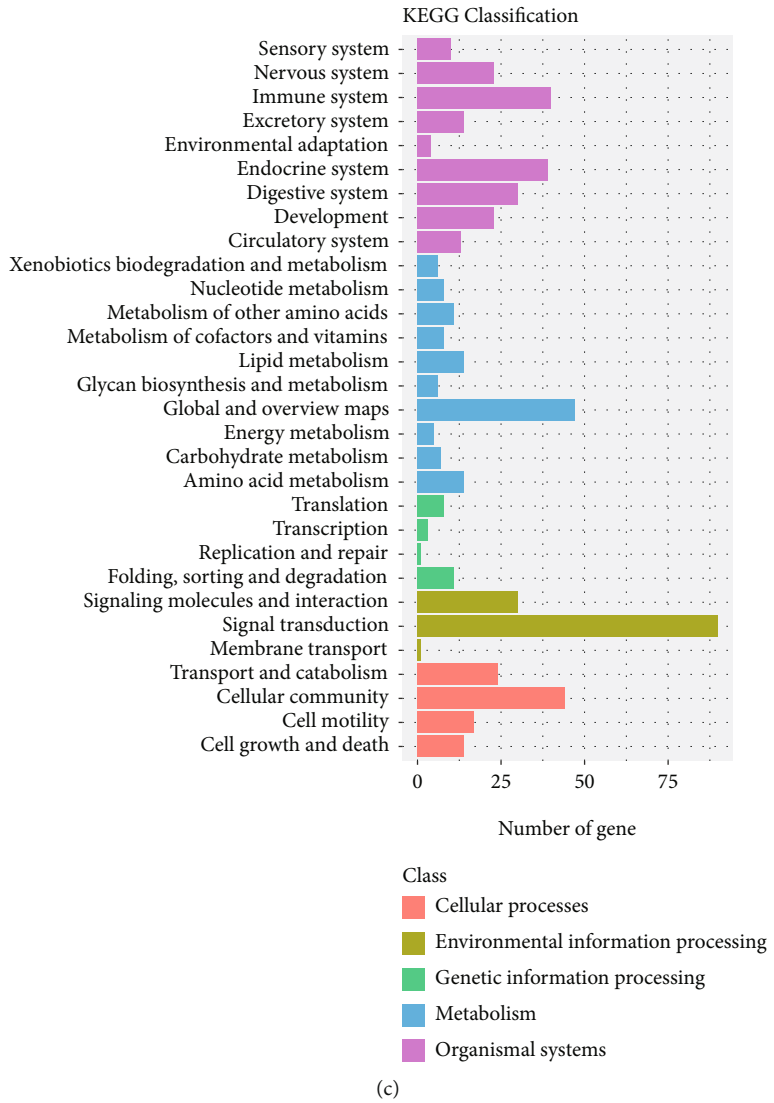

(c)

Figure 3: Continued.

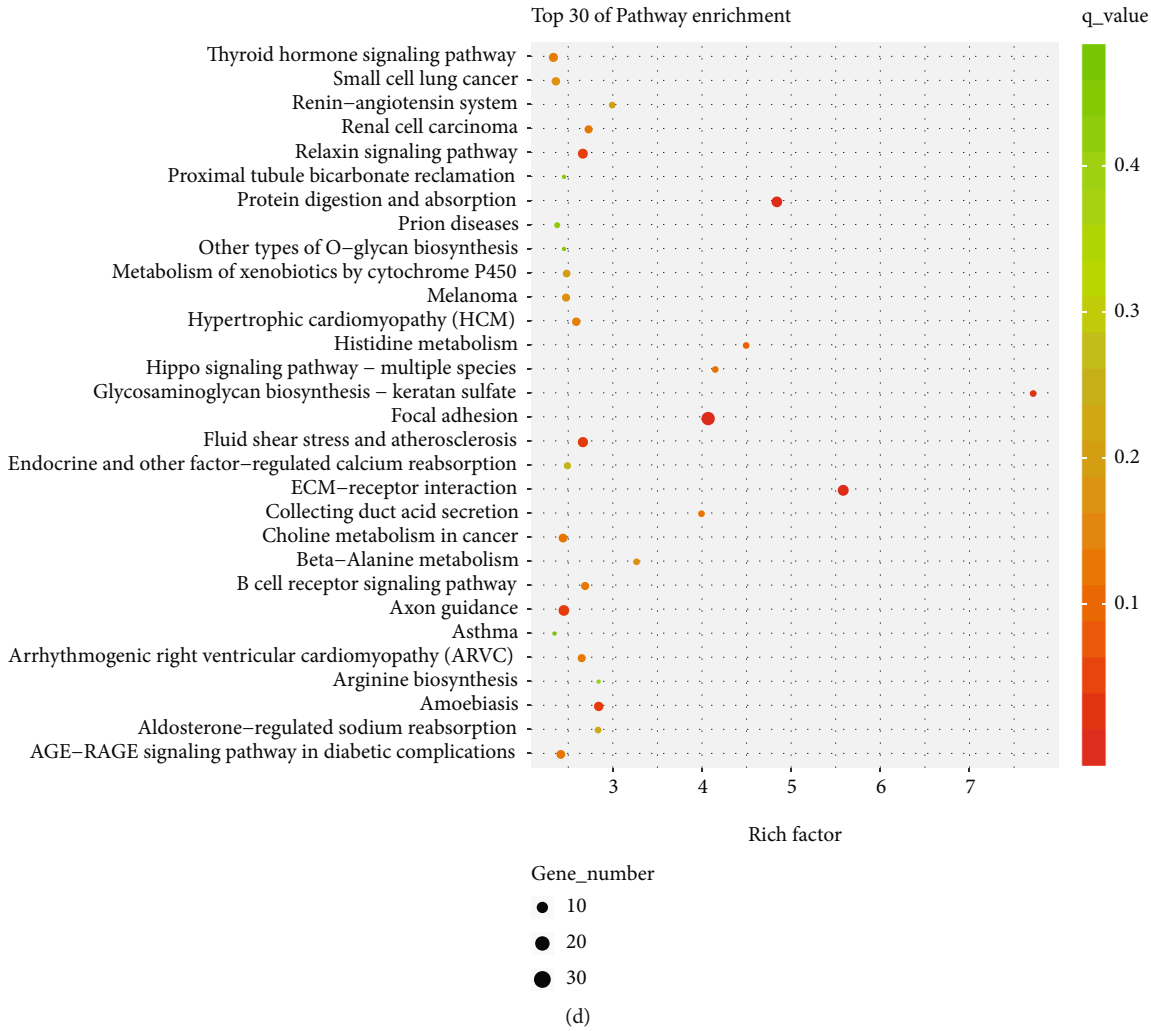

Figure 3: Gene ontology analysis and KEGG analysis of differentiated expressed genes in stria vascularis of *Slc26a4* deletion.

through the pigmentation of the intermediate cells [14], and the lateral wall appears darker and more obvious in *Slc26a4*$^{+/+}$ mice when compared to *Slc26a4*$^{-/-}$ (Figure 1(a)).

The inner layer of the SV is formed by marginal cells facing the endolymph [10]. Therefore, we used the actin stain phalloidin, to profile the structure of these marginal cells in SV. Indeed, enlargement of marginal cells was seen in *Slc26a4*$^{-/-}$ mice, while the marginal cells from *Slc26a4*$^{+/+}$ mice were normal in both size and organization [15] (Figure 1(b)).

3.2. Transcript Regulation in the Stria Vascularis Caused by Slc26a4 Deletion. To determine the role of *SLC26A4* in the function of the cochlea, wildtype and *Slc26a4*$^{-/-}$ mice were sacrificed and their SV were carefully isolated. Total RNA from pairs of SVs was extracted and then sent for next-generation sequencing and data from each sample generated on average 24-Mb of clean reads, after low-quality filtering, and these clean reads were mapped for reference. Each of the data sets contained 24-Mb reads and a mapping rate of 92–93%. Moreover, we counted the number of identified expressed genes and calculated their proportion and distribution to the total gene number in the database for each sample. The correlation for gene expression levels among the samples is a key criterion to determine whether the experiments are reliable and whether the samples chosen are reasonable, and principal component analysis was performed to assess gene expression levels (Figure 2(a)).

Volcano and Scatter plots showed differentially expressed transcripts for a fold change of >2 in the *Slc26a4* deficient group when compared to the wildtype group (183 upregulated genes and 63 downregulated genes) (Figures 2(b) and 2(c)).

3.3. Gene Ontology Analysis of the Differential Genes. To better understand the associated functions of these differentially expressed genes in *Slc26a4*-mediated cochlear function, gene ontology (GO) analysis was used to perform enrichment analysis and classifications (Figures 3(a) and 3(b)). GO analysis identified enriched biological processes associated with "biological adhesion," "cellular component organization or biogenesis," "multicellular organismal processes," and "developmental processes," indicating that a strong multicellular organism biogenesis process occurred during the *Slc26a4*-mediated maintenance of cochlear homeostasis. Furthermore,

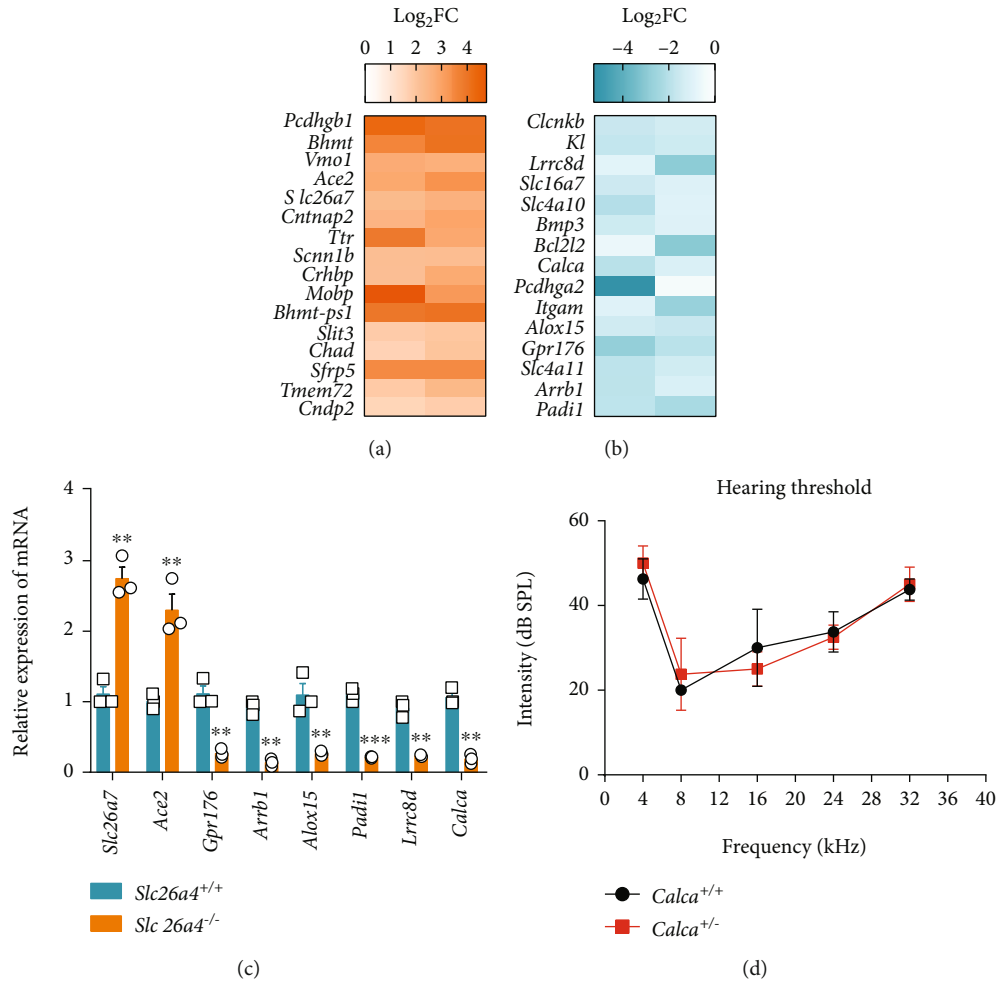

FIGURE 4: Validation of differentiated expressed genes in stria vascularis of *Slc26a4* deletion. (a, b) Heatmap indicated selected upregulated genes (a) and downregulated genes (b) in *Slc26a4*$^{-/-}$ SVs. (c) Quantitative RT-PCR analysis of expression of indicated genes in *Slc26a4*$^{-/-}$ SVs. (d) ABR test of wildtype and *Calca*$^{+/-}$ mice. $^{*}p < 0.05$ and $^{**}p < 0.01$ by the unpaired *t*-test (c). Data are from three independent experiments with biological duplicates in each (c, d; mean ± s.e.m. of $n = 3$ duplicates).

enriched cellular component terms associated with "membrane," "organelle," "extracellular region," and "membrane-enclosed lumen" were identified implying that diverse cellular components were involved in *Slc26a4*-mediated cochlear function. Enriched molecular functions were defined as associated with "structural molecule activity," "catalytic activity," and "molecular transducer activity," indicating that formation of organelle structure and intracellular signal transduction were the major molecular functions for *Slc26a4*.

3.4. Analysis of Important KEGG Pathways. We next used the differential genes for KEGG pathway enrichment, and the results showed that genes involving in the "ECM-receptor interaction pathway," "focal adhesion pathway," "aldosterone-regulated sodium reabsorption pathways," and "taste transduction pathways" were significantly enriched, indicating that loss of *Slc26a4* genes may lead to disrupted transmembrane cell communication and transport in the SV (Figures 3(c) and 3(d)).

Collectively, GO and KEGG pathway analysis suggested an essential role for *SLC26A4* in the regulation of extracellular structure formation, cell-to-cell or cell-to-ECM adhesion, and transmembrane transport.

3.5. Validation of Selected Genes. Several important upregulated and downregulated genes are represented as shown in the heatmap (Figures 4(a) and 4(b)). Quantitative RT-PCR results validated the differential expression of selected candidate genes, including *Padi1*, *Arrb1*, *Ace2*, *Gpr176*, *Lrrc8d*, *Alox15*, and *Calca* (Figure 4(c)).

We noted that one of the important downregulated genes in the SV of *Slc26a4* deficient mice was *Gpr176*, which encodes a G-protein-coupled receptor [16] and has previously been reported to be associated with adult-onset autosomal dominant cerebellar ataxia, with deafness and narcolepsy [17]. Quantitative RT-PCR analysis confirmed the downregulation of *Gpr176* in the SV of *Slc26a4*$^{-/-}$ mice (Figure 4(c)), suggesting a reduction of *GPR176*-mediated signaling upon *Slc26a4* deficiency.

Another important gene found was *Calca* and therefore, we generated a *Calca* knockout mouse using CRISPR/Cas9

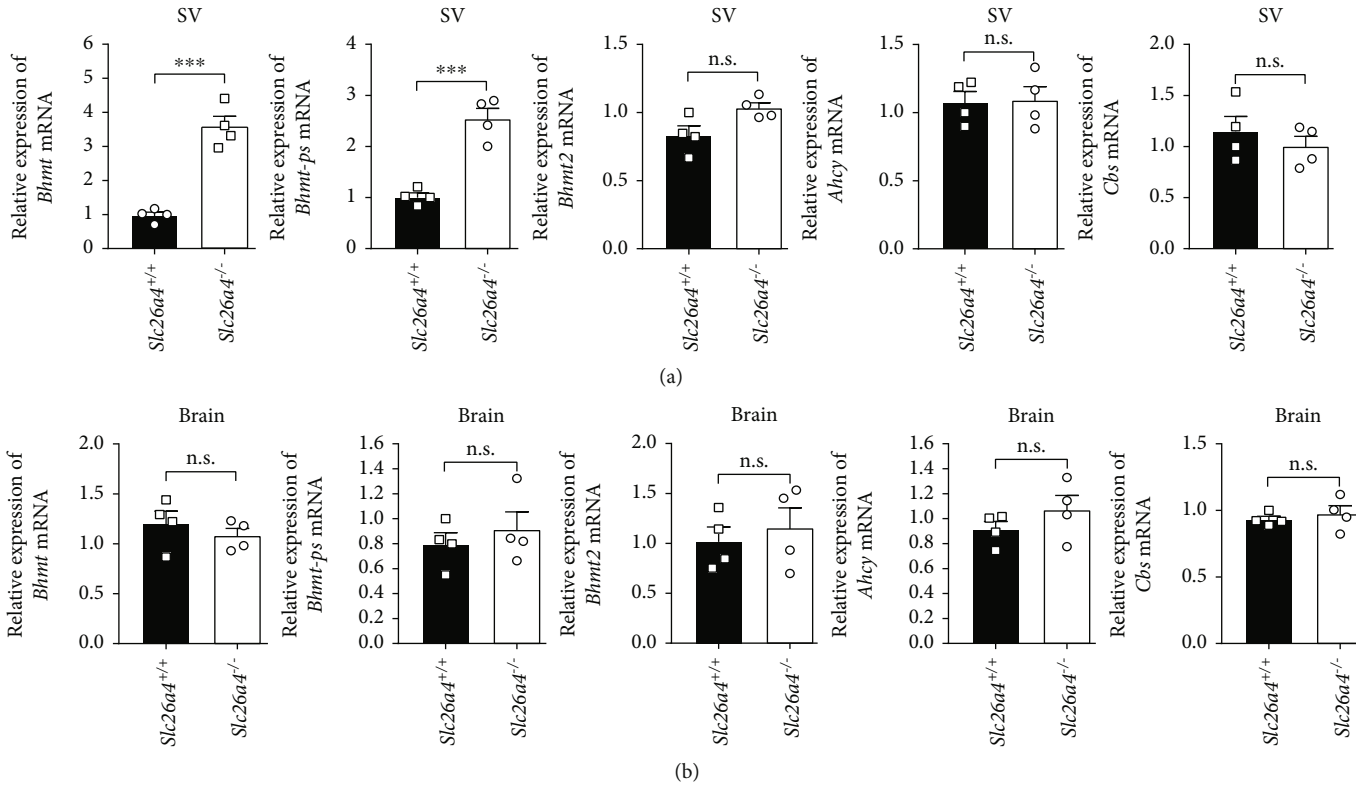

Figure 5: Altered expression of Hcy metabolism enzymes in *Slc26a4*$^{-/-}$ SVs. (a, b) Quantitative RT-PCR analysis of expression of Hcy metabolism enzymes in *Slc26a4*$^{-/-}$ SVs (a) or brains (b). n.s.: no significance. $^{*}p < 0.05$ and $^{**}p < 0.01$ by the unpaired t-test (c). Data are from three independent experiments with biological duplicates in each (a, b; mean ± s.e.m. of $n = 3$ duplicates).

technology and carefully examine its ABR threshold. The results showed that *Calca*$^{+/-}$ mice had equivalent hearing to the wildtype controls (Figure 4(d)), suggesting that at least heterozygous deletion of *Calca* had no significant effect on hearing.

3.6. Altered Hcy Metabolism in the Stria Vascularis of Slc26a4$^{-/-}$ *Mice.* We next determined the expression of *Bhmt*, as well as several other enzymes required for Hcy metabolism including *Bhmt2*, *Ahcy*, and *Cbs* in the SV and brain from *Slc26a4*$^{-/-}$ mice using quantitative RT-PCR. The results showed that *Slc26a4* deficiency significantly increased *Bhmt* expression in the SV but not the brain, while the expressions of other enzymes involved in Hcy metabolism were similar in both groups (Figures 5(a) and 5(b)). Interestingly, we also observed a significant increase in the *Bhmt* pseudogene (*Bhmt-ps)*, in the SV of *Slc26a4*$^{-/-}$ mice but not in brain, which was similar to the levels of *Bhmt* itself, suggesting that there may be a common regulation of *Bhmt* and *Bhmt-ps* in the SV. Thus, we applied immunostaining assays using an anti-Hcy polyclonal antibody to measure levels in the SV from wildtype and *Slc26a4*$^{-/-}$ mice and found that Hcy levels were dramatically decreased in the SV of *Slc26a4*$^{-/-}$ mice (Figure 6(a)). However, we did not observe a significant change in serum Hcy levels in these mice when compared to the wild types, based on an anti-Hcy ELISA (Figures 6(b) and 6(c)).

4. Discussion

Hearing loss could be caused by genetic factors, aging, chronic cochlear infections, infectious diseases, ototoxic drugs, and noise exposure [18–24]. Most of the hearing loss is due to the damage of hair cells and spiral ganglion neurons and has been extensively investigated in many previous studies [25–30], while the detailed mechanism of stria vascularis-related hearing loss, such as Pendred syndrome, has not been well known. *SLC26A4* affects cochlear function both in humans and mice; however, the mechanism by which *SLC26A4* achieves this is unclear [15]. Transcriptome sequencing has been extensively used in many previous studies to investigate the detailed mechanism in the inner ear [31–37]. In our study, we applied a transcriptome sequencing approach to examine the levels of differentially expressed genes in the SV from *Slc26a4*$^{-/-}$ mice. Using bioinformatic analysis, we identified 183 upregulated genes and 63 downregulated genes in the SV associated with *Slc26a4* depletion. Furthermore, the cellular functions of these genes are related to cell communication, extracellular matrix organization, and transmembrane transportation. Therefore, our findings suggest a novel mechanism by which *SLC26A4* can affect cochlear function.

Previous studies have shown that macrophage invasion contributes to degeneration of the SV in the *Slc26a4*$^{-/-}$ mouse model [14, 38]. Consistent with this, we found an additional

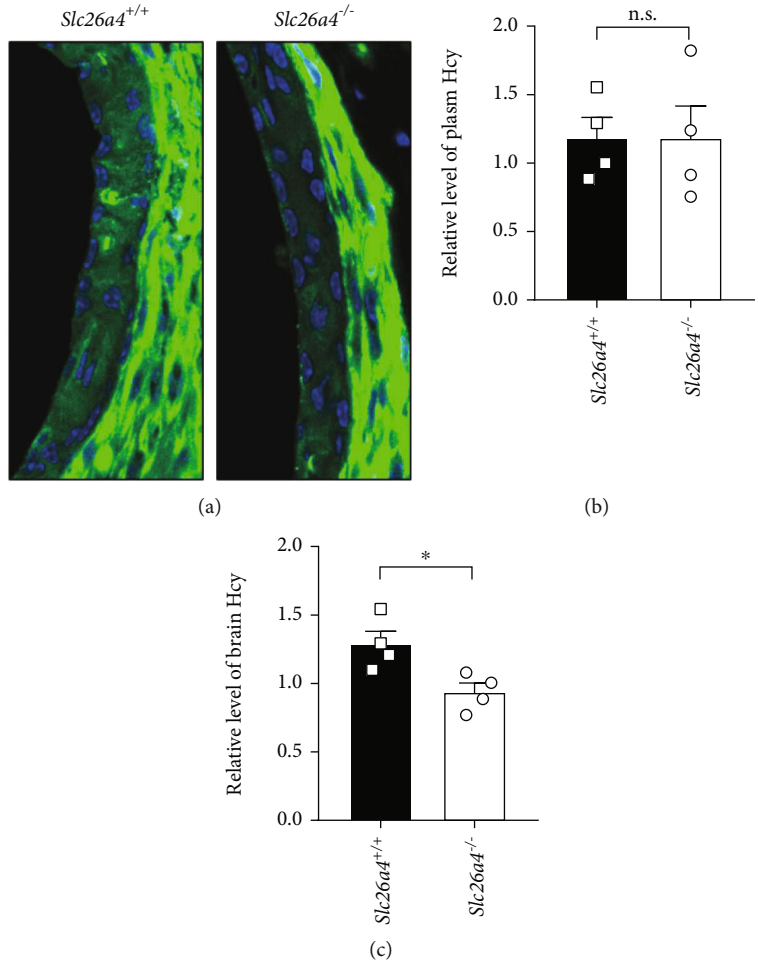

Figure 6: Altered Hcy metabolism in *Slc26a4*$^{-/-}$ SVs. (a) Stria vascularis from wildtype or *Slc26a4*$^{-/-}$ mice were coated on coverlips and sent for immunostaining against Hcy. (b, c) Elisa assay of Hcy level in plasma (b) and brain (c) from wildtype or *Slc26a4*$^{-/-}$ mice. n.s.: no significance. $^{*}p < 0.05$ by the unpaired t-test (b, c). Data are from three independent experiments with biological duplicates in each (a, b, c; mean ± s.e.m. of $n = 3$ duplicates).

two well-characterized inflammation regulating genes, *Alox15*, that encoded arachidonate 15-lipoxygenase [39] and *Arrb1*, encoding β-arrestin 1 [40, 41], in top downregulated genes in the SV of *Slc26a4*$^{-/-}$ mice. Quantitative RT-PCR results also showed that the expression levels of *Arrb1* and *Alox15* were decreased in the SV of these knockout mice. These findings suggest a possible role for tissue inflammation in the degeneration of the SV in the Pendred syndrome mouse model [42, 43].

The *Calca* gene, encoding calcitonin and alpha-calcitonin gene-related peptide [44], is one of the top downregulated genes found in our study. As reported in a previous study, *Calca* is expressed in mouse cochlea at an early stage during development [45]. We therefore obtained a *Calca* mutant mouse to determine whether the low expression of *Calca* affected hearing. Since *Calca* plays a critical role in multiorgan development [46, 47], *Calca*$^{-/-}$ mice, created by CRISPR/-Cas9 methodology, were unhealthy and died soon after birth. Therefore, we were forced to generate a *Calca*$^{+/-}$ heterozygous mouse model to determine hearing. The ABR result showed that there was no difference in the hearing threshold between the wildtype and the *Calca*$^{+/-}$ animals. No significant hearing loss may be due to the heterozygotic nature of the mice used. Therefore, further research is needed to determine whether more subtle, or hidden hearing loss is present in these mice. Also, a new *Calca* minus model is needed to further investigate its effect upon hearing.

Our transcriptome sequencing results found that the most distinctive upregulated gene in the SV from *Slc26a4*$^{-/-}$ mice was *Bhmt*, which encodes betaine Hcy S methyltransferase, whose activity is required for the transfer of a methyl group from betaine to Hcy, a nonproteinaceous sulfur amino acid [48, 49]. Malfunction of *Bhmt* leads to hyperhomocysteinemia and several previous epidemiological and experimental studies have revealed a correlation between hyperhomocysteinemia and hearing loss [50]. Previous study showed that Hcy level plays an important part in keeping the integrity of SV, which is the foundation of SV to establish the EP [51]. We consistently observed a dramatic decrease in Hcy from the SV of *Slc26a4*$^{-/-}$ mice when compared to wildtypes, and recently, nutritional imbalance is emerging as a causative factor associated with hearing loss. Furthermore, Teresa Partearroyo et al. have reported that *Bhmt* plays a central role in the homeostasis

of methionine metabolism in the cochlea and its deficiency in mice causes increased susceptibility to noise-induced hearing loss [52, 53]. Moreover, a decrease in *Bhmt* expression and an increase of Hcy in the SV is thought to explain the hearing loss phenotype seen in *Cx30*$^{-/-}$ mice [54]. However, one difference between our findings and previous studies is that in the SV of *Slc26a4*$^{-/-}$ mice, *Bhmt* is upregulated, which leads to decreased amounts of Hcy, which is part of the folate and methionine cycles. The elevated expression of *Bhmt* leads to an increased consumption of Hcy and folate and production of methionine and S-Adenosylmethionine, which serve as the major donors of methyl groups in the synthesis of hormones, nucleotides, and membrane lipids. It is speculated that the altered expression of *Bhmt* results in a dramatic change in multiple biochemical reactions and a disruption of nutrient homeostasis in the endolymph. However, whether the decrease in Hcy levels accounts for cochlear dysfunction and hearing loss in Pendred syndrome mouse models requires further investigation.

5. Conclusion

Transcriptomic profiling revealed that *Slc26a4* deficiency significantly affected the expression of genes associated with cell adhesion, transmembrane transport, and the biogenesis of multicellular organisms. The altered expression of *Bhmt* results in a dramatic change in multiple biochemical reactions and a disruption of nutrient homeostasis in the endolymph which may contribute to hearing loss of *Slc26a4* knockout mouse.

Data Availability

Data are available from the author Wenyue Xue (xuecindy0107@163.com) upon reasonable request and with permission of the Department of Otolaryngology-Head and Neck Surgery, Shanghai Jiao Tong University Affiliated Sixth People's Hospital.

Conflicts of Interest

The authors declare that there is no conflict of interest regarding the publication of this paper.

Authors' Contributions

Wenyue Xue and Yuxin Tian have contributed equally to this work.

Acknowledgments

The authors would like to express their gratitude to EditSprings (https://www.editsprings.com/) for the expert linguistic services provided. This study was supported by the grants from the general program grants of the Natural Science Foundation of China [grant number: 81770998, 82071040].

References

[1] Z. Zhang, J. Wang, C. Li, W. Xue, Y. Xing, and F. Liu, "Gene therapy development in hearing research in China," *Gene Therapy*, vol. 27, no. 7-8, pp. 349–359, 2020.

[2] H. J. Park, S. Shaukat, X. Z. Liu et al., "Origins and frequencies of SLC26A4 (PDS) mutations in east and south Asians: global implications for the epidemiology of deafness," *Journal of Medical Genetics*, vol. 40, no. 4, pp. 242–248, 2003.

[3] R. K. Jackler and A. De La Cruz, "The large vestibular aqueduct syndrome," *The Laryngoscope*, vol. 99, no. 12, pp. 1238–1243, 1989.

[4] P. Wangemann, K. Nakaya, T. Wu et al., "Loss of cochlear HCO^{3-} secretion causes deafness via endolymphatic acidification and inhibition of Ca2+ reabsorption in a Pendred syndrome mouse model," *American Journal of Physiology Renal Physiology*, vol. 292, no. 5, pp. F1345–F1353, 2007.

[5] H. Amlal, S. Petrovic, J. Xu et al., "Deletion of the anion exchanger Slc26a4 (pendrin) decreases apical Cl−/HCO3− exchanger activity and impairs bicarbonate secretion in kidney collecting duct," *American Journal of Physiology-Cell Physiology*, vol. 299, no. 1, pp. C33–C41, 2010.

[6] T. Ito, X. Li, K. Kurima, B. Y. Choi, P. Wangemann, and A. J. Griffith, "Slc26a4-insufficiency causes fluctuating hearing loss and stria vascularis dysfunction," *Neurobiology of Disease*, vol. 66, pp. 53–65, 2014.

[7] X. Li, F. Zhou, D. C. Marcus, and P. Wangemann, "Endolymphatic Na(+) and K(+) concentrations during cochlear growth and enlargement in mice lacking Slc26a4/pendrin," *PLoS One*, vol. 8, no. 5, article e65977, 2013.

[8] H. M. Kim and P. Wangemann, "Failure of fluid absorption in the endolymphatic sac initiates cochlear enlargement that leads to deafness in mice lacking pendrin expression," *PLoS One*, vol. 5, no. 11, article e14041, 2010.

[9] C. Madden, M. Halsted, J. Meinzen-Derr et al., "The influence of mutations in the SLC26A4 gene on the temporal bone in a population with enlarged vestibular aqueduct," *Archives of Otolaryngology – Head & Neck Surgery*, vol. 133, no. 2, pp. 162–168, 2007.

[10] P. Wangemann, E. M. Itza, B. Albrecht et al., "Loss of KCNJ10 protein expression abolishes endocochlear potential and causes deafness in Pendred syndrome mouse model," *BMC Medicine*, vol. 2, no. 1, p. 30, 2004.

[11] D. C. Marcus, T. Wu, P. Wangemann, and P. Kofuji, "KCNJ10 (Kir4.1) potassium channel knockout abolishes endocochlear potential," *American Journal of Physiology-Cell Physiology*, vol. 282, no. 2, pp. C403–C407, 2002.

[12] T. Ito, A. Nishio, P. Wangemann, and A. J. Griffith, "Progressive irreversible hearing loss is caused by stria vascularis degeneration in an Slc26a4-insufficient mouse model of large vestibular aqueduct syndrome," *Neuroscience*, vol. 310, pp. 188–197, 2015.

[13] H. Chen, Y. Xing, Z. Zhang et al., "Coding-in-noise deficits are not seen in responses to amplitude modulation in subjects with cochlear synaptopathy induced by a single noise exposure," *Neuroscience*, vol. 400, pp. 62–71, 2019.

[14] R. Singh and P. Wangemann, "Free radical stress-mediated loss of Kcnj10 protein expression in stria vascularis contributes to deafness in Pendred syndrome mouse model," *American Journal of Physiology Renal Physiology*, vol. 294, no. 1, pp. F139–F148, 2008.

[15] I. E. Royaux, I. A. Belyantseva, T. Wu et al., "Localization and functional studies of pendrin in the mouse inner ear provide insight about the etiology of deafness in pendred syndrome," *Journal of the Association for Research in Otolaryngology*, vol. 4, no. 3, pp. 394–404, 2003.

[16] M. Doi, I. Murai, S. Kunisue et al., "Gpr176 is a Gz-linked orphan G-protein-coupled receptor that sets the pace of circadian behaviour," *Nature Communications*, vol. 7, no. 1, article 10583, 2016.

[17] Care4Rare Canada Consortium, K. D. Kernohan, L. Cigana Schenkel et al., "Identification of a methylation profile for DNMT1-associated autosomal dominant cerebellar ataxia, deafness, and narcolepsy," *Clinical Epigenetics*, vol. 8, no. 1, p. 91, 2016.

[18] Y. Liu, J. Qi, X. Chen et al., "Critical role of spectrin in hearing development and deafness," *Science Advances*, vol. 5, no. 4, article eaav7803, 2019.

[19] S. Gao, C. Cheng, M. Wang et al., "Blebbistatin inhibits neomycin-induced apoptosis in hair cell-like HEI-OC-1 cells and in cochlear hair cells," *Frontiers in Cellular Neuroscience*, vol. 13, p. 590, 2020.

[20] Y. Zhang, W. Li, Z. He et al., "Pre-treatment with fasudil prevents neomycin-induced hair cell damage by reducing the accumulation of reactive oxygen species," *Frontiers in Molecular Neuroscience*, vol. 12, p. 264, 2019.

[21] S. Zhang, Y. Zhang, Y. Dong et al., "Knockdown of Foxg1 in supporting cells increases the trans-differentiation of supporting cells into hair cells in the neonatal mouse cochlea," *Cellular and Molecular Life Sciences: CMLS*, vol. 77, no. 7, pp. 1401–1419, 2020.

[22] F. Qian, X. Wang, Z. Yin et al., "The slc4a2b gene is required for hair cell development in zebrafish," *Aging*, vol. 12, no. 19, pp. 18804–18821, 2020.

[23] H. Zhou, X. Qian, N. Xu et al., "Disruption of Atg7-dependent autophagy causes electromotility disturbances, outer hair cell loss, and deafness in mice," *Cell Death & Disease*, vol. 11, no. 10, p. 913, 2020.

[24] F. Tan, C. Chu, J. Qi et al., "AAV-ie enables safe and efficient gene transfer to inner ear cells," *Nature Communications*, vol. 10, no. 1, p. 3733, 2019.

[25] Z. H. He, S. Y. Zou, M. Li et al., "The nuclear transcription factor FoxG1 affects the sensitivity of mimetic aging hair cells to inflammation by regulating autophagy pathways," *Redox Biology*, vol. 28, p. 101364, 2020.

[26] W. Liu, X. Xu, Z. Fan et al., "Wnt signaling activates TP53-induced glycolysis and apoptosis regulator and protects against cisplatin-induced spiral ganglion neuron damage in the mouse cochlea," *Antioxidants & Redox Signaling*, vol. 30, no. 11, pp. 1389–1410, 2019.

[27] R. Guo, M. Xiao, W. Zhao et al., "2D Ti3C2TxMXene couples electrical stimulation to promote proliferation and neural differentiation of neural stem cells," *Acta Biomaterialia*, 2020.

[28] J. Qi, Y. Liu, C. Chu et al., "A cytoskeleton structure revealed by super-resolution fluorescence imaging in inner ear hair cells," *Cell Discovery*, vol. 5, no. 1, p. 12, 2019.

[29] Z. He, L. Guo, Y. Shu et al., "Autophagy protects auditory hair cells against neomycin-induced damage," *Autophagy*, vol. 13, no. 11, pp. 1884–1904, 2017.

[30] L. Liu, Y. Chen, J. Qi et al., "Wnt activation protects against neomycin-induced hair cell damage in the mouse cochlea," *Cell Death & Disease*, vol. 7, no. 3, article e2136, 2016.

[31] C. Cheng, Y. Wang, L. Guo et al., "Age-related transcriptome changes in Sox2+ supporting cells in the mouse cochlea," *Stem Cell Research & Therapy*, vol. 10, no. 1, p. 365, 2019.

[32] Q. Fang, Y. Zhang, X. Chen et al., "Three-dimensional graphene enhances neural stem cell proliferation through metabolic regulation," *Frontiers in Bioengineering and Biotechnology*, vol. 7, p. 436, 2020.

[33] M. Tang, J. Li, L. He et al., "Transcriptomic profiling of neural stem cell differentiation on graphene substrates," *Colloids and surfaces B: Biointerfaces*, vol. 182, article 110324, 2019.

[34] Y. Zhang, L. Guo, X. Lu et al., "Characterization of Lgr6+ cells as an enriched population of hair cell progenitors compared to Lgr5+ cells for hair cell generation in the neonatal mouse cochlea," *Frontiers in Molecular Neuroscience*, vol. 11, p. 147, 2018.

[35] D. You, L. Guo, W. Li et al., "Characterization of Wnt and Notch-responsive Lgr5+ hair cell progenitors in the striolar region of the neonatal mouse utricle," *Frontiers in Molecular Neuroscience*, vol. 11, p. 137, 2018.

[36] S. Zhang, Y. Zhang, P. Yu et al., "Characterization of Lgr5+ progenitor cell transcriptomes after neomycin injury in the neonatal mouse cochlea," *Frontiers in Molecular Neuroscience*, vol. 10, p. 213, 2017.

[37] C. Cheng, L. Guo, L. Lu et al., "Characterization of the transcriptomes of Lgr5+ hair cell progenitors and Lgr5- supporting cells in the mouse cochlea," *Frontiers in Molecular Neuroscience*, vol. 10, p. 122, 2017.

[38] S. V. Jabba, A. Oelke, R. Singh et al., "Macrophage invasion contributes to degeneration of stria vascularis in Pendred syndrome mouse model," *BMC Medicine*, vol. 4, no. 1, p. 37, 2006.

[39] S. Uderhardt, M. Herrmann, O. V. Oskolkova et al., "12/15-lipoxygenase orchestrates the clearance of apoptotic cells and maintains immunologic tolerance," *Immunity*, vol. 36, no. 5, pp. 834–846, 2012.

[40] T. J. Frederick and S. D. Miller, "Arresting autoimmunity by blocking beta-arrestin 1," *Nature Immunology*, vol. 8, no. 8, pp. 791-792, 2007.

[41] Y. Shi, Y. Feng, J. Kang et al., "Critical regulation of CD4+ T cell survival and autoimmunity by beta-arrestin 1," *Nature Immunology*, vol. 8, no. 8, pp. 817–824, 2007.

[42] L. A. Everett, I. A. Belyantseva, K. Noben-Trauth et al., "Targeted disruption of mouse Pds provides insight about the inner-ear defects encountered in Pendred syndrome," *Human Molecular Genetics*, vol. 10, no. 2, pp. 153–161, 2001.

[43] Z. Su, H. Xiong, Y. Liu et al., "Transcriptomic analysis highlights cochlear inflammation associated with age-related hearing loss in C57BL/6 mice using next generation sequencing," *PeerJ*, vol. 8, article e9737, 2020.

[44] A. Schoe, E. de Jonge, R. J. Klautz, J. T. van Dissel, and E. van de Vosse, "Single-nucleotide polymorphisms in the CALCA gene are associated with variation of procalcitonin concentration in patients undergoing cardiac surgery," *American Journal of Respiratory and Critical Care Medicine*, vol. 194, no. 6, pp. 767–769, 2016.

[45] J. S. Wu, P. Vyas, E. Glowatzki, and P. A. Fuchs, "Opposing expression gradients of calcitonin-related polypeptide alpha (Calca/Cgrpα) and tyrosine hydroxylase (Th) in type II afferent neurons of the mouse cochlea," *The Journal of Comparative Neurology*, vol. 526, no. 3, pp. 425–438, 2018.

[46] C. P. Camacho, S. C. Lindsey, M. C. Melo et al., "Measurement of calcitonin and calcitonin gene-related peptide mRNA

refines the management of patients with medullary thyroid cancer and may replace calcitonin-stimulation tests," *Thyroid*, vol. 23, no. 3, pp. 308–316, 2013.

[47] L. Pacifico, J. F. Osborn, F. Natale, F. Ferraro, M. De Curtis, and C. Chiesa, "Procalcitonin in pediatrics," *Advances in Clinical Chemistry*, vol. 59, pp. 203–263, 2013.

[48] S. L. Yang, S. S. Aw, C. Chang, S. Korzh, V. Korzh, and J. Peng, "Depletion of Bhmt elevates sonic hedgehog transcript level and increases β-cell number in zebrafish," *Endocrinology*, vol. 152, no. 12, pp. 4706–4717, 2011.

[49] J. C. Evans, D. P. Huddler, J. Jiracek et al., "Betaine-homocysteine methyltransferase: zinc in a distorted barrel," *Structure*, vol. 10, no. 9, pp. 1159–1171, 2002.

[50] R. Martínez-Vega, T. Partearroyo, N. Vallecillo, G. Varela-Moreiras, M. A. Pajares, and I. Varela-Nieto, "Long-term omega-3 fatty acid supplementation prevents expression changes in cochlear homocysteine metabolism and ameliorates progressive hearing loss in C57BL/6J mice," *The Journal of Nutritional Biochemistry*, vol. 26, no. 12, pp. 1424–1433, 2015.

[51] T. Partearroyo, N. Vallecillo, M. A. Pajares, G. Varela-Moreiras, and I. Varela-Nieto, "Cochlear homocysteine metabolism at the crossroad of nutrition and sensorineural hearing loss," *Frontiers in Molecular Neuroscience*, vol. 10, p. 107, 2017.

[52] R. Martínez-Vega, F. Garrido, T. Partearroyo et al., "Folic acid deficiency induces premature hearing loss through mechanisms involving cochlear oxidative stress and impairment of homocysteine metabolism," *The FASEB Journal*, vol. 29, no. 2, pp. 418–432, 2015.

[53] T. Partearroyo, S. Murillo-Cuesta, N. Vallecillo et al., "Betaine-homocysteineS-methyltransferase deficiency causes increased susceptibility to noise-induced hearing loss associated with plasma hyperhomocysteinemia," *The FASEB Journal*, vol. 33, no. 5, pp. 5942–5956, 2019.

[54] M. Cohen-Salmon, B. Regnault, N. Cayet et al., "Connexin30 deficiency causes instrastrial fluid-blood barrier disruption within the cochlear stria vascularis," *Proceedings of the National Academy of Sciences of the United States of America*, vol. 104, no. 15, pp. 6229–6234, 2007.

Hindawi
Neural Plasticity
Volume 2021, Article ID 5524381, 9 pages
https://doi.org/10.1155/2021/5524381

Research Article

Identification and Characterization of a Cryptic Genomic Deletion-Insertion in *EYA1* Associated with Branchio-Otic Syndrome

Hao Zheng,[1,2] Jun Xu,[3,4,5] Yu Wang,[1] Yun Lin,[3,4,5] Qingqiang Hu,[1] Xing Li,[1] Jiusheng Chu,[1] Changling Sun,[6] Yongchuan Chai,[3,4,5] and Xiuhong Pang[1]

[1]*Department of Otolaryngology-Head and Neck Surgery, Taizhou People's Hospital, The Fifth Affiliated Hospital of Nantong University & Clinical Hospital of Dalian Medical University, Taizhou, Jiangsu, China*
[2]*Department of Clinical Medicine, Medical School of Nantong University, Nantong, Jiangsu, China*
[3]*Department of Otolaryngology-Head and Neck Surgery, The Ninth People's Hospital, Shanghai Jiaotong University School of Medicine, Shanghai, China*
[4]*Ear Institute, Shanghai Jiaotong University School of Medicine, Shanghai, China*
[5]*Shanghai Key Laboratory of Translational Medicine on Ear and Nose Diseases, Shanghai, China*
[6]*Department of Otolaryngology-Head and Neck Surgery, Affiliated Hospital of Jiangnan University, Wuxi, Jiangsu, China*

Correspondence should be addressed to Changling Sun; winterc126@sina.com, Yongchuan Chai; cycperfect@163.com, and Xiuhong Pang; pxhzxy@163.com

Received 23 February 2021; Accepted 19 March 2021; Published 7 April 2021

Academic Editor: Geng lin Li

Branchio-oto-renal spectrum disorder (BORSD) is characterized by hearing loss accompanied by ear malformations, branchial cysts, and fistulae, with (branchio-oto-renal syndrome (BORS)) or without renal abnormalities (BOS (branchio-otic syndrome)). As the most common causative gene for BORSD, dominant mutations in *EYA1* are responsible for approximately 40% of the cases. In a sporadic deaf patient diagnosed as BOS, we identified an apparent heterozygous genomic deletion spanning the first four coding exons and one 5′ noncoding exon of *EYA1* by targeted next-generation sequencing of 406 known deafness genes. Real-time PCR at multiple regions of *EYA1* confirmed the existence of this genomic deletion and extended its 5′ boundary beyond the 5′-UTR. Whole genome sequencing subsequently located the 5′ and 3′ breakpoints to 19268 bp upstream to the ATG initiation codon and 3180 bp downstream to exon 5. PCR amplification across the breakpoints in both the patient and his parents showed that the genomic alteration occurred *de novo*. Sanger sequencing of this PCR product revealed that it is in fact a GRCh38/hg38:chr8:g.71318554_71374171delinsTGCC genomic deletion-insertion. Our results showed that the genomic variant is responsible for the hearing loss associated with BOS and provided an example for deciphering such cryptic genomic alterations following pipelines of comprehensive exome/genome sequencing and designed verification.

1. Introduction

Branchio-oto-renal spectrum disorder (BORSD) characterized by malformations of the outer, middle, and inner ear associated with conductive, sensorineural, or mixed hearing loss, branchial cysts and fistulas, and renal abnormalities comprises branchio-oto-renal (BOR) syndrome (BOR1: #113650, BOR2: #610896) and branchio-otic syndrome (BOS) (BOS1: #602588, BOS3: #608389) [1, 2], two phenotypes that differ only by the presence or absence of renal abnormalities. BORSD affects about 1 in 40000 children including 2% of profoundly deaf children [3, 4]. Same to other dominant disorders, the offspring of BOR/BOS individuals are at a 50% risk of inheriting the pathogenic variant. Once the pathogenic variant has been identified in an affected family member, prenatal testing for a pregnancy or preimplantation genetic diagnosis (PGD) becomes possible [5, 6].

The known disease-causing genes for BOR/BOS are *EYA1* (#601653; located in 8q13.3), *SIX1* (#601205; located in 14q23.1), and *SIX5* (#600963; located in 19q13.32), in which *EYA1* is the most frequent gene responsible for about 40% of affected patients [7]. *EYA1*, the human homolog of the Drosophila eyes absent gene, acts as a protein phosphatase and transcriptional coactivator [8, 9]. Eya1 homozygous-deficient mice lack ears and kidneys, and Eya1 heterozygous-deficient mice present with phenotypes resembling BOR syndrome [10, 11]. The majority of disease-associated missense mutations cluster in the conserved C-terminal 271-residue Eya domain (ED) of *EYA1* (321-592 residues) [12]. Otherwise, the N-terminal domain of *EYA1* (1-320 residues) is poorly conserved and can attenuate the catalytic activity of Eya to achieve transactivation when bound to a DNA-binding protein [9, 13]. To date, more than 190 mutations in *EYA1* have been found to be associated with BOR/BOS, of which copy number variants (CNVs) account for about 17.1-20% (http://www.hgmd.cf.ac.uk/ac/all.php, last updated in April 2019) [7, 14, 15].

CNVs, DNA segments including deletions, duplications, and complex rearrangements which exceed 1 kb, are a major source of genome diversity in human populations [16, 17] and have been implicated in a variety of human diseases and cancers [18, 19]. Large CNVs, especially the heterozygous ones, however, were hard to be detected by the conventional mutation screening methods such as polymerase chain reaction (PCR) amplification and Sanger sequencing. With the wide application of various genome sequencing technologies, an increasing number of rare CNVs have been found to play a vital role in genetic etiology of hearing loss [20, 21]. But so far, there is no recognized pipeline for the detection of cryptic genomic alterations that are hard to detect by conventional methods.

In this study, we reported how multiple genomic sequencing methods including targeted NGS, real-time PCR, WGS, and Sanger sequencing were applied comprehensively to identify a heterozygous 55618 bp genomic deletion-insertion of *EYA1* gene in a sporadic patient with BOS. This may provide an example for deciphering such cryptic genomic alterations following pipelines of comprehensive exome/genome sequencing and designed verification.

2. Materials and Methods

2.1. Editorial Policies and Ethical Considerations. All subjects in this study gave written, informed consent to participate in this study. Identifying information will not be included in the manuscript unless the information is essential for scientific purposes. This study was approved by the Ethics Committee of Taizhou People's Hospital, the Fifth Affiliated Hospital of Nantong University, and was compliant with the Declaration of Helsinki.

2.2. Subjects and Clinical Examinations. The proband II-1 and his parents (I-1 and I-2) were recruited by the Department of Otolaryngology—Head and Neck Surgery, Taizhou People's Hospital, Jiangsu Province (Figure 1(a)). Comprehensive clinical history was taken, and a detailed physical examination was performed in all subjects with special attentions to audiological, branchial, renal, olfactory, cardiac, ophthalmologic, skeletal, mental, intestinal, and dermatologic abnormalities. The hearing loss was confirmed by otoscopy, pure-tone audiometry (PTA), immittance, distortion product otoacoustic emission (DPOAE), and auditory brainstem response (ABR). The malformation of the middle and inner ear was confirmed by high-resolution CT (HRCT) and magnetic resonance imaging (MRI). Renal abnormalities were excluded by ultrasound and renal function test. Phenotypes of BOS/BOR were evaluated by the diagnostic criteria described previously [7]. Major criteria are branchial anomalies, deafness, preauricular pits, and renal anomalies. Minor criteria are external ear anomalies, middle ear anomalies, inner ear anomalies, preauricular tags, and others, including facial asymmetry and palate abnormalities.

2.3. Targeted NGS of 406 Deafness Genes. Genomic DNA was extracted from the whole blood using the Blood DNA Kit (TIANGEN BIOTECH, Beijing, China). Sequencing of all 406 deafness-related genes was completed by targeted next-generation sequencing (NGS) using the MyGenotics gene enrichment system (Panel1-V4, MyGenotics, Boston, MA, USA) and the Illumina HiSeq 2000 sequencer (Illumina, San Diego, CA, USA) as previously described (Supplementary Table S1) [22]. The reads were aligned to HG19 using the BWA software, and the variants were called using the Genome Analysis Toolkit (GATK), both with the default parameters. The copy numbers of related genes were obtained through CapCNV analysis followed by CNVkit protocol (https://cnvkit.readthedocs.io/en/stable/pipeline.html). SNVs and indels were presented using Variant Call Format (VCF) version 4.1 and annotated using the ANNOVAR software. Data analysis and bioinformatics processing were performed as previously described [22].

Possible pathogenic effect of the missense mutations was evaluated by computational tools including CADD, Exome Variant Server, gnomAD, MutationTaster, PolyPhen-2, 1000 genomes, PhastCons, Phylop, PROVEAN (cut-off score < –2.5), and SIFT (cut-off score < 0.05).

2.4. Real-Time PCR. To verify the existence and explore approximate breakpoint position of the suspected heterozygous genomic deletion related to exons 1-5 in *EYA1* found by targeted NGS of 406 deafness genes (Figure 2(a)), primers were designed in its upstream, middle, and downstream regions, including 5′-end upstream region, noncoding 5′-UTR, exon 2, exon 5, and exon 6 (Figure 2(b)). The primers were designed by the PRIME3 software online (http://frodo.wi.mit.edu/cgi-bin/primer3/primer3_www.cgi). Real-time PCR was performed in the proband, his unaffected parents, and a normal-hearing control on the 7300 Real-Time PCR System (Applied Biosystems) using SYBR® Premix Ex Taq™ (Takara Bio Company). Each reaction was repeated three times and the average Ct was recorded [21].

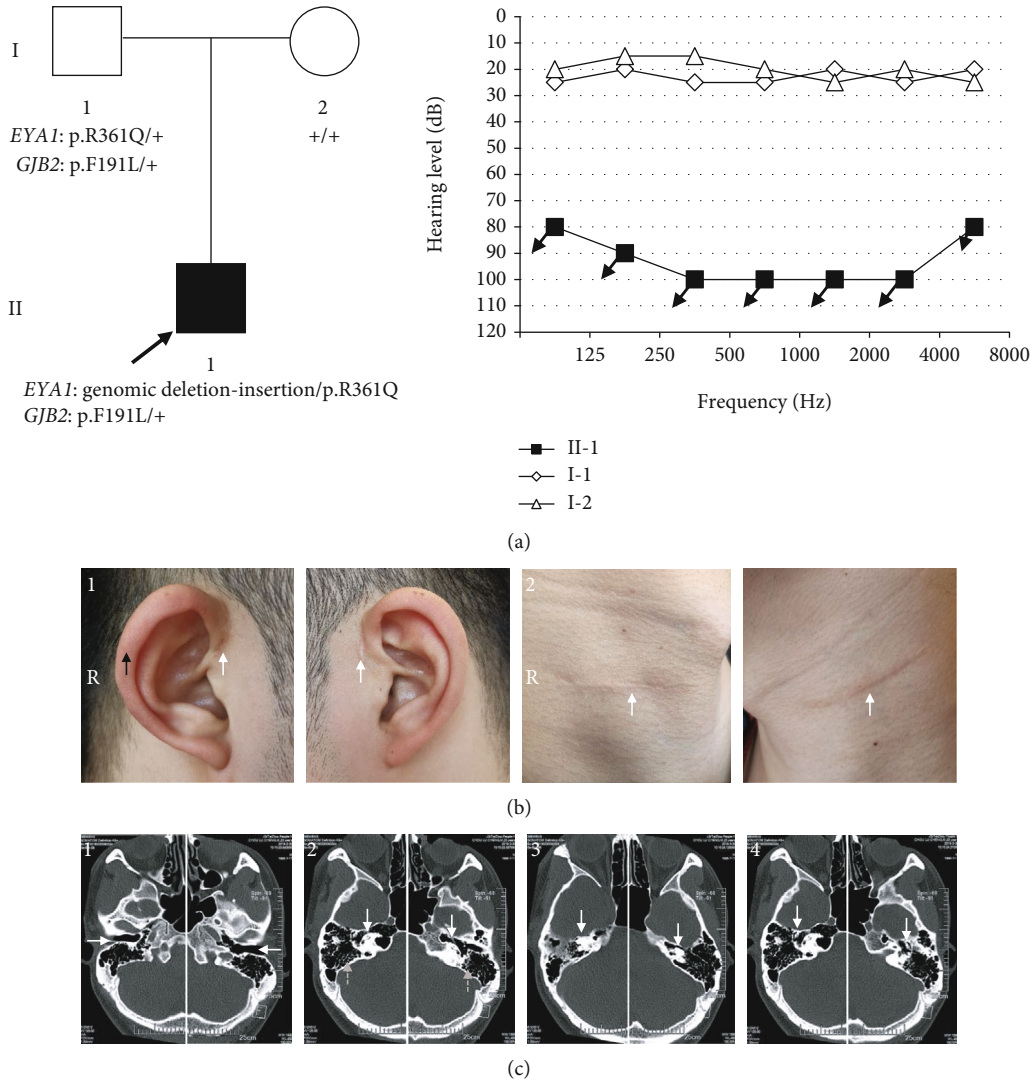

Figure 1: Pedigree, genotype, and phenotype characterization of the family. (a) Pedigree, genotype, and audiograms. Proband II-1 is pointed by the black arrow, and hearing loss is indicated by the black square. The audiograms showed profound sensorineural hearing loss in II-1 and normal hearing loss in his parents. (b) Right cup-shaped outer ear is showed by a black arrow in b1; two white arrows in b1 and b2 indicate bilateral surgical scars of preauricular fistula and cervical branchial cyst, respectively. (c) Findings in temporal HRCT: c1: bilateral lower external auditory canals; c2: white solid and grey dotted arrows indicate cochlear hypoplasia and overgasification of mastoid cells, respectively; c3: malformed semicircular canal; c4: deformed ossicular chain.

2.5. Whole Genome Sequencing. To judge whether the heterozygous deletion involved upstream genes or not and search for the exact breakpoint position of 5′- and 3′-end, whole genome sequencing was selected (Figure 2(c)). Paired-end DNA libraries were prepared according to the manufacturer's instructions (Illumina TruSeq Library Construction). DNA libraries were sequenced on Illumina HiSeq X according to the manufacturer's instructions for paired-end 150 bp reads. The average sequencing depth ranged from 31.35 to 57.77, and 90.1% to 99.2% of whole genome were covered at least 20. Reads (without barcode) were aligned to HG19 using SpeedSeq. Single nucleotide variants, insertions, deletions, and indels calling were performed using Genome Analysis Toolkit v2.1. Structure variants and copy number variants were analyzed in SpeedSeq. Annotations of single nucleotide variants, indels, structure variants, and copy number variants were performed with ANNOVAR [23].

2.6. Sanger Sequencing. To verify the results of WGS, a single PCR amplification was performed in the proband across the break junction (Figure 2(d)). The exact break junction and additional insertion were identified by sequencing of this PCR product. The same PCR amplification was used to detect the novel CNV in unaffected parents and a normal-hearing control (forward primer F1: 5′-ATCTGTGGCCC CCAAATACTTC-3′; reverse primer R1: 5′-AGGTCCT CTGCCCATTATTTGA-3′; PCR product size: 244 bp) (Figure 2(d)). In addition, a second PCR was performed

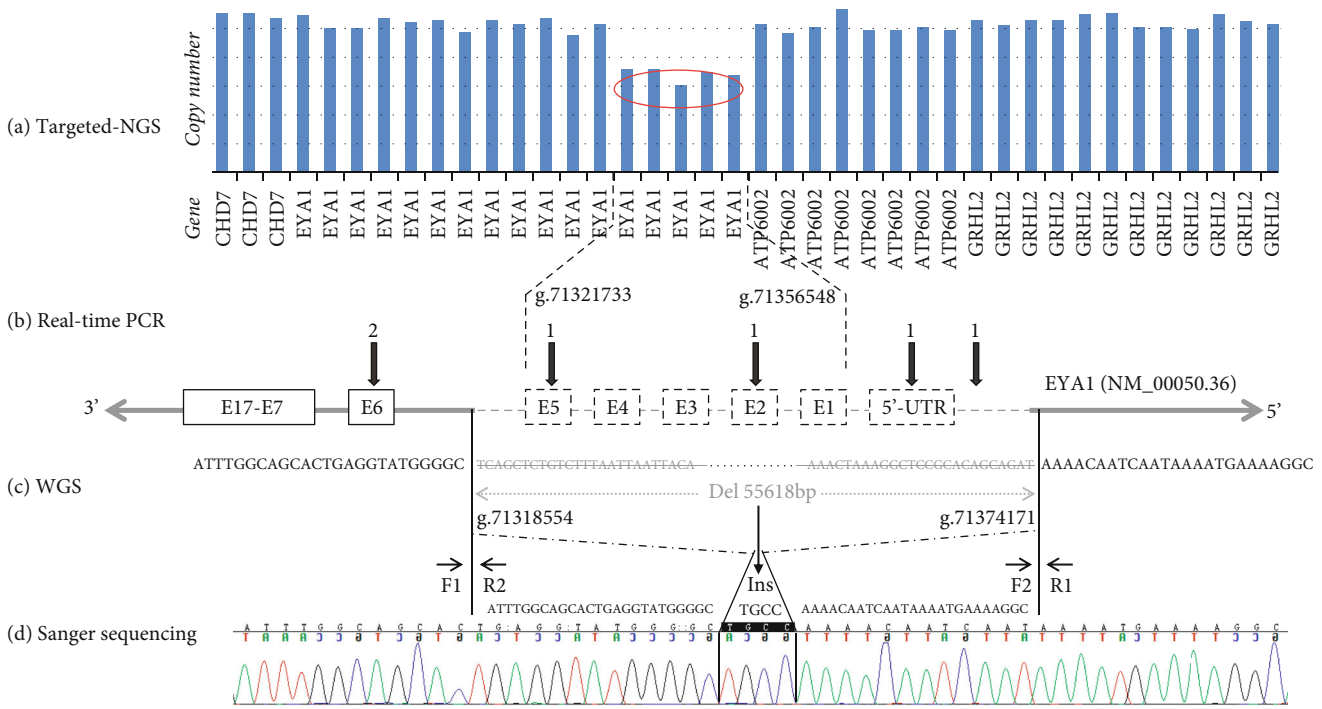

Figure 2: The process of identifying CNV. (a) The red oval indicates the region of deletion detected by targeted NGS. (b) Results of real-time PCR: 1 and 2 indicate copy number; black arrows: primer position; E: exon; left grey arrow: the 3′-end; right grey arrow: the 5′-end. (c) Grey words: region of deletion; F and R: forward and reverse primer; Ins: insertion. (d) Sequence diagram of 244 bp PCR product. 4 bases between the two black vertical lines were additional insertion.

to amplify across the 5′ breakpoint from the wild-type allele (forward primer F2: 5′-TTAGACCAGACACAAA AGCAACTCC-3′; reverse primer R1: 5′-AGGTCCTCT GCCCATTATTTGA-3′; PCR product size: 364 bp) (Figure 2(d)), and a third PCR was performed to amplify across the 3′ breakpoint from the wild-type allele (forward primer F1: 5′-ATCTGTGGCCCCCAAATACTTC-3′; reverse primer R2: 5′-AGAAAGGGATTTTCTAAAGCCATCA-3′; PCR product size: 559 bp) (Figure 2(d)). The CNV was determined as heterozygous if all PCR products were amplified and as homozygous if only the 244 bp but not the 364 bp and 559 bp products were amplified. No CNV was detected when only 364 bp and 559 bp were amplified. This CNV was subsequently screened in 400 ethnically matched normal controls (data not shown) and excluded benign CNV listing in the Database of Genomic Variants (http://dgv.tcag.ca/dgv/app/about?ref=).

3. Results

3.1. Clinical Characteristics. The sporadic patient II-1 was found with bilateral congenital profound sensorineural hearing loss (Figure 1(a)), right cup-shaped outer ear, bilateral old surgical scars of congenital preauricular fistula, and cervical branchial cysts (Figure 1(b)). Bilateral lower external auditory canals, enlarged middle ear cavity, overgasification of mastoid cells, malformed ossicular chain, cochlear hypoplasia in immature apical turn and absence of the middle turn, malformed semicircular canals, and abnormal internal auditory canals were found by temporal bone HRCT (Figure 1(c)). Renal and other abnormalities were excluded after a series of detailed clinical examinations.

3.2. Screening for All Known Deafness Genes by Targeted NGS. Five heterozygous variants were submitted by targeted NGS of 406 known deafness genes in this patient: a genomic deletion spanning coding exon 2-6 in *EYA1* (GRCh38/h38: chr8: 71321733-71356548) (Figure 2(a)), c.1082G>A (p.Arg361Gln) in *EYA1* (NM_000503.6), c.571T>C (p.Phe191Leu) in *GJB2* (NM_004004.6), c.2575C>G (p.Gln859Glu) in *TCOF1* (NM_001135243), and c.685T>C (p.Tyr229His) in *KARS* (NM_001130089) (Figure 3). Possible pathogenic effect of the missense mutations was evaluated by computational tools (Table 1). Variants p.Arg361Gln (rs145219836) in *EYA1* and p.Phe191Leu (rs397516878) in *GJB2* were proved to be inherited from his unaffected father, while p.Gln859Glu (rs201043592) in *TCOF1* and p.Tyr229-His (rs150529876) in *KARS* were from his unaffected mother (Figure 3 and Table 1).

3.3. Verify the Existence of the Deletion by Real-Time PCR. To verify if the genomic deletion found by targeted NGS existed or not, the DNA segments in 5′-upstream region, 5′-UTR, exon 2, exon 5, and exon 6 were detected quantitatively, and their copy numbers were 1, 1, 1, 1, and 2, respectively (Figure 2(b)). The genomic deletion was proved to exist and its 3′-end breakpoint located within exon 5-exon 6. But where the 5′-end breakpoint was and whether the

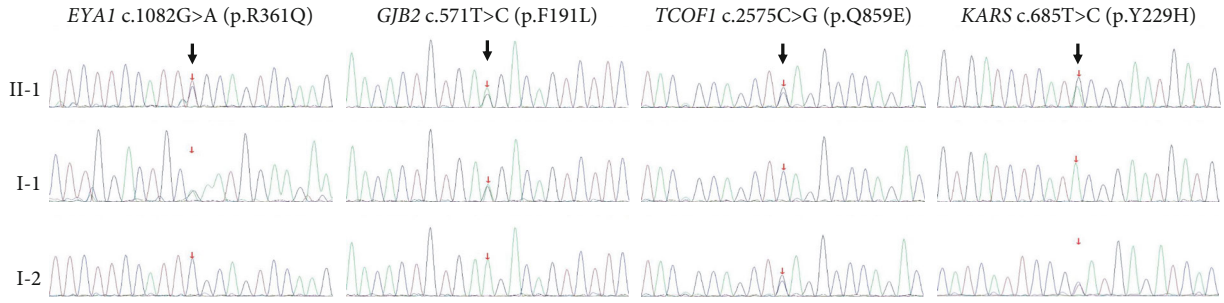

Figure 3: Sequencing diagram of 4 missense variants in patient II-1, unaffected parents I-1/I-2. Black arrow: changed base position.

deletion involved upstream genes or not need further exploration.

3.4. Breakpoints of the Deletion Identified by WGS. To explore where the 5′-end breakpoint was and whether the deletion involved upstream genes or not, WGS was selected. 55618 bp genomic deletion located in chromosome 8q13.3 was identified from g.71318554 to g.71374171 (19268 bp upstream to initiation codon ATG and 3180 bp downstream to exon 5), which involved 5′ upstream, noncoding 5′-UTR and exon 1, coding exons 2-5, intron 1-4, and partial intron 5 (Figure 2(c)).

3.5. True Genomic CNV Was Identified by Sanger Sequencing. The breakpoints detected by WGS were verified exactly the same by amplification of the 244 bp product across 5′ and 3′ breakpoints. Notably, an additional 4 bp insertion not detected by WGS was identified by Sanger sequencing. So a novel deletion-insertion variant GRCh38/hg38:chr8:g.71318554_71374171delinsTGCC spanned 5′-UTR, exons 1 to 5, was identified in our study (Figure 2(d)). 559 bp and 364 bp products amplified successfully suggested that the deletion-insertion variant was a heterozygous one. Meanwhile, these three fragments (559 bp, 364 bp, and 244 bp) also amplified in unaffected parents and one normal-hearing control, only fragments of 559 bp and 364 bp but 244 bp amplified successfully in them (Figure 4).

Moreover, the novel deletion-insertion variant in *EYA1* was not found in 400 ethnically matched normal controls and was ruled out as a benign CNV listed in the Database of Genomic Variants (DGV, http://dgv.tcag.ca/dgv/app/about?ref=).

4. Discussion

Hearing loss is one of the major disabilities worldwide, which is often induced by loss of sensory hair cells in the inner ear cochlea [24–28]. Hearing loss could be caused by genetic factors, aging, chronic cochlear infections, infectious diseases, ototoxic drugs, and noise exposure [29–37]; and genetic factors account for more than 60% of hearing loss. According to phenotypes of BOS/BOR evaluated by the diagnostic criteria described previously [7], BOS was diagnosed in our sporadic patient with three major criteria of branchial anomaly, deafness, and preauricular pits and three minor criteria of external, middle, and inner ear anomalies. In contrast to the deformities of the ear reported in a previous study which showed atresia or stenosis in the external auditory canal, reduction in size of the middle ear space and hypoplastic mastoid cells [2], enlarged middle ear cavity, and overgasification of mastoid cells were discovered in our study (Figure 1(c)). In addition, the lower position of bilateral external auditory canals was first reported. High heterogeneity of phenotypes in BOR spectrum disease was further confirmed by our findings [7].

A heterozygous missense variant p.Arg361Gln and a genomic CNV GRCh38/hg38:chr8:g.71318554_71374171delins TGCC in *EYA1* were identified simultaneously in our study. The former was suggested to be a nonpathogenic variant due to inheriting from his phenotypically normal father and benign predicted result of PolyPhen-2, PROVEAN, and SIFT (Figures 1 and 3, Table 1). The latter, a novel genomic deletion-insertion variant spanned 5′-UTR, exons 1 to 5, involving 5′-UTR and N-terminal domain, was very likely to be a pathogenic mutation, due to it being not found in his phenotypically normal parents (Figure 4) and 400 ethnically matched normal controls, and was ruled out as a benign CNV listed in the DGV. *De novo* mutation was proved by the parental origin of variants p.Arg361Gln in *EYA1*, p.Phe191Leu in *GJB2*, p.Gln859Glu (rs201043592) in *TCOF1*, and p.Tyr229His in *KARS* (Figures 1 and 3, Table 1). This result further proved previous opinion about high *de novo* rate in *EYA1* [38].

To date, two pathogenic mutations c.241C>T (p.Gln81Ter) and c.229C>T (p.Arg77Ter) (NM_000503.6) involving exons 1-5 are reported in previous study. They are predicted to be pathogenic due to loss of function from truncated or absent protein (https://www.ncbi.nlm.nih.gov/clinvar/variation). These two pathogenic mutations were included in the range of the novel genomic CNV discovered in our study. Haploinsufficiency seems to be the most likely explanation for BOR-related phenotypes in cases with nonsense and large deletions leading to similar disease phenotypes [39, 40]. In addition, the presence of the N-terminal domain significantly attenuates the phosphatase activity of Eya [9]. It has been proposed that the ED domain of Eya acts as an autoinhibitor of the transactivation potential of the N-terminal domain [41]. A decreased ability in binding to special proteins of N-terminal domain caused by haploinsufficiency led to a decline in transactivation of EYA1, which was very likely the pathogenic mechanism of the genomic deletion-insertion mutation identified in our study [9, 13].

Table 1: Pathogenic prediction by computational tools.

Gene	Mutation	CADD-phred	Exome Variant Server	gnomAD	1000G	MutationTaster	PhastCons scores*	Phylop score†	PolyPhen-2 (HumVar score)	PROVEAN (score)‡	SIFT (score)§	Origin
EYA1	p.Arg361Gln c.1082G>A rs145219836	26.7	Not present	0.0005	0.0002	Disease causing (0.999)	0.995	6.162	Benign (0.123)	Neutral (-1.86)	Tolerated (0.114)	I-1
GJB2	p.Phe191Leu c.571T>C rs397516878	27.0	Not present	0.000149	0.0002	Disease causing (0.999)	1	5.159	Possibly damaging (1)	Deleterious (-5.72)	Damaging (0.006)	I-1
TCOF1	p.Q859E c.2575C>G rs201043592	11.16	Not present	0.000107	0.0005	Polymorphism	0.139	1.479	Benign (0.301)	Neutral (-1.56)	Damaging (0.046)	I-2
KARS	p.Y229H c.685T>C rs150529876	15.34	Not present	0.001161	0.0032	Polymorphism	0.006	-0.014	Benign (0.275)	Neutral (0.36)	Tolerated (0.593)	I-2

Note: *The values vary between 0 and 1; the closer the value is to 1, the more probable the nucleotide is conserved. †The values between -14 and +6, sites predicted to be conserved are assigned positive scores, while sites predicted to be fast evolving are assigned negative scores. ‡Negative and positive scores indicate deleterious and neutral, respectively, with cut-off score set at -2.5. §The value ranges from 0 (deleterious) to 1 (neutral) with cut-off score set at 0.05.

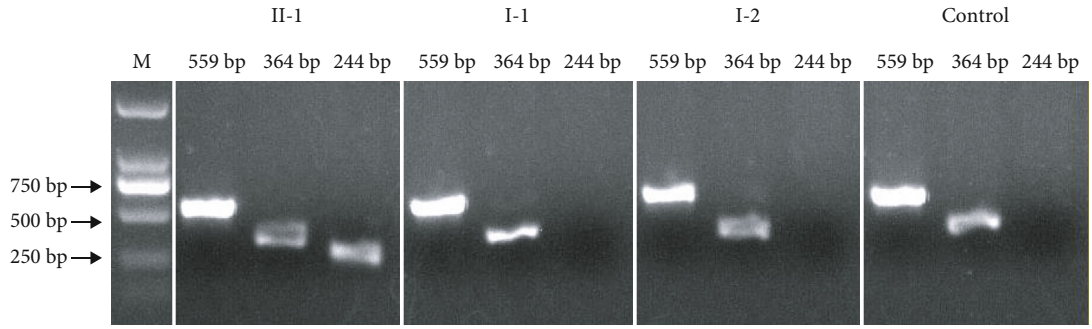

Figure 4: Electrophoresis gel figure of 244 bp, 364 bp, and 559 bp PCR product in patient II-1, unaffected parents I-1/I-2, and control. M: marker.

So far, no specialized detection scheme was considered reasonable for rapid and economical detection of cryptic genomic CNVs. In our study, by applying multiple genomic testing methods step by step to identify a potential heterozygous genomic CNV (Figure 2), a rational pipeline for detecting cryptic genomic CNVs appeared to have been successfully established. Since most of the pathogenic mutations are located in the coding region and its flanking sequences and the cost of targeted NGS and WES is relatively lower than that of WGS, researchers often choose one of them to search for pathogenic mutations first. A potential heterozygous genomic deletion involving exon 1-exon 5 of *EYA1* was reported by targeted NGS (Figure 2(a)). To verify whether the deletion existed and the range of 5′- and 3′-end breakpoints, real-time PCR was considered as the preferred method for quantification [21]. Unfortunately, while confirming the presence of the deletion, 5′-end breakpoint region could not be evaluated by real-time PCR (Figure 2(b)). Considering economy, accuracy, time, and manpower saving, WGS was selected to detect the exact breakpoints. Encouragingly, the position of 5′- and 3′-end breakpoints detected by WGS was proved perfectly accurate by Sanger sequencing (Figures 2(c) and 2(d)). However, if there was no verification by Sanger sequencing, the "TGCC" insertion that WGS failed to detect would have been missed (Figure 2(d)). In the process of detection, we discovered that all molecular detection methods applied above had their own special advantages and disadvantages; reasonable and comprehensive application of them was of great significance for the efficient detection of cryptic heterozygous genomic CNV. Targeted NGS and WES only detected exons and their flanking sequences, but not noncoding regions, so they can only provide clues for the possible existence of CNVs. Fortunately, due to no restriction on the region of primers for quantitative detection, real-time PCR can well make up for the defects of targeted NGS and WES and can confirm the existence of CNV and the range of its breakpoints no matter in coding or noncoding regions. When the region of CNV breakpoints cannot be determined, WGS can be selected to find the breakpoints accurately in the genomic level. However, given that the read length of WGS is about 150-200 bp, short fragment may be missed for complex CNVs, such as deletion-insertion. As the most accurate sequencing technology, Sanger sequencing can detect each base missed by WGS in targeted amplified region and thus dig out the true genomic CNVs. So we suggested that the reasonable application of the above sequencing methods step by step can be used as a pipeline for detection of cryptic genomic CNVs in our future work.

According to the parental origin and pathogenic prediction of computational tools, missense p.Arg361Gln in *EYA1*, p.Gln859Glu (rs201043592) in *TCOF1*, and p.Tyr229His in *KARS* were considered as benign variants (Figures 1 and 3, Table 1). Although p.Phe191Leu in *GJB2* was listed as uncertain significance in ClinVar (https://www.ncbi.nlm.nih.gov/clinvar), it was regarded as a recessive inherited pathogenic one in our daily counseling work according to functional study [42]. Unfortunately, biallelic pathogenic mutations c.235delC and c.176_191del of *GJB2* were identified in his girlfriend with nonsyndromic profound hearing loss. According to the law of autosomal recessive inheritance, the offspring of the proband and his girlfriend is at a 50% risk of inheriting biallelic pathogenic variants of *GJB2*. To *EYA1*, also 50% of their offspring should be affected with BOR spectrum diseases in an autosomal dominant way. Therefore, it was of great significance to identify the genetic pathogenic factors for them, which provides a theoretical basis for prenatal diagnosis or PGD to get healthy offspring. Given that the chance of conceiving healthy offspring naturally was only 25%, we suggested that PGD technology was their best choice.

5. Conclusion

In conclusion, a novel heterozygous *de novo* genomic deletion-insertion in *EYA1*, GRCh38/hg38:chr8:.71318554_71374171delinsTGCC, was very likely the pathogenic cause for the patient with BOS due to a decline in transactivation of EYA1 resulting from haploinsufficiency. Through genetic counseling, the disease from *EYA1* and *GJB2* in the offspring of the patient can be avoided in the process of subsequent reproduction. Our results provided an example for deciphering such cryptic genomic alterations following pipelines of comprehensive exome/genome sequencing and designed verification.

Data Availability

All the sequencing data supporting the conclusions of the study can be obtained by contacting Xiuhong Pang via email (pxhzxy@163.com).

Conflicts of Interest

The authors declare no conflict of interest.

Authors' Contributions

XP, YC, and CS conceived and designed the experiments. HZ, JX, YL, and YW performed the experiments. XP, YC, HZ, and CS analyzed the data. XP, QH, XL, and JC collected the samples and reviewed the phenotypes. HZ and XP wrote the paper. All authors reviewed the manuscript. Hao Zheng, Jun Xu, and Yu Wang contributed equally to this work and share first authorship.

Acknowledgments

We would like to thank the family for agreeing to include their details. The Government of China is also acknowledged for providing research grant. This research was supported by grants from the National Natural Science Foundation of China (81700920 to X.P.), the Natural Science Foundation of Jiangsu Province (BK20191229 to X.P.), the Fifth "333 Project" Scientific Research Foundation of Jiangsu Province (BRA2019192 to X.P.), the Medical Scientific Research Project from Health and Family Planning Commission of Jiangsu Province (H201666 to X.P.), the Science and Technology Commission of Shanghai Municipality (14DZ2260300 to Y.C.), and the Medical Top-Notch Young Talents Program of Wuxi (BJ2020043 to C.S.).

Supplementary Materials

Supplementary Table S1: 406 causative genes for deafness were screened by targeted NGS. *(Supplementary Materials)*

References

[1] A. Kochhar, S. M. Fischer, W. J. Kimberling, and R. J. Smith, "Branchio-oto-renal syndrome," *American Journal of Medical Genetics. Part A*, vol. 143A, no. 14, pp. 1671–1678, 2007.

[2] R. J. H. Smith, *Branchiootorenal spectrum disorder*, M. P. Adam, H. H. Ardinger, R. A. Pagon, S. E. Wallace, and B. LJH, Eds., GeneReviews((R)), Seattle (WA), 1993.

[3] F. C. Fraser, J. R. Sproule, F. Halal, and J. M. Optiz, "Frequency of the branchio-oto-renal (BOR) syndrome in children with profound hearing loss," *American Journal of Medical Genetics*, vol. 7, no. 3, pp. 341–349, 1980.

[4] C. Stinckens, L. Standaert, J. W. Casselman et al., "The presence of a widened vestibular aqueduct and progressive sensorineural hearing loss in the branchio-oto-renal syndrome. A family study," *International Journal of Pediatric Otorhinolaryngology*, vol. 59, no. 3, pp. 163–172, 2001.

[5] S. Kumar, K. Deffenbacher, C. W. R. J. Cremers, G. van Camp, and W. J. Kimberling, "Branchio-oto-renal syndrome: identification of novel mutations, molecular characterization, mutation distribution, and prospects for genetic testing," *Genetic Testing*, vol. 1, no. 4, pp. 243–251, 1997.

[6] T. Matsunaga, M. Okada, S. Usami, and T. Okuyama, "Phenotypic consequences in a Japanese family having branchio-oto-renal syndrome with a novel frameshift mutation in the gene EYA1," *Acta Otolaryngol*, vol. 127, no. 1, pp. 98–104, 2007.

[7] E. H. Chang, M. Menezes, N. C. Meyer et al., "Branchio-oto-renal syndrome: the mutation spectrum in EYA1 and its phenotypic consequences," *Human Mutation*, vol. 23, no. 6, pp. 582–589, 2004.

[8] P. X. Xu, J. Cheng, J. A. Epstein, and R. L. Maas, "Mouse Eya genes are expressed during limb tendon development and encode a transcriptional activation function," *Proceedings of the National Academy of Sciences of the United States of America*, vol. 94, no. 22, pp. 11974–11979, 1997.

[9] J. P. Rayapureddi and R. S. Hegde, "Branchio-oto-renal syndrome associated mutations in eyes absent 1 result in loss of phosphatase activity," *FEBS Letters*, vol. 580, no. 16, pp. 3853–3859, 2006.

[10] P. X. Xu, J. Adams, H. Peters, M. C. Brown, S. Heaney, and R. Maas, "Eya1-deficient mice lack ears and kidneys and show abnormal apoptosis of organ primordia," *Nature Genetics*, vol. 23, no. 1, pp. 113–117, 1999.

[11] P. X. Xu, W. Zheng, C. Laclef et al., "Eya1 is required for the morphogenesis of mammalian thymus, parathyroid and thyroid," *Development*, vol. 129, no. 13, pp. 3033–3044, 2002.

[12] S. Abdelhak, V. Kalatzis, R. Heilig et al., "Clustering of mutations responsible for branchio-oto-renal (BOR) syndrome in the eyes absent homologous region (eyaHR) of EYA1," *Human Molecular Genetics*, vol. 6, no. 13, pp. 2247–2255, 1997.

[13] K. Ikeda, Y. Watanabe, H. Ohto, and K. Kawakami, "Molecular interaction and synergistic activation of a promoter by Six, Eya, and Dach proteins mediated through CREB binding protein," *Molecular and Cellular Biology*, vol. 22, no. 19, pp. 6759–6766, 2002.

[14] E. Razmara, F. Bitarafan, E. Esmaeilzadeh-Gharehdaghi, N. Almadani, and M. Garshasbi, "The first case of NSHL by direct impression on *EYA1* gene and identification of one novel mutation in *MYO7A* in the Iranian families," *Iranian Journal of Basic Medical Sciences*, vol. 21, no. 3, pp. 333–341, 2018.

[15] Y. H. Ahn, C. Lee, N. K. D. Kim et al., "Targeted exome sequencing provided comprehensive genetic diagnosis of congenital anomalies of the kidney and urinary tract," *Journal of Clinical Medicine*, vol. 9, no. 3, p. 751, 2020.

[16] L. Feuk, A. R. Carson, and S. W. Scherer, "Structural variation in the human genome," *Nature Reviews. Genetics*, vol. 7, no. 2, pp. 85–97, 2006.

[17] The 1000 Genomes Project Consortium, P. H. Sudmant, T. Rausch et al., "An integrated map of structural variation in 2,504 human genomes," *Nature*, vol. 526, no. 7571, pp. 75–81, 2015.

[18] C. T. Watson, M. B. Tomas, A. J. Sharp, and H. C. Mefford, "The genetics of microdeletion and microduplication syndromes: an update," *Annual Review of Genomics and Human Genetics*, vol. 15, no. 1, pp. 215–244, 2014.

[19] S. Girirajan, C. D. Campbell, and E. E. Eichler, "Human copy number variation and complex genetic disease," *Annual Review of Genetics*, vol. 45, no. 1, pp. 203–226, 2011.

[20] X. Pang, Y. Chai, L. He et al., "A 7666-bp genomic deletion is frequent in Chinese Han deaf patients with non-syndromic enlarged vestibular aqueduct but without bi-allelic *SLC26A4* mutations," *International Journal of Pediatric Otorhinolaryngology*, vol. 79, no. 12, pp. 2248–2252, 2015.

[21] X. Pang, H. Luo, Y. Chai et al., "A 1.6-Mb microdeletion in chromosome 17q22 leads to NOG-related symphalangism spectrum disorder without intellectual disability," *PLoS One*, vol. 10, no. 3, article e0120816, 2015.

[22] L. He, X. Pang, H. Liu, Y. Chai, H. Wu, and T. Yang, "Targeted next-generation sequencing and parental genotyping in sporadic Chinese Han deaf patients," *Clinical Genetics*, vol. 93, no. 4, pp. 899–904, 2018.

[23] Z. Cen, Z. Jiang, Y. Chen et al., "Intronic pentanucleotide TTTCA repeat insertion in the SAMD12 gene causes familial cortical myoclonic tremor with epilepsy type 1," *Brain*, vol. 141, no. 8, pp. 2280–2288, 2018.

[24] Y. Liu, J. Qi, X. Chen et al., "Critical role of spectrin in hearing development and deafness," *Science Advances*, vol. 5, no. 4, article eaav7803, 2019.

[25] Y. Wang, J. Li, X. Yao et al., "Loss of CIB2 causes profound hearing loss and abolishes mechanoelectrical transduction in mice," *Frontiers in Molecular Neuroscience*, vol. 10, p. 401, 2017.

[26] J. Qi, Y. Liu, C. Chu et al., "A cytoskeleton structure revealed by super-resolution fluorescence imaging in inner ear hair cells," *Cell Discovery*, vol. 5, no. 1, p. 12, 2019.

[27] Z. H. He, S. Y. Zou, M. Li et al., "The nuclear transcription factor FoxG1 affects the sensitivity of mimetic aging hair cells to inflammation by regulating autophagy pathways," *Redox Biology*, vol. 28, p. 101364, 2020.

[28] J. Qi, L. Zhang, F. Tan et al., "Espin distribution as revealed by super-resolution microscopy of stereocilia," *American Journal of Translational Research*, vol. 12, no. 1, pp. 130–141, 2020.

[29] C. Zhu, C. Cheng, Y. Wang et al., "Loss of ARHGEF6 causes hair cell stereocilia deficits and hearing loss in mice," *Frontiers in Molecular Neuroscience*, vol. 11, p. 362, 2018.

[30] S. Gao, C. Cheng, M. Wang et al., "Blebbistatin inhibits neomycin-induced apoptosis in hair cell-like HEI-OC-1 cells and in cochlear hair cells," *Frontiers in Cellular Neuroscience*, vol. 13, 2020.

[31] Y. Zhang, W. Li, Z. He et al., "Pre-treatment with fasudil prevents neomycin-induced hair cell damage by reducing the accumulation of reactive oxygen species," *Frontiers in Molecular Neuroscience*, vol. 12, p. 264, 2019.

[32] F. Qian, X. Wang, Z. Yin et al., "The *slc4a2b* gene is required for hair cell development in zebrafish," *Aging (Albany NY)*, vol. 12, no. 19, pp. 18804–18821, 2020.

[33] H. Zhou, X. Qian, N. Xu et al., "Disruption of Atg7-dependent autophagy causes electromotility disturbances, outer hair cell loss, and deafness in mice," *Cell Death & Disease*, vol. 11, no. 10, p. 913, 2020.

[34] C. Cheng, Y. Wang, L. Guo et al., "Age-related transcriptome changes in Sox2+ supporting cells in the mouse cochlea," *Stem Cell Research & Therapy*, vol. 10, no. 1, p. 365, 2019.

[35] Z. He, L. Guo, Y. Shu et al., "Autophagy protects auditory hair cells against neomycin-induced damage," *Autophagy*, vol. 13, no. 11, pp. 1884–1904, 2017.

[36] W. Liu, X. Xu, Z. Fan et al., "Wnt signaling activates TP53-induced glycolysis and apoptosis regulator and protects against cisplatin-induced spiral ganglion neuron damage in the mouse cochlea," *Antioxidants & Redox Signaling*, vol. 30, no. 11, pp. 1389–1410, 2019.

[37] Y. Zhang, S. Zhang, Z. Zhang et al., "Knockdown of *Foxg1* in Sox9+ supporting cells increases the trans-differentiation of supporting cells into hair cells in the neonatal mouse utricle," *Aging (Albany NY)*, vol. 12, no. 20, pp. 19834–19851, 2020.

[38] T. L. Stockley, R. Mendoza-Londono, E. J. Propst, S. Sodhi, L. Dupuis, and B. C. Papsin, "A recurrent EYA1 mutation causing alternative RNA splicing in branchio-oto-renal syndrome: implications for molecular diagnostics and disease mechanism," *American Journal of Medical Genetics. Part A*, vol. 149A, no. 3, pp. 322–327, 2009.

[39] N. Huang, I. Lee, E. M. Marcotte, and M. E. Hurles, "Characterising and predicting haploinsufficiency in the human genome," *PLoS Genetics*, vol. 6, no. 10, article e1001154, 2010.

[40] P. D. Brophy, F. Alasti, B. W. Darbro et al., "Genome-wide copy number variation analysis of a branchio-oto-renal syndrome cohort identifies a recombination hotspot and implicates new candidate genes," *Human Genetics*, vol. 132, no. 12, pp. 1339–1350, 2013.

[41] S. J. Silver, E. L. Davies, L. Doyon, and I. Rebay, "Functional dissection of eyes absent reveals new modes of regulation within the retinal determination gene network," *Molecular and Cellular Biology*, vol. 23, no. 17, pp. 5989–5999, 2003.

[42] C. Ambrosi, A. E. Walker, A. D. DePriest et al., "Analysis of trafficking, stability and function of human connexin 26 gap junction channels with deafness-causing mutations in the fourth transmembrane helix," *PLoS One*, vol. 8, no. 8, article e70916, 2013.

Hindawi
Neural Plasticity
Volume 2021, Article ID 5517209, 8 pages
https://doi.org/10.1155/2021/5517209

Research Article

Evaluation of Clinical Graded Treatment of Acute Nonsuppurative Otitis Media in Children with Acute Upper Respiratory Tract Infection

Wei Meng, Dong-Dong Huang, Guang-Fei Li, Zi-Hui Sun, and Shuang-Ba He

Department of Otorhinolaryngology Head and Neck Surgery, Nanjing Tongren Hospital, School of Medicine, Southeast University Nanjing, China

Correspondence should be addressed to Shuang-Ba He; hesb@njtrh.org

Received 11 January 2021; Revised 23 February 2021; Accepted 12 March 2021; Published 5 April 2021

Academic Editor: Geng lin Li

Objective. To treat children with acute nonsuppurative otitis media induced by acute upper respiratory tract infection of varying severity and evaluate its therapeutic effects. *Materials and Methods*. Patients from the emergency department with acute nonsuppurative otitis media were followed up between September 2015 and December 2018. A total of 420 patients were classified into grades I to III according to tympanic membrane intactness and systemic reactions and treated according to grading. *Results*. Grade I patients showed no significant difference in the recovery of acute symptoms whether antibiotics are used or not. Grade II patients, after 3 months of follow-up, showed no tympanic membrane perforation, and 9 cases of binaural B-type children did not improve but were cured by operation. In grade III patients, after treatment for 4 hours in the experimental group 3, the earache subsided, 1 case had tympanic membrane perforation, and the patients recovered after 2 weeks (64/92) and after 3 months (28/92) of drug treatment. After treatment for 4 h in the control group 3, the earache eased, and 3 patients developed tympanic membrane perforation and were treated for 3 months. 4 binaural B-type children did not improve but recovered after surgical treatment. *Conclusion*. Grade I patients could be closely followed up by clinical observation. For anti-inflammatory patients with grade II disease, treatment has therapeutic significance. For patients with grade III, some patients still have TMP, but the use of cephalosporin third-generation drugs plus an appropriate amount of hormone therapy is effective in reducing symptoms and tympanic local reactions.

1. Introduction

Acute otitis media (AOM) is one of the most common diseases in children in the otolaryngology department. AOM is an infection of the mucosa in the middle ear cavity caused by bacteria and/or viruses, directly entering the tympanum through the eustachian tube and is usually followed by a common cold [1]. AOM is more common in children between the ages of 6 months and 3 years. The three most common bacterial infections are *Streptococcus pneumoniae* (25-50%), *Haemophilus influenzae* (15-30%), and *Moraxella catarrhalis* (3-20%). AOM is classified into acute nonsuppurative otitis media and acute suppurative otitis media. Acute nonsuppurative otitis media refers to the tubal pharynx, mouth, and cartilage segments, inflammatory mucosal hyperemia, swelling, and congestion after acute upper respiratory tract infection and may be accompanied by bacteria or viruses via the eustachian tube, directly into the middle ear cavity, resulting in an inflammatory reaction in the middle ear mucosa. In the early acute inflammatory stage, it is accompanied by changes in the tympanic membrane and inflammatory serous or mucous exudation changes in the middle ear cavity in the late stage. The disease often coexists with upper respiratory tract infection and can include recurrent attacks, sudden onset, and one or more symptoms. The symptoms of acute nonsuppurative otitis media are mainly local symptoms, such as ear pain which is persistent and can be characterized by irritability, sometimes covering and pulling ears, most often affecting sleep. Only those having an upper respiratory tract infection in the early stage can

present with fever. Signs seen in the early stage are mild congestion, depression of the tympanic membrane, and deformation of the light cone. Tympanic effusion shows a dull, pale yellow, or amber, tympanic membrane sometimes with an arc-shaped liquid level line. Acute suppurative otitis media refers to its pathological change, which is caused by a large amount of middle ear exudate formed by the negative pressure of the middle ear in the early stage, which becomes the culture medium of bacteria, leading to continuous invasion of the suppurative bacteria through the eustachian tube, resulting in high reproduction rate, responsible for the absorption of toxins causing systemic fever symptoms. Its pathological manifestations are congestion and swelling of middle ear mucosa, increased purulent secretion, hyperemia and convex tympanic membrane, and even perforation and purulent discharge. Intracranial and extracranial complications may occur if the infection involves suppuration of the mastoid cavity without timely drainage. In addition to the symptoms of local persistent ear pain and infant earache, the symptoms may also be accompanied by systemic symptoms such as high fever, crying, nausea, and vomiting, and the symptoms will be relieved after purulent ear discharges. Some children experienced early hearing loss. Symptoms include enlarged and convex tympanic membrane hyperemia areas, disappearance of tympanic membrane sign, rupture of tension part, perforation, pus overflow, and sometimes redness behind the ears.

The treatment of acute otitis media in children is mainly through the application of antibacterial drugs combined with other symptomatic treatments. Indications for the use of antibacterial drugs for acute otitis media in children are suspected nonsuppurative otitis media and suppurative otitis media caused by bacterial infection, especially in severe cases (ear purulent or with high fever $\geq 39^{\circ}C$) and young children, who should be treated with antibacterial drugs in time [2–8].

The three common pathogenic bacteria in children with acute otitis media include Streptococcus pneumoniae, Haemophilus influenzae, and Moraxella catarrhalis. Oral amoxicillin is recommended as the first-line medication to effectively fight against moderately sensitive strains of penicillin, and the course of treatment is 7-10 days [6]. Alternatively, macrolide oral azithromycin, which has a high tissue concentration in the middle ear mastoid infection site, has a significant effect on intracellular bacteria such as nonclassified Haemophilus influenzae, with a short course of treatment, long action time, and good compliance and is also suitable for those allergic to penicillin drugs [7, 8]. If the above drugs are ineffective, second- or third-generation cephalosporins can also be selected.

Because the shape of the tympanic membrane is very important for the diagnosis of diseases and judging the severity of lesions, this study classified children's acute otitis media according to pain score and tympanic membrane shape. Patients with perforation and purulent tympanic membrane or accompanied by systemic symptoms are definitively diagnosed with acute suppurative otitis media, and patients with acute nonsuppurative otitis media were classified and treated individually in order to establish a reasonable threshold for emergency medical treatment and procedures for children with acute nonsuppurative otitis media, while focusing on assessing the eustachian tube function and reducing complications.

Table 1: The basic situation of the researcher.

Gender	Quantity	Age	Height (cm)	Weight (kg)
Male	208	4.81 ± 2.29	99.8 ± 10.13	21.1 ± 3.14
Female	212	4.75 ± 2.27	99 ± 10.98	19.6 ± 3.08

The inclusion criteria, based on China's "Guidelines for the diagnosis and treatment of otitis media in children" 2015 diagnostic criteria, were as follows: (1) age 2-14 years, (2) 48 h within a sudden occurrence, (3) earache, (4) tympanic membrane intact with acute congestion, (5) middle ear effusion, and (6) a history of upper respiratory tract infection before onset.

The exclusion criteria were as follows: (1) tympanic tube and cochlear implants, (2) external ear canal redness or pus, (3) congenital head deformity, and (4) other serious infections, such as renal insufficiency, heart failure, malignant tumors, immune dysfunction, or other serious diseases.

2. Subjects and Methods

2.1. Subjects. The subjects of this study were children with acute nonsuppurative otitis media (2-14 years old, 208 males and 212 females) with an average age of 4.12 ± 2.31 years (Table 1).

This study included 420 cases: 293 cases of single ear, 127 cases of both ears, 106 cases of hernias, and 10 cases of recurrent episodes (repeated more than three times). These cases were classified into grades I to III based on the tympanic membrane intactness and systemic reactions.

2.2. Grading Criteria: Severity Grading of Acute nonsuppurative Otitis Media. Grade I: the tympanic membrane is mainly in the hammer bone, a small tympanic membrane, no effusion, normal shape, pain score of 4–6 points, and transient attack.

Grade II: tympanic membrane congestion is obvious, involving most of the tympanic membrane, no effusion, the shape is normal, a pain score of 6–8 points, and a transient attack.

Grade III: tympanic membrane congestion, effusion or empyema, obvious bulging of the tympanic membrane tension, pain score higher than 8 points, children with persistent ear pain, ear nausea, and symptoms may be accompanied with fever (Figure 1).

There were 147 cases of grade I, which were randomized into two groups: experimental group 1, which was administered oral antibiotics for 3 days (61 cases) and control group 1 without antibiotic administration (86 cases). There were 150 cases of grade II, which were randomized into two groups: experimental group 2 with oral antibiotics for 5–7 days (69 cases) and control group 2,with analgesic therapy which did not use antibiotics (81 cases). There were 123 cases of grade III, which were randomized into two groups: experimental group 3, which received a course of three-generation

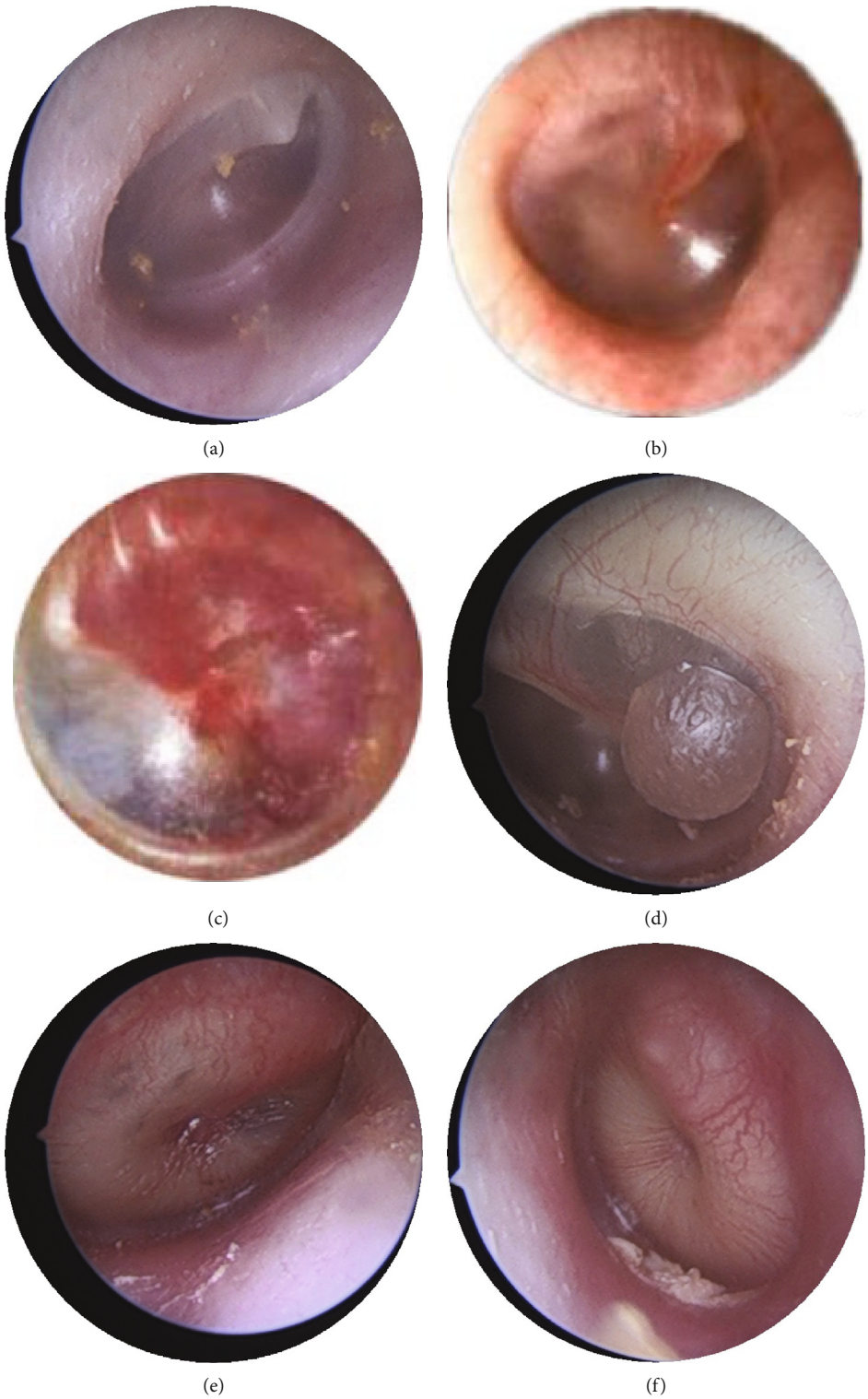

(a) (b) (c) (d) (e) (f)

Figure 1: Continued.

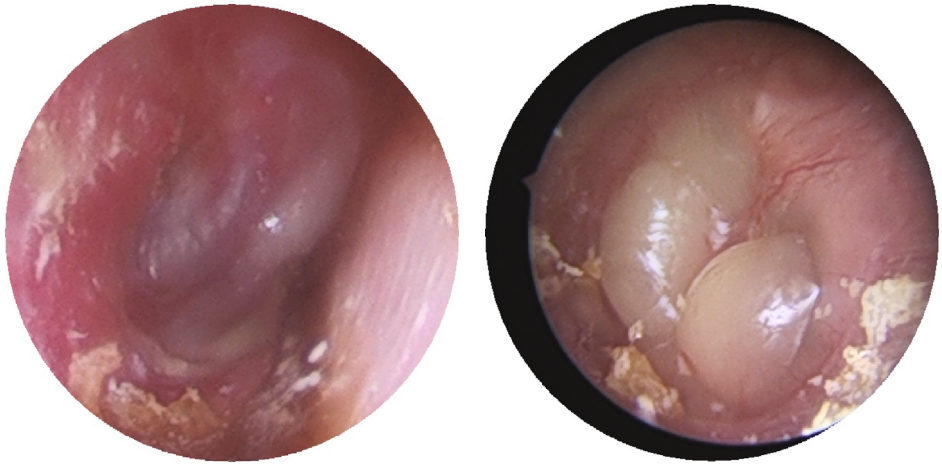

(g) (h)

Figure 1: Grading criteria: severity grading of acute nonsuppurative otitis media: (a) normal, (b) grade I, (c) grade II, and (d)–(h) grade III.

Table 2: Efficacy rating.

Cure	All symptoms disappeared or the total score before and after treatment decreased by >80%
Better	Part of the symptoms disappeared or the total score decreased by 30%-80% before and after treatment
Invalid	No improvement in symptoms or a total score reduction of<30% before and after treatment
Aggravation	Increased symptoms or increased total score before and after treatment

Follow-up table of acute otitis media

Patient name: Age:

Height: Weight:

Family contact:

Time of onset: Duration:

Accompanying symptoms: fever (yes no) ; change of mind (yes no)

Pain level:

0 2 4 6 8 10

Tympanic membrane morphology

See drawing for the hyperemic range, swelling (yes no)

Tympanogram: Left Right

Treatment regimen:

The next review:

Figure 2: Clinical follow-up table of acute otitis media.

cephalosporins with appropriate steroid hormone by intravenous drip for 1 day (92 cases) and control group 3, who received oral antibiotics for 5–7 days (31 cases) and analgesic therapy.

2.3. Selection Criteria for Anti-Inflammatory Drugs. Based on common bacterial infections, third-generation cephalosporins are considered more sensitive, and the side effects are also reduced. For glucocorticoids, it is recommended to use sodium methylprednisolone succinate for injection (based on the weight of the patient, 1-2 mg/kg).

2.4. Efficacy Evaluation. Two weeks after the patient's acute symptoms subsided, the tympanogram was reviewed; if the tympanogram was type A, the treatment was terminated; if the tympanogram was type B or C, the patient was transferred to the late follow-up treatment (Table 2).

2.5. Late Follow-Up Treatment. According to the situation, the corresponding treatment was followed up for treatment review. After a three-month conservative treatment (nasal hormone and oral discharge), the patient was observed for recurrence, adenoid hypertrophy, and swelling of the eustachian tube and pharyngeal mucosa, then treated by adenoidectomy and tympanic tube implantation, if warranted by the observation (Figure 2).

2.6. Statistical Methods. The data were statistically analyzed using SPSS software (version 19.0), and the measurement data were expressed as mean ± SD. The comparison between groups was made using the paired t-test and Chi-square test. Statistical significance was set at $P < 0.05$.

3. Results

3.1. Grade I. In 147 patients with grade I, the symptoms of earache in the experimental group 1 and control group 1

were transient, and there was no significant difference in the recovery of symptoms. 34 children had both ears of C-type, and nasal symptoms were treated with nasal hormones. In the last month, both groups were converted to type A; patients in class I were treated with antibiotics. There was no significant difference in clinical outcomes.

3.2. Grade II. Children with grade II (150cases), experimental group 2 (69 cases), and control group 2 (81 cases) were treated with no perforation of the tympanic membrane and children with sputum; there was no significant difference in pain relief and control.

Among the children with grade II (43/150) both ears type B, (31/150) binaural type C, and 9 cases of children with binaural type B after 3 months of standardized follow-up treatment were treated with surgery and the remaining patients recovered. In the experimental group, 23 patients with a b-tympanogram before treatment were treated, and 1 patients were treated. In the control group, 20 patients had a b-tympanogram before treatment and 8 patients after treatment. Apply the Chi-square test ($t = 6.203$, $P < 0.05$), there was a significant difference in negative pressure in the experimental group compared to the control group in the treatment of tympanic effusion (Tables 3–6).

3.3. Grade III. In grade III (123 cases), experimental group 3 (92/123) cases were treated with antibiotics and hormones once. Earache and ear swelling symptoms recovered quickly, and there was only 1 case of tympanic membrane perforation (TMP). After two weeks of tympanogram review, 64/92 patients recovered, and the remaining patients recovered after 1–3 months of conservative treatment. None of the patients underwent surgery.

In the control group 3, 31 of 123 patients were treated with antibiotics alone and 5 children with TMP. Ear pain and ear swelling symptoms partially recovered slowly. After two weeks of tympanogram review, 3/31 patients recovered, and the remaining patients recovered after 1–3 months of conservative treatment. 4 cases of B-type children with standard treatment for 3 months did not improve, and treatment was performed with adenoid radiofrequency ablation+tympanic membrane transplantation. After extubating, the patient healed (Tables 7 and 8).

There was a significant difference of the experimental group compared to the control group in the treatment of TMP, in the Chi-square test ($t = 8.297$, $P < 0.05$).

Table 3: Pain score.

	Experimental group 2	Control group 2
Before treatment	7.2 ± 0.84	7.17 ± 0.76
After treatment	1 ± 0.71	2.4 ± 1.34
t	21.54	19.26
P	<0.05	<0.05

Table 4: Tympanic membrane morphology changers.

	Tympanic membrane congestion	Tympanic effusion
Experimental group before treatment	Serious	Presence
Experimental group after treatment	Lighten	Regression
Control group before treatment	Serious	Presence
Control group after treatment	Lighten	Regression

Table 5: The tympanic negative pressure of both ears before treatment.

	A	C	B
Experimental group	13	19	23
Control group	21	12	20

Table 6: The tympanic negative pressure of both ears after 3 months of treatment.

	A	C	B
Experimental group	44	10	1
Control group	41	4	8

Table 7: Pain score after 4 hours.

	Experimental group3	Control group3
Before treatment	9.34 ± 1.31	9.5 ± 1.30
After treatment	0.8 ± 0.84	2.4 ± 0.64
t	26.87	24.79
P	<0.05	<0.05

4. Discussion

AOM is a common and frequently occurring disease in children. The onset was sudden, and some lesions exhibited a self-healing tendency [9–11]. Clinical diagnosis is often performed in pediatric or otolaryngology head and neck surgery emergency departments, requiring more visits to the pediatric department [12–14]. Because of the lack of later clinical observation and follow-up, related research on the disease is gradually gaining attention from domestic otolaryngology head and neck surgery departments, with the main research focusing on the use of antibiotics. According to reports from the United States on the treatment of children with AOM and the self-healing tendency of AOM, observation treatment is under consideration [15–19].

In clinical observation, the tympanic membrane morphology is the gold standard for the diagnosis of AOM in children [20–25]. The researchers divided the clinically enrolled children with AOM into tympanic membrane morphology, accompanying symptoms, and children's crying degree and divided them into three grades. The corresponding treatments were then performed.

Table 8: Tympanic membrane morphology changers after 4 hours.

	Tympanic membrane congestion	Tympanic membrane dilating	Tympanic effusion
Experimental group before treatment	Serious	Serious	Presence
Experimental group after treatment	Lighten	Regression	Regression
Control group before treatment	Serious	Serious	Presence
Control group after treatment	Lighten	Invalid	Not subsided

Conclusions from clinical studies were as follows:

(1) The symptoms of earache in children with grade I were transient, even when antibiotic treatment was taken, and there was no significant difference in the recovery of acute symptoms. Some children had nasal congestion, and ear symptoms were treated with nasal hormones in the presence of nasal symptoms. Type A, whether antibiotic treatment was used or not, there was no significant difference in clinical effects; therefore, children with grade I can be observed, and no anti-inflammatory treatment is necessary

(2) Children with grade II tumors should receive antibiotics to treat tympanic effusion. Negative pressure in patients treated with antibiotics was better than that in patients not treated with antibiotics. Children with grade II are recommended to receive oral antibiotics to strengthen the tympanic effusion for the treatment of negative pressure

(3) Children with grade III disease should be treated immediately with hormones and anti-inflammatory agents. After earache, the relief of other ear swelling symptoms was obvious. These agents are known to have a certain effect in preventing perforation of the tympanic membrane. After a three-month follow-up and observation period, it was observed that anti-inflammatory and hormonal treatments have a significant effect on accelerating the regression of tympanic effusion in late stages

The investigators believe that the clinical treatment of acute nonsuppurative otitis media in children caused by an acute upper respiratory tract infection should be treated by evaluating the degree of severity, the absence of excessive intake of antibiotics for the treatment of low-grade disease, and insufficient treatment of more serious grades [26–30]. In case of incomplete remission, some patients may have prolonged symptoms, resulting in future hearing loss and cholesteatoma formation [31, 32]. Effective and not excessive treatment, clinical summarizing of the standardized treatment mode, convenient and quick referral modes, effective follow-up systems, and minimization of the impact of AOM on patients are the focus of this research. Through outpatient follow-up observation and appropriate treatment, the researchers improved the attention of the patient' s family members, reduced the occurrence of clinical symptoms caused by AOM, and treated the children in a timely manner, including those whose treatment was initially ineffective and required repeated treatment [33–37].

Given that clinical work requires special treatment, researchers carried out pediatrics and otolaryngology head and neck surgery and referred all patients with upper respiratory tract infection with acute ear pain to the otolaryngology head and neck specialist for grading, appropriate treatment program, and specialized disease treatment [38–40]. The process attempted to avoid shortcomings in the pediatric and otolaryngology departments by using clinical scales, speeding up the diagnosis, standardizing diagnosis and treatment processes, and facilitating scientific research data and follow-up of clinical treatment effects [41, 42].

The relationship between tympanic effusion in children with AOM and secretory otitis media is still not clear. These two diseases have complex connections in children. It is certain, however, that the two diseases mutually promote and create a vicious cycle therefore requiring close follow-up observations and treatment. Finally, the relationship between these two diseases is an important direction for future research.

5. Conclusions

This study showed no significant difference in clinical in 147 grade I patients regardless of antibiotic treatment. A total of 150 patients had grade II tumors that were treated with antibiotics for tympanic effusion. Negative pressure was significantly different in patients treated with antibiotics compared to those without antibiotic treatment. In 123 grade III patients who underwent hormone therapy, regardless of the ear pain after medication, the relief of ear swelling symptoms was obvious, and the perforation of the tympanic membrane was prevented. The acceleration of the regression of tympanic effusion was also observed in the late stage.

Data Availability

The data used to support the findings of this study are available from the corresponding author upon request.

Conflicts of Interest

The authors declare that there are no conflicts of interest regarding the publication of this paper.

Authors' Contributions

Wei Meng and Dong-dong Huang designed and conducted the experiments. Guang-Fei Li and Zi-Hui Sun contributed to the data analysis and interpretation. Shuang-Ba He

contributed to the manuscript writing. All authors have read and approved the final manuscript.

Acknowledgments

This study was supported by the Jiangsu Provincial Natural Science Foundation (No. BK20161116) and the Nanjing Medical Science and Technique Development Foundation (No. QRX17033). We would like to thank Editage (http://www.editage.cn) for the English language editing.

References

[1] K. A. Daly, H. J. Hoffmen, K. J. Kvaerner et al., "Epidemiology, natural history, and risk factors: panel report from the Ninth International Research Conference on Otitis Media," *International Journal of Pediatric Otorhinolaryngology*, vol. 74, no. 3, pp. 231–240, 2010.

[2] A. Ruohola, O. Meurman, S. Nikkari et al., "Microbiology of acute otitis media in children with tympanostomy tubes: prevalences of bacteria and viruses," *Clinical Infectious Diseases*, vol. 43, no. 11, pp. 1417–1422, 2006.

[3] N. Le Saux, I. Gaboury, M. Baird et al., "A randomized, double-blind, placebo-controlled noninferiority trial of amoxicillin for clinically diagnosed acute otitis media in children 6 months to 5 years of age," *CMAJ*, vol. 172, no. 3, pp. 335–341, 2005.

[4] P. Matzneller, S. Krasniqi, M. Kinzig et al., "Blood, tissue, and intracellular concentrations of azithromycin during and after end of therapy," *Antimicrobial Agents and Chemotherapy*, vol. 57, no. 4, pp. 1736–1742, 2013.

[5] B. Biner, C. Celtik, N. Oner et al., "The comparison of single-dose ceftriaxone, five-day azithromycin, and ten-day amoxicillin/clavulanate for the treatment of children with acute otitis media," *The Turkish Journal of Pediatrics*, vol. 49, no. 4, pp. 390–396, 2007.

[6] D. P. McCormick, T. Chonmaitree, C. Pittman et al., "Nonsevere acute otitis media: a clinical trial comparing outcomes of watchful waiting versus immediate antibiotic treatment," *Pediatrics*, vol. 115, no. 6, pp. 1455–1465, 2005.

[7] P. Little, C. Gould, I. Williamson, M. Moore, G. Warner, and J. Dunleavey, "Pragmatic randomised controlled trial of two prescribing strategies for childhood acute otitis media," *BMJ*, vol. 322, no. 7282, pp. 336–342, 2001.

[8] A. Hoberman, J. L. Paradise, D. J. Burch et al., "Equivalent efficacy and reduced occurrence of diarrhea from a new formulation of amoxicillin/clavulanate potassium(Augmentin)for treatment of acute otitis media in children," *The Pediatric Infectious Disease Journal*, vol. 16, no. 5, pp. 463–470, 1997.

[9] J. H. Powers, "Diagnosis and treatment of acute otitismedia:evaluating the evidence," *Infectious Disease Clinics of North America*, vol. 12, pp. 409–426, 2007.

[10] R. P. Venekamp, R. A. Damoiseaux, and A. G. Schilder, "Acute otitis media in children," *American Family Physician*, vol. 95, no. 2, pp. 109-110, 2017.

[11] H. Atkinson, S. Wallis, and A. P. Coatesworth, "Acute otitis media," *Postgraduate Medicine*, vol. 127, no. 4, pp. 386–390, 2015.

[12] A. K. C. Leung and A. H. C. Wong, "Acute otitis media in children," *Recent Patents on Inflammation & Allergy Drug Discovery*, vol. 11, no. 1, pp. 32–40, 2017.

[13] K. M. Harmes, R. A. Blackwood, H. L. Burrows, J. M. Cooke, R. V. Harrison, and P. P. Passamani, "Otitis media: diagnosis and treatment," *American Family Physician*, vol. 88, no. 7, pp. 435–440, 2013.

[14] A. S. Lieberthal, A. E. Carroll, T. Chonmaitree et al., "The diagnosis and management of acute otitis media," *Pediatrics*, vol. 131, p. 964, 2013.

[15] C. R. Paul and M. A. Moreno, "Acute otitis media," *JAMA Pediatrics*, vol. 174, no. 3, p. 308, 2020.

[16] N. Shirai and D. Preciado, "Otitis media: what is new?," *Current Opinion in Otolaryngology & Head and Neck Surgery*, vol. 27, no. 6, pp. 495–498, 2019.

[17] A. Leichtle, T. K. Hoffmann, and M. C. Wigand, "Otitis media: definition, pathogenesis, clinical presentation, diagnosis and therapy," *Laryngo- Rhino- Otologie*, vol. 97, no. 7, pp. 497–508, 2018.

[18] G. Isaacson, "Otoscopic diagnosis of otitis media," *Minerva Pediatrica*, vol. 68, no. 6, pp. 470–477, 2016.

[19] J. Rodríguez, D. Pavez, R. Pérez, and J. Cofré, "Recomendaciones para el diagnóstico y tratamiento antimicrobiano de la otitis media aguda en pediatría," *Revista Chilena de Infectología*, vol. 36, no. 4, pp. 497–504, 2019.

[20] I. N. Protasova, O. V. Per'yanova, and T. S. Podgrushnaya, "Acute otitis media in the children: etiology and the problems of antibacterial therapy," *Vestnik Otorinolaringologii*, vol. 82, no. 2, pp. 84–89, 2017.

[21] American Academy of Pediatrics Subcommittee on Management of Acute Otitis Media, "Diagnosis and management of acute otitis media," *Pediatrics*, vol. 113, no. 5, pp. 1451–1465, 2004.

[22] Chinese Physician Association Pediatrics Branch Children's Otolaryngology Committee, "Children's otitis media diagnosis and treatment - clinical practice guide (2015)," *Chinese Journal of Practical Pediatrics*, vol. 31, no. 2, pp. 81–84, 2016.

[23] G. Dickson, "Acute otitis media," *Primary Care*, vol. 41, no. 1, pp. 11–18, 2014.

[24] K. Ramakrishnan, R. A. Sparks, and W. E. Berryhill, "Diagnosis and treatment of otitis media," *American Family Physician*, vol. 76, no. 11, pp. 1650–1658, 2007.

[25] F. Felix, G. A. Gomes, G. A. P. S. Cabral, J. R. Cordeiro, and S. Tomita, "The role of new vaccines in the prevention of otitis media," *Brazilian Journal of Otorhinolaryngology*, vol. 74, no. 4, pp. 613–616, 2008.

[26] W. Coronell-Rodríguez, C. Arteta-Acosta, N. Alvis-Zakzuk, and N. Alvis-Guzmán, "Costs of acute otitis media in children in a city of the Colombian Caribbean coast," *Biomédica*, vol. 39, no. 1, pp. 75–87, 2019.

[27] A. Laulajainen-Hongisto, A. A. Aarnisalo, and J. Jero, "Differentiating acute otitis media and acute mastoiditis in hospitalized children," *Current Allergy and Asthma Reports*, vol. 16, no. 10, p. 72, 2016.

[28] N. Juilland, P. Vinckenbosch, and C. Richard, "Otite moyenne aiguë et complications à court terme [acute otitis media and short-term complications]," *Revue Médicale Suisse*, vol. 12, no. 506, pp. 338–340, 2016, 342-3.

[29] A. Syggelou, V. Fanos, and N. Iacovidou, "Acute otitis media in neonatal life: a review," *Journal of Chemotherapy*, vol. 23, no. 3, pp. 123–126, 2011.

[30] A. S. Lieberthal, "Acute otitis media guidelines: review and update," *Current Allergy and Asthma Reports*, vol. 6, no. 4, pp. 334–341, 2006.

[31] M. V. Subbotina, "The clinical classification of acute otitis media with special reference to tympanometry," *Vestnik Otorinolaringologii*, vol. 82, no. 6, pp. 85–88, 2017.

[32] M. E. Pichichero and J. R. Casey, "Acute otitis media disease management," *Minerva Pediatrica*, vol. 55, no. 5, pp. 415–438, 2003.

[33] R. H. Schwartz and D. M. Schwartz, "Acute otitis media: diagnosis and drug therapy," *Drugs*, vol. 19, no. 2, pp. 107–118, 1980.

[34] P. Amrhein, A. Hospach, C. Sittel, and A. Koitschev, "Akute otitis media bei Kindern," *HNO*, vol. 61, no. 5, pp. 374–379, 2013.

[35] J. A. Rosenfeld and G. Clarity, "Acute otitis media in children," *Primary Care*, vol. 23, no. 4, pp. 677–686, 1996.

[36] G. Worrall, "Acute otitis media," *Canadian Family Physician*, vol. 53, no. 12, pp. 2147-2148, 2007.

[37] M. M. Rovers, P. Glasziou, C. L. Appelman et al., "Antibiotics for acute otitis media: a meta-analysis with individual patient data," *Lancet*, vol. 368, no. 9545, pp. 1429–1435, 2006.

[38] D. Hurst, "Efficacy of allergy immunotherapy as a treatment for patients with chronic otitis media with effusion," *International Journal of Pediatric Otorhinolaryngology*, vol. 72, no. 8, pp. 1215–1223, 2008.

[39] P. Sommerfleck, M. E. G. Macchi, S. Pellegrini et al., "Acute otitis media in infants younger than three months not vaccinated against Streptococcus pneumoniae," *International Journal of Pediatric Otorhinolaryngology*, vol. 6, no. 6, pp. 976–980, 2013.

[40] H.-J. Lee, S.-K. Park, K. Y. Choi et al., "Korean clinical practice guidelines: otitis media in children," *Journal of Korean Medical Science*, vol. 8, no. 8, pp. 835–848, 2012.

[41] K. Kitamura, Y. Iino, Y. Kamide et al., "Clinical practice guidelines for the diagnosis and management of acute otitis media (AOM) in children in Japan-2013 update," *Auris, Nasus, Larynx*, vol. 2, no. 2, pp. 99–106, 2015.

[42] A. Coco, L. Vernacchio, T. M. Hors, and A. Anderson, "Management of acute otitis media after publication of the 2004 AAP and AAFP clinical practice guideline," *Pediatrics*, vol. 2, no. 2, pp. 214–220, 2010.

Hindawi
Neural Plasticity
Volume 2021, Article ID 5520794, 10 pages
https://doi.org/10.1155/2021/5520794

Review Article

Mitochondrial Dysfunction and Sirtuins: Important Targets in Hearing Loss

Lingjun Zhang, Zhengde Du, and Shusheng Gong

Department of Otorhinolaryngology, Beijing Friendship Hospital, Capital Medical University, 95 Yongan Road, Xicheng District, Beijing 100050, China

Correspondence should be addressed to Shusheng Gong; gongss1962@163.com

Received 7 January 2021; Revised 9 February 2021; Accepted 2 March 2021; Published 15 March 2021

Academic Editor: Renjie Chai

Mitochondrial dysfunction has been suggested to be a risk factor for sensorineural hearing loss (SNHL) induced by aging, noise, ototoxic drugs, and gene. Reactive oxygen species (ROS) are mainly derived from mitochondria, and oxidative stress induced by ROS contributes to cochlear damage as well as mitochondrial DNA mutations, which may enhance the sensitivity and severity of hearing loss and disrupt ion homeostasis (e.g., Ca^{2+} homeostasis). The formation and accumulation of ROS further undermine mitochondrial components and ultimately lead to apoptosis and necrosis. SIRT3–5, located in mitochondria, belong to the family of sirtuins, which are highly conserved deacetylases dependent on nicotinamide adenine dinucleotide (NAD^+). These deacetylases regulate diverse cellular biochemical activities. Recent studies have revealed that mitochondrial sirtuins, especially SIRT3, modulate ROS levels in hearing loss pathologies. Although the precise functions of SIRT4 and SIRT5 in the cochlea remain unclear, the molecular mechanisms in other tissues indicate a potential protective effect against hearing loss. In this review, we summarize the current knowledge regarding the role of mitochondrial dysfunction in hearing loss, discuss possible functional links between mitochondrial sirtuins and SNHL, and propose a perspective that SIRT3–5 have a positive effect on SNHL.

1. Introduction

Hearing loss is a common sensory disorder with high prevalence. About 500 million people in the world suffer from hearing loss [1]. It can not only cause impaired communication, but also affect the physical and mental health of individuals and social and economic development. It has been proposed that the elderly with hearing loss have higher rates of dementia, depression, and death [2]. Hearing loss is often classified as conductive, sensorineural, or mixed according to anatomical deficit [2, 3]. Sensorineural hearing loss is caused by dysfunction of cochlea or auditory nerve, which is the commonest in adult primary care [2, 3].

Many previous studies have suggested that mitochondrial dysfunction is involved in the etiology of several types of sensorineural hearing loss (SNHL), such as noised-induced hearing loss (NIHL), age-related hearing loss (ARHL), ototoxic drug-induced hearing loss (ODIHL), and inherited hearing loss. In most mammalian cells, mitochondria are the main source of reactive oxygen species (ROS) [4, 5, 6]. Increased ROS formation results in further damage to the mitochondrial structure, including mitochondrial membranes, mitochondrial DNA (mtDNA), respiratory chain proteins, and nuclear DNA related to mitochondrial functions [7]. SNHL occurs because of the irreversible damage to hair cells (HCs) and spiral ganglion neurons (SGNs), both of which have very limited regeneration ability in adult mice cochlea [8, 9, 10, 11, 12, 13].

Sirtuins are histone deacetylases dependent on NAD^+ that remove various cellular proteins' acyl modifications [14]. They regulate metabolism, differentiation, stress responses, apoptosis, and the cell cycle [15, 16]. Seven members of the sirtuin family (named SIRT1–7) have been identified with different locations in the cell. Recent studies have revealed that mitochondrial sirtuins, especially SIRT3, modulate ROS levels in hearing loss pathologies and indicated that SIRT4 and SIRT5 may have a potential protective effect against hearing loss. In this review, we focus on

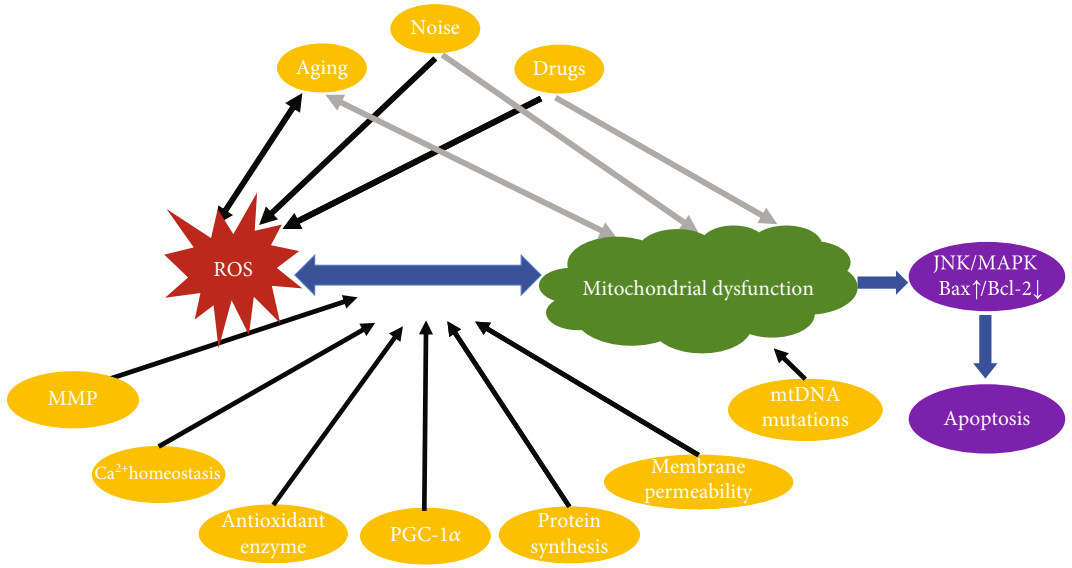

Figure 1: Stimulations induce ROS and mitochondrial dysfunction and finally cells' apoptosis. Diagram showing aging, noise, and drugs could induce ROS and the probable mechanism to lead to mitochondrial dysfunction, moreover, the interaction between ROS and mitochondrial dysfunction.

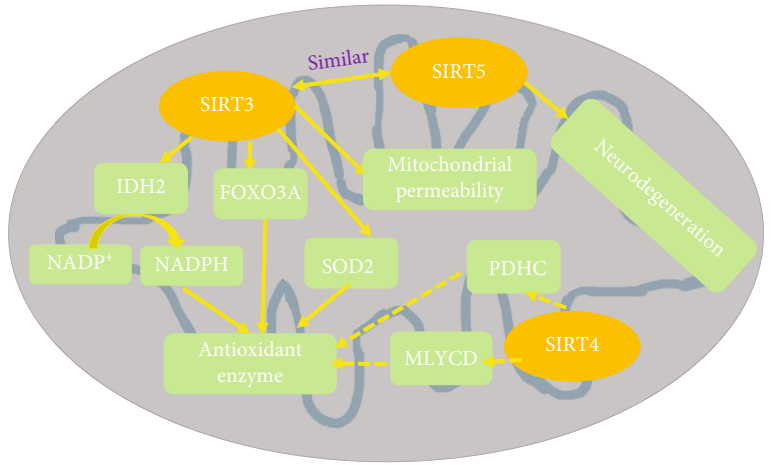

Figure 2: Regulation of ROS and protection of mitochondria by sirtuins. The diagram showing possible signaling ways of mitochondrial sirtuins (SIRT3~5) to reduce level of ROS and resist oxidative reaction. Solid lines represent considerable evidence for an interaction while dashed lines suggest putative interactions.

mitochondrial dysfunction and the role of mitochondrial sirtuins in SNHL, as shown in Figures 1 and 2.

2. Hearing Loss and Mitochondrial Dysfunction

2.1. Age-Related Hearing Loss (ARHL). ARHL, or presbycusis, is a progressive decline in hearing function that is the most prevalent type of SNHL in the elderly [17, 18, 19, 20]. It is characterized by higher hearing thresholds, beginning at high frequencies and spreading toward low frequencies, accompanied by the loss of HCs and SGNs from the basal to apical turn [21, 22, 23, 24, 25, 26]. The mechanism underlying ARHL is considered to be multifactorial, involving environmental and hereditary factors, but remains unclear. Extensive evidence suggests that mitochondria make a large contribution to the pathology of ARHL.

A previous study proposed that the accumulation of mtDNA mutations could result in age-related degenerative diseases like ARHL [27]. Major mtDNA mutations arise in the genes encoding mitochondrial oxidative phosphorylation complexes, resulting in an impairment of its activity [28]. Transgenic PolgA mice with knockout of the functional nuclear gene that encodes the polymerase helping repair damaged mtDNA, POLG D257A, developed hearing loss more rapidly and earlier than their wild-type counterparts. Furthermore, 10-month old PolgA mice showed severe sensorineural degeneration in the basal turn and neural degeneration in the apical turn, including clumping of surviving neurons in the cochlea [29]. On the other hand, mtDNA

mutations affect cochlear function by leading to not only mitochondrial dysfunction but also energy metabolic disturbances and induction of apoptosis [30].

Extensive experimental evidence indicates that oxidative stress and ROS are closely associated with the development of ARHL. A suitable model of the senescence-accelerated mouse prone 8 (SAMP8) has been established to study the impact of the aging process on various parameters. In SAMP8 mice, oxidative stress, changes in antioxidant enzyme levels, and impairment in activities of complexes I, II, and IV were shown to be involved in premature ARHL [31]. Moreover, the level of 7,8-dihydro-8-oxoguanine, a crucial biomarker of mitochondrial and nuclear DNA damage in HCs and SGNs [32], increased with aging and mitochondriogenesis decreased, as assessed by the activity of citrate synthase and the ratio of mtDNA to nuclear DNA [31]. After exposure to H_2O_2 (0.1 mM) for only 1 h *in vitro*, House Ear Institute-Organ of Corti 1 auditory cells presented with premature senescence, leading to a lower mitochondrial membrane potential (MMP), breakdown of the mitochondrial fusion/fission balance, destruction of mitochondrial morphology, and collapse of the mitochondrial network [33]. Furthermore, oxidative stress and an accumulation of ROS increased expression of the mitochondrial proapoptotic gene Bcl-2-antagonist/killer 1 (Bak) to induce apoptosis. Suppression or deletion of Bak reduced apoptotic cell death of SGNs and HCs and prevented ARHL [34, 35].

As the major source of ROS, mitochondria contain a complex antioxidant system to resist the destructive effects of these species. Isocitrate dehydrogenase 2 (IDH2), which can convert $NADP^+$ to NADPH, is crucial in the mitochondrial response to oxidative stress. In male mice, IDH2 deficiency accelerated the ARHL process, along with increased oxidative DNA damage and apoptosis and a loss of SGNs and HCs [36]. Superoxide dismutase 1 (SOD1-) knockout mice also exhibited premature ARHL, characterized by an early loss of HCs, severe degeneration of SGNs, and leanness of the stria vascularis [37].

Glutathione peroxidase 1 (Gpx1) also has important antioxidant properties. Mice with deletion of Gpx1 showed higher hearing thresholds at high frequencies and extensive damage of HCs [34]. $Ggt1^{dwg/dwg}$ mice, with deletion of the γ-glutamyl transferase 1 gene that encodes an antioxidant enzyme crucial for resynthesizing reduced glutathione (GSH), exhibited an extremely rare type of cochlear pathology in which the function of outer hair cells (OHCs) was unaffected while inner hair cells (IHCs) were unusually and selectively lost. Furthermore, treatment with N-acetyl-L-cysteine could completely prevent the hearing deficit and IHC loss in these mice [38]. In addition, administration of EUK-207, a synthetic SOD/catalase drug, attenuated the senescence phenotype *in vitro* and mitigated ARHL in SAMP8 mice by increasing the expression of FOXO3A and the mRNA and protein levels of manganese SOD (Mn-SOD) and catalase [39].

Peroxisome proliferator-activated receptor γ coactivator 1α (PGC-1α) could regulate mitochondrial biogenesis and upregulate the expression of oxidative stress-related genes, including Gpx1, catalase, and Mn-SOD genes [40, 41]. Overexpression of PGC-1α, with a consequent rise in nuclear respiratory factor 1 and mitochondrial transcription factor A, resulted in reduced damage to mtDNA and decreased apoptosis in the strial marginal cell aging model harboring mtDNA4834 deletion [34, 42, 43].

2.2. Noise-Induced Hearing Loss (NIHL). Excessive exposure to noise from recreation, the environment, and various occupations can lead to hearing loss, known as NIHL, which is one of the most prevalent types of SNHL. Its typical characteristics are an increased hearing threshold, tinnitus, decreased speech discrimination score, and auditory processing disorders [44]. Higher frequencies are preferentially affected, creating a V-shaped dip or notch, around 4 or 6 kHz [45]. The cochlear injury following noise exposure is mainly caused by mechanical damage and biochemical pathways. Generally, OHCs are more sensitive to noise exposure than IHCs [28].

ROS production was observed as an early event in cochlear damage after noise exposure [46]. As the major source of ROS, mitochondria are assumed to be damaged and, in turn, increase the accumulation of ROS. It has also been reported that mitochondrial ROS provide feedback regulation after metabolic excess, autophagy, and the inflammatory response [44]. ROS generate lipid peroxidation products, such as 8-iso-prostaglandin F2α, that reduce blood flow in the cochlea [47], finally resulting in apoptosis [44]. Ischemia may lead to cochlear hypoxia and lower adenosine triphosphate (ATP) levels and further increase the generation of ROS. On the other hand, mitochondria possess a potent antioxidant enzyme system to scavenge ROS, relying on the NADPH pool. Mn-SOD heterozygous knockout mice had worse hearing thresholds, particularly at 4 kHz, and greater damage of OHCs in all cochlear turns after noise exposure and exacerbation of NIHL [14]. In another study, Gpx1-knockout mice exhibited greater HC and nerve fiber loss with higher auditory brainstem response thresholds [48].

Calcium homeostasis is also a significant factor in the occurrence and development of NIHL. After noise exposure, the level of free Ca^{2+}increased immediately in HCs [43, 49]; the probable ion channels allowing entry are L-type Ca^{2+} and P2X2 ATP-gated channels [50]. Mitochondria modulate cellular calcium homeostasis through selective calcium entry channels, the mitochondrial calcium uniporter (MCU), and the sodium-calcium exchanger with the function of extruding calcium from mitochondria [51]. Inhibiting the MCU in CBA/J mice attenuated the loss of sensory HCs, synaptic ribbons, and the NIHL process. Furthermore, MCU-knockout mice showed resistance to noise-induced seizures and recovery of IHC synaptic connections, the auditory brainstem response, and wave I amplitude after noise exposure [51]. Mitochondrial Ca^{2+} overload not only results in a decline in the MMP and overproduction of ROS but also triggers ROS-independent apoptotic and necrotic cell death pathways [50, 52, 53].

Before there is a permanent threshold shift caused by noise exposure, the level of 5′-AMP-activated protein kinase (AMPK) is elevated in the spiral ligament of cochlea, in addition to an increased level of phospho-c-Jun N-terminal

kinase, and this mediates the activation of apoptosis [54, 28]. Apoptosis occurs through both extrinsic and intrinsic pathways; the latter is activated by the change of mitochondrial membrane permeability. In addition to ROS, cytochrome C and caspase-independent apoptosis-inducing factor increase membrane permeability [28, 50, 55].

2.3. Ototoxic Drug-Induced Hearing Loss (ODIHL). Platinum-based anticancer drugs, such as cisplatin, and aminoglycoside antibiotics are clinically common ototoxic drugs [56, 57, 58]. Platinum-based anticancer drugs are widely adopted to treat different kinds of cancer, and aminoglycosides are broad-spectrum antibiotics used to treat many life-threatening bacterial infections. Both can lead to hearing loss at high frequencies and preferential damage to OHCs at the cochlea basal turn [43, 59, 60–62, 63, 64].

The ototoxicity of both cisplatin and aminoglycoside antibiotics is modulated by genetic factors, and mitochondrial mutations are well-defined risk factors. Individuals bearing the mtDNA mutation A1555G in the 12S ribosomal RNA gene suffer more profound hearing loss [56, 65, 66]. C1494T is the second most common mutation identified, especially in Chinese populations [67, 68, 69]. Mutations in thiopurine S-methyltransferase (TMPT) and catechol O-methyltransferase (COMT) are related to earlier onset and greater severity of hearing loss induced by cisplatin in children [70]. However, a more recent study revealed that variations in the TMPT or COMT genes may not correspond to cisplatin ototoxicity and did not affect hearing damage induced by cisplatin in mice. Thus, the precise role of these genes in cisplatin ototoxicity remains unclear [71].

Mitochondrial dysfunction and ROS are the main initiators of ODIHL. Aminoglycoside antibiotics, such as gentamicin, tend to accumulate in the mitochondria of HCs through nonselective mechanoelectrical transducer cation channels expressed on the stereociliary membranes of HCs [72–74, 75, 76]. Administration of gentamicin can directly inhibit mitochondrial protein synthesis [28], trigger opening of the mitochondrial permeability transition pore, and lower the MMP [77]. Aminoglycosides can induce the release of arachidonic acid, leading to lipid peroxidation and generation of ROS [78, 79, 80, 81]. The ototoxic effect of aminoglycosides has been proposed to be linked to the formation of iron-aminoglycoside complexes that promote the formation of ROS [82]. Downregulation of tRNA5-methylaminomethyl-2-thiouridylate methyltransferase, a mitochondrial protein, significantly made HEI-OC1 auditory cells more sensitive to damage induced by neomycin [80]. Aminoglycosides also dysregulate calcium homeostasis, facilitating the transfer of Ca^{2+} into mitochondria [83]. Elevation of mitochondrial Ca^{2+} levels promotes both mitochondrial oxidation and cytoplasmic ROS prior to cell death [84]. In an *in vitro* study, mitochondria-specific ROS formation was evaluated in cochlear explants after exposure to gentamicin, which was accompanied by a reduction of NAD(P)H and the MMP [85]. ROS formation in HCs in response to cisplatin leads to depletion of NADPH and binding to the sulfhydryl groups of enzymes [28, 86]. Cisplatin could stimulate the activity of NADPH oxidase 3, a relevant source of ROS, to elevate ROS levels [87]. Oxidative stress induced by cisplatin could lead to GSH depletion, increased lipid peroxidation, and an imbalance of the oxidant/antioxidant systems [43].

Mitochondrial apoptotic pathways are activated following both cisplatin and aminoglycoside cochlear injury through the Bcl-2 family of proteins. After cisplatin treatment, the level of Bax was increased and the level of Bcl-2 was decreased in HCs, spiral ganglia, and the lateral wall [88]. Pretreatment with an adenovector expressing human Bcl-2 (Ad.11D.Bcl-2) could protect HCs and preserve hearing in mice treated with gentamicin [89].

2.4. Inherited Hearing Loss. Sensorineural hearing loss which mainly causes by mutation of genes, known as inherited hearing loss, has been identified more common due to the development of science and technology [90, 91, 92]. Its clinical and genetical characteristics are very heterogeneous [93]. Though the mechanism of many cases remains unclear, large evidence has proved that it has much to do with the mitochondrial function.

13 crucial polypeptides of oxidative phosphorylation were encoded by mitochondrial genome [94]. Mutation in the mitochondria DNA has been proved to be related to the maternally inherited susceptibility in both syndromic and nonsyndromic hearing loss [93]. Mitochondrial disorders including Kearns-Sayre syndrome, MELAS syndrome, and MERRF syndrome are always accompanied by syndromic hearing loss [94]. In view of nonsyndromic hearing loss, extensive research has been carried out to identify the role of A1555G and C1494T mutations in 12S rRNA and emphasize the high susceptibility to hearing loss induced by drugs such as cisplatin and aminoglycoside [95, 65, 66, 96]. Mutation of 7505A>G in the $tRNA^{Ser(UCN)}$ would lead to mitochondrial dysfunction by lowering the activity of cellular respiratory chain and the level of ATP, MMP, and over produce ROS [97], finally induce cell apoptosis [98]. Other variants in the $tRNA^{Ser(UCN)}$ including A7445G, T7505C, T7510C, and T7511C alter mitochondrial translation and function, involving in SNHL [95, 99, 100, 101].

The phenotypic expression of variants in mitochondrial DNA could be modulated by nuclear modifier genes, which may also play an important role in inherited hearing loss. Fan et al. had found that the interaction between p.191Gly>-Val mutation in mitochondrial tyrosyl-tRNA synthetase 2 (YARS2) and the 7511A>G mutation in $tRNA^{Ser(UCN)}$caused hearing loss [102]. Moreover, in the study of Chinese families, people who suffer both mutations present much higher penetrance of hearing loss than those who carry only one [102]. Mtu1 is a tRNA-modifying enzyme and mtu1 knockout zebrafish exhibited a smaller number of hair cells and reductions in the hair bundle densities in the auditory and vestibular organs [103]. Deletion of Gtpbp3 also resulted in impairment of mitochondria function in zebrafish, which provided novel opportunities for studying pathophysiology of mitochondrial disorders [104].

Much more mitochondrial gene loci associated with hearing loss have been discovered due to advanced technology. Mitochondrial dysfunction caused by mtDNA mutations are one of the major molecular mechanisms

responsible for deafness. However, many cases remained unclear. We hope more research will be carried out in the future.

3. Sirtuins and Function

Sirtuins were originally described in yeast and named Sir2, with seven Sir2 homologs (SIRT1-7) discovered. Sirtuins consume NAD^+ to deacetylate lysine residues and generate nicotinamide and $2'$-O-acetyl-ADP-ribose [105]. The crucial function of sirtuins is to sense and regulate cellular metabolic responses [106, 107]. They display diverse subcellular localizations in the cell. In the nucleus, there are mainly SIRT1, SIRT6, and SIRT7, whereas in the cytoplasm, SIRT2 is located. SIRT3, SIRT4, and SIRT5 are predominantly located in the mitochondria [16] and are the main focus of this review. SIRT3 is the principal mitochondrial deacetylase, whereas SIRT4 and SIRT5 only have weak deacetylase functions [108]. However, SIRT5 has robust demalonylase, desuccinylase, and deglutarylase activities [109], and SIRT4 can regulate lipoamidation [110].

3.1. SIRT3. SIRT3 is the main deacetylase in mitochondria, and its expression is the highest in tissues with vigorous metabolism such as the liver, kidney, and heart [111]. SIRT3 level increases under calorie restriction, fasting, and exercise training in different tissues [112, 113]. Acetyl-CoA synthetase 2 was the first reported target of SIRT3 [114]. However, further research revealed that SIRT3 also affected a diverse range of target proteins and participated in all major biochemical reactions and metabolic activities of mitochondria, including the respiratory chain, antioxidant defenses, and apoptosis [15, 16].

SIRT3 is an important factor involved in resisting various mitochondrial stresses, especially by utilizing cellular antioxidant systems to combat oxidative stress. SOD2, which reduces ROS levels and protects against oxidative stress, is activated by SIRT3-mediated deacetylation [115]. SIRT3 deacetylates and activates IDH2, the major source of NADPH in mitochondria, which helps maintain GSH levels [16, 15, 116]. Deacetylation of FOXO3A, a forkhead transcription factor, by SIRT3 activates the transcription of SOD2, catalase, and other crucial antioxidant genes and protects mitochondria from further oxidative stress [117, 118]. Another key stress-sensitive pathway in mitochondria affected by SIRT3 is the mitochondrial permeability transition pore. SIRT3 deacetylates cyclophilin D [119] and mitochondrial fusion protein optic atrophy protein 1. These proteins affect mitochondrial dynamics and the MMP [120].

SIRT3 plays important roles in a wide range of diseases, including hearing loss. As mentioned above, ROS and mitochondrial dysfunction have much to do with the etiology of SNHL. SIRT3 deacetylates and activates the antioxidant system in mitochondria to reduce the level of ROS induced by noise, aging, or drugs and maintain mitochondrial permeability through deacetylation of proteins. Under caloric restriction, deacetylation and activation of IDH2 by SIRT3 increased the levels of NADPH and GSH in mitochondria, thus preventing ARHL in wild-type, but not SIRT3-knockout mice [112]. Similarly, overexpression of SIRT3 in mice aided in preventing NIHL. Administration of the NAD^+ precursor nicotinamide riboside to mice prevented the degeneration of spiral ganglia neurites and NIHL by activating the NAD^+-SIRT3 pathway, and these protective effects were abrogated with SIRT3 deletion [121]. Adjudin, a lonidamine analog, could protect cochlear HCs from gentamicin-induced damage mediated by the SIRT3-ROS axis [122].

3.2. SIRT4. SIRT4 is widely expressed and abundant in pancreatic β-cells, kidney, heart, brain, and liver [123, 110]. It has been reported that SIRT4 has no detectable NAD^+-dependent deacetylase activity and function through NAD^+-dependent ADP-ribosylation [16, 123]. Few studies have been carried out in other tissues, except pancreatic ß-cells, and the precise enzymatic functions of SIRT4 remain unclear. ATP is indispensable for insulin secretion by pancreatic β-cells, and SIRT4 inhibits the activity of glutamate dehydrogenase (GDH) to reduce the amount of ATP produced by the catabolism of glutamate and glutamine [124, 16]. Mice deficient in SIRT4 or subjected to calorie restriction exhibited upregulation of amino acid-stimulated insulin secretion [123]. It is interesting that SIRT3 deacetylates and activates GDH, indicating that this enzyme may be regulated by both SIRT3 and SIRT4 [124, 125]. SIRT4 knockdown also caused increased fatty acid oxidation dependent on SIRT1, respiration, and AMPK phosphorylation [126].

Compared with those on SIRT3, there have been fewer studies on the regulation of SIRT4. Recent research suggests that SIRT4 may be involved in ROS homeostasis by the pyruvate dehydrogenase complex and GDH and fatty acid oxidation through malonyl-CoA decarboxylase [110, 127], ultimately reducing ROS production, that is, may have potentially optimistic effect in preservation of hearing function. However, there are studies showing that increased activity of SIRT4 may raise ROS levels in murine cardiomyocytes [128, 129]. Nevertheless, the precise mechanism of SIRT4 enzymatic activity is unknown, though it may play a role in hearing loss. Further studies are needed to identify the mechanism underlying SIRT4 function.

3.3. SIRT5. Unlike other sirtuins, SIRT5 primarily originated from prokaryotes [130], with high expression in various tissues such as the heart, brain, and liver. [131]. The function of SIRT5 has generally become an important research topic.

SIRT5-deficient mice show no detectable alterations in the whole acetylation state of mitochondria, indicating there is a specific acetyl substrate for SIRT5 or alternative functions [132]. And global protein hypermalonylation and hypersuccinylation are observed, indicating that SIRT5 catalyzes lysine demalonylation and desuccinylation reactions in mammals [133]. One target of SIRT5 is carbamoyl phosphate synthetase 1 (CPS1). This enzyme has been identified as the key rate-determining step of the urea cycle for detoxification and removal of ammonia. SIRT5 upregulates CPS1 activity through deacetylation and desuccinylation, and this function is absent in SIRT5-deficient mice [124, 134, 15]. In mice overexpressing SIRT5, the CPS1 protein was more deacetylated and activated in the liver than in wild-type mice [135].

In terms of occurrence and development of SNHL, SIRT5 has been demonstrated to contribute to ROS homeostasis and attenuate oxidative stress. It may reduce ROS levels and oxidative stress through a mechanism similar to that of SIRT3, by deacetylation of FOXO3A and desuccinylation of IDH2, so that it may have optimistic effect on preserve hearing function [136, 137]. Another study showed that SIRT5 enhanced SOD1-mediated ROS reduction by desuccinylation [138]. Recent evidence suggests that SIRT5 plays a potential protective role against neurodegeneration, which is a common phenomenon in SNHL. Although the mechanism remains undetermined, SIRT5 may protect neurons by limiting overproduction of ROS directly and controlling systemic ammonia levels indirectly [139].

4. Conclusion

Although extensive research is required to probe the pathology of hearing loss, a causative role for mitochondrial dysfunction remains one of the most solid theories. Mitochondrial sirtuins (SIRT3-5) are intimately linked to responses to stress, such as oxidative stress, metabolic regulation, and apoptosis, all of which are related to the occurrence and development of hearing loss. Moreover, we have reasons to believe SIRT3-5 have positive effect on SNHL. Moving forward, it is important to determine the precise activities of mitochondrial sirtuins as crucial targets to help prevent and cure hearing loss.

Data Availability

The data that support the findings of this study are openly available from the corresponding author upon reasonable request.

Conflicts of Interest

The authors declare that there is no conflict of interests regarding the publication of this paper.

Acknowledgments

We would like to thank all the authors who contributed to this special issue. This work was supported by grants from the National Natural Science Foundation of China (Grant Nos. 81830030, 81771016, and 81700917).

References

[1] T. Vos, C. Allen, M. Arora et al., "Global, regional, and national incidence, prevalence, and years lived with disability for 310 diseases and injuries, 1990-2015: a systematic analysis for the Global Burden of Disease Study 2015," *The Lancet*, vol. 388, no. 10053, pp. 1545–1602, 2016.

[2] L. L. Cunningham and D. L. Tucci, "Hearing loss in adults," *The New England Journal of Medicine*, vol. 377, no. 25, pp. 2465–2473, 2017.

[3] C. L. Nieman and E. S. Oh, "Hearing loss," *Annals of Internal Medicine*, vol. 173, no. 11, pp. ITC81–ITC96, 2020.

[4] H. Zhou, X. Qian, N. Xu et al., "Disruption of Atg7-dependent autophagy causes electromotility disturbances, outer hair cell loss, and deafness in mice," *Cell Death & Disease*, vol. 11, no. 10, p. 913, 2020.

[5] J. F. Turrens, "Mitochondrial formation of reactive oxygen species," *The Journal of Physiology*, vol. 552, no. 2, pp. 335–344, 2003.

[6] R. S. Balaban, S. Nemoto, and T. Finkel, "Mitochondria, oxidants, and aging," *Cell*, vol. 120, no. 4, pp. 483–495, 2005.

[7] N. D. Bonawitz, M. S. Rodeheffer, and G. S. Shadel, "Defective mitochondrial gene expression results in reactive oxygen species-mediated inhibition of respiration and reduction of yeast life span," *Molecular and Cellular Biology*, vol. 26, no. 13, pp. 4818–4829, 2006.

[8] T. Wang, R. Chai, G. S. Kim et al., "Lgr5+ cells regenerate hair cells via proliferation and direct transdifferentiation in damaged neonatal mouse utricle," *Nature Communications*, vol. 6, no. 1, 2015.

[9] S. Zhang, Y. Zhang, Y. Dong et al., "Knockdown of Foxg1 in supporting cells increases the trans-differentiation of supporting cells into hair cells in the neonatal mouse cochlea," *Cellular and Molecular Life Sciences*, vol. 77, no. 7, pp. 1401–1419, 2020.

[10] Y. Zhang, S. Zhang, Z. Zhang et al., "Knockdown of Foxg1 in Sox9+ supporting cells increases the trans-differentiation of supporting cells into hair cells in the neonatal mouse utricle," *Aging (Albany NY)*, vol. 12, no. 20, pp. 19834–19851, 2020.

[11] S. Zhang, D. Liu, Y. Dong et al., "Frizzled-9+ supporting cells are progenitors for the generation of hair cells in the postnatal mouse cochlea," *Frontiers in Molecular Neuroscience*, vol. 12, 2019.

[12] R. Guo, X. Ma, M. Liao et al., "Development and application of cochlear implant-based electric-acoustic stimulation of spiral ganglion neurons," *ACS Biomaterials Science & Engineering*, vol. 5, no. 12, pp. 6735–6741, 2019.

[13] S. Zhang, R. Qiang, Y. Dong et al., "Hair cell regeneration from inner ear progenitors in the mammalian cochlea," *American Journal of Stem Cells*, vol. 9, no. 3, 2020.

[14] A. Tuerdi, M. Kinoshita, T. Kamogashira et al., "Manganese superoxide dismutase influences the extent of noise-induced hearing loss in mice," *Neuroscience Letters*, vol. 642, pp. 123–128, 2017.

[15] B. Osborne, N. L. Bentley, M. K. Montgomery, and N. Turner, "The role of mitochondrial sirtuins in health and disease," *Free Radical Biology & Medicine*, vol. 100, pp. 164–174, 2016.

[16] W. He, J. C. Newman, M. Z. Wang, L. Ho, and E. Verdin, "Mitochondrial sirtuins: regulators of protein acylation and metabolism," *Trends in Endocrinology and Metabolism*, vol. 23, no. 9, pp. 467–476, 2012.

[17] S. Someya, T. Yamasoba, R. Weindruch, T. A. Prolla, and M. Tanokura, "Caloric restriction suppresses apoptotic cell death in the mammalian cochlea and leads to prevention of presbycusis," *Neurobiology of Aging*, vol. 28, no. 10, pp. 1613–1622, 2007.

[18] M. Knipper, P. Van Dijk, I. Nunes, L. Rüttiger, and U. Zimmermann, "Advances in the neurobiology of hearing disorders: recent developments regarding the basis of tinnitus and hyperacusis," *Progress in Neurobiology*, vol. 111, pp. 17–33, 2013.

[19] C. Cheng, Y. Wang, L. Guo et al., "Age-related transcriptome changes in Sox2+ supporting cells in the mouse cochlea," *Stem Cell Research & Therapy*, vol. 10, no. 1, p. 365, 2019.

[20] Z.-D. Du, S. Yu, Y. Qi et al., "NADPH oxidase inhibitor apocynin decreases mitochondrial dysfunction and apoptosis in the ventral cochlear nucleus of D-galactose-induced aging model in rats," *Neurochemistry International*, vol. 124, pp. 31–40, 2019.

[21] E. M. Keithley, C. Canto, Q. Y. Zheng, N. Fischel-Ghodsian, and K. R. Johnson, "Age-related hearing loss and the ahl locus in mice," *Hearing Research*, vol. 188, no. 1-2, pp. 21–28, 2004.

[22] Y. Liu, J. Qi, X. Chen et al., "Critical role of spectrin in hearing development and deafness," *Science Advances*, vol. 5, no. 4, article eaav7803, 2019.

[23] Z.-h. He, S.-y. Zou, M. Li et al., "The nuclear transcription factor FoxG1 affects the sensitivity of mimetic aging hair cells to inflammation by regulating autophagy pathways," *Redox Biology*, vol. 28, p. 101364, 2020.

[24] X. Fu, X. Sun, L. Zhang et al., "Tuberous sclerosis complex-mediated mTORC1 overactivation promotes age-related hearing loss," *The Journal of Clinical Investigation*, vol. 128, no. 11, pp. 4938–4955, 2018.

[25] Y. Ding, W. Meng, W. Kong, Z. He, and R. Chai, "The role of FoxG1 in the inner ear," *Frontiers in Cell and Development Biology*, vol. 8, article 614954, 2020.

[26] Z.-D. Du, S.-G. Han, T.-F. Qu et al., "Age-related insult of cochlear ribbon synapses: an early-onset contributor to D-galactose-induced aging in mice," *Neurochemistry International*, vol. 133, article 104649, 2020.

[27] A. W. Linnane, T. Ozawa, S. Marzuki, and M. Tanaka, "Mitochondrial DNA mutations as an important contributor to ageing and degenerative diseases," *The Lancet*, vol. 333, no. 8639, pp. 642–645, 1989.

[28] T. Kamogashira, C. Fujimoto, and T. Yamasoba, "Reactive oxygen species, apoptosis, and mitochondrial dysfunction in hearing loss," *BioMed Research International*, vol. 2015, Article ID 617207, 7 pages, 2015.

[29] B. K. Crawley and E. M. Keithley, "Effects of mitochondrial mutations on hearing and cochlear pathology with age," *Hearing Research*, vol. 280, no. 1-2, pp. 201–208, 2011.

[30] S. Someya, T. Yamasoba, G. C. Kujoth et al., "The role of mtDNA mutations in the pathogenesis of age-related hearing loss in mice carrying a mutator DNA polymerase γ," *Neurobiology of Aging*, vol. 29, no. 7, pp. 1080–1092, 2008.

[31] J. Menardo, Y. Tang, S. Ladrech et al., "Oxidative stress, inflammation, and autophagic stress as the key mechanisms of premature age-related hearing loss in SAMP8 mouse cochlea," *Antioxidants & Redox Signaling*, vol. 16, no. 3, pp. 263–274, 2012.

[32] S. Tanrıkulu, S. Doğru-Abbasoğlu, A. Özderya et al., "The 8-oxoguanine DNA N-glycosylase 1 (hOGG1) Ser326Cys variant affects the susceptibility to Graves' disease," *Cell Biochemistry and Function*, vol. 29, no. 3, pp. 244–248, 2011.

[33] T. Kamogashira, K. Hayashi, C. Fujimoto, S. Iwasaki, and T. Yamasoba, "Functionally and morphologically damaged mitochondria observed in auditory cells under senescence-inducing stress," *NPJ Aging and Mechanisms of Disease*, vol. 3, no. 1, p. 2, 2017.

[34] C. Fujimoto and T. Yamasoba, "Oxidative stresses and mitochondrial dysfunction in age-related hearing loss," *Oxidative Medicine and Cellular Longevity*, vol. 2014, Article ID 582849, 6 pages, 2014.

[35] S. Someya, J. Xu, K. Kondo et al., "Age-related hearing loss in C57BL/6J mice is mediated by Bak-dependent mitochondrial apoptosis," *Proceedings of the National Academy of Sciences of the United States of America*, vol. 106, no. 46, pp. 19432–19437, 2009.

[36] K. White, M.-J. Kim, C. Han et al., "Loss of IDH2 accelerates age-related hearing loss in male mice," *Scientific Reports*, vol. 8, no. 1, p. 5039, 2018.

[37] E. M. Keithley, C. Canto, Q. Y. Zheng, X. Wang, N. Fischel-Ghodsian, and K. R. Johnson, "Cu/Zn superoxide dismutase and age-related hearing loss," *Hearing Research*, vol. 209, no. 1-2, pp. 76–85, 2005.

[38] D. Ding, H. Jiang, G.-D. Chen et al., "N-acetyl-cysteine prevents age-related hearing loss and the progressive loss of inner hair cells in γ-glutamyl transferase 1 deficient mice," *Aging (Albany NY)*, vol. 8, no. 4, pp. 730–750, 2016.

[39] N. Benkafadar, F. François, C. Affortit et al., "ROS-induced activation of DNA damage responses drives senescence-like state in postmitotic cochlear cells: implication for hearing preservation," *Molecular Neurobiology*, vol. 56, no. 8, pp. 5950–5969, 2019.

[40] J. St-Pierre, S. Drori, M. Uldry et al., "Suppression of reactive oxygen species and neurodegeneration by the PGC-1 transcriptional coactivators," *Cell*, vol. 127, no. 2, pp. 397–408, 2006.

[41] P. I. Merksamer, Y. Liu, W. He, M. D. Hirschey, D. Chen, and E. Verdin, "The sirtuins, oxidative stress and aging: an emerging link," *Aging (Albany NY)*, vol. 5, no. 3, pp. 144–150, 2013.

[42] X.-Y. Zhao, J.-L. Sun, Y.-J. Hu et al., "The effect of overexpression of PGC-1α on the mtDNA4834 common deletion in a rat cochlear marginal cell senescence model," *Hearing Research*, vol. 296, pp. 13–24, 2013.

[43] C. Fujimoto and T. Yamasoba, "Mitochondria-targeted antioxidants for treatment of hearing loss: a systematic review," *Antioxidants (Basel)*, vol. 8, no. 4, p. 109, 2019.

[44] A. R. Fetoni, F. Paciello, R. Rolesi, G. Paludetti, and D. Troiani, "Targeting dysregulation of redox homeostasis in noise-induced hearing loss: oxidative stress and ROS signaling," *Free Radical Biology & Medicine*, vol. 135, pp. 46–59, 2019.

[45] O. S. Hong, M. J. Kerr, G. L. Poling, and S. Dhar, "Understanding and preventing noise-induced hearing loss," *Disease-a-Month*, vol. 59, no. 4, pp. 110–118, 2013.

[46] S. M. Vlajkovic, K.-H. Lee, A. C. Y. Wong et al., "Adenosine amine congener mitigates noise-induced cochlear injury," *Purinergic Signal*, vol. 6, no. 2, pp. 273–281, 2010.

[47] J. M. Miller, J. N. Brown, and J. Schacht, "8-iso-prostaglandin F(2alpha), a product of noise exposure, reduces inner ear blood flow," *Audiology & Neuro-Otology*, vol. 8, no. 4, pp. 207–221, 2003.

[48] K. K. Ohlemiller, S. L. McFadden, D.-L. Ding, P. M. Lear, and Y.-S. Ho, "Targeted mutation of the gene for cellular glutathione peroxidase (Gpx1) increases noise-induced hearing loss in mice," *Journal of the Association for Research in Otolaryngology*, vol. 1, no. 3, pp. 243–254, 2000.

[49] A. Fridberger, A. Flock, M. Ulfendahl, and B. Flock, "Acoustic overstimulation increases outer hair cell Ca2+ concentrations and causes dynamic contractions of the hearing organ," *Proceedings of the National Academy of Sciences of the United States of America*, vol. 95, no. 12, pp. 7127–7132, 1998.

[50] A. Kurabi, E. M. Keithley, G. D. Housley, A. F. Ryan, and A. C.-Y. Wong, "Cellular mechanisms of noise-induced hearing loss," *Hearing Research*, vol. 349, pp. 129–137, 2017.

[51] X. Wang, Y. Zhu, H. Long et al., "Mitochondrial calcium transporters mediate sensitivity to noise-induced losses of hair cells and cochlear synapses," *Frontiers in Molecular Neuroscience*, vol. 11, 2019.

[52] T. N. Le, L. V. Straatman, J. Lea, and B. Westerberg, "Current insights in noise-induced hearing loss: a literature review of the underlying mechanism, pathophysiology, asymmetry, and management options," *Journal of Otolaryngology - Head & Neck Surgery*, vol. 46, no. 1, p. 41, 2017.

[53] S. Orrenius, B. Zhivotovsky, and P. Nicotera, "Regulation of cell death: the calcium-apoptosis link," *Nature Reviews. Molecular Cell Biology*, vol. 4, no. 7, pp. 552–565, 2003.

[54] R. Nagashima, T. Yamaguchi, N. Kuramoto, and K. Ogita, "Acoustic overstimulation activates 5′-AMP-activated protein kinase through a temporary decrease in ATP level in the cochlear spiral ligament prior to permanent hearing loss in mice," *Neurochemistry International*, vol. 59, no. 6, pp. 812–820, 2011.

[55] S. W. Tait and D. R. Green, "Caspase-independent cell death: leaving the set without the final cut," *Oncogene*, vol. 27, no. 50, pp. 6452–6461, 2008.

[56] J. Schacht, A. E. Talaska, and L. P. Rybak, "Cisplatin and aminoglycoside antibiotics: hearing loss and its prevention," *The Anatomical Record: Advances in Integrative Anatomy and Evolutionary Biology*, vol. 295, no. 11, pp. 1837–1850, 2012.

[57] H. Li, Y. Song, Z. He et al., "Meclofenamic acid reduces reactive oxygen species accumulation and apoptosis, inhibits excessive autophagy, and protects hair cell-like HEI-OC1 cells from cisplatin-induced damage," *Frontiers in Cellular Neuroscience*, vol. 12, p. 139, 2018.

[58] W. Liu, X. Xu, Z. Fan et al., "Wnt signaling activates TP53-induced glycolysis and apoptosis regulator and protects against cisplatin-induced spiral ganglion neuron damage in the mouse cochlea," *Antioxidants & Redox Signaling*, vol. 30, no. 11, pp. 1389–1410, 2019.

[59] M. Jiang, T. Karasawa, and P. S. Steyger, "Aminoglycoside-induced cochleotoxicity: a review," *Frontiers in Cellular Neuroscience*, vol. 11, p. 308, 2017.

[60] Z. Zhong, X. Fu, H. Li et al., "Citicoline protects auditory hair cells against neomycin-induced damage," *Frontiers in Cell and Development Biology*, vol. 8, 2020.

[61] S. Gao, C. Cheng, M. Wang et al., "Blebbistatin inhibits neomycin-induced apoptosis in hair cell-like HEI-OC-1 cells and in cochlear hair cells," *Frontiers in Cellular Neuroscience*, vol. 13, 2020.

[62] Z. He, L. Guo, Y. Shu et al., "Autophagy protects auditory hair cells against neomycin-induced damage," *Autophagy*, vol. 13, no. 11, pp. 1884–1904, 2017.

[63] Z. He, Q. Fang, H. Li et al., "The role of FOXG1 in the postnatal development and survival of mouse cochlear hair cells," *Neuropharmacology*, vol. 144, pp. 43–57, 2019.

[64] Y. Zhang, W. Li, Z. He et al., "Pre-treatment with fasudil prevents neomycin-induced hair cell damage by reducing the accumulation of reactive oxygen species," *Frontiers in Molecular Neuroscience*, vol. 12, p. 264, 2019.

[65] T. Nguyen and A. Jeyakumar, "Genetic susceptibility to aminoglycoside ototoxicity," *International Journal of Pediatric Otorhinolaryngology*, vol. 120, pp. 15–19, 2019.

[66] Z. Gao, Y. Chen, and M. X. Guan, "Mitochondrial DNA mutations associated with aminoglycoside induced ototoxicity," *Journal of Otology*, vol. 12, no. 1, pp. 1–8, 2017.

[67] H. Zhao, R. Li, Q. Wang et al., "Maternally inherited aminoglycoside-induced and nonsyndromic deafness is associated with the novel C1494T mutation in the mitochondrial 12S rRNA gene in a large Chinese family," *American Journal of Human Genetics*, vol. 74, no. 1, pp. 139–152, 2004.

[68] D. Han, P. Dai, Q. Zhu et al., "The mitochondrial $tRNA^{Ala}$ T5628C variant may have a modifying role in the phenotypic manifestation of the 12S rRNA C1494T mutation in a large Chinese family with hearing loss," *Biochemical and Biophysical Research Communications*, vol. 357, no. 2, pp. 554–560, 2007.

[69] Q. Wang, Q.-Z. Li, D. Han et al., "Clinical and molecular analysis of a four-generation Chinese family with aminoglycoside-induced and nonsyndromic hearing loss associated with the mitochondrial 12S rRNA C1494T mutation," *Biochemical and Biophysical Research Communications*, vol. 340, no. 2, pp. 583–588, 2006.

[70] the CPNDS Consortium, C. J. D. Ross, H. Katzov-Eckert et al., "Genetic variants in TPMT and _COMT_ are associated with hearing loss in children receiving cisplatin chemotherapy," *Nature Genetics*, vol. 41, no. 12, pp. 1345–1349, 2009.

[71] J. J. Yang, J. Y. S. Lim, J. Huang et al., "The role of inherited TPMT and COMT genetic variation in cisplatin-induced ototoxicity in children with cancer," *Clinical Pharmacology and Therapeutics*, vol. 94, no. 2, pp. 252–259, 2013.

[72] J. Qi, L. Zhang, F. Tan et al., "Espin distribution as revealed by super-resolution microscopy of stereocilia," *American Journal of Translational Research*, vol. 12, no. 1, 2020.

[73] J. Qi, Y. Liu, C. Chu et al., "A cytoskeleton structure revealed by super-resolution fluorescence imaging in inner ear hair cells," *Cell Discovery*, vol. 5, no. 1, 2019.

[74] X. Yu, W. Liu, Z. Fan et al., "c-Myb knockdown increases the neomycin-induced damage to hair-cell-like HEI- OC1 cells in vitro," *Scientific Reports*, vol. 7, no. 1, 2017.

[75] A. Li, D. You, W. Li et al., "Novel compounds protect auditory hair cells against gentamycin-induced apoptosis by maintaining the expression level of H3K4me2," *Drug Delivery*, vol. 25, no. 1, pp. 1033–1043, 2018.

[76] W. Marcotti, S. M. van Netten, and C. J. Kros, "The aminoglycoside antibiotic dihydrostreptomycin rapidly enters mouse outer hair cells through the mechano-electrical transducer channels," *The Journal of Physiology*, vol. 567, no. 2, Part 2, pp. 505–521, 2005.

[77] N. Dehne, U. Rauen, H. de Groot, and J. Lautermann, "Involvement of the mitochondrial permeability transition in gentamicin ototoxicity," *Hearing Research*, vol. 169, no. 1-2, pp. 47–55, 2002.

[78] J. Guo, R. Chai, H. Li, and S. Sun, "Protection of hair cells from ototoxic drug-induced hearing loss," in *Advances in Experimental Medicine and Biology*, vol. 1130, pp. 17–36, Springer, 2019.

[79] M. Guan, Q. Fang, Z. He et al., "Inhibition of ARC decreases the survival of HEI-OC-1 cells after neomycin damage in vitro," *Oncotarget*, vol. 7, no. 41, pp. 66647–66659, 2016.

[80] Z. He, S. Sun, M. Waqas et al., "Reduced TRMU expression increases the sensitivity of hair-cell-like HEI-OC-1 cells to neomycin damage in vitro," *Scientific Reports*, vol. 6, no. 1, 2016.

[81] S. Sun, M. Sun, Y. Zhang et al., "In vivo overexpression of X-linked inhibitor of apoptosis protein protects against neomycin-induced hair cell loss in the apical turn of the cochlea during the ototoxic-sensitive period," *Frontiers in Cellular Neuroscience*, vol. 8, 2014.

[82] E. M. Priuska and J. Schacht, "Formation of free radicals by gentamicin and iron and evidence for an iron/gentamicin complex," *Biochemical Pharmacology*, vol. 50, no. 11, pp. 1749–1752, 1995.

[83] R. Esterberg, D. W. Hailey, A. B. Coffin, D. W. Raible, and E. W. Rubel, "Disruption of intracellular calcium regulation is integral to aminoglycoside-induced hair cell death," *The Journal of Neuroscience*, vol. 33, no. 17, pp. 7513–7525, 2013.

[84] R. Esterberg, T. Linbo, S. B. Pickett et al., "Mitochondrial calcium uptake underlies ROS generation during aminoglycoside-induced hair cell death," *Journal of Clinical Investigation*, vol. 126, no. 9, pp. 3556–3566, 2016.

[85] D. E. Desa, M. Bhanote, R. L. Hill et al., "Second-harmonic generation directionality is associated with neoadjuvant chemotherapy response in breast cancer core needle biopsies," *Journal of Biomedical Optics*, vol. 24, no. 8, pp. 1–14, 2019.

[86] H. C. Jensen-Smith, R. Hallworth, and M. G. Nichols, "Gentamicin rapidly inhibits mitochondrial metabolism in high-frequency cochlear outer hair cells," *PLoS One*, vol. 7, no. 6, article e38471, 2012.

[87] D. Mukherjea, S. Jajoo, T. Kaur, K. E. Sheehan, V. Ramkumar, and L. P. Rybak, "Transtympanic administration of short interfering (si)RNA for the NOX3 isoform of NADPH oxidase protects against cisplatin-induced hearing loss in the rat," *Antioxidants & Redox Signaling*, vol. 13, no. 5, pp. 589–598, 2010.

[88] S. A. Alam, K. Ikeda, T. Oshima et al., "Cisplatin-induced apoptotic cell death in Mongolian gerbil cochlea," *Hearing Research*, vol. 141, no. 1-2, pp. 28–38, 2000.

[89] S. C. Pfannenstiel, M. Praetorius, P. K. Plinkert, D. E. Brough, and H. Staecker, "Bcl-2 gene therapy prevents aminoglycoside-induced degeneration of auditory and vestibular hair cells," *Audiology & Neuro-Otology*, vol. 14, no. 4, pp. 254–266, 2009.

[90] Y. Wang et al., "Loss of CIB2 causes profound hearing loss and abolishes mechanoelectrical transduction in mice," *Frontiers in Molecular Neuroscience*, vol. 10, 2017.

[91] C. Zhu, C. Cheng, Y. Wang et al., "Loss of ARHGEF6 causes hair cell stereocilia deficits and hearing loss in mice," *Frontiers in Molecular Neuroscience*, vol. 11, 2018.

[92] Y. He, X. Lu, F. Qian, D. Liu, R. Chai, and H. Li, "Insm1a is required for zebrafish posterior lateral line development," *Frontiers in Molecular Neuroscience*, vol. 10, 2017.

[93] H. Kremer, "Hereditary hearing loss; about the known and the unknown," *Hearing Research*, vol. 376, pp. 58–68, 2019.

[94] M. X. Guan, "Molecular pathogenetic mechanism of maternally inherited deafness," *Annals of the New York Academy of Sciences*, vol. 1011, no. 1, pp. 259–271, 2004.

[95] Y. Ding, J. Leng, F. Fan, B. Xia, and P. Xu, "The role of mitochondrial DNA mutations in hearing loss," *Biochemical Genetics*, vol. 51, no. 7-8, pp. 588–602, 2013.

[96] F. Meng, Z. He, X. Tang et al., "Contribution of the $tRNA^{Ile}$ 4317A->G mutation to the phenotypic manifestation of the deafness-associated mitochondrial 12S rRNA 1555A->G mutation," *The Journal of Biological Chemistry*, vol. 293, no. 9, pp. 3321–3334, 2018.

[97] L. Xue, Y. Chen, X. Tang et al., "A deafness-associated mitochondrial DNA mutation altered the $tRNA^{Ser(UCN)}$ metabolism and mitochondrial function," *Mitochondrion*, vol. 46, pp. 370–379, 2019.

[98] F. Qian, X. Wang, Z. Yin et al., "The *slc4a2b* gene is required for hair cell development in zebrafish," *Aging (Albany NY)*, vol. 12, no. 19, pp. 18804–18821, 2020.

[99] X. Tang, R. Li, J. Zheng et al., "Maternally inherited hearing loss is associated with the novel mitochondrial $tRNA^{Ser(UCN)}$ 7505T>C mutation in a Han Chinese family," *Molecular Genetics and Metabolism*, vol. 100, no. 1, pp. 57–64, 2010.

[100] R. Li, K. Ishikawa, J.-H. Deng et al., "Maternally inherited nonsyndromic hearing loss is associated with the T7511C mutation in the mitochondrial $tRNA^{Ser(UCN)}$ gene in a Japanese family," *Biochemical and Biophysical Research Communications*, vol. 328, no. 1, pp. 32–37, 2005.

[101] V. Labay, G. Garrido, A. C. Madeo et al., "Haplogroup analysis supports a pathogenic role for the 7510T>C mutation of mitochondrial tRNA(Ser(UCN)) in sensorineural hearing loss," *Clinical Genetics*, vol. 73, no. 1, pp. 50–54, 2008.

[102] W. Fan, J. Zheng, W. Kong et al., "Contribution of a mitochondrial tyrosyl-tRNA synthetase mutation to the phenotypic expression of the deafness-associated $tRNA^{Ser(UCN)}$ 7511A>G mutation," *The Journal of Biological Chemistry*, vol. 294, no. 50, pp. 19292–19305, 2019.

[103] Q. Zhang, L. Zhang, D. Chen et al., "Deletion of Mtu1 (Trmu) in zebrafish revealed the essential role of tRNA modification in mitochondrial biogenesis and hearing function," *Nucleic Acids Research*, vol. 46, no. 20, pp. 10930–10945, 2018.

[104] D. Chen, F. Li, Q. Yang et al., "The defective expression of _gtpbp3_ related to tRNA modification alters the mitochondrial function and development of zebrafish," *The International Journal of Biochemistry & Cell Biology*, vol. 77, Part A, pp. 1–9, 2016.

[105] J. M. Denu, "The Sir2 family of protein deacetylases," *Current Opinion in Chemical Biology*, vol. 9, no. 5, pp. 431–440, 2005.

[106] B. Schwer and E. Verdin, "Conserved metabolic regulatory functions of sirtuins," *Cell Metabolism*, vol. 7, no. 2, pp. 104–112, 2008.

[107] M. C. Haigis and D. A. Sinclair, "Mammalian sirtuins: biological insights and disease relevance," *Annual Review of Pathology*, vol. 5, no. 1, pp. 253–295, 2010.

[108] E. Verdin, M. D. Hirschey, L. W. S. Finley, and M. C. Haigis, "Sirtuin regulation of mitochondria: energy production, apoptosis, and signaling," *Trends in Biochemical Sciences*, vol. 35, no. 12, pp. 669–675, 2010.

[109] J. Du, Y. Zhou, X. Su et al., "Sirt5 is a NAD-dependent protein lysine demalonylase and desuccinylase," *Science*, vol. 334, no. 6057, pp. 806–809, 2011.

[110] R. A. Mathias, T. M. Greco, A. Oberstein et al., "Sirtuin 4 is a lipoamidase regulating pyruvate dehydrogenase complex activity," *Cell*, vol. 159, no. 7, pp. 1615–1625, 2014.

[111] B.-H. Ahn, H.-S. Kim, S. Song et al., "A role for the mitochondrial deacetylase Sirt3 in regulating energy homeostasis," *Proceedings of the National Academy of Sciences of the United States of America*, vol. 105, no. 38, pp. 14447–14452, 2008.

[112] S. Someya, W. Yu, W. C. Hallows et al., "Sirt3 mediates reduction of oxidative damage and prevention of age-related hearing loss under caloric restriction," *Cell*, vol. 143, no. 5, pp. 802–812, 2010.

[113] M. . D. Hirschey, T. Shimazu, E. Jing et al., "SIRT3 deficiency and mitochondrial protein hyperacetylation accelerate the development of the metabolic syndrome," *Molecular Cell*, vol. 44, no. 2, pp. 177–190, 2011.

[114] W. C. Hallows, S. Lee, and J. M. Denu, "Sirtuins deacetylate and activate mammalian acetyl-CoA synthetases," *Proceedings of the National Academy of Sciences of the United States of America*, vol. 103, no. 27, pp. 10230–10235, 2006.

[115] R. Tao, M. C. Coleman, J. D. Pennington et al., "Sirt3-mediated deacetylation of evolutionarily conserved lysine 122 regulates MnSOD activity in response to stress," *Molecular Cell*, vol. 40, no. 6, pp. 893–904, 2010.

[116] W. Yu, K. E. Dittenhafer-Reed, and J. M. Denu, "SIRT3 protein deacetylates isocitrate dehydrogenase 2 (IDH2) and regulates mitochondrial redox status," *The Journal of Biological Chemistry*, vol. 287, no. 17, pp. 14078–14086, 2012.

[117] A. H. H. Tseng, S.-S. Shieh, and D. L. Wang, "SIRT3 deacetylates FOXO3 to protect mitochondria against oxidative damage," *Free Radical Biology & Medicine*, vol. 63, pp. 222–234, 2013.

[118] C. Han and S. Someya, "Maintaining good hearing: calorie restriction, Sirt3, and glutathione," *Experimental Gerontology*, vol. 48, no. 10, pp. 1091–1095, 2013.

[119] X. Qiu, K. Brown, M. D. Hirschey, E. Verdin, and D. Chen, "Calorie restriction reduces oxidative stress by SIRT3-mediated SOD2 activation," *Cell Metabolism*, vol. 12, no. 6, pp. 662–667, 2010.

[120] S. A. Samant, H. J. Zhang, Z. Hong et al., "SIRT3 deacetylates and activates OPA1 to regulate mitochondrial dynamics during stress," *Molecular and Cellular Biology*, vol. 34, no. 5, pp. 807–819, 2014.

[121] K. . D. Brown, S. Maqsood, J.-Y. Huang et al., "Activation of SIRT3 by the NAD^+ precursor nicotinamide riboside protects from noise-induced hearing loss," *Cell Metabolism*, vol. 20, no. 6, pp. 1059–1068, 2014.

[122] Y. Quan, L. Xia, J. Shao et al., "Adjudin protects rodent cochlear hair cells against gentamicin ototoxicity via the SIRT3-ROS pathway," *Scientific Reports*, vol. 5, no. 1, 2015.

[123] M. C. Haigis, R. Mostoslavsky, K. M. Haigis et al., "SIRT4 inhibits glutamate dehydrogenase and opposes the effects of calorie restriction in pancreatic β cells," *Cell*, vol. 126, no. 5, pp. 941–954, 2006.

[124] D. B. Lombard, D. X. Tishkoff, and J. Bao, "Mitochondrial sirtuins in the regulation of mitochondrial activity and metabolic adaptation," *Handbook of Experimental Pharmacology*, vol. 206, pp. 163–188, 2011.

[125] C. Schlicker, M. Gertz, P. Papatheodorou, B. Kachholz, C. F. W. Becker, and C. Steegborn, "Substrates and regulation mechanisms for the human mitochondrial sirtuins Sirt3 and Sirt5," *Journal of Molecular Biology*, vol. 382, no. 3, pp. 790–801, 2008.

[126] N. Nasrin, X. Wu, E. Fortier et al., "SIRT4 regulates fatty acid oxidation and mitochondrial gene expression in liver and muscle cells," *The Journal of Biological Chemistry*, vol. 285, no. 42, pp. 31995–32002, 2010.

[127] G. Laurent, N. . J. German, A. . K. Saha et al., "SIRT4 coordinates the balance between lipid synthesis and catabolism by repressing malonyl CoA decarboxylase," *Molecular Cell*, vol. 50, no. 5, pp. 686–698, 2013.

[128] Y.-X. Luo, X. Tang, X.-Z. An et al., "SIRT4 accelerates Ang II-induced pathological cardiac hypertrophy by inhibiting manganese superoxide dismutase activity," *European Heart Journal*, vol. 38, no. 18, pp. 1389–1398, 2017.

[129] A. Lang, S. Grether-Beck, M. Singh et al., "MicroRNA-15b regulates mitochondrial ROS production and the senescence-associated secretory phenotype through sirtuin 4/SIRT4," *Aging (Albany NY)*, vol. 8, no. 3, pp. 484–505, 2016.

[130] R. A. Frye, "Phylogenetic classification of prokaryotic and eukaryotic Sir2-like proteins," *Biochemical and Biophysical Research Communications*, vol. 273, no. 2, pp. 793–798, 2000.

[131] E. Michishita, J. Y. Park, J. M. Burneskis, J. C. Barrett, and I. Horikawa, "Evolutionarily conserved and nonconserved cellular localizations and functions of human SIRT proteins," *Molecular Biology of the Cell*, vol. 16, no. 10, pp. 4623–4635, 2005.

[132] D. B. Lombard, F. W. Alt, H.-L. Cheng et al., "Mammalian Sir2 homolog SIRT3 regulates global mitochondrial lysine acetylation," *Molecular and Cellular Biology*, vol. 27, no. 24, pp. 8807–8814, 2007.

[133] C. Peng, Z. Lu, Z. Xie et al., "The first identification of lysine malonylation substrates and its regulatory enzyme," *Molecular & Cellular Proteomics*, vol. 10, no. 12, p. M111.012658, 2011.

[134] T. Nakagawa, D. J. Lomb, M. C. Haigis, and L. Guarente, "SIRT5 deacetylates carbamoyl phosphate synthetase 1 and regulates the urea cycle," *Cell*, vol. 137, no. 3, pp. 560–570, 2009.

[135] M. Ogura, Y. Nakamura, D. Tanaka et al., "Overexpression of SIRT5 confirms its involvement in deacetylation and activation of carbamoyl phosphate synthetase 1," *Biochemical and Biophysical Research Communications*, vol. 393, no. 1, pp. 73–78, 2010.

[136] L. Zhou, F. Wang, R. Sun et al., "SIRT5 promotes IDH2 desuccinylation and G6PD deglutarylation to enhance cellular antioxidant defense," *EMBO Reports*, vol. 17, no. 6, pp. 811–822, 2016.

[137] Y. Wang, Y. Zhu, S. Xing, P. Ma, and D. Lin, "SIRT5 prevents cigarette smoke extract-induced apoptosis in lung epithelial cells via deacetylation of FOXO3," *Cell Stress & Chaperones*, vol. 20, no. 5, pp. 805–810, 2015.

[138] Z.-F. Lin, H.-B. Xu, J.-Y. Wang et al., "SIRT5 desuccinylates and activates SOD1 to eliminate ROS," *Biochemical and Biophysical Research Communications*, vol. 441, no. 1, pp. 191–195, 2013.

[139] R. A. H. van de Ven, D. Santos, and M. C. Haigis, "Mitochondrial sirtuins and molecular mechanisms of aging," *Trends in Molecular Medicine*, vol. 23, no. 4, pp. 320–331, 2017.